12.12.90

UCM

BJR

THE BRITISH JOURNAL OF RADIOLOGY

Volume 62 Number 743 November 1989

CUK-H06093-19-P25850.

19

X-ray Diagnosis • Ultrasound • Interventional Radiology
Radiotherapy • Oncology • Hyperthermia
Nuclear Medicine • Nuclear Magnetic Resonance
Radiation Physics • Radiobiology • Radiation Protection

BJR is published by The British Institute of Radiology BIR

For Quality Assurance in Radiation Therapy...

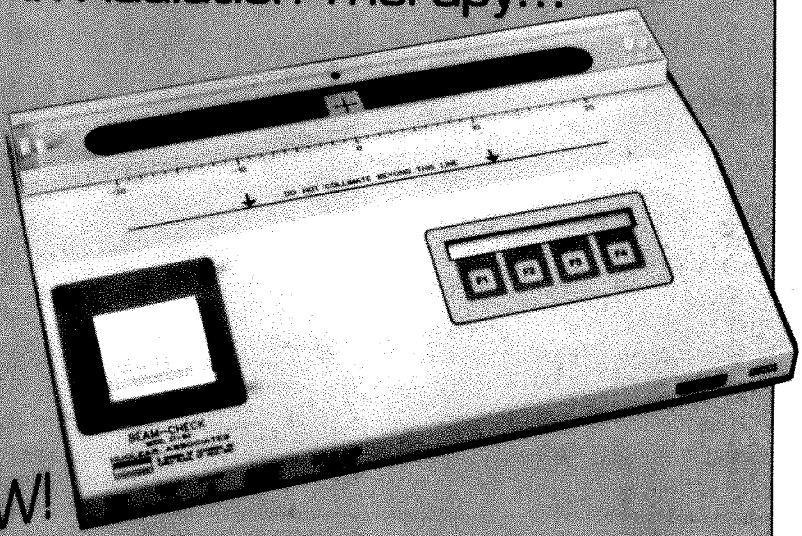

NEW!

BEAM-CHECK™*

Light & Radiation Field Analyzer

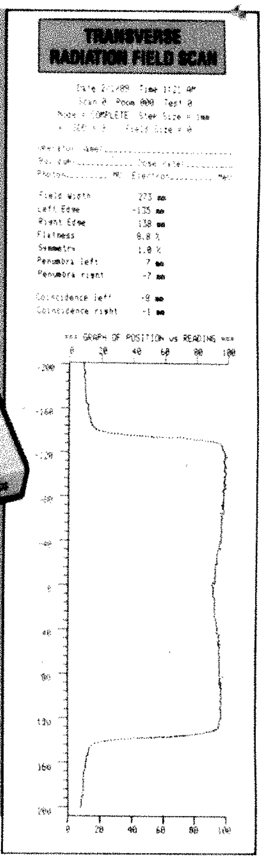

TRANSVERSE RADIATION FIELD SCAN

```
Scan 0  Room 000  Test 0
Mode = COMPLETE  Step Size = 1mm

Field Width          273 mm
Left Edge           -135 mm
Right Edge           138 mm
Flatness             0.8 %
Symmetry             1.0 %
Penumbra left          7 mm
Penumbra right        -7 mm

Coincidence left      -9 mm
Coincidence right     -1 mm

*** GRAPH OF POSITION vs READING ***
```

Printed Output of Radiation Field Scan

- Checks light field and radiation field coincidence.
- Analyzes radiation field for flatness, symmetry, and penumbral size.
- Built-in graphics printer provides hardcopy outputs of scan information.
- Single axis diode scanner.
- Self-contained, no cables to attach.

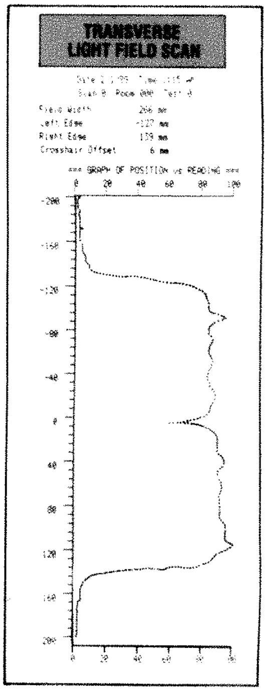

TRANSVERSE LIGHT FIELD SCAN

```
Scan 0  Room 000  Test 0
Field Width          266 mm
Left Edge           -127 mm
Right Edge           139 mm
Crosshair Offset       6 mm

*** GRAPH OF POSITION vs READING ***
```

Printed Output of Light Field Scan

*Developed by Lawrence E. Reinstein, Ph.D.,
Radiation Oncology Department,
State University of New York at Stony Brook.

For more information, request Bulletin 430-14

NUCLEAR ASSOCIATES

VICTOREEN

Division of VICTOREEN, INC.
100 VOICE ROAD • P.O. BOX 349
CARLE PLACE, NY 11514-0349 U.S.A.
(516) 741-6360 • FAX (516) 741-5414
A Member of THE TALBEX GROUP, PLC

TM, Victoreen, Inc.

P25850

BJR THE BRITISH JOURNAL OF RADIOLOGY

Established 1896

The Editorial Committee

Honorary Editors
D. G. Shaw, FRCP, FRCR
N. J. McNally, BSc, MSc, PhD

Deputy Editor
C. K. Bomford, BSc, MPhil, FInstP
D. M. King, MB, BS, FRCR, DMRD

Associate Editors
P. Armstrong, MB, BS, FRCR, DMRD
H. Baddeley, MB, BS, DMRD, FRCR, MRACR
P. R. Blake, MD, MB, BS, BSc, FRCR
J. A. Bullimore, MB, BS, MRCS, LRCP, DMRT, FRCR
R. G. Dale, MSc, PhD, CPhys, FInstP
P. Dawson, BSc, PhD, MB, BS, MRCP, MInstP, FRCR
S. Dische, MD, FRCR
F. A. Duck, PhD, MIEEE
A. H. Freeman, MB, BS, FRCR
R. M. Harrison, BSc, MSc, PhD, FInstP
J. W. Hopewell, BSc, PhD
H. W. C. Loose, DMRD, FRCR
A. M. Peters, BSc, MSc, MB, ChB, MD, MRCPath
D. W. Pilling, MB, ChB, DCH, DMRD, FRCR
J. F. Reidy, MB, BS, FRCP, FRCR
J. R. K. Savage, DSc
R. A. Shields, PhD
D. M. Tait, MB, ChB, MRCP, FRCR
J. Tudor, MB, BS, FRCR
A. R. Valentine, MB, BS, MRCS, LRCP, FRCR, DMRD
G. H. Whitehouse, MB, BS, FRCP, FRCR, DMRD
A. G. Wilson, FRCP, FRCR
E. P. Wraight, MB, BChir, PhD, DMRT

Associate Editors Overseas
S. G. A. Chenery, PhD, FCCPM (North America)
B. J. Cremin, MD, FRCR, FRACR (South Africa)
R. Fox, DPhil (Australia)
M. Takahashi, MD (Japan)
D. M. Taylor, DSc, CChem, FRSC (Continental Europe)

Managing Editor: T. R. Hogan, BSc, PhD

The British Journal of Radiology is published monthly by the British Institute of Radiology, 36 Portland Place, London W1N 4AT. Telephone 01-580 4189 (editorial). Editorial communications should be addressed to the Honorary Editors in accordance with the Instructions to Authors published in the January issue each year, and copies of which may be obtained from the Managing Editor upon request.

Advertisements. Communications should be addressed to the Advertising Manager at the above address. Tel. 01-631 1168.

Subscriptions. The monthly fulfilment and distribution are carried out by Butterworth Scientific Ltd, PO Box 63, Westbury House, Bury Street, Guildford, Surrey GU2 5BH, UK. Telephone 0483 300966.

UK and Overseas subscription orders should be sent to: Westbury Subscription Services, PO Box 101, Sevenoaks, Kent TN15 8PL, UK. Telephone 0732 885833. Telex 95678. Facsimile 0732 884079. Cable Westbury, Sevenoaks, Kent. North American orders should be sent to: Journals Fulfilment Department, Butterworths, 80 Montvale Avenue, Stoneham, MA 02180, USA. Telex 880052. Telephone (617) 438 8464.

The annual subscription to *The British Journal of Radiology* (12 issues) for UK readers is £115.00. Overseas rates are £125.00. These prices include delivery by sea mail; airmail rates are available on request. Copies of this journal sent to subscribers in Bangladesh, Canada, India, Japan, Pakistan, Sri Lanka and USA are air-speeded for quicker delivery at no extra cost. Subscriptions are on a calendar year basis only.

All claims for unfulfilled subscriptions should be sent to Westbury Subscription Services at the above address.

Back issues prior to the current volume are available from Wm Dawson & Sons Ltd, Cannon House, Folkestone, Kent, England CT19 5EE. Telephone 0303 57421.

US mailing agents: Mercury Airfreight International Ltd Inc. Second class postage paid at Rahway, NJ, USA. Postmaster: send address corrections to The British Journal of Radiology, c/o Mercury Airfreight International Ltd Inc., 10B Englehard Avenue, Avenel, NJ 07001, USA.

THE BRITISH INSTITUTE OF RADIOLOGY

BIR

Founded 1897
Incorporated by Royal Charter
Patron: Her Majesty The Queen

The British Institute of Radiology is an association of persons interested in radiology and allied subjects. Meetings are held monthly from October until May. Particulars of membership and other information may be obtained on application to the General Secretary at the Institute, 36 Portland Place, London W1N 4AT.
Telephone: 01-580 4085 and 01-580 4189.
Cable Address: Britology, London W1.

President
C. R. Hill, BA, PhD, DSc, FIEE, FInstP

Honorary Secretaries
M. Gowland, MB, ChB, FRCR, MRCP(Hon)
M. P. Law, BSc, PhD

Honorary Treasurer
D. S. McIntosh, BSc, PhD, ARIC, MPS

General Secretary
Susan M. Johnstone, BA

SCHERING

Ultra-comfortable contrast medium

ULTRAVIST

iopromide

Prescribing Information: Presentation Intravascular injections of non-ionic iopromide in strengths of 240mg, 300mg and 370mg of iodine/ml. **Uses** Delineation of the vascular and renal systems. **Dosage and Administration** Intravenous urography: Adult minim
doses: Ultravist 370: 0.8ml/kg body weight; Ultravist 300: 1ml/kg body weight; Ultravist 240: 1.3ml/kg body weight. Computed Tomography: Cranial CT: Ultravist 240: 1.5-2.5ml/kg body weight; Ultravist 300: 1-2ml/kg body weight; Ultravist 370: 1-1.5ml/kg
weight. Whole-body CT: Dosage depends on investigation and scanner. Angiography: Dosage (6-80ml) depends on age, weight, cardiac output, general condition, and investigation. **Contra-indications, Warnings, etc** Contra-indications: Possible hypersensiti
contrast media, thyrotoxicosis, cardiac decompensation, hysterosalpingography during pregnancy, acute pelvic inflammation. Warnings, etc: Caution if there is: severe hepatic or renal impairment; cardiac or circulatory insufficiency; cerebral arterioscler
cerebral spasmodic conditions; epilepsy; juvenile-onset or long-standing diabetes; pulmonary emphysema; poor general health; hyperthyroidism, multiple myeloma; a history of allergy, especially if patient has received a contrast medium before. Use d
preganancy only if essential. Do not mix contrast media and anti-allergic agents. With multiple myeloma, juvenile-onset or long-standing diabetes, polyuria, oliguria, gout or marasmus, do not restrict fluids. First correct disturbances of water and electro
With phaeochromocytoma, premedicate with an alpha-blocker. Administer Ultravist to recumbent patients and closely observe for at least 30 minutes. The capacity of the thyroid to take up iodine is reduced. If marked side-effects or suspected allergic rea
occur during injection, and do not disappear when it is interrupted, stop the investigation. Even minor side-effects may be signs of severe reaction. Life-threatening side-effects include hypotensive collapse, circulatory failure, ventricular fibrillation, cardiac
pulmonary oedema, anaphylactic shock or other allergic manifestations and convulsions or other cerebral symptoms. **List Price:** Ultravist 370 1x100ml £43.39. **Product Licence No:** 0053/0173 Ultravist 240; 0053/0174 Ultravist 300; 0053/0175 Ultravis
Product Licence Holder: Schering Health Care Limited, The Brow, Burgess Hill, West Sussex RH15 9NE. Further information is available on request from: Schering Health Care Limited, Hospital Diagnostics and Pharmaceuticals, The Brow, Burge
West Sussex, RH15 9NE. 'Ultravist' is a registered trade mark.

SHCL UV 11

VOL 62 NO 743 NOVEMBER 1989

The British Journal of Radiology

Contents

Papers

Page

Sequential imaging of post-operative thrombus using the In-111-labelled platelet-specific monoclonal antibody P256 963
A. W. J. Stuttle, J. Klosok, A. M. Peters and J. P. Lavender

^{99}Tc^{m}-HMPAO single photon emission computed tomography in partial epilepsy: a preliminary report 970
D. F. Smith, F. W. Smith, R. S. G. Knight, R. C. Roberts and H. G. Gemmell

Total abdominal and pelvic ultrasound: incidental findings and a comparison between outpatient and general practice referrals in 1000 cases 974
P. Mills, A. E. A. Joseph and E. J. Adam

Can ultrasound replace the intravenous urogram in preliminary investigation of renal tract disease? A prospective study 977
H. G. Lewis-Jones, G. H. R. Lamb and P. L. Hughes

Ultrasound-guided, histological, fine-needle biopsy from suspect parathyroid tumours: success-rate and reliability of histological diagnosis 981
S. Karstrup, A. Glenthøj, B. Hainau, L. Hegedüs, S. Torp-Pedersen and H. H. Holm

The value of transoesophageal ultrasonography in the management of a mediastinal foregut cyst 986
J. E. Page, A. G. Wilson and M. A. de Belder

A quality assessment of the effects of a hydrogenous filter on a p(66)Be(40) neutron beam 989
J. P. Slabbert, P. J. Binns, H. L. Jones and J. H. Hough

Ovarian failure following abdominal irradiation in childhood: the radiosensitivity of the human oocyte 995
W. H. B. Wallace, S. M. Shalet, J. H. Hendry, P. H. Morris-Jones and H. R. Gattamaneni

A physical evaluation of the imaging performance of a high-resolution fluorography system 999
A. R. Cowen

Surface heating of diagnostic ultrasound transducers 1005
F. A. Duck, H. C. Starritt, G. R. ter Haar and M. J. Lunt

Technical note

The use of an infrared touch-screen to control the sensitivity of ultrasound scanners in clinical practice 1014
S. D. Pye, V. Elliott, I. Marshall, D. Millar, S. Robertson, W. N. McDicken and S. R. Wild

Case reports

Ultrasonographic appearances of parathyroid carcinoma 1017
B. D. Daly, S. L. Coffey and M. Behan

Uterine leiomyomata: sonographic mimicry 1019
R. L. Borgstein, J. J. Shaw and R. H. Pearson

Ductal adenoma of the breast: mammographic appearances and pathological correlation 1021
E. Moskovic and S. Ramachandra

Agenesis of the salivary glands: a report of two cases 1023
A. M. Whyte and M. W. J. Hayward

An illustrative case: enough to raise one's blood pressure 1026
J. Herbetko, V. Batty and J. G. B. Millar

Case of the month

Common symptom: uncommon cause 1029
K. T. Tung and G. F. Wilson

Short communication

Control of patient positioning for fast neutron therapy using positron emission tomography 1031
S. Vynckier, F. Vanneste, F. Richard, A. Bol, C. Michel and A. Wambersie

Correspondence

An interesting radiation protection finding around a linear accelerator 1033
T. Conere, H. Weatherburn and B. Wassem

Visits to controlled areas in X-ray departments 1033
B. A. Goddard

British standards specification for balloon dilatation catheters 1034
G. Hartnell

Radiological appearances of colonic ring staple anastomoses 1034
T. Y. K. Chan and T. Davidson

Authors' reply 1034
B. D. Daly and B. M. Crowley

Book reviews

Pioneers in angiography. The Portuguese School of Angiography, 2nd edn. *J. A. Veiga-Pires and R. G. Grainger* (Eds) 1035

Atlas of normal roentgen variants that may simulate disease, 4th edn *T. E. Keats* 1035

Frontiers in European radiology 5. *A. L. Baert, E. Boijsen, W. A. Fuchs and F. H. W. Heuck* (Eds) 1035

Vascular anatomy of the spinal cord. Neuroradiological investigations and clinical syndromes. *A. K. Thron* 1036

Clinical imaging of the cerebello-pontine angle. *A. Valavanis, O. Schubiger and T. P. Naidich* 1036

Breast cancer detection: mammography and other methods in breast imaging, 2nd edn. *L. W. Bassett and R. H. Gold* (Eds) 1036

BIR Bulletin *facing page* 1036

Featured in the next issue

Double-contrast computed tomographic arthrography of the shoulder joint
J. V. Cook and R. Tayar

Demonstration of osteochondritis dissecans of the talus by coronal computed tomographic arthrography
A. M. Davies and V. N. Cassar-Pullicino

Sublethal damage repair and radiosensitivity of human squamous cell carcinoma cells grown with different culture techniques
J. H. M. Schwachöfer, R. P. M. A. Crooijmans, J. van Gasteren, J. Hoogenhout, C. R. Jerusalem and H. B. Kal

© 1989. The British Institute of Radiology. This publication is copyright under the Berne Convention and the Universal Copyright Convention. All rights reserved, apart from any relaxations permitted under national copyright laws, no part of this publication may be reproduced, stored in a retrieval system or transmitted in any form or by any means without the prior permission of the copyright owners. Permission is not, however, required to copy abstracts of papers or of articles on condition that a full reference to the source is shown. Multiple copying of the contents of the publication without permission is always illegal. Published by The British Institute of Radiology, 36 Portland Place, London W1N 4AT. Origination by BPCC Whitefriars Ltd, Tunbridge Wells, and printed and bound in Great Britain by BPCC Wheatons Ltd, Exeter.

ISSN 0007 1285

VOL 62 NO 744 DECEMBER 1989

The British Journal of Radiology

Contents

Papers

Page

Ultrasound-guided chemical parathyroidectomy in patients with primary hyperparathyroidism: a prospective study 1037
S. Karstrup, I. Transbøl, H. H. Holm, A. Glenthøj and L. Hegedüs

Double-contrast CT arthrography of the shoulder joint 1043
J. V. Cook and R. Tayar

Demonstration of osteochondritis dissecans of the talus by coronal CT arthrography 1050
A. M. Davies and V. N. Cassar-Pullicino

The influence of Buscopan on adverse reactions to intravascular contrast media 1056
S. Sharma, M. Rajani, A. Khosla, N. Misra and R. K. Goulatia

The correlation of histopathological, microradiographic and ultrasound features in diseases of the prostate gland 1059
D. R. Jones, G. J. Griffiths, M. C. Parkinson, K. T. Evans, E. E. Roberts, R. Ll. Davies, T. J. Harrison and W. B. Peeling

Low-field cine MRI in aortic valve disease 1063
M. J. Metcalfe, R. A. Jones, T. W. Redpath, F. W. Smith, K. Jennings and S. Walton

Gadolinium-enhanced magnetic resonance imaging of spinal tumours 1067
C. I. Rothwell, T. Jaspan, B. S. Worthington and I. M. Holland

Periventricular enhancement: a non-pathognomonic sign of intracerebral tumours 1075
P. A. Murray, A. N. Harnett, P. I. Thompson, M. Charlesworth and P. N. Plowman

Modulation in the radiosensitivity of MCF-7 human breast carcinoma cells by 17B-estradiol and tamoxifen 1079
D. E. Wazer, O. F. Tercilla, P.-S. Lin and R. Schmidt-Ullrich

Sublethal damage repair and radiosensitivity of human squamous cell carcinoma cells grown with different culture techniques 1084
J. H. M. Schwachöfer, R. P. M. A. Crooijmans, J. van Gesteren, J. Hoogenhout, C. R. Jerusalem and H. B. Kal

Case reports

Burkitt's lymphoma following treatment for Hodgkin's disease 1089
A. C. R. Robinson, G. G. Khoury and D. Carney

Induced fluid movement within a giant ovarian cyst demonstrated by echo-planar imaging 1091
B. S. Worthington, B. Chapman, R. Ordidge, R. Coxon, M. K. Stehling, E. M. Symonds and P. Mansfield

Sonographic demonstration of renal tumour extension into the contralateral renal vein 1093
P. Carvalho.

Spontaneous regression of multiple bone metastases in malignant melanoma 1095
M. E. A. O'Connor, B. W. E. M. Powell, J. M. O'Connell and C. L. Harmer

Spontaneous pneumothorax with metastatic seminoma 1100
A. J. Chippindale, B. Patel and B. Eddelston

Case of the month

A painful knee 1103
A. M. Davies and N. Evans

Short communication

A radiological feature to assist in the diagnosis of intestinal obstruction 1105
J. Walker and H. Carty

Correspondence

A localized hypersensitivity reaction to co-trimoxazole in a pre-irradiated field simulating recall phenomenon
I. L. Atahan, F. H. Akyol, M. Gürkaynak, H. Alanyali and E. Özyar 1107

Kinetics of recovery from sublethal radiation damage
R. Guttenberger and H. D. Thames 1107

Authors' reply
J. W. Hopewell and G. M. J. M. van den Aardweg 1109

The immediate film in intravenous urography
J. G. B. Russell and J. M. Weller 1110

Lung cancer: tissue characterization by MRI T_1, T_2 values *in vitro* and role of histopathology 1111
S. S. Ranade, P. N. Trivedi and V. S. Bamane

The potential value of hyperthermia in the management of human immunodeficiency virus infection
K. D. Cochran and H. Weatherburn 1112

Proceedings

Proceedings of the British Institute of Radiology
Clinical relevance of radiobiological models, 26 May 1989 1113
Radiology in AIDS, 19 January 1989 1117

Book reviews

Computed tomography of the abdomen in adults. 85 radiological exercises for students and practitioners. *A. Wackenheim and A. Badoz* 1118
Blood flow in artificial organs and cardiovascular prostheses. Oxford Medical Engineering Series, No. 8. *J. C. Barbenel, A. C. Fisher, J. D. S. Gaylor, W. J. Anderson and C. D. Sheldon* (Eds) 1118
Anatomy and MRI of the joints. A multiplanar atlas. *W. D. Middleton and T. L. Lawson* (Eds) 1118
Nuclear medicine. Self-assessment in radiology and imaging, No. 5. *S. Karimjee, A. Thomas and W. Taylor* 1119
Practical NMR imaging. *M. A. Foster and J. M. S. Hutchison* (Eds) 1119
Manual of nuclear medicine procedures. *R. Mistry* 1119
Assessing the skeletal maturity of the hand wrist: Fels method. *A. F. Roche, W. C. Chumlea and D. Thissen* 1120
Glucagon in 1987: gastrointestinal and hepatobiliary physiology diagnosis and treatment. *J. Picazo* (Ed.) 1120
Recent developments in nonionic contrast media. *V. Taenzer and S. Wende* (Eds) 1121
Imaging techniques in orthopaedics. *C. S. B. Galasko and I. Isherwood* (Eds) 1121
Appropriate diagnostic technology in the management of cardiovascular diseases, Technical report series 771. *World Health Organization* 1121
Radiology of the foot and ankle. *T. H. Berquist* (Ed.) 1121
Radiology of the oesophagus. *D. N. Hüpscher* 1122
Principles of radiopharmacology. *H. Deckard and P. H. Cox* 1122
An atlas of planar and SPECT bone scans. *I. Gogelman and B. D. Collier* 1122

Index to Vol. 62 *follows text*
BIR Bulletin *follows index*

Featured in the next issue

MR: boundless possibilities . . . or possible boundaries? (Silvanus Thompson Lecture)
I. R. Young

Randomized trial of laser-assisted passage through occluded femoro-popliteal arteries
W. D. Jeans, P. Murphy, A. O. Hughes, M. Horrocks and R. N. Baird

Assessment and comparison of chest radiography in the United States and in Sweden
W. K. Leitz, B. R. K. Hedberg-Vikström, B. J. Conway, C. K. Showalter and F. G. Reuter

© 1989: The British Institute of Radiology. This publication is copyright under the Berne Convention and the Universal Copyright Convention. All rights reserved, apart from any relaxations permitted under national copyright laws, no part of this publication may be reproduced, stored in a retrieval system or transmitted in any form or by any means without the prior permission of the copyright owners. Permission is not, however, required to copy abstracts of papers or of articles on condition that a full reference to the source is shown. Multiple copying of the contents of the publication without permission is always illegal. Published by The British Institute of Radiology, 36 Portland Place, London W1N 4AT. Origination by BPCC Whitefriars Ltd, Tunbridge Wells, and printed and bound in Great Britain by BPCC Wheatons Ltd, Exeter.
ISSN 0007 1285

1989, *The British Journal of Radiology*, 62, 963–969

VOLUME 62 NUMBER 743 NOVEMBER 1989

The British Journal of Radiology

Sequential imaging of post-operative thrombus using the In-111-labelled platelet-specific monoclonal antibody P256

By *A. W. J. Stuttle, J. Klosok, A. M. Peters and J. P. Lavender

Departments of Diagnostic Radiology and Orthopaedic Surgery, Hammersmith Hospital, Du Cane Road,
London W12 0HS

(*Received May 1989 and in revised form June 1989*)

Abstract. Eleven patients undergoing total hip replacement were studied by radioimmunoscintigraph for development of post-operative thrombus. Images were obtained using the ^{111}In-labelled Fab′ fragment of a monoclonal antibody (P256) directed against human platelets. Six patients showed focal accumulation of radioactivity in the lower limbs. Three of these had contrast venograms that were all positive for thrombus. Two of these six patients showed evidence of pulmonary localization of P256-Fab′ and this correlated with positive ventilation/perfusion scintigraphy in one of the patients. Sequential imaging with ^{111}In-P256 Fab′ not only established a diagnosis of deep venous thrombus but also provided useful information regarding its natural history.

Venous thrombosis in the leg veins is seen in 20–30% of patients following surgery, increasing to 50% after hip surgery (Kakkar, 1977). Although it is a cause of widespread morbidity and mortality, our knowledge of its natural history and outcome is limited. As a result, management is uncertain and subject to wide differences of opinion.

What is the relationship between venous thrombosis and pulmonary embolism (PE)? Because of difficulties in the clinical diagnosis of PE, the only accurate data on this question must be based on pulmonary angiography or ventilation/perfusion imaging. A number of such studies are available including one by Browse et al (1976), who showed an incidence of venous thrombosis in 17 out of 50 (34%) and of PE in 12 out of 50 (24%) post-operative patients. These data on venous thrombosis are based on ascending venography performed prospectively and on the use of radioiodinated fibrinogen. Both these diagnostic methods have disadvantages: venography can only be performed on one occasion whilst labelled fibrinogen is insensitive to thrombus in the thigh and pelvis and liable to false positive results due to protein extravasation and focal venous dilation. More recently, Doppler ultrasound has been used to measure venous flow during calf compression. However, a non-obstructing thrombus is not detected and, again, upper femoral and pelvic thrombus is missed.

Indium-111-hydroxyquinoline-labelled platelets have been found useful for the detection of thrombus but have not gained widespread use because of the time and technical skill required in the labelling procedure. We have recently described an ^{111}In-labelled monoclonal antibody (P256), which binds to the IIb/IIIa glycoprotein complex on the platelet surface, for thrombus detection (Peters et al, 1986; Stuttle et al, 1988a). Intravenous injection of this tracer results in rapid *in vivo* labelling of platelets, thereby avoiding the need for cell separation. Imaging of platelet uptake on deep venous thrombus (DVT) in the leg can readily be seen with a gamma camera.

P256 whole antibody and its F(ab′)$_2$ fragment have been shown to cause dose related aggregation of platelets *in vitro* and this is a serious disadvantage. The monovalent Fab′ fragment, however, does not cause activation of platelets, despite binding with relatively high affinity (Stuttle et al, 1988b). The Fab′ fragment is therefore undergoing evaluation in our unit. In this paper we report on its application in the detection and natural history of post-operative DVT in a small group of patients undergoing total hip replacement (THR).

Materials and methods

Production of radiolabelled P256 Fab′

P256 is a mouse monoclonal antibody of isotype IgG$_1$. It was originally derived from fusion of the P3-NS1/-1-Ag4-1 myeloma cell line with spleen cells from BALB/c mice immunized with human peripheral blood mononuclear cells as described elsewhere (Bai et al, 1984). Purified Fab′ fragment, prepared by digestion of P256 whole antibody with papain (Parham et al, 1982) and radiolabelled with ^{111}In via the bifunctional chelate diethylenetriaminepenta-acetic acid (DTPA) (Hnatowich et al, 1983), was supplied by Amersham

---

*Author for correspondence.

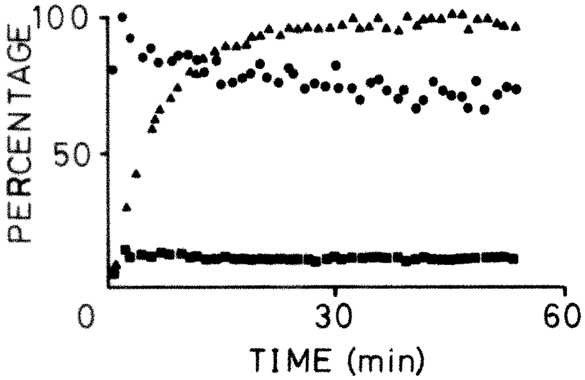

Figure 1. Time–activity curves of liver (■), spleen (▲) and cardiac blood pool (●) for ^{111}In-labelled P256 Fab′. Dynamic acquisition was performed on a 1-min time frame for 45 min following injection of P256 Fab′. Results were calculated from the mean counts per pixel in the appropriate region of interest with blood and spleen expressed as a percentage of their respective maxima and liver expressed as a percentage of the splenic maxima.

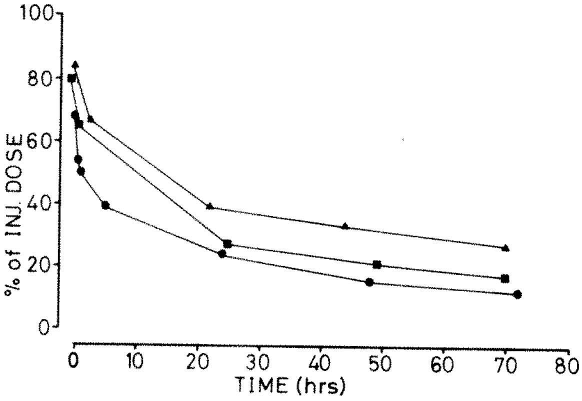

Figure 2. Total blood clearance of ^{111}In-P256 Fab′ in three patients following the first administration.

International plc. Specific activity at the time of injection was between 70 and 120 MBq/mg protein, with a radiochemical purity of >95%. The percentage immunoreactivity of the ^{111}In-labelled fragment was 70–80%.

Patient selection

This study was approved by the local ethical committee and the Administration of Radioactive Substances Advisory Committee. Eleven patients (eight female, three male) undergoing THR were sequentially recruited to the study (age range 54–82 years). Informed consent was obtained.

Study protocol

Patients were injected with approximately 100 μg ^{111}In-DTPA-P256 Fab′ between 24 and 96 h after THR. Following the first injection, images were obtained at 24-h intervals for 3 days at which time a second injection of P256 Fab′ was administered and imaging continued for a further 3 days. Static 5-min images were obtained on each occasion with an LFOV gamma camera (IGE 400A), fitted with a parallel-hole, medium-energy collimator and on-line to a MDSA^2 computer. In some patients, dynamic imaging of the liver and spleen was performed using a 1-min frame rate for 45 min following the first or second injection of P256 Fab′. Blood samples were taken at 5 min, 60 min, between 2 and 5 h and at 24-h intervals following injection of P256 Fab′. Duplicate blood samples were anticoagulated with lithium heparin and EDTA. Lithium heparin (chosen to avoid the possibility of chelation of ^{111}In from platelet-associated Fab′ fragments) samples were used to measure cell-associated and cell-free radioactivity. The EDTA samples were used to obtain blood cell profiles using an automated blood analyser (Sysmex).

In three patients, total urine output following the first injection of P256 Fab′ was collected for 3 days and analysed for ^{111}In radioactivity.

Analysis of blood and urine samples

Three 200 μl aliquots of whole blood were placed into LP3 tubes (Sarstedt), and the remainder of the blood

Table I. Sites of focal accumulation in six THR patients

Case no.	Time after first injection (h)									Time after second injection (h)								
	24			48			72			24			48			72		
	T	C	L	T	C	L	T	C	L	T	C	L	T	C	L	T	C	L
1	0	2	0	0	1	0	0	1	0	0	0	0	0	0	0	0	0	0
2	ND			0	2	0	*			—			—			—		
3	0	3	0	0	3	0	0	3	0	0	2	1	0	2	1	0	2	0
4	0	3	2	2	3	2	2	3	2	2	3	1	*			—		
5	ND			0	3	0	0	3	0	0	3	0	2	3	0	2	3	0
6	0	3	0	0	3	0	0	3	0	0	3	0	0	3	0	0	3	0

T = thigh; C = calf; L = lung. Localization was scored on a 0–3 basis as follows: very marked (3), marked (2), visible (1) or absent (0). ND = not done, *patient withdrew from study.

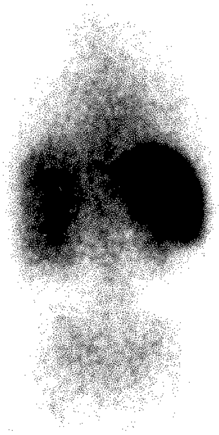

Figure 3. Anterior view of whole-body distribution for P256 Fab′ (female, 65 years) 24 h following the first administration.

sample centrifuged at 1000 *g* for 15 min at room temperature to obtain cell-free plasma. Three 200 μl aliquots of cell-free plasma were also removed for subsequent measurement of radioactivity. All blood samples were processed within 30 min of removal from the patient. For each 24-h urine sample obtained, total volume was measured and 3 × 1 ml portions removed for counting. Whole blood, cell-free plasma and urine samples were counted in a gamma scintillation counter (Canberra-Packard). Mean results for each of the three aliquots were corrected for total blood volume, calculated from the patient's height and weight (Hurley, 1975), or total urine volume, decay corrected from the time of injection and expressed as a percentage of the injected dose.

Results

In vivo kinetics

Time–activity curves of liver, spleen and cardiac blood pool for P256 Fab′ (Fig. 1) were similar to those reported for ^{111}In-labelled platelets (Peters et al, 1985), P256 whole antibody (Peters et al, 1986) and P256 F(ab′)$_2$ (Stuttle et al, 1988a). Time to equilibration for splenic uptake was approximately 20 min with no evidence of reversible hepatic accumulation. Blood clearance of radioactivity (Fig. 2) was rapid over 24 h and followed by a slower rate of clearance up to 96 h at which time approximately 20% of the dose remained in the circulation. The percentage of circulating activity that was cell-associated was initially 60–70% and rose to 80–90% after 24 h. Analysis of urine activity in three patients demonstrated a loss of 16.3, 13.7 and 13.8% of the injected dose in 72 h with a loss in the first 24 h of 7.7, 8.1 and 6.1%. Whole-body distribution 24 h after injection (Fig. 3) was similar to that expected for labelled platelets.

Imaging

Of the 11 patients, six showed focal accumulation of radioactivity in the lower limb, consistent with platelet accumulation on thrombus. Table I summarizes the results for sites of focal accumulation with respect to time in these patients. Case 4 received the first injection of antibody fragment 48 h after surgery. The scintigrams, taken 24 h later, showed evidence of a left calf vein thrombus and pulmonary embolism. This localization of activity was seen on all subsequent images (Fig. 4). Ascending venography demonstrated the presence of a small thrombus in a perforating vessel of the mid left calf (not shown). A ventilation/perfusion scan showed a mismatched defect consistent with pulmonary embolus (Fig. 5). Although not seen at 24 h, focal

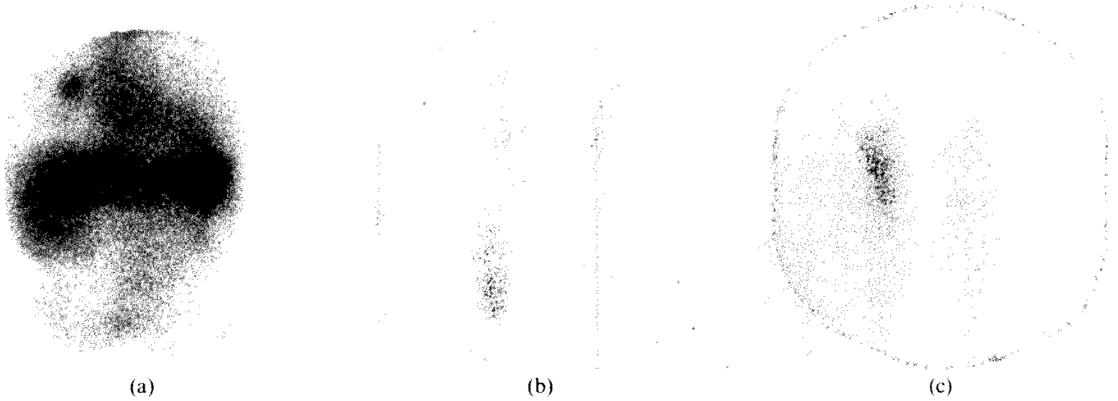

(a) (b) (c)

Figure 4. (a) Anterior view obtained 24 h after first administration showing marked focal accumulation in the right pulmonary artery. (b) Posterior view of the calf 24 h after injection showing focal accumulation in the left calf region, which (c) was more marked at 72 h.

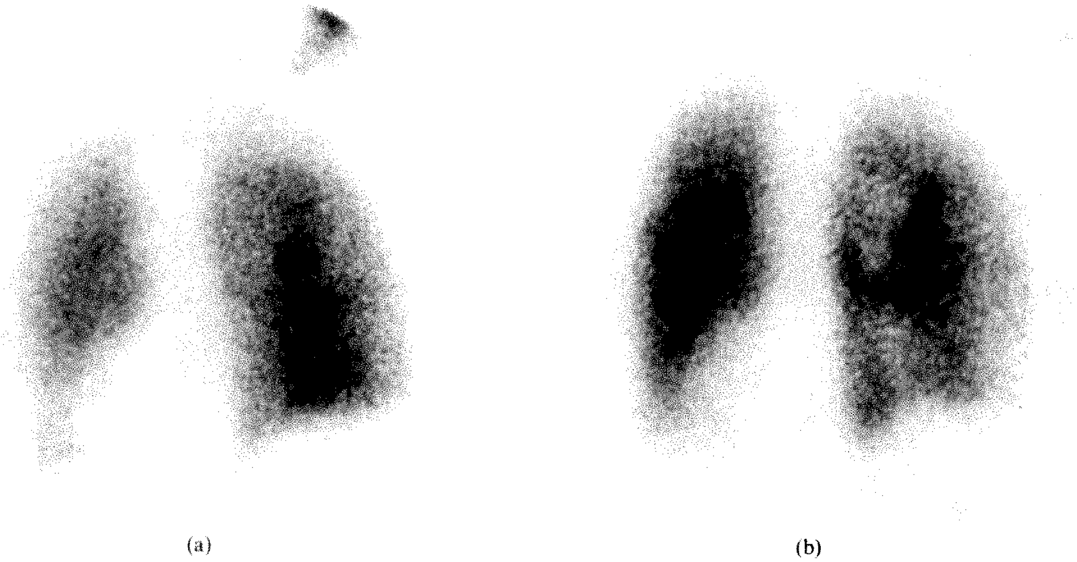

(a) (b)

Figure 5. Right posterior oblique projection of (a) ventilation and (b) perfusion scan for Case 4. Ventilation/perfusion scanning was performed at 48 h after the first administration of P256 Fab′.

accumulation of radioactivity in the thigh was apparent in this patient at 48 h following the first injection of P256 Fab′ (Fig. 6), suggesting the appearance of fresh thrombus in this region or an embolus from the calf region. At this time the patient was asymptomatic but was nonetheless anticoagulated with heparin on the basis of these scintigraphic findings. Within 24 h of anticoagulation, the patient bled into her operation site and therapy was stopped. Ten days later the patient developed chest pain consistent with pulmonary embolus and a ventilation/perfusion scan demonstrated perfusion defects in both lungs that were not matched on

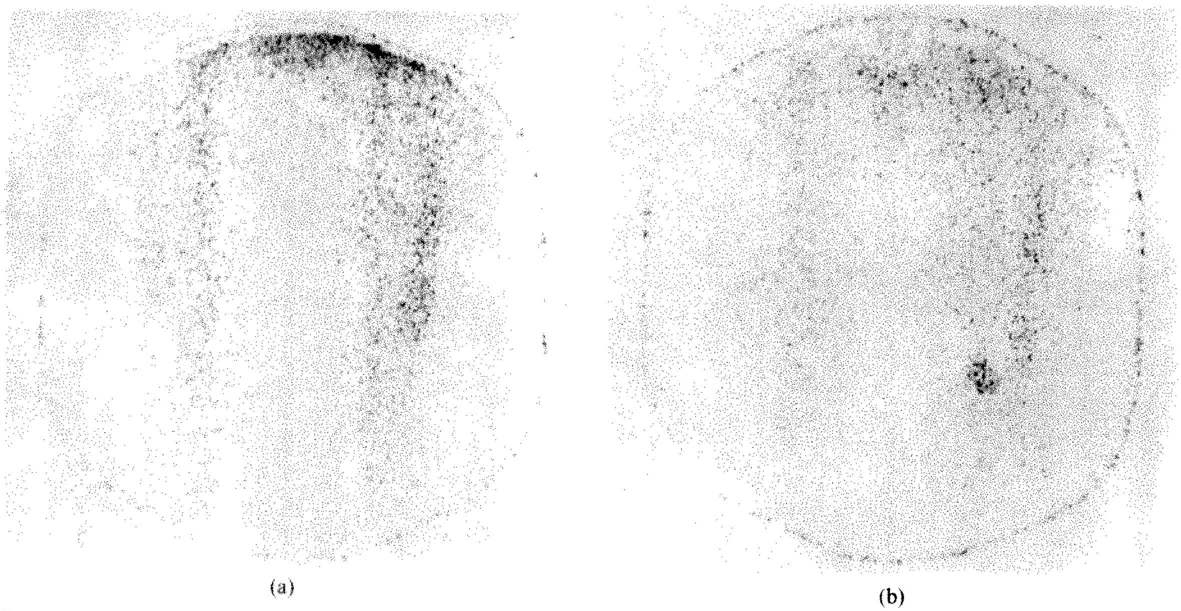

(a) (b)

Figure 6. Anterior view of the thigh at (a) 24 h and (b) 48 h in Case 4 showing the appearance of accumulation in the left thigh region between 24 and 48 h post-injection.

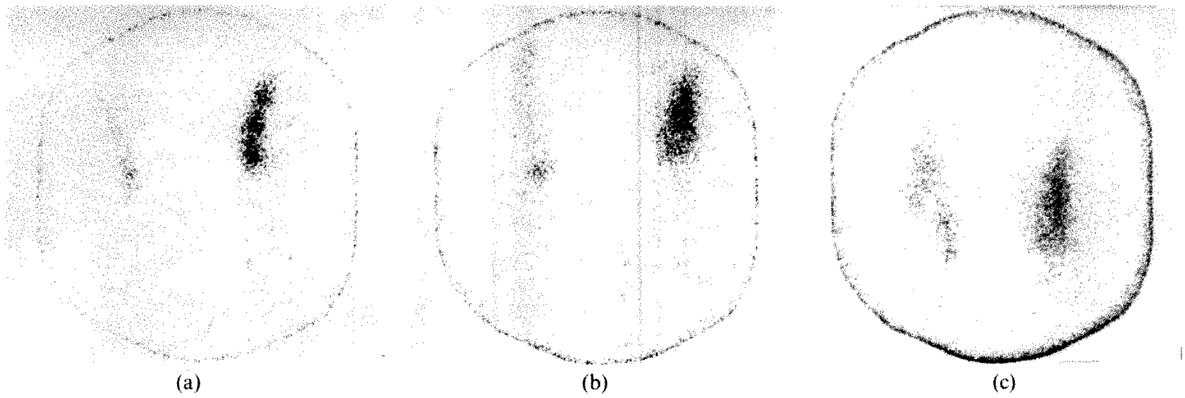

Figure 7. Posterior view of the calf region in Case 5 showing bilateral focal accumulation of P256 Fab′ (a) 48 h after the first injection, (b) 24 h and (c) 72 h following the second injection of P256 Fab′.

ventilation imaging. These defects were significantly more marked in comparison with the first ventilation/perfusion scan.

Case 5 showed bilateral focal accumulation of radioactivity in the calf region with a more marked uptake on the operated side (Fig. 7). This latter thrombus was confirmed by ascending venography and the patient was placed on low-dose heparin therapy. Despite this treatment the focal accumulation in the contralateral limb was seen to increase (Fig. 7) with simultaneous appearance of further activity in the thigh region on the same side (Fig. 8). Although the patient had no symptoms of calf thrombus or pulmonary embolus, a ventilation/perfusion scan 16 days later showed mismatched defects indicative of pulmonary embolus.

Case 6 demonstrated bilateral focal accumulation of ^{111}In in the calf region (Fig. 9), which was apparent throughout the 6 days of imaging. A venogram of the right leg performed 24 h following the second injection was negative, although a bilateral venogram performed 4 days later confirmed the presence of thrombi in both legs (Fig. 10). A review of the first venogram showed that the involved vein was not filling with contrast medium. The venogram of the left leg demonstrated propogation of thrombus towards the popliteal fossa, which presumably occurred subsequent to P256 Fab′ scintigraphy.

Discussion

We have previously demonstrated that the monovalent Fab′ fragment differs from the whole antibody and F(ab′)$_2$ fragment of P256 in that it does not cause aggregation of platelets *in vitro* up to saturating concentrations (Stuttle et al, 1988b). P256 Fab′ fragment thus represents a safer reagent for *in vivo* applications since it is unlikely to cause platelet activation even in patients with thrombocytopenia.

Following intravenous administration, P256 Fab′ rapidly binds to platelets giving rise to a biodistribution similar to that of platelets labelled "conventionally" *in vitro* with a lipophilic complex like ^{111}In-oxine. Dynamic imaging performed over the liver and spleen indicated that platelets were rapidly labelled with P256 Fab′, were functionally intact and showed no evidence of activation such as reversible hepatic accumulation (Peters et al, 1985). Blood clearance of radioactivity was more rapid than seen with conventionally labelled platelets. Although there was evidence of urinary clearance of ^{111}In, this was not sufficient to account for the fall in the circulating activity. Several possibilities exist to explain

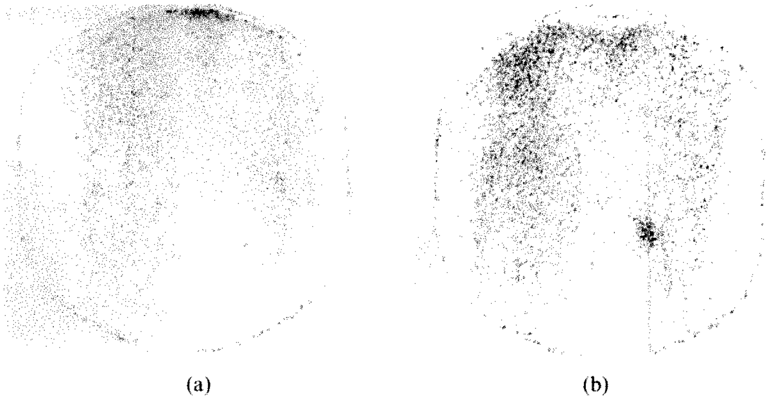

Figure 8. Anterior scintigrams of the pelvic region in Case 5 obtained at (a) 24 and (b) 48 h after P256 Fab′ injection showing increasing focal accumulation of ^{111}In in the left thigh.

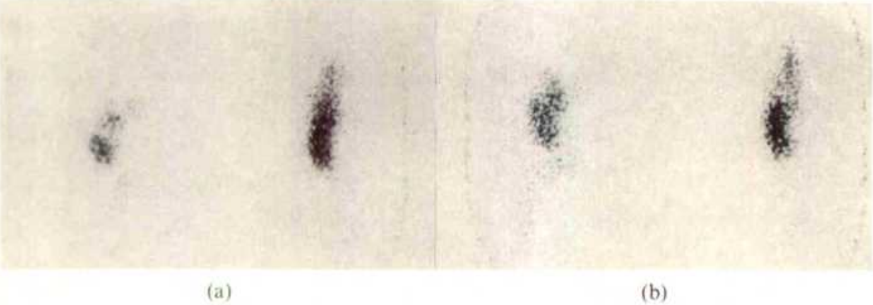

Figure 9. P256 Fab′ scintigram in Case 6 showing bilateral uptake in the calf region (a) 24 and (b) 72 h following the second injection.

this rapid clearance rate. Free antibody may be cleared from the circulation resulting in a shift of the equilibrium in favour of dissociation from the platelet surface. However, analysis of spleen/liver count-rate ratios for P256 Fab′ did not show a marked decrease with time as would be expected in the event of removal of free antibody by the liver. Another possibility would be an increased removal by the liver and spleen of platelets carrying P256 Fab′. Again the available evidence does not support this as there was no alteration in the circulating platelet count in any of the patients studied, although this may reflect removal of a small population of platelets carrying a relatively high concentration of P256 Fab′. Furthermore, dynamic imaging showed that

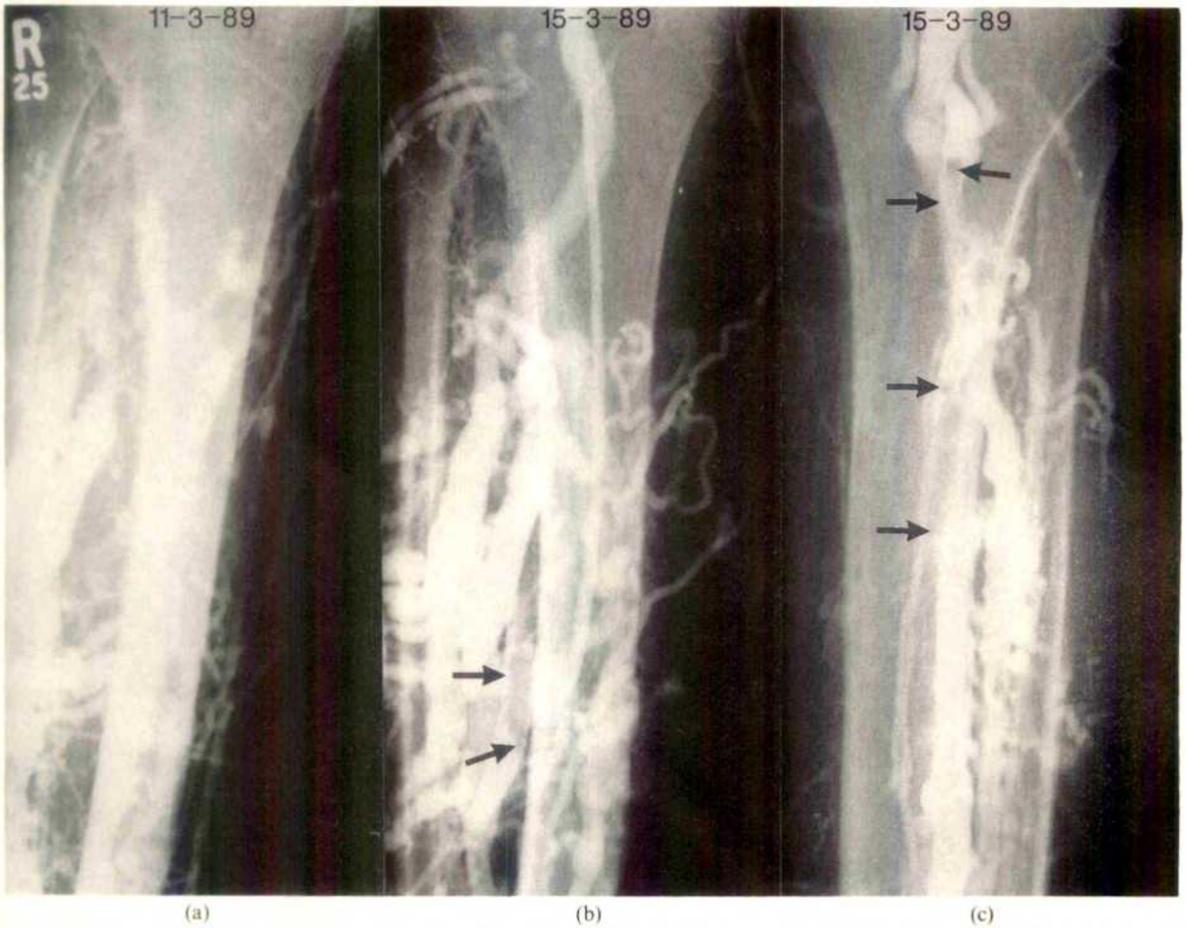

Figure 10. Venogram of the right calf in Case 6 performed at (a) 24 h after the second injection and repeated in the (b) right calf and (c) left calf 4 days later. The initial venogram of the right calf failed to show the presence of thrombus; however, the repeat venogram (b) clearly demonstrated thrombus. In retrospect it was found that the affected vessel was not filling with contrast medium at the time of the first venogram.

the splenic pool reached a plateau at 20 min with no subsequent increase, suggesting no selective splenic sequestration (Peters et al, 1984). From the images obtained in this study there was no evidence for removal of P256 Fab′ by any route other than liver, spleen and kidney. It is hoped that further work in an experimental animal model may resolve these questions.

In this short series of 11 patients, we demonstrated a 55% incidence of thrombus by P256 Fab′ scintigraphy. Confirmation of thrombus by ascending venography was sought in only three cases. It is interesting that in one patient the initial venogram failed to demonstrate thrombus, although when repeated 4 days later, confirmed the presence of a small thrombus in the calf region. The scintigram of this lesion showed clear evidence of focal accumulation, which raises the likelihood that this technique may prove a very sensitive method for thrombus detection. In all six patients who showed focal accumulation of tracer, thrombus was present primarily in the calf veins and developed during the first 48 h following surgery. This is in contrast to venographic studies (Stamatakis et al, 1977) in patients undergoing THR, which has indicated thrombus formation in response to local trauma in the femoral vein. In two patients, thrombus was seen in the femoral vein but appeared in the region of Hunter's canal and not adjacent to the operative site. It is interesting to note that thrombus was seen to extend in spite of low-dose heparin in one patient. In two patients showing focal pulmonary localization of P256 Fab′, there was evidence to suggest that this arose from the calf vein thrombus rather than thrombus in the femoral region. This is also in contrast to previous studies, which have suggested that pulmonary embolus usually arises from femoral, rather than calf, thrombus (Sagar et al, 1976).

Direct imaging of thrombus in pulmonary vessels has been seen with ^{111}In-hydroxyquinoline labelled platelets (Sostman et al, 1982; Clarke-Pearson et al, 1985; Pope & Sostman, 1986). It seems likely that rapid blood clearance of this tracer is a factor that promotes imaging of platelet accumulation in pulmonary thrombus. Although the accuracy of this tracer for pulmonary embolic disease will await a more extended study, these preliminary findings encourage the hope that a single agent may identify both aspects of thrombo-embolic disease.

In conclusion, ^{111}In-P256 Fab′ results in high-resolution images of thrombus in deep veins of the legs and pulmonary vessels. It can be used in a novel way to follow the natural history of thrombo-embolic disease, not only improving clinical management but also allowing greater insight into the sequence of events that occurs in this widespread disorder.

Acknowledgments

A. W. J. S. is supported by Amersham International plc. We are grateful to Ms B. Henderson and Ms D. Knight for expert technical assistance and the Department of Haematology for performing blood profiles.

References

BAI, Y., DURBIN, H. & HOGG, N., 1984. Monoclonal antibodies specific for platelet glycoproteins react with human monocytes. *Blood, 64*, 139–146.

BROWSE, N. L., CLEMENSON, G., BATEMAN, N. T., GAUNT, J. I. & CROFT, D. N., 1976. Effect of intravenous dextran 70 and pneumatic leg compression on incidence of postoperative pulmonary embolism. *British Medical Journal, ii*, 1281–1284.

CLARKE-PEARSON, D. L., COLEMAN, R. E., SIEGEL, R., SYNAN, I. S. & PETRY, N., 1985. Indium-111 platelet imaging for the detection of deep venous thrombosis and pulmonary embolism in patients without symptoms after surgery. *Surgery, 98*, 98–103.

HNATOWICH, D., LAYNE, W. W., CHILDS, R. L., LANTEIGNE, D. & DAVIS, M. A., 1983. Radioactive labelling of antibody: a simple and efficient method. *Science, 220*, 613–615.

HURLEY, P. J., 1975. Red cell and plasma volumes in normal adults. *Journal of Nuclear Medicine, 16*, 46.

KAKKAR, V. V., 1977. Fibrinogen uptake test for detection of deep vein thrombosis: a review of current practice. *Seminars in Nuclear Medicine VII, 3*, 229–244.

PARHAM, P., ANDROLEWICZ, M. J., BRODSKY, F. M., HOLMES, N. J. & WAYS, J. P., 1982. Monoclonal antibodies: purification, fragmentation and application to structural and functional studies of class I MHC antigens. *Journal of Immunological Methods, 53*, 133–173.

PETERS, A. M., LAVENDER, J. P., NEEDHAM, S. G., LOUTFI, I., SNOOK, D., EPENETOS, A. A., LUMLEY, P., KEERY, R. J. & HOGG, N., 1986. Imaging thrombus with radiolabelled monoclonal antibody to platelets. *British Medical Journal, 293*, 1525–1527.

PETERS, A. M., SAVERYMUTTU, S. H., MALIK, F., IND, P. W. & LAVENDER, J. P., 1985. Intrahepatic kinetics of indium-111 labelled platelets. *Thrombosis Haemostasis, 54*, 595–598.

PETERS, A. M., SAVERYMUTTU, S. H., WONKE, B., LEWIS, S. M. & LAVENDER, J. P., 1984. The interpretation of platelet kinetic studies for the identification of sites of abnormal platelet destruction. *British Journal of Haematology, 57*, 637–649.

POPE, C. F. & SOSTMAN, H. D., 1986. Radioisotope labelled platelets in medical diagnosis. *Investigative Radiology, 21*, 611–617.

SAGAR, S., NAIRN, D., STAMATAKIS, J. D., MAFFEI, F. H., HIGGINS, A. F., THOMAS, D. P. & KAKKAR, V. V., 1976. Efficacy of low-dose heparin in prevention of extensive deep-vein thrombosis in patients undergoing total-hip replacement. *Lancet, i*, 1151–1154.

SOSTMAN, H. D., HEUMANN, R. D., LOKE, J., ZOGHBI, S. S., THAKUR, M. L., GREENSPAN, R. H. & GOTTSCHALK, A., 1982. Detection of pulmonary embolism in man with 111-In-labelled autologous platelets. *American Journal of Roentgenology, 138*, 945–947.

STAMATAKIS, J. D., KAKKAR, V. V., SAGAR, S., LAWRENCE, D., NAIRN, D. & BENTLEY, P. G., 1977. Femoral vein thrombosis and total hip replacement. *British Medical Journal, ii*, 223–225.

STUTTLE, A. W. J., PETERS, A. M., LOUTFI, I., LUMLEY, P., GEORGE, P. & LAVENDER, J. P., 1988a. Use of an anti-platelet monoclonal antibody F(ab′)2 fragment for imaging thrombus. *Nuclear Medicine Communications, 9*, 647–655.

STUTTLE, A. W. J., RITTER, J. M., PETERS, A. M. & LAVENDER, J. P., 1988b. *In vitro* studies with an anti-platelet monoclonal antibody: P256. *Nuclear Medicine Communications, 9*, 813–815.

1989, *The British Journal of Radiology*, 62, 970–973

^{99}Tc^m-HMPAO single photon emission computed tomography in partial epilepsy: a preliminary report

By D. F. Smith, MRCP(UK), *F. W. Smith, MD, FFR, R. S. G. Knight, MRCP(UK),
†R. C. Roberts, DPhil, MRCP(UK) and ‡H. G. Gemmell, PhD

Departments of Neurology and *Nuclear Medicine, Aberdeen Royal Infirmary, Foresterhill, Aberdeen,
†Section of Neurology, Department of Medicine, Ninewells Hospital and Medical School, Dundee and
‡Department of Biomedical Physics, University of Aberdeen, Aberdeen

(*Received January 1989 and in revised form June 1989*)

Abstract. In the pre-operative assessment of patients being considered for temporal lobe surgery, accurate lateralization and localization of the epileptic focus is mandatory. Surface electroencephalography (EEG) can be misleading and confirmatory evidence, preferably non-invasive, of the site of the epileptic focus is valuable. Sixteen patients with partial epilepsy, six of whom were considered to be good surgical candidates, had technetium-99m hexamethylpropylene amine oxime (^{99}Tc^m-HMPAO) scanning. In those patients with poor epileptic control and a well localized EEG focus, there was a correlation between EEG and HMPAO scan abnormalities, whilst in all patients where no correlation existed, the HMPAO scan was normal. We conclude that ^{99}Tc^m-HMPAO single photon emission computed tomography may be a useful non-invasive, adjunctive investigation in the pre-operative assessment of patients with partial epilepsy.

Positron emission tomography (PET) and single photon emission computed tomography (SPECT) are being increasingly used in the investigation of patients with partial epilepsy, particularly those being considered for temporal lobe surgery (Engel, 1987).

Using these methods, zones of interictal hypometabolism/hypoperfusion and ictal hypermetabolism/hyperperfusion have been demonstrated. Positron emission tomographic scanning is not generally available and of the radiopharmaceuticals available for SPECT scanning, ^{99}Tc^m-HMPAO offers several advantages (Anderson et al, 1987). This paper presents the preliminary findings of the use of ^{99}Tc^m-HMPAO SPECT in patients with partial epilepsy and indicates its potential value in a well defined group of patients.

Methods

Sixteen patients, age range 17–58 years, were studied. All had partial epileptic seizures, either simple or complex, consistent with temporal lobe origin and some had generalized seizures. Duration of epilepsy varied between 1 and 34 years. All patients were reported to have a focal electroencephalographic abnormality. The electroencephalograms (EEGs) were reviewed and foci strictly defined as being well or poorly lateralized and localized. All patients had normal cerebral CT scans. The project was ethically approved and informed consent was obtained from all patients.

The patients were divided into two groups. Those in Group A (six patients) had poorly controlled epilepsy (> 1 seizure/week), a well lateralized temporal EEG focus and were considered to be good candidates for temporal lobe surgery while those in Group B (10 patients) had better control of epilepsy, a poorly defined EEG focus or both of these features.

Images of the brain were made between 20 min and 1 h after the intravenous injection of 750 mBq of ^{99}Tc^m-HMPAO in a volume of 2.5 ml using an International General Electric 400A Rotating Head gamma camera. Horizontal slices were taken at an angle of 5° below the orbito-meatal line to produce better images of the temporal lobes. All scans were interpreted blind, the reporter being aware of neither the control of epilepsy nor the lateralization or localization of the EEG abnormality. All patients had interictal HMPAO SPECT scans and these were considered to be abnormal if a localized zone of hypoperfusion was present.

Results

Results are summarized in Figs 1 and 2 and Tables I–III. Figure 1 shows the normal SPECT scan of a Group

Table I. ^{99}Tc^m-HMPAO SPECT in Group A patients with poorly controlled epilepsy and well localized EEG focus

Case no.	EEG	CT	HMPAO SPECT
1	R, T	N	N
2	L, T	N	L, T/P
3	L, T	N	L, T
4	L, T	N	L, T/P
5	R, T	N	R, T
6	L, T	N	L, T

N = normal; L = left; R = right; T = temporal; P = parietal.

Address correspondence to: Dr D. F. Smith, Department of Neurological Sciences, Walton Hospital, Rice Lane, Liverpool L9 1AE.

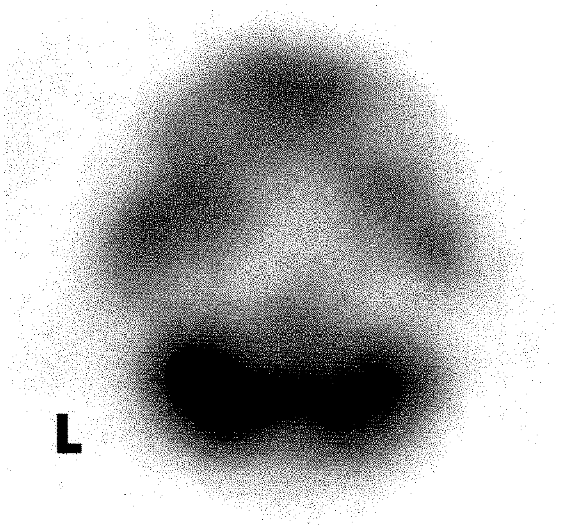

Figure 1. Normal transverse section through the cerebellum and the anterior of both temporal lobes using ^{99}Tc^m-HMPAO.

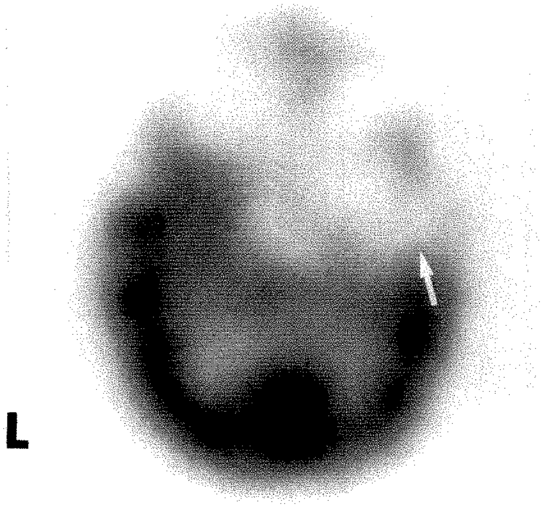

Figure 2. Epileptic focus (white arrow) in right temporal lobe shows no uptake of ^{99}Tc^m-HMPAO.

B patient and Fig. 2 demonstrates the abnormal scan of a Group A patient. In Group A (Table I) Case 1 had a normal SPECT scan. Cases 2–6 had SPECT abnormalities that corresponded with the EEG focus in both lateralization and localization. In Group B (Table II) none of eight patients with a poorly defined EEG focus, irrespective of control of epilepsy, had abnormal SPECT scans. One of two patients with well defined EEG foci and better epilepsy control had a corresponding SPECT abnormality. Table III summarizes all the HMPAO SPECT findings and indicates that in all cases where EEG and SPECT did not correlate, SPECT was normal.

Discussion

Positron emission tomography provides a quantitative assessment of regional cerebral metabolism. An interictal zone of hypometabolism, when present, is considered to be a reliable indicator of the site of the epileptic lesion (Engel et al, 1982a,b,c). However, PET is expensive to install and operate and is thus not available for widespread use (Smith et al, 1987). Single photon emission computed tomography provides a qualitative assessment of regional cerebral blood flow. Results similar to PET (interictal hypoperfusion and ictal hyperperfusion) have been demonstrated with this method. ^{123}IMP is cyclotron produced and therefore not

Table II. ^{99}Tc^m-HMPAO SPECT in Group B patients with better control of epilepsy, a poorly defined EEG focus or both these features

Subgroup	Case no.	EEG	CT	HMPAO SPECT
1. Poor control Not well localized	1	L	N	N
EEG focus	2	L	N	N
2. Better control Not well localized	1	R	N	N
EEG focus	2	R	N	N
	3	Bilateral	N	N
	4	R	N	N
	5	R	N	N
	6	L	N	N
3. Better control Well localized	1	R, F/T	N	N
EEG focus	2	L, T	N	L, T

N = normal; L = left; R = right; F = frontal; T = temporal.

Table III. Summary of the HMPAO SPECT results

	Result
GROUP A	
Poor control Well localized EEG focus Surgical candidates	5/6 had correlation between EEG and SPECT
GROUP B	
Subgroups 1 and 2 Poor or better control, not well localized EEG focus	0/8 had correlation between EEG and SPECT
Subgroup 3 Better control but well localized EEG	1/2 had correlation between EEG and SPECT

In all cases where EEG and SPECT did not correlate, SPECT was normal.

generally available (Smith et al, 1987). ^{133}Xe requires a rapidly rotating, highly sensitive, brain-dedicated SPECT to produce images of reasonable quality (Anderson et al, 1987). Hexamethylpropylene amine oxime was first produced by Amersham International plc in 1985. It can be combined with ^{99}Tc^{m} pertechnetate to produce a lipophilic chelate that rapidly crosses the blood–brain barrier and is thereafter converted to a hydrophilic substance that does not readily diffuse back into the systemic circulation. Thus the initial tracer distribution, which closely resembles cerebral blood flow (Sharp et al, 1986) remains constant for up to 24 h. These physical properties and the type of radiation emitted from ^{99}Tc^{m}-HMPAO make this technique suitable for use on conventional single-head rotating gamma cameras available in most nuclear medicine departments.

Surgery should be considered in any epileptic patient who has failed to respond to optimal anticonvulsant therapy and whose prognosis for spontaneous recovery is poor (Roberts, 1989). The major problem in patient selection is the accurate lateralization and localization of the epileptic focus. The presence of a consistent, well localized, interictal spike focus or ictal activity provides good evidence of the epileptogenic site. However, the surface EEG may reveal no clear focus, bilateral independent spike foci or indeed, rarely, the focus may be falsely lateralized to the homotopic contralateral cortex (Dreifuss, 1987). Hence a battery of clinical, psychological, imaging and electrographic investigations are used to provide localizing data and the more independent investigations that concur as to the source of the epilepsy the more confident the surgical approach that can be made (Engel, 1987).

Positron emission tomography has demonstrated interictal hypometabolism and ictal hypermetabolism providing useful lateralizing and localizing information in up to 70% of patients undergoing temporal lobe surgery (Engel et al, 1984). Similar images to PET have been demonstrated using SPECT but the latter only provides qualitative information and the spatial resolution is poorer. However, a recent review questions the clinical relevance of these factors (Editorial, 1989). The principal advantages of SPECT are lesser cost and widespread availability. In addition, ictal SPECT scanning is technically easier and probably provides more significant information than ictal PET scans. No direct comparison between ^{99}Tc^{m}-HMPAO SPECT and PET has yet been made.

Several studies of HMPAO SPECT in epilepsy are reported. The technique was more sensitive than CT scanning (Biersack et al, 1985) and as sensitive as MRI scanning (Stefan et al, 1987) in detecting epileptic foci. In a recent study of 19 patients, HMPAO SPECT is reported to be better than CT or surface EEG in "diagnosing the localization" in temporal lobe epilepsy (Lassen, 1988). In 21 children with epilepsy, HMPAO SPECT correlated well with EEG in those with normal CT scans and with EEG, CT and subsequent pathological findings in those with abnormal CT scans (Lambert et al, 1988). The use of HMPAO SPECT during WADA (intracarotid sodium amytal) testing is reported in three patients. Using this technique rapid alterations of hemispheric and cerebellar perfusion can be monitored and correct lateralization of speech dominance, where this is in doubt, may be possible (Biersack et al, 1987).

Both SPECT and PET are likely to become established parts of epilepsy research and management (Editorial, 1989). In this preliminary study, ^{99}Tc^{m}-HMPAO SPECT appeared to correlate with surface EEG in patients with poorly controlled epilepsy who had a well localized EEG focus. Since HMPAO SPECT was normal in patients with better control of epilepsy, the finding of interictal hypoperfusion may be related to seizure frequency. We believe that the current main clinical application of HMPAO SPECT is as an adjunctive, pre-operative investigation in patients being considered for temporal lobe surgery. Further study comparing clinical presentation, EEG, SPECT, histology and surgical outcome is required.

References

Anderson, A. R., Friberg, H., Lassen, N. A., Kristensen, K. & Neirinckx, R. D., 1987. Serial studies of cerebral blood flow using ^{99}Tc^{m} HMPAO: a comparison with ^{133}Xe. *Nuclear Medicine Communications, 8,* 549–557.

Biersack, H. J., Linke, D., Brassel, F., Reichmann, K., Kurthen, M., Durwen, H. F., Reuter, B. M., Wappenschmidt, S. T. J. & Stefan, H., 1987. Technetium-99m HM-PAO brain SPECT in epileptic patients before and during unilateral hemispheric anaesthesia (WADA test): report of three cases. *Journal of Nuclear Medicine, 28,* 1763–1767.

Biersack, H. J., Reichmann, K., Winkler, C., Stefan, H., Kuhnen, K., Bulau, P., Penin, H., Tyrrell, D. A., Nierinckx, R. D. & Gruner, K. R., 1985. ^{99m}Tc-labelled hexamethyl propylene amine oxime photon emission scans in epilepsy. *Lancet, ii,* 1436–1437.

Dreifuss, F. E., 1987. Goals of surgery for epilepsy. In *Surgical Treatment of the Epilepsies,* ed. by J. Engel Jr (Raven Press, New York), pp. 31–49.

Editorial, 1989. SPECT and PET in epilepsy. *Lancet, i,* 135–137.

ENGEL, J. JR, 1987. Approaches to the localisation of the epileptogenic lesion. In *Surgical Treatment of the Epilepsies*, ed. by J. Engel Jr (Raven Press, New York), pp. 75–96.

ENGEL, J. JR, BROWN, W. J., KUHL, D. E., PHELPS, M. E., MAZZIOTTA, J. C. & CRANDALL, P. H., 1982a. Pathological findings underlying focal temporal lobe hypometabolism in partial epilepsy. *Annals of Neurology, 12*, 518–528.

ENGEL, J. JR, KUHL, D. E., PHELPS, M. E. & CRANDALL, P. H., 1982b. Comparative localisation of epileptic foci in partial epilepsy by PET and · EEG. *Annals of Neurology, 12*, 524–537.

ENGEL, J. JR, KUHL, D. E., PHELPS, M. E. & MAZZIOTTA, J. C., 1982c. Interictal cerebral glucose metabolism in partial epilepsy in relation to EEG changes. *Annals of Neurology, 12*, 510–517.

ENGEL, J., SUTHERLING, W. W., CAHAN, L., CRANDALL, P. H., KUHL, D. E. & PHELPS, M. E., 1984. The role of positron emmision tomography in the surgical therapy of epilepsy. In *Advances in Epileptology: XVth Epilepsy International Symposium*, ed. by R. J. Porter (Raven Press, New York), pp. 427–432.

LAMBERT, R., GILDAY, D. L., ASH, J. M., HWANG, P. A., KEM, R. Z. & OGUNMEKAN, A. D., 1988. Interictal SPECT-HMPAO and epilepsy in children. *Journal of Nuclear Medicine, 29*, 792.

LASSEN, N. A., 1988. Cerebral blood flow by SPECT for side localization and differential diagnosis in temporal lobe epilepsy. *Journal of Nuclear Medicine, 29*, 916.

ROBERTS, R. C., 1989. Surgery for epilepsy. *Proceedings of the Royal College of Physicians of Edinburgh, 19*, 43–50.

SHARP, P. F., SMITH, F. W., GEMMELL, H. G., LYALL, D., EVANS, N. J. S., GVOZODANOVIC, D., DAVIDSON, J., TURRELL, D. A., PICKETT, R. D. & NIERINCKX, R. D., 1986. Technetium ^{99}m-HMPAO stereoisomers as potential agents for imaging regional cerebral blood flow (rCBF). *Journal of Nuclear Medicine, 27*, 171–177.

SMITH, F. W., GEMMELL, H. G. & SHARP, P. F., 1987. The use of ^{99}Tc^{m} HMPAO for the diagnosis of dementia. *Nuclear Medicine Communications, 8*, 573–580.

STEFAN, H., KUHNEN, C., BIERSACK, H. J. & REICHMANN, K., 1987. Initial experience with 99m Tc-hexamethylpropylene amine oxime (HM-PAO) single photon emission computed tomography (SPECT) in patients with focal epilepsy. *Epilepsy Research, 1*, 234–238.

1989, *The British Journal of Radiology*, 62, 974–976

Total abdominal and pelvic ultrasound: incidental findings and a comparison between outpatient and general practice referrals in 1000 cases

By P. Mills, MRCP, A. E. A. Joseph, MSc, FRCR and *E. J. Adam, MRCP, FRCR

Department of Diagnostic Radiology, St George's Hospital, Blackshaw Road, Tooting, London SW17

(*Received February 1989 and in revised form June 1989*)

Abstract. Ultrasound examination is a rapid and non-invasive method of examing the abdomen. Opinions differ as to whether the entire abdomen and pelvis should be examined in all cases or whether examination can be confined to the region of suspected pathology. The aim of this study was to evaluate the diagnostic yield of total abdominal and pelvic ultrasound examination in patients referred for primary diagnostic ultrasound and with particular reference to specific symptoms. The results of 1000 examinations were analysed. In 25% of patients, a significant abnormality was found and almost one-third of these were incidental findings. The incidence of abnormalities was not significantly different between patients referred via their general practitioners and those referred via the hospital outpatients department. We recommend total abdominal and pelvic examination in all cases regardless of the presenting symptoms.

Abdominal ultrasound is a valuable means of rapidly assessing the upper abdomen and pelvis. A satisfactory examination is possible in most cases. A recent review of patients referred for primary diagnostic ultrasound, rather than for follow-up of known pathology, has illustrated the high diagnostic yield of the technique in both outpatient referred cases and in patients referred by their general practitioners (Colquhoun et al, 1988). Other authors have shown a high yield of abnormalities that were found incidentally during abdominal ultrasound examination (Adam et al, 1984; Paakkala et al, 1987; Verbanck et al, 1988).

The aim was to determine whether the diagnostic yield is sufficiently high to justify examination of the entire abdomen and pelvis in all patients referred for diagnostic ultrasound, or whether examination can be confined to the site of suspected pathology. The diagnostic yield from abdominal and pelvic ultrasound in patients referred with specific symptoms was analysed. A further aim was to determine the diagnostic yield in patients referred directly by their general practitioners compared with those referred via the hospital outpatients department.

Method

We have reviewed retrospectively the abdominal and pelvic ultrasound scan findings in 1000 patients. Five hundred patients were referred directly by their general practitioners and 500 were referred via the hospital outpatients department. Hospital inpatients were excluded. The data were drawn from a daybook in which the patient's name, age, clinical details given on the request form and the result of the scan are recorded. The patients were all fasted for 6 h prior to their examination. The scans were performed (by two consultants (A.E.A.J. and E.J.A.) and/or four senior registrars) using a Technicare Autosector (real time) and a 5 MHz transducer. Children and adolescents aged under 18 years were excluded and only patients attending for primary diagnostic ultrasound were included.

The findings of the examination were then classified into one of three groups: no abnormality, minor abnormality and significant abnormality. The scans classified as "no abnormality" were entirely normal. Minor abnormalities were renal cysts, ovarian cysts, prostatic enlargement, fatty infiltration of the liver, ectatic aorta, liver congestion, liver haemangioma, renal scarring, pleural effusion, fibroids and moderate splenomegaly. The significant abnormalities were divided into two groups: moderate lesions and lesions requiring further investigation and treatment. Moderate lesions were gallstones, aortic aneurysm <5 cm in diameter, hepatitis, pelvic inflammatory disease, chronic pancreatitis, hepatosplenomegaly and hiatus hernia. Lesions classified as requiring further action were hydronephrosis, renal calculi, hepatic fibrosis, single kidney, adnexal mass, lymphoma, polycystic ovaries, pancreatic mass, duodenal and antral wall thickening, liver metastases, thickened bowel wall, aortic aneurysm >5 cm in diameter, aortic dissection, adrenal mass, bleeding ovarian cyst, gastric carcinoma, pregnancy, tubal pregnancy, colonic carcinoma and prostatic carcinoma.

Results

The most common reason for referral was for examination of the gallbladder in order to detect gallstones. A total of 407 patients in the study group (40.7%) were referred with the symptom of right upper quadrant pain and the clinical suspicion of gallstones. A further 157 patients (15.7%) were referred with non-specific abdo-

---

*Author for correspondence.

Table I. Incidence of gallstones in different groups

Result of scan	%
Overall incidence of gallstones	10.5
Gallstones diagnosed incidentally	2.9
Patients presenting with right upper quadrant pain ($n = 407$)	
Gallstones present	18
Normal	71
Other abnormality	11
Patients presenting with non-specific abdominal pain ($n = 157$)	
Gallstones present	9
Normal	74.5
Other abnormality	16.5

minal pain. The ultrasound findings in these two groups are shown in Table I together with the overall incidence of gallstones and the proportion of gallstones that were incidental findings. Forty-four patients in the right upper quadrant pain group were found to have a significant abnormality other than gallstones during the ultrasound scan. In 12 patients, the abnormality was thought to be responsible for the patient's symptoms. For example, right renal calculi were found in three cases, an echogenic pancreas consistent with pancreatitis in four cases and duodenal or antral wall thickening in five cases. These five cases were confirmed to have peptic ulceration at subsequent endoscopy. In the remainder of cases an incidental abnormality was found. These were polycystic kidneys (2), single kidney (4), hepatic fibrosis (2), solid renal tumour (1), pleural effusion (2), hepatitis (6), adnexal mass (1), horseshoe kidney (2), hiatus hernia (5), renal scarring (4), liver haemangioma (1), fibroids (1) and splenomegaly (1).

Another common reason for referral was for the investigation of pelvic pain. Fifty-five patients (5.5%) were referred with pelvic pain. The ultrasound findings are shown in Table II. In nine patients (16%), a significant abnormality that was extrapelvic was found. These were hydronephrosis (2), renal scarring (1), hepatitis (2), ascites (1), thickened bowel (1), mass in the right iliac fossa (1) and a mass in the renal pelvis that was later shown to represent transitional cell carcinoma. Furthermore, in 14 patients who were referred for examination of the upper abdomen, a pelvic abnormality was discovered. These were carcinoma of the bladder (1), adnexal mass (4), ovarian cyst (2), thickened bowel (2), fibroids (4) and tubal pregnancy (1). Subsequent follow-up has shown that 10 of these diagnoses were accurate. The false positive diagnoses were adnexal mass (3) and tubal pregnancy (1). These 14 patients were fasted prior to their examination so their bladders were not full. This probably explains the four false positive diagnoses in whom a clinical examination and a repeat ultrasound scan showed no abnormality.

Table II. Ultrasound findings in 55 patients referred with pelvic symptoms

Results	%
Pelvic abnormality	38
Normal	45
Extrapelvic abnormality	17

Table III. Incidental findings

	%
Proportion of abnormalities that were incidental findings	9.1
Proportion of *significant* lesions of those diagnosed incidentally	32

Overall, in 91 patients of the original 1000, incidental significant abnormalities were found during the ultrasound examination. For example, in five patients referred because of right upper quadrant pain, a single kidney was discovered. The proportions of findings that were incidental are shown in Table III and the significant lesions that were correctly diagnosed incidentally are shown in Table IV. We have attempted to follow-up those who had significant lesions, with the following exceptions: patients diagnosed as having a single kidney were not followed-up as no further action was taken in these cases because none had renal pathology; patients with gallstones, aortic aneurysm and polycystic kidneys were not followed-up as these lesions are easily recognized using ultrasound and it was considered that no further confirmation of the diagnosis was required. Of the remainder, the diagnosis was accurate in 23, incorrect in seven and no follow-up was available in eight. The false positive diagnoses were adnexal mass (3), tubal pregnancy (1), pelvic inflammatory disease (1) and renal calculus (2). Our main source of error was in overdiagnosing lesions in the pelvis. Again, this may have occurred because the patients did not have full bladders. Of the 91 patients in whom a significant lesion was found incidentally, 84.6% were true positive diagnoses, 7.7% were false positive and in 7.7% no follow-up was available.

Table V shows a comparison of the ultrasound findings between patients referred directly by their general practitioners and those referred via the hospital outpatients department. The age range and mean of the two groups were similar. The principal difference between the two groups was that more minor abnormalities were

Table IV. Significant lesions that were correctly diagnosed incidentally

Gallstones	29	Ascites	1
Renal calculus	9	Aortic dissection	1
Splenomegaly	8	Polycystic ovaries	1
Hydronephrosis	7	Hepatitis	1
Hepatic fibrosis	5	Renal mass	1
Single kidney	5	Carcinoma of bladder	1
Chronic pancreatitis	3		
Polycystic kidneys	2		
Aortic aneurysm	2		

Table V. Comparison of the results of the ultrasound scans between the general practice (GP) and outpatients department (OPD) referral groups

Result of scan	GP referrals ($n=500$)	OPD referrals ($n=500$)
Age range (mean) in years	20–92 (47)	19–84 (52)
No abnormality	51.8%	38.4%
Minor abnormality	21.4%	38.8%
Significant abnormality	26.8%	22.8%
Moderate	18.8%	13%
Requiring investigation or treatment	8%	9.8%

found in the outpatient referral group. However, in the more important significant abnormality section, there was no significant difference between the two groups.

Discussion

Colquhoun et al (1988) have recently reported the findings in 1861 patients referred for primary diagnostic abdominal ultrasound. They state that, in patients referred for gallbladder examination, it is appropriate to examine the gallbladder and bile ducts alone, as the incidence of a significant abnormality being found if these two structures are normal is 1.5% or less. However, the symptoms on which the suspicion of gallstones is raised are usually vague and non-specific. For this reason and because of the number of significant non-biliary abnormalities that we have found, we do not adhere to this policy. In our series of 407 patients referred for gallbladder examination because of right upper quadrant pain, a significant non-biliary abnormality was found in 11%. In the group of patients referred because of non-specific abdominal symptoms, such as pain or nausea, the incidence of significant abnormality (excluding gallstones) was 16.5%.

Colquhoun et al (1988) also state that abnormalities revealed in lower abdominal examinations were related only to the pelvic organs in their series. They recommend that examination of patients with pelvic symptoms may be confined to this area. In our group of patients referred for examination of the pelvis, there was a 16% incidence of significant non-pelvic pathology.

There have been several other reports of the diagnostic yield from abdominal ultrasound. The overall incidence of gallstones has been reported as varying from 12 up to 30% (Sorensen & Hasch, 1985; Fitzgerald & Keeling, 1988). Paakkala et al (1987) have reported a rate of 15% incidental pathological findings, although they do not specify the lesions that were classified as pathological. In our series, 9.1% of the total number of abnormalities were found incidentally but these constituted almost a third of all significant abnormalities.

We believe that examination of the entire abdomen and pelvis is worthwhile in all patients, regardless of their symptoms, because the probability of finding a significant abnormality, unrelated to the original site of symptoms, is significant. A previous study of 650 patients attending for ultrasound examination at this hospital showed that the rates of organ visualization were satisfactory in the majority of patients (Adam et al, 1985). In our experience, examining the entire abdomen and pelvis prolongs the examination by approximately 25%. A thorough examination at the time of first referral prevents further referrals for examination of other sites.

This study confirms further the statements of Colquhoun et al (1988) and Sorensen and Hasch (1985), that the diagnostic yield is as high in patients referred directly by their general practitioners as in those referred via the hospital outpatients department. It is, therefore, our policy to offer open access to ultrasound facilities for general practitioners.

References

Adam, E. J., Creagh-Barry, M. & Joseph, A. E. A., 1984. Total abdominal scanning in 650 patients: rates of visualisation and pathology. *British Journal of Radiology, 58*, 695.

Colquhoun, I. R., Saywell, W. R. & Dewbury, K. C., 1988. An analysis of referrals for primary diagnostic ultrasound to a general X-ray department. *British Journal of Radiology, 61*, 297–300.

Fitzgerald, E. J. & Keeling, P. N. W., 1988. Ultrasound as part of a "one day" gastroenterology service: a pilot study. Presented at the meeting of the British Medical Ultrasound Society, Glasgow, December 5–7, 1988. *British Journal of Radiology, 62*, 638–639.

Paakkala, T., Mattson, J., Koivisto, E. & Lehtinen, E. 1987. The accuracy and value of abdominal ultrasonography. *VI European Congress of Radiology Abstracts Book*, p. 193.

Sorensen, K. & Hasch, E., 1985. Ultrasonic diagnosis in patients referred from general practice. *Ugeskrift for Laeger, 147*, 121–123.

Verbanck, J. J., Van Aelst, F., Rutgeerts, L., Demuynck, H., Ghillebert, G. et al. 1988. The impact of routine admission abdominal sonography on patient care. *Journal of Clinical Ultrasound, 16*, 651–654.

1989, *The British Journal of Radiology*, 62, 977–980

Can ultrasound replace the intravenous urogram in preliminary investigation of renal tract disease? A prospective study

By H. G. Lewis-Jones, DMRD, MRCP, FRCR, G. H. R. Lamb DMRD, FRCR and P. L. Hughes, DMRD, FRCR,

Department of Radiology, Royal Liverpool Hospital, Prescot Street, Liverpool L7 8XP

(*Received February 1989 and in revised form May 1989*)

Abstract. The intravenous urogram has long been the mainstay of urinary tract imaging in adult practice. It has been shown recently that in many clinical situations the routine use of intravenous urography is no longer justified and in some situations avoidance of adverse contrast reactions, reduced examination time and significant cost reduction. In order to assess the clinical and financial aspects of a change in practice in our department, a prospective study was undertaken over a total of 10 weeks when 328 patients who were referred for intravenous urography were also examined independently by ultrasound combined with the plain abdominal radiograph. The results were compared and in 81.4% of cases the two techniques yielded identical information. Ultrasound plus a plain abdominal radiograph provided more diagnostic information in a further 12.5% of cases, whilst intravenous urography was more informative in only 6.1%. The findings of the study are discussed by considering the main clinical groups and comparing the relative yields of ultrasound and urography. A scheme of routine urinary tract investigations using ultrasound and the plain abdominal radiograph is proposed. We estimate a 58% reduction in number of urographic examinations while retaining diagnostic accuracy. The financial and planning implications for our department are discussed.

Ultrasound is playing an ever-increasing role in the evaluation of adult renal tract disease and for certain indications it has been advocated as the investigation of choice.

In order to evaluate the potential of ultrasound as the preliminary investigation for the adult urological system, this prospective study comparing ultrasound and the intravenous urogram was undertaken.

Methods

Three hundred and twenty-eight patients attending for urography over a 10-week period were also examined independently by ultrasound.

Urography was performed following a full-length control radiograph of the abdomen. Radiographs were exposed at 1, 5 and 19 min with abdominal compression unless contraindicated. A full-length compression release radiograph was recorded as well as a separate full-bladder view. All radiographs were assessed at the time by a staff radiologist.

Ultrasound examination was then performed by a different senior staff radiologist and only the control abdominal radiograph was available for inspection. The kidneys were examined using either a Diasonics 3.5 MHz sector scanner or an Aloka 3.5 MHz linear array. The bladder was examined again after voiding before returning the patient for the final post-micturition radiograph.

The two investigations were performed independently by two senior staff radiologists and results compared.

Results

Patients were subdivided according to indication as stated on the request form. Abnormal findings were confirmed where possible by follow-up of the patient. The overall results are shown in Table I. Whenever ultrasound was performed for imaging the renal tract, a plain abdominal radiograph was also available for inspection.

Discussion

Each group is considered according to indication.

Haematuria

It is hard to conceive that many patients with haematuria would be considered to have had complete and satisfactory urinary tract imaging without intravenous urography. The poor sensitivity of ultrasound for urothelial tumours of the renal pelvis, ureters, bladder base and bladder fundus is well recognized (Itzchak et al, 1981). Ultrasound failed in this study to detect one renal pelvis transitional cell carcinoma and two bladder tumours that were demonstrated at urography. This suggests that, for the investigation of haematuria, the intravenous urogram (IVU) should be maintained for initial examination, whilst ultrasound remains complementary in selected cases.

Patients presenting with a recently diagnosed bladder neoplasm require assessment of the upper tracts by urography; the phenomenon of multifocal urothelial neoplasms is well recognized (Smart, 1964). This is often the premise on which patients are referred for routine urographic follow-up, yet it has also been shown that such subsequent tumours occur at a rate similar to that found in the general population (Walzer & Soloway, 1983). These patients will have routine cystoscopy independent of the result of any bladder imaging and would therefore only benefit from urography in the presence of haematuria and a negative cystoscopy.

P25850

Table I. Overall study results

Indication	Total number	Ultrasound equal to IVU	Ultrasound more informative	IVU more informative
Haematuria	89	68	18	3
Bladder neoplasm follow-up	15	14	—	1
Bladder outflow tract obstruction	51	42	7	2
Urinary tract infection	39	33	3	3
Loin pain	48	40	1	7
Pre-operative assessment	22	18	2	2
Frequency or incontinence	19	18	—	1
Hypertension	18	17	1	—
Trauma	11	9	2	—
Miscellaneous	16	8	7	1
Total number	328	267	41	20
%		81.4	12.5	6.1

Bladder outflow tract obstruction

In this study, ultrasound generally provided more information regarding prostatic enlargement, bladder wall changes and post-micturition residue, although it did not detect two bladder diverticula sited at the fundus. No other advantage of urography was shown and this is certainly supported by the literature (Bauer et al, 1980). These authors also point out, however, that in the presence of haematuria, urography remains indicated. De Lacey has recently gone further and has suggested that unless the patient is to be treated conservatively, and in the absence of haematuria, no renal imaging is necessary at all (De Lacey et al, 1988).

Urinary tract infection

Urinary tract infections are common in women under 40 years of age, who constituted 80% of patients in this group, and in these cases it is particulary desirable to avoid radiation exposure. We found no abnormalities in this group requiring treatment or further investigation and numerous studies have commented on the minimal pick-up rate of pathology in urological examinations for this indication (Fair et al, 1979; De Lange & Jones, 1983; Mogensen & Hansen, 1983). The presence of risk factors such as diabetes mellitus, a history of calculi, unusual pathogens and possibly pyelonephritis, would reduce the reluctance to perform an IVU.

Loin pain

The IVU in this situation provided more diagnostic information than ultrasound. Urography clearly demonstrated two cases of ureteric obstruction due to lucent calculi, one of congenital pelvi-ureteric junction obstruction and two cases with appearances suggesting recently passed calculi. Ultrasound, however, did demonstrate appropriate upper tract changes with no cause shown on the plain radiograph. In none of the cases studied was ultrasound or the plain radiograph normal when a significant abnormality had been shown at urography.

However, studies have demonstrated (Erwin et al, 1984; Hill et al, 1985) that, in acute obstruction, ultrasound may not show dilatation of the upper tracts suggesting it is not suitable as an initial method of investigation. In patients with clinical renal colic, therefore, the IVU remains appropriate but in patients with non-specific loin or abdominal pain with normal urinalysis, usually being investigated as outpatients, ultrasound remains adequate. Also included in this group were nine patients referred for follow-up of renal calculi. In all nine cases, the plain radiograph provided all the necessary information while ultrasound demonstrated any serial upper tract changes.

Pre-operative assessment

Urography prior to colorectal and gynaecological surgery has already been questioned in the literature (Sack, 1979; Phillips et al, 1983). In two cases, urography showed clearly the level of ureteric obstruction due to tumour, while in two further cases, ultrasound demonstrated the pelvic mass causing ureteric obstruction. Ultrasound detected upper tract changes in all the abnormal cases and proceeding to urography in these cases would appear logical.

The remaining groups contained small patient numbers and included indications such as frequency, incontinence, hypertension, chronic renal failure, transplanted kidneys and neurogenic bladders. In all these groups the incidence of pathology was extremely low and ultrasound detected all significant abnormalities. A small group of patients were referred with suspected renal trauma. In this situation the importance of documenting the presence of two functioning kidneys necessitates the IVU. We would recommend the use of a single-shot IVU combined with ultrasound as the latter has proven more sensitive in detecting perinephric collections.

Table II outlines the proposed scheme of investigation incorporating ultrasound as the initial method of examination. The number of IVUs that were rendered unnecessary by adopting this scheme are also shown for each indication.

Conclusions

In this small pilot study, we have demonstrated that ultrasound combined with a plain abdominal radiograph can be used as the initial investigation of patients with suspected urinary tract disease. Proceeding directly to urography in selected patients, as we have outlined, would produce a 58% reduction in the number of urograms performed while retaining diagnostic accuracy.

During the financial year of this study, we performed 2800 IVU examinations. The consumable costs of a single IVU examination were estimated at £25 for a non-ionic contrast medium examination and £15 for an ionic contrast medium examination. The consumable costs include contrast medium, injection materials, X-ray film and associated sundries. During the period of this study the ratio of non-ionic to ionic examinations was 42% to 58% with a calculated total consumable cost of £53 760. This study has shown a potential 58% reduction in intravenous urography and therefore a potential saving of £31 180. The consumable costs of ultrasound, estimated at £1.10 per examination, reduces the saving to £28 100 and if, as is suggested, a plain abdominal radiograph is also performed, the final potential consumable saving totals £26 500. Many X-ray departments are now using non-ionic contrast media for intravenous urography and this will of course increase the consumable cost savings considerably.

Patient benefits include reduced radiation dose, avoidance of adverse contrast medium reactions, reduced examination time and a more pleasant and acceptable examination, in general, while retaining diagnostic accuracy.

Such a change of policy would involve altered departmental planning. The sudden increase in ultrasound workload has been anticipated in our department by replacing a plain tomographic unit due for renewal with a new ultrasound unit. We have observed radiographic and radiological practice in the department and found that one radiologist and radiographer can examine the renal tract at the rate of six to eight patients per hour. The IVU occupies a radiographer for 50–55 min per pair of examinations and the radiologist's contribution for injection, radiograph review and reporting time consumes 9 min on average per patient. Therefore, when comparing IVU with ultrasound, the radiologist's input is comparable in terms of examination time while there is a definite saving in radiographer's time, which can be redeployed within the department. This, however, must be balanced against the need for increased training of radiographic and radiological staff in ultrasound.

The study highlights the potential of ultrasound to

Table II. Proposed scheme of investigation

Indication	Method of investigation (a) first choice (b) second choice	No. of IVUs replaced by ultrasound
Haematuria	(a) IVU (b) Ultrasound if indicated by IVU	0
Bladder neoplasm follow-up	(a) Ultrasound (b) Haematuria plus normal cystoscopy — IVU	15
Bladder outflow tract obstruction	(a) Ultrasound (b) With haematuria — IVU	40
Urinary tract infection	(a) Ultrasound (b) Complicated infection — IVU	33
Loin pain		
Renal colic	(a) IVU	
Loin/abdominal pain	(a) Ultrasound	25
Pre-operative assessment	(a) Ultrasound (b) Upper tract changes — proceed to IVU	20
Trauma	(a) IVU — single shot (b) Ultrasound if indicated by IVU	0
Incontinence Frequency and dysuria Renal failure Renal transplants Miscellaneous	(a) Ultrasound	57

Total number of IVUs replaced by ultrasound was 190 (58% of total referred for IVU).

influence our day-to-day practice for the good and merits, we feel, a more long-term study of its role in the investigation of the renal tract.

References

BAUER, D. L., GARRISON, R. W. & MCROBERTS, J. W., 1980. The health and cost implications of routine excretory urography before transurethral prostatectomy. *Journal of Urology*, *123*, 386–389.

DE LACEY, G., JOHNSON, S. & MEE, D., 1988. Prostatism: how useful is routine imaging of the urinary tract? *British Medical Journal*, *296*, 965–967.

DE LANGE, H. E. & JONES, B., 1983. Unnecessary intravenous urography in young women with recurrent urinary tract infections. *Clinical Radiology*, *34*, 551–553.

ERWIN, B. C., CARROLL, B. A. & SOMMER, F. G., 1984. Renal colic: the role of ultrasound in initial evaluation. *Radiology*, *152*, 147–150.

FAIR, W. R., MCCLENNAN, B. L. & JOST, R. G., 1979. Are excretory urograms necessary in evaluating women with urinary tract infection? *Journal of Urology*, *121*, 313–315.

HILL, M. C., RICH, J. I., MARDIAT, J. G. & FINDER, C. A., 1985. Sonography *vs* excretory urography in acute flank pain. *American Journal of Roentgenology*, *144*, 1235–1238.

ITZCHAK, Y., SINGER, D. & FISCHELOVITCH, Y., 1981. Ultrasonographic assessment of bladder tumours. I. Tumour detection. *Journal of Urology*, *126*, 31–33.

MOGENSEN, P. & HANSEN, L. K., 1983. Do intravenous urography and cytoscopy provide important information in otherwise healthy women with recurrent urinary tract infection? *British Journal of Urology*, *55*, 261–263.

PHILLIPS, R., HITTINGER, R., SAUNDERS, V., BLESOVSKY, L., STEWART-BROWN, S. & FIELDING, P., 1983. Pre-operative urography in large bowel cancer: a useless investigation? *British Journal of Surgery*, *70*, 425–427.

SACK, R. A., 1979. The value of intravenous urography prior to abdominal hysterectomy for gynecologic disease. *American Journal of Obstetrics and Gynecology*, *134*, 208–212.

SMART, J. G., 1964. Renal ureteric tumours in association with bladder tumours. *British Journal of Urology*, *36*, 380–390.

WALZER, Y. & SOLOWAY, M., 1983. Should the follow-up of patients with bladder cancer include routine excretory urography? *Journal of Urology*, *130*, 672–673.

1989, *The British Journal of Radiology*, 62, 981–985

Ultrasound-guided, histological, fine-needle biopsy from suspect parathyroid tumours: success-rate and reliability of histological diagnosis

By S. Karstrup, MD, *A. Glenthøj, MD, *B. Hainau, MD, †L. Hegedüs, MD, S. Torp-Pedersen, MD and H. H. Holm, MD, PhD

Departments of Ultrasound, *Pathology and †Internal Medicine and Endocrinology, University Hospital, Herlev, Denmark

(*Received April 1989*)

Abstract. Ultrasound-guided, fine-needle tissue biopsies were performed in 60 suspected parathyroid tumours in 55 consecutive patients with biochemically proven hyperparathyroidism. The specimens were randomly arranged and re-read "blind" by two pathologists. The interobserver agreement, corrected for chance agreement, was 0.92 (= kappa coefficient). Twenty-three of the 60 suspect parathyroid tumours were verified histologically following surgery. No diagnostic errors were seen but the percentage of insufficient biopsies from suspect parathyroid tumours or surgically verified parathyroid tumours was high (45 and 47%, respectively). We conclude that a reliable tissue diagnosis can be made by ultrasound-guided, fine-needle tissue biopsy. However, when the material is insufficient for histological diagnosis, we recommend the additional use of ultrasound-guided, fine-needle aspiration for cytology or parathyroid hormone determination.

Several studies have confirmed the success of ultrasound in localizing enlarged parathyroid glands in the neck (Butch et al, 1985; Winzelberg, 1987). However, there is difficulty in distinguishing enlarged parathyroid glands from nodular thyroid lesions, as these may show a similar echopattern (Rastad et al, 1984a; Solbiati et al, 1985; Karstrup et al, 1988c). To ensure a reliable diagnosis of the ultrasonographically suspect parathyroid gland, the use of ultrasound-guided, fine-needle aspiration (FNA) for parathyroid hormone (PTH) measurement (Doppman et al, 1983; Karstrup et al, 1985, 1988a) or cytological examination (Solbiati et al, 1983; Rastad et al, 1984b; Karstrup et al, 1988a) has also been suggested. In addition, previous reports have called attention to the possibility of ultrasound-guided, fine-needle tissue biopsy (FNTB) for histological examination (Charboneau et al, 1983; Karstrup et al, 1986, 1988a).

The aim of the present study was to assess the success-rate in obtaining small tissue cores for histological examination from suspected parathyroid tumours in a consecutive series of patients with hyperparathyroidism. Additionally, we wanted to evaluate the reliability of the histological diagnosis.

Materials and methods

During the period from 1986 to 1988, ultrasound-guided FNTB was performed in 60 suspected parathyroid tumours in 55 consecutive patients (46 women and nine men) with biochemically proven hyperparathyroidism (46 patients with primary disease and nine patients with hyperparathyroidism secondary to kidney disease). The median age was 60 years (range 25–81 years).

All the specimens were collected retrospectively, randomly arranged and re-read independently by two pathologists who had no access to clinical data. Both had at least 5 years experience in microscopic examination of endocrine tissue. Only three final conclusions were possible: parathyroid tissue, non-parathyroid tissue or insufficient material for examination. In addition, the pathologists were asked to describe the findings in the specimens.

The ultrasound examinations were performed with a 6 or 7 MHz sector scanner (Brüel and Kjaer) mounted with a needle-steering device for precise ultrasound-guided punctures. The ultrasound-guided, fine-needle biopsies were performed using a 0.8 mm (21-gauge) Sure-cut needle (TSK Laboratory). The principles of the Sure-cut needle have been described in detail by Torp-Pedersen et al (1984, 1985). All the fine-needle biopsies were carried out under local anaesthesia. Initially, an outer guide needle (1.2 mm) was introduced into the skin and neck muscle. The fine needle was passed through the guide needle following an electronic puncture line (Figs 1, 2).

The tissue cores were expelled on to a sterile piece of paper, fixed in formalin (Torp-Pedersen et al, 1985) and then stained using haematoxylin and eosin (Fig. 3). Immunostaining with antibody against thyroglobulin was employed if needed.

The ultrasonically measured volume of suspect parathyroid tumours was approximated to half of the product of maximum length, width and depth.

Statistical analysis for unpaired data was performed using the Mann-Whitney test. The kappa coefficient was

---

Address correspondence to: Steen Karstrup, MD, Department of Diagnostic Ultrasound, Herlev Hospital, University of Copenhagen, DK-2730 Herlev, Denmark.

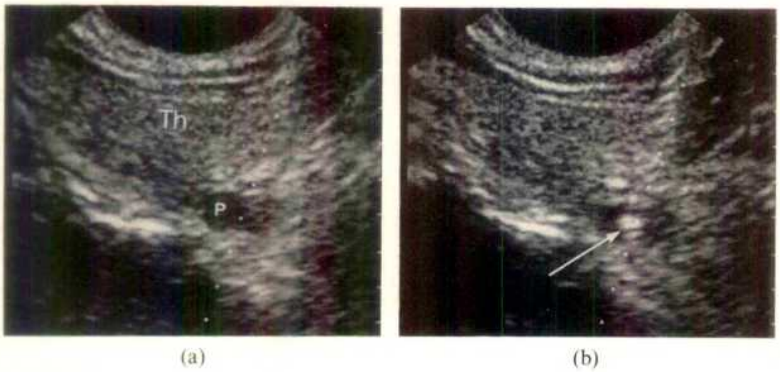

Figure 1. Longitudinal scan of the neck showing a parathyroid tumour (P) before (a) and during (b) ultrasound-guided fine-needle tissue biopsy. The arrow indicates the tip of the Sure-cut needle. Th = thyroid gland.

calculated to test the observer agreement (Koran, 1975; Fleiss, 1981). Probability values <0.05 were regarded as significant.

Results

Table I shows the agreement of the two pathologists (I and II). In three cases they disagreed on the histological examination but in all of these, Observer I did not find the material sufficient for a histological diagnosis. The kappa coefficient was calculated as 0.92.

In 57 of the 60 specimens from suspect parathyroid tumours, both pathologists agreed on the following microscopical findings: parathyroid (21), non-parathyroid (12; thyroid 8, striated muscle 3, lymphatic tissue 1) and insufficient material (24; blood 10, connective tissue 4, injured tissue 5, no material for examination 5). The success rate in obtaining tissue for histological diagnosis from suspect parathyroid tumours was 55% [(21 + 12) out of 60]. In three cases, one of the pathologists found it necessary to perform immunostaining with antibody against thyroglobulin before a final diagnosis could be made.

Twenty-three of the suspected parathyroid tumours (19 patients) were histologically verified following neck surgery. Both pathologists agreed on the histological diagnosis of all the specimens obtained by ultrasound-guided FNTB. Table II compares the histological findings of FNTB and the surgical specimens. No false positive or false negative findings were encountered. However, in 10 of the 23 suspected parathyroid tumours (43%), the material was insufficient for a histological diagnosis.

The approximated volume of the 10 parathyroid tumours from which sufficient material was obtained (Table II) ranged from 0.5 to 15.8 ml (median 1.0 ml) and the volume of the nine parathyroid tumours from which insufficient material was obtained ranged from 0.14 to 2.2 ml (median 1.0 ml). No significant difference ($p > 0.05$) was found between the two groups.

No complications were observed following ultrasound-guided FNTB. In patients operated on, no signs of haematoma or extraglandular fibrosis were encountered.

Discussion

Ultrasonography has proved a useful method in localizing enlarged parathyroid glands in the neck. However, the main difficulty with ultrasonography has been in discriminating parathyroid tumours from thyroid nodules, especially if they are protruding from the posterior surface of the thyroid gland. Less commonly, lymphnodes or deep muscular tissue have been misinterpreted as being parathyroid tumours (Reading et al, 1982; Rastad et al, 1984a; Butch et al, 1985; Winzelberg, 1987; Karstrup et al, 1988c). All the mentioned causes

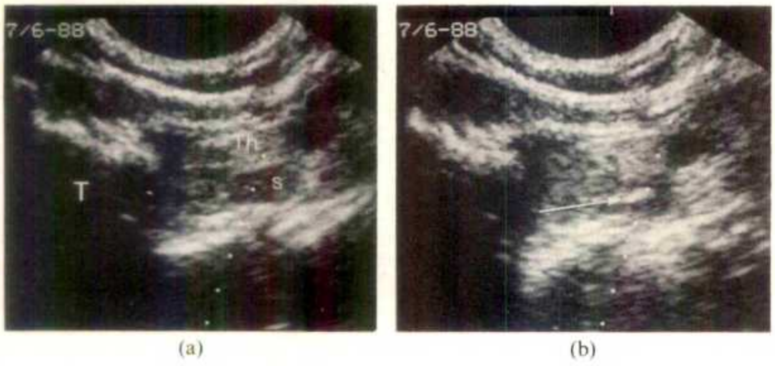

Figure 2. Transverse scan of the neck in a patient with primary hyperparathyroidism. (a) The left thyroid lobe is seen with echo-poor lesions. The lesion (s) was suspected of being a parathyroid tumour. T = trachea; Th = thyroid gland. (b) The tip of the Sure-cut needle (arrow) is seen inside the lesion. Histological examination disclosed thyroid tissue.

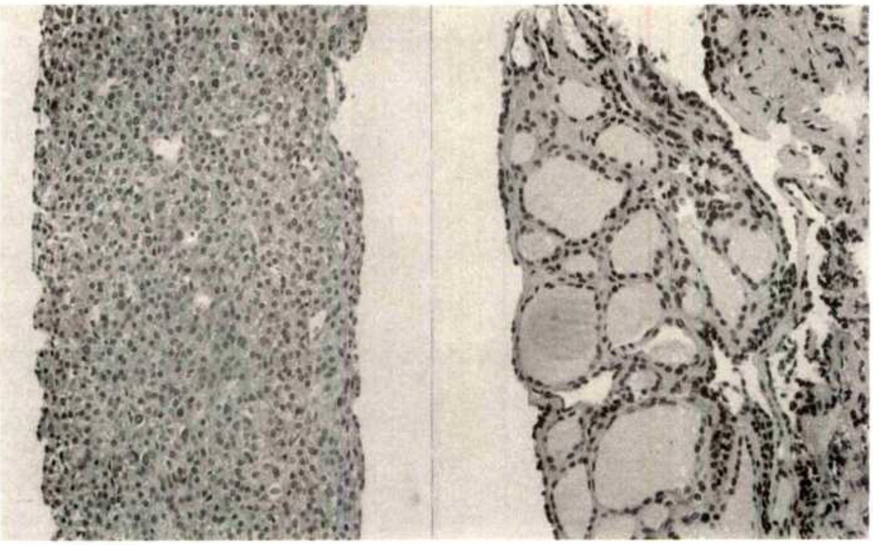

(a) (b)

Figure 3. Histological specimens from Sure-cut biopsies. (a) Parathyroid tissue with chief cells arranged in a solid/trabecular pattern (haematoxylin and eosin × 116). (b) Thyroid tissue showing follicles with accumulation of colloid (haematoxylin and eosin × 154).

of false positive ultrasound findings were observed in the present study.

The histological appearance of parathyroid tissue is well known to pathologists, as histological examinations are routinely performed on specimens following neck surgery (Grimelius et al, 1986). In contrast, cytological identification of parathyroid cells—and discrimination from thyroid cells—has been reported to be more difficult (Zajicek, 1974; Söderström, 1983; Gutekunst et al, 1986; Glenthøj & Karstrup, 1989). This is the main reason for performing FNTB for histological examination. Another reason is that the technique of performing ultrasound-guided FNTB and the handling of the material does not differ from FNTB obtained from other tumour lesions in the body (Torp-Pedersen et al, 1985), an advantage in routine daily practice. Other

Table I. Agreement of two observers (I and II) in histological examination of ultrasound-guided FNTB from 60 suspected parathyroid tumours

Observer II	Observer I			
	Parathyroid	Non-parathyroid	Insufficient material	Total
Parathyroid	21	0	3	24
Non-parathyroid	0	12	0	12
Insufficient material	0	0	24	24
Total	21	12	27	60

$$\text{Kappa coefficient} = \frac{\text{observed agreement} - \text{chance agreement}}{1 - \text{chance agreement}} = \frac{0.95 - 0.36}{1 - 0.36} = 0.92$$

Table II. Comparison of the histological diagnosis of FNTB and surgical verified specimens in 23 suspected parathyroid tumours

Surgery	Ultrasound-guided FNTB			
	Parathyroid	Non-parathyroid	Insufficient material	Total
Parathyroid	10	0	9	19
Non-parathyroid	0	3	1	4
Total	10	3	10	23

Predictive value of parathyroid diagnosis (10/10 × 100%) = 100% (69–100%).
Predictive value of non-parathyroid diagnosis (3/3 × 100%) = 100% (29–100%).
Retrieval rate (13/23 × 100%) = 57% (35–77%). 95% confidence limits in parentheses.

possible techniques for reliable identification of parathyroid glands have been reported. Thus, ultrasound-guided FNA and immunochemical determination of a high PTH content in the aspirates (Doppman et al, 1983; Karstrup et al, 1985; Gutekunst et al, 1986; Karstrup et al, 1988a). Although, this method seems to be very accurate, it requires special techniques not routinely available in all radiological departments.

The results disclosed no cases of disagreement between the two pathologists with regard to organ diagnosis, and the observer agreement, corrected for chance agreement, was found to be high. Furthermore, in the group of patients who underwent surgery no diagnostic errors were encountered. Based on these results we find that a reliable tissue diagnosis can be made by use of ultrasound-guided FNTB. However, the negative outcome from this study was a high percentage of insufficient material obtained from suspected parathyroid tumours or surgically verified parathyroid tumours [45% (27/60) and 47% (9/19), respectively]. A reason seems to be the difficulties of obtaining tissue cores when dealing with cystic and/or necrotic tumours or tumours with a soft consistency. These limitations in the use of the Sure-cut needle have also been reported in other organs (Torp-Pedersen et al, 1985).

By using the Sure-cut needle for histological sampling from suspected parathyroid tumours, a high percentage of inadequate biopsies is to be expected. In those cases where, on inspection, there is an evident tissue core from a suspect parathyroid tumour, we find this sufficient for a morphological diagnosis. However, in those cases where there is doubt or if no tissue core can be seen, we recommend the use of ultrasound-guided FNA for cytology and/or parathyroid hormone determination. The FNA can be carried out through the previously inserted guide needle causing only minimal additional strain on the patient (Karstrup et al, 1988a).

By combining ultrasonography and FNTB, a reliable tissue diagnosis can be obtained, thus forming the basis of ultrasound-guided, percutaneous inactivation of parathyroid tumours (Solbiati et al, 1985; Karstrup et al, 1987, 1988b). A positive parathyroid verification might aid and even quicken the clinical evaluation of patients suspected of hyperparathyroidism, particularly in patients with concurrent hypercalcaemic diseases and in patients presenting with severe hypercalcaemic symptoms (Reading et al, 1982). Finally, a pre-operative diagnosis has been of value in patients with ectopic parathyroid tissue and in patients requiring re-explorations (Charboneau et al, 1983; Gooding et al, 1985).

References

Butch, R. J., Simeone, J. F. & Mueller, P. R., 1985. Thyroid and parathyroid ultrasonography. *Radiologic Clinics of North America, 23*, 57–71.

Charboneau, J. W., Grant, C. S., James, E. M., Goellner, J. R. & Hodgson, S. F., 1983. High-resolution ultrasound guided percutaneous needle biopsy and intraoperative ultrasonography of cervical parathyroid adenoma in a patient with persistent hyperparathyroidism. *Mayo Clinic Proceedings, 58*, 497–500.

Doppman, L. J., Krudy, A. G., Marx, J. S., Saxe, A., Schneider, P., Norton, A. J., Spiegel, M. A., Dowms, W. R., Schaaf, M., Brennan, E. M., Schneider, B. A. & Auerbach, D. G., 1983. Aspiration of enlarged parathyroid glands for parathyroid hormone assay. *Radiology, 148*, 31–35.

Fleiss, J. L., 1981. *Statistical Methods for Rates and Proportions*, 2nd edn (Wiley, New York).

Glenthøj, A. & Karstrup, S., 1989. Parathyroid identification by ultrasonically guided aspiration cytology: is a correct cytological identification possible? *Acta Pathologica, Microbiologica et Immunologica Scandinavica, 97*, 497–502.

Gooding, A. W. G., Clark, O. H., Stark, D. D., Moss, A. A. & Montgomery, K. C., 1985. Parathyroid aspiration biopsy under ultrasonic guidance in the postoperative hyperparathyroid patient. *Radiology, 155*, 193–196.

Grimelius, R., Åkerström, G., Johansson, H., Ljunghall, S. & Rastad, J., 1986. The role of pathology in diagnosis and surgical decision-making. In *Progress in Surgery, 18*, ed. by E. H. Forthmann (Karger, Basel), pp. 80–92.

Gutekunst, R., Valesky, A., Borisch, B., Hafferman, W., Kiffner, E., Thiess, E., Lohrs, U. & Scriba, P. C., 1986. Parathyroid localization. *Journal of Clinical Endocrinology and Metabolism, 63*, 1390–1393.

Karstrup, S., Hegedüs, L., Torp-Pedersen, S. & Holm, H. H., 1985. Ultrasonically guided fine needle aspirations of suspect parathyroid tissue to determine parathyroid hormone concentration. *British Journal of Medicine, 290*, 284.

Karstrup, S., Glenthøj, A., Torp-Pedersen, S., Nielsen, L. & Hegedüs, L., 1986. Ultrasonically guided fine needle biopsy for histological sampling of suspect parathyroid tissue. *British Journal of Radiology, 59*, 507–509.

Karstrup, S., Holm, H. H., Torp-Pedersen, S. & Hegedüs, L., 1987. Ultrasonically-guided percutaneous inactivation of parathyroid tumours. *British Journal of Radiology, 60*, 667–670.

Karstrup, S., Glenthøj, A., Torp-Pedersen, S., Hegedüs, L. & Holm, H. H., 1988a. Ultrasonically guided fine needle aspiration of suggested enlarged parathyroid glands. *Acta Radiologica, 29*, 213–216.

Karstrup, S., Lohela, P., Apaja-Sarkkinen, M., Borgmästars, H. & Holopeinen, O., 1988b. Non-operative inactivation of a parathyroid tumour in a patient with hypercalcaemic crisis. *Acta Medica Scandinavica, 224*, 187–188.

Karstrup, S., Hegedüs, L. & Holm, H. H., 1988c. Parathyroid ultrasonography in patients with primary hyperparathyroidism. *Danish Medical Bulletin, 35*, 583–585.

Koran, M. L., 1975. The reliability of clinical methods, data and judgements. *New England Journal of Medicine, 13*, 642–646.

Rastad, J., Lindgren, P. G., Ljunghall, S., Johansson, H., Malmaeus, J., Rudberg, C. & Åkerström, G., 1984a. Ultrasound scanning for pre-operative location of parathyroid tumours. *Acta Chirurgica Scandinavica, 150*, 199–204.

Rastad, J., Johansson, H., Lindgren, G. P., Ljunghall, S., Stenkvist, B. & Åkerström, G., 1984b. Ultrasonic localization and cytologic identification of parathyroid tumours. *World Journal of Surgery, 8*, 501–508.

Reading, C. C., Charboneau, W. J., James, M. E., Karsell, R. P., Purnell, C. D., Grant, S. C. & van Heerden, A. J., 1982. High resolution parathyroid sonography. *American Journal of Roentgenology, 139*, 539–546.

Söderström, N., 1983. Identification of normal tissue by aspiration cytology. In *Clinical Aspiration Cytology*, ed. by A. J. Linsk & S. Franzen (J. B. Lippincott, Philadelphia), pp. 14–15.

SOLBIATI, L., MONTALI, G., CROCE, F., BELLOTTI, E., GIANGRANDE, A. & RAVETTO, C., 1983. Parathyroid tumours detected by fine-needle aspiration biopsy under ultrasonic guidance. *Radiology, 148*, 793–797.

SOLBIATI, L., GIANGRANDE, H., DE PRA, L., BELLOTTI, E., CANTU, P. & RAVETTO, C., 1985. Percutaneous ethanol injection of parathyroid tumours under US guidance: treatment of secondary hyperparathyroidism. *Radiology, 155*, 607–610.

TORP-PEDERSEN, S., JUUL, N. & VYBERG, M., 1984. Histological sampling with a 23 gauge modified Menghini needle. *British Journal of Radiology, 57*, 151–154.

TORP-PEDERSEN, S., VYBERG, M., JUUL, N. & SEHESTED, M., 1985. Fine needle histological sampling. In *Interventional Ultrasound*, ed. by H. H. Holm & J. K. Kristensen (Munksgaard, Copenhagen), pp. 35–40.

WINZELBERG, G. C., 1987. Parathyroid imaging. Diagnosis and treatment. *Annals of Internal Medicine, 107*, 64–70.

ZAJICEK, J., 1974. Aspiration biopsy cytology. In *Monographs in Clinical Cytology*, ed. by G. L. Wied (Karger, Basel), pp. 87–88.

1989, *The British Journal of Radiology*, 62, 986–988

The value of transoesophageal ultrasonography in the management of a mediastinal foregut cyst

By J. E. Page, MRCP, FRCR, A. G. Wilson, FRCP, FRCR and *M. A. de Belder, MA, MRCP

Departments of Diagnostic Radiology and *Cardiology, St George's Hospital, London SW17 0QT

(*Received May 1989*)

Abstract. Mediastinal foregut cysts account for approximately 10% of primary mediastinal masses. The differentiation of these cysts from other mediastinal masses is important, especially if a policy of aspiration and observation of cysts is adopted. Computed tomography (CT) is generally regarded as the definitive imaging modality in these cases, but it may occasionally fail to identify the cystic nature of the mass. We report a case in which transoesophageal ultrasound contributed to the diagnosis and demonstrated features of the cyst contents that were not visible on CT.

There have been a number of papers advocating conservative management of mediastinal foregut cysts by aspiration, so avoiding thoracotomy (Schwartz et al, 1986; Kuhlman et al, 1988; Wittich et al, 1988). The differentiation of solid from cystic mediastinal masses is critical if this approach is to be used. In most cases this is straightforward, since the computed tomography (CT) number of mediastinal cyst contents is usually in the region of 0–20 Hounsfield units (HU), consistent with their cystic nature (Kuhlman et al, 1988). However, much higher attenuation values, well into the soft-tissue range, have been recorded (Nakata et al, 1982).

Confusion that might result with such lesions can be avoided with ultrasound examination, which will also characterize the cyst contents and appearance of the cyst wall that may be of diagnostic value. Vascular relationships may also be determined without the need for intravenous contrast medium. Transthoracic sonography is not usually helpful because of interference produced by air in the lungs and by the bony skeleton, except in children. However, transoesophageal ultrasonography overcomes these difficulties. The case illustrates the use of this technique in combination with CT and percutaneous needle aspiration in the assessment of a mediastinal foregut cyst.

Case report

A 48-year-old woman presented to her GP with mild discomfort in the chest and left shoulder. A chest radiograph at this time showed a well defined left paratracheal mass (Fig. 1), and she was therefore referred for further investigation.

At the time of referral she was asymptomatic and clinical examination was unremarkable. A barium swallow showed a slight extrinsic impression of the oesophagus. Computed tomography confirmed a 4 cm diameter posterior mediastinal mass. This was a well defined, ovoid structure lying immediately behind and to the left of the trachea, closely related to the superior aspect of the aortic arch (Fig. 2). The CT number of the mass was 15–20 HU consistent with a cyst. The lesion did not enhance following intravenous contrast medium.

Transoesophageal ultrasonography was performed using a 5 MHz, phased-array transducer incorporating colour-coded Doppler. The examination, carried out under light sedation, revealed a 4 cm, fluid-filled mass closely related to the postero-lateral part of the aortic arch (Fig. 3). It was adjacent to a vertebral body and contained sludge, which moved with gravity on moving the patient to a supine position and then back again to the left lateral position. Colour Doppler imaging revealed flow in the left pulmonary artery and the descending aorta, but there was no evidence of blood flow in or out of the cyst. The examination lasted 12 min.

Percutaneous cyst aspiration was carried out under fluoroscopic control and local anaesthetic. Fifteen millilitres of turbid, creamy fluid were removed for analysis and cytology confirmed the presence of amorphous debris with a small number of neutrophils, foamy macrophages and cholesterol crystals. Unfortunately, there was no epithelial component present to determine the aetiology of the cyst and no malignant cells were seen. Biochemical analysis of the fluid showed a high sodium and chloride content with low levels of cholesterol and protein. Bacteriological cultures were negative.

Following aspiration, a chest radiograph showed considerable decrease in size of the cyst. It was concluded that this patient had a mediastinal foregut cyst of indeterminate nature. There was no evidence of malignancy and it was thought unlikely to be causing her symptoms, which had settled spontaneously. It was felt that thoracotomy was not justified and the patient was well 6 months later.

Discussion

Computed tomography is probably the imaging technique of choice in the investigation of mediastinal masses. Intravenous contrast medium enhancement is usually necessary to delineate vascular relationships and differentiation of solid and cystic masses is not always

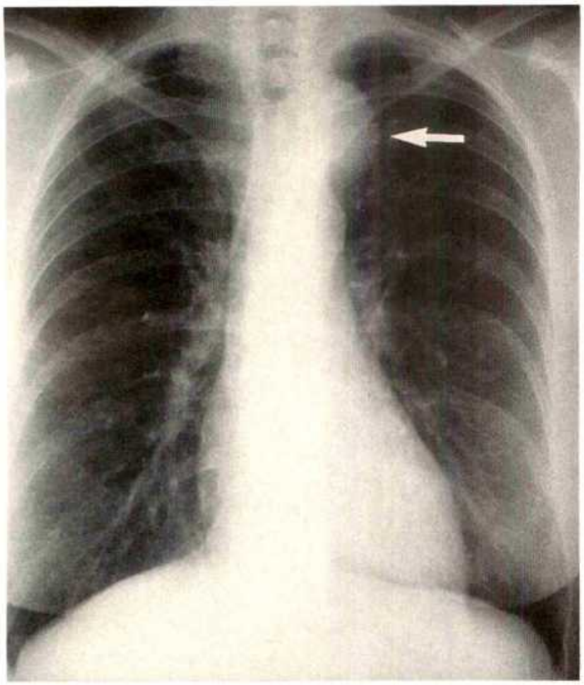

Figure 1. Chest radiograph showing a mass of soft-tissue density above the aortic arch (arrow).

possible (Schwartz et al, 1986). Benign mediastinal foregut cysts account for approximately 10% of primary mediastinal masses (Kirwan et al, 1973; Fitch et al, 1986). These cysts are said to have a characteristic appearance on CT, being smooth, round or oval structures of homogeneous density that do not enhance following intravenous contrast medium (Kuhlman et al, 1988). Their location in the posterior mediastinum (bronchogenic and enterogenous cysts), paratracheal or subcarinal region (bronchogenic cysts) is also typical (Sirivella et al, 1985). The appearances are said to be so characteristic that thoracotomy may be avoided in asymptomatic patients on the basis of these appearances (Fitch et al, 1986).

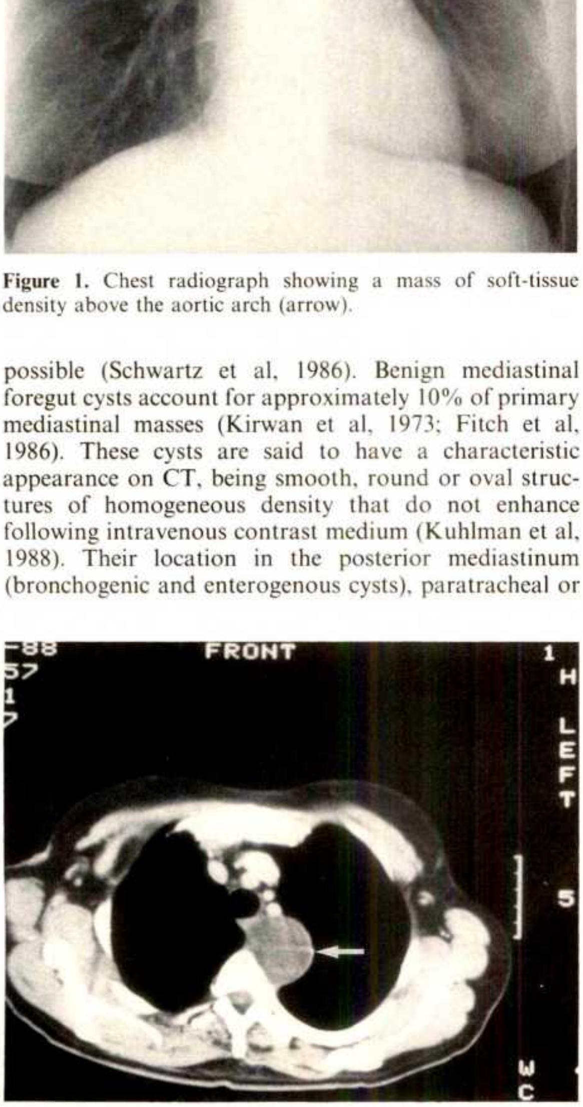

Figure 2. Computed tomographic scan showing the non-enhancing mass lying postero-lateral to the trachea and between the left subclavian artery and the spine (arrow).

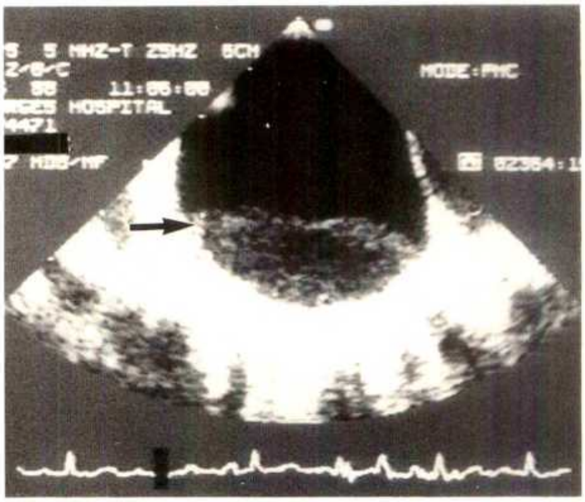

Figure 3. Transoesophageal ultrasonography confirms the cystic nature of the mass and its relationship to the great vessels. The layering of "sludge" is clearly demonstrated (arrow).

One possible source of confusion, however, is the CT number of these cysts. Although typically close to water or fluid density, *i.e.* up to 20 HU (Kuhlman et al, 1988), there have been a number of reports of foregut cysts with higher CT numbers in the range of solid masses. Values in the 26–35 HU range are not uncommon (Fitch et al, 1986) and even higher values of 89 and 97 HU have been recorded (Nakata et al, 1982). These numbers are well into the soft-tissue range and may be much higher than many solid organs, such as kidney (30 HU), spleen and pancreas (40 HU). The nature of the cyst contents varies from serous to turbid or mucous and this may account for the range of attenuation values (Fitch et al, 1986). Increased calcium levels and cellular content have also been implicated (Schwartz et al, 1985). High CT numbers could lead to misclassification of a cyst as solid.

Ultrasound has a useful role to play in the differentiation of solid and cystic mediastinal masses (Goldberg, 1973), particularly in infants and children in whom it is easier to find a suitable acoustic window (Snyder et al, 1985; Fitch et al, 1986). Transoesophageal ultrasound was described by Frazin and co-workers (1976). It is mainly used in the assessment of cardiac disease (Gussenhoven et al, 1986; Sutherland & Roelandt, 1988); scans are usually performed on unsedated patients but mild sedation may be used in anxious patients. The technique takes 5–10 min to perform, is well tolerated and safe (de Belder et al, 1988; Geibel et al, 1988). This method has been used by one other group in the assessment of solid mediastinal lesions

(Borner et al, 1988), although this is the first reported case of the use of transoesophageal ultrasonography in the investigation of mediastinal cysts and illustrates its advantages in the assessment of possible cystic structures. Transoesophageal ultrasonography also has the capacity to identify fluid-filled spaces regardless of CT number, although this was not a problem in this particular case. It does not require intravenous contrast medium to ascertain relationship to vascular structures and it may reveal more information concerning the nature of the cyst contents.

Aspiration of mediastinal cysts has been performed for both diagnostic and therapeutic purposes. The most favoured routes appear to be transbronchial or transoesophageal (Schwartz et al, 1986; Kuhlman, 1988), although percutaneous aspiration has been reported under CT control (Wittich et al, 1988). In this case, percutaneous needle sampling of the cyst contents was performed under fluoroscopic control. Unfortunately, no epithelial component was aspirated (this occurs in up to 20% of cases (Sirivella et al, 1985)) and hence a specific diagnosis was not possible.

There is still controversy over long-term management of these patients. Infection is a serious complication, occurring at any time, and, because of this risk, some authors advocate thoracotomy, even in asymptomatic patients (Kirwan et al, 1973; Sirivella et al, 1985). Aspiration and/or drainage and follow-up is considered satisfactory in asymptomatic patients by others, including ourselves (Schwartz et al, 1986; Wittich et al, 1988; Kuhlman et al, 1988).

Although we do not advocate the use of transoesophageal ultrasound in the evaluation of all mediastinal masses, it is a relatively quick and safe procedure, which may provide valuable information not obtained from CT when a cystic lesion is suspected.

References

Borner, N., Lorenz, J., Jakob, H. G. & Schweden, F., 1988. Mediastinal lymph node enlargement evaluated by transoesophageal echography. Presented at the International Symposium on Transoesophageal Echocardiography, Mainz, West Germany, December 1988.

de Belder, M. A., Fox, M., Leech, G. & Camm, A. J., 1988. Transoesophageal echocardiography in unsedated patients: technique and patient tolerance. Presented at the International Symposium on Transoesophageal Echocardiography, Mainz, West Germany, December 1988.

Fitch, S. J., Tonkin, I. L. D. & Tonkin, A. K., 1986. Imaging of foregut duplication cysts. *Radiographics, 6,* 189–201.

Frazin, L., Talano, J. V., Stephanides, L., Loeb, H. S., Kopel, L. & Gunnar, R. M., 1976. Esophageal echocardiography. *Circulation, 54,* 102–108.

Geibel, A., Kasper, W., Behroz, A., Przewolka, U., Meinertz, T. & Just, H., 1988. Risk of transesophageal echocardiography in awake patients with cardiac diseases. *American Journal of Cardiology, 62,* 337–339.

Goldberg, B. B., 1973. Mediastinal ultrasonography. *Journal of Clinical Ultrasound, 1,* 114–119.

Gussenhoven, E. J., Taams, M. A., Roelandt, J. R. T. C., Ligtvoet, K. M., McGhie, J., van Herwerden, L. A. & Cahalan, M. K., 1986. Transoesophageal two-dimensional echocardiography: its role in solving clinical problems. *Journal of the American College of Cardiology, 8,* 975–979.

Kirwan, W. O., Walbaum, P. R. & McCormack, R. J. M., 1973. Cystic intrathoracic derivatives of the foregut and their complications. *Thorax, 28,* 424–428.

Kuhlman, J. E., Fishman, E. K., Wang, K. P., Zerhouni, E. A. & Siegelman, S. S., 1988. Mediastinal cysts: diagnosis by CT and needle aspiration. *American Journal of Roentgenology, 150,* 75–78.

Nakata, H., Nakayama, C., Kimoto, T., Nakayama, T., Tsukamoto, Y., Nobe, T. & Suzuki, H., 1982. Computed tomography of mediastinal bronchogenic cysts. *Journal of Computer Assisted Tomography, 6,* 733–738.

Schwartz, A. R., Fishman, E. K. & Wang, K. P., 1986. Diagnosis and treatment of a bronchogenic cyst using transbronchial needle aspiration. *Thorax, 41,* 326–327.

Schwartz, D. B., Beals, T. F., Wimbish, K. J. & Hammersley, J. R., 1985. Transbronchial fine needle aspiration of bronchogenic cysts. *Chest, 88,* 573–575.

Sirivella, S., Ford, W. B., Zikria, E. A., Miller, W. H., Samadani, S. R. & Sullivan, M. E., 1985. Foregut cysts of the mediastinum. *Journal of Thoracic and Cardiovascular Surgery, 90,* 776–782.

Snyder, M. E., Luck, S. R., Hernandez, R., Sherman, J. O. & Raffensperger, J. G., 1985. Diagnostic dilemmas of mediastinal cysts. *Journal of Pediatric Surgery, 20,* 810–815.

Sutherland, S. G. & Roelandt, J. R. T. C., 1988. Oesophageal echocardiography. *British Heart Journal, 60,* 1–3.

Wittich, G. R., Karnel, F., Schurawitzki, H. & Jantsch, H., 1988. Percutaneous drainage of mediastinal pseudocysts. *Radiology, 167,* 51–53.

1989, *The British Journal of Radiology*, 62, 989–994

A quality assessment of the effects of a hydrogenous filter on a p(66)Be(40) neutron beam

By J. P. Slabbert, BSc(Hons), P. J. Binns, MSc, H. L. Jones, BSc and J. H. Hough, PhD
National Accelerator Centre, PO Box 72, Faure 7131, South Africa

(Received September 1988 and in final form June 1989)

Abstract. Recent measurements in a p(62)Be(36) neutron therapy beam have shown that the quality of the in-phantom beam changes with depth. This variation can be ascribed to the presence of a relatively large low-energy neutron component emanating from the neutron source. As part of the pre-clinical calibration programme at a newly commissioned neutron therapy facility, radiobiological and microdosimetric observations were made to determine the magnitude of this effect on a p(66)Be(40) beam and to evaluate the hardening effect of a hydrogenous filter. The reported data identify a correlation between the two assays and quantify a linear relationship between y^* and filter thicknesses $\leqslant 6$ cm. Using the data obtained in the study, a filter thickness was selected to comply with clinical requirements. By employing lineal energy spectra, it is demonstrated that subtle changes in beam quality may be quantified in a reproducible manner without resorting to time-consuming radiobiological studies.

The p + Be reaction is now well established as the reaction of choice for providing a high-intensity source of fast neutrons suitable for therapy. A singular disadvantage remains, however, when compared with the d + Be reaction, and that is the presence of a prominent low-energy component attributed to evaporation neutrons as demonstrated by Johnsen (1977). These low-energy neutrons can prove clinically undesirable if they affect the consistency of the beam. Any such effect will manifest itself in a variation in beam quality with depth when in-phantom measurements are performed in an unfiltered beam. The effect is due principally to preferential scattering of the low-energy component out of the beam, which renders a more energetic radiation field at greater depths within the scattering medium. This "hardening" of the beam was predicted by Amols et al (1977). In a radiobiological study performed by Hall et al (1982) using 43 MeV protons on a thick target, an 8–12% variation in the relative biological effectiveness (RBE) was observed when exposing V79 cells at different depths (2 and 12 cm). Although this quality change could be eliminated by means of a 4 cm thick hydrogenous filter, these authors subsequently adopted the use of a thin target (Hall et al, 1983).

The present study, undertaken at the recently completed neutron therapy facility of the National Accelerator Centre (NAC) near Cape Town (Jones et al, 1988), was prompted by the apparent contrasting results obtained at Clatterbridge [p(62)Be(36)] using different biological end-points (Bewley et al, 1987; Hornsey & Meyers, 1987). The aim of the investigation was to quantify the effect that low-energy neutrons have on the quality of a p(66)Be(40) beam and, if any, to minimize this effect with the incorporation of a hydrogenous filter.

Whilst the dominant characteristics of the neutron radiation are determined by the reaction type and target thickness, the design of the target assembly and the collimator system can modify the quality of the beam. At the NAC, protons are accelerated to 66 MeV and impinge upon a 19.6 mm thick Be target. Only 40 MeV of the incident beam energy is dissipated in the target, which is encapsulated in a 0.55 mm thick Cu cylinder. A 2 mm air gap allows for possible heat expansion of the Be. The protons are finally brought to rest in a 1 mm Cu plate, which is cooled on both front and back surfaces by 1 mm of water. The end of the Cu target assembly is 3 mm thick. The beam is pre-collimated by 13 cm of steel before passing through twin transmission chambers mounted 21 cm beyond the target. No flattening filters were used in the beam.

Methods

Radiobiological assay

V79 hamster fibroblasts were employed for this assay, with cell survival serving as the biological end-point. To ensure maximum precision in the estimation of survival levels the idea of a self-contained set of measurements was followed (Hall & Kellerer, 1979) and one set of survival curves (four in all) was obtained from the same cell population. These cells are routinely cultured as monolayers in minimum essential medium (Gibco), supplemented with 10% fetal calf serum and antibiotics (penicillin and streptomycin). Two days before the scheduled irradiation, the cell line was subcultured from the growing stock. The cells are then partially confluent on the day of irradiation. Four hours prior to irradiation the cells were detached from the growth surface by a 1:1 mixture of EDTA (0.1%) and trypsin (0.25%). Following a single dilution route, appropriate cell numbers were seeded in 4 ml complete medium in 25 cm^2 tissue-culture flasks (Falcon). Cell numbers were sufficient for the formation of approximately 200 colonies per flask. Three flasks were seeded for each dose point on each of the four survival curves (at 2.5 and 15 cm depth, with and without filtration). For a specific dose point, each of the flasks (12 in all) were seeded from a common cell suspension using the same pipette. Upon completion of this preparation the cells were returned to the incubator (5% CO_2 in air at 37°C) and allowed to attach to the surface of the culture flask.

Before irradiation the flasks were filled with complete medium, capped and sealed with Parafilm. Using two jigs, the flasks were orientated such that charged particle equilibrium was realized in the tissue culture medium (for cells at 2.5 cm) and with the attached cells located at the specified depth. To minimize possible biological variations, all the flasks for a specific dose point (at 2.5 and 15 cm depths) were irradiated simultaneously for each filtration condition. After the cells at the 2.5 cm position had received their prescribed dose, this jig was removed and the irradiation of the cells at 15 cm continued. This interruption did not exceed 1 min. The dose rate at 2.5 cm depth was 0.4 Gy min^{-1}. After irradiation the flasks were returned to the incubator where they remained for 6 days. Thereafter the flasks were rinsed with Dulbecco's phosphate-buffered saline, the colonies fixed with methanol–acetic acid in water (1:1:3) and stained with 0.01% amidoblack. Only colonies comprising 50 or more cells were scored.

Irradiations were performed in a 60 cm × 60 cm × 60 cm water phantom, with and without a 5 cm thick polythene filter placed at the exit aperture of the collimator. The front surface of the water phantom was located at a source–surface distance (SSD) of 150 cm. The three flasks, spanning a lateral distance of 11.5 cm, were positioned symmetrically about the central axis in a 20 cm × 20 cm field. At both depths, with and without filtration, absorbed dose measurements in the off-centre flasks did not differ by more than 2% from those measured on the central axis. The revised dosimetry protocol (Minjheer et al, 1987) was adhered to throughout for the assessment of the total absorbed dose. Dose measurements were performed with a 0.5 cm^3 tissue-equivalent ionization chamber (Exradin Model T2) flushed with methane-based tissue-equivalent (TE) gas.

Microdosimetric evaluation

Compared with conventional absorbed dose determinations where a hydrogenous/non-hydrogenous detector pair is used, the application of tissue-equivalent proportional counter (TEPC) measurements permits a far more comprehensive evaluation of beam quality. The experimental method and data analysis employed are described in a recent intercomparison study (Binns & Hough, 1988). Several modifications have since been implemented to extend the lower lineal energy limit and facilitate more exacting data collection. Propane instead of methane-based TE gas was used at a pressure of 8.7 kPa to simulate a 2 μm mean chord length in unit density tissue. Pulse height data covering three lineal energy ranges were accumulated simultaneously and the raw data binned into 40 logarithmic intervals per decade. Unless specified, only total dose parameters are reported.

The investigation was conducted in two phases (I and II). Initially, lineal energy spectra were evaluated in a 20 cm × 20 cm field at two depths (2.5 and 15 cm), with and without a 5 cm thick polythene filter. As an indicator of biological relevance, the microdosimetric parameter y^* [dose mean lineal energy corrected for saturation (International Commission on Radiation Units and Measurements (ICRU), 1983] was calculated (Menzel, 1984). Having identified a significant variation in y^* under these conditions, a more extensive series of measurements was proposed in order to optimize the filter thickness. Measurements at 2.5 and 15 cm depths (without filtration) were repeated some months later and significant differences again observed. Thereafter the counter was repositioned at 2.5 cm depth and the filtration thickness varied from 1 to 7 cm.

Table I. Parameters describing survival curves obtained at different depths in a water phantom with and without a 5 cm thick polythene filter (field size 20 cm × 20 × cm). For constants α and β the 95% confidence errors are stated in parentheses. The coefficients α and β describing the linear-quadratic fit to the experimental data are covariant parameters. Assuming this mathematical property as premise, the 95% confidence limits were used to calculate limiting $\bar{D}$ values

Filtration (cm)	Depth (cm)	α (× 10) (Gy^{-1})	β (× 10) (Gy^{-2})	$\bar{D}$ (Gy)
0	2.5	4.76 (0.54)	1.12 (0.12)	1.38 (0.05)
0	15.0	3.72 (1.35)	1.14 (0.31)	1.55 (0.05)
5	2.5	3.98 (0.79)	1.08 (0.20)	1.52 (0.07)
5	15.0	4.39 (0.99)	0.93 (0.25)	1.51 (0.09)

Results

In fitting curves to the surviving fractions $S(D)$, the linear-quadratic model

$$S(D) = \exp[-(\alpha D + \beta D^2)]$$

was adopted and the coefficients α and β determined (Table I). Included in the tabulation are mean inactivation dose values $\bar{D}$ (Kellerer & Hug, 1972) calculated from these coefficients. In contrast to D_0 values (ICRU, 1979), which are calculated from the distal portion of the survival curve, $\bar{D}$ values are determined by integration over the complete dose range and are hence dominated by the surviving fractions at low doses. This single parameter description of cell survival has been used extensively for intercomparison purposes (Fertil et al, 1984) and a recent analysis has highlighted the correlation between survival data in the first decade and tumour response (Elkind, 1988).

Figure 1 shows survival data obtained at two depths without the use of a hardening filter and indicates that the beam is more effective at shallow depths. The quality of the beam remains unaffected at different depths when a 5 cm thick polythene filter is used (Fig. 2). Moreover, the survival data at 2.5 cm depth with filtration yield a curve indistinguishable from that at 15 cm depth without filtration. The statistical difference, however,

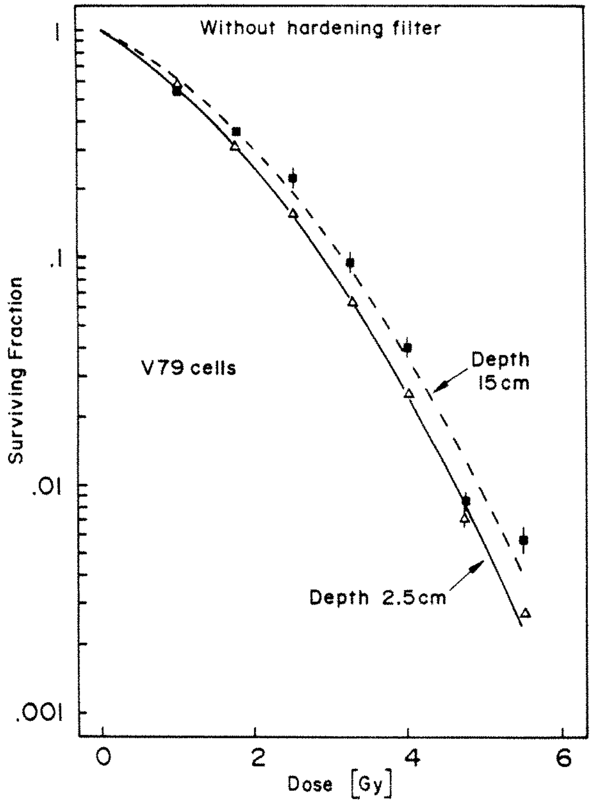

Figure 1. Survival fractions determined at (△) 2.5 and (■) 15 cm depths with no hardening filter. Where larger than the symbols, the error bars indicate one standard deviation.

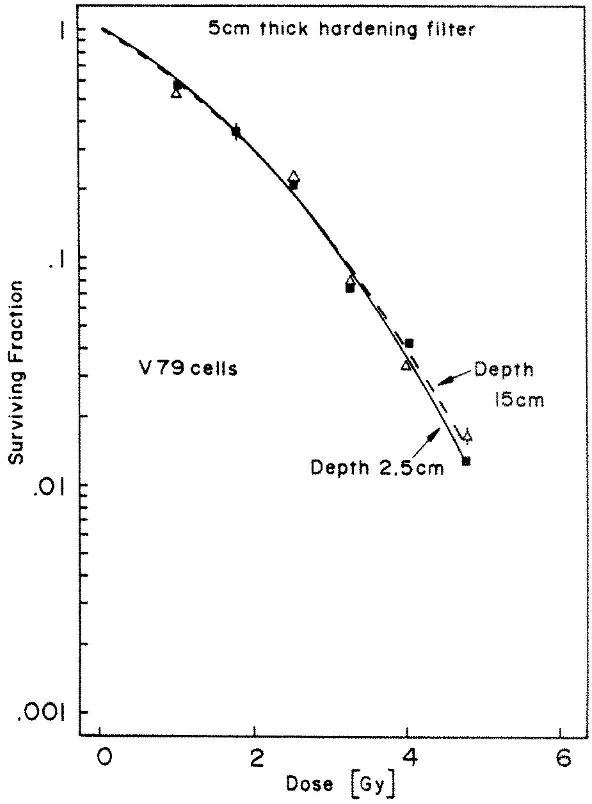

Figure 2. Survival fractions determined at different depths after incorporating a hardening filter (5 cm polythene). Symbols and error bars as in Fig. 1.

between all the data sets is best illustrated by the 95% confidence ellipses (Skokal & Rohlf, 1969) drawn in Fig. 3, where the ellipse on the right-hand side (no filtration, 2.5 cm depth) is clearly separated from the others. A difference is also indicated by the ratios of the $\bar{D}$ values: 1.12 ± 0.05 (no filter) and 1.01 ± 0.07 (5 cm polythene). The data plotted in Fig. 4, (lower curve) were obtained by calculating the relative effectiveness (RE) at the 40% survival level, which approximates to clinically prescribed doses. This value is simply the quotient of the doses required to produce the same effect $[D_{\mathrm{n}(15\,\mathrm{cm})}/D_{\mathrm{n}(2.5\,\mathrm{cm})}]$. The RE value determined some months later with a different cell population using a 3 cm thick filter correlates well with the earlier data.

Lineal energy spectra determined at 2.5 cm depth for varying polythene thicknesses are shown in Fig. 5. The hardening of the beam with increasing filtration is demonstrated by fewer slow recoil protons ($14 < y < 140\ \mathrm{keV}\ \mu\mathrm{m}^{-1}$) and an increase in the fast recoil proton component ($1 < y < 14\ \mathrm{keV}\ \mu\mathrm{m}^{-1}$). Above the proton edge, located at approximately $140\ \mathrm{keV}\ \mu\mathrm{m}^{-1}$, no distinct differences could be observed for the filtered spectra. The evaluated microdosimetric parameters are summarized in Table II. For consistency, a common

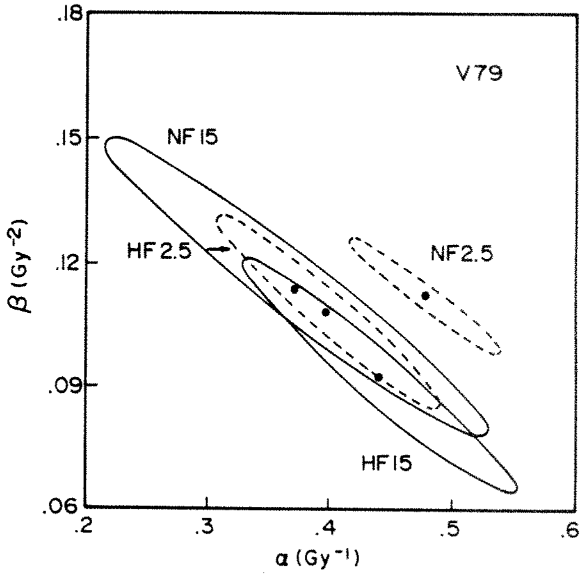

Figure 3. 95% confidence ellipses depicting the relationship between α and β, the parameters describing the linear-quadratic fit to survival curve data. HF symbolizes the use of a 5 cm thick hydrogenous (polythene) filter whilst NF indicates no filtration.

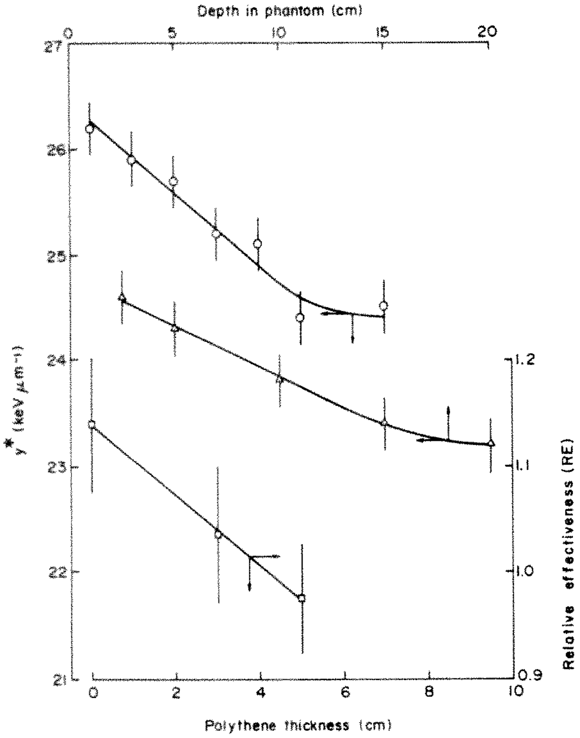

Figure 4. The upper curve (○) depicts the variation of y^*, at a depth of 2.5 cm, with increasing filtration (polythene) whilst the lower curve (□), reflects a similar trend for the relative effectiveness of the beam (20 cm × 20 cm field). 95% confidence limits for the RE values are indicated in the lower curve. The middle curve (△) shows the variation in y^* with depth in the water phantom (10 cm × 10 cm field). The latter data were obtained after a 2.5 cm thick polythene filter had been installed in the isocentric gantry.

Table II. Microdosimetric parameters (for events > 1 keV μm^{-1}) evaluated from lineal energy spectra determined for different depths and filtration conditions. The field size was set at 20 cm × 20 cm throughout

Phase	Depth (cm)	Filter (cm)	$\bar{y}_F$ (keV μm^{-1})	$\bar{y}_D$ (keV μm^{-1})	y^* (keV μm^{-1})
I	2.5	0	8.22	76.6	26.6
		5	7.41	76.0	24.8
	15.0	0	7.60	75.4	25.1
		5	7.51	76.0	24.8
II	2.5	0	8.48	78.8	26.2
		1	8.37	79.4	25.9
		2	8.36	80.9	25.7
		3	8.11	79.2	25.2
		4	8.02	79.4	25.1
		5[a]	—	—	24.4
		7	7.80	78.2	24.5
	15.0	0	7.82	76.0	24.7

[a] Limited machine time for Phase II did not permit a repeat measurement with the 5 cm thick filter. Taking into account the 1.5% difference between Phase I and Phase II data (2.5 and 15 cm depths without filtration), the y^* value was adjusted accordingly.

cut-off of 1 keV μm^{-1} was applied to these spectra before calculating the tabulated values. Measurements at 2.5 and 15 cm depth with a 5 cm filter yielded identical y^* values (Phase I) and spectra that were indistinguishable from each other over the entire lineal energy range. Experimental errors of 6%, 2% and 1% are associated with $\bar{y}_F$, $\bar{y}_D$ and y^*, respectively (Binns & Hough, 1988). An acceptable overall agreement between Phase I and Phase II observations was found and similar trends noted: decreasing $\bar{y}_F$ and y^* with increasing depth (without filtration); with $\geqslant$5 cm polythene the values at 2.5 and 15 cm depth are in good agreement with one another. Whilst no deduction can be made for $\bar{y}_D$, a clear trend in y^* values with filter thickness is apparent in Phase II. The latter is illustrated by the upper curve in Fig. 4.

In seeking a compromise between filtration effect and diminished dose-rate, a 2.5 cm thick polythene filter was selected and inserted in the isocentric head, approximately 15 cm from the target assembly. Unfortunately it was not possible to obtain microdosimetric spectra with the filter positioned at the collimator aperture prior to its permanent installation. However, a series of

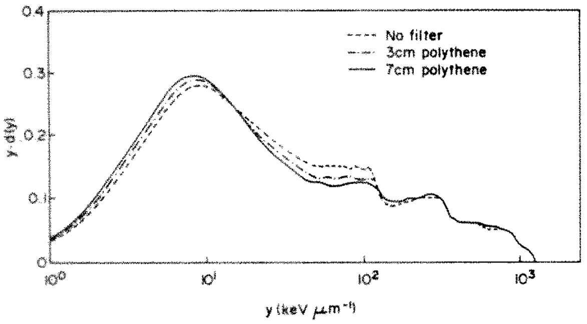

Figure 5. Lineal energy spectra determined at 2.5 cm depth in a 20 cm × 20 cm field without filtration (- - -) and with a 3 (—·—) and (——) 7 cm thick polythene filter.

Table III. Microdosimetric parameters and photon fractions determined at different depths in the p(66)Be(40) therapy beam (10 cm × 10 cm field) after insertion of a beam hardening filter (2.5 cm polythene)

Depth (cm)	$\bar{y}_F$ (keV μm^{-1})	$\bar{y}_D$ (keV μm^{-1})	y^* (keV μm^{-1})	y^*_n (keV μm^{-1})	D_G (%)
2.5	4.3	85.5	24.6	25.6	4.7
5	4.2	84.0	24.3	25.3	4.9
10	4.0	84.7	23.8	24.9	5.3
15	3.9	83.4	23.4	24.5	5.4
20	3.8	84.0	23.2	24.3	5.7

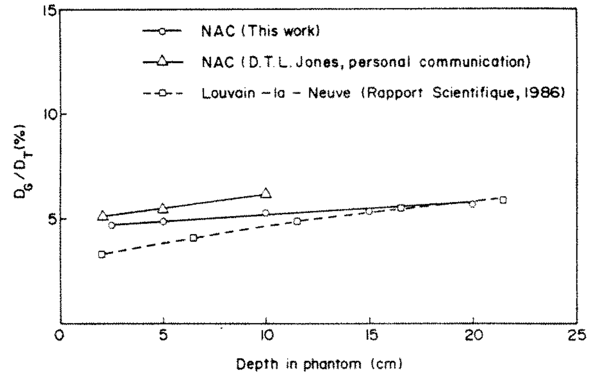

Figure 6. Photon dose fractions determined from lineal energy spectra measured at different depths in a 60 cm × 60 cm × 60 cm water phantom for a 10 cm × 10 cm field (○) after the installation of a 2.5 cm polythene filter in the isocentric gantry. The triangles (△) represent values determined in the same beam using the paired-chamber technique. Gamma fractions measured at Louvain-la-Neuve are also shown (□).

measurements was performed at a later stage to determine the in-phantom photon component as a function of depth. The evaluated parameters (for a 10 cm × 10 cm field) are summarized in Table III and the middle curve in Fig. 4 depicts the variation of y^* with depth. The photon component D_G of the beam was assessed by fitting a ^{60}Co event size spectrum to each of the measured total event size spectra (Menzel & Waker, 1976). By subtracting the photon component, y^*_n values (neutrons only) were calculated and show a trend very similar to that observed for y^*, affirming the dominance of high-LET recoils. Photon dose fractions are shown in Fig. 6, together with values determined from the paired-chamber technique. Comparative data from the therapy beam at Louvain-la-Neuve, where 2 cm of polythene filtration is used (Vynckier et al, 1983), are also depicted.

Discussion

The upper curve in Fig. 4 implies that a 6 cm thick polythene filter is required to eliminate any measurable variation in beam quality attributable to the presence of low-energy neutrons. This microdosimetric evaluation is underlined by the data obtained from the radiobiological assay (lower curve). Unfortunately the consequent reduction in dose-rate precludes the use of a 6 cm thick filter in clinical applications. Moreover, the design specifications of the target assembly restricts proton currents to 30 μA, thereby excluding the option of using a thinner target. The choice of a 2.5 cm thick polythene filter appeared the most appropriate compromise with only an ensuing reduction in dose-rate of approximately 15%. The in-phantom variation of y^* using this filter is shown in the middle curve in Fig. 4. Smaller y^* values are obtained in this instance because all the measurements were performed in a smaller field (10 cm × 10 cm).

Table IV. Dose fractions determined at 2.5 cm depth for varying filter thickness (20 cm × 20 cm field)

Filter (cm)	$1 \leq y < 14$ (keV μm^{-1})	$14 \leq y < 140$ (keV μm^{-1})	$y \geq 140$ (keV μm^{-1})
0	0.463	0.392	0.145
3	0.483	0.368	0.149
7	0.500	0.350	0.150

By dividing the spectrum into three lineal energy regions (Table IV), the changes observed in Fig. 5 may be quantified. The lower interval (1–14 keV μm^{-1}) embraces the fast-proton and electron recoil distributions, whilst slow-proton recoils contribute principally to the central portion of the spectrum (14–140 keV μm^{-1}). The distribution above 140 keV μm^{-1} is determined by heavy-ion recoils and α particles produced via nuclear reactions. Application of the polythene filter preferentially reduces the slow-proton contribution to the spectrum. This enhances the number of fast-proton events, which in turn leads to a small increase in the heavy-ion dose component.

The photon fractions evaluated from the probability distributions are in acceptable agreement with the values determined by means of the paired-chamber technique (Fig. 6). The present data also concur with that of Louvain-la-Neuve at depths greater than 15 cm and indicate a larger in-air γ component at the NAC.

The purpose of this investigation was to determine whether the presence of a low-energy neutron component in the beam would significantly affect the quality of the radiation under therapy conditions. Radiobiological findings, supported by microdosimetric evaluations, indicated the need for a hydrogenous filter. The analysis of lineal energy spectra demonstrated that subtle changes in beam quality can be quantified in a reproducible manner without resorting to time-consuming radiobiological studies. Moreover, the presented microdosimetric data demonstrate the use of Rossi-type proportional counters for evaluating different target designs, thicknesses and backings.

Acknowledgments

The authors wish to thank those who contributed to the success of the reported measurements: Dr D. T. L. Jones (NAC, Faure), Dr L. Böhm (Tygerberg Hospital, Cape Town), Dr J. S. Galpin (CSIR, Pretoria) and the cyclotron operating staff.

References

AMOLS, H. I., DICELLO, J. F., AWSCHALOM, M., COULSON, L., JOHNSEN, S. W. & THEUS, R. B., 1977. Physical characterization of neutron beams produced by protons and deuterons of various energies bombarding beryllium and lithium targets of several thicknesses. *Medical Physics*, *4*, 486–493.

BEWLEY, D. K., HALL, E. J. & CULLEN, B. M., 1987. Relative biological effectiveness as a function of neutron energy and depth in phantom. *British Journal of Radiology*, *60*, 313–314.

BINNS, P. J. & HOUGH, J. H., 1988. Lineal energy measurements in two fast neutron beams: d(16)+Be and p(66)+Be. *Radiation Protection Dosimetry, 23*, 385–388.

ELKIND, M. M., 1988. The initial part of the survival curve: does it predict the outcome of fractionated radiotherapy? *Radiation Research, 114*, 425–436.

FERTIL, B., DERTINGER, H., COURDI, A. & MALAISE, E. P., 1984. Mean inactivation dose: a useful concept for intercomparison of human cell survival curves. *Radiation Research, 99*, 73–84.

HALL, E. J. & KELLERER, A., 1979. Review of RBE data for cells in culture. In *High LET Radiations in Clinical Radiotherapy*, ed. by G. W. Barendsen, J. Broerse & K. Bruer (Pergamon Press, Oxford), pp.171–174.

HALL, E. J., ZAIDER, M., BIRD, R. & ASTOR, M., 1982. Radiobiological studies with therapeutic neutron beams generated by $p^+ \rightarrow Be$ or $d^+ \rightarrow Be$. *British Journal of Radiology, 55*, 640–644.

HALL, E. J., ZAIDER, M., BIRD, R. & ROBERTS, W., 1983. Radiobiological studies with therapeutic neutron beams generated by $p^+ \rightarrow Be$ or $d^+ \rightarrow Be$ (Letter to the Editor). *British Journal of Radiology, 56*, 349–350.

HORNSEY, S. & MYERS, R., 1987. Changes of quality in neutron beam with depth measured by jejunal microcolonies. *British Journal of Radiology, 60*, 315.

ICRU, 1979. *Quantitative Concepts and Dosimetry in Radiobiology*, Report 30 (ICRU, Washington DC).

—— 1983. *Microdosimetry*, Report 36 (ICRU, Washington DC).

JOHNSEN, S. W. 1977. Proton-beryllium neutron production at 25–55 MeV. *Medical Physics, 4*, 255–258.

JONES, D. T. L., YUDELEV, M. & HENDRIKSE, W. L. J., 1988. Physical characteristics of the South African high energy neutron therapy facility. *Radiation Protection Dosimetry, 23*, 365–368.

KELLERER, A. M. & HUG, O., 1972. Theory of dose-effect relationships. In *Encyclopedia of Medical Radiology* (Springer Verlag, Berlin), pp. 1–42.

MENZEL, H. G. & WAKER, A. J., 1976. Gamma dose contributions derived from energy deposition spectra. In *Basic Physical Data for Neutron Dosimetry* (Commission of European Communities, Luxembourg), EUR 5629e, pp. 179–183.

MENZEL, H. G., 1984. Proportional counter measurements in neutron therapy beams. In *Advances in Dosimetry for Fast Neutrons and Heavy Charged Particles for Therapy Applications* (IAEA, Vienna), pp. 105–126.

MIJNHEER, B. J., WOOTTEN, P., WILLIAMS, J. R., EENMAA, J. & PARNELL, C. J., 1987. Uniformity in dosimetry protocols for therapeutic applications of fast neutron beams. *Medical Physics, 14*, 1020–1026.

RAPPORT SCIENTIFIQUE, 1986. *Rapport Scientifique de l'Utilisation du Cyclotron et des Activites de l'Unité de Physique Nucléaire*, (Université Catholique de Louvain), p. 76.

SKOKAL, R. R. & ROHLF, F. J. 1969. In *Biometry* (W. H. Freeman & Company, San Francisco).

VYNCKIER, S., PIHET, P., FLÉMAL, J. M., MEULDERS, J. P. & WAMBERSIE, A., 1983. Improvement of a p(65)+Be neutron therapy beam for therapy at Cyclone, Louvain-la-Neuve. *Physics in Medicine and Biology, 28*, 685–691.

1989, *The British Journal of Radiology*, *62*, 995–998

Ovarian failure following abdominal irradiation in childhood: the radiosensitivity of the human oocyte

By W. H. B. Wallace, S. M. Shalet, *J. H. Hendry, †P. H. Morris-Jones and †H. R. Gattamaneni

Departments of Endocrinology, *Radiobiology and †Paediatric Oncology, Christie Hospital and Holt Radium Institute, Manchester

(*Received May 1989 and in revised form July 1989*)

Abstract. Ovarian function has been studied sequentially since 1975 in 19 patients treated in childhood for an intra-abdominal tumour with surgery and whole abdominal radiotherapy (total dose 30 Gy). Eleven patients received chemotherapeutic agents that are not known to cause gonadal dysfunction. All but one patient have developed ovarian failure with persistently elevated gonadotrophin levels (FSH and LH >32 IU/litre) and low serum oestradiol values (<40 pmol/litre) before the age of 16 years. The majority ($n = 12$) did not progress beyond breast stage I without sex steroid replacement therapy. As the number of oocytes within the ovary declines exponentially by atresia from approximately 2 000 000 at birth to approximately 2000 at the menopause, we have been able to estimate that the LD_{50} for the human oocyte does not exceed 4 Gy.

Information on the effect of radiation on ovarian function in humans has come from patients who have been treated in the past with low doses of irradiation for infertility (Kaplan, 1958), higher doses to induce an artificial menopause (Peck et al, 1940; Doll & Smith, 1968) and doses received incidentally by the ovary during the treatment of abdominal tumours (Shalet et al, 1976).

Lushbaugh and Casarett (1976) reported that a rapidly induced permanent menopause was evident after 6 Gy in women who were aged 40 years or more. In young women higher doses are required to induce the same effect. As the germ cell population is non-renewing from birth and declines exponentially by atresia with age, this differential effect of age on radiation-induced sterility is most readily explained by a gradual reduction in the initial complement of oocytes (Shalet, 1983).

There have been few studies of ovarian function following ovarian irradiation, uncomplicated by the effects of other cytotoxic agents, in humans. Shalet et al (1976) observed ovarian failure in all 18 patients who had received whole abdominal radiotherapy (20–30 Gy) in childhood for an abdominal malignancy. Himelstein-Braw et al (1977) studied ovarian morphology following abdominal irradiation in seven patients who had received whole abdominal radiotherapy (20–30 Gy). They found that follicle growth was inhibited and the number of oocytes was markedly reduced in the majority of their patients.

We have recently reviewed the natural history of ovarian function (Wallace et al, 1989) in 53 patients treated in childhood for an abdominal malignancy with surgery and radiotherapy. The outlook for normal ovarian function following whole abdominal irradiation was poor. By further study of 19 of these patients we describe how we have been able to estimate an upper limit for the LD_{50} of the human oocyte, which is significantly less than the value of 6–18 Gy quoted in the literature (Bianchi, 1983).

Materials and methods

Since 1975 we have followed sequentially 19 female patients who have been treated in childhood since 1966 at the Christie Hospital for an intra-abdominal tumour with external whole abdominal radiotherapy, surgery and chemotherapy. Twelve patients had a diagnosis of Wilm's tumour, three patients had a unilateral ovarian dysgerminoma and one patient each had an adrenal carcinoma, sacro-coccygeal teratoma, rhabdomyosarcoma of the bladder, and an abdominal neuroblastoma. The median age at diagnosis was 4 years (range 1.3–13.1 years).

The 19 patients (Table I) include every female child who received a total dose of 30 Gy (16–26 fractions in 21–38 days) to the whole abdomen at this Institute since 1966. Radiotherapy was delivered using a two-field technique by either a linear accelerator or a telecobalt machine to a field defined superiorly by the dome of the diaphragm and inferiorly by the superior border of the ischial tuberosity. Shielding was applied throughout to the femoral heads and acetabula, and in the Wilm's tumour patients to the unaffected kidney after 20 Gy. Both ovaries lay within the irradiation field although their exact anatomical position has not been defined. Eight patients received no chemotherapy and the remaining 11 patients received chemotherapeutic agents that are not known to damage the gonad (vincristine, adriamycin and actinomycin D).

The pubertal status of each patient was recorded according to the criteria of Tanner (1962). Blood was taken from each subject at each consultation before the onset of ovarian failure and assayed for FSH, LH and oestradiol using standard radioimmunoassays. Ovarian failure was defined as being either pubertal failure, *i.e.* a

---

Correspondence to: Dr S. M. Shalet, Department of Endocrinology, Christie Hospital, Wilmslow Road, Withington, Manchester M20 9BX.

failure to undergo or to complete pubertal development, or a premature menopause with the onset of secondary amenorrhoea before the age of 40 years, both in the presence of persistently elevated gonadotrophin levels (FSH and LH >32 IU/litre) and a low serum oestradiol concentration (<40 pmol/litre). The age at which ovarian failure was diagnosed was the age when the above criteria were first met.

The LD_{50} of the oocyte was defined as follows. Assuming an exponential decline in the oocyte population with increasing age, and a similar rate of atresia of unirradiated follicles and of follicles surviving irradiation injury, the shorter latency time to ovarian failure after irradiation can be related to the amount of depletion of the oocyte population by given doses of irradiation (Fig. 1).

The germ cell population of the ovary at birth is about 2 000 000, it is non-renewing and it has been shown from histological measurements to decline approximately exponentially by atresia with age (Baker, 1971). The precise number of oocytes remaining at the menopause is unclear; linear extrapolation from the work of Block (1952), who counted the number of follicles present in the ovaries of 43 women ranging in age from 6 to 44 years and who died accidentally, indicated 2200 primordial follicles would still be present at the menopause. However, this may be an overestimate as Richardson et al (1987) in a recent study of the number of follicles present in the ovaries of pre-, peri- and post-menopausal women, found that the rate of follicle loss appears to accelerate in the decade before the menopause. Therefore for the purpose of this study the oocyte population at the menopause is considered not to exceed 2200.

Figure 1 describes the exponential fall in the oocyte population with increasing age, with an estimated 2200 oocytes remaining at the time of the menopause at the average age of 50 years. If the surviving germ cell population after irradiation declines by atresia at the same rate as an unirradiated population, as indicated in rats (Beaumont, 1964), then we can estimate the surviving fraction of oocytes for each patient who has developed ovarian failure. This assumes that the ovary following irradiation is depleted of oocytes comparable to the state approaching the normal menopause, and that oocytes which do survive irradiation are available for recruitment and mature normally (Himmelstein-Braw et al, 1977). For illustration, we have shown a patient (Case 12) who developed ovarian failure at the age of 15.9 years after receiving radiotherapy (total dose 30 Gy) at the age of 1.7 years. The surviving fraction of oocytes is calculated as shown.

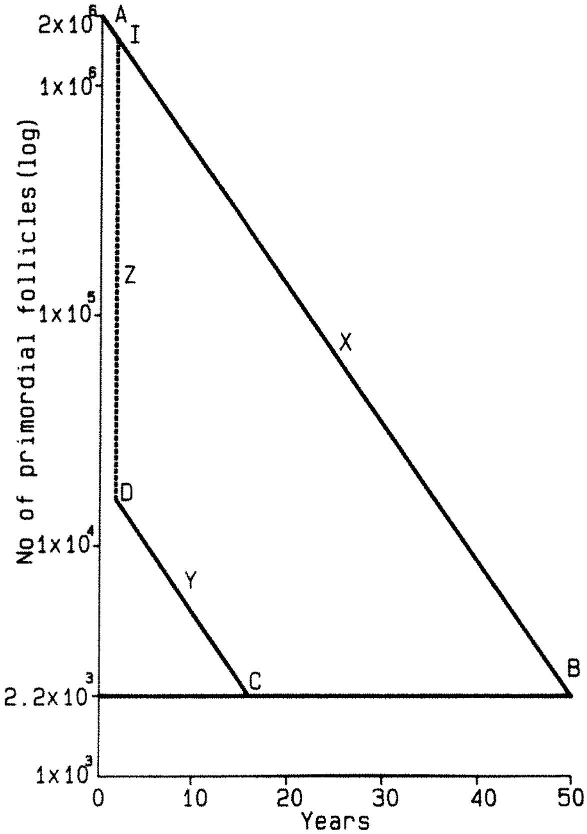

Figure 1. Exponential fall in number of primordial follicles with increasing time: estimation of surviving oocyte fraction. Point A: The number of primordial follicles present at birth is ~2 000 000 (Baker, 1971). Point B: The number of primordial follicles remaining at the menopause from linear extrapolation from the work of Block (1952) is ~2200 and may be less (Richardson et al, 1987). The average age of the menopause in this country is 50 years. Line X: The number of primordial follicles declines exponentially by atresia with increasing age. Point C: Represents, for illustration, the age at which Case 12 developed ovarian failure (15.9 years). Line Y: This line represents the rate of decline of the surviving fraction of oocytes after irradiation. As oocytes die in interphase within a few hours of irradiation it can be assumed that the decline in the surviving oocytes occurs at the same rate as for an unirradiated ovary. Line Z: Case 12 received 30 Gy to both ovaries at the age of 1.7 years and this line represents the oocyte cell kill for this patient. Point D: Surviving number of primordial follicles after irradiation (1.55×10^4). Point I: Represents the average number of primordial follicles present at time of irradiation (1.55×10^6). The surviving fraction is calculated to be:

$$\frac{\text{Point D}}{\text{Point I}} \times 100 = \frac{1.55 \times 10^4}{1.55 \times 10^6} \times 100 = 1\%.$$

Results

Eighteen out of 19 patients who have received megavoltage whole abdominal radiotherapy (see Table I) developed ovarian failure with the majority ($n = 12$) not progressing beyond breast stage I without sex steroid replacement therapy. One patient (Case 19) treated for a Wilm's tumour in 1972 at the age of 6.8 years surprisingly has normal ovarian function at the age of 23 years.

Figure 2 demonstrates the estimation of the LD_{50} for the human oocyte. The surviving fraction of oocytes for each of the patients has been calculated by the method

Table I. Age at irradiation, age at diagnosis of ovarian failure and surviving fraction of oocytes

Case	Age at irradiation (years)	Ovarian failure diagnosed (years)	Surviving fraction of oocytes (%)
1	13	14.1	0.75
2	2	13.1	0.65
3	4	13.2	0.65
4	5	12.8	0.6
5	13	15.7	1
6	8	12	0.6
7	3	11.9	0.6
8	2	9.7	0.4
9	4	10.5	0.5
10	4	10.4	0.5
11	2	14.3	0.8
12	2	15.9	1
13	11	13.9	0.8
14	12	12.6	0.6
15	4	13.6	0.7
16	1	11.7	0.6
17	6	12	0.6
18	3	11.1	0.55
19	7	NF	N/A

NF: normal ovarian function; N/A: not applicable.

as demonstrated above for Case 12 and the values, which range from 0.5 to 1.0%, are shown in Table I. Assuming exponential inactivation of the oocytes with increasing (fractionated) dose, the LD$_{50}$ is about 4 Gy and the D$_0$ (LD$_{63}$ or 37% survival) about 6 Gy.

Discussion

There are marked diferences reported in the radiosensitivity of the oocyte between species, with mouse oocytes (LD$_{50}$, 0.15 Gy) being seven times more sensitive than rat oocytes (LD$_{50}$, 1 Gy), which are about 50 times more sensitive than those of the monkey (LD$_{50}$, 50 Gy) (Baker, 1971). The stage of development of the oocyte is important, with the primordial oocyte of guinea-pigs, monkeys and humans being more radioresistant than oocytes in growing follicles; the reverse is true in mice (Bianchi, 1983). The effect of dose fractionation on the human oocyte is unclear (International Commission on Radiological Protection (ICRP), 1984); there is a sparing effect in mice but the reverse is true for monkeys (Bianchi, 1983).

Information on the radiosensitivity of the human oocyte has come from a wide range of sources. Kaplan (1958) reported a series of 700 women who had received 0.6 Gy to the ovaries over 2 weeks as treatment for infertility. There were 308 conceptions and no reported deleterious effects on the ovaries. Several studies have reported the dose of radiation required to induce an artificial menopause in the treatment of benign gynaecological disorders. Peck et al (1940) reported that a dose of 625 roentgens (approximately 6 Gy) produced permanent castration in a group of 72 patients, most of whom were over 40 years at treatment. Doll and Smith (1968) reviewed over 2000 women who were treated for menorrhagia and referred to a dose of 5–10.5 Gy as being sufficient to induce a permanent menopause in 97% of their patients. Lushbaugh and Casarett (1976) concluded that the dose of radiation required to induce an artificial menopause in women over the age of 40 years is around 6 Gy, while younger women require 20 Gy to induce permanent sterility with 95% confidence. Larger doses received by children as part of the treatment of abdominal tumours (20–30 Gy) have been reported to cause ovarian failure (Shalet et al, 1976; Wallace et al, 1989) and a reduction in the number of primordial follicles on morphological examination (Himmelstein-Braw et al, 1977).

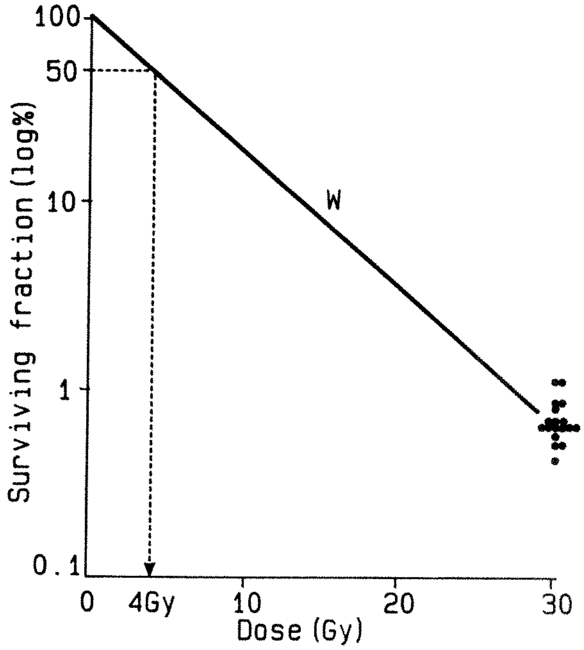

Figure 2. Dose–response relationship for the human oocyte. The surviving fraction of oocytes for each patient has been calculated from Fig. 1 (see Table I, method as shown for Case 12), and plotted against the dose of radiation received by the ovaries. Line W: Represents the estimated (fractionated) dose–response relationship for the human oocyte from which the LD$_{50}$ can be estimated not to exceed 4 Gy.

The LD$_{50}$ for human oocytes has been estimated to be 6–18 Gy (Bianchi, 1983). Baker (1971) has suggested that extrapolation from the rhesus monkey may be justifiable on the grounds that it has a 28-day menstrual cycle and similar ovarian development to women.

Our assumption that the rate of decline of the surviving fraction of oocytes is not greater than that for an unirradiated ovary seems tenable for two reasons. Oocytes die in interphase within a few hours of irradiation, they become pyknotic and are removed by phagocytosis within a few days (Lindop, 1969). Evidence following irradiation of fetal rat ovaries has shown that severely damaged germ cells degenerate rapidly and are eliminated from the ovary within a few days of exposure. Furthermore there is evidence that the subsequent rate of depletion of oocytes is lower in irradiated animals than in controls (Beaumont, 1964). If this is the case in the human then the surviving fraction would be less than we have estimated for each patient, consistent with a more radiosensitive oocyte than we have predicted and a lower LD_{50}.

As the effect on fertility of fractionating the dose is uncertain (ICRP, 1984), it has not been possible to correct the data for differences in dose per fraction. Hence the present LD_{50} could be considered as an upper limit, the value for single doses thus being <4 Gy. Interestingly this is similar to the values quoted for male cells at a corresponding stage of development (meiotic prophase) (Meistrich & van Beek, 1989).

Ovarian failure is often difficult to diagnose biochemically between 5 and 10 years of age (Whitehead et al, 1982). Therefore for some of these girls it is possible that ovarian failure due to follicular depletion occurred sooner than diagnosed. This would also make our estimate of the LD_{50} too high.

Premature ovarian failure has been described after whole abdominal irradiation (Shalet et al, 1976), craniospinal radiotherapy (Livesey & Brook, 1988) and flank radiotherapy (Wallace et al, 1989). The dose of irradiation received by an ovary is dependent on the position in relation to the radiation field, which can be determined by pelvic ultrasound examination. If the dose received by the ovary furthest from the radiation field is calculated, then the present analyses indicate that the surviving fraction of oocytes can be estimated and the predicted age at ovarian failure determined assuming an average complement of oocytes for age at the time of irradiation. This may provide a factual basis for fertility counselling in such patients.

Acknowledgments

This work was supported by a grant from the Leukaemia Research Fund.

References

Ash, P., 1980. The influence of radiation on fertility in man. *British Journal of Radiology*, *53*, 271–278.

Baker, T. G., 1971. Radiosensitivity of mammalian oocytes with particular reference to the human female. *American Journal of Obstetrics and Gynecology*, *110*, 746–761.

Beaumont, H. M., 1964. The short-term effects of acute X-radiation on oogonia and oocytes. *Proceedings of the Royal Society*, *161*, 550–570.

Bianchi, M., 1983. Cytotoxic insult to germinal tissue, part 2; The ovary. In *Cytotoxic Insult to Tissue Effects on Cell Lineages*, ed. by C. S. Potten & J. H. Hendry (Churchill-Livingstone, Edinburgh), pp. 309–328.

Block, E., 1952. Quantitative morphological investigations of the follicular system in women: variations at different ages. *Acta Anatomica*, *14*, 108–123.

Doll, R. & Smith, P. G., 1968. The long term efects of X irradiation in patients treated for metropathia haemorhagica. *British Journal of Radiology*, *41*, 362–368.

Hendry, J. H., 1988. Considerations of long-term radiation injury in nonhemopoietic tissues. In *Hematopoesis: Long-term Effects of Chemotherapy and Radiation*, ed. by N. G. Testa & R. P. Gale (Marcel Dekker, New York), pp. 247–277.

Himmelstein-Braw, R., Peters, H. & Faber, M., 1977. Influence of irradiation and chemotherapy on the ovaries of children with abdominal tumours. *British Journal of Cancer*, *36*, 269–275.

ICRP, 1984. *Nonstochastic Effects of Ionising Radiation*, ICRP Publication 41 (Pergamon Press, Oxford).

Kaplan, I. I., 1958. The treatment of female sterility with X-ray therapy directed to the pituitary and ovaries. *American Journal of Obstetrics and Gynecology*, *76*, 447–453.

Lindop, P. J., 1969. The effects of radiation on rodent and human ovaries. *Proceedings of the Royal Society of Medicine*, *62*, 144–148.

Livesey, E. A. & Brook, C. G. D., 1988. Gonadal dysfunction after treatment of intracranial tumours. *Archives of Disease in Childhood*, *63*, 495–500.

Lushbaugh, C. C. & Casarett, G. W., 1976. The effect of gonadal irradiation in clinical radiation therapy: a review. *Cancer*, *37*, 1111–1120.

Meistrich M. L. & van Beek, M. E. A. B., 1987. Radiation sensitivity of the human testis. In *Advances in Radiation Biology: Relative Radiation Sensitivities of Human Organ Systems 11*, ed. by J. T. Lett and K. I. Altman (Academic Press, California).

Peck, W. S., McGreer, J. T., Kretzschmar, N. M. & Brown, W. E., 1940. Castration of the female by irradiation. *Radiology*, *34*, 176–183.

Richardson, S. J., Senikas, V. & Nelson, J. F., 1987. Follicular depletion during the menopausal transition: evidence for accelerated loss and ultimate exhaustion. *Journal of Clinical Endocrinology and Metabolism*, *65*, 1231–1237.

Shalet, S. M., Beardwell, C. G., Morris-Jones, P. H., Pearson, D. & Orrell, D. H., 1976. Ovarian failure following abdominal irradiation in childhood. *British Journal of Cancer*, *33*, 655–658.

Shalet, S. M., 1983. Disorders of the endocrine system due to radiation and chemotherapy. *Clinical Endocrinology*, *18*, 637–659.

Tanner, J. M., 1962. *Growth at Adolescence* (Blackwell, Oxford).

Wallace, W. H. B., Shalet, S. M., Crowne, E. C., Morris-Jones, P. H. & Gattamaneni, H. R., 1989. Ovarian failure following abdominal irradiation in childhood: Natural history and prognosis. *Clinical Radiology*, in press.

Whitehead, E., Shalet, S. M., Morris-Jones, P. M., Beardwell, C. G. & Deakin, D. P., 1982. Gonadal function after combination chemotherapy for Hodgkin's disease in childhood. *Archives of Disease in Childhood*, *47*, 287–291.

1989, *The British Journal of Radiology*, 62, 999–1004

A physical evaluation of the imaging performance of a high-resolution fluorography system

By A. R. Cowen, BSc

The Radiological Imaging Group, University of Leeds, Department of Medical Physics, The General Infirmary, Leeds LS1 3EX

(Received January 1989 and in revised form May 1989)

Abstract. A physical evaluation of the imaging performance of a unique high-resolution fluorography system is presented. Measurements have been made of contrast performance, unsharpness (modulation transfer function) and noise (Wiener spectrum and threshold contrast detectability), and the results have been compared with those measured from medium-fast calcium tungstate and rare-earth screen–film combinations and a standard fluorography system. The results have proved sufficiently encouraging that a full-scale trial is now underway to evaluate the system's performance in routine clinical application.

In 1985 Cowen et al proposed a design for a fluorographic imaging system for use in Bucky radiography. Central to this proposal was the need to implement an X-ray image intensifier of adequate spatial resolution (de Lacey et al, 1983). Following a comment by Kühl et al (1977), the author postulated that a significant improvement in spatial resolution might be achieved by using an X-ray image intensifier of reduced input phosphor screen thickness. It was appreciated from the outset that a significant reduction in conversion factor (G_x) would result. The device would therefore be unsuitable for use in TV fluoroscopy but in fluorography might provide the image quality needed to compete with screen–film radiography. An X-ray image intensifier tube with this specification has been manufactured and supplied to this department for physical and subsequently clinical evaluation. This article describes a physical evaluation of the image quality of the high-resolution fluorography system that has been developed.

The high-resolution fluorography system

This investigation of the high-resolution (HR) fluorography system was carried out in the Radiological Imaging Laboratory of the Department of Medical Physics during 1987. For the purpose of these tests the HR image intensifier was mounted inside a specially constructed, rigid, aluminium support frame. Subsequently the HR system was installed in a DL14 floating-top Bucky table. The Anodica 100 mm fluorography camera was attached at right angles to the optical distributor, providing convenient access to both the 100 mm film supply and take-up cassettes. This small-format camera was originally designed to operate in serial mode at acquisition rates of up to six frames per second. For the purpose of Bucky fluorography, serial mode acquisition is unnecessary and manual operation is satisfactory; therefore, the fluorographic system was not interfaced to the X-ray generator and the motorized film transport mechanism was disabled. The push-button service control was used to transport the film in and out of the exposure gate providing full manual control of system operation. The test films were processed through a Kodak M8 processor (development temperature 33°C) by kind permission of the Diagnostic Radiology Department of the General Infirmary.

Calibrating the HR system

Following installation, the system was carefully calibrated as regards radiological speed, optical focusing and focal uniformity. These features are examined in turn below.

Fluorographic speed

The HR image intensifier differed from the standard production model in that the input phosphor layer had been reduced in thickness by a factor of approximately 3. The conversion factor was determined using a Philips Roentgen-Photometer under calibrated measurement conditions (*viz.* 75 kV plus 1.5 mm copper filtration and an input exposure rate of 25 μC kg^{-1} s^{-1}); the resulting G_x values are listed in Table I. The HR image intensifier exhibited an approximately three-fold reduction in G_x compared with 14-inch systems of standard design.

As this was the first device of its kind we had no precedent as to the optimum operating exposure levels. An investigation of acceptable operating radiological speeds was carried out using a PTW-DALi exposure-meter and a Victoreen portable densitometer. Radiological speed is defined as the reciprocal of the radiation exposure (measured in μC kg^{-1}). In the 14 and 10 inch field selections speed was calibrated using a peak X-ray tube voltage of 75 kV and a 1.5 mm copper filter in the beam. In the 6-inch field, calibration was carried out using 55 kV and a 5 mm thick aluminium filter. The reason for this was that in clinical Bucky fluorography the 6-inch field would be largely reserved for such applications as paediatric radiology and, in adults, radiography of the extremities where low-energy X-ray beams are used.

Within limits, the speed of a fluorographic system can be varied by programming different iris diaphragm diameters. Maximum radiological speed is achieved

Table I. Measured characteristics of the HR fluorography system

Nominal image Intensifier field (inch)	Measured field size (cm)	G_x (Cd m^{-2}/mR s^{-1})	Geometrical distortion		Contrast ratio		Spatial resolution limit (c mm^{-1})
			Integral (%)	Differential (%)	10% area	1% area	
14	32	30	7.3	21.4	15.3	10.2	3.2
10	24	14.5	1.6	4.3	15.7	10.9	4.3
6	16	7	—	—	17.2	12.1	5.6

when the iris diaphragm is fully open, providing maximum light transfer to the film: this condition was denoted the *high-speed* (HS) option. The resulting speed in the three field selections reduces in proportion to the areas of the input fields. The HS option is used in applications in which the minimization of radiation dose is an important clinical consideration. In addition to this a *high-definition* (HD) option was provided in order to improve signal-to-noise ratio in those clinical examinations in which high image fidelity is required. In the three field selections the HD selections are approximately a quarter of the speed of the corresponding HS selections. In clinical application this would mean that prior to making an exposure the radiographer would have to select both the field size and radiological speed appropriate to that particular patient and examination. The latter is a similar selection process to that made in traditional radiography where the radiographer has to select the appropriate screen–film combinations. Table II summarizes the speeds of the HR fluorography system compared with those of the Du Pont screen–film combination and standard 14-inch fluorography units used in the General Infirmary.

Sizing, focusing and geometry

The image intensifier high-tension (HT) electrode voltages were set according to the values recommended by the equipment manufacturers. The resulting image intensifier field coverage was measured using an enlarged version (38 cm diameter) of the Leeds Matrix test object M1 (Hay et al, 1985) with an SID of 1 m. The results are listed in Table I. The test object enabled us simultaneously to assess the degree of geometrical distortion of the HR image tube. Overall, the geometrical distortion visible on film was acceptable in the 14-inch field, small in the 10 inch and negligible in the 6 inch: integral and differential distortion figures are listed in Table I. Further details on the measurement of geometrical distortion and reference results obtained from a conventional X-ray image intensifier were published in FAXIL (1983).

The focusing eletrode voltages were optimized using an array of Hüttner no. 18 resolution gratings made of 80 μm thick lead and which included a range of spatial frequencies up to 7.1 cycles (c) mm^{-1}. The focusing criterion we adopted demanded the best overall spatial resolution throughout a quality area of the image intensifier corresponding to a circle of diameter 60% of that of the input window. Focusing of the image intensifier was carried out by viewing the output screen via the primary objective lens using a collimator comprising a Minolta telephoto lens combined with a Minolta monocular viewing attachment. The collimator had previously been focused at infinity using a test lightbox. The adjustment of the focusing electrode voltage was monitored using a Fluke digital voltmeter attached to the appropriate measuring point on the HT power unit. The final focus values were noted and periodically checked during subsequent use for the purposes of quality control.

A series of test images were then recorded on film over a range of 100 mm camera lens focus settings. In an effort to ensure optimum optical focusing the iris diaphragm was set to maximum diameter thereby mini-

Table II. Calibration of the radiological speeds of the MR fluorography system

Radiographic systems [Speed (μC Kg^{-1})$^{-1}$]		50 μm 14 inch XRII Fluorography								
		Detail Cr4 (0.7)	QD Cr4 (2)	Par speed Cr4 (2.8)	Hi plus Cr4 (5.6)	QIII		Standard fluorography		
						Cr7 (9)	Cr4 (18)	6″ (22)	10″ (32)	14″ (48)
(50 μm) 14 inch Fluorography	6 inch		↑D		S↑					
	10 inch				↑D		S↑			
	14 inch					↑D			S↑	
						←	4 : 1		→	

mizing depth of focus and a unity neutral density filter was placed in the optical path in order temporarily to slow the system down (by a factor of 10) to minimize X-ray quantum mottle. Mean spatial resolution values measured over the defined quality area from 100 mm film samples are listed in Table I. Following these measurements the neutral density filter was removed.

Physical evaluation of HR fluorography

In this section we will describe the measurement of the contrast, spatial and noise performance of the HR fluorography system.

Contrast performance

The contrast performance of a Bucky fluorography system is strongly influenced by the H and D curves of the film used. A variety of types of 100 mm fluorography films had previously been evaluated (FAXIL, 1983) and from this data we selected Kodak X-omat GR 100 mm film. This film exhibits a low base-plus-fog level with medium to high contrast rendition characteristics that are particularly useful in the reproduction of fine detail in bone while retaining adequate soft-tissue latitude. The average and maximum gamma values of Kodak X-omat GR film are 2.62 and 3.10, respectively. This can be compared with values between 2.9 and 5 and 2.2 and 2.9 for high-contrast and wide-latitude radiographic film, respectively (Hay et al, 1981). Figure 1 compares the sensitometric characteristics of X-omat GR with Du Pont Cronex 4 and Cronex 6-plus (latitude) radiographic films.

In traditional radiography it is normal practice to use a moving Bucky grid to reduce patient X-ray scatter but at the same time prevent reproduction of any structural inhomogeneities in the grid. It proved impossible to accommodate a moving grid in our HR fluorography installation for mechanical reasons. As predicted by the author (Cowen et al, 1985), the new image tube reproduced the structure of the standard static grid supplied with it, markedly degrading the quality of the final images. After evaluating several types of static grid a Smit-Roentgen carbon-fibre-covered and interspaced grid was used (60 lines cm^{-1}, 12:1 ratio and focal distance 100 cm). This grid exhibited good scatter rejection over the range of kilovoltages required (50–85 kV). Grid structure noise was negligible apart from a degree of fine linear structure at very low X-ray tube voltage selections. The grid was incorporated in a mounting arrangement that would facilitate its removal when examining babies, young paediatric subjects and extremities of adults.

The input phosphor screen of the HR image intensifier has an estimated detective quantum efficiency of approximately one-third of that of the equivalent standard image tube (*viz.* 0.15 *cf* 0.45). Before this study the author was concerned that the comparatively high degree of transmission of X rays into the body of the HR image tube might result in scatter processes that would degrade image contrast. The contrast loss of the image intensifier tube was measured by recording fluorographic images of 3 mm thick lead discs of diameter 10% and 1% of that of each image field. Fluorographic images were recorded in all three field sizes and the films were scanned using a Joyce Loebl 3CS microdensitometer. Following correction for the characteristic of the X-GR film, the effective contrast ratios were calculated (Table I). Comparing these results with those previously obtained on standard 14-inch systems, no evidence of a deterioration in contrast performance with the thin phosphor image tube was found. It must be stressed that these figures represent the contrast ratios of the total fluorographic system (including lenses, optical distributor and camera) and not of the image tube alone.

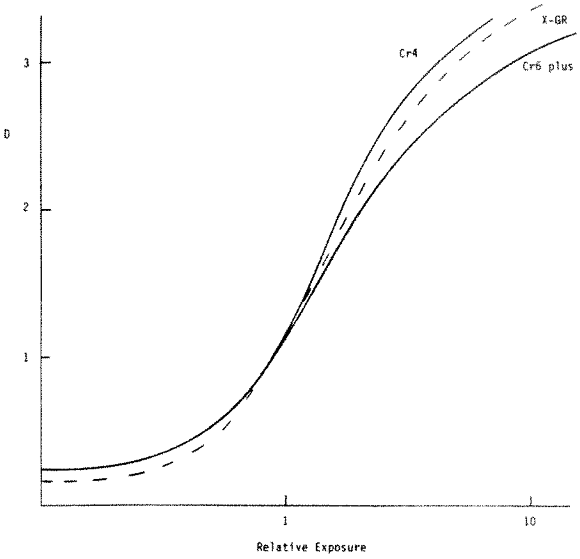

Figure 1. Film sensitometry of Kodak X-omat GR 100 mm film compared with Du Pont Cronex 4 and Cronex 6-plus radiographic films.

In a fluorographic examination, irradiation of the X-ray image intensifier from regions of the patient of high X-ray transmission or direct (unattenuated) radiation results in flare and contrast loss within the final image. In systems that incorporate television fluoroscopy the operator observes a live image depicting the patient positioning and the degree of X-ray beam collimation. Therefore, the operator is able to take immediate measures to adjust the collimating diaphragm to ameliorate the effects of any highlight flare and contrast loss caused by patient X-ray scatter and internal scatter processes. The HR fluorography system did not incorporate TV fluoroscopy and therefore did not provide these visual cues. Although this did not prove a significant problem in this laboratory study it could have caused difficulties in any subsequent clinical use. To ease this problem we decided to implement a collimation system that would prevent inadvertent irradiation of the periphery of the image field outside the active imaging area. Two sets of three circular lead collimators

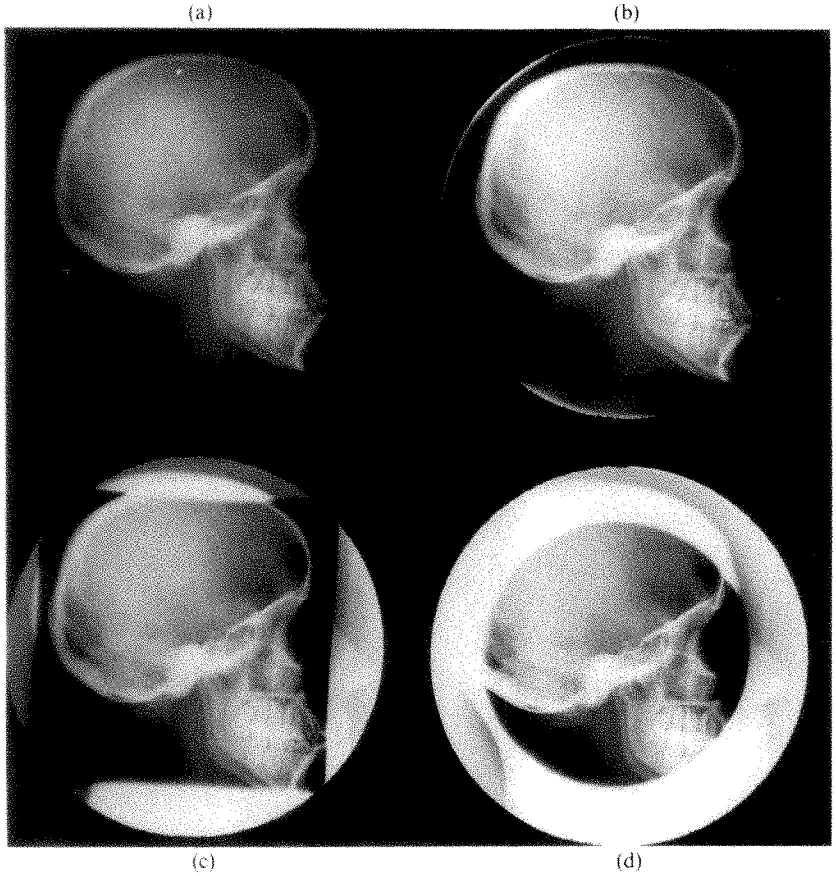

Figure 2. Scatter reduction in HR fluorography. (a) HR fluorogram (10-inch field) of a skull phantom using no collimation. (b) Effect of pre-collimation. (c) Effect of pre- and post-collimation. (d) Effect of over-collimation.

(mounted on aluminium substrates), matched to the three image intensifier field selections, were manufactured. The first set of collimators (known as pre-collimators) were attached to the diaphragm box providing the basic circular collimation of the X-ray field matched to the input fields of the image tube. An interlock arrangement was incorporated into the diaphragm box to ensure that the appropriate collimator was always used. The second set (known as post-collimators) are positioned in the plane of the input window of the X-ray image intensifier. The effect of circular pre- and post-collimation in minimizing both patient and internal scatter can be judged from Fig. 2. Figure 2a is an HR fluorogram (10-inch field) of a skull phantom using no collimation of the X-ray beam resulting in an unacceptable loss of contrast. Provision of firstly pre-collimation, Fig. 2b, and then post-collimation, Fig. 2c, significantly improves the contrast rendition of the system. Further reduction of the X-ray field using collimators appropriate to the 6-inch field selection results in further improvement in image quality, Fig. 2d.

Image sharpness

The spatial imaging performance of the HR fluorography system was assessed by measuring the modulation transfer function (MTF). This measurement was based on the method described by Pei-Jan Lin (1982), who carried out a field evaluation of the standard 14-inch image intensifier. Test films of the unsharpness profile, produced by imaging a 30 μm wide slit in a lead plate, were scanned using a Joyce Loebl 3CS microdensitometer. Following correction of the data for the H and D curve of the X-GR film the MTF was calculated using the Fast Fourier Transform algorithm and a Tektronix 4052A microcomputer. The MTFs of the HR (50 μm) image intensifier system exhibited a progressive improvement with the selection of smaller fields. Figure 3 compares these MTFs with that of the 10-inch field selection of a standard 14-inch system published by Pei-Jan Lin (1982). The superior MTF of the HR system is clearly demonstrated. In addition, the HR system's MTFs have been compared with that produced by a medium-fast conventional ($CaWO_4$) radiographic screen–film combination (*viz.* Du Pont Par Speed and Cronex 4 film). The MTF of the HR system compares favourably with this combination, suggesting that HR fluorography would provide adequate sharpness for a wide range of classical radiographic studies. Other studies (not reproduced here) showed that at low to medium spatial frequencies, HR fluorography exhibits a similar MTF to Du Pont Detail screens. At high spatial frequencies ($>5\ \mathrm{c\,mm^{-1}}$) the latter is clearly superior.

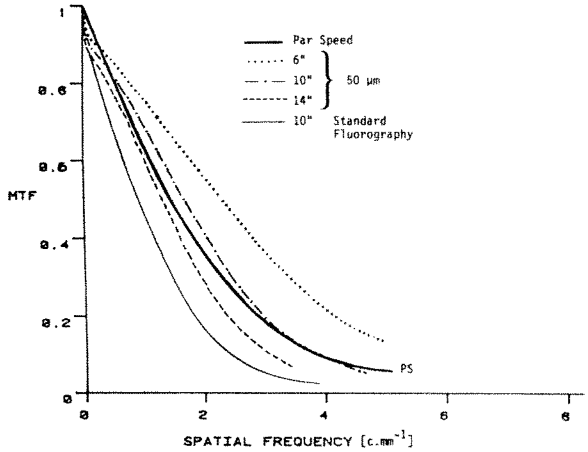

Figure 3. Modulation transfer function of the HR fluorography system in 14 (– – –), 10 (—·—) and 6 inch (. . .) fields compared with standard fluorography (——) and medium to fast screen–film radiography (——).

These results would indicate that HR fluorography may not be suitable for radiographic examinations that demand the highest spatial fidelity.

Image noise

In common with all other fluorography systems, the HR device is subject to a variety of noise processes that can degrade image quality (Cowen et al, 1983, 1984). Noise in the HR fluorography process was assessed by measuring the Wiener spectra from film samples exposed under both HS and HD conditions; the results are presented in Fig. 4. The Wiener spectrum of the Kodak X-omat GR fluorographic film was also measured by exposing film samples to light of the appropriate spectrum using the procedure described in FAXIL (1983). The Wiener spectra were measured by using an analog measuring system, first described by Hay et al (1981). The noise power spectral density was expressed in units of μm^2 and was measured over a spatial frequency range between 0.1 to 20 c mm^{-1}, as measured in the plane of the film. This measure represents the situation when the 100 mm fluorogram is viewed directly with no optical magnification. The difference in X-ray quantum noise in the HD and HS selections is reflected in the lower noise power density at low to medium spatial frequencies. The reduction in noise power does not correlate with the four-fold difference in radiation exposure used in those two dose selections. Theoretically one would expect a similar (four-fold) reduction in noise power but in practice a reduction of approximately half this magnitude is found. This result would indicate the presence of a significant contribution of structure mottle in the HR fluorography images. A similar effect has been described by Cowen et al (1983). At medium to high spatial frequencies the Wiener spectra in the HS and HD selections cross over; this effect was not expected and we have no explanation for it. At very high spatial frequencies the Wiener spectra exhibited by the fluorographic system coalesced with that of the X-GR film grain. Also included in Fig. 4 are the Wiener spectra produced by a medium-speed radiographic screen–film combination (Du Pont Par Speed plus Cronex 4) and a fast rare-earth screen–film combination (Du Pont Quanta III plus Cronex 4). The Par Speed–Cronex 4 screen–film combination exhibits similar noise power density to the HS fluorography speed selection. The Quanta III screens exhibited the greatest noise power, while the HD selection exhibited the lowest.

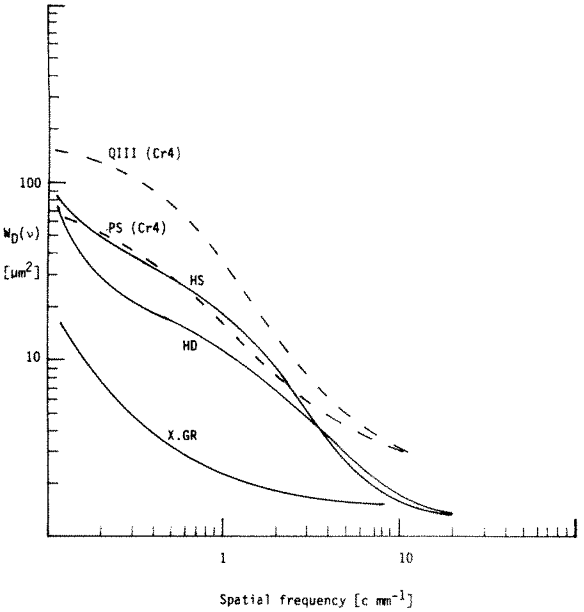

Figure 4. Wiener spectra of HR fluorography in HS and HD speed selections compared with medium to fast and rare-earth screen–film radiography.

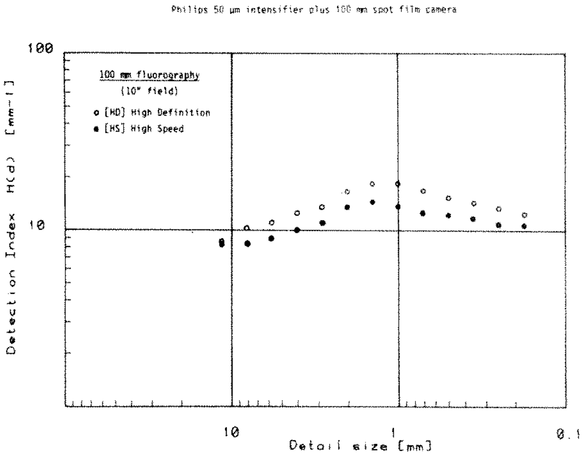

Figure 5. Threshold detection index curves produced by the HR fluorography system in HS (●) and HD (○) speed selections.

The presence of noise not only detracts from the aesthetic quality of an image but also limits the sensitivity with which an observer can detect low-contrast signals in that image. It is possible to quantify the impact of image noise on the visual detectability of low-contrast details by using a device such as Leeds test object type T0.9F (Cowen et al, 1983). This test object comprises an array of circular test details of varying (and calibrated) contrast and diameter. Six images of T0.9F were produced using the HR fluorography system in the 10-inch mode and using both HS and HD speed selections. The test images were viewed by two experienced observers and average threshold contrasts C_T for each detail diameter d were determined. Results are presented in Fig. 5 as a threshold detection index diagram $H_T(d)$, where $H_T(d) = [C_T(d)\ d]^{-1}$ (see Cowen et al, 1983). Figure 5 indicates that the HD selection produced a significant improvement in threshold contrast detectability compared with HS. In theory, for X-ray quantum limited imaging one would expect a two-fold increase in detection index while in practice only a 30% improvement was achieved. This again illustrates the important influence of structure mottle in the HR fluorographic imaging system (see also Cowen et al, 1983).

Discussion

A physical assessment of the image quality of a high-resolution Bucky fluorography unit has been carried out under laboratory conditions. A range of objective and subjective measurements have been performed on the HR fluorography system and the results have been compared with those produced by typical rare-earth and medium to fast tungstate screen–film combinations and a standard fluorography system. The MTF and measured noise power (Wiener spectra) produced by the HR system compared favourably with the conventional imaging modalities. A significant contribution from structure mottle was measured in the HR fluorography system and its limiting effect on image quality (low-contrast detectability) was confirmed.

This investigation also presented the author with the opportunity to optimize a range of equipment features that influence image quality and the system's ergonomics. These include selection of anti-scatter grid, collimation of the X-ray beam and the provision of operator-selectable radiological speeds (HS and HD).

The improvement in physical image quality produced by the HD selection has been established in this study. However, the wider radiological implications of the HD option will have to be evaluated in detail during a clinical trial. A digital scout-shot facility, using a CCD TV camera plus digital video framestore, which will provide the radiographer with an immediate feedback on patient positioning and exposure conditions, is now under development. The digital scout-shot facility should produce several practical advantages including reducing the reject-radiograph rate, increasing patient throughput and saving radiographer time and patient dose. Future directions for this research might include an investigation of the HR tube and the image transducer in a digital Bucky fluorography system.

The results of this study proved sufficiently encouraging that a full-scale clinical trial is now being instituted under the supervision of Dr R. S. Bury of the Diagnostic Radiology Department. In this trial the HR system will operate for 12 months with a radiographic workload typical of that of a traditional Bucky room. The aim of this trial is to establish the extent to which HR fluorography can replace classical radiography and also gather detailed information regarding the financial, radiological and ergonomic implications of using the HR small-format technique.

Acknowledgments

I wish to thank Philips Medical Systems (both in the Netherlands and the UK) and my colleagues in the General Infirmary for their scientific, technical and clinical support of this project.

References

COWEN, A. R., HAY, G. A. & COLEMAN, N. J., 1983. *A physical Comparison between 100 mm Fluorography and Full-size Radiography*. DHSS Reports on Image Forming Systems no. 11, STB/5/83 (HMSO, London).

COWEN, A. R., HAYWOOD, J. M., CLARKE, O. F. & ROUSE, S., 1984. Digital grey-scale fluorography: a new approach to digital radiographic imaging. *British Journal of Radiology*, *57*, 533–538.

COWEN, A. R., CLARKE, O. F. & HAYWOOD, J. M., 1985. High resolution fluorographic imaging. *British Journal of Radiology*, *58*, 570–572.

DE LACEY, G., PARIS, F. A. & HORSFIELD, D., 1983. *Assessment of a Picker System 1200 for 100 mm Fluorography*. DHSS Equipment Assessment Report no. STB/12/83 (HMSO, London).

FAXIL, 1983. *A Comparative Assessment of the Sensitometric Characteristics of 100 mm and 105 mm Fluorographic Films*. DHSS Reports on Image Forming Systems no. 12, STB/6/83 (HMSO, London).

HAY, G. A., COWEN, A. R. & COLEMAN, N. J., 1981. *Measurements on Du Pont Screen–Film Systems*. DHSS Reports on Image Forming Systems no. 4, STB/3/81 (HMSO, London).

HAY, G. A., CLARKE, O. F., COLEMAN, N. J. & COWEN, A. R., 1985. A set of X-ray quality control test objects for TV fluoroscopy. *British Journal of Radiology*, *58*, 335–344.

KÜHL, W. & SCHRIJVERS, J. E., 1977. Design aspects of X-ray image intensifiers. *Acta Electronica*, *20(i)*, 41–51.

1989, *The British Journal of Radiology*, *62*, 1005–1013

Surface heating of diagnostic ultrasound transducers

By F. A. Duck, PhD, H. C. Starritt, MSc, *G. R. ter Haar, PhD and †M. J. Lunt, PhD

Medical Physics Department, Royal United Hospital, Bath BA1 3NG, *Institute of Cancer Research, Royal Marsden Hospital, Sutton SM2 5NG and †Medical Physics Department, Poole General Hospital, Poole BH15 2JB

(*Received March 1989 and in revised form May 1989*)

Abstract. Surface temperatures of a variety of transducers used with common commercial ultrasonic diagnostic equipment have been measured. Transducers operating in imaging mode, in both continuous and pulsed Doppler modes, and in mixed modes were investigated. A total of 30 transducers and scan-heads used with equipment from 10 manufacturers were examined, including a range of array types, mechanical sectors and continuous-wave Doppler transducers. Measurements were made using an infrared radiometer, or a thermocouple probe, with the transducers operating in air. Surface temperatures of 13 transducers operating in imaging mode were found to be in the range 0.0–13.1°C above ambient after 5 min operation. Some transducers operating in pulsed Doppler mode reached considerably higher temperatures. The most extreme example increased the surface temperature by 36.5°C after 1 min and reached a steady-state temperature of almost 80°C. Transducers operating at these temperatures cannot be retained on the skin of a conscious subject without pain, and will cause skin burns within a brief period of time. A linear relationship has been demonstrated between temperature increase and spatial-average acoustic intensity. The rate of increase in air was found to be about 10 times greater for pulsed arrays than for continuous-wave Doppler transducers.

Medical ultrasonic transducers do not transfer all the applied electrical power into acoustic power. The balance between electrical and acoustic power is lost as thermal energy in the transducer drive, with much of the energy being deposited in the transducer itself. This paper is a report of temperature increases measured on the surface of a number of clinical ultrasound transducers in current use, and on the skin temperatures induced following application of particular transducers. A full analysis of the thermal responses of ultrasonic transducers is beyond the scope of this paper although some discussion is included regarding the factors that may be controlling the observed temperatures.

It has been known for some time that the application of some continuous-wave (CW) Doppler transducers may cause the skin temperature to rise. Filipczyński (1978) reported measurements of skin temperature following the application of two different CW Doppler transducers, using a thermal imaging camera. An increase of 12.5°C was measured after a 9.5 MHz transducer used with a Parks 806 Doppler flowmeter had been applied to the skin for 100 s. The rise in temperature was attributed mainly to the absorption of ultrasound by the tissue, although it was also noted that "the probe itself produces additional heat due to internal losses in the piezoelectric material and due to absorption in the plastic layer covering the transducer surface". Filipczyński reported a maximum skin temperature of 41°C, which is physiologically acceptable. Reporting on a second Doppler instrument with a spatial-average intensity of 100 mW cm^{-2}, he found a temperature increase of only 2.3°C. At this time these temperature observations generated only passing interest.

At about the same time, one of us (M.J.L.) carried out measurements of the heating of air of a 9.5 MHz Parks transducer similar to that reported by Filipczyński, demonstrating that higher temperatures would be generated when the transducer was driven off resonance. Using a small bead thermistor attached to the front of the probe, a peak temperature of 67°C was observed at 9.3 MHz, from a room temperature of 25°C. At resonance the highest temperature reached was 59°C. At the time, these elevated temperatures were not considered important because of the small physical size of the transmitting element (0.1 cm^2) and because no particular sensation of excessive warmth was noticed during use. In addition, a low power output was available, which resulted in maximum transducer temperatures about 15°C lower than those reached by the higher output. The lower power was commonly sufficient for normal clinical use. Carson et al (1978) reported that the intensity of the Parks probe was clearly the highest in a wide survey of imaging and CW Doppler transducers in use at that time, with the intensity at the transducer face measuring 375 mW cm^{-2}. By comparison, the highest intensity from any other commercial CW Doppler unit was given as 93 mW cm^{-2}, and the highest from a pulsed imaging transducer only about 1 mW cm^{-2}. The issue of transducer heating was subsequently ignored.

More recently, however, significantly higher powers have become more widely used with the introduction of pulsed Doppler and duplex systems (Duck et al, 1987). In addition, there has been a general recent trend in both imaging and Doppler applications for acoustic output to increase with the introduction of each new generation of diagnostic systems (Duck, 1989). The study reported here is therefore intended to document the current state of transducer heating in diagnostic ultrasound.

Knowledge of the extent to which the transducer is a thermal source is also necessary in the context of predictions of tissue temperature rises. Safety considerations require estimations of tissue temperature that include beam power, frequency and shape, and ultrasound absorption [American Institute of Ultrasound in Medicine (AIUM) 1988]. If the transducer itself is a heat source, the thermal pattern predicted close to the skin may be modified considerably, and it will be necessary to introduce an additional term into the calculation. Calculations of this type have been reported by Nyborg (1988).

Outline theory

The initial rate of temperature rise $\Delta T/\Delta t$ in the transducer can in principle be derived if the specific heat capacity C of the transducer is known:

$$\frac{\Delta T}{\Delta t}=\frac{P_t}{mC} \tag{1}$$

where m is the mass of the transducer and P_t is the power dissipated in it. In reality the transducer is composite, consisting of the piezoelectric element, backing material and overlying layers each with its own thermal capacity. Each of these three components will commence heating depending on its own properties and on the proportion of the total energy lost in each. The surface temperature will be affected by each depending on its depth within the transducer head. For simplicity, the following discussion assumes that the transducer is a single thermal unit.

The heating can be assumed to occur in a slab whose area A is defined by the piezoelectric element being driven, and whose thickness may include the faceplate and backing material in addition to the piezoelectric element itself. Equation (1) may therefore be rewritten as:

$$\frac{\Delta T}{\Delta t}=\frac{P_t}{Ad\rho C} \tag{2}$$

where ρ and d are the effective density and thickness of the transducer.

The transducer efficiency ε may be defined as the proportion of the total electrical power P emitted as acoustic power P_a, under normal acoustic load. Operating into such a load:

$$P_t=P-P_a=P_a[(1-\varepsilon)/\varepsilon]$$

and so from Equation (2):

$$\frac{\Delta T}{\Delta t}=\frac{P_a}{A}\frac{(1-\varepsilon)}{\varepsilon d\rho C}=I\frac{(1-\varepsilon)}{\varepsilon d\rho C} \tag{3}$$

where I is the spatial average acoustic intensity at the transducer face.

Operating into air, all the power is dissipated in the transducer and, provided that ε is low and the transducer impedance is altered little, $P_t\simeq P=P_a/\varepsilon$. In this case:

$$\frac{\Delta T}{\Delta t}=\frac{P_a}{A}\frac{1}{\varepsilon d\rho C}=I\frac{1}{\varepsilon d\rho C} \tag{4}$$

Thus for a transducer operating in air the heating rate is increased by a factor $1/(1-\varepsilon)$ in comparison with the rate when the transducer is operating into a normal acoustic load, such as the skin. In both cases $\Delta T/\Delta t$ is proportional to the source intensity I.

If the heat generation is considered to be primarily or only restricted to the peizoelectric plate, Equation (4) can be developed further. The thickness of the plate is approximately related to its resonant frequency f by $d=v/2f$ where v is the velocity of sound in the piezoelectric material. Equation (4) may be re-written as:

$$\frac{\Delta T}{\Delta t}=If\frac{2}{\varepsilon v\rho C} \tag{5}$$

The rate of temperature rise of the transducers would therefore be expected to be greater for higher-frequency transducers with the same efficiency and intensity.

The efficiency ε of the transducer depends on both its mechanical design and the manner in which it is electrically driven. The piezoelectric material used has an associated dissipation that depends on the material. The efficiency ε also depends on the coupling of energy into the backing material and into the load. Additionally, the operational efficiency depends on the spectrum of the electrical excitation. The greatest efficiency is achieved by driving the transducer continuously at its resonant frequency. At frequencies away from resonance the efficiency decreases in a manner given by the Q of the transducer. An example from our measurements showed that the efficiency of a 9.5 MHz CW Doppler transducer reduced from 0.17 at resonance to 0.038 at 10.0 MHz. These estimates of efficiency were obtained from measurements of electrical power delivered to the transducer, and measured total acoustic power using an ultrasonic force balance (Lunt & Ashley, 1979). When transducers are driven for broad-band pulse operation, some proportion of the electrical power will be contained in spectral components at which the transducer is less efficient in converting electrical to ultrasonic energy. Thus the operational efficiency of a transducer will be lower when pulsed than when operating continuously at its resonant frequency.

The efficiencies of medical transducers are not well documented. According to estimates provided by manufacturers, modern undamped CW Doppler transducers may exhibit efficiencies which reach 40% to 50%, whilst the efficiency of a damped transducer, operating at resonance, is probably no more than 10% to 20%. However, as noted above, the operational efficiency of a damped transducer when driven under broad-band conditions may be considerably lower than this. Some further discussion is included towards the end of this paper.

The final temperature reached by the transducer will depend on the rate of heat loss to the surrounding environment. This will include the tissue in contact with the transducer and the transducer holder, and will also depend on the environmental air temperature.

The experimental study

Two sets of measurements were carried out and will be reported separately. In the first, the transducer under study was operated in air and the temperature at the surface of the transducer measured. The second study investigated the skin surface temperature resulting from the application of the transducer.

Transducer heating in air

Initial observations were carried out using one of a set of seven liquid-crystal sheets (Edmund Scientific Co, New Jersey, USA). Each sheet measured 10 cm × 15 cm and the overall temperature range extended from 19 to 49°C. The transducer under study was mounted with its face horizontal and a sheet covering a suitable temperature range laid on the surface of the transducer. These observations allowed a general examination of the temperatures reached and the rates of temperature rise. Perhaps more usefully, the spatial pattern of heating on the transducer face could be observed, identifying regions of the transducer being used, particularly for pulsed Doppler or M-mode transmission. For quantitative thermometry, however, the use of liquid-crystal sheets lacks precision.

The measurement of surface temperature was made in the majority of cases using one of two infrared radiometers; the C-600M Biotherm Infrared Thermometer (Linear Laboratories, Los Altos, California, USA) or the Heimann KT-41 radiometer (Heimann GMBH, Wiesbaden, West Germany). The KT-41 was used for the majority of the measurements and has a precision of ±0.01°C. The C-600M was used for measurements of higher surface temperatures, above 40°C, and has a precision of ±0.1°C. For two of the transducers studied, temperatures in excess of 50°C were achieved and for these highest temperatures a needle-mounted copper–constantan thermocouple was used for the measurement. The radiometers were both calibrated at 30°C using an AGA black-body reference source. Strictly, many of the transducers studied were not "black-body radiators". The radiometers, however, detect and respond to infrared radiation and in the temperature range under study most dull, matt surfaces may be considered as black-body radiators. As confirmation, spot measurements were made on several of the transducers under steady-state conditions using the needle thermocouple. Radiometer and thermocouple measurements differed by no more than 0.5°C under all circumstances, within the temperature range 25–40°C.

Prior to the thermal measurement, total acoustic power was measured where possible using a radiation force balance (Duck et al, 1985), and the drive conditions for maximum power determined. Specific conditions varied widely, with total power in pulsed Doppler operation depending on the sample gate-length and depth, and Doppler-shift range (*i.e.* repetition frequency) as well as on output power control. The force balance could not be used to measure accurately acoustic power in imaging mode, and instead it was used to establish the machine settings giving highest output for imaging, since for some scanners acoustic power depends on the focusing conditions selected. The absolute accuracy of total power measurement was probably no better than ±20%, taking account of all factors, including calibration and beam position and direction. The dimensions of the transducer active area were also recorded. Approximate estimates were used where documentation was lacking and the active piezoelectric element could not be inspected directly.

Experimentally the transducer to be studied was mounted in a stand with its emitting face pointing horizontally, and the radiometer directed towards the transducer surface at a distance of 5–10 mm. Since all equipment was studied in the clinical room in which it was normally used, the thermal environment was largely uncontrolled with "cold" transducers starting at between 24 and 29°C. For this reason temperature increases are reported rather than absolute temperatures. The temperature rises at 1 min, ΔT_1, and at 5 min, ΔT_5, after switch-on are given in Tables I and II. Also given are the identification of the type and mode of operation of each transducer and, for CW Doppler, pulsed Doppler and single-element pulse–echo transducers, the total acoustic power. A total of 30 different transducers were examined, operating with 12 machines from 10 different manufacturers. The transducers included linear, curved and sector arrays, mechanical sectors, including one annular array, and Doppler-only transducers. They were operated in imaging, pulsed Doppler, continuous-wave Doppler and mixed modes.

A finite temperature increase was observed for all transducers operating in Doppler mode (Table I). The range of Doppler acoustic power was 6.2–315 mW and the 1 min temperature rise ranged from 0.7 to 36.5°C. Broadly, higher powers generated higher temperatures, but other factors including transducer size, frequency and efficiency are important [see Equations (4) and (5)]. Two phased-array transducers operating with the same duplex scanner (E/1/1, E/1/2) became particularly hot, reaching maximum absolute temperatures of 67.6 and 79.2°C. Although not included in the table of results, a linear array used in pulsed Doppler mode with the same equipment was also observed to reach a temperature in excess of 50°C.

The temperature increases in air of transducers operating in imaging mode (Table II) varied from 0°C to a maximum increase at 5 min of 13.1°C (see also "Note added in revision"). For those arrays operating in combined imaging and M-mode the measurements were made over the emitting portion of the M-mode line. Three transducers operating with machine C emitted an M-line pulse continually, even when the operator was using only the real-time image. The one annular array measured differed notably in its time progression of temperature increase (A/1/3, see Fig. 1). It had not approached thermal equilibrium at 5 min and continued to increase in temperature appreciably from 4.1°C at 5 min to 6.5°C at 10 min. Figure 1 shows selected examples of temperature rise with time.

Equation (4) shows that a linear relationship might be

Table I. Measured transducer surface temperature increases in air at 1 min (ΔT_1) and at 5 min (ΔT_5) in Doppler modes

Manufacturer/ machine/ transducer	Type	Frequency (MHz)	Area (cm^2)	Acoustic power (mW)	Temperature increase	
					ΔT_1 (°C)	ΔT_5 (°C)
Continuous wave						
G/1/1	D/PA	3.5	1.6	84	2.7	4.5
D/1/1	MS	3.5	2.8	78	3.1	8.2
C/1/4	D	5	1.9	24	1.0	1.7
G/1/3	D	3.0	0.9	15	1.6	2.7
I/1/4	D/PA	1.9	0.9	30	1.5	3.1
Pulsed						
C/1/1	PA	5	2.2	36	8.2	12.5
E/1/1	PA	3.5	2.2	315	30.5[a]	42.0[a]
E/1/2	PA	5	1.0	90	36.5[a]	52.2[a]
E/1/3	PA	3.5	1.5	43	10.0[a]	13.0[a]
G/1/1	PA	3.5	3.2	18	2.2	2.9
G/1/2	PA	2.5	4.1	74	2.6	4.2
I/1/1	PA	2.5	5.0	23	1.4	2.3
I/1/2	PA	3.5	4.0	33	3.4	5.4
I/1/3	PA	5	2.2	14	3.2	5.4
A/1/1	MS	2.25	1.3	23	3.8	5.9
A/1/2	MS	5	0.3	6.2	1.3	2.2
B/2/1	MS	7.5	0.3	6.5	2.0	3.2
D/1/1	MS	3.5	2.8	110	4.7	8.2
D/1/2	MS	5	2.3	105	3.4	8.9
B/1/1	D	2	1.0	11	0.7	1.7
B/1/2	D	3	1.0	11	1.2	2.0
B/1/3	D	5	0.2	7.5	1.7	2.0

PA, phased array; MS, mechanical sector; D, Doppler-only transducer; D/PA, CW Doppler transducer incorporated into a phased-array scan-head.
[a] Measured using a needle-mounted thermocouple.

expected between the initial rate of temperature rise and I, the source intensity. Where possible I was calculated and values plotted against the 1 min temperature rise, ΔT_1 (Fig. 2). (The 1 min rise was assumed to be approximately linearly related to the initial rate.) Three groups of transducers are identified. Group 1 includes all pulsed transducers except mechanical sectors, and consists mainly of phased arrays operating in pulsed Doppler mode, in which the piezoelectric element lies close to the transducer surface. Group 2 are mechanical sectors operating in pulsed Doppler mode, in which the transducer is surrounded by a fluid coupling medium. Group 3 includes transducers designed specifically as Doppler transducers to operate with long tone-bursts or continuously.

Least-squares linear-regression analysis was carried on the measured values from each group separately. Results obtained using thermocouple measurements have been omitted from the analysis since the thermal load resulting from the contact of the thermocouple on the transducer was observed to slow its rate of temperature rise, and may have also reduced slightly the measured temperatures at the highest values. Where available, radiometer measurements at lower powers were included for those transducers otherwise measured with the thermocouple.

Analysis of the Group 1 transducers, the pulsed transducers excluding mechanical sectors, gave the following expressions

$$\Delta T_1 = 0.25 + 0.301I \qquad r = 0.958 \qquad (6a)$$

$$\Delta T_5 = 0.34 + 0.492I \qquad r = 0.964 \qquad (6b)$$

where ΔT_1 and ΔT_5 are in °C and I is the spatial-average intensity at the transducer in mW cm^{-2}. The correlation coefficient of acoustic power against ΔT_1 was lower ($r = 0.920$).

The regression of ΔT against the product If [Equation (5)] was also calculated:

$$\Delta T_1 = 0.016 + 0.0883If \qquad r = 0.990 \qquad (7a)$$

$$\Delta T_5 = -0.115 + 0.1473If \qquad r = 0.956 \qquad (7b)$$

where f is in MHz.

For Group 2, the mechanical sectors, the correlation coefficient was only 0.526, presumably because of the wider range of design of these mechanical scan-heads. The associated linear-regression expression was felt to have little predictive value and is omitted.

Table II. Measured transducer surface temperature increases in air at 1 min (ΔT_1) and at 5 min (ΔT_5) in imaging and mixed modes

Manufacturer/ machine/ transducer		Type	Frequency (MHz)	Area (cm^2)	Temperature increase	
					ΔT_1 (°C)	ΔT_5 (°C)
Imaging only						
H/1/1		B	3.5	1.3	0.0	0.0
J/1/1		B	3.5	2.8	0.5	1.2
J/1/2		B	5	1.3	0.6	1.3
E/1/1		PA	3.5	4.5	8.2	13.1
I/1/1		PA	2.5	5.0	0.0	0.0
I/1/2		PA	5	2.2	3.8	5.8
E/1/4		LA	3.5	13	3.4	5.8
F/1/1		LA	3.5	17	0.0	0.0
F/1/2		LA	5	9.0	0.4	0.6
A/2/1		CA	3.5	7.5	0.5	1.7
A/1/1		MS	2.25	1.3	0.8	1.7
A/1/2		MS	5	0.3	0.4	1.2
A/1/3		AA	3.5	3.3	1.7	4.1
Mixed mode						
C/1/1	with M-mode	PA	5	2.2	6.9	10.5
C/1/2	with M-mode	CA	3.75	7.0	3.1	5.2
C/1/3	with M-mode	LA	7.5	5.0	3.3	5.3
G/1/2	colour flow	PA	2.5	4.1	1.2	1.6
I/1/2	colour flow	PA	3.5	4.0	3.7	5.7
I/1/3	colour flow	PA	5	2.2	4.4	7.0

B, single element; PA, phased array; LA, linear array; CA, curved array; AA, annular array; MS, mechanical sector.

For the CW Doppler transducers, Group 3, linear-regression analysis yielded

$$\Delta T_1 = 0.61 + 0.0353I \qquad r = 0.896 \qquad (8a)$$

$$\Delta T_5 = 1.28 + 0.0503I \qquad r = 0.808 \qquad (8b)$$

The regression lines represented by Equations (6a) and (8a) are included in Fig. 2.

Skin temperatures

The skin temperature following application of the transducer was measured for a limited number of transducers. In particular, the effect of transducers operating with duplex system "E" were studied, since this gave the greatest temperature rises in air. The skin temperature of the inner forearm was measured using a radiometer before applying the transducer to the skin, and again immediately following the removal of transducer. Since the presence of coupling gel on the skin modifies its emissivity (Filipczyński, 1978), measurements were made either with minimal use of gel or following complete removal of the gel from the skin. It is recognized that poor acoustic coupling will result in a greater power dissipation in the transducer than with good coupling, and hence possibly greater heating. However, no substantial differences were observed in skin heating depending on the quality of coupling, resulting possibly from the generally low efficiency of these transducers [see Equations (3) and (4)].

For practical purposes two broad categories of use can be envisaged under which transducers may warm the skin. In the first category, the transducers may be placed on the skin "cold" and then activated. In this case the transducer heating would be expected to be slowed and reduced from the case in air by two mechanisms: first, a fraction of the power previously dissipated in the transducer will now be emitted, and secondly, the tissue will probably act as a more effective heat-sink than air, especially if the skin circulation becomes enhanced. The second broad category is when the transducer is powered by the scanner in air before application to the skin. Some transducers continue to receive electrical power even when the image is frozen. Even those more common systems in which the power is switched off when the freeze button is operated may in practice be left active whilst not in use. The illustrative examples reported below were intended to take account of these alternative modes of use.

A cold transducer on the skin surface for 1 min caused a slight (about 1°C) reduction in temperature when the power was off. Probe E/1/1 operating in imaging mode warmed the skin by 2.4°C in 1 min when switched on from cold. When applied to the skin having been powered in air for several minutes, again operating in imaging mode, the skin temperature rose 3.7°C from 32.5 to 36.2°C in 1 min. In pulsed Doppler mode it was not possible to hold the E/1/1 or E/1/2 probes, which

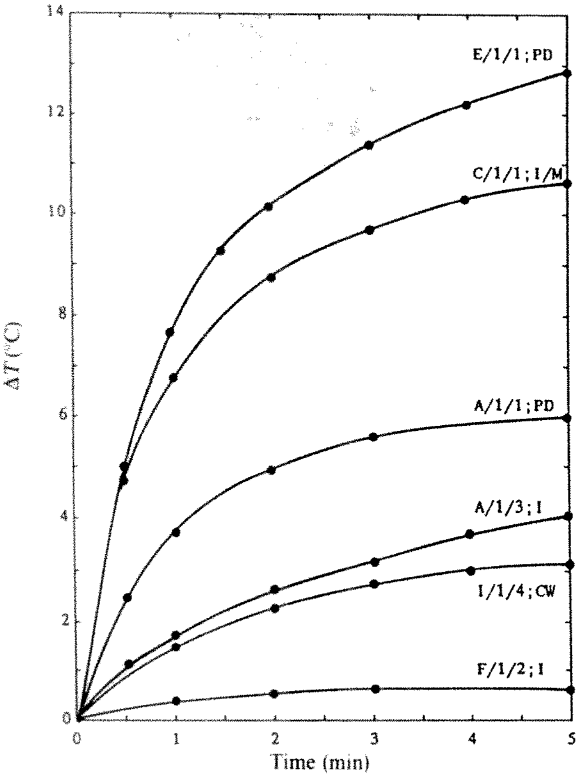

Figure 1. Surface temperature increase with time for selected transducers. E/1/1, pulsed Doppler, phased array, 3.5 MHz; C/1/1, imaging/M-mode, phased array, 5 MHz; A/1/1, pulsed Doppler, mechanical sector, 2.25 MHz; A/1/3, imaging, annular array, 3.5 MHz; I/1/4, CW Doppler, Doppler-only transducer in phased-array scan-head, 1.9 MHz; F/1/2, imaging, linear array, 5 MHz.

generated the greatest heat, on the skin for long under drive conditions without experiencing considerable discomfort and pain. Following about 45 s from cold, the E/1/1 transducer raised the skin temperature to 42.9°C, and a temperature of 41.6°C was observed following about 30 s application of the E/1/2 probe. Both transducers could reach sufficiently high temperatures if left operating in pulsed Doppler mode in air to cause immediate pain when applied to the skin.

The thermal effect of these particularly hot transducers was imaged using a pyroelectric videcon camera (Series 75, Insight Visions Systems Ltd, Malvern England). Figure 3 shows the thermal images after the application of the E/1/1 phased-array transducer operating in pulsed Doppler mode to the inner forearm. The dynamic range of the image is about 9°C and the skin temperature about 32.5°C. A square region of raised temperature (>40°C) is seen on the skin and is still clearly visible 30 s later. Figure 4 shows a similar pattern of elevation of skin temperature following the use of the E/1/1 transducer in imaging mode.

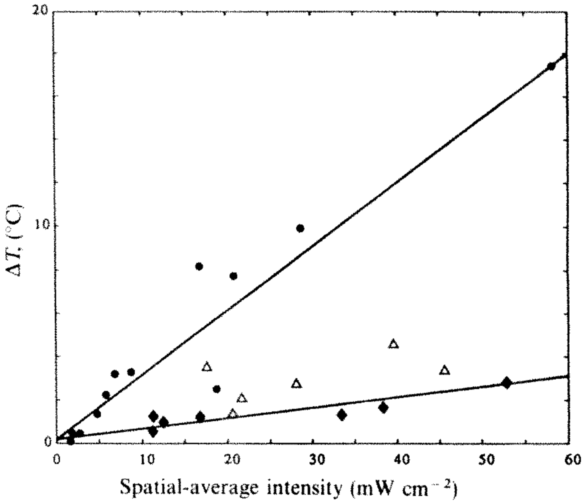

Figure 2. Surface temperature at 1 min (ΔT_1) against spatial-average intensity at the transducer. ●, Group 1, pulsed transducers excluding mechanical sectors; △, Group 2, mechanical sectors; ◆, Group 3, CW Doppler transducers. Linear-regression equations for Groups 1 and 3 are given in Equations (6a) and (8a).

Discussion

The temperatures that have been measured at the surfaces of diagnostic ultrasound transducers demonstrate that consideration of transducer temperature is essential during the design of safe diagnostic ultrasound systems. The empirical expressions [Equations (6), (7) and (8)] may allow a reasonable estimate to be made of the expected transducer surface temperature when operated in air, from a knowledge of total acoustic power and transducer area. This estimate assumes that the thermal, electrical and piezoelectric characteristics of other chosen transducers are comparable to those in this study. A temperature increase in air after 1 min at the surface of pulsed Doppler transducers (excluding mechanical sectors) of about 0.3°C per mW cm^{-2} would seem to be fairly widely applicable for both pulsed Doppler and M-mode operation (see "Note added in revision" at the end of this paper). Whilst transducers can also heat when operated in imaging mode, it should not be assumed that they necessarily heat at a similar rate, and we present no evidence relating heating in imaging mode to intensity.

At first sight the lower value of about 0.035°C per mW cm^{-2} for CW Doppler transducers seems surprising [Equation (8a)]. Nevertheless, the observed low heating of CW Doppler transducers matches well with Filipczyński's results. In his paper, one system, operating at 100 mW cm^{-2} ($\pm 20\%$), gave a skin temperature of 2.3°C at 60 s. Equation (8a) predicts a temperature of 4.1 ± 0.7°C for the same transducer operating in air. Similarly for the Parks 806 probe using an intensity of 375 mW cm^{-2} (Carson et al, 1978), a temperature rise of 13.8°C is predicted in air, in comparison with a skin

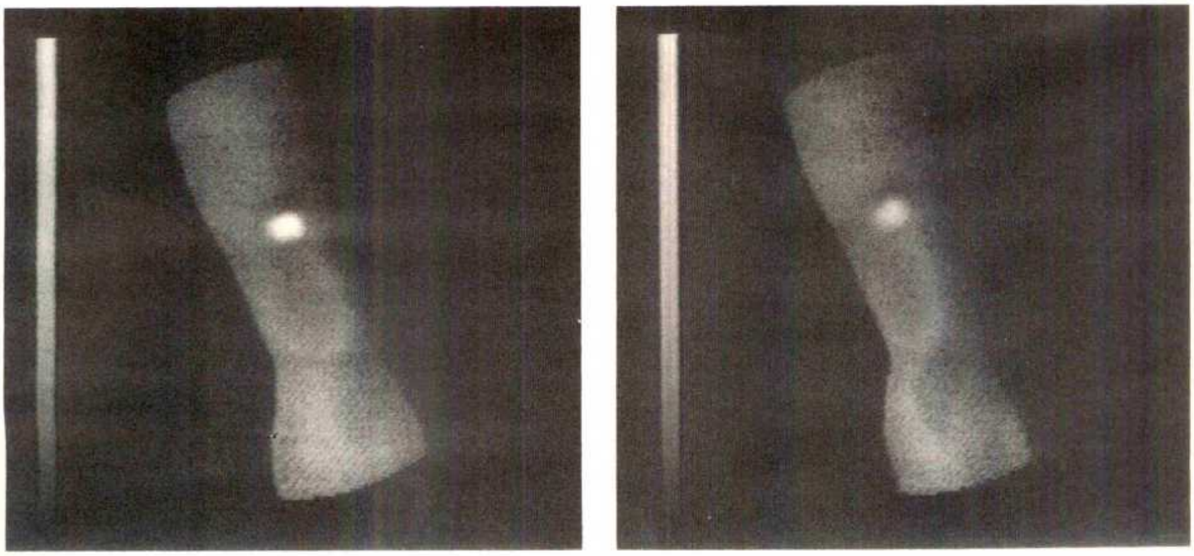

(a) (b)

Figure 3. Thermal images following the application of phased-array E/1/1 operating in pulsed Doppler mode to the inner forearm (a) immediately after the transducer was removed and (b) about 30 s later. Displayed temperature range about 9°C. Skin temperature 32.5°C.

temperature increase of 12.5°C measured by Filipczyński. For reasons already discussed, skin temperatures would be expected to be lower than transducer temperatures in air. The almost ten-fold difference in heating rate in air between these two classes of transducers needs some explanation. Since $\Delta T/\Delta t \propto 1/\varepsilon$ [Equation (4)], transducers with lower efficiency operating in air will heat more than those with greater efficiency, under otherwise similar conditions. It is known that CW Doppler transducers are designed to be more efficient than the more heavily damped transducers intended for pulse–echo applications, but only by a factor of three or four at most. The required ten-fold difference in efficiency cannot be accounted for by considering only the difference in design. The explanation must lie in the part that the bandwidth of the electrical drive plays in determining the operational efficiency of the pulsed transducer when in use. It is perfectly possible that the efficiency of a damped transducer could be reduced from 10–20% at resonance to 5% or less when pulsed, due only to the higher losses associated with those frequencies in the drive that are converted with lower efficiency by the transducer.

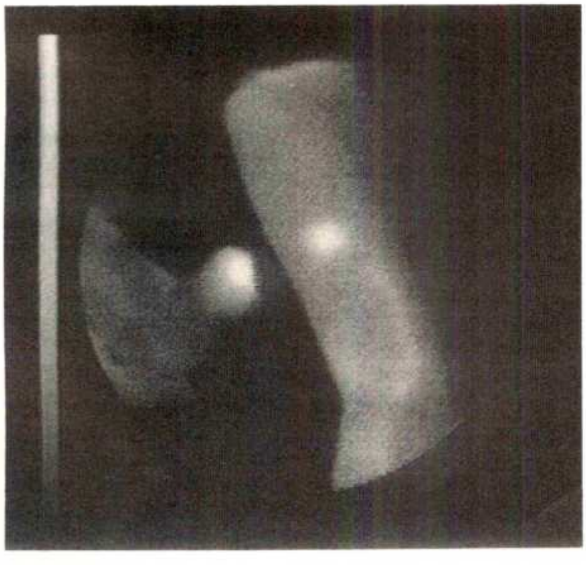

Figure 4. Thermal image immediately following the application of phased-array E/1/1 operating in imaging mode to the inner forearm. Scaling as Fig. 3.

The piezoelectric plate itself (rather than the backing or facing material) would seem to be the major site of heat generation, and this is supported by the experimental result that the highest correlation coefficient was obtained when the thickness of the piezoelectric plate was included in the analysis [Equation (7a)]. The relatively small mass of the piezoelectric plate will experience a greater increase in temperature than would occur if the same energy were deposited in the greater mass of the surrounding material. A simple example serves to illustrate this. Consider a transducer with $\varepsilon = 0.2$ and a measured acoustic output of 50 mW. Operating in air, 250 mW is dissipated in the transducer. Assume that this is equally shared between the piezoelectric plate and the surrounding backing and facing material. A typical mass of a piezoelectric plate is about 1 g, and assuming a specific thermal capacity, C, of 1 J g^{-1} °C^{-1} the initial temperature rise of the plate is 0.0125°C s^{-1} [Equation (1)], or 7.5°C in 1 min ignoring conduction losses. If the remaining 125 mW is dissipated in only 10 g of surrounding material, and this is probably a conservative estimate, the temperature rise in this material would only be one-tenth of that of the piezoelectric plate, assuming the same value of C. For the mechanical sectors, one must suppose that the piezoelectric element experiences similar heating to other pulsed transducers, but that this is not detected at the surface of the transducers because of the thermal capacity and insulation provided by the scan head. Further detailed theoretical and experimental studies will be required to investigate fully these problems.

From a clinical viewpoint it seems surprising that the excessively high temperatures observed with one scanner have not apparently been noticed before. Temperatures this high on the skin will cause full thickness burns. Moritz and Henriques (1947), in a classic paper, reported a series of carefully controlled experiments on pig and human skin exposed to temperatures in the range 44–100°C for periods of time lasting from 1 s at the highest temperatures to 8 h at the lowest. From their compiled results it is possible to predict that a full burn could occur, for example, following a 1 min exposure at 53°C, or 5 s at 60°C. The actual skin temperature, and hence its liability to damage, will depend partly on the thermal properties of the applied surface, which in these experiments was a flowing heated fluid. Good conductors such as metals cause higher skin temperatures than poor conductors such as wood, with plastic materials comparable to the transducer face plates probably lying between these extremes. Further discussion of these and other relevant issues is given by the British Standards Institution (BSI, 1983).

Given the relatively wide use of the equipment in question, it would have been expected that some evidence of skin reaction from these high temperatures would have been seen clinically. Several reasons for the absence of such reports may be suggested. First, they were not expected. Patients are known to report periodically that some sensation is experienced when an ultrasound transducer is held on the skin. A common response might well be that "it is not possible to feel ultrasound", a response that in general may be justified. Secondly, the particularly high temperatures reported were generated only under specific operating conditions, which may be used only rarely. In addition, a moving transducer will be less likely to raise the skin to a hazardous temperature than a stationary transducer. Clearly a conscious patient would report vigorously if a transducer operating at an excessive temperature were to be applied to the skin. Equally clearly a sedated patient, or a neonate, may not inform and severe burning could result. Furthermore, some individuals demonstrate reduced temperature sensitivity, and could remain unaware of elevated skin temperatures. As an additional point it may be added that oesophageal transducers operate in a region of minimal sensory nerve endings and are surrounded by tissue at approximately core temperature. At least one manufacturer, aware of thermal problems in this context, has incorporated a thermistor to sense transducer temperature and which causes the transducer power to cease if the temperature becomes too high.

British Standard 5724 (BSI, 1979) based on IEC 601/1, limits the allowed temperature for applied parts not intended to supply heat to the patient to less than 41°C. In this survey, whilst we have found only one scanner that caused transducers to exceed this limit in air, it will be necessary to study further the behaviour of all transducers under conditions of skin contact. For instance, it may be possible to raise the skin temperature to greater than 41°C by operating a pulsed Doppler or M-mode line having previously increased the surface temperature of the transducer by skin contact whilst imaging. Such considerations need full evaluation and involve concerns outside the general safety standard of BS 5724, Part 1.

The only ultrasonic standards relating in any way to the temperature rises reported here are the Japanese standards, which set exposure limits that depend on the spatial-average intensity at the transducer (Maeda & Ide, 1986). In these standards, for normal B-mode operation a spatial-average intensity of 10 mW cm^{-2} is permitted. This is allowed to increase to 40 mW cm^{-2} for cardiac M-mode operation and to 100 mW cm^{-2} for cranial A-mode operation. The use of Equation (6a) predicts that the 1 min temperature rise for pulsed probes (excluding mechanical sectors) under these conditions would be 3.3, 12.3 and 32.6°C, respectively.

The temperature limit of 41°C defined by IEC 601/1 allows an ambient temperature of up to 25°C. Setting ΔT_5 as the difference, 16°C, it is possible to use Equations (6b) and (8b) to predict upper limits for the acoustic intensity at the transducer that would generate a transducer surface temperature of 41°C after 5 min operation in air. The values are 31.8 mW cm^{-2} for pulsed transducers and 293 mW cm^{-2} for CW Doppler transducers. Probes intended for intraluminal use, for example oesophageal, rectal or vaginal transducers, may be assumed to operate from a starting temperature of 37°C. For such probes it would be reasonable to limit their temperature rise to 4°C and the limiting intensities in this case are 7.9 mW cm^{-2} for pulsed transducers and 73.2 mW cm^{-2} for CW Doppler transducers.

Conclusions

The surface temperatures of 30 diagnostic ultrasound transducers operating in air have been measured. Temperature increases were observed for transducers operating in imaging mode, pulsed Doppler mode and in continuous-wave Doppler mode. Generally these increases were only of a few degrees centigrade. However, extreme examples were observed where, for example, one transducer operating in pulsed Doppler mode reached a surface temperature of almost 80°C.

Analysis of the temperature increases showed that pulsed transducers (except mechanical sectors) operating in pulsed Doppler mode gave a transducer surface temperature rise in air after 1 min of about 0.3°C per mW cm^{-2}, the intensity being averaged over the transducer surface. Transducers for continuous-wave Doppler use gave a 1 min temperature rise of about 0.035°C per mW cm^{-2}. Whilst the correlation between temperature rise and intensity for mechanical sector scan-heads was poor, the surface temperatures were generally intermediate between those found on other pulsed transducers and the temperatures of CW Doppler transducers. Increases in temperature during imaging operation were also observed, but the relationship between temperature rise and source intensity was not quantified.

Upper limits for intensity at the transducer, based on considerations of transducer heating in air, are about 30 mW cm^{-2} for damped pulse transducers, and 300 mW cm^{-2} for CW Doppler transducers. Intensities from intraluminal probes should not exceed one-quarter of these values.

Acknowledgments

We are very grateful to those colleagues who have made available to us the clinical scanners evaluated in this survey, all of which were in steady clinical use. We would also like to note the considerable help given by Mr Francis Ring, both with advice and with the loan of the radiometers and the pyroelectric videcon camera, without which the study would not have been possible. The manufacturers of equipment E/1 have been informed of the temperatures reported above, and are at present modifying the conditions that give rise to them.

Note added in revision

Since these measurements were made, we have investigated a further duplex scanner, from a manufacturer not represented in the survey. Four curved arrays were studied, operating in B, M and pulsed Doppler modes. For both M and pulsed Doppler modes the 1 min temperature rise, ΔT_1, was between -31% and $+11\%$ of the rise predicted by Equation (6a), with an average error of -14.3%. At 5 min the range of discrepancy between predicted and observed temperature rise [Equation (6b)] was -24% to $+27\%$ with an average of -4.1%. Greater errors were observed from predictions using Equations (7a) and (7b) (which include frequency) and gave a worst-case overestimate of 59% at 1 min and 85% at 5 min for a 5 MHz transducer. These measurements give an initial indication of the predictive quality of these equations and suggest that Equations (6a) and (6b) might prove to be more accurate than Equations (7a) and (7b).

For one of the 5 MHz arrays operating in imaging mode alone, the increase in surface temperature at 5 min, ΔT_5, was 28.2°C, reaching a maximum temperature of 54.5°C. This temperature exceeded the highest temperature reported above for imaging mode (see E/1/1, Table II).

References

AIUM, Bioeffects Committee, 1988. Bioeffects considerations for the safety of diagnostic ultrasound. *Journal of Ultrasound in Medicine*, 7, S1–S38.

BSI, 1979. *Medical Electrical Equipment Part 1. Specifications for General Safety Requirements*. British Standard BS 5724 (BSI, London).

——1983. *Medical Information on Human Reaction to Skin Contact with Hot Surfaces*. BSI Published Document PD 6504 (BSI, London).

Carson, P. L., Fischella, P. R. & Oughton, T. V., 1978. Ultrasonic power and intensities produced by diagnostic ultrasound equipment. *Ultrasound in Medicine and Biology*, *3*, 341–350.

Duck, F. A., 1989. Output data from European studies. Proceedings of the Second WFUMB Symposium on Safety and Standardisation in Medical Ultrasound. *Ultrasound in Medicine and Biology*, *15*, Suppl. 1, 61–64.

Duck, F. A., Starritt, H. C., Aindow, J. D., Perkins, M. A. & Hawkins, A. J., 1985. The output of pulse-echo ultrasound equipment: a survey of powers, pressures and intensities. *British Journal of Radiology*, *58*, 989–1001.

Duck, F. A., Starritt, H. C. & Anderson, S. P., 1987. A survey of the acoustic output of ultrasonic Doppler equipment. *Clinical Physics and Physiological Measurement*, *8*, 39–49.

Filipczyński, L., 1978. Measurement of the temperature increases generated in soft tissue by ultrasonic diagnostic Doppler equipment. *Ultrasound in Medicine and Biology*, *4*, 151–155.

Lunt, M. J. & Ashley, B., 1979. A simple radiation balance for measuring ultrasonic power. *Journal of Medical Engineering and Technology*, *3*, 194–197.

Maeda, K. & Ide, M., 1986. The limitation of the ultrasound intensity from diagnostic devices in the Japanese industrial standards. *IEEE Transactions on Ultrasonics Ferroelectrics and Frequency Control*, *UFFC-33*, 241–244.

Moritz, A. R. & Henriques, F. C. Jr., 1947. Studies of thermal injury II. The relative importance of time and surface temperature in the causation of cutaneous burns. *American Journal of Pathology*, *23*, 695–720.

Nyborg, W. L., 1988. Solutions of the bio-heat equation. *Physics in Medicine and Biology*, *33*, 785–792.

1989, *The British Journal of Radiology*, 62, 1014–1016

Technical note

The use of an infrared touch-screen to control the sensitivity of ultrasound scanners in clinical practice

By S. D. Pye, PhD, V. Elliott, DCR(R), DMU, I. Marshall, DCR(R), D. Millar, DCR(R), S. Robertson, DCR(R), W. N. McDicken, PhD and S. R. Wild, DMRD, FRCR, FRCPE

Departments of Medical Physics and Medical Engineering and Radiology, Western General Hospital, Edinburgh EH4 2XU

(Received April 1989 and in revised form June 1989)

Real-time ultrasound involves rapid scanning through the body and easy control manipulation is essential. The sensitivity settings of a scanner (also referred to as the time gain compensation (TGC) settings) are crucial in obtaining good image quality. However, many ultrasound scanners only allow the operator a limited scope for adjusting the sensitivity, and often it is only possible to change the slope or overall level of the TGC or to alter the TGC at a few depth ranges. No commercially available scanners allow the operator to alter the sensitivity in small regions of the image despite the common experience that a diagnosis is often made by examining in detail a particular area of an image.

One approach to this problem is to automate fully the sensitivity controls (McDicken et al, 1974; DeClercq & Maginness, 1975; Pye et al, 1988). Another approach is to make the sensitivity controls more flexible and easier to use. In order to explore the potential of more flexible methods of sensitivity control, an infrared touch-screen has been used in conjunction with a microcomputer to control the sensitivity of a real-time scanner. This system has been evaluated clinically in routine obstetric scanning.

Instrumentation

The touch-screen is manufactured by Microvitec Ltd, and comprises an array of infrared emitters and detectors plus control logic mounted in a frame that fits around a 14-inch monitor screen. The maximum resolution of the array is 120 divisions horizontally by 90 vertically. The touch-screen is linked to a mechanical sector scanner via a microcomputer (Cromemco, Model CS-2). The touch-screen passes to the microcomputer the co-ordinates of points close to the screen where the infrared beams are broken by an object such as a finger. The alternative to using an infrared touch-screen was to use a touch-sensitive membrane covering the face of the monitor.

The infrared screen has two advantages: (a) the infrared beams are invisible and so, unlike the membrane, they do not degrade the image and (b) the infrared beams lie slightly in front of the monitor screen so that the position of a pointing finger can be registered without smearing the monitor with coupling gel. The microcomputer receives co-ordinate data in cartesian form and converts it to polar values for the 90° sector image. The microcomputer also controls the sensitivity of the scanner by controlling the gain of the receiver electronics. Only in this way is it possible to operate over the whole dynamic range of the signal, which is necessary to improve the image quality. The details of the electronics linking the microcomputer and the scanner are described by Pye et al (1986). The touch-screen and image monitor are mounted on top of the scanner so that the screen can easily be seen and reached by the operator without disturbing the position of his or her scanning arm. Several modes of operation were tried.

1. Selecting a region of the image by touching a single point and then altering the sensitivity around that point.
2. Defining a sector shape by touching three points on the image and then altering the sensitivity within the sector.
3. Controlling the size of the change in sensitivity using a separate control box, or using the touch-screen itself.

A particularly useful method of adjusting the sensitivity was found to be by touching the image at one point and then altering the sensitivity in an area of approximately 3 cm^2 around it. This was applied to making biparietal diameter (BPD) measurements, where the sensitivity could be lowered for the skull echoes on both sides of the fetal head without affecting the presentation of important structures within the head. In this way the operator is still able to check that the correct section through the head has been achieved.

The most acceptable method of controlling the size of the sensitivity change was using a small control box mounted just below the image monitor. The control box has two push buttons—one button to increase the sensitivity and the other to decrease it. By keeping one of the buttons depressed, the sensitivity rises or falls at a rate set by the microcomputer software; 10 dB s^{-1} was found to be a suitable rate. Having adjusted the sensitivity at one location in the image, another location can be selected and its sensitivity adjusted. Any number of locations can be set in this way, although in practice a maximum of three was used. Simultaneously pressing both buttons on the control box instructs the microcomputer to remove the sensitivity changes introduced by the touch-screen. The number of regions in the image that have been modified is recorded on the visual display unit of the microcomputer. In a final version of the system this information could be displayed more clearly either by using a separate grey shade image of the sensitivity values, or by using a graphics overlay on the echo image to indicate the modified regions. The overlay would switch on automatically for a few seconds whenever the touch-screen was activated and then switch off so as not to obscure the image.

Clinical evaluation

The touch-screen has been used in routine obstetric scanning in 120 pregnancies with gestations between 8 and 40 weeks. Patients were scanned by four experienced radiographers and pairs of images were obtained, one using the touch-screen sensitivity control and the

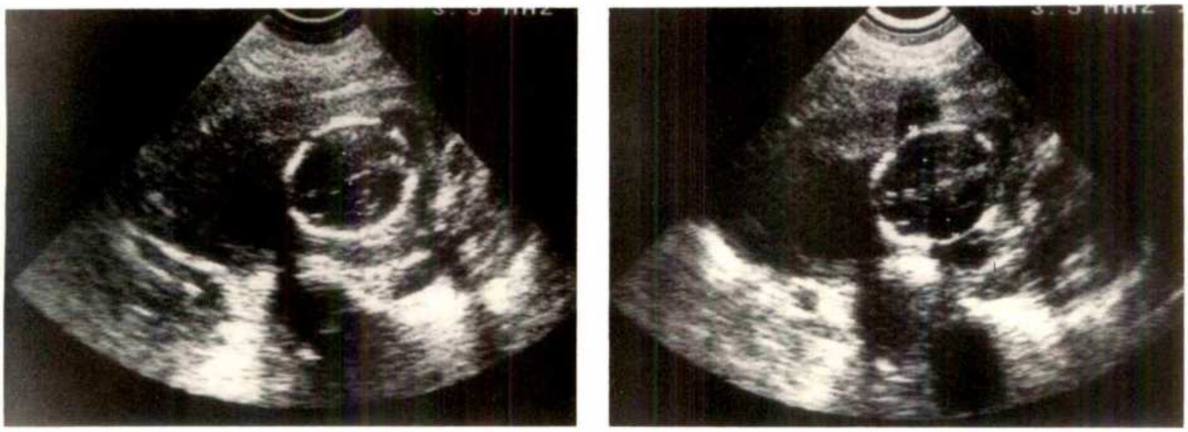
(a) (b)

Figure 1. Biparietal diameter measurement of a 16-week fetus (a) using the scanner's TGC controls and (b) using the touch-screen to bring skull echoes out of saturation.

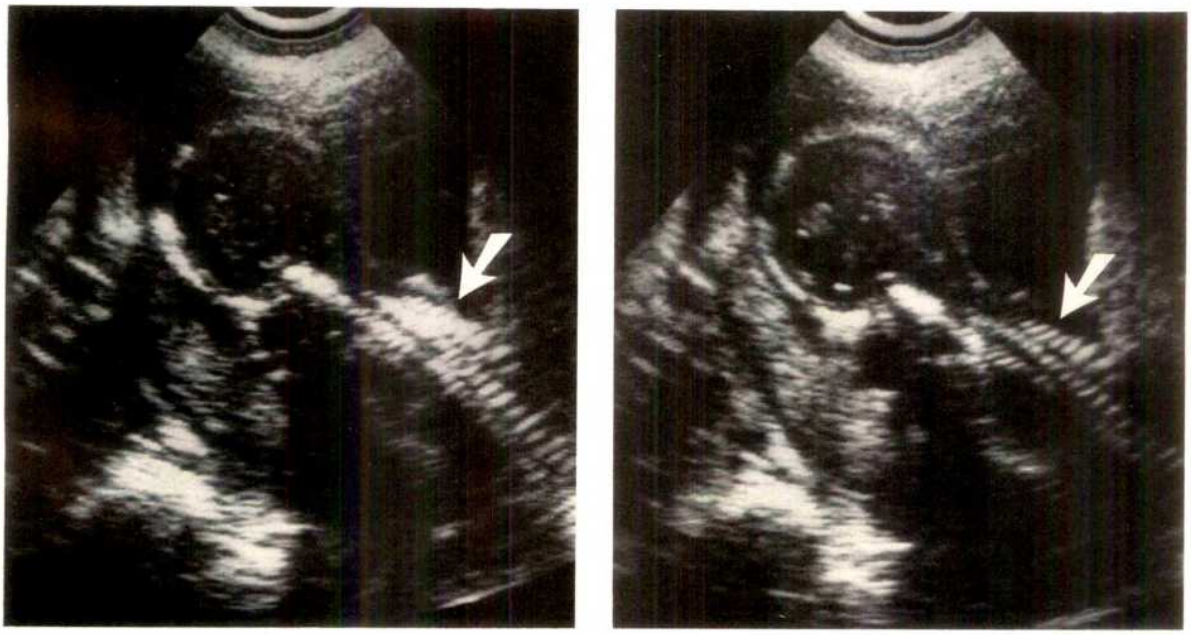
(a) (b)

Figure 2. The head and spine of a 16-week fetus (a) using the scanner's TGC controls and (b) using the touch-screen to image the vertebrae more clearly (arrows).

other using the scanner's own sensitivity controls. The effect of the touch-screen could then be seen by comparing the images, which were recorded on single-sided emulsion film. The situations in which the touch-screen was used are described below.

1. Reduction of saturated fetal skull echoes (79 patients). The most striking results were obtained in this application. Reducing the sensitivity at the fetal skull changed broad, saturated skull echoes to fine, well defined echo lines. All the operators commented that they found these much easier to use for BPD measurement than the broader skull echoes present without the touch-screen. An example is shown in Fig. 1. Because fetal movement frequently occurred between taking BPD measurements with and without the use of the touch-screen, it was not possible to determine whether the touch-screen improved the accuracy of the BPD measurements.
2. Reduction of saturated echoes from the fetal spine, particularly the cervical and sacral regions, so as to image individual vertebrae more clearly. This is illustrated in Fig. 2. (46 patients.)
3. Adjustment of the sensitivity at the ends of fetal longbones to enable them to be measured more easily (18 patients).
4. Adjustment of the sensitivity settings when scanning early pregnancies to image the fetus more clearly before making a crown–rump length measurement (three patients).
5. Adjustment of the sensitivity so as to improve visualization of the fetal aorta, the placenta, fetal kidney and depth of liquor (four patients).

The most useful feature of the touch-screen was that it allowed the sensitivity of the scanner to be reduced in localized areas so as to bring saturated echoes within the dynamic range of the receiving amplifier in the scanner. The applications of increasing the sensitivity rather than reducing it were fewer. This was chiefly because in the regions where it was desired to visualize structures, such as regions of shadowing, raising the sensitivity simply increased the amount of noise, indicating that the signal level in the shadowed region had already fallen below the noise level.

One application in which several of the operators had hoped to improve the image was when making a BPD measurement with the fetal head close to the skin surface and the probe. However, this was not successful as most of the poor image quality in this situation was in fact due to poor ultrasound beam shape and not to the sensitivity settings.

Conclusions

The results of the clinical evaluation show that touch-screen computing techniques are well suited to controlling the sensitivity of ultrasound scanners. Instead of having to manipulate several controls whose function is often difficult to relate to the image, the operator can simply point to or outline the region in the image where the sensitivity is to be altered. This has been found to facilitate the measurement of fetal structures and to give clear visualization of the fetal spine.

References

DeClercq, A. & Maginness, M. G., 1975. Adaptive gain control for dynamic ultrasound imaging. In *IEEE Ultrasonics Symposium Proceedings, 1975*, IEEE Cat. No. 75 CHO 994-4SU (Institute of Electrical and Electronic Engineers, New York), pp. 59–63.

McDicken, W. N., Evans, D. H. & Robertson, D. A. R., 1974. Automatic sensitivity control in diagnostic ultrasonics. *Ultrasonics, 12*, 173–176.

Pye, S. D., McDicken, W. N., Wild, S. R. & Anderson, T., 1986. Automatic swept gain in ultrasonic imaging. In *Physics in Medical Ultrasound*, IPSM Report 47, ed. by J. A. Evans (Institute of Physical Sciences in Medicine, York), pp. 173–175.

Pye, S. D., Wild, S. R. & McDicken, W. N., 1988. Clinical trial of a new adaptive TGC system for ultrasound imaging. *British Journal of Radiology, 61*, 523–526.

1989, *The British Journal of Radiology*, *62*, 1017–1019

Case reports

Ultrasonographic appearances of parathyroid carcinoma

By B. D. Daly, MRCPI, FFR(RCSI), FRCR, S. L. Coffey, MRCPI, FFR(RCSI) and M. Behan, MRCP, FRCR

Department of Radiology, Mater Hospital, Dublin 7, Eire

(*Received July 1988*)

Real-time ultrasonography of the neck is currently recommended as an initial imaging technique in the investigation of hyperparathyroidism (Butch et al, 1985). Pathological parathyroid glands in patients with hyperparathyroidism may be detected with an overall accuracy of 93% (Graif et al, 1987). Parathyroid carcinoma is a rare tumour, which accounts for 1–4% of all cases of primary hyperparathyroidism (Schantz & Castleman, 1973; van Heerden et al, 1979). Although the sonographic features of carcinoma of the parathyroid have been reported recently (Kinoshita et al, 1985; Edmunson et al, 1986), the conclusions have been conflicting. We describe the sonographic appearances of parathyroid carcinoma in two patients with evidence of invasion of surrounding structures, and discuss the brief literature on the use of ultrasound for the pre-operative diagnosis of this rare tumour. Scans were performed with a real-time electronically focused, linear array probe with a water-bath.

Case reports

Case 1

A 45-year-old woman was admitted for investigation of a lump on the left side of her neck. She had no symptoms of hyperparathyroidism. A small nodule was palpable in the left lobe of the thyroid gland. Physical examination was otherwise normal. Routine biochemistry showed an elevated serum calcium of 3.75 mmol/litre (normal range 2.20–2.63 mmol/litre). Ultrasound of the neck demonstrated an irregular 3 cm × 2 cm × 2 cm solid mass in the posterior aspect of the left lobe of the thyroid, extending to the common carotid artery and to the pre-vertebral muscles, with which there was no interface (Fig. 1). The mass was hypoechoic relative to the thyroid with a mixed pattern of medium and low echogenicity and had irregular margins (Fig. 2).

At surgery, a solid mass measuring 3 cm in maximum diameter was found on the posterior aspect of the left lobe of the thyroid gland. The mass was adherent to the surrounding structures, including the oesophagus. No lymphadenopathy was noted. A left thyroid lobectomy was performed.

Histological examination showed that the tumour consisted of parathyroid chief cells with abnormal morphology and dense fibrous trabeculae. Areas of microcalcification and necrosis were also present. The margins of the tumour had invaded the thyroid capsule microscopically. The pathological diagnosis was parathyroid carcinoma.

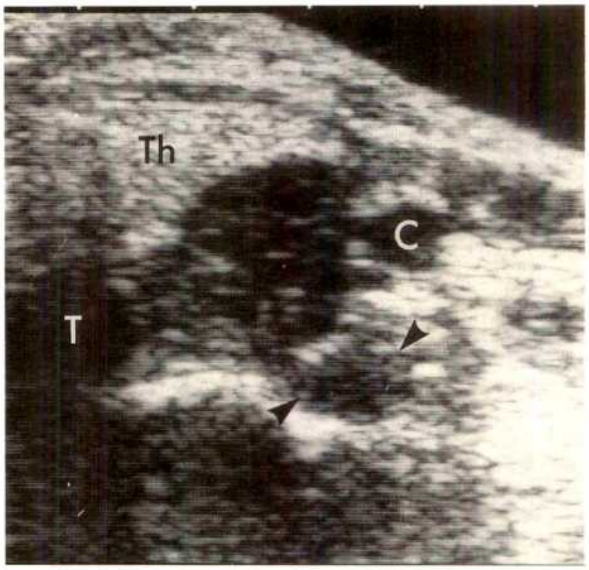

Figure 1. *Case 1.* Transverse view. The hypoechoic parathyroid carcinoma lies behind the echogenic left lobe of thyroid (Th) and extends posteriorly to the pre-vertebral muscles (arrows). (T = tracheal shadow; C = carotid artery.)

Case 2

A 61-year-old woman was investigated for symptoms of lethargy and bone pain of 9 months duration. She had lost 13 kg in weight and had developed persistent hoarseness. No abnormality was noted in the neck on physical examination. The right vocal cord was paralysed on pre-operative laryngoscopy. Serum calcium was 3.69 mmol/litre (normal range 2.20–2.63 mmol/litre).

Ultrasound showed a single, lobulated, 3.0 cm × 1.8 cm × 1.0 cm, mainly hypoechoic, solid lesion in the posterior aspect of the right lobe of the thyroid gland, which was closely applied to the trachea on its medial edge (Fig. 3). The borders of the mass were markedly irregular (Fig. 4) and it extended posteriorly through the thyroid capsule into the neurovascular bundle (Fig. 5).

At surgery, a tumour measuring 3 cm in maximum diameter was intimately adherent to the posterior aspect of the lower pole of the right lobe of the thyroid gland. The tumour enveloped the recurrent laryngeal nerve and was fixed to the trachea and oesophagus. Partial excision of the wall of the trachea was required to effect complete removal. No lymphadenopathy was identified. Histological examination showed abnormal large cells resembling parathyroid chief cells.

Address correspondence to: Dr B. D. Daly, Radiology Department, St James' University Hospital, Becket Street, Leeds LS9 7TF.

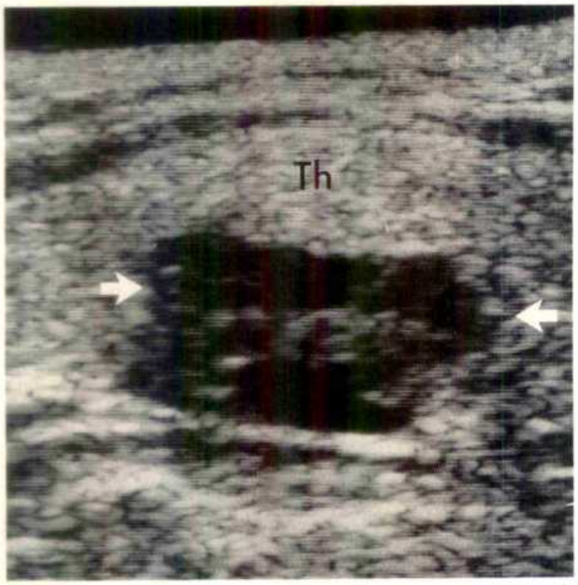

Figure 2. *Case 1.* Longitudinal view. Parathyroid carcinoma with mixed, low-echo texture and poorly defined margins (arrows) in keeping with local infiltration of the surrounding echogenic thyroid gland (Th).

Numerous areas of fibrous tissue within the tumour were invaded by the sheets of abnormal parathyroid cells. The microscopic and macroscopic features were considered typical of parathyroid carcinoma.

Discussion

The ultrasonographic appearances of parathyroid carcinoma have been previously described in a series of eight cases by Edmunson et al (1986). In that series the neoplasms were predominantly hypoechoic relative to the surrounding thyroid tissue, with a lobulated contour. Two of the cases in their series contained both hyper- and hypoechoic regions. The average diameter of the tumours was 2.4 cm. They concluded that in the absence of signs of frank invasion, which were noted in only two cases in their series, parathyroid carcinoma could not be differentiated accurately from parathyroid adenoma on ultrasound appearances alone.

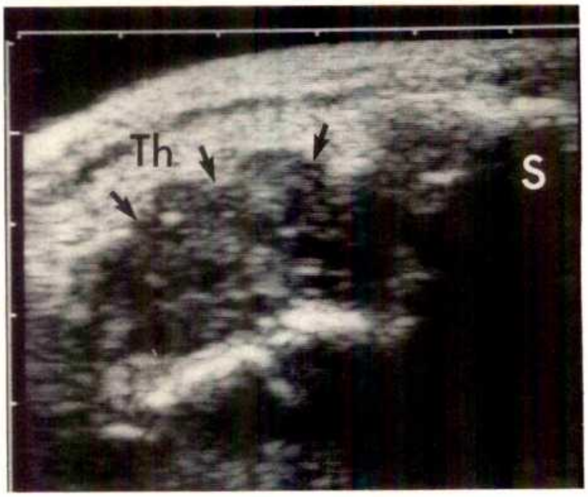

Figure 4. *Case 2.* Longitudinal view. Marked irregularity of tumour margins (arrows) and mixed internal echo texture are shown (S = sternal shadow; Th = thyroid).

Two further cases of parathyroid carcinoma have been described by Kinoshita et al (1985). Both of these

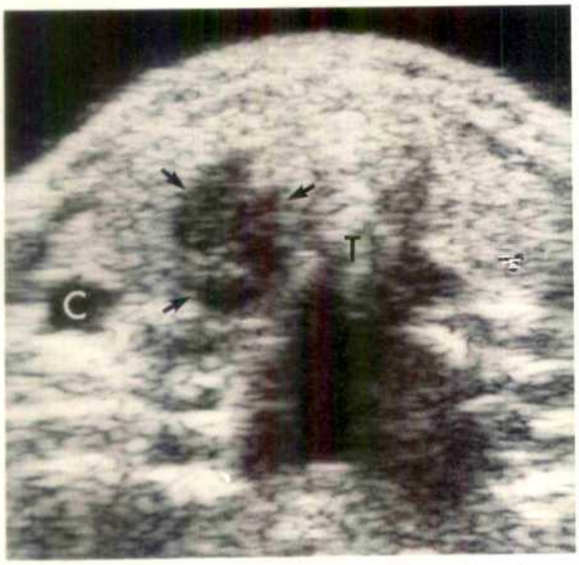

Figure 3. *Case 2.* Transverse view. Parathyroid carcinoma (arrows) lying adjacent to the trachea (T = trachea; C = carotid artery).

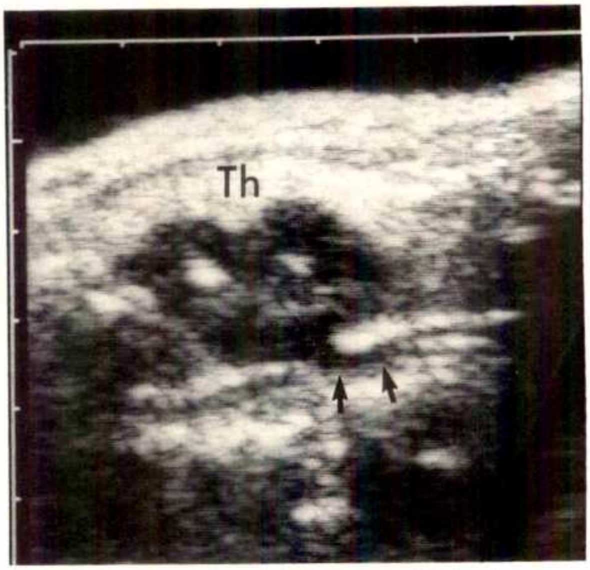

Figure 5. *Case 2.* Longitudinal view. Invasion of the neurovascular bundle by tumour (arrows) (Th = thyroid).

1989, *The British Journal of Radiology*, *62*, 1019–1021

cases were isoechogenic with the adjacent thyroid gland. Both tumours measured more than 2 cm in maximum diameter. The authors concluded that, where the echogenicity of a parathyroid tumour was high, it was more likely to be a carcinoma than an adenoma.

A single case of parathyroid carcinoma reported by Reading et al (1982) was hypoechoic relative to the surrounding thyroid gland, measured 2 cm in maximum diameter and was indistinguishable from parathyroid adenomas of similar size reported in the same series.

Both of the tumours described by us are similar in size to those previously reported, with maximum diameters of 3 cm in both cases. All of the parathyroid carcinomas reported to date have been 2 cm or more in diameter, which is larger in size than the average parathyroid adenoma (Graif et al, 1987), though some overlap of size does occur. The mixed, predominantly hypoechoic, internal echo pattern seen in both cases is also non-specific and may be seen with the degenerative changes that can develop in large parathyroid adenomas (Lees, 1987). However, in both of our cases the tumours had markedly lobulated and irregular margins on ultrasound, which were interpreted as suggestive of malignancy. Local invasion was also apparent, with extension of tumour posteriorly and loss of definition of the normal posterior margin of the thyroid gland in Case 1 and invasion of the neurovascular bundle by tumour in Case 2. The appearances were confirmed subsequently on pathological examination.

The pre-operative differentiation of parathyroid carcinoma from parathyroid adenoma is of considerable importance to the surgeon, warning of the need for more radical surgery. The suspicion that a parathyroid tumour may be carcinomatous may also help the pathologist, as the histopathological features of parathyroid carcinoma are difficult to distinguish from those of parathyroid adenoma and are often only made in retrospect with the development of local recurrence or metastases (van Heerden et al, 1979). Edmunson et al (1986) have suggested that gross invasion of surrounding structures by tumour is the only reliable sonographic feature that can distinguish parathyroid carcinoma from a large parathyroid adenoma. We would suggest, however, that where more subtle signs of local invasion and marked irregularity of tumour margins are noted, as in the two cases reported here, then malignancy should be suspected, especially where the tumour is 2 cm or more in diameter.

Acknowledgments

We would like to thank Mr George Scully for photographic illustrations and Mrs Patricia Grace for the manuscript.

References

Butch, J. R., Simeone, J. F. & Mueller, P. R., 1985. Thyroid and parathyroid ultrasonography. *Radiologic Clinics of North America*, *23*, 57–71.

Edmunson, G. R., Charboneau, J. W., James, E. M., Reading, C. C. & Grant, C. S., 1986. Parathyroid carcinoma: high frequency sonographic features. *Radiology*, *161*, 65–67.

Graif, M., Itzchak, Y., Strauss, S., Dolev, E., Mohr, R. & Wolfstein, I., 1987. Parathyroid sonography: diagnostic accuracy related to shape, location and texture of the gland. *British Journal of Radiology*, *60*, 439–443.

Kinoshita, Y., Fukase, M., Uchihashi, M., Takenaka, M., Hishikawa, R., Nakada, M., Nonaka, H., Kondo, T. & Fugita, T., 1985. Significance of pre-operative use of ultrasonography in parathyroid neoplasms: comparison of sonographic textures with histologic findings. *Journal of Clinical Ultrasound*, *13*, 457–460.

Lees, W. R., 1987. Ultrasound. In *Textbook of Radiology and Imaging*, ed. by D. Sutton (Churchill Livingstone, Edinburgh), Ch. 67, p. 1806.

Reading, C. C., Charboneau, J. W., James, E. M., Karsell, P. R., Purnell, D. C., Grant, C. S. & van Heerden, J. A., 1982. High resolution parathyroid sonography. *American Journal of Roentgenology*, *139*, 539–546.

Schantz, A. & Castleman, B., 1973. Parathyroid carcinoma: a study of 70 cases. *Cancer*, *31*, 600–605.

Van Heerden, J. A., Weiland, L. H., Remine, W. H., Walls, J. T. & Purnell, D. C., 1979. Cancer of the parathyroid glands. *Archives of Surgery*, *114*, 475–479.

Uterine leiomyomata: sonographic mimicry

By R. L. Borgstein, FRCR, J. J. Shaw, MRCOG and R. H. Pearson, FRCR

Departments of Radiology and Obstetrics and Gynaecology, Queen Mary's University Hospital, Roehampton Lane, London

(*Received March 1989 and in revised form May 1989*)

Leiomyomata (fibroids) are the commonest uterine tumours and they may vary widely in their sonographic appearance. We describe a case in which the appearance was that of a missed abortion and discuss the limitations of ultrasound in the differential diagnosis of fibroids. This case also highlights some of the benefits of per-operative sonography.

Case report

A 43-year-old Caucasian woman presented with heavy vaginal bleeding 4 days after the end of a normal period. On

---

Address correspondence to: Dr R. L. Borgstein, Radiology Department, The London Hospital, Whitechapel, London E1 1BB.

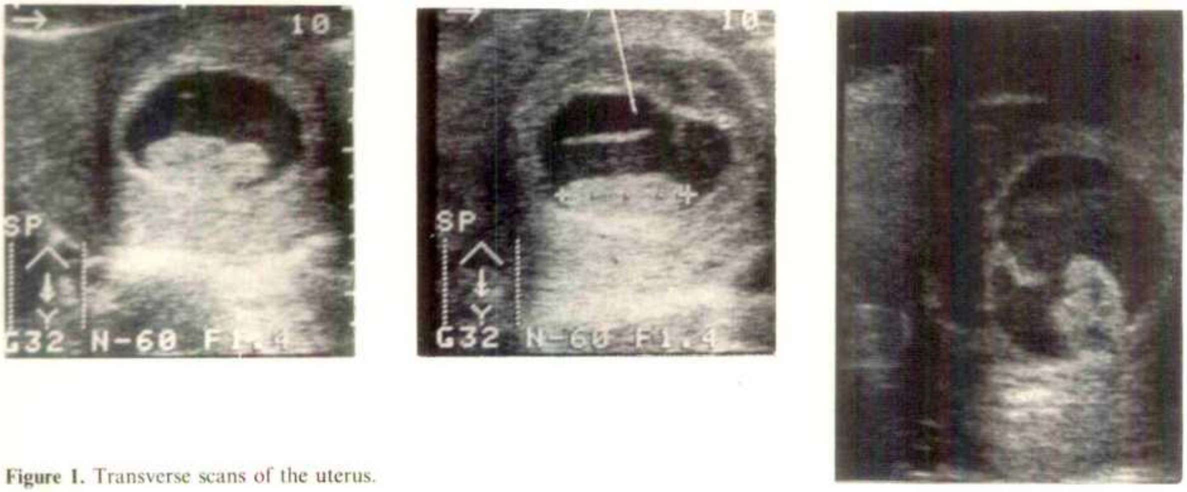

Figure 1. Transverse scans of the uterus.

admission she was found to be febrile and tachycardic. Examination revealed a tender, 15-week-size uterus, normal adnexae and no evidence of peritonism. A provisional diagnosis of degenerating fibroid was made and the patient was admitted for rest, observation and analgesia.

An ultrasound scan the next day was reported as follows: uterus 60 mm × 44 mm × 58 mm; remains of fetus seen; crown–rump length 38 mm (10–11 weeks). Placental tissue is noted on the anterior wall of the uterus with cystic areas within. A provisional diagnosis is missed abortion (Fig. 1).

On the basis of this report an evacuation of retained products of conception (ERPC) was performed. The uterine cavity was found to be deviated to the right but empty on curettage. The patient was re-scanned the same day; the previous findings remained unchanged and mobility of the "fetus" demonstrated by scanning in the upright position (Fig. 2). As the initial ERPC had been unsuccessful, a further evacuation was attempted under ultrasound guidance. The "sac" was found to be to the left of, and separate from, the uterine cavity.

It became apparent that we had been misled by an unusual appearance of a degenerating fibroid. Despite conservative management, the patient's condition did not improve and a total abdominal hysterectomy was carried out. Histology confirmed a solitary, degenerating, intramural fibroid.

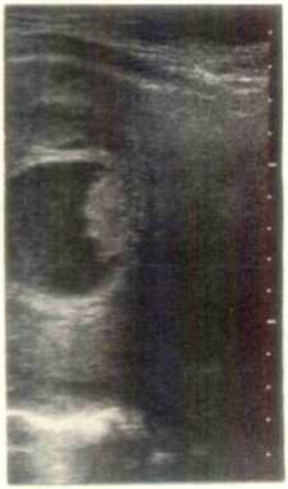

Figure 2. Longitudinal scan in the erect position.

Discussion

Uterine leiomyomata occur in 20–30% of women over 30 years of age and are often multiple. Depending on their location within the uterine wall, they are divided into submucous, intramural and subserous. They can also occur completely separate from the uterus, *e.g.* in the broad ligament, and retroperitoneally (Sarti, 1987). Hyaline and cystic degeneration are very common; calcification occurs infrequently, in less than 10% of cases (Blaustein, 1982).

The typical ultrasonographic appearance has been described as a homogeneous, hypoechoic area within the uterine wall causing deformity of contour. This seldom presents diagnostic difficulty unless located on the posterior or lateral aspects of the uterus, where it may be indistinguishable from an adnexal or pouch of Douglas mass (Sanders & James, 1985). With improved resolution it is now appreciated that there is a wider range of normal echo-texture depending on the ratio of fibrous tissue to smooth muscle (Sanders & James, 1985).

However, it is the degenerating fibroid that produces the more bizarre appearances that may cause diagnostic difficulty, particularly, as with this patient, if taken out of clinical context. The ischaemic degenerative process results in increased echogenicity and a more heterogeneous pattern. The differential diagnosis then includes uterine malignancy and gestational trophoblastic disease, as well as some solid ovarian tumours (Sarti, 1987).

With more extensive degeneration, cystic changes occur that appear as echolucent areas with posterior enhancement. These may coalesce to form larger, single (as in this case) or multiple cavities, the latter resembling a multiloculated ovarian tumour (Delarue et al, 1987).

Calcification within a fibroid appears as areas of increased echogenicity; often irregularly distributed throughout the mass. As the calcium content increases, acoustic shadowing is noted. With further calcification only an echogenic rim is visible, simulating a fetal head or fetal parts if incomplete (Lev-Toaff et al, 1987; Baltarowich et al, 1988).

In up to 98% of patients, fibroids are multiple (Sanders & James, 1985). This may cause considerable deformity of the uterine cavity, and in a woman of child-bearing age, care must be taken not to miss an early gestational sac (Grainger & Allison, 1986; Baltarowich et al, 1988).

Uterine leiomyomata have been shown to exhibit a wide range of sonographic appearances but this is the first report of a fibroid so convincingly mimicking a missed abortion. Equally misleading was the appearance of the anterior wall resembling placental tissue, albeit with cystic changes.

The role of ultrasound in obstetrics and gynaecology is no longer limited to its diagnostic aspects. It is becoming increasingly valuable in "blind" therapeutic procedures (as illustrated). Guidance through difficult terminations of pregnancy and even transvaginal extraction of submucous fibroids have been described (Darney, 1985).

Acknowledgments

We would like to express our thanks to Miss R. Dodd and Miss D. Z. Mohammed of the Ultrasound Department, and to the Photographic and Medical Illustration Departments, of Queen Mary's University Hospital.

References

Baltarowich, O. H., Kurtz, A. B., Pennell, R. G., Needleman, L., Vilaro, M. M. & Goldberg, B. B., 1988. Pitfalls in the sonographic diagnosis of uterine fibroids. *American Journal of Roentgenology*, *151*, 725–728.

Blaustein, A. (Ed.), 1982. *Pathology of the Female Genital Tract*, 2nd edn (Springer-Verlag, New York), pp. 353–356.

Darney, P., 1985. Sonographically guided extraction of a submucous myoma. *Obstetrics and Gynaecology*, *66*, 731–732.

Delarue, T., de Bosschère, J. P. & Lepechoux, Y., 1987. Un piège échographique: la dégénérescence pseudokystique des myomes utérins. *Journal de Gynecologie, Obstetrique et Biologie de la Reproduction*, *16*, 614–616.

Grainger, R. G. & Allison, D. J., 1986. *Diagnostic Radiology* (Churchill Livingstone, London), pp. 1606–1607.

Lev-Toaff, A. S., Coleman, B. G., Arger, P. H., Mintz, M. C., Arenson, R. L. & Toaff, M. E., 1987. Leiomyomas in pregnancy: sonographic study. *Radiology*, *164*, 375–380.

Sanders, R. C. & James, A. E., 1985. *Principles and Practice of Ultrasonography in Obstetrics and Gynaecology*, 3rd edn (Appleton Century Crofts, Norwalk, Connecticut), pp. 540–542.

Sarti, D. A., 1987. *Diagnostic Ultrasound. Text and Cases* (Year Book Medical Publishers Inc., Chicago), p. 691.

Ductal adenoma of the breast: mammographic appearances and pathological correlation

By E. Moskovic, MRCP, FRCR and *S. Ramachandra, MB, BS

Departments of Radiology and *Histopathology, Royal Marsden Hospital, Fulham Road, London SW3 6JJ

(*Received January 1989 and in revised form May 1989*)

Ductal adenoma of the breast is a little known and only recently described lesion. However, it is an important diagnosis to make since it is benign, despite simulating malignancy on both clinical examination and mammography.

Case report

A 72-year-old woman was referred to the Breast Unit at the Royal Marsden Hospital, complaining of a feeling of "thickening" within the lateral aspect of the left breast. Clinical examination revealed no discrete mass but there was a slight area of nodularity lateral to the left nipple, which was asymmetrical when compared with the corresponding area on the right.

Mammography was performed (Fig. 1) and revealed an area of grouped microcalcification deep and lateral to the left nipple with no associated soft-tissue mass. The calcifications were irregular and clustered, with a linear element. In view of the morphology of the calcification, biopsy was recommended on mammographic grounds, and together with the clinical findings, a diagnosis of malignancy was suspected.

Needle localization of the radiologically suspicious area was undertaken and subsequent surgical biopsy performed. The patient made an uneventful recovery.

The excised specimen was radiographed prior to histological examination (Fig. 2) and the calcification was noted to appear more discrete than on the pre-operative mammogram.

Pathological findings

The specimen comprised breast tissue within which there was a fairly well circumscribed nodule 0.8 cm in maximum diameter with a firm, white, gritty cut surface. This corresponded with the calcified area on the specimen radiograph. The surrounding breast tissue appeared unremarkable. On microscopic examination, a ductal adenoma was seen (Fig. 3). Papillary structures were absent but there were foci of myo-epithelial cell hyperplasia and prominent apical snouting of epithelial cells. A striking feature was the presence of large numbers of calcispherules, both within glandular lumina as well as in the

---

Address correspondence to: E. Moskovic, Department of Radiology, The Brompton Hospital, Fulham Road, London SW3 6HP.

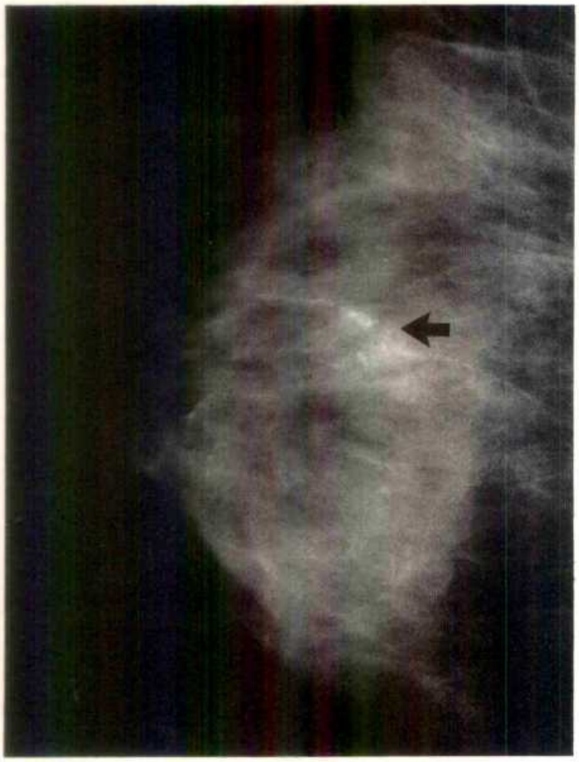

Figure 1. Left oblique mammogram showing an area of amorphous microcalcification (arrowed).

connective tissue stroma (Fig. 4). The edge of the lesion was fairly well circumscribed, but in one area the glands appeared to merge irregularly into surrounding fibrous tissue, mimicking infiltration. Mitoses were sparse.

The histological features conformed to those that have been described by Azzopardi and Salm (1984). The rest of the breast showed involutional changes, foci of duct ectasia and fibrosis.

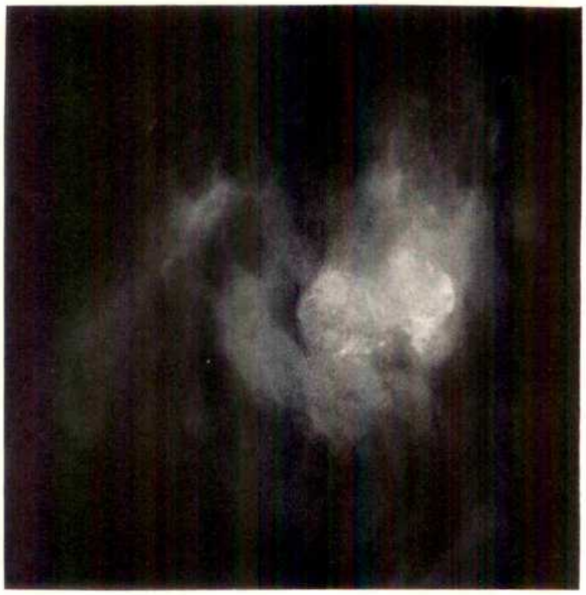

Figure 2. Detail of specimen radiograph following excision. The microcalcification appears better circumscribed.

Discussion

The term "ductal adenoma" of the breast was proposed in 1984 by Azzopardi and Salm following a review of 24 cases of this condition for which no description could be found in the existing literature. It is a benign, glandular entity arising in the more peripheral breast ducts, presenting often with a palpable lump, and, unlike the intraduct papilloma, not associated with a nipple discharge.

Of the 24 cases first described, the mean age was 51 years with only five patients younger than 40 years. Calcification was noted to be fairly common (nine out of 24 cases), but although some of these lesions were

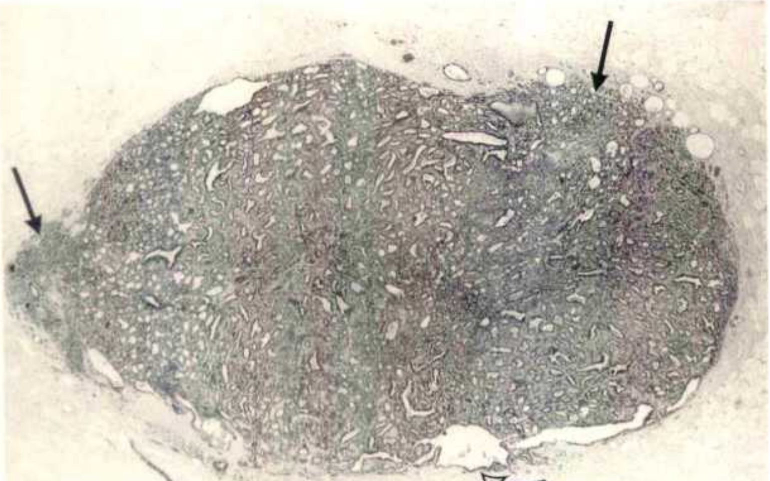

Figure 3. Histology of the ductal adenoma: low-power view. The remains of a duct lumen are seen (open arrow). The edge of the lesion is well defined but apparent "invasion" of the surrounding stroma is seen in two areas (arrows). Haematoxylin and eosin × 19.

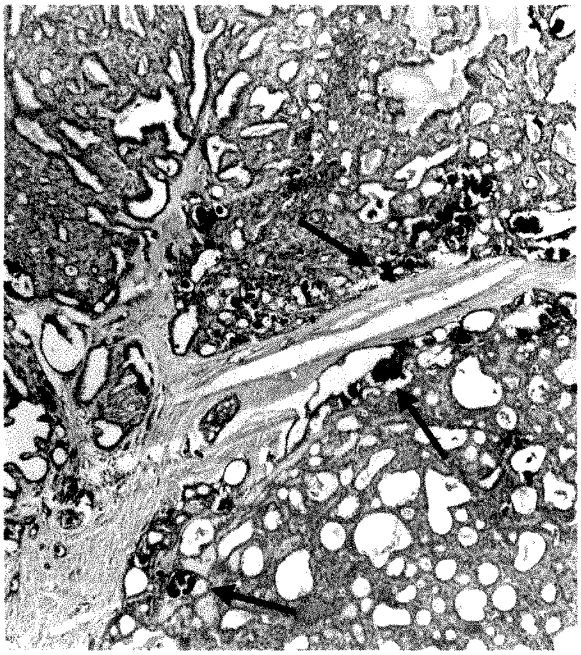

Figure 4. Histology at a higher magnification showing numerous calcispherules (arrows). Haematoxylin and eosin ×113.

detected radiologically, the mammographic appearances were not described. A fibrotic local reaction also occurs with apparent "invasion" of surrounding tissue, which has been mistaken previously, at frozen section, for malignancy. Multifocality was also seen in 10 cases.

The combination of a clinically palpable mass with radiologically suspicious calcification, histologically simulating a carcinoma, causes justifiable concern in an older patient. Therefore, the accurate identification of this tumour as an innocent lesion by fine-needle aspiration cytology and/or biopsy is necessary.

The radiological differential diagnosis lies between carcinoma, especially in the older patient, and fibrocystic disease including sclerosing adenosis.

Histologically, the ductal adenoma differs from the more common intraduct papilloma by the absence of papillary structures. It demonstrates a variety of patterns with glandular proliferation being the dominant feature. In some cases the presence of marked sclerosis and paucity of epithelial elements may cause difficulty in distinguishing the lesion from a sclerosing papilloma, or even sclerosing adenosis. It may bear a resemblance to the extremely rare pleomorphic salivary type adenoma of the breast (van der Walt et al, 1982), with which it has probably been confused in the past.

Ductal adenoma of the breast has been documented recently in a surgical journal (Scicolone et al, 1986) as causing confusion by mimicking a carcinoma, but we can find no reference to it in the radiological literature and its mammographic appearances to date have not been well described.

In conclusion, we feel that wider awareness of this benign entity amongst radiologists, surgeons and pathologists will minimize risk of confusion with a carcinoma. With the advent of the National Breast Screening Programme, we anticipate the discovery of more of these lesions, and hope that further information regarding their radiological appearances will become available.

Acknowledgments

Our thanks go to Dr Colin Parsons and Dr Cyril Fisher for their valuable advice and to Miss E. Rhatigan for typing the manuscript.

References

AZZOPARDI, J. G. & SALM, R., 1984. Ductal adenoma of the breast: a lesion which can mimic carcinoma. *Journal of Pathology*, *144*, 15–23.

VAN DER WALT, J. D. & ROHLOVA, B., 1982. Pleomorphic adenoma of the human breast. A report of a benign tumour closely mimicking a carcinoma clinically. *Clinical Oncology*, *8*, 361–365.

SCICOLONE, G., ZEN, F., VISONA, A., MOTTERVAN, F., CONTIN, F., BANO, A. & VINCENTINI, A., 1986. Ductal adenoma of the breast, correlation between clinico-radiological and pathological aspects. *Chirugia Italiana*, *38*, 543–548.

Agenesis of the salivary glands: a report of two cases

By A. M. Whyte, FFDRCSI, DDRRCR, FRCR and M. W. J. Hayward, FRCS, FRCR

Department of Radiology, University Hospital of Wales, Heath Park, Cardiff

(*Received September 1988 and in revised form May 1989*)

Congenital absence of the major salivary glands is uncommon with only a few reported cases in the world literature. Agenesis may be partial or total; the more severely affected patients suffer from a dry mouth, an increased rate of dental decay and difficulty in wearing dentures. Following exclusion of the more common causes of a dry mouth by the clinician, the diagnosis of salivary gland agenesis can be confirmed by computed tomography (CT) and a $^{99}Tc^{m}$-pertechnetate scintiscan.

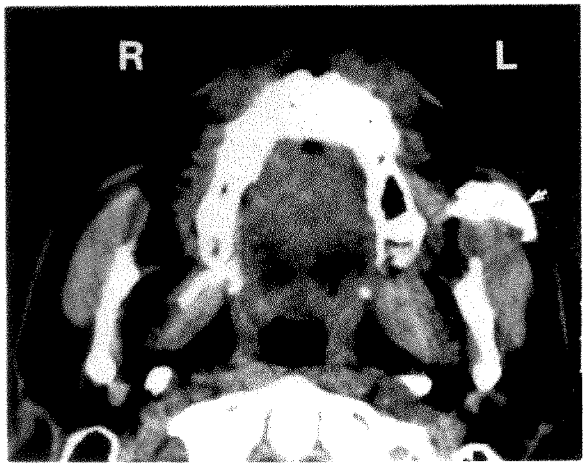

Figure 1. Computed tomographic scan showing absence of the parotid glands, which are replaced by fat (L + 58, W 250). There is a collection of Lipiodol ultrafluid anterior to the left masseter muscle (arrow).

Case reports

A 34-year-old man presented with a 9-month history of a slowly enlarging mass in the left cheek. On examination there was a small mass situated deep within the left cheek adjacent to the buccal mucosa. Intra-oral examination revealed an adequate amount of saliva, the dental decay rate was not excessive and there was absence of the parotid papillae. Computed tomography demonstrated a small collection of contrast medium from a previously attempted sialogram just anterior to the left masseter muscle and corresponding to the palpable mass. The injection of Lipiodol ultrafluid had been made at a site presumed to be the left parotid papilla. An incidental finding was bilateral absence of the parotid glands, the glandular beds being filled with fat (Fig. 1).

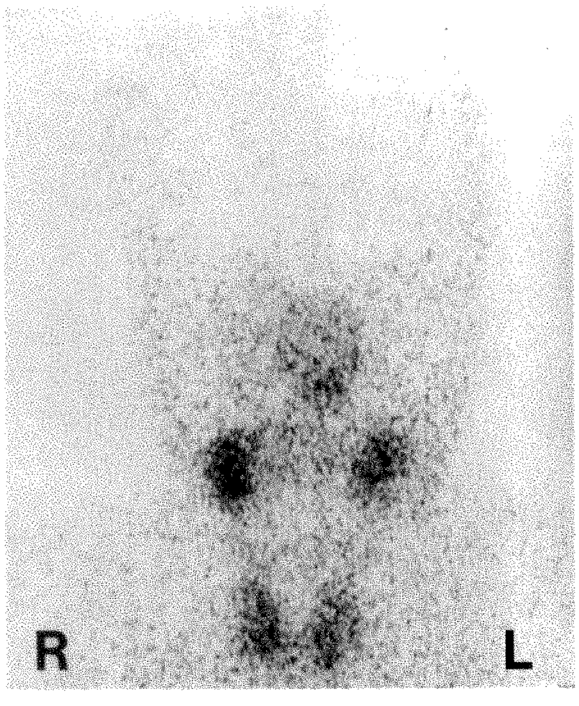

Figure 2. A ^{99}Tc^{m}-pertechnetate scintiscan demonstrating normal uptake in the submandibular glands and minor secretory glands of the nasal cavity and pharynx but no uptake in the parotid glands.

A ^{99}Tc^{m}-pertechnetate scintiscan demonstrated normal uptake of radionuclide by the submandibular glands and the minor secretory glands of the oral and nasal cavities (Fig. 2). The lesion in the left cheek was excised and found to be a cystic pleomorphic adenoma. It had presumably arisen within a minor salivary gland or possibly accessory parotid tissue.

Case 2

A 23-year-old woman presented with a long-standing complaint of a dry mouth. There was no significant medical history and the patient was not taking any medication. Intra-oral examination revealed marked dryness of the oral mucosa and there was bilateral absence of the parotid papillae and submandibular duct orifices. The patient's oral hygiene was excellent and there was little dental decay or tooth loss. Computed tomography demonstrated absence of the major salivary glands (Fig. 3). A ^{99}Tc^{m}-pertechnetate scintiscan confirmed the absence of uptake into the major salivary glands. Activity was seen in the minor secretory glands of the mouth, nose and pharynx (Fig. 4).

Discussion

Diminution in production of saliva leading to xerostomia may be primary, where a pathological lesion is present in the salivary glands, or secondary, where the salivary glands are normal and there is usually a metabolic upset or disturbance of the neurosecretory mechanism. Drugs acting by this secondary mechanism usually have anticholinergic or sympathomimetic activity and are the commonest cause of a dry mouth.

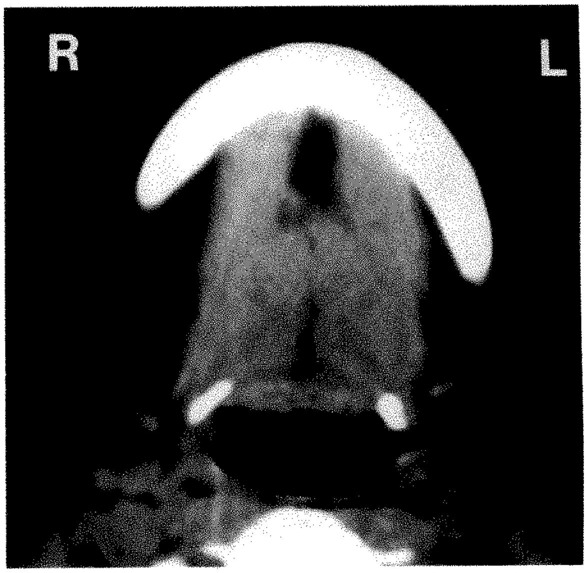

Figure 3. Computed tomographic scan demonstrating absence of the submandibular glands and replacement by fat (L + 50, W 250).

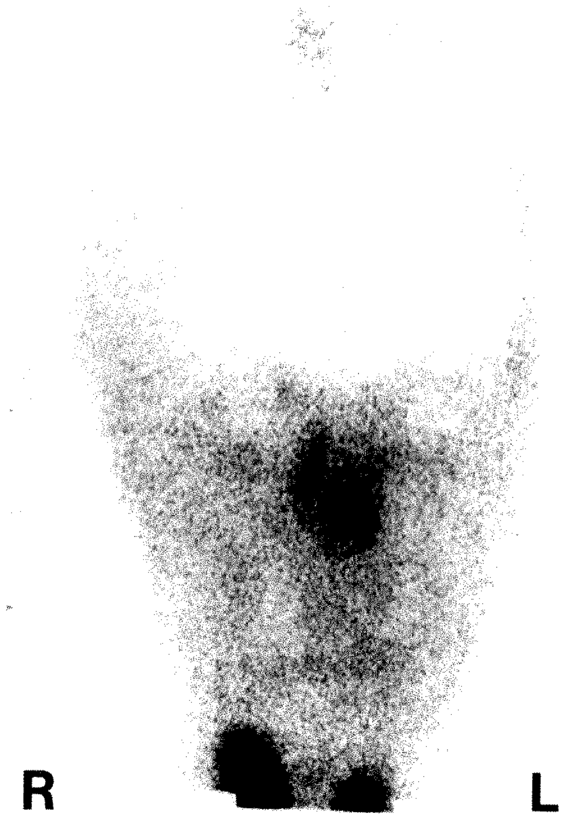

Figure 4. Total absence of uptake in the parotid and submandibular glands shown on scintigraphy.

Sjogren's syndrome, the commonest cause of primary xerostomia, results from autoimmune damage to the glands. Other causes of primary xerostomia include irradiation, recurrent infection and, rarely, agenesis of the major salivary glands (Mason & Chisholm, 1975). There are 28 reported cases of salivary gland agenesis in the world literature including the two current cases (Table I). This can be familial, usually with an autosomal dominant pattern of inheritance (Wiesenfield et al, 1983) and there is also a recognized association with lacrimal punctum aplasia and agenesis of the lacrimal glands themselves (Caccamise & Townes, 1980). Parotid gland agenesis can also be a feature of first and second bronchial arch anomalies occasionally being seen in mandibulofacial dysostosis (Cohen, 1974) and in those cases of hemifacial microsomia with marked facial soft-tissue and cranial nerve defects (David et al, 1987).

Table I. Reported cases of salivary gland agenesis

Reference	New cases reported	Other cases reviewed	Total
Mason & Chisholm (1975)	1	—	1
Smith & Smith (1977)	1	15	16
Wiesenfield et al (1983)	1	8	9
Whyte & Hayward (this study)	2	—	2
Total			28

The salivary glands originate from proliferating buds of epithelium that arise from the primitive oral cavity between the 4th and 12th week of intrauterine life. The parotid glands develop first followed by the submandibular, sublingual and minor salivary glands (Wiesenfield et al, 1983).

Agenesis of the major glands may be partial or total. Clinical suspicion of agenesis should arise when the papillae of the salivary gland ducts are absent. Total agenesis leads to marked reduction in salivary flow although some saliva will be produced by the minor salivary glands. This usually leads to an increased incidence of oropharyngeal infection including dental caries, premature loss of the dentition and extreme difficulty in wearing dentures (Mason & Chisholm, 1975). Partial agenesis would be expected to cause less severe symptoms and sequelae. The submandibular, sublingual and minor salivary glands make the most significant contribution to resting salivary flow and, as in the first case, parotid gland aplasia may not be noticed by the patient (Wisenfield et al, 1983). Management is supportive, including saliva substitutes, mouthwashes and rigorous oral hygiene.

Computed tomography and magnetic resonance imaging (MRI) are both capable of demonstrating the anatomical absence of major salivary gland tissue, the glandular beds being replaced by fat. ^{99}Tc^{m}-pertechnetate scintiscanning is a complementary examination in that it shows functioning salivary gland tissue, including the minor secretory glands of the nasal cavity and oropharynx, that are beyond the resolution of CT or MRI. Normally, the radionuclide is accumulated by salivary duct epithelium, maximum activity in the gland being attained 10–20 min after administration (Davies, 1980). Any cause of primary xerostomia can lead to disturbance in the active transport mechanism and reduced or absent uptake into the major salivary glands. Agenesis is unique in that there will be no evidence of glandular tissue on CT or MRI, whereas in conditions such as Sjogren's syndrome, glandular tissue, albeit abnormal, will still be present. Correlation of these imaging studies with the clinico-pathological findings allows a specific diagnosis of agenesis to be made.

Acknowledgments

We would like to thank Dr D. Murray Walker who referred the patients and Miss Diane Webb for typing the manuscript.

References

CACCAMISE, W. C. & TOWNES, P. L., 1980. Congenital absence of the lacrimal puncta associated with alacrima and aptyalism. *American Journal of Opthalmology*, *89*, 62–65.

COHEN, M. M., 1974. Mandibulofacial dysostosis. In *Birth Defects*, ed. by D. Bergsma (Williams and Wilkins, Baltimore), p. 465.

David, D. J., Mahatumarat, C. & Cooter, R. D., 1987. Hemifacial microsomia: a multisystem classification. *Plastic and Reconstructive Surgery*, *80*, 525–533.

Davies, E. R., 1980. Radioisotope imaging. In *A Textbook of Radiology and Imaging*, ed. by D. Sutton (Churchill Livingstone, London), p. 1337.

Mason, D. K. & Chisholm, D. M., 1975. *Salivary Glands in Health and Disease* (W. B. Saunders, London), pp. 120–124.

Smith, N. J. D. & Smith, P. B., 1977. Congenital absence of the major salivary glands. *British Dental Journal*, *142*, 259–260.

Wisenfield, D., Ferguson, M. M., Allan, C. J., McMillan, N. C. & Scully, C. M., 1983. Bilateral parotid gland aplasia. *British Journal of Oral Surgery*, *21*, 175–178.

An illustrative case: enough to raise one's blood pressure

By J. Herbetko, MRCP, FRCR, V. Batty, MSc, FRCR and *J. G. B. Millar, MSc, FRCP

Department of Radiology, Southampton General Hospital, Tremona Road, Southampton S09 4XY and
*Department of Medicine, Southampton University, Southampton

(*Received November 1988 and in revised form June 1989*)

A 64-year-old man was noted, during investigation of labile hypertension, to have marked central obesity and a plethoric facies. Tests revealed diabetes mellitus and consistently elevated urinary excretion of vanillylmandelic acid (VMA) at 1066, 661 and 500 μmol/24 h (normal range 7–85).

Imaging with meta-iodobenzylguanidine (MIBG) showed increased uptake in the region of the left adrenal gland (Fig. 1), and subsequent computed tomographic (CT) scans are illustrated in Fig. 2. A repeat CT scan 7 months following surgery is illustrated in Fig. 3.

On the basis of the first CT scan, further investigations were undertaken.

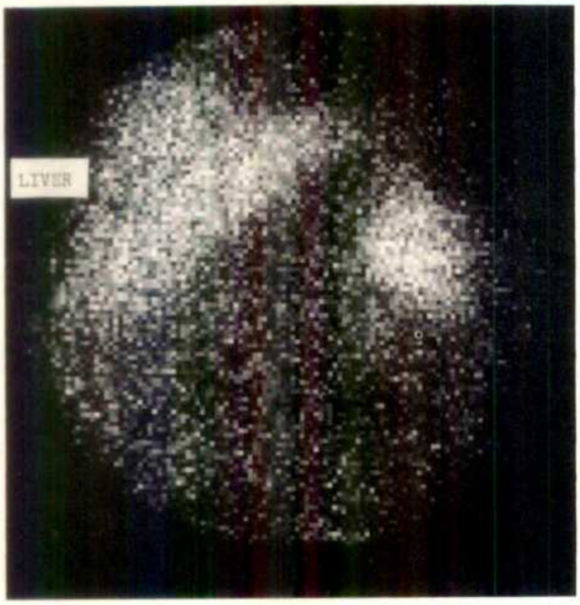

Figure 1. A MIBG image showing uptake in the liver and the left adrenal gland.

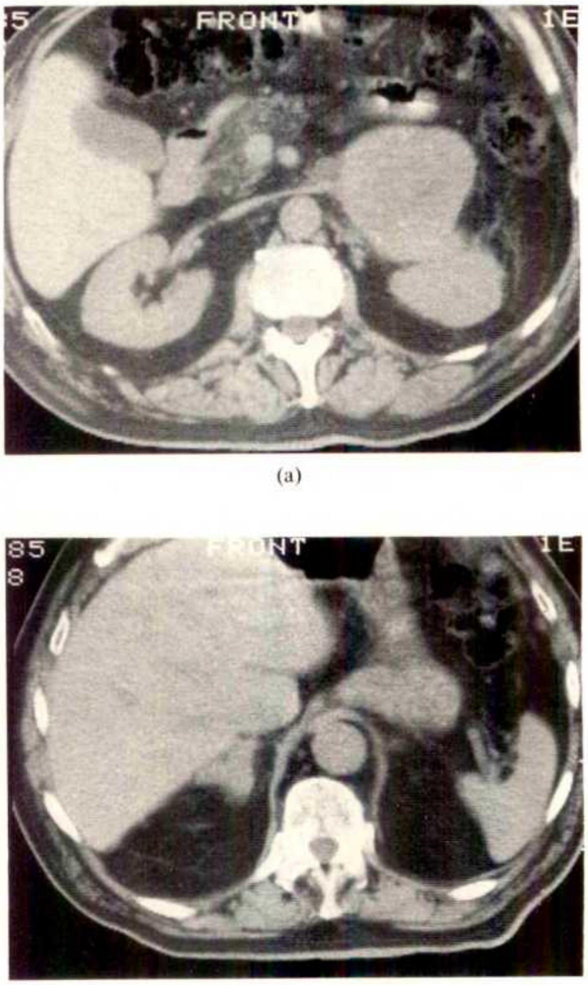

(a)

(b)

Figure 2. Abdominal CT images prior to surgery.

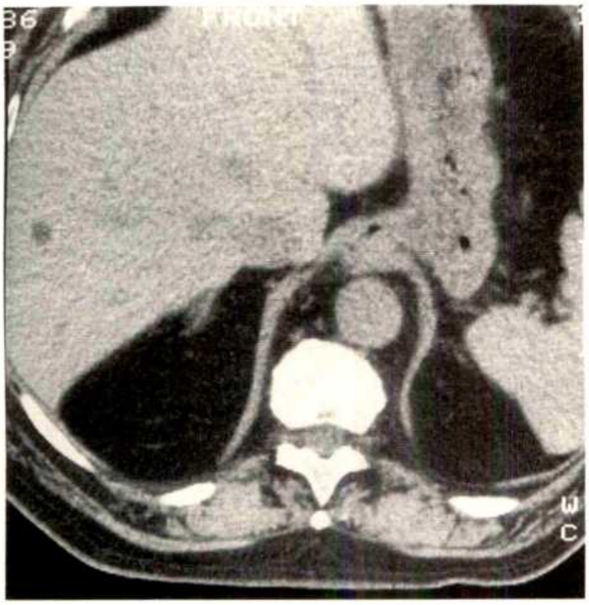

Figure 3. Abdominal CT image 7 months post-surgery.

The biochemical findings together with the MIBG image are diagnostic of a phaeochromocytoma.

The CT scan shows the presence of an 8 cm mass containing flecks of calcium, replacing the left adrenal gland, which confirms this diagnosis. In addition, there is marked hypertrophy of the right adrenal gland with preservation of its normal configuration, together with abundant retroperitoneal fat deposition.

These findings of adrenal hyperplasia and an abundant amount of fat can occur in Cushing's syndrome and this was confirmed on biochemical testing. Serum cortisol at 9.00 a.m. was >1932 nmol/litre (normal 200–700) and at 12.00 p.m. was 1874 nmol/litre (normal <200). On both low (0.5 mg 6-hourly) and high (2 mg 6-hourly) doses of dexamethasone, serum cortisol at 9.00 a.m. was >1932 nmol/litre. Plasma adrenocorticotrophin hormone (ACTH) at 9.00 a.m. was 399 ng/litre (normal <80). Plasma corticotrophin releasing factor (CRF) was 270 ng/litre (normal <100). At operation, high levels of both ACTH and CRF were found in the left adrenal vein compared with the superior vena cava. While lacking some of the features often seen in Cushing's syndrome (*e.g.* striae), the patient's appearance was highly suggestive of it.

Surgical removal of the phaeochromocytoma resulted in the return to normal of the right adrenal gland on subsequent CT 7 months later (Fig. 3), and the circulating levels of ACTH and CRF post-operatively were 24 ng/litre and <20 ng/litre, respectively. Serum cortisol levels were low, implying an inadequate stimulus to the remaining adrenal gland, and steroid support was therefore necessary post-operatively. Blood pressure and blood sugars returned to normal.

Histologically, the excised mass was a benign phaeochromocytoma. Tumour extracts were examined by radioimmunoassay and chromatography and shown to contain high concentrations of CRF and ACTH compared with normal adrenal gland tissue. The ACTH detected was not the high molecular weight form usually secreted by ectopic tumours. Tumour staining with ACTH anti-serum was negative although it has been postulated that a low storage capacity may be associated with a high secretion rate. Fuller biochemical details of this case have been reported elsewhere (Jessop et al, 1987).

At follow-up 3 years after diagnosis, the patient remained biochemically normal, apart from needing steroid support, and tumour-free.

Discussion

The commonest presentation of phaeochromocytoma is persistent hypertension although classically, but less commonly, this can be labile and severe. There are multiple additional symptoms reflecting catecholamine secretion, including anxiety attacks, tremor, sweating, arrhythmias and alteration of bowel habit.

In suspected cases of phaeochromocytoma, initial investigations are primarily biochemical with particular emphasis on 24 h urinary levels of adrenaline, noradrenaline, dopamine and their metabolites.

If the diagnosis is confirmed or if clinical suspicion remains high, then it is reasonable to proceed with radionuclide imaging with iodo-131-MIBG, if this is available, followed by CT. Alternatively, as CT is very reliable in locating phaeochromocytoma in the adrenal glands, this can be performed first followed by MIBG imaging if the tumour is ectopic.

Wide-field imaging at 24, 48 and 72 h following intravenous injection of MIBG has a high sensitivity in locating phaeochromocytomas, and has the advantage over CT in readily locating the 10% of cases that are extra-adrenal or multiple, in particular when these tumours are small or located in unusual sites such as the bladder or cardiac muscle.

The majority of extra-adrenal phaeochromocytomas occur in neural crest cells along the sympathetic chain adjacent to the abdominal aorta (Organ of Zuckerkandl) (Johnson et al, 1985). In addition, the 10% of malignant phaeochromocytomas will show concentration of radionuclide in metastatic lesions.

Cushing's syndrome occurs with increased blood levels of glucocorticoid steroids. These are either ACTH-dependent as seen in Cushing's disease, ectopic ACTH syndromes or iatrogenic ACTH administration, or non-ACTH-dependent as seen in adrenal adenoma, adrenal carcinoma or iatrogenic corticosteroid administration.

Ectopic ACTH is produced by a number of tumours including oat cell carcinoma, carcinoid, thymic malignancy, medullary carcinoma of the thyroid, islet cell tumours of the pancreas and, very rarely, phaeochromocytoma (Davies et al, 1982).

Hypertension is said to be commoner in the ectopic

ACTH syndromes and levels of ACTH and related hormones are generally higher.

In addition, weight loss, muscle weakness, pigmentation, fluid retention and hirsuitism are also commoner, whilst weight gain, obesity and striae are unusual.

Of the 18 previously reported cases of phaeochromocytoma producing ectopic ACTH, 17 were women and all tumours were benign and solitary (Fiorica et al, 1983; Lamovec et al, 1984; Shroeder et al, 1984; Bruining et al, 1985; Beaser et al, 1986).

References

BEASER, R. S., GUAY, A. T., LEE, A. K., SILVERMAN, M. L. & FLINT, L. D., 1986. An adrenocorticotrophic hormone-producing pheochromocytoma: diagnostic and immunohistochemical studies. *Journal of Urology, 135*, 10–13.

BRUINING, H. A., ONG, E. G. L., GERSHUNY, A. R. & LAMBERTS, S. W. J., 1985. Cushing's syndrome and phaechromocytoma caused by an adrenal tumour, also containing met-encephalin and somatostatin: a case report. *World Journal of Surgery, 9*, 639–642.

DAVIES, C. J., JOPLIN, G. F. & WELBOURN, R. B., 1982. Surgical management of the ectopic ACTH syndrome. *Annals of Surgery, 196*, 246.

FIORICA, V., MALES, J. L., KEM, D. C., DEBAULT, L. E. & KNICKERBOCKER, F. M., 1983. Cushing's syndrome from an ACTH-secreting pheochromocytoma. *Journal of the Oklahoma State Medical Association, 76*, 45–50.

JESSOP, D. S., CUNNAH, D., MILLAR, J. G. B., NEVILLE, E., COATES, P., DONIACH, I., BESSER, G. M. & REES, L. H., 1987. A phaeochromocytoma presenting with Cushing's syndrome associated with increased concentrations of circulating corticotrophin-releasing factor. *Journal of Endocrinology, 113*, 133–138.

JOHNSON, C. M., SHEEDY, P. F., WELCH, T. J. & HATTERY, R. R., 1985. CT of the adrenal medulla. *Seminars in Ultrasound, CT and MR, 6*, 219–239.

LAMOVEC, J., MEMOLI, V. A., TERZAKIS, J. A., SOMMERS, S. C. & GOULD, V. E., 1984. Pheochromocytoma producing immunoreactive ACTH with Cushing's syndrome. *Ultrastructural Pathology, 7*, 41–48.

SHROEDER, J. O., ASA, S. L., KOVACS, K., KILLINGER, D., HADLEY, G. L. & VOLPE, R., 1984. Report of a case of phaeochromocytoma producing immunoreactive ACTH and beta-endorphin. *Journal of Endocrinological Investigation, 7*, 117–121.

1989, *The British Journal of Radiology*, 62, 1029–1030

Case of the month

Common symptom: uncommon cause

By Kean T. Tung MA, MRCP and Graham F. Wilson FRCR, FFRRCSI

Department of Radiology, St Thomas' Hospital, Lambeth Palace Road, London SE1

(*Received June 1988 and in revised form July 1988*)

A 48-year-old Bangladeshi man presented with a 2-month history of low lumbar back pain radiating down the right leg. Otherwise he felt well and in particular suffered no cough, fever or weight loss.

Examination revealed local tenderness over the lower lumbar spine with decreased range of movements but no neurological deficit. The remainder of the physical examination was normal.

The chest radiograph (Fig. 1), lateral radiograph of the lumbar spine (Fig. 2) and ultrasound scan of the porta hepatis (Fig. 3) are shown below.

What is the most likely diagnosis?

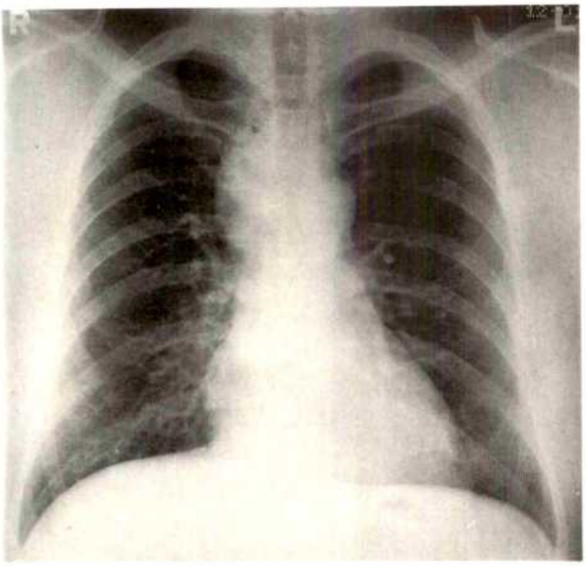

Figure 1. Chest radiograph.

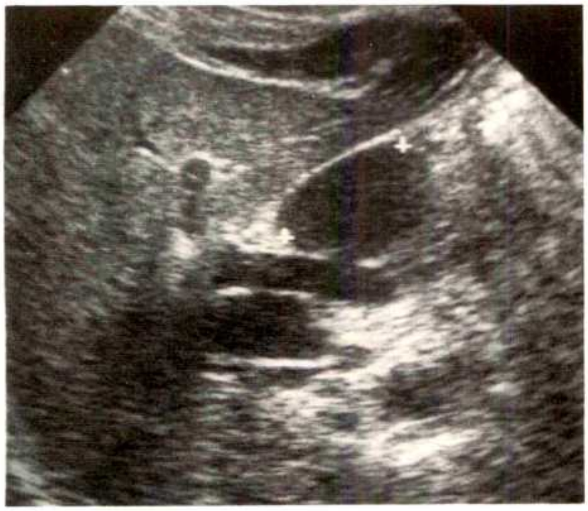

Figure 3. Oblique longitudinal ultrasound scan through the porta hepatis; remainder of abdomen was normal.

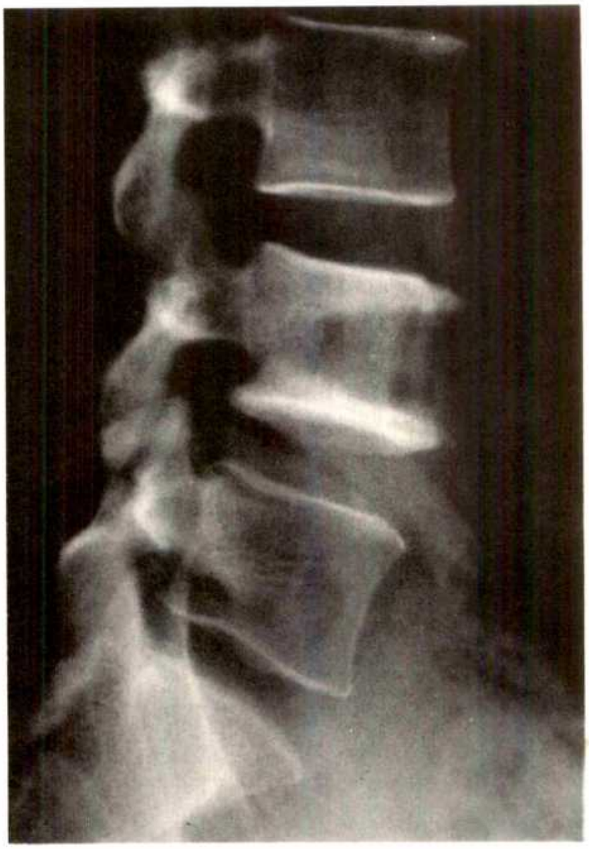

Figure 2. Lateral radiograph of the lower lumbar spine.

The chest radiograph shows right paratracheal lymphadenopathy with normal hila and clear lungs. The radiograph of the lumbar spine shows a wedge-shaped lytic defect with sclerotic margins in the anterior part of the body of L4 with normal adjacent end-plates and disc spaces. The ultrasound scan of the porta hepatis shows a round, hypoechoic mass typical of an enlarged lymph node lying anterior to the portal vein, which is seen entering the liver and dividing into right and left branches. Posterior to the portal vein, the inferior vena cava is seen running obliquely through the plane of the section.

Mediastinoscopy and biopsy of the paratracheal nodes demonstrated giant-cell granulomata and acid-fast bacilli on Ziehl-Nielson staining, confirming tuberculous lymphadenitis. The patient was started on antituberculous therapy comprising rifampicin, isoniazid and ethambutol. A follow-up chest radiograph at 3 months showed reduction in size of the paratracheal lymphadenopathy but the lumbar spine appearances were not significantly changed.

Discussion

Tuberculous lymphadenitis is still the most common form of non-pulmonary tuberculosis in England and Wales (National Survey of Tuberculosis Notifications, 1980), most often involving the cervical nodes. These patients usually present with neck swelling or minor constitutional symptoms. Abdominal lymphadenitis is unusual in developed countries, although in one survey of abdominal tuberculosis using computed tomography evaluation, adenopathy, including enlarged porta hepatis nodes, was the most common finding (Hulnick et al, 1985).

Skeletal tuberculosis accounts for almost 15% of non-pulmonary cases and lesions in the thoracic and lumbar vertebrae predominate. Infection is presumed to have spread by a haematogenous route from an infected focus elsewhere or alternatively from involved para-aortic lymph nodes in direct contact with vertebral bodies.

The most common radiological appearance is that of disc space narrowing with erosion of the adjacent end-plates but the subligamentous erosion of the anterior part of the vertebral body without disc involvement is a well recognized form (Chapman et al, 1979). Such anterior erosions may produce "gouge" defects similar to those occasionally seen in lymphoma. A destructive lesion with or without marginal sclerosis confined to a single vertebral body with normal adjacent discs and vertebrae is also a characteristic finding in spinal tuberculosis in patients originating from India, Africa and the Caribbean.

The differential diagnosis in our case includes lymphoma although the distribution of involved nodes with no peripheral lymphadenopathy and the unifocal bone involvement at presentation makes this diagnosis less likely.

In conclusion, the diagnosis of tuberculous lymphadenitis must be considered in Asian patients who present with unusual lymphadenopathy and destructive spinal lesions.

References

CHAPMAN, M., MURRAY, R. O. & STOKER, D. J., 1979. Tuberculosis of the bones and joints. In *Radiology of Tuberculosis*, ed. by B. Felson (Grune and Stratton, New York), pp. 80–96.

HULNICK, D. H., MEGIBOW, A. J., NAIDICH, D. P., HILTON, S., CHO, K. C. & BALTHAZAR, E. J., 1985. Abdominal tuberculosis: CT evaluation. *Radiology*, *157*, 198–204.

NATIONAL SURVEY OF TUBERCULOSIS NOTIFICATIONS IN ENGLAND AND WALES, 1978–79. Report from the Medical Research Council Tuberculosis and Chest Diseases Unit, 1980. *British Medical Journal*, *281*, 895–898.

1989, *The British Journal of Radiology*, *62*, 1031–1032

Short communication

Control of patient positioning for fast neutron therapy using positron emission tomography

By S. Vynckier, PhD, F. Vanneste, MSc, F. Richard, MD, *A. Bol, PhD, *C. Michel, PhD and A. Wambersie, MD, PhD

UCL-Cliniques Universitaires St-Luc, Brussels and *Positron Tomography Laboratory, Louvain-la-Neuve, Belgium

(*Received February 1989 and in revised form April 1989*)

With conventional photon therapy, radiographs are widely used for the verification of patient positioning. This method cannot be used with neutrons because of the poor sensitivity of standard films to neutrons compared with γ rays. In addition, there is little difference in energy absorption between bone and soft tissue for these neutron beams (Bewley et al, 1973; Catterall & Bewley, 1979).

The problem can be solved by introducing into the collimator, at the target position, a diagnostic X-ray tube (Risler & Wootton, 1988). Another approach entails visualizing the neutron-induced activity within the patient using positron emission tomography (PET). At high neutron energies, short-lived positron emitters are produced (Kleck et al, 1988; Vynckier et al, 1988) with activities sufficiently high to be visualized; the dose-equivalent rate close to the patient as a result of this activation is $\sim 30\,\mu\text{Sv h}^{-1}$ immediately after irradiation (Tatcher et al, 1987). The same approach was reported recently for pion radiotherapy (Goodman et al, 1986).

At Louvain-la-Neuve, fast neutron therapy is performed with fixed vertical neutron beams produced by 65 MeV protons on a beryllium target (*i.e.* p(65)+Be). The physical characteristics of the beam (*e.g.* percentage depth–dose and scattering) are comparable to those of an 8 MV photon beam (Vynckier et al, 1983). The neutron energy spectrum reaches a maximum of 65 MeV and has a mean energy of $\sim$ 30 MeV.

The PET camera is located in the same building, close to the neutron therapy room. The scanner is an ECATIII (model PT911/01) PET camera from CTI. The gantry consists of a ring with 512 BGO detectors, coupled to 512 phototubes. The spatial resolution in the tomographic plane is $\sim$8 mm with the filtering conditions generally used for reconstruction (Hoffman et al, 1986). In order to ensure reproducibility, the same flat bed is used at the PET scanner as at the neutron therapy facility. The scan plane is identified by skin marks and laser beams.

The positron emitters produced were identified as ^{15}O and ^{11}C, with half-lives of 122 s and 20.3 min, respectively. These are produced predominantly from the ^{16}O(n,2n)^{15}O and the ^{12}C(n,2n)^{11}C reactions. These reactions have a maximum in their cross-sections around 30 MeV and a threshold around 20 MeV. The ^{13}N positron emitter (from the ^{14}N(n,2n)^{13}N reaction and with a half-life of 9.9 min) was not identified owing to a lower nitrogen concentration in tissue.

The patient scan is taken approximately 5 min after irradiation for a scan time of 10 min. At that moment, the total activity in the patient is typically 2–3 MBq depending on the dose given. In order to correct for attenuation inside the patient, a 10-min transmission scan is taken directly after the emission scan, under the same conditions, using an external ring source. The patient and lung contours can easily be drawn on the reconstructed attenuation image. In order to avoid distortion in the activity distribution when more than one field is given shortly after each other, the fields are currently scanned one by one on successive days.

As an example, the treatment of a 26-year-old man with a neurofibrosarcoma of the mediastinum is discussed. A neutron boost was applied with two parallel, opposed, oblique neutron beams avoiding the spinal cord. The dose distribution is presented in Fig. 1. Positioning of these oblique fields was difficult since only a vertical neutron beam is available. A control with a PET scan was therefore useful.

The resulting PET scan is shown in Fig. 2. It illustrates the transmission scans and the activity distributions for the oblique neutron fields. The decrease with depth of activity corresponds with the decrease of absorbed dose with depth. A comparison with a conventional CT scan proves that no activity was found in the spinal cord region (*i.e.* no absorbed dose), which proves that the oblique neutron fields were well positioned. The induced activity of the oblique posterior field was counted 2 min later than in the anterior field, which explains the lower activity. This method is particulary powerful since the PET scan can easily be obtained with the dose of one fraction. In case of unsatisfactory positioning, corrections can be made the next day.

For other diagnostic verifications, more sections should be made when the sensitive structure bends. If a high-quality picture is required, this should be taken at the next therapy session.

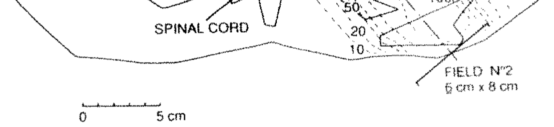

Figure 1. Dose distributions for the treatment of neurofibrosarcoma of the mediastinum with two oblique neutron fields. Isodose values are normalized to the dose at the specification point (+).

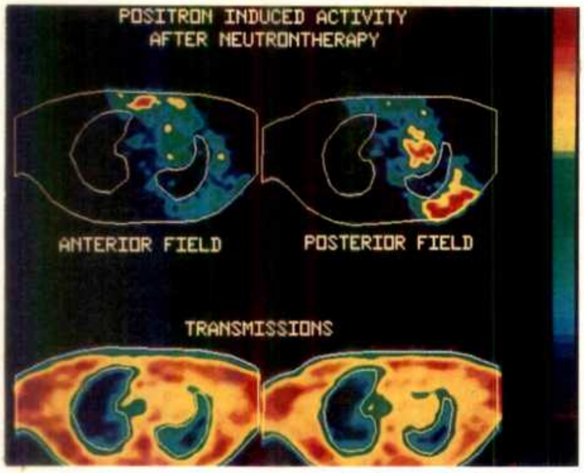

Figure 2. Positron emission tomographic images for the oblique anterior (left) and the oblique posterior (right) neutron field. The corresponding transmission scans are shown at the bottom of the figure.

It can be concluded that PET can be used to control the patient beam positioning. However, this approach has two important limitations.

1. The measurements have to be performed immediately after the therapy session because of the short half-lives of the positron emitters. Therefore, the PET facility has to be located close to the treatment facility.
2. High neutron energies are required (at least p(40) + Be) since the cross-sections of these reactions have a threshold around 20 MeV.

References

Bewley, D. K., Catterall, M. & Page, B. C., 1973. Medical radiography with fast neutrons. *British Journal of Radiology*, *46*, 24–29.

Catterall, M. & Bewley, D. K., 1979. In *Fast Neutrons in the Treatment of Cancer* (Academic Press, London).

Goodman, G. B., Lam, G. K. Y., Harrison, R. W., Bergstrom, M., Martin, W. R. & Pate, B. D., 1986. The use of positron emission tomography in pion radiotherapy. *International Journal of Radiation Oncology, Biology, Physics*, *12*, 1867–1871.

Hoffman, E. J., Phelps, M. E., Huang, S. C., Collard, P. E., Bidaut, L. M., Schwab, R. L. & Ricci, A. R., 1986. Dynamic, gated and high resolution imaging with ECAT III. *IEEE Transactions in Nuclear Science*, *33*, 452–455.

Kleck, J., Smathers, J., Myers, L., Mandelkern, M. & Digby, W., 1988. Fast neutron dosimetry using positron emission tomography. Proceedings of the World Congress on Medical Physics and Biomedical Engineering, San Antonio, 1988. *Physics in Medicine and Biology*, *33*, Suppl. 1, 5.

Risler, R. & Wootton, P., 1988. On the use of a separate X-ray portal film system with a leaf collimator for neutron therapy. Proceedings of the European Cyclotron Meeting, Uppsala, 1988, in press.

Tatcher, M., Rosenberg, I. & Couch, J. G., 1987. Dose to radiotherapy technologists from activation of patients at a fast neutron therapy facility. *Health Physics*, *53*, 311–312.

Vynckier, S., Pihet, P., Flémal, J. M., Meulders, J. P. & Wambersie, A., 1983. Improvement of a p(65) + Be neutron beam for therapy at Cyclone, Louvain-la-Neuve. *Physics in Medicine and Biology*, *28*, 685–691.

Vynckier, S., Vanneste, F., Richard, F. & Wambersie, A., 1988. Treatment planning for neutron therapy. *Radiation Protection Dosimetry*, *23*, 463–469.

1989, *The British Journal of Radiology*, *62*, 1033–1034

Correspondence

(The Editors do not hold themselves responsible for opinions expressed by correspondents)

An interesting radiation protection finding around a linear accelerator

THE EDITOR—SIR,

While commissioning an Asea Brown Boveri (ABB) Dynaray-LA20 linear accelerator, some unexpected results were obtained during radiation leakage measurements around the treatment head, as reported below.

Basically, radiation dose measurements were being made to confirm that the accelerator complied with International Electrotechnical Commission (IEC) requirements, as specified by BS 5724, Section 2.1 (British Standards Institution (BSI), 1984). These were undertaken using a Nuclear Enterprises Ionex dosemeter Type 2500/3 in conjunction with a Farmer Type 2571 0.6 cm^3 thimble ion chamber, following the protocol detailed in paragraph 31.3 of BS 5724, Section 2.1.

Consequently, the collimators were closed and the small residual aperture covered by three-tenth-value layers of lead, and readings were taken over a 2 m radial plane perpendicular to the beam axis at 1 m from the X-ray focus (*i.e.* in the isocentre plane). Typical results are detailed in Table I and are expressed as a percentage of the main beam set dose; the uncertainty in each result does not exceed ±1.5% of the stated value. Whilst the readings generally were within the specification of the IEC/BSI, it was noted that these did not increase with increasing radial distance from the isocentre and, most surprisingly, the measured values for photons generated at 6 MV exceeded those for 16 MV photons. As may be seen from Table II, the magnitude of the 6 MV measurements are reduced more significantly than those at 16 MV, when the measuring chamber was screened by a 50 mm block of lead; this confirms the lower quality of the leakage radiation at 6 MV. A radiograph, using Kodak XV2 film and taken previously at the collimator housing, had revealed two radiation "hot spots" for 16 MV photons. Following these results, this procedure was repeated and a further radiograph was taken with 6 MV photons; this revealed a larger, quite separate, "hot spot" that had not appeared on the 16 MV radiograph. For nominal beam qualities of 6 MV, the magnitude of radiation scatter laterally in cGy mA^{-1} min^{-1} differs by a factor of ~2 (Karzmark & Pering, 1973).

Table I. Comparison of percentage of set doses obtained at various radial distances from the isocentre using 16 MV and 6 MV generated photons

	Distance from isocentre (m)		
	0.5	1.0	1.5
% of set dose for 16 MV photons	0.02	0.03	0.01
% of set dose for 6 MV photons	0.06	0.14	0.06

Table II. Comparison of percentage of set doses obtained at 1.0 m distance from the isocentre for 16 MV and 6 MV generated photons with and without an extra 50 mm lead shielding for the measurement chamber

	Photon beam (MV)	
	16	6
% of set dose without 50 mm lead shielding	0.03	0.14
% of set dose with 50 mm lead shielding	0.02	0.02

In this case, this would appear to be compensated by the electron beam current being approximately 2.5 times greater at 6 MV than 16 MV; however, filtration and, consequently, mean spectral energy may differ. A definitive conclusion cannot, therefore, be reached but the results in Table I appear to be, at least in part, explicable by the greater magnitude of lateral scattering as a consequence of the greater beam current of the 6 MV beam. Variations in the path thickness of the head attenuation at different distances from the beam axis may also be a factor in explaining the variation in radiation dose with radial distance from the beam isocentre.

ABB have now produced modifications to the head shielding for this series of accelerators and the leakage has been greatly diminished. Whilst the findings for our particular installation are now acceptable, it may nevertheless be prudent, in the general case, not to assume that protection problems with dual photon energy accelerators will diminish at the lower beam quality. It is essential that measurements be undertaken at all beam qualities or misleading findings may result.

Yours, etc.,

TOM CONERE
HENRY WEATHERBURN
*BERNARD WASSEM

Department of Bio-Medical Physics
and Bio-Engineering,
University Medical Buildings,
Foresterhill, Aberdeen AB9 2ZD and
*Asea Brown Boveri,
CH-5401 Baden,
Switzerland

(*Received June 1989*)

References

BSI, 1984. *Medical Electrical Equipment, Section 2.1*, BS 5724 (British Standards Institution, London).

KARZMARK, C. J. & PERING, N. C., 1973. *Physics in Medicine & Biology*, *18*, 321–354.

Visits to controlled areas in X-ray departments

THE EDITOR—SIR,

The Southampton Health District receives many requests from school children who wish to visit X-ray departments as part of their school activities. Such visits could prove beneficial in terms of future recruitment.

Although some Health Authorities insist that no person under 18 years of age should be admitted to controlled areas in X-ray departments, it was recently agreed by members of the Southampton Radiation Protection Supervisors' Committee that such visits should be permitted. Members of staff in X-ray departments have been told that school children and all visitors may visit controlled areas providing they are supervised at all times and are fully subjected to the Local Rules and systems at work.

It was felt that the standard of protection is high in such areas and that there should be no problem, providing visitors are stationed behind the protective screens away from the primary beam and scattered radiation.

The rule that no one under 18 years of age can be employed to work in controlled areas still applies. My colleagues and I would welcome any comments on this decision.

Yours, etc.,
B. A. GODDARD

District Management Offices,
Western Hospital,
Oakley Road, Millbrook,
Southampton S09 4WQ
(*Received June 1989*)

(*It has just been drawn to our attention that this letter appeared in* Radiography Today, *August 1989.*)

British Standards specification for balloon dilatation catheters

THE EDITOR—SIR,

Some of your readers may like to know that a draft specification for balloon dilatation catheters has been prepared by the British Standards Institution. This draft is now available for public comment and can be obtained from the Sales Administration (Drafts), British Standards Institution, Linford Wood, Milton Keynes, MK1 46LE. Apparently the cost for this is £8.

Anyone wishing to comment on this draft specification can communicate their comments directly to the British Standards Institution. I represent the Royal College of Radiologists on the committee that developed this draft standard and I will also be happy to receive any comments from interested cardiologists and radiologists working in this field.

Yours, etc.,
GEORGE HARTNELL

Department of Radiology,
Bristol Royal Hospital for Sick Children,
St Michael's Hill,
Bristol BS2 8BJ
(*Received June 1989*)

Radiological appearances of colonic ring staple anastomoses

THE EDITOR—SIR,

We read with interest the article in *BJR* by Dr Daley and Mr Crowley (1989) relating the plain radiographic appearances of colonic staple ring to possible anastomotic dehiscence. They suggest that urgent water-soluble contrast medium enema should be performed to confirm the diagnosis. While agreeing with the principle, we would like to point out that the risk to a low rectal anastomosis with such a confirmatory enema must be seriously considered. To minimize such a risk, post-operative rectal examination is kept to a minimum and contrast enema is sometimes delayed for 14 to 21 days to allow the anastomosis to heal (Heald & Leicester, 1981). A soft Foley catheter can be used in place of the more rigid enema tube, although catheter trauma may still be implicated in the disruption of the anastomosis (Shorthouse et al, 1982). A covering colostomy in the presence of a high-risk anastomosis provides a convenient alternative route for contrast medium administration. As this obviates the risk of per rectum investigation, loopography is understandably favoured by some surgeons prior to colostomy closure.

Another relevant point is the difference between radiological and clinical leakage. One wonders if this difference is at least in part attributed to by the use of enema tubes and we would agree that a pre-contrast plain radiograph is mandatory to assess the integrity of the staple ring. A study of pre- and post-contrast staple ring apearances would determine whether radiological leakage is in any way associated with possible enema tube trauma.

Yours, etc.,
T. Y. K. CHAN
*T. DAVIDSON

Department of Radiology,
St Thomas' Hospital,
London SE1 and
*Department of Surgery,
Westminster Hospital,
London SW1P
(*Received May 1989*)

(*Authors' reply*)

THE EDITOR—SIR,

We welcome the comments of Mr Chan and Mr Davidson on our paper. We would, however, emphasize that we have recommended an urgent water-soluble "contrast" enema only in those cases where both a disrupted staple ring and the clinical situation have suggested dehiscence of the anastomosis. As illustrated by Case 6 in our series, early disruption of the staple ring alone is not invariably associated with anastomotic dehiscence.

We would also make the observation that contrast enemas via a colostomy site are also associated with a significant incidence of complications such as perforation and are especially hazardous if a catheter balloon is inflated within the colostomy (Ansell, 1976).

Yours, etc.,
B. D. DALY
B. M. CROWLEY

Department of Radiology,
St James' Hospital,
Beckett Street,
Leeds LS9 7TF
(*Received June 1989*)

References

ANSELL, G., 1976. *The Alimentary Tract in Complications in Diagnostic Radiology* (Blackwell, Oxford), pp. 333–369.

HEALD, R. J. & LEICESTER, R. J., 1981. The low stapled anastomosis. *British Journal of Surgery, 68*, 333–337.

SHORTHOUSE, A. J., BARTRAM, C. I., EYERS, A. A. & THOMPSON, J. P. S., 1982. The water soluble contrast enema after rectal anastomosis. *British Journal of Surgery, 69*, 714–717.

1989, *The British Journal of Radiology*, *62*, 1035–1036

Book reviews

Pioneers in Angiography. The Portuguese School of Angiography, 2nd edn. Ed. by J. A. Veiga-Pires and Ronald G. Grainger, pp. 192, 1987 (MTP Press, Lancaster).
ISBN 0-85200-828-7

Sir Hugh Cairns, in introducing Almeida Lima's book *Cerebral Angiography* (Oxford University Press, 1949)—the first English textbook on the subject—wrote: "The reader cannot but be impressed at how much was discovered in the early stages in Lisbon, and how little has since been added." Lima is said to have performed the first (cut-down) carotid angiogram in England in the 1930s during the 3 years that he spent in London acquiring neurosurgical skills from Cairns. However, Lima himself credited Norman Dott, the Edinburgh neurosurgeon, as being the British pioneer.

The origin of angiography in Portugal in 1927 is a fascinating story, and this book is the second English edition of a Portuguese *Festschrift* produced a decade ago to celebrate the 50th anniversary. The story is quite as exciting and improbable as the 15th century discovery of the sea-route to India, in which the Portuguese also held a monopoly. The Portuguese School of Angiography was founded by Egaz Moniz, professor of neurology in Lisbon and an intellectual polymath of Renaissance proportion. Among others, he filled the posts of ambassador to Spain, foreign minister and senior Portuguese delegate to Versailles, but his main interest lay in experimental medicine; in 1949 he received the Nobel Prize for discovering the operation of pre-frontal leucotomy. As a result of his innovative genius and perseverance, he successfully carried out the first human angiogram on 28th June 1927. By injecting a 25% solution of sodium iodide, he succeeded in recording intracranial arteries deviated by a pituitary tumour. In 1934 Moniz summarized the conclusions of his experiments in a work which was virtually the first angiographic textbook, *L'Angiographie Cérébrale* (Masson).

The gist of this book concerns the critical first 4 years of experiments (1927–31), the events of which are described by several of Moniz's acolytes. Distinguished Portuguese and foreign doctors (also Moniz himself) reminisce briefly over these heady days, and North Europeans and Americans trace the Lisbon link in angiography to their parts of the world. Moniz's success encouraged others around him. Theirs are names now largely forgotten, yet each was an experimenter in his own right and the father of his particular branch of angiography:

Acute and peripheral vessels—Reynaldo dos Santos;
Lung and heart—Lopo de Carvalho;
Lymph vessels—Hermani Monteiro;
Peripheral veins—Jao Cid dos Santos (Reynaldo's son);
Portal veins—A. de Sousa Pereira;
Rapid film changer (Radiocarousel)—Pereira Caldes.

World radiology owes a debt of gratitude to Portuguese medicine for offering the possibility of performing all types of angiography. Thus wrote Olle Olsson in 1981, and this book goes some way to pay that debt. I enjoyed reading the flowery Lusitanian phrases (wisely not clipped in translation to modern English usage) and the pioneers' reminiscences of the birth of angiography. All science historians must own a copy of this book, and all radiologists will find a professional connection within its pages to stimulate their interests.

E. H. Burrows

Atlas of Normal Roentgen Variants That May Simulate Disease, 4th edn. By Theodore E. Keats, pp. xv + 1085, 1988 (Year Book Medical Publishers, Chicago), £97.50.
ISBN 0-8151-5047-4

"Keat's Atlas" with its three previous editions has become established as a virtually essential bench book in all radiodiagnostic departments. Its continuing popularity has resulted in a fourth edition. How does it differ from the third? One thousand and eighty-five pages against 923, 3.56 kg against 3.51 kg, a much enlarged section on the cervical spine, increased coverage of joints and a general updating. The price is only a little more than the third edition. If one does not have any edition, one should probably rectify this promptly; if one owns the third, one might think that another £97 is not worth the difference in content; if the proud owner of earlier editions, it is probably worth giving them away and trading up to this new volume.

Donald Shaw

Frontiers in European Radiology 5. Ed. by A. L. Baert, E. Boijsen, W. A. Fuchs and F. H. W. Heuck, pp. vi + 176, 1988 (Springer-Verlag, Berlin), DM 180.
ISBN 3-540-17636-5 (Berlin)
0-387-17636-5 (New York)

The 5th issue of *Frontiers in European Radiology* contains four chapters. The first (by J. Buck) is on "Angiocinedensitometry of renal blood circulation by electrocardiogram-controlled injection and computer assisted evaluation". This is an experimental technique that very few radiologists will be familiar with. Angiocinedensitometry has so far not been applied widely to study circulation in various organs in a clinical setting and is not likely to in the future. Details of the method and experimental application in animals and in some patients are described. There is also a critical analysis of the limitations. The text is very well referenced but when one looks at the date of some of the references one appreciates that in the last few years this method of studying the circulation has not made any significant advance.

The second chapter (by Ch. L. Zollikofer) discusses the "Experimental basis of percutaneous transluminal angioplasty". This is an outstanding review providing very valuable information to all vascular radiologists. The field is covered very widely. The author discusses the mechanisms, macroscopic and microscopic changes in vessels following the procedure, as well as pharmacological phenomena and metabolic changes in the arterial wall following angioplasty. Finally he discusses the characteristics and physical properties of balloon catheters. This chapter is a very valuable contribution since percutaneous angioplasty is now such a well established procedure. The availability of such basic information is of great help to those interested in the technique. The review is also very well referenced.

The third chapter (by J. Pirschel) deals with "Ultrasound examination of the breast—diagnostic information related to mammography". This contribution is rather shorter, analyses the ultrasound examination of the breast and assesses its diagnostic value. It is a useful review and provides a very helpful evaluation of the indications and disadvantages of sonography compared with mammography.

The fourth chapter (by D. Poos and P. Capesius) discusses the value of "Computerized tomography in the diagnosis of pituitary microadenoma". This short review is of rather limited value since the information imparted is now well established and has been published extensively. On the other hand, for those who are interested in this particular subject it is quite helpful in view of the extensive references provided. The book is well produced, easily read and well annotated. Illustrations, too, are of good quality and clearly labelled. For the size of book (176 pages) it is rather expensive; nevertheless, there is a lot of valuable information that can only be found by a literature search. For this reason the book should be available in the libraries of all X-ray departments that are involved in the techniques discussed.

R. E. STEINER

Vascular Anatomy of the Spinal Cord. Neuroradiological Investigations and Clinical Syndromes. By Armin K. Thron; with Ch. Rossberg and A. Mironov (collaborators), pp. vi + 114, 1988 (Springer-Verlag, Vienna), DM 98.
ISBN 3-211-82015-9 (Vienna)
0-387-82015-9 (New York)

In this book a detailed description of the anatomy and physiology of the arterial supply and venous drainage of the spinal cord, nerve roots and spinal meninges is presented. Pathological processes affecting the spinal circulation and, in particular, the pathophysiology of angiomas, arterio-venous anomalies, compressive lesions and vascular obstructions are discussed. The book is logically arranged, well written and superbly illustrated, with photographs and diagrams of the surface vessels and injected specimens. Excellent radiographs include post-mortem and *in vivo* angiograms of the normal and of the various conditions presented. All the illustrations are adequately labelled and well described. The literature review is up to date and the book provides a clear exposition of current knowledge.

The book is highly specialized and is essential reading only for radiologists with a particular interest in spinal angiography. However, the author presents in an interesting manner the circulation disorders of the spinal contents and, in particular, the pathophysiology of angiomatous malformations and the mechanisms of production of symptoms; the book is good value for money and well indexed and it should be available for reference in departmental and medical libraries.

B. KENDALL

Clinical Imaging of the Cerebello-pontine Angle. By A. Valavanis, O. Schubiger and T. P. Naidich, pp. x + 202, 1987 (Springer-Verlag, Berlin), DM 198.
ISBN 3-540-16553-3 (Berlin)
0-387-16553-3 (New York)

This monograph is based on experience of 275 cases of cerebello-pontine (CP) angle mass lesion collected by its Swiss and American authorship. The majority (60%) of these are, of course, acoustic neurinomas, but a wide spectrum of pathology accounts for the remainder, and these are described and illustrated.

Introductory chapters cover an historical review of the subject, anatomy of the CP angle, and brief descriptions of the available computed tomography (CT) based imaging techniques such as water-soluble contrast media, and gas cisternography. The description of positive contrast medium injection prior to CT is slightly contentious; if contrast medium were run up following lumbar puncture with the patient in lateral decubitus position, one could then avoid the need for 60° head down tilting of a prone patient that is described. Furthermore, the standard technique for lateral cervical puncture in the UK is with the patient prone whereas this book describes a lateral decubitus position using undercouch fluoroscopy.

Abnormalities on plain radiography in the investigation of acoustic neurinoma are described but not illustrated, and it is perhaps a little frustrating that the authors do not comment on their use or advocacy of such studies.

Similarly, vertebral angiography is described in the context of acoustic neurinoma, but the reader is left wondering whether the authors believe it to be required prior to surgery.

The major part of the book sequentially describes the conditions comprising the differential diagnosis of a CP angle mass, including acoustic neurinoma, meningioma, epidermoid, arachnoid cyst, chordoma, rarer neurinomas, metastases, vascular malformations, etc. These are invariably illustrated by several excellent examples. The book closes with a chapter on magnetic resonance imaging with superlative images including examples of gadolinium enhancement. Finally, one of the book's strengths is the copious referencing of the text, more than 600 in all.

In summary, a comprehensive up-to-date account of CP angle imaging is presented here. Although for a necessarily limited and specialist readership, this book provides an excellent text and atlas. It can be highly recommended to all those neuroradiologists and neuroscientists who want to study the subject in more detail than given in standard radiological textbooks. It is handsomely produced and is good value for money.

A. R. VALENTINE

Breast Cancer Detection; Mammography and Other Methods in Breast Imaging, 2nd edn. Ed. by Lawrence W. Bassett and Richard H. Gold, pp. xvi + 204, 1987 (Grune & Stratton, Orlando), $59.00.
ISBN 0-8089-1842-7

The objective of the book is to set out the relative merits and limitations of the imaging methods currently available for breast cancer diagnosis. This is accomplished in a fair and accurate way. It is especially directed at those who "are seeking guidance on mammographic interpretation and in the selection of breast imaging equipment".

The expert authors who have contributed chapters are all well known and include Leicester Kalisher, Stephen Feig, Ed Sickles, Wende Logan, Myron Moskowitz and Richard Gold. Each selection is easily read, laid out in a logical way and contains a large volume of information. Some chapters are more relevant than others. The authors state that thermography is included simply because it is still in use in some centres and there are chapters on light scanning and magnetic resonance imaging since these are techniques still under evaluation. However, the main thrust relates to X-ray mammography including chapters on interpretation, mammographic technique, "the team approach", pre-operative localization, specimen radiology, magnification and the benefits and risks of the technique. The book has only 204 pages so to cover all of these subjects well, virtually every sentence carries an important message.

The editorial standard is very high with attractive page layout and good quality images. The text is complemented by a large number of relevant illustrations.

The book can be thoroughly recommended as a comprehensive introduction to mammography. The information provided here together with familiarity with an atlas of mammography, such as that written by Tabar, would provide the foundation necessary to start reporting mammograms.

C. A. PARSONS

1989, *The British Journal of Radiology*, 62, 1037–1042

VOLUME 62 NUMBER 744 DECEMBER 1989

The British Journal of Radiology

Ultrasound-guided chemical parathyroidectomy in patients with primary hyperparathyroidism: a prospective study

By Steen Karstrup, MD, *Ib Transbøl, MD, PhD, Hans Henrik Holm, MD, PhD, †Anders Glenthøj, MD and ‡Laszlo Hegedüs, MD

Departments of Ultrasound, †Pathology and ‡Internal Medicine and Endocrinology, Herlev Hospital, University of Copenhagen and *Department of Internal Medicine, Division of Endocrinology, Hvidovre Hospital, University of Copenhagen, Denmark

(*Received June 1989*)

Abstract. Twenty of 31 consecutive ultrasound examined patients with primary hyperparathyroidism were selected for treatment with ultrasound-guided percutaneous injection of ethanol (96%) into biopsy-verified solitary parathyroid tumours following a strict protocol with regard to dose, number of treatments and a minimum of 6 months follow-up. Of 18 patients completing the above protocol, a biochemical improvement was observed in 12, of whom eight became normocalcaemic during the follow-up period of 6 months after the last treatment. An obvious clinical improvement was seen in eight of the patients. In four patients, a unilateral vocal cord paralysis was observed, but was permanent in only one patient. Progressive fibrosis of the parathyroid tumours following injections impeded the intraglandular dissemination of ethanol. Another problem noted was the inability of ultrasound to detect multiglandular involvement. We find ultrasound-guided chemical parathyroidectomy an attractive alternative to surgery in patients who are not well suited for surgical intervention. However, the technique has not been fully developed, and in the present study, possible improvements are indicated.

The ability of ultrasound to localize enlarged parathyroid glands has been well documented since the first report by Arima et al (1975) (Butch et al, 1985; Winzelberg, 1987). A recent development in parathyroid ultrasonography has been the application of ultrasound-guided fine-needle aspiration biopsies (Solbiati et al, 1983; Rastad et al, 1984; Karstrup et al, 1988a) or histological microcore biopsies (Karstrup et al, 1989) in order to secure a reliable tissue diagnosis of the ultrasound-suspect parathyroid tumours.

The ability to place needles precisely in parathyroid tumours has provided new possibilities of percutaneous treatment. Preliminary results of percutaneous inactivation of parathyroid tumours using injection of absolute ethanol was first reported by Solbiati et al (1985). In six out of seven patients with hyperparathyroidism as a result of kidney disease, a clinical and biochemical improvement was observed following treatment. In addition, successful inactivation of hyperactive parathyroid adenomas in patients with primary hyperparathyroidism (PHPT) has been reported by Karstrup et al (1987, 1988b).

This treatment has hitherto been offered only to a few highly selected patients. Preliminary results have been promising. To evaluate the possible role and present limitations of the procedure, we present the results of ultrasound-guided chemical parathyroidectomy in a consecutive series of patients with PHPT.

Materials and methods

Patient selection

Thirty-one consecutive patients (26 females and five males) presenting with PHPT were examined. Median age was 62 years (range 39 to 81 years). The patients were selected according to the criteria given in Table I. Based on these criteria, 11 patients were excluded from the study because of non-visualization of a parathyroid tumour (six), mental instability (two), two preferred surgical treatment and one patient was excluded because

Table I. Pretreatment criteria for ultrasound-guided chemical parathyroidectomy

1. Ultrasound-detected solitary parathyroid tumour.
2. Parathyroid verification by ultrasound-guided fine-needle biopsy:
   (a) parathyroid cells with increased PTH content and/or
   (b) parathyroid tissue.
3. Normal function of vocal cords examined by indirect laryngoscopy.
4. Patient compliance.
5. Patient acceptance.

Address correspondence and reprint requests to: Steen Karstrup, MD, Department of Ultrasound, Herlev Hospital, DK-2730 Herlev, Denmark.

Table II. Patient data and ultrasound findings

Patients			Ultrasound findings		Ultrasound-guided biopsy		
No.	Age	Sex	Size (ml)	Site	Tissue	Cells	PTH gradient PT/TH (μg/l)
1	65	F	0.3	LI	None	+	5.2/0.3
2	68	M	1.0	LI	+	+	160/0.5
3	60	F	2.0	LS	+	+	4.7/0.3
4	42	F	1.0	RI	+	+	1.2/0.3
5	72	F	1.0	LI	+	+	20/2.6
6	69	M	0.2	LI	+	+	7.5/0.3
7	63	F	0.2	RI	+	+	17/0.3
8	66	F	1.0	LI	+	?	2.5/0.3
9	41	F	1.6	LI	+	+	385/0.3
10	47	M	0.3	RS	+	+	0.3/0.3
11	56	F	0.6	LS	+	+	34/1.2
12	60	F	0.9	RS	+	+	15/0.3
13	70	F	0.8	LS	+	+	4/0.3
14	49	M	0.3	LI	None	+	0.4/0.3
15	50	F	1.0	LS	+	+	39/7.4
16	81	F	0.8	RI	None	+	2.1/1.2
17	79	F	1.0	LI	None	+	40/0.3
18	49	F	1.0	LI	+	+	7.3/6.4
19*	74	F	0.9	RI	+	+	3.4/0.5
20*	41	F	0.6	RI	+	+	1.7/0.3

RS = right superior; RI = right inferior; LS = left superior; LI = left inferior; PT = parathyroid; TH = thyroid.
+ = positive verification; ? = non-conclusive examination; none = no tissue for examination.
*Patients excluded during the period of treatment.

of an abnormal indirect laryngoscopy. Thus, 20 patients (16 females and four males) (Table II) entered the study. Median age was 65 years (range 41 to 81 years).

Design of study

Ninety-six per cent ethanol was used. The dose was calculated as half of the volume of the parathyroid tumour (half of the product of maximum length, width and depth). A maximum of three treatments with an interval of 1 month between treatments was given. Routine blood tests including serum concentrations of ionized calcium, total calcium and C-terminal parathyroid hormone (PTH) were performed prior to treatment—generally 1 month after the ultrasound-guided biopsy—as well as during the period of treatment. Following the last treatment, blood tests were carried out after 3 and 6 months. Indirect laryngoscopy was performed routinely before treatment and after the final treatment.

Technique for examination and treatment

The ultrasound examinations were performed with a 7 MHz sector scanner (Brüel and Kjaer) mounted with a needle steering device for precise ultrasound-guided punctures. Tissue diagnosis was obtained using fine-needle (0.6 mm) aspirations for cytological examinations (Glenthøj & Karstrup, 1989) and immunochemical PTH measurements (Doppman et al, 1983; Karstrup et al, 1988a). Histological diagnoses were obtained using a 21-gauge (0.8 mm) cutting needle (Sure-cut) (Karstrup et

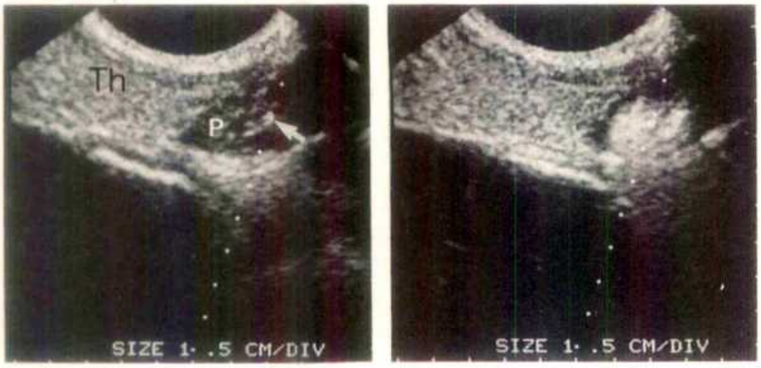

Figure 1. Longitudinal scans of the neck showing a parathyroid tumour (P) (Th = thyroid gland). In (a) the needle-tip echo is seen inside the parathyroid tumour (arrow). In (b) the parathyroid tumour has become echogenic following intraglandular injection of ethanol.

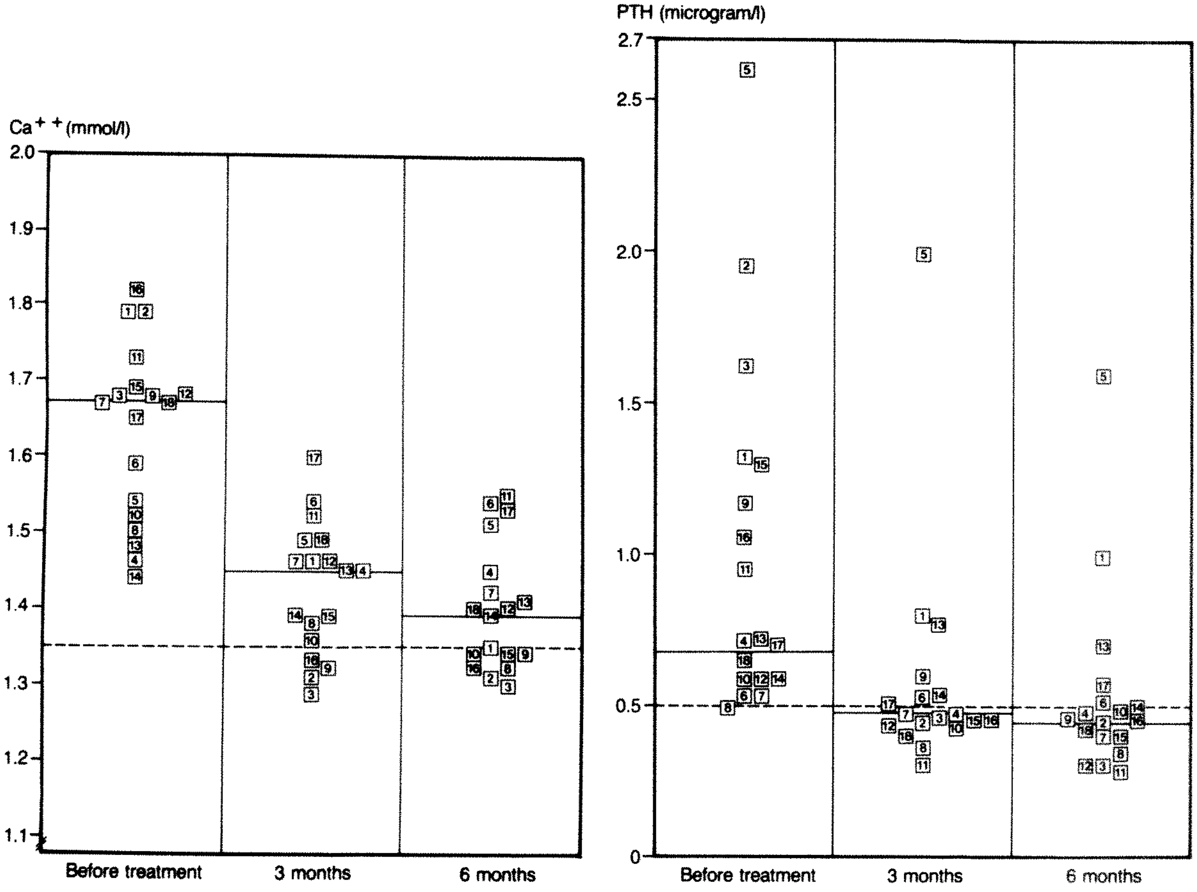

(a)

(b)

Figure2. (a) Serum levels of ionized calcium (Ca++) before treatment and 3 and 6 months after the last treatment. (b) Serum levels of parathyroid hormone (PTH) before treatment and 3 and 6 months after the last treatment. The dotted lines indicate the upper limit of the normal range. The solid lines indicate the median values.

al, 1989). All the fine-needle biopsies were performed according to principles previously described (Karstrup et al, 1988a).

Usually, the alcohol injection was performed on an outpatient basis with local anaesthesia. Initially, an outer guide needle (1.2 mm) was introduced through the skin and into the neck muscles. A 0.6 mm fine needle was inserted through the guide needle following an electronic puncture line (Fig. 1). When the needle-tip echo was seen inside the parathyroid tumour, ethanol was injected under continuous ultrasound guidance. During the first treatment, the ethanol was deposited centrally in the parathyroid tumour. During subsequent treatments, deposition of ethanol in non-fibrotic parts of the parathyroid tumour was attempted. All injections were recorded on videotapes. The procedure lasts 10–20 min.

Statistical analysis was performed using Wilcoxon's test for paired data. Probability values less than 0.05 were regarded as significant.

Informed consent was obtained in every case and the study followed the principles of the Helsinki Declaration II and was approved by the local ethical committee.

Results

The serum concentrations of ionized calcium and PTH in each patient before and after the treatment are given in Fig. 2. Two patients were excluded from the study during the period of treatment. One patient was lost to follow-up owing to discovery of a breast tumour, and another because of a transient paralysis of the vocal cord following the first treatment.

At 3 and 6 months after the last treatment, a significant decrease in serum concentration of ionized calcium, total calcium and PTH was demonstrated ($p<0.0001$). The median values and 95% confidence limits during the follow-up period are indicated in Table III. Eight patients had evident clinical improvement following the treatment (Table IV).

In the group of patients presenting with only kidney stones the follow-up period has been too short for

Table III. Biochemical values in 18 patients before and following treatment

	Ionized calcium	Total calcium	PTH
	(normal range 1.15–1.35 mmol/l)	(normal range 2.20–2.70 mmol/l)	(normal range 0.21–0.50 μg/l)
Before treatment			
Median	1.67	2.94	0.68
95% CL of median	1.50–1.69	2.77–3.09	0.57–1.7
Range	1.44–1.82	2.65–3.27	0.49–2.60
No. of patients with normal values	0 (0%)	3 (17%)	1 (6%)
3 months			
Median	1.45	2.53	0.47
95% CL of median	1.36–1.49	2.48–2.64	0.44–0.54
Range	1.29–1.60	2.37–2.80	0.31–2.00
No. of patients with normal values	4 (22%)	14 (78%)	11 (61%)
6 months			
Median	1.39	2.52	0.46
95% CL of median	1.34–1.45	2.45–2.59	0.41–0.53
Range	1.30–1.55	2.13–2.78	0.28–1.60
No. of patients with normal values	8 (44%)	15 (83%)	13 (72%)

CL = confidence limits.

Table IV. Clinical findings in 20 patients before and after treatment

Case no.	Main clinical manifestations	Associated disease	No. of treatments	Clinical improvement	Complication of treatment	OP
1	Fatigue	COLD, toxic goitre	3	None	None	No
2	Acute hypercalcaemic symptoms	Ischaemic heart disease	1	Yes	None	No
3	Skeletal pain	Non-toxic goitre	2	Yes	None	No
4	Fatigue	Toxic goitre	3	None	None	Yes
5	Skeletal pain	Hypertension	3	None	None	Yes
6	Asymptomatic	—	3	None	None	Yes
7	Nephrolithiasis	—	3	—	Vocal cord paralysis, permanent	Yes
8	Anorexia, weight loss	—	3	Yes	None	No
9	Nephrolithiasis	—	3	—	None	No
10	Nephrolithiasis	Hypertension	3	—	Vocal cord paralysis, 2 months	No
11	Skeletal pain	—	3	Yes	None	No
12	Swellings and pain of joints	—	3	Yes	None	No
13	Nephrolithiasis	Toxic goitre	3	—	None	No
14	Nephrolithiasis	—	3	—	None	No
15	Fatigue, muscle weakness	Rheumatoid arthritis	3	Yes	None	No
16	Acute hypercalcaemic symptoms	—	2	Yes	Vocal cord paralysis, 3 months	No
17	Fatigue, depression	Cerebral stroke	3	None	None	No
18	Fatigue, muscle weakness	Astrocytoma, epilepsy	3	Yes	None	No
19*	Asymptomatic	Hypertension	1	—	Vocal cord paralysis, 1 month	Yes
20*	Asymptomatic	Hypertension (breast tumour)	2	—	None	Yes

OP = operation (neck surgery); COLD = chronic obstructive lung disease.
*Patients excluded during the period of treatment.

conclusions. Additionally, it was the impression of the authors that patients generally felt an unspecific increase in mental as well as physical well-being. No scientific quantification of this was attempted.

Complications following treatment

In four patients, unilateral vocal cord paralysis was observed following treatment (Table IV). In three patients, this was transient lasting from 1 to 3 months. However, the recurrent laryngeal nerve paralysis seems to be permanent (12 months) in one patient who at present has no symptoms of hoarseness. No other complications were observed.

During the alcohol injection, most patients complained of moderate pain extending unilaterally to the jaw and teeth, disappearing immediately when injections were stopped.

Patients operated on

Six patients underwent operation (Table IV). In two patients (Cases 4 and 6), diffuse hyperplasia of the parathyroid glands was diagnosed. In the remaining four patients, a solitary parathyroid adenoma was found in accordance with the ultrasound findings. In the one patient with a permanent vocal cord paralysis, the parathyroid tumour was found to be surrounded by fibrosis involving the recurrent laryngeal nerve making surgery unusually difficult.

Patients initially excluded from the study

Of the 11 patients initially excluded, eight underwent neck surgery and all had a solitary parathyroid adenoma. Five of these adenomas were localized in accordance with the ultrasound findings, but three were found in the upper mediastinum.

Discussion

The fact that enlarged parathyroid glands can be detected by ultrasound and a correct tissue diagnosis made by ultrasound-guided fine-needle biopsies provide new possibilities for percutaneous treatment. The present study was prompted by preliminary observations in which parathyroid adenomas have been successfully inactivated using percutaneous injections of ethanol under continuous ultrasound guidance (Karstrup et al, 1987, 1988b).

Twenty of 31 patients examined (65%) were included in the treatment study. The main reason for exclusion was non-visualization of a parathyroid tumour, of which three were localized in areas inaccessible to ultrasound. Only two patients were actively excluded because of possible hypercalcaemic symptoms (mental instability). Selection of patients was thus not based on biochemical values or the clinical presentation.

In 14 of the ultrasound-suspect parathyroid tumours in the treatment group, a combined histological, cytological and immunochemical verification of parathyroid tissue was obtained using ultrasound-guided biopsies. In the remaining six tumours, at least two biopsy tests were positive for parathyroid tissue. In those cases with no response to treatment, reasons other than a wrong diagnosis should be sought.

The main reason for the choice of a maximum of three treatments was to balance what could be regarded as ethically permissible in changing the treatment in a consecutive group of patients of whom many were fit for surgery and the possibility of achieving normocalcaemia (Karstrup et al, 1987, 1988b). All patients were referred for surgical treatment or medical follow-up 6 months after the last treatment.

Treatment was given at 1-month intervals so it was possible to evaluate the biochemical values and stop if normocalcaemia was achieved. Three patients became normocalcaemic following one or two treatments. However, this rule also caused some problems. Generally, during the second and third treatment, the parathyroid tumours became harder to puncture, probably due to development of fibrosis. In subsequent treatments, more punctures (two to three) often had to be performed in order to inject the alcohol selectively into soft areas inside the tumour. Furthermore, the dose of ethanol often had to be reduced owing to inability to inject the estimated volume.

The injections into progressively harder tumours obviously increased the risk of ethanol escaping outside, either along the needle tract or through previously made puncture holes, because of the simultaneous application of an increased intraglandular pressure. In three of four patients, vocal cord paralysis occurred during the second or third treatment. One of these patients had evidence of extraglandular fibrosis found during neck surgery. All these patients had small tumours (< 1 ml). Fibrotic changes were especially pronounced in one patient in whom the parathyroid tumour could be palpated as a hard nodule following treatment.

Following treatment, an obvious improvement of biochemical values was observed in 12 patients, of whom eight achieved normocalcaemia. However, the serum concentrations of ionized calcium were, in general, found to be distributed in the upper normal range. A longer period of medical follow-up will be necessary to see if permanent cure has been achieved. Of the remaining four patients with biochemical improvement, three are now followed by blood tests and one patient has undergone neck surgery. At present, 11 of the patients with biochemical improvement are followed medically, as their remaining clinical manifestations do not indicate surgical intervention. Such a strategy has also been proposed by others (Lafferty & Hubay, 1989).

In six patients completing the treatment protocol, no obvious biochemical or clinical improvement was observed. Four of these patients underwent neck surgery. Two had a solitary parathyroid adenoma removed and two had parathyroid hyperplasia diagnosed, of which only one enlarged parathyroid gland was verified on ultrasound. The number of patients reported with PHPT as a result of diffuse hyperplasia of the parathyroid glands usually range between 10 and 15% (Trigonis et al, 1983; Kristoffersen et al, 1987), or possibly even higher (McGarity et al, 1981; Palmer et al, 1987). Such patients are not well suited for this treatment and were excluded from the study. Small hyperplastic parathyroid glands may not be visualized on ultrasound (Simeone et al, 1981; Rastad et al, 1984).

In the remaining two patients with unaltered hyperparathyroidism, surgery has been precluded because of cardiovascular and pulmonary risks. Surgical parathyroidectomy is generally safe. However, patients with concommitant chronic diseases and old patients represent a high surgical risk group (Hoff et al, 1983; Kristoffersen et al, 1987; Christensen et al, 1988; Lafferty & Haubay, 1989). In such patients chemical parathyroidectomy is attractive. In fit patients, the usefulness of the treatment is still questionable as six of 18 patients (33%) had no benefit from the treatment. This number might even be higher with increasing periods of follow-up. In addition, it is difficult to exclude cases of primary parathyroid hyperplasia and the treatment is not without a risk for vocal cord paralysis.

From our experiences, we feel the interval between treatments should be shortened to avoid multiple punctures and intraglandular injections into partly fibrotic tumours. The dose of ethanol should not exceed half of the volume of the parathyroid tumour and the dose should be estimated individually depending on intraglandular dissemination. The number of treatments offered to the patients remains unclear. We give as few treatments as necessary, and feel a maximum of three treatments is appropriate. Additional treatments could be considered depending on the patients biochemical and clinical status. Unlimited treatments in a patient fit for surgery should be avoided.

We have now started to treat and follow-up patients with concurrent chronic diseases, patients of high age, patients presenting with severe symptomatic hypercalcaemia and the few patients who refuse surgery to evaluate further this technique.

Acknowledgments

We thank Ulla Boutrup, RN, for her invaluable assistance with the interventional procedures.

References

Arima, M., Yoki, H. & Sonada, T., 1975. Preoperative identification of tumour of the parathyroid by ultrasonic tomography. *Surgery, Gynecology and Obstetrics, 141,* 242–244.

Butch, R. J., Simeone, J. F. & Mueller, P. R., 1985. Thyroid and parathyroid ultrasonography. *Radiologic Clinics of North America, 23,* 57–71.

Christensen, P., Hessov, I., Mosekilde, L. & Nielsen, F., 1988. Operative treatment of primary hyperparathyroidism (English abstract). *Ugeskrift for Laeger, 150,* 2527–2530.

Doppman, L. J., Adrian, G. K., Stephen, J. M., Saxe, A., Schneider, P., Norton, J. A., Spiegel, A. M., Downs, R. W., Schoof, N., Brennan, M. E., Schneider, A. B. & Auerbach, G. D., 1983. Aspiration of enlarged parathyroid glands for parathyroid hormone assay. *Radiology, 148,* 31–35.

Glenthøj, A. & Karstrup, S., 1989. Parathyroid identification by ultrasonically guided aspiration cytology. Is correct cytological identification possible? *APMIS, 97,* 497–502.

Hoff, V. W., Ballardie, F. W. & Bicknell, E. J., 1983. Primary hyperparathyroidism: the case for medical management. *British Medical Journal, 287,* 1605–1608.

Karstrup, S., Holm, H. H., Torp-Pedersen, S. & Hegedüs, L., 1987. Ultrasonically guided percutaneous inactivation of parathyroid tumours. *British Journal of Radiology, 60,* 667–670.

Karstrup, S., Glenthøj, A., Torp-Pedersen, S., Hegedüs, L. & Holm, H. H., 1988a. Ultrasonically guided fine needle aspiration of suggested enlarged parathyroid glands. *Acta Radiologica, 29,* 213–216.

Karstrup, S., Lohela, P., Apaja-Sarkkinen, M., Borgmästars, H. & Holopeinen, O., 1988b. Non-operative inactivation of a parathyroid tumour in a patient with hypercalcaemic crisis. *Acta Medica Scandinavica, 224,* 187–188.

Karstrup, S., Glenthøj, A., Hainau, B., Hegedüs, L., Torp-Pedersen, S. & Holm, H. H., 1989. Ultrasound-guided histological fine-needle biopsy from suspect parathyroid tumours: Success rate and reliability of histological diagnosis. *British Journal of Radiology, 62,* in press.

Kristofferson, A., Dahlgren, K., Grandstad, B. & Järhult, J., 1987. Primary hyperparathyroidism in Northern Sweden. *Surgery, Gynecology and Obstetrics, 164,* 119–123.

Lafferty, W. F. & Haubay, A. C., 1989. Primary hyperparathyroidism. A review of the long-term surgical and nonsurgical morbidities as a basis for rational approach to treatment. *Archives of Internal Medicine, 149,* 789–796.

McGarity, C. W., Matews, H. W., Fullenwider, T., Isaacs, W. J. & Miller, A. D., 1981. The surgical management of primary hyperparathyroidism. A personal series. *Annals of Surgery, 143,* 744–804.

Palmer, M., Ljunghall, S., Åkerström, G., Adami H. O., Bergström, R., Grimelius, L., Rudberg, C. & Johansson, H., 1987. Patients with primary hyperparathyroidism operated on over a 24-year period. Temporal trends of clinical and laboratory findings. *Journal of Chronic Diseases, 40,* 121–130.

Rastad, J., Johanson, H., Lindgren, G. P., Ljunghall, S., Stenkvist, B. & Åkerström, G., 1984. Ultrasonic localization and cytological identification of parathyroid tumours. *World Journal of Surgery, 8,* 501–508.

Simeone, J. F., Mueller, P. R., Ferucci, T. J., Van Sonnenberg, E., Wang, C-A., Hall, A. D. & Wittenberg, J., 1981. High-resolution real time sonography of the parathyroid. *Radiology, 141,* 745–751.

Solbiati, L., Montali, G., Croce, F., Bellotti, E., Giangrande, A. & Ravetto, C., 1983. Parathyroid tumors detected by fine-needle aspiration biopsy under ultrasonic guidance. *Radiology, 148,* 793–797.

Solbiati, L., Giangrande, A., De-Pra, L., Bellotti, E., Cantu, P. & Ravetto, C., 1985. Percutaneous ethanol injection of parathyroid tumours under US guidance: treatment of secondary hyperparathyroidism. *Radiology, 155,* 607–610.

Trigonis, C., Hamberger, B., Farnebo, L. O., Abarca, J. & Grandberg, O. P., 1983. Primary hyperparathyroidism. *Acta Chirurgica Scandinavica, 149,* 675–679.

Winzelberg, G. C., 1987. Parathyroid imaging. Diagnosis and treatment. *Annals of Internal Medicine, 107,* 64–70.

1989, *The British Journal of Radiology*, 62, 1043–1049

Double-contrast computed tomographic arthrography of the shoulder joint

By J. V. Cook, MRCP, FRCR and R. Tayar, FRCR

Department of Radiology, St Helier Hospital, Carshalton

(Received February 1989 and in revised form July 1989)

Abstract. Dislocation of the shoulder joint can cause post-traumatic injury to certain anatomical structures, which may lead to recurrent dislocation. The operative visualization of some of these abnormalities may be difficult and their identification preoperatively allows selection of the appropriate surgical approach and avoids the necessity for lengthy surgery. Fifty-one patients with a history of recurrent dislocation, single dislocation or suspected recurrent subluxation as a cause of pain were examined over a 3-year period by double-contrast computed tomographic (CT) arthrography. Thirty-five patients had a demonstrable abnormality and 13 were considered suitable for surgical intervention on radiological criteria. A further 12 patients were advised to have surgery on a combination of clinical and radiological grounds. Eleven of these have so far had surgery, eight of which required an arthrotomy and the CT findings have been confirmed in all these cases. The results of CT arthrography in the patients examined are reported and the technique, normal anatomy and pathological findings are described. The technique is suggested as the imaging method of choice in recurrent dislocation.

The stability of the shoulder joint depends on a series of structures that are described as anterior and posterior capsular mechanisms. Anteriorly, these are the glenoid labrum (which adds depth to the shallow glenoid), synovial membrane and capsule, anterior glenohumeral ligaments and the subscapularis muscle and tendon. The posterior capsular mechanism consists of the glenoid labrum, synovial membrane and capsule and the posterior tendinous rotator cuff and associated muscles. Injury to any of these structures, singly or in combination, can result in recurrent dislocation.

Instability of the glenohumeral joint may be difficult to diagnose clinically and not all the injuries may be easily identified surgically, which can lead to continued post-operative disability. The purpose of this retrospective study was to determine the role of double-contrast computed tomographic (CT) arthrography in the pre-operative assessment of these patients.

Methods

Fifty-one patients referred for suspected instability of the shoulder joint were evaluated by double-contrast CT arthrography. Five millilitres of contrast medium (iopamidol 200) and 10–15 ml of air were introduced into the shoulder joint using the conventional approach with a 22 G needle under fluoroscopic control. This allows optimal distension of the joint without causing discomfort.

Plain double-contrast views of the shoulder were taken to assess the integrity of the rotator cuff and the patient was then positioned in the scanner with the arm slightly internally rotated in a neutral position. This demonstrates the anterior labrum to best advantage. However, when there was a suspicion of posterior instability, scans were also taken with the arm in slight external rotation to show this area optimally.

Studies were performed using a Siemens DRH scanner and 4 or 8 mm contiguous sections were taken using a target magnification of the region of interest from just beneath the acromioclavicular joint to just below the glenohumeral joint. Images were routinely recorded with a wide window setting of 800/250.

The CT scans were reported with particular attention paid to the glenoid labrum, looking for detachment of the labrum with or without underlying fracture of the glenoid, stripping of the joint capsule from the labrum or glenoid and presence of a humeral defect.

Normal anatomy

The glenohumeral joint has a propensity for dislocation because of a large redundant capsule with its three anterior thickenings forming the glenohumeral ligaments and the shallowness of the glenoid fossa in relation to the humeral head.

Contiguous axial sections through the joint show the normal variations at each level. A superior section taken at the level of the coracoid process (Fig. 1) shows the humeral head to be rounded. At this level, the presence of a Hill–Sachs defect (Fig. 4), which is a compression fracture of the superolateral aspect of the humeral head, can be ascertained. On more inferior sections, a depression in this area is commonly seen (Fig. 5) due to the concavity that is normally present between the greater tuberosity and the humeral head and should not be misinterpreted as a Hill–Sachs defect.

At the level of Fig. 1, the superior glenohumeral ligament is identified. It is a small ligament, which contributes little to the stability of the joint and may be identified separately or continuous with the long head of

---

Address correspondence to: J. V. Cook; present address: Department of Radiology, St George's Hospital, Blackshaw Road, Tooting, London.

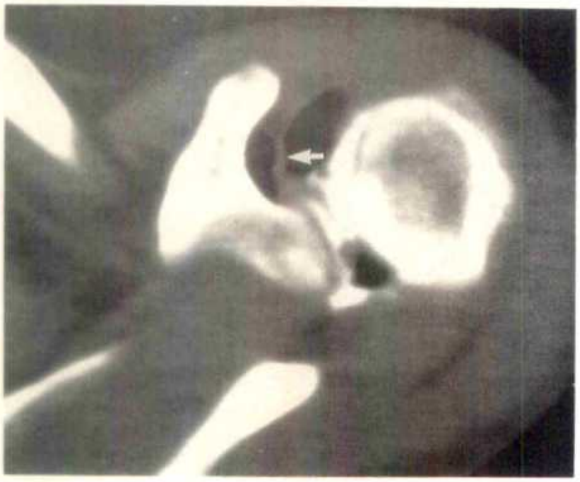

Figure 1. Superior section at the level of the base of the coracoid process shows the anterior capsule and superior glenohumeral ligament (arrow).

biceps, which it accompanies to the supraglenoid tubercle.

A section through the middle of the glenohumeral joint (Fig. 2) demonstrates the labrum, capsular insertions and bicipital sheath. The glenoid labrum is a rim of fibrous tissue that is firmly attached to the glenoid and contributes stability by adding depth to the fossa. It blends superiorly with the long head of biceps. The anterior glenoid labrum has a constant triangular appearance on cross-section, whereas the posterior labrum is normally rounded (Fig. 2a) but may be slightly notched, and this should not be mistaken for an early tear (Rafii et al, 1986).

The fibrous capsule is a redundant structure of variable size, which is easily distended with air allowing better visualization of the intracapsular structures. Posteriorly, the capsule has a constant insertion directly onto the labrum. However, anteriorly, the capsule has a variable insertion (Rothman et al, 1975) and may be inserted directly onto the labrum (Type 1), the glenoid neck (Type 2) or more medially along the scapular neck (Type 3) (Fig. 3). In the latter two types, the capsular insertion may appear continuous with the neck of the glenoid or separated from it by a thin band of soft tissue that includes the periosteum. The Type 3 insertion is usually associated with a large subscapular bursa, which is one of two constant recesses of the fibrous capsule. The second recess is that which forms the bicipital sheath, which is usually seen as an air-filled structure (Fig. 2a) and absence of the tendon within the sheath has been documented in cases of ruptured bicipital tendon (Deutch et al, 1984).

Type 3 insertion of the capsule is also associated with a deficiency of the middle glenohumeral ligament. The middle glenohumeral ligament is a major factor in providing joint stability. It is of variable size, and examination of cadavers show it to be poorly developed in a third of patients who are predisposed to dislocation (DePalma et al, 1949). Conversely, a small subscapularis bursa is associated with a well-developed ligament, which may be up to 2 cm wide.

The middle glenohumeral ligament may be identified on CT (Fig. 2c) if there is some prolapse of the capsule beyond the ligament. However, it is not seen with sufficient frequency to allow accurate assessment of its integrity or degree of development. A Type 3 insertion of the capsule and large subscapular bursa suggest a congenital deficiency.

The inferior glenohumeral ligament is usually only identified as ridges along the capsule on more inferior sections but does play an increasing role in anteroinferior stability when the shoulder is in abduction.

The capsule is reinforced by the tendons of the rotator cuff. Anteriorly, stability is provided by the subscapularis muscle and tendon, which sweep laterally to be inserted into the humeral head (Fig. 3). It is identified as it straddles the capsule and in some patients is noted to be hypoplastic. Posteriorly, joint stability is provided by infraspinatus and teres minor muscles. The capsule is reinforced superiorly by supraspinatus, which is the tendon that ruptures most frequently in an injury to the rotator cuff, and inferiorly by the long head of triceps.

Results

Fifty-one patients with suspected joint instability were examined over a 3-year period by double-contrast CT arthrography. Thirty-seven patients were male and 14 were female. The age range was from 12 to 80 years. Thirty-five patients had a documented history of recurrent dislocation occurring over a 1–11 year period. Six patients presented with persistent pain after a single episode of dislocation. Eight patients simply complained of discomfort or stiffness; two of these patients had previously had anterior bone block surgery for recurrent dislocation. Two patients complained of some instability and were found to have posterior subluxation clinically. Eleven patients underwent surgery, eight of whom had an arthrotomy and a further five patients are on the waiting list.

The most common abnormality in those with recurrent dislocation was thinning of the anterior labrum (Fig. 5), which was present in 14 patients, of which nine had a Hill–Sachs defect (62%) (Fig. 4). Three patients had an isolated Hill–Sachs defect. Thinning of the anterior labrum was considered to be present when it was disproportionate to the width of the remainder of the labrum or when there was a loss of its normal triangular appearance. If attrition of the anterior labrum was suspected, further 4 mm contiguous scans were found to be helpful.

Recurrent dislocation

In the group of patients with recurrent dislocation, three had rotator cuff tears (Fig. 6), two of which have been confirmed surgically. Six patients had Bankart

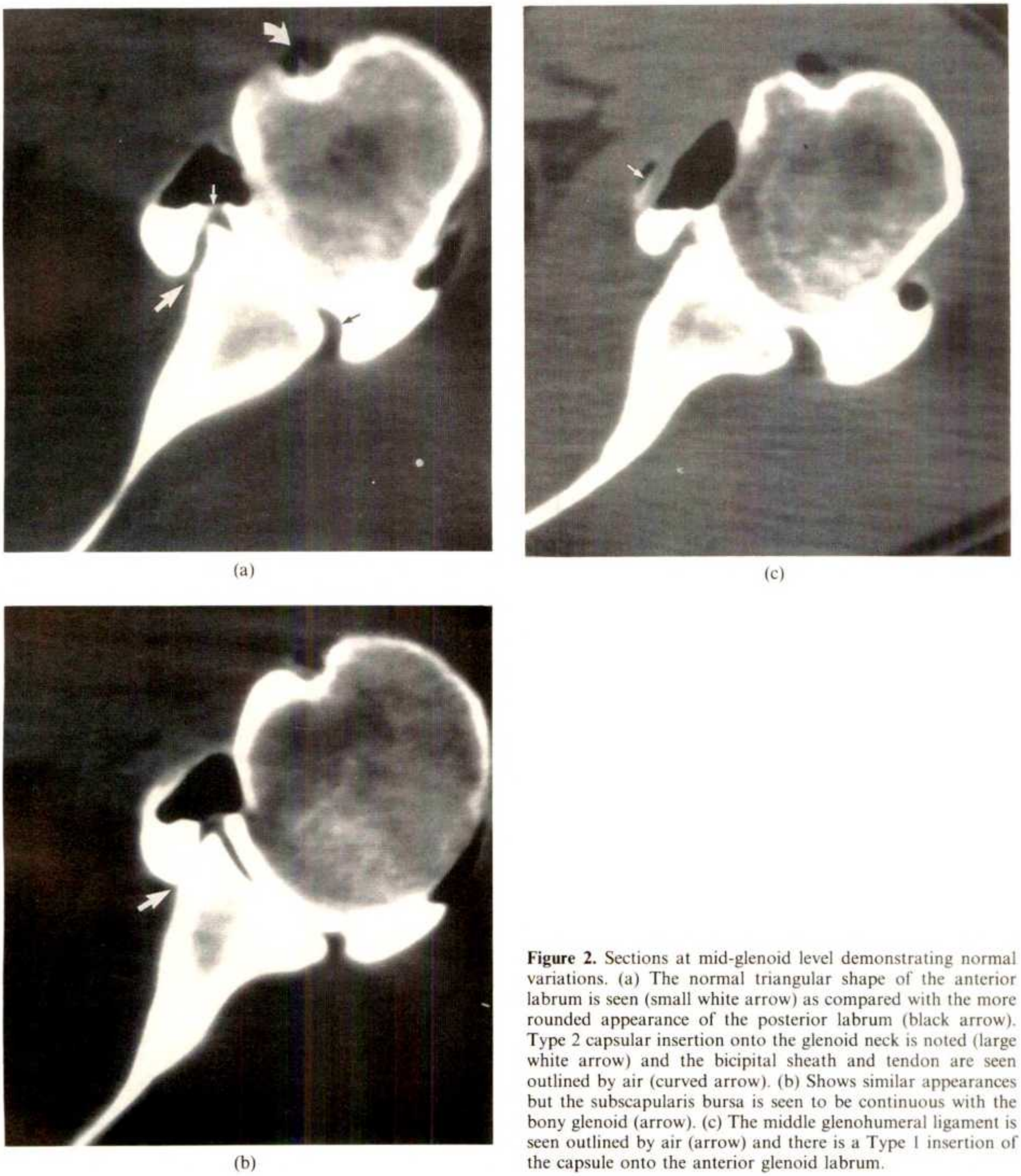

(a)

(c)

(b)

Figure 2. Sections at mid-glenoid level demonstrating normal variations. (a) The normal triangular shape of the anterior labrum is seen (small white arrow) as compared with the more rounded appearance of the posterior labrum (black arrow). Type 2 capsular insertion onto the glenoid neck is noted (large white arrow) and the bicipital sheath and tendon are seen outlined by air (curved arrow). (b) Shows similar appearances but the subscapularis bursa is seen to be continuous with the bony glenoid (arrow). (c) The middle glenohumeral ligament is seen outlined by air (arrow) and there is a Type 1 insertion of the capsule onto the anterior glenoid labrum.

lesions (disruption of the anterior labrum; Fig. 7), three of which have been confirmed surgically. Two of these patients originally decided against surgery—but following further episodes of dislocation they decided to have surgery, which was successful. The patients underwent a Putti Platt repair, a Putti Platt repair with stapling of the anterior capsule to the anterior glenoid and a Putti Platt repair with particular double breasting of a lax subscapularis muscle, respectively. The latter patient was noted to have a large redundant subscapularis bursa on CT arthrography. The three remaining patients are awaiting surgery; one is to have an anterior

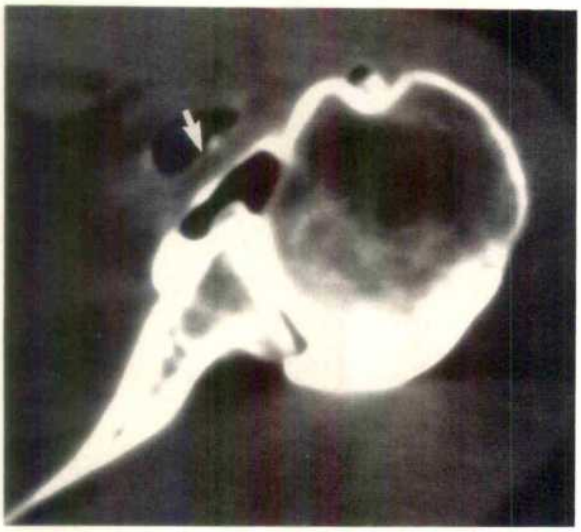

Figure 3. Section through lower glenoid shows the subscapularis tendon (arrow) and Type 3 insertion of the capsule anteriorly.

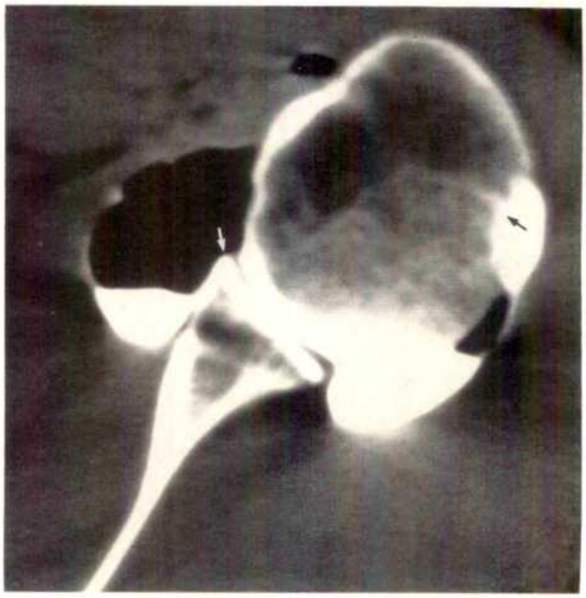

Figure 5. Section at midglenoid level shows marked attrition of anterior labrum (white arrow). Normal concavity between the greater tuberosity and humeral head is seen posteriorly (black arrow).

bone graft in addition to the anterior repair because of a large Bankart lesion and underlying glenoid defect.

One patient who had marked stripping of the anterior capsular insertion (Fig. 8) and elevation of the subscapularis bursa also had surgery where the findings were confirmed.

Eight patients were considered radiologically normal and none have had surgery. However, six of these patients were recommended for physiotherapy. None have had any further episodes of dislocation during a 1–3 year period.

Four patients underwent surgery because of a combination of a long history of recurrent dislocation, clinical instability and demonstration of thinning of the

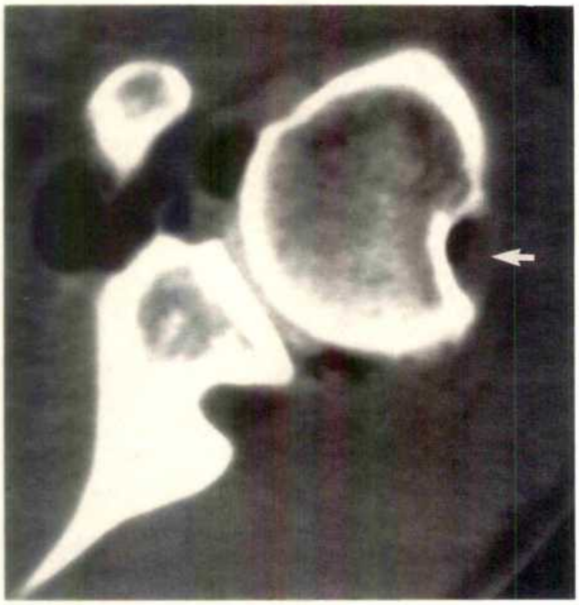

Figure 4. Section at the level of the coracoid process demonstrates a Hill–Sachs defect (arrow).

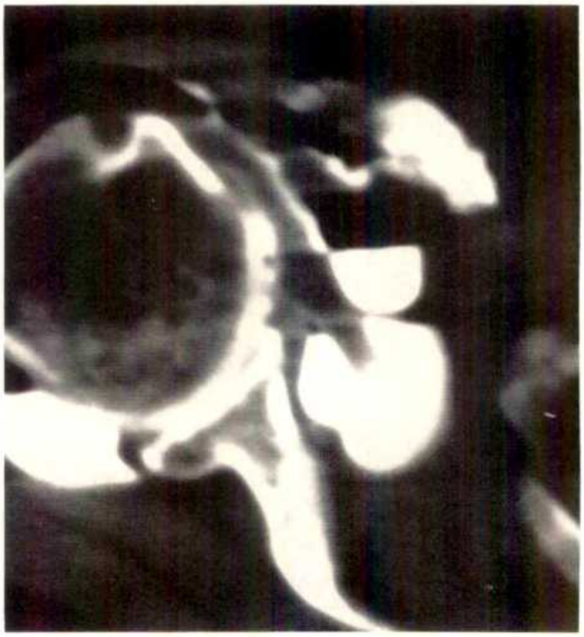

Figure 6. Air and contrast medium is seen in the soft tissues surrounding the joint following a supraspinatus tear.

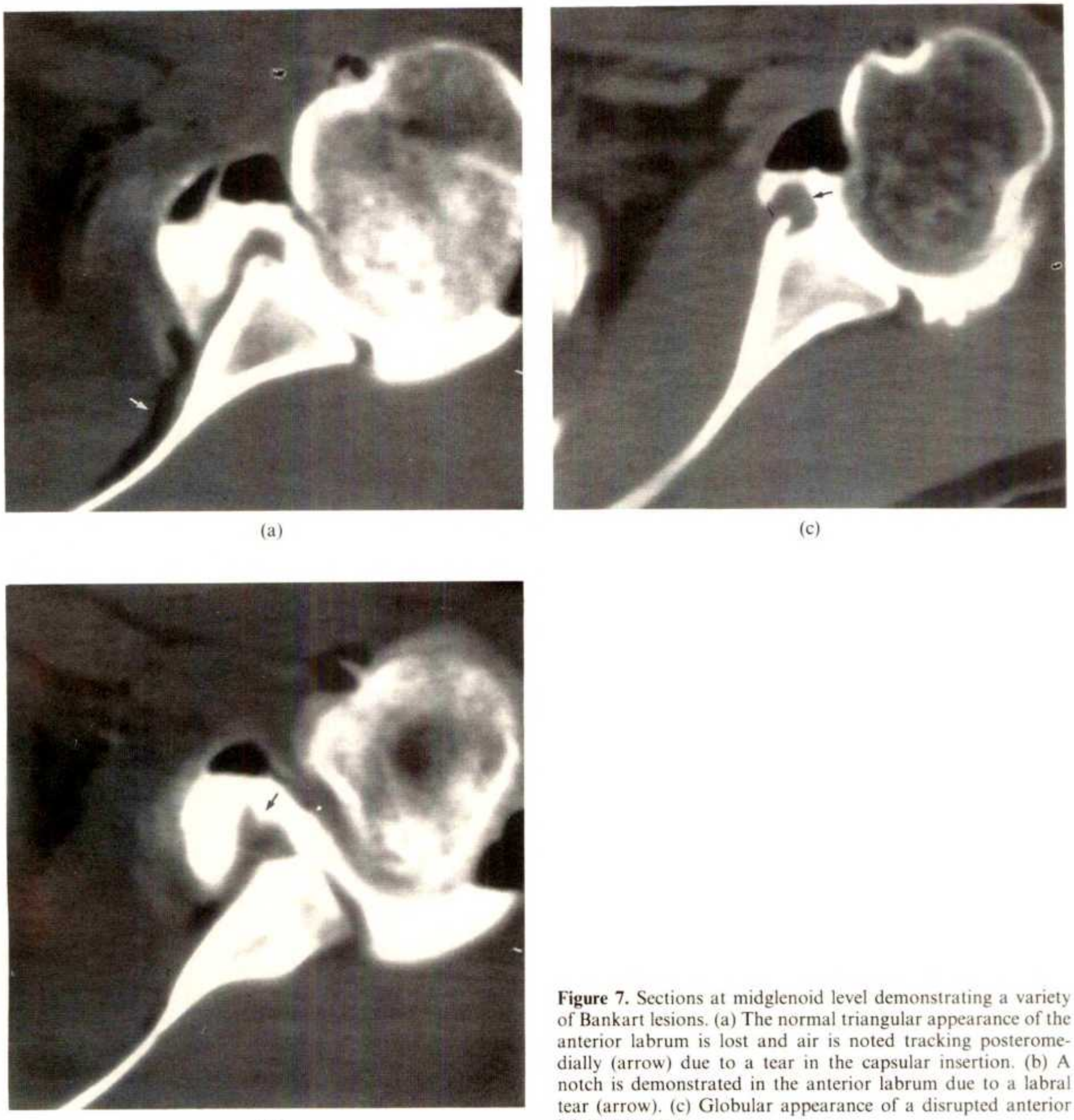

(a)

(c)

(b)

Figure 7. Sections at midglenoid level demonstrating a variety of Bankart lesions. (a) The normal triangular appearance of the anterior labrum is lost and air is noted tracking posteromedially (arrow) due to a tear in the capsular insertion. (b) A notch is demonstrated in the anterior labrum due to a labral tear (arrow). (c) Globular appearance of a disrupted anterior labrum (arrow).

anterior labrum as corroborative evidence on CT examination. One patient had an arthrotomy, which confirmed the anterior labrum attrition and a normal posterior labrum. As this was a retrospective study, the remaining patients had Putti Platt anterior repairs without opening the joint, as was indicated radiologically, and therefore the degree of anterior labrum thinning could not be confirmed nor the absence of intracapsular pathology verified. However, all these patients have had a satisfactory result from their surgery and have no significant residual symptoms.

Single dislocation

Surprisingly, all six patients with a history of only a single dislocation were found to have an abnormality. This was thought to be due to the severity of the initial traumatic episode leading to early symptoms and signs. One patient had thinning of the anterior labrum and

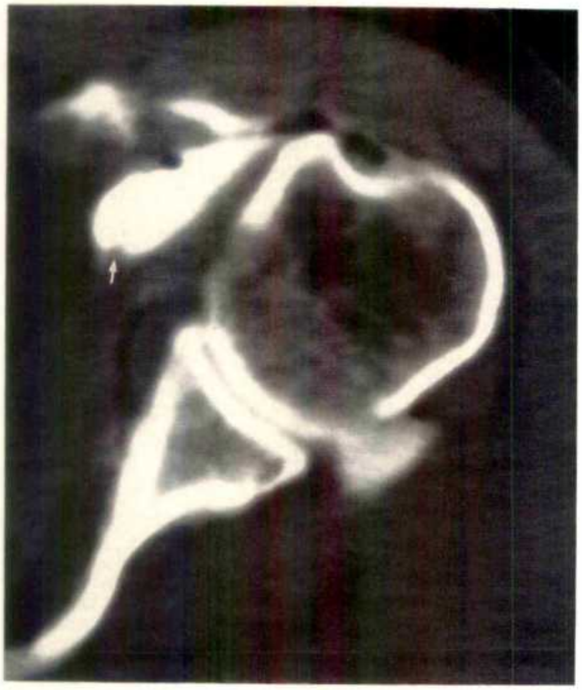

Figure 8. Marked elevation of the subscapularis bursa is noted due to a significant tear of the anterior capsular insertion (arrow).

one patient had an isolated Hill–Sachs defect. The latter can occur after an isolated incident and does not necessarily indicate chronic dislocation.

The remaining four patients had a Bankart lesion (this patient has so far declined surgery), a tear of the supraspinatus (confirmed at surgery), a minor stripping of the anterior capsule insertion and a fracture of the greater tuberosity, respectively.

Posterior dislocation

Two patients complained of pain and were found to have clinical evidence of posterior subluxation. One of these patients had attrition of the posterior labrum whereas the other patient was considered normal. Neither had surgical exploration and both responded to non-surgical treatment.

Pain

Eight patients complained of pain without instability. One was found to have acromioclavicular joint subluxation and responded to hydrocortisone injections, three patients had osteoarthritis that responded to anti-inflammatory agents, two patients had an adhesive capsulitis following previous joint surgery and both responded to manipulation under anaesthetic and hydrocortisone injections. Two patients were considered to be normal on CT examination.

Discussion

Clinical assessment of the shoulder is often difficult. Some patients have a history of 20–30 dislocations whereas others only have pain due to chronic subluxation. Several authors have studied the mechanisms involved in causing recurrent dislocation (Bankart, 1938; Townley, 1950; Mosely & Overgaard, 1962; Symeonides, 1972), which include normal anatomical variants and pathological entities. They require a different therapeutic approach and cannot be diagnosed on clinical evaluation alone.

Arthrotomy and surgical evaluation of the intra-articular anatomy in every case results in the prolongation of operating time with a resultant increase in operation risks, both local and general.

A pre-operative technique that could identify tendon, capsular and intra-articular abnormalities would allow appropriate selection of patients for surgery and would also indicate which patients required more extensive surgical exploration, including an arthrotomy.

Single-contrast arthrography was first performed in 1939 (Lindblom & Palmer, 1939) and was very helpful in the diagnosis of rotator cuff tears. Double-contrast arthrography was first reported by Goldman and Ghelman (1978). Identification of the labrum with this technique often requires tomography to avoid pooling of contrast medium obscuring the labrum. Tomography requires precision and maintenance of an oblique position without movement, experience in interpretation and involves a large radiation dose.

Double-contrast CT is now considered the imaging technique of choice in the pre-operative evaluation of the unstable shoulder.

Turkel et al (1981) investigated the mechanisms preventing glenohumeral joint dislocation by anatomical dissections. They found that at 0° of abduction, the subscapularis muscle mostly stabilizes the joint; at 45° of abduction, the subscapularis muscle, middle glenohumeral ligament and antero-superior fibres of the inferior glenohumeral ligament provide stability. As the shoulder approaches 90° of abduction, the inferior glenohumeral ligament plays a more major role.

Anterior dislocation usually occurs in external rotation, abduction, hyperextension or a combination of these. Bankart (1938) originally considered that an intact labrum was essential in the prevention of dislocation. However, Townley (1950) found that, if the glenoid labrum was removed from a posterior approach in cadavers and the anterior capsular mechanism left intact, it was physically impossible to cause anterior dislocation. Most authors also now agree that deficiency or damage to the middle glenohumeral ligament is one of the more important factors in causing anterior dislocation.

Detachment of the capsule from the glenoid and involving disruption of the middle glenohumeral ligament is common in young patients and does not heal spontaneously. Smaller capsular rents without damage to the middle glenohumeral ligament are more common in the elderly and do not usually require surgical intervention or lead to recurrent dislocation.

Those with a congenital predisposition to dislocation tend to suffer far less traumatic dislocations. There may not be any definite antecedent history and they normally reduce spontaneously. The abnormalities that can be identified are a capacious subscapularis bursa and absence of the middle glenohumeral ligament. Thinning of the anterior labrum due to continued wear and tear may also be seen as a secondary feature, which is useful corroborative evidence in those patients who do not have an obvious history of chronic subluxation.

Patients who have a long history of recurrent dislocation and usually have predisposing capsular laxity and congenital deficiency of the glenohumeral ligament normally undergo a surgical procedure that involves an anterior approach and refashioning of a short anterior capsule. The operation necessitates division and repair of the subscapularis muscle, which thus gets shortened and the combined technique re-establishes the anterior capsular mechanism.

In traumatic dislocation, as the humeral head dislocates, it may tear or crush the labrum, causing detachment of the anterior capsule from the bony glenoid, tear the rotator cuff, fracture the glenoid or cause an impaction fracture resulting in the Hill–Sachs defect. These abnormalities, singly or in combination, lead to recurrent episodes of instability. This form of post-traumatic injury may occur after a single violent episode or may occur in patients with a predisposition to recurrent dislocation who have had several episodes that have resulted in secondary damage.

The presence of this post-traumatic intracapsular injury leads to the continued morbidity of patients who simply undergo anterior capsule refashioning without opening of the joint. Post-operative recurrence rates vary from 1 to 8%, depending on the technique involved. Morrey and James (1976) and Singson et al (1987) studied patients with recurrent dislocation following surgical repair and found on double-contrast CT that incomplete operative visualization of intra-articular anatomy had resulted in an inadequate repair.

Double-contrast CT arthrography has been found to be helpful in the identification of capsular and intracapsular pathology. It is a simple technique to perform, which avoids unnecessary discomfort and radiation dose to the patient. It is accurate in its diagnosis of intra-articular abnormalities that would otherwise need arthrotomy and prolonged surgery to identify. The technique is recommended and has been shown to contribute to the safety and success of any operative intervention.

Acknowledgments

We would like to thank Mr G. Kavanagh for referring the patients for CT scanning and the Medical Photography Department at St Helier Hospital for their invaluable assistance in preparing the photographs from the original radiographs.

References

Bankart, A. S. B., 1938. The pathology and treatment of recurrent dislocation of the shoulder joint. *British Journal of Surgery, 26*, 23–29.

DePalma, A. F., Callery, G. & Bennet, G. A., 1949. Variational anatomy and degenerative lesions of the shoulder joint. *American Academy of Orthopedic Surgeons Instructional Course Lectures, 6*, 255.

Deutch, A. L., Resnick, D., Mink, J. H., Berman, J. L., Cone, R. O., Resnick, C. S., Danzig, L. & Guerra, J., 1984. Computed and conventional tomography of the glenohumeral joint: normal anatomy and clinical experience. *Radiology, 153*, 603–609.

Goldman, A. B. & Ghelman, B., 1978. The double contrast arthrogram. *Radiology, 127*, 655–663.

Lindblom, K. & Palmer, I., 1939. Arthrography and roentgenography in ruptures of tendons of the shoulder joint. *Acta Radiologica, 20*, 548–562.

Morrey, B. F. & James, J. M., 1976. Recurrent anterior dislocation of the shoulder, long-term follow-up of Putti Platt and Bankart procedures. *Journal of Bone and Joint Surgery, 58A*, 252–256.

Moseley, H. F. & Overgaard, B., 1962. The anterior capsular mechanism in recurrent anterior dislocation of the shoulder. *Journal of Bone and Joint Surgery, 44B*, 913–927.

Rafii, M., Firooznia, H., Golimbu, C., Minkoff, J. & Bonamo, J., 1986. CT arthrography of the shoulder. *American Journal of Roentgenology, 146*, 361–367.

Rothman, R. H., Marvel, J. P. & Heppenstall, R. B., 1975. Anatomic considerations in the glenohumeral joint. *Orthopedic Clinics of North America, 6*, 341–352.

Shuman, W. P., Kilcoyne, R. F., Matsen, F. A., Rogers, J. V. & Mack, L. A. 1983. Double contrast computed tomography of the glenoid labrum. *American Journal of Roentgenology, 141*, 581–584.

Singson, R. D., Feldman, F., Bigliani, L. U. & Rosenberg, Z. S., 1987. Recurrent shoulder dislocation after surgical repair: double contrast CT arthrography. *Radiology, 164*, 425–428.

Symeonides, P. P., 1972. The significance of the subscapularis muscle in the pathogenesis of recurrent anterior dislocation of the shoulder. *Journal of Bone and Joint Surgery, 54B*, 913–927.

Townley, C. O., 1950. The capsular mechanism in recurrent dislocation of the shoulder. *Journal of Bone and Joint Surgery, 32A*, 370–380.

Turkel, S. J., Panio, I. M. W., Marshall, J. L. & Girgis, F. G., 1981. Stabilizing mechanisms preventing anterior dislocation of the glenohumeral joint. *Journal of Bone and Joint Surgery, 63A*, 1208–1217.

1989, *The British Journal of Radiology*, 62, 1050–1055

Demonstration of osteochondritis dissecans of the talus by coronal computed tomographic arthrography

By A. M. Davies, DMRD, FRCR and *V. N. Cassar-Pullicino, DMRD, FRCR

Departments of Radiology, Royal Orthopaedic Hospital, Birmingham and *Robert Jones and Agnes Hunt Orthopaedic Hospital, Oswestry

(*Received May 1989 and in revised form August 1989*)

Abstract. Ten cases of osteochondritis dissecans of the talus are reviewed. Coronal computed tomographic arthrography identified the precise location in each case and consistently revealed the extent of the lesion to be greater than that apparent on the plain radiographs. The talar cartilage over the lesion was shown to be thinned in four cases, deficient in two, and fissuring of the cartilage was demonstrated in four. Subarticular cysts were identified in all but two cases and contrast medium was shown to enter the cysts in two cases indicating a communication with the ankle joint. The aetiology and relevance of these findings to treatment are discussed.

The appropriate treatment for osteochondritis dissecans (OD) of the talus depends on accurate delineation of the extent of the lesion and the integrity of the overlying cartilage. The osseous abnormality is usually initially identified on routine plain radiographs of the ankle. Supplementary views ("mortise", etc.) can prove helpful in detecting subtle lesions (Yvars, 1976; Smith et al, 1977; Newberg, 1979; Thompson & Loomer, 1984) as can scintigraphy (Burkus et al, 1984).

Clearer definition of the lesion can be achieved with plain tomography (Smith et al, 1977; Burkus et al, 1984), axial computed tomography (CT) (Reis et al, 1982; Zinman & Reis, 1982; Solomon et al, 1986) or coronal CT (Firooznia et al, 1983). The cartilagenous component of the lesion can only be visualized in the presence of intra-articular contrast medium and can be shown by arthrography, with or without plain tomography (Freiberger et al, 1979; Goldman, 1984) and by axial CT arthrography (Tehranzadeh & Gabriele, 1984).

However, with axial imaging the plane of the cartilagenous defect parallels the imaging plane and is therefore poorly demonstrated. Direct coronal CT arthrography (CCTA) is preferable because the plane of the osteochondral separation is perpendicular to the plane of imaging (Heare et al, 1988). We review our experience of CCTA in a series of 10 patients with OD of the talus.

Patients and methods

In a 6-month period, 10 patients with the diagnosis of OD of the talus were identified from plain radiographs of the ankle. The relevant past medical history, presenting complaint and plain radiographic findings were recorded. In four patients, plain direct coronal CT of the talus was obtained before the contrast examination was performed.

Three millilitres of non-ionic contrast medium (300 mgI/ml) mixed with 0.1ml of adrenaline (1 in 1000) were injected into the tibio-talar joint under screening control. On removal of the needle, antero-posterior, lateral and oblique radiographs were obtained as in a conventional ankle arthrogram examination.

The patients were then transferred to the CT suite and placed supine on the scanning couch with the knees partially flexed and the soles of the feet placed symmetrically flat on the table. The gantry was then angled (10–20°) towards the knees to approximate the coronal plane of the talus and 2 mm contiguous slices on a high-resolution mode were performed with a Siemens DRH scanner. Initially, images of both hindfeet were obtained followed by expanded images of the OD.

Results

There were seven male and three female patients ranging in age from 28 to 54 years (mean 36 years). Complaints varied in severity from discomfort with strenuous sporting activities to more severe ankle pain. The duration of symptoms ranged from 8 months to 7 years (mean 3 years). Five patients gave a history of antecendent minor trauma to the ankle which at the time required no investigation or treatment. One patient originally presented with traumatic dislocation of the tibio-talar joint and bimalleolar fractures with an intact talus. The remaining four patients were unable to attribute the onset of symptoms to prior trauma.

Plain radiographs of the ankle revealed chronic osteochondral defects of the dome of the talus. There were nine postero-medial lesions (four right, five left) and one antero-lateral lesion (left). Employing the Berndt & Harty classification, six Stage III lesions were identified (Berndt & Harty, 1959), indicating that a discrete fragment of bone was visible within the osseous defect. The remaining four cases exhibited subarticular cyst formation with irregularity of the overlying articular cortex in one. In one patient, two loose bodies were shown to be

---

Address correspondence to: Dr A. M. Davies, Consultant Radiologist, Department of Radiology, Royal Orthopaedic Hospital, Woodlands, Northfield, Birmingham B31 2AP.

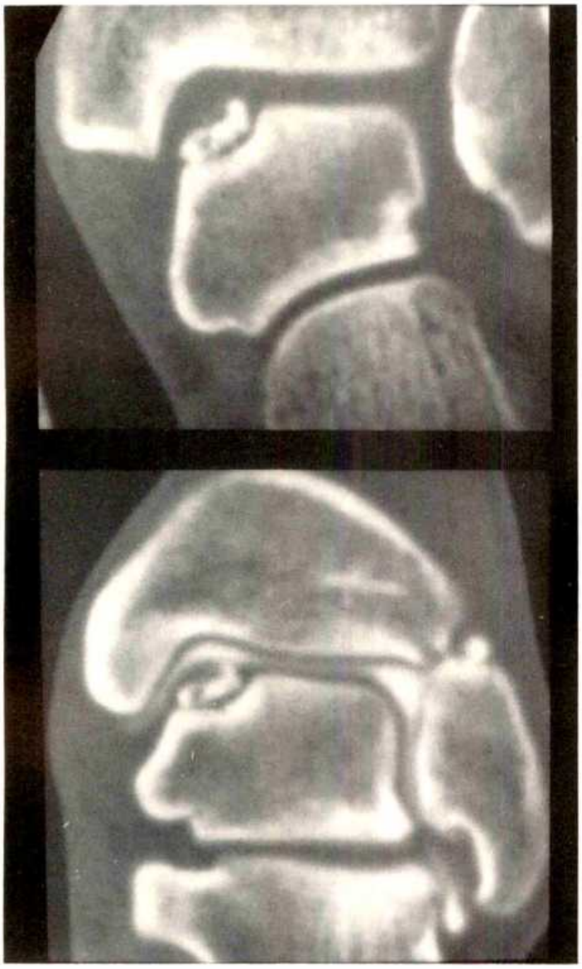

Figure 1. Pre- and post-contrast coronal CT showing a single osseous fragment with intact overlying cartilage.

lying in the posterior joint recess on the lateral radiograph.

Coronal CT arthrography delineated the cartilage over the talar dome and distal tibia in all 10 cases and showed that the subchondral component within the talus was consistently far more extensive than suggested by the plain radiographs. Within the talar lesions, discrete but non-detached osseous fragments (*i.e.* overlying cartilage intact) with a surrounding area of ill defined sclerosis were present in five cases. The fragments were solitary in two cases (Fig. 1) and multiple in three (Fig. 2). Loose bodies were identified in the posterior recess of the ankle joint in two cases and a partially detached osteochondral body in one (Fig. 3). The cartilage of the dome of the talus overlying the defect was thinned in four cases and locally deficient in two. Fissuring of the talar cartilage indicated by fine curvilinear extension of contrast medium into the chondral plate was present in four cases (Fig. 2). Thinning of the adjacent tibial cartilage was identified in three cases,

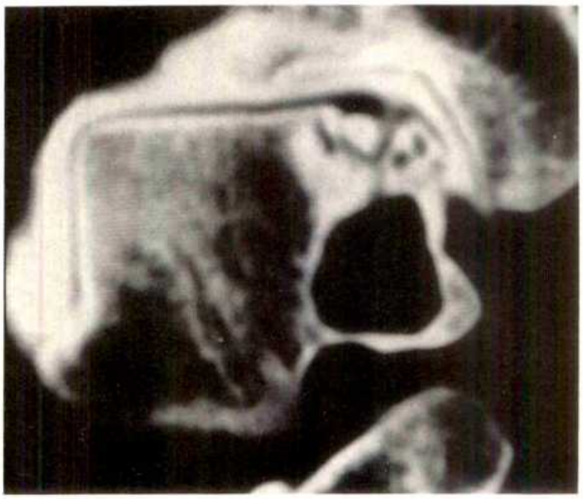

Figure 2. Coronal CT arthrography showing a contrast-medium-filled cartilage fissure extending down to osseous fragmentation and a large subchondral geode (14 mm diameter).

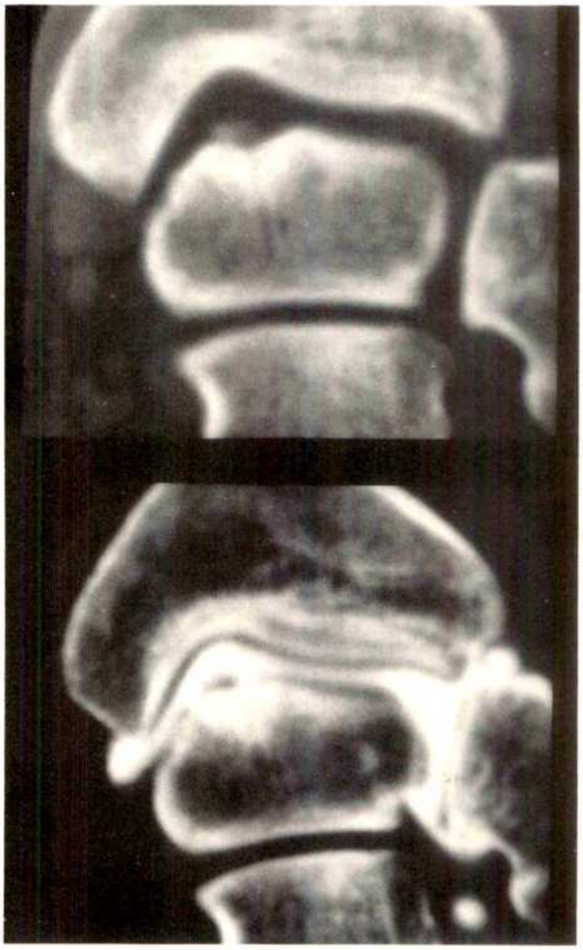

Figure 3. Pre- and post-contrast coronal CT showing an almost completely detached osteochondral fragment.

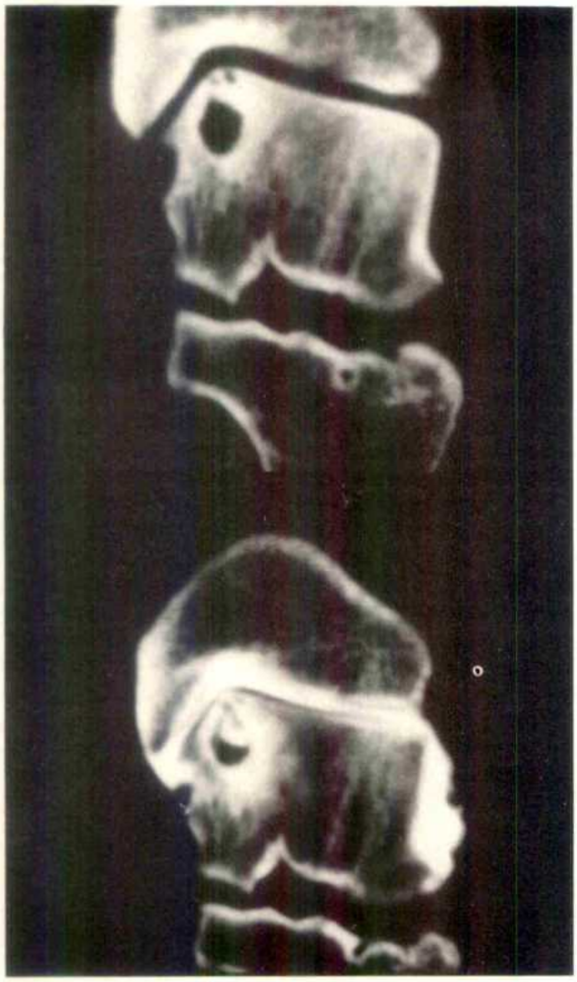

Figure 4. Pre- and post-contrast coronal CT showing contrast medium entering a subarticular cyst.

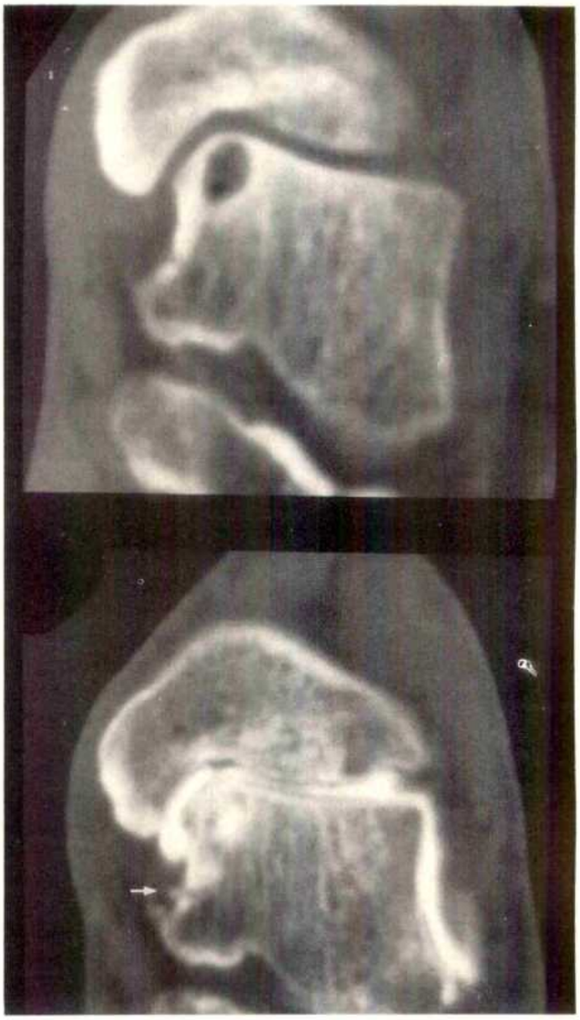

Figure 5. Pre- and post-contrast coronal CT showing communication between the ankle joint and subarticular cyst with contrast medium passing through a defect in the medial cortex of the talus (arrow).

one of which revealed a degenerate vacuum phenomenon in the medial joint space on the pre-contrast examination.

In all but two cases the OD was associated with the formation of subarticular cysts, which tended to be multiple and varied in size from several millimetres (Figs 4, 5) to a geode of 14 mm in diameter (Fig. 2). Contrast medium was demonstrated entering the subarticular cysts in the two cases in which the overlying cartilage was deficient (Figs 4, 5). In one of these cases the contrast medium also showed communication with the soft tissues via a small defect in the medial cortex of the talus (Fig. 5).

The CT of the contralateral asymptomatic ankle included in the examination revealed similar, but less pronounced, osseous changes in four of the 10 cases.

Discussion

Osteochondral defects of the talus account for approximately 4% or all cases of osteochondritis (Lindholm et al, 1980). Originally known as osteochondritis dissecans of the talus (Kappis, 1922; Rendu, 1932; Fairbank, 1933), the current terminology is confusingly varied (Flick & Gould, 1985). Similar lesions, suggesting a traumatic origin, have been called transchondral fractures (Berndt & Harty, 1959; Davidson et al, 1967), osteochondral fractures (Yvars, 1976; Newberg, 1979; Canale & Belding, 1980; Pettine & Morrey, 1987), flake fractures (Marks, 1952), chip fractures (Coltart, 1952) and dome fractures of the talus (Mukherjee & Young, 1973).

The aetiology remains controversial, with two theories: trauma (Berndt & Harty, 1959) and ischaemia (Ray & Coughlin, 1947). The former postulates that the lesion results from non-union of an acute osteochondral fracture; the latter that separation of a loose fragment of cartilage and subchondral bone follows localized vascular damage. Since the ischaemia is thought to be induced by repetitive minor injuries, it is trauma, be it acute or chronic, that is considered the major factor in the development of OD of the talus (McCullough & Venugopal, 1979). An incidence of over 80% of patients with OD of the talus following a single acute traumatic episode is quoted by many published reports (Davidson et al, 1967; Alexander & Lichtman, 1980; Canale & Belding, 1980; Pettine & Morrey, 1987). However, as in the current series, postero-medial lesions may occur in the absence of any history of trauma (Marks, 1952; Yvars, 1976, Canale & Belding, 1980). The presence of an apparently intact talus on the initial radiographs of the patient with a fracture dislocation of the ankle joint might tend to contradict the acute traumatic hypothesis. It is conceivable, however, that a postero-medial lesion, which is thought to follow a compressive injury (Berndt & Harty, 1959), may not be visible on an antero-posterior radiograph as the abnormality does not affect the highest point of the talar dome.

A bilateral distribution, as revealed on CT in four cases in our series, is well recognized in OD particularly when involving the femoral condyles. The changes in the contralateral talus were always less pronounced, which may explain the lack of symptoms. Repetitive trauma would seem to be the likely aetiology in these cases as it is improbable that a single acute episode of sufficient severity would be sustained by both ankles simultaneously without a positive history.

The cartilage can only be visualized in the presence of intra-articular contrast medium and that part overlying the OD can only be assessed accurately when the plane of imaging is perpendicular to the cartilage and the OD (Heare et al, 1988). Theoretically, coronal reformatting of axial images would give the same information, but it is unlikely that sufficient resolution would be achieved to demonstrate fine detail such as fissures in the cartilage (Fig. 2).

The management of patients with OD of the talus is also controversial. Lesions in children will tend to heal either spontaneously or following immobilization, whilst healing in the adult is exceptional rather than routine (Lee & Mercurio, 1981). Long-term follow-up of adult patients shows little change in the radiographic appearance and osteoarthritis is a rare sequel (McCullough & Venugopal, 1979; Bauer et al, 1987). The nature and extent of surgical treatment depends on the integrity of the overlying cartilage (Lee & Mercurio, 1981; Pritsch et al, 1986).

An undetached osseous fragment remains avascular as the underlying layer of fibrous tissue acts as a barrier to capillary ingrowth, although the cartilage continues to be intact and viable as the chondrocytes receive nutrition from the synovial fluid (Flick & Gould, 1985; Greenspoon & Rosman, 1987). Drilling across the fibrocartilaginous area between the fragment and host bone may be necessary to induce vascularization and bony union. This can be achieved either by a transarticular approach or in a retrograde manner with or without an osteotomy of the medial malleolus. Postponing surgery does not adversely affect the ultimate outcome in the majority of patients (Alexander & Lichtman, 1980) although prompt excision is advocated for those patients with a Type IV lesion (Berndt & Harty, 1959) in which a detached osteochondral fragment is present (Pettine & Morrey, 1987).

In the presence of subarticular cysts (Figs 2, 4, 5), curettage and bone grafting is required. Large cysts (geodes) are a rare but recognized finding (Yvars, 1976; Yuan et al, 1979) and are ideally demonstrated by both CT (Fig. 2) and magnetic resonance (Dalinka et al, 1989). Four patients in the current series exhibited a fissure through the talar cartilage extending into the neck of the cyst (Fig. 2) and in a further two cases contrast medium was shown to pass into the cavity of a cyst (Figs 4, 5). In none of these cases were the fissures or communication between the joint and cyst visible on the conventional arthrograms. Comparison of the pre- and post-contrast CT examinations was helpful in distinguishing between a small quantity of contrast medium within a cyst and osteocartilaginous debris.

Two theories exist to explain the pathogenesis of subarticular cysts (Resnick & Niwayama, 1988). The first, synovial fluid intrusion, suggests that synovial fluid herniates through the cartilage in response to an elevated intra-articular pressure thus forming the cyst. The second, bony contusion, postulates that the cysts are foci of necrosis due to stress in the subchondral bone (Rhaney & Lamb, 1955). The presence of communication between the articular cavity and the cyst (Figs 4, 5) has been cited in support of the intrusion theory. The absence of communication has been put forward in support of the contusion theory. However, the conclusion that a failure to demonstrate a communication on conventional ankle arthrography is evidence against the synovial intrusion theory (Yuan et al, 1979) is obviously incorrect as this study reveals the superiority of CCTA in this respect. It is also conceivable that at some stage in the development of a subchondral cyst the communicating channel may become occluded with fibrocartilaginous material thereby preventing contrast medium entering the cyst cavity. The converse may also occur in that a non-communicating cyst may subsequently rupture or erode to produce a communication secondarily.

This study confirms the findings of Heare and co-workers who demonstrated the value of CCTA in the delineation of OD of the talus in four patients (Heare et al, 1988). Although no comparison with conventional arthrotomography was performed in either study, as an adequate concentration of contrast medium could not be maintained for both examinations, our previous experience with similar cases confirms the superiority of CCTA in this context. In expressing a preference for CCTA, the radiation dose need not influence the choice, as it equals or is less than that required for conventional tomography (Zinman & Reis, 1982; Tehranzadeh & Gabriele, 1984).

The cartilage of the talus may be visualized directly by arthroscopy of the ankle (Carson & Andrews, 1988) and has been advocated in the assessment and treatment of OD of the talus (Parisien, 1986; Pritsch et al, 1986). A lack of correlation between the plain radiographic features and the appearances at arthroscopy has been found (Pritsch et al, 1986). In one current case, however, the patient also underwent arthroscopy and similar appearances to CCTA were demonstrated. Similarly, Heare and co-workers did not perform a comparison between the two techniques but did show close correlation in one of their four cases who also underwent arthroscopy (Heare et al, 1988). We therefore have no reason to doubt the accuracy of CCTA in demonstrating the integrity of the cartilage and consider it preferable to arthroscopy as the first investigation, as it is cheaper, less invasive and has the additional advantage of revealing the subchondral element of the lesion. In addition, the limited manoeuverability at arthroscopy means that it can be difficult to see the postero-medial dome of the talus, which was the commonest site for OD in this study.

Magnetic resonance of the ankle joint may ultimately supersede CCTA (Yulish et al, 1987) but not until it becomes universally available.

References

Alexander, A. H. & Lichtman, D. M., 1980. Surgical treatment of transchondral talar-dome fractures: long term follow up. *Journal of Bone and Joint Surgery, 62A*, 646–652.

Bauer, M., Jonsson, K. & Linden, B., 1987. Osteochondritis dissecans of the ankle. *Journal of Bone and Joint Surgery, 69B*, 93–96.

Berndt, A. L. & Harty, M., 1959. Transchondral fractures (osteochondritis dissecans) of the talus. *Journal of Bone and Joint Surgery, 41A*, 988–1020.

Burkus, J. K., Sella, E. J. & Southwick, W. O., 1984. Occult injuries of the talus diagnosed by bone scan and tomography. *Foot and Ankle, 4*, 316–324.

Canale, S. T. & Belding, R. H., 1980. Osteochondral lesions of the talus. *Journal of Bone and Joint Surgery, 62A*, 97–102.

Carson, W. G. & Andrews, J. R., 1988. Arthroscopy of the ankle. *Seminars in Orthopaedics, 3*, 123–129.

Coltart, W. D., 1952. Aviators astralgus. *Journal of Bone and Joint Surgery, 34B*, 545–566.

Dalinka, M. K., Kricun, M. E., Zlatkin, M. B. & Hibbard, C. A., 1989. Modern diagnostic imaging in joint disease. *American Journal of Roentgenology, 152*, 229–240.

Davidson, A. M., Steel, H. D., Mackenzie, D. A. & Penny, J. A., 1967. A review of 21 cases of transchondral fractures of the talus. *Journal of Trauma, 7*, 378–415.

Fairbank, H. A. T., 1933. Osteochondritis dissecans. *British Journal of Surgery, 21*, 67–82.

Firooznia, H., Golimbu, C. & Rafii, M., 1983. Computed tomography in the detection of joint disorders. *Orthopaedic Review, 12*, 69–82.

Flick, A. B. & Gould, N., 1985. Osteochondritis dissecans of the talus (transchondral fractures of the talus): review of the literature and new surgical approach for medial dome lesions. *Foot and Ankle, 5*, 165–185.

Freiberger, R. H., Kaye, J. J. & Spiller, J., 1979. Ankle arthrography. In *Arthrography* (Appleton-Century-Crofts, New York), pp. 239, 255, 256.

Goldman, A. B., 1984. Ankle arthrography. In *Procedures in Skeletal Radiology* (Grune & Stratton, Orlando), pp. 204–205.

Greenspoon, J. & Rosman, M., 1987. Medial osteochondritis of the talus in children. Review and new surgical management. *Journal of Paediatric Orthopaedics, 7*, 705–708.

Heare, M. M., Gillespy, T. & Bittar, E. S., 1988. Direct coronal computed tomography arthrography of osteochondritis dissecans of the talus. *Skeletal Radiology, 17*, 187–189.

Kappis, M., 1922. Weitere beiträge zur traumatisch-mechanischen enstehung der "spontanen" knorpelabiosungen. *Deutsche Zeitschrift für Chirurgie, 171*, 13–29.

Lee, C. K. & Mercurio, C., 1981. Operative treatment of osteochondritis dissecans *in situ* by retrograde drilling and cancellous bone grafting: a preliminary report. *Clinical Orthopaedics and Related Research, 158*, 129–136.

Lindholm, T. S., Osterman, K. & Vankka, E., 1980. Osteochondritis dissecans of the elbow, ankle and hip: a comparison study. *Clinical Orthopaedic and Related Research, 148*, 245–253.

Marks, K. L., 1952. Flake fractures of the talus progressing to osteochondritis dissecans. *Journal of Bone and Joint Surgery, 34B*, 90–92.

McCullough, C. J. & Venugopal, V., 1979. Osteochondritis dissecans of the talus: the natural history. *Clinical Orthopaedics and Related Research, 144*, 264–268.

Mukherjee, S. J. & Young, A. B., 1973. Dome fractures of the talus: a report of 10 cases. *Journal of Bone and Joint Surgery, 55B*, 319–326.

Newberg, A. H., 1979. Osteochondral fractures of the dome of the talus. *British Journal of Radiology, 52*, 105–109.

Parisien, J. S., 1986. Arthroscopic treatment of osteochondral lesions of the talus. *American Journal of Sports Medicine, 14*, 211–217.

Pettine, K. A. & Morrey, B. F., 1987. Osteochondral fractures of the talus. *Journal of Bone and Joint Surgery, 69B*, 89–92.

Pritsch, M., Horoshovski, H. & Farine, I., 1986. Arthroscopic treatment of osteochondral lesions of the talus. *Journal of Bone and Joint Surgery, 68A*, 862–864.

Ray, R. B. & Coughlin, E. J., 1947. Osteochondritis dissecans of the talus. *Journal of Bone and Joint Surgery, 29*, 697–706.

Reis, N. D., Zinman, C., Besser, M. I. B., Shifrin, L. Z., Folman, Y., Torem, S., Froindlich, D. & Zaklad, H., 1982. High resolution computerised tomography in clinical orthopaedics. *Journal of Bone and Joint Surgery, 64B*, 20–24.

Rendu, A., 1932. Fracture intra-articulaire parcellaire de la poulie astraglienne. *Lyon Médecine, 150*, 220–222.

Resnick, D. & Niwayama, G., 1988. *Diagnosis of Bone and Joint Disorders*, 2nd edn (W. B. Saunders, Philadelphia), pp. 1375–1381.

Rhaney, K. & Lamb, D. W., 1955. The cysts of osteoarthritis of the hip: a radiological and pathological study. *Journal of Bone and Joint Surgery, 37B*, 663–675.

Smith, G. R., Winquist, R. A., Allan, N. K. & Northrop, C. H., 1977. Subtle transchondral fractures of the talar dome: a radiological perspective. *Radiology, 124*, 667–673.

Solomon, M. A., Gilula, L. A., Oloff, L. M. & Oloff, J., 1986. CT scanning of the foot and ankle. 2: Clinical applications and review of the literature. *American Journal of Roentgenology, 146*, 1204–1214.

Tehranzadeh J. & Gabriele, O. F., 1984. Intra-articular calcified bodies: detection by computed arthrotomography. *Southern Medical Journal, 77*, 703–710.

Thompson, J. P. & Loomer, R. L., 1984. Osteochondral lesions of the talus in a sports medicine clinic. *American Journal of Sports Medicine, 12*, 460–463.

YUAN, H. A., CADY, R. B. & DEROSA, C., 1979. Osteochondritis dissecans of the talus associated with subchondral cysts. *Journal of Bone and Joint Surgery, 61A*, 1249–1251.

YULISH, B. S., MULOPOLOS, G. P., GOODFELLOW, D. B., BRYNA, P. J., MODIC, M. T. & DOLLINGER, B. M., 1987. Magnetic resonance imaging of osteochondral lesions of the talus. *Journal of Computer Assisted Tomography, 11*, 246–301.

YVARS, M. F., 1976. Osteochondral fractures of the dome of the talus. *Clinical Orthopaedics and Related Research, 114*, 185–191.

ZINMAN, C. & REIS, N. D., 1982. Osteochondritis dissecans of the talus: use of a high resolution computed tomography scanner. *Acta Orthopaedica Scandinavica, 53*, 697–700.

1989, *The British Journal of Radiology*, 62, 1056–1058

The influence of Buscopan on adverse reactions to intravascular contrast media

By Sanjiv Sharma, MD, Mira Rajani, MD, Anil Khosla, MD, Nalinikant Misra MD and R. K. Goulatia, MD

Department of Radiodiagnosis, Cardiothoracic and Neurosciences Centre, All India Institute of Medical Sciences, New Delhi, India

(*Received May 1989 and in revised form July 1989*)

Abstract. We have analysed the ability of prior intravenous Buscopan (hyoscine butylbromide) injection to influence the incidence and severity of adverse reactions to intravascularly administered, iodinated, ionic contrast medium in 258 consecutive digital subtraction angiographic (DSA) examinations. Adverse reactions were seen in 7.9% of the intravenous and 2.4% of the intra-arterial DSA examinations. The incidence of adverse reactions with and without prior Buscopan injection during intravenous DSA examinations was 8.2% and 7.1%, respectively and during intra-arterial DSA examinations was 5.6% and 1.5%, respectively. This difference is not statistically significant (χ^2-test). We conclude that prior intravenous injection of Buscopan has no influence on the incidence or severity of adverse reactions to intravascular contrast media.

Adverse reactions to intravascular contrast media can be considered broadly as two groups. The first group includes those associated with either the use of large doses of contrast medium, as in angiocardiography, high-dose urography and accidental overdosage, or injection of a concentrated bolus of contrast medium delivered to a critical area such as the myocardium, brain, spinal cord or kidneys. Adverse reaction in such situations is dose related, and is produced by the physical and chemical characteristics of the contrast medium. Such reactions can be predicted to some extent on the basis of the results of animal experiments (Ansell, 1975).

The second group of adverse reactions occur in a susceptible patient in response to a dose of contrast medium that would be harmless to most patients. These reactions cannot be predicted beforehand and are called idiosyncratic reactions. Their pathogenesis is not clearly understood (Ansell, 1975).

Increased cholinergic activity secondary to cholinesterase inhibition by contrast media has been implicated in the mechanism of these adverse reactions (Dawson & Edgerton, 1983; Manhire et al, 1984). It has also been suggested that the effect of some antihistamines in preventing these adverse reactions was due to their anticholinergic rather than antihistaminic activity (Inman, 1952). In a preliminary communication, Hartnell and Hemingway (1988) have recently reported that prior injection of Buscopan (hyoscine butylbromide) in digital subtraction angiography (DSA) results in fewer side-effects from intravascularly administered contrast media. Evaluation of the abdominal vessels by DSA provides an ideal situation to test this hypothesis since prior intravenous Buscopan injection is usually necessary to control intestinal peristalsis to obtain diagnostically adequate angiograms.

We have planned the present study to assess the influence of prior intravenously administered Buscopan on the incidence and severity of adverse reactions to contrast media during subsequent DSA examinations.

Materials and methods

The influence of intravenous Buscopan on contrast-medium-induced adverse effects in 258 consecutive DSA examinations has been studied.

These reactions have been classified as minor (usually subside without treatment), intermediate (usually require some form of treatment, but there is no undue alarm for the patient's safety, and the response to the treatment is usually rapid), severe (there is often fear for the patient's life and intensive treatment is usually required) and death (Ansell, 1975). We have followed the classification for the clinical features as described by Ansell (1970). The patients were divided into two groups.

Group A patients were studied by intravenous route and in all cases a small volume (25–30 ml) bolus of Urografin 370 (Schering AG) was delivered to the mid-right atrium via a high-flow pigtail catheter. These patients were subdivided into two groups: those who received prior Buscopan injection and those who did not. Buscopan was given as a bolus injection of 20–40 mg, administered via the right atrial catheter 5 min before the bolus injection of contrast medium. All the patients were subsequently monitored for contrast-medium-related reactions for up to 6 h after the examination.

Group B patients underwent direct intra-arterial DSA examination by the percutaneous transfemoral route and a 1:1 dilution of Urografin 370 was delivered to the aorta or its branches. These patients were also subdivided into two groups: those who received Buscopan

---

Address correspondence to: Dr Sanjiv Sharma, Department of Radiodiagnosis, Cardiothoracic Centre, All India Institute of Medical Sciences, Ansari Nagar, New Delhi 110029, India.

Table I. Influence of Buscopan on adverse reactions to intravascular contrast media

	Number of patients	Number of patients with adverse reactions	%
Group A: Intravenous DSA	89	7	7.9
Buscopan given	61	5	8.2
Buscopan not given	28	2	7.1
Group B: Intra-arterial DSA	169	4	2.4
Buscopan given	36	2	5.6
Buscopan not given	133	2	1.5

injection prior to DSA and those who did not. Buscopan (20–40 mg) was administered as a bolus injection in a peripheral vein 5 min prior to angiography. The adverse reactions were monitored in a similar manner.

Results

A total of 258 consecutive DSA examinations was assessed. The patients were divided into two groups based on the route of contrast medium administration. Adverse reactions to contrast media were seen in 7.9% of intravenous and 2.4% of intra-arterial examinations. The incidence of adverse reactions with and without Buscopan injections in both the groups is summarized in Table I.

Group A consisted of 89 patients who underwent intravenous DSA (IV-DSA) and Group B consisted of 169 patients who underwent intra-arterial DSA (IA-DSA). Adverse reactions in Group A included nausea and vomiting (five patients), rigors (three patients), urticarial rashes (three patients) and unilateral orbital oedema (two patients); all reactions subsided with symptomatic treatment. Four patients in this group had more than one adverse reaction.

In Group B, adverse reactions included rigors (two patients), nausea and vomiting (one patient), urticarial rash (one patient) and facial oedema (one patient); all reactions subsided with symptomatic treatment. One patient in this group also had more than one adverse reaction. We have applied the χ^2-test to data from both groups and the difference in the incidence of adverse reactions with and without Buscopan injection was not found to be statistically significant.

Discussion

No unifying theory explains all the adverse reactions to intravascular contrast media (Lasser, 1984). These adverse reactions have been known to be related to the hyperosmolarity, allergic potential and the chemotoxicity of the iodinated contrast media (Ansell et al, 1980; Dawson & Edgerton, 1983; Lasser,1985; McClennan, 1987).

Lasser and Lang (1966) reported that contrast media inhibit the enzyme cholinesterase resulting in reduced hydrolysis of acetylcholine, and hence an increased cholinergic activity. Subsequently, Lalli (1980) suggested that the cholinergic pathways could also be stimulated by the effect of the contrast media on the central nervous system. The resultant increased cholinergic activity has been postulated as responsible for the various adverse reactions to contrast media (Herxheimer, 1956; Lasser & Lang, 1966; Boijsen et al, 1971; Coel & Lasser, 1971; Higgins, 1977; Littner et al, 1977; Ansell et al, 1980; Dawson & Edgerton, 1983).

The preliminary report by Hartnell and Hemingway (1988) studied the effect of Buscopan on adverse reactions in 34 patients undergoing DSA. In 17 patients who received Buscopan, there were no significant adverse reactions (one patient reported slight nausea). In the other 17 patients who did not receive Buscopan, there were four (23%) severe reactions (the nature of which was not specified). In contrast to that study, we found that prior Buscopan injection did not influence the incidence or severity of contrast-medium-related adverse reactions. The incidence of adverse reactions with and without prior Buscopan injections was 8.2% and 7.1%, respectively, during IV-DSA and 5.6% and 1.5%, respectively, during IA-DSA examinations (Table I).

We conclude that Buscopan has no influence on the incidence or severity of adverse reactions to intravascular contrast media. The use of Buscopan in DSA examinations should be limited to its ability to improve the image by controlling intestinal peristalsis.

Acknowledgment

We are grateful to Dr D. R. Sundaram of the Department of Biostatics for his help in the statistical analysis of the data.

References

ANSELL, G., 1970. Adverse reactions to contrast agents. *Investigative Radiology*, *5*, 374–391.

—— 1975. Contrast media toxicity. In *Recent Advances in Radiology*, ed. by T. Lodge & R. E. Steiner (Churchill Livingstone, New York), pp. 335–350.

ANSELL, G., TWEEDIE, M. C. K., WEST, C. R., EVANS, P. & COUCH, LO., 1980. The current status of reactions to intravenous contrast media. *Investigative Radiology*, *15*, S32–S39.

BOIJSEN, E., DAHN, I. & HALLBOOK, T., 1971. Haemodynamic effect of contrast medium in arteriography of legs. *Acta Radiologica Diagnosis*, *11*, 295–309.

COEL, M. N. & LASSER, E. C., 1971. A pharmacological basis for peripheral vascular resistance changes with contrast media injections. *American Journal of Roentgenology*, *111*, 802–806.

DAWSON, P. & EDGERTON, D., 1983. Contrast media and enzyme inhibition. I. Cholinesterase. *British Journal of Radiology*, *56*, 653–656.

HARTNELL, G. G. & HEMINGWAY, A. P., 1988. Contrast medium reactions—does Buscopan reduce them? *British Journal of Radiology*, *61*, 652.

HERXHEIMER, A., 1956. The nervous pathway mediating cholinergic urticaria. *Clinical Science*, *15*, 195–203.

HIGGINS, C. B., 1977. Effects of contrast media on the conducting system of the heart. *Radiology*, *124*, 599–604.

INMAN, G. K. E., 1952. A comparison of urographic contrast media, with particular reference to the aetiology and prevention of certain effects. *British Journal of Radiology*, *25*, 625–631.

LALLI, A. F., 1980. Contrast media reactions: data analysis and hypothesis. *Radiology*, *134*, 1–12.

LASSER, E. C., 1984. Adverse reactions to contrast media. In *Radiocontrast Agents*, ed. by M. Sovak (Springer, New York), pp. 525–532.

—— 1985. Etiology of anaphylactoid responses: the promise of non-ionics. *Investigative Radiology*, *20*, S79–S83.

LASSER, E. C. & LANG, J. H., 1966. Acetylcholinesterase inhibition by some organic contrast agents. *Investigative Radiology*, *2*, 237–242.

LITTNER, M. R., ROSENFIELD, A. T., ULRICH, S. & PUTNAM, C. E., 1977. Evaluation of bronchospasm during excretory urography. *Radiology*, *124*, 117–122.

MANHIRE, A. R., DAWSON, P. & DENNET, R., 1984. Contrast agent induced emesis. *Clinical Radiology*, *35*, 369–370.

MCCLENNAN, B. L., 1987. Low osmolality contrast media: premises and promises. *Radiology*, *162*, 1–8.

1989, *The British Journal of Radiology*, 62, 1059–1062

The correlation of histopathological, microradiographic and ultrasonographic features in disease of the prostate gland

By *‡D. R. Jones, FRCSE, †G. J. Griffiths, MD, FRCR, §M. C. Parkinson, BSc, MD, FRCPath, *K. T. Evans, FRCP, FRCR, FFR(RSCI), DMRD, *E. E. Roberts, MSc, DCR, *R. Ll. Davies, MSc, PhD, MIBiol, CBiol, *T. J. Harrison and ‡W. B. Peeling, MA, FRCS

Department of *Diagnostic Radiology, University of Wales, College of Medicine, Cardiff, Departments of †Radiology and ‡Urology, St Woolos Hospital, Newport and §St Peter's Hospitals, The Institute of Urology, London, relocated to the Bland-Sutton Institute, Middlesex Hospital, London

(*Received December 1988 and in revised form June 1989*)

Abstract. The histopathological, microradiographic and ultrasonographic features of corresponding areas of 100 cadaveric prostates were examined and correlated statistically to investigate their relationship. Benign glands are seen to be related to reticular structure and mid-range echoes. Benign prostatic hyperplasia is related to microadenomatous structure and mid-range echoes, whilst cancer is related to amorphous structure and low echoes. A small number of cancers have irregular calcification present and these tumours are related to high echoes. The structure of the prostate gland is therefore related to its pathology and explains its ultrasound echogenicity.

Per-rectal ultrasonography has been shown to be useful in the diagnosis of prostatic disease (Peeling et al, 1979; Brooman et al, 1981). However, the echogenicity and mechanism of its production has been a subject of much debate and controversy. "Grey scale" ultrasonography using improved equipment has been described (Harada et al, 1980), but the advent of "tissue texture analysis" has led to diverging reports as to how cancer is represented (Greenberg et al, 1981; Rifkin et al, 1983; Dahnert et al, 1986; Lee et al, 1986).

The sensitivity of per-rectal ultrasonography was shown in a retrospective study by Rifkin et al in 1986, but difficulties in differentiating cancer from benign conditions were described and correlation with the histopathology of whole prostates was suggested as a means of understanding the representation of the different disease processes.

A cadaver study has been carried out (Jones et al, 1989) and a visual correlation made of the histopathology, microradiography and ultrasonography of the prostate. A classification of the structural appearances of the prostate gland has also been made (Davies et al, 1988), in which regular, microadenomatous, reticular and amorphous structure was described. The statistical relationship of these features to the mechanism of production of the ultrasonic echoes has been investigated.

Materials and methods

Using a technique of histopathology, microradiography and per-rectal ultrasonography of cadaver specimens (Jones et al, 1989), the features in 100 prostates were examined. Statistical correlations were made between the histopathological features (benign, fat, calcification, benign hyperplasia and malignant), the microradiographic features (regular, microadenomatous, reticular and amorphous structure) and the ultrasound features (high echoes, hyperechoic; mid-range echoes, isoechoic; low echoes, hypoechoic).

With legal and ethical consent, the specimens, suspended in a Perspex tank, were scanned transversely in 0.5 cm steps within 48 h of death. After processing, they were sectioned precisely at the levels of scanning for histopathology and microradiography. Each section ($n = 543$) was analysed in 16 areas (using a 4×4 grid system). The presence or absence of each feature was recorded and the extent (percentage) of the features in each prostate calculated using a Fortran computer program. The relationships of the percentage of each feature were statistically correlated using the "mini-tab" computer statistics program.

Results

The periurethral muscle and periprostatic fat were seen to relate strongly to hypoechoic and hyperechoic echoes ($r = 0.91$, $r = 0.93$; $p < 0.001$), respectively, on ultrasonography. Ultrasound was also shown to be reliable and sensitive in identifying prostatic calcification ($r = 0.904$, $p < 0.001$).

Table I. The relationship between structure and pathology

Structure	Benign		Malignant	
	(r)	(p)	(r)	(p)
Regular	+0.128	>0.05	−0.344	<0.001
Microadenomatous	+0.441	<0.001	−0.271	<0.01
Reticular	+0.592	<0.001	−0.651	<0.001
Amorphous	−0.683	<0.001	+0.818	<0.001

Address offprint requests to Mr D. R. Jones, Department of Urology, Leeds General Infirmary, Leeds.

Table II. The relationship between echogenicity and pathology

Echogenicity	Benign		Malignant (no calcification)	
	(*r*)	(*p*)	(*r*)	(*p*)
Low echo	−0.238	<0.01	+0.336	<0.001
Mid-range echo	+0.302	<0.001	−0.331	<0.001
High echo	−0.007	>0.05	−0.014	>0.05

Relationship to structure and echogenicity

Benign hyperplasia. This was seen to be positively related to microadenomatous and reticular structure, and inversely related to the presence of amorphous structure; there was no statistical relationship to regular structure (Table I).

The presence of benign hyperplasia was also seen to be positively related to mid-range echoes and inversely related to low echoes; high echoes have no relationship (Table II).

Cancer. It was shown that cancer is strongly associated with amorphous architecture on microradiography and inversely related to microadenomatous, reticular and regular structure (Table I). Malignancy (without microcalcification) was seen to relate positively to low echoes and inversely to mid-range echoes (Table II). High echoes have no statistical relationship to cancer when microcalcification is absent, but malignancy was related to high echoes if microcalcification was present.

Differential relationship of structure to benign or malignant prostates (Table III)

The percentage of microadenomatous structure in benign and malignant glands was not found to be significantly different, which is probably because microadenomatous structure is often partly and not completely destroyed by some cancers. However, benign and malignant glands contain a significantly different amount of reticular, amorphous and regular structure.

An increased percentage of cancer in the gland was related to the percentage of amorphous structure present, and inversely related to the percentage of microadenomatous, reticular and regular structure (Table IV).

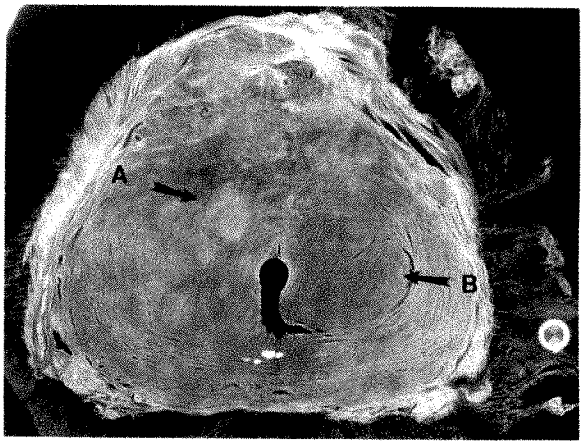

Figure 1. Microradiograph of prostatic carcinoma. A = Amorphous structure (carcinoma); B = benign structure.

It was concluded that cancer is amorphous on microradiography with destruction of all other types of structure (Fig. 1).

Differential relationship of echogenicity to benign or malignant prostates (Table V)

The percentage of low and mid-range echoes from benign and malignant glands was found to be significantly different; however, in the absence of microcalcification, the percentage of high echoes was not significantly different.

The effects on echogenicity of an increased percentage of cancer in the gland are detailed in Table VI. An increased percentage resulted in a significantly increased percentage of low echoes and a decreased percentage of mid-range echoes that was not significant, although cancer had significantly fewer ultrasonic mid-range echoes than benign disease. An increased percentage of cancer in the gland also resulted in a decreased percentage of high echoes. Cancer, therefore, had no significant effect on high echoes although there was a tendency to reduce them, and when microcalcification was present, it caused high echoes.

It was concluded that cancer causes low ultrasonic echoes with loss of mid-range echoes (Fig. 2). A few cancers have high echoes, which are due to associated microcalcification.

Table III. The differential relationship of structure to the presence of benign or malignant prostates

Structure	Benign	Malignant	*t*-test	*p*	Significant
Amorphous	14.4%[a]	49.9%	−7.8	<0.001	+
Regular	37.1%	23.3%	+3.3	<0.01	+
Microadenomatous	11.7%	8.7%	+1.3	>0.05	—
Reticular	36.5%	18.0%	+4.8	<0.001	+

[a] Consists mainly of muscle.

Table IV. The correlation of an increasing percentage of malignancy on structure

	Correlation (r)	p	Significant
Amorphous	+0.795	<0.001	+
Regular	−0.275	<0.01	+
Microadenomatous	−0.544	<0.001	+
Reticular	−0.707	<0.001	+

Relative echogenicity of prostatic cancer

Of the 29 cancers examined, 19 (66%) were hypoechoic, four (14%) were isoechoic and six (20%) were hyperechoic (Table VII). This is similar to findings in clinical practice, but differences will be present as incidental cancers are present in the cadaver study. All isoechoic cancers were incidental findings, being confined tumours and measuring $\leqslant 5$ mm.

On separating cancers into confined and unconfined groups (Table VIII), seven (44%) of the confined cancers were hypoechoic with four (25%) isoechoic and five (31%) hyperechoic. However, unconfined cancers were mainly hypoechoic (12, 92%) with only one (8%) hyperechoic and isoechoic tumours were absent.

Relationship of cancer to gland shape

Benign glands had a mild tendency to become more irregular with age ($r=0.128$) but this was not significant ($p>0.05$). The shape of malignant glands was significantly different from benign glands ($t=5.736$, $p<0.001$) being more irregular.

Irregularity of the gland shape was seen to relate to the size of the tumour ($r=0.555$, $p=0.001$). Tumours, if present in crescent, semicircular or round glands, were all equal to or less than 0.5 cm diameter. In asymmetrical and irregular glands, tumours were any size, including small tumours.

Relationship of echogenicity to tumour size

Hypoechoic cancers were seen to be distributed throughout the full range of tumour sizes (mean = 3.16 cm), whereas isoechoic cancers were all less than 0.5 cm in diameter and produced no structural change on microradiography. Hyperechoic cancers were smaller (mean = 1.02 cm) than hypoechoic cancers and all except one were confined to the gland. This may have a prognostic significance.

Table VI. The correlation of an increasing percentage of malignancy on echogenicity

	Correlation (r)	p	Significant
Low echoes	+0.254	<0.01	+
Mid-range echoes	−0.138	>0.05	−
High echoes	−0.311	<0.001	+

Table VII. Echogenicity of the cancers ($n=29$)

Echogenicity	n	Calcification	Structure
Hypoechoic	19 (66%)	No calcification in tumour	Amorphous
Isoechoic	4 (14%)	Calcification when present in benign distribution	Structured (no structural change present)
Hyperechoic	6 (20%)	Calcification in tumour	Amorphous

Table VIII. Echogenicity of confined and unconfined cancers

Echogenicity	Confined ($n=16$)		Unconfined ($n=13$)	
	No.	%	No.	%
Hypoechoic	7	44	12	92
Isoechoic	4	25	0	0
Hyperechoic	5	31	1	8

Discussion and conclusions

The technique of microradiography has enabled the structure of the prostate gland to be examined (Davies, 1986; Davies et al, 1988). It has been shown that there are four types of structure (regular, microadenomatous, reticular and amorphous), which are present in the different disease states of the gland. These relate to the disease processes present and its resulting ultrasound echogenicity.

The muscle of the gland has an amorphous structure that results in low echoes; the fat around the gland produces high echoes.

Benign glands are related to reticular structuring and this produces mid-range echoes. Benign hyperplasia produces a microadenomatous type of structure (Fig. 3) and this also produces mid-range echoes that are of a more coarse nature. Benign hyperplasia is inversely

Table V. The differential relationship of echogenicity to the presence of benign or malignant prostates

Echogenicity	Benign	Malignant	t-test	p	Significant
Low echoes	18.5[a]	29.7%	−3.1	<0.01	+
Mid-range echoes	66.9%	56.5%	+3.7	<0.001	+
High echoes	10.8%	14.4%	+1.9	>0.05	−

[a] Mainly from periurethral muscle.

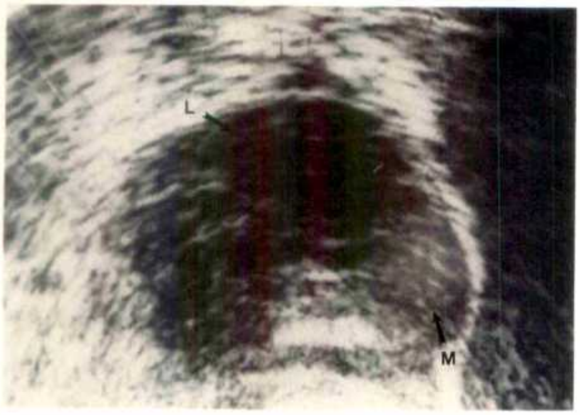

Figure 2. Per-rectal ultrasound of prostatic carcinoma. M = Mid-range echoes from benign structure; L = low echoes from amorphous malignant structure with breach of capsule.

related to amorphous structure and low echoes, *i.e.* inversely related to loss of structure and loss of mid-range echoes.

Cancer is related to amorphous structure and inversely to all other types of structure (Fig. 1). It is related to low echoes and to loss of mid-range echoes (Fig. 2), but in some tumours where microcalcification is present, high echoes occur.

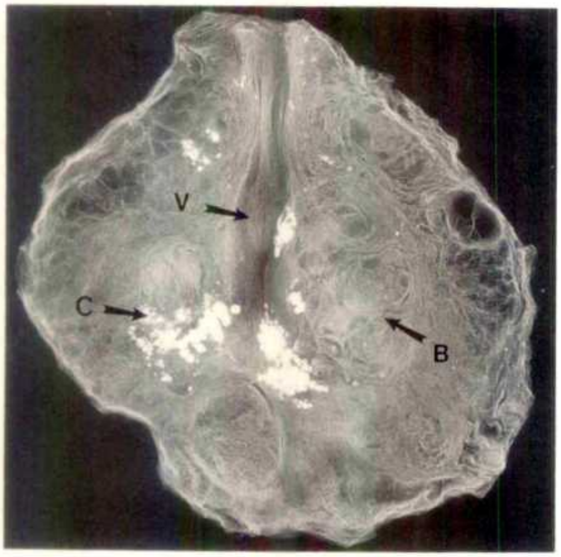

Figure 3. Microradiography of benign prostatic hypertrophy. B = Benign prostatic hyperplasia (microadenomatous type); C = calcification; V = verumontanum.

Acknowledgments

We are grateful to the Departments of Medical Statistics and Pathology and the Medical Workshop for their assistance in performing this work. We are indebted to the Medical Research Council for their support of this project.

References

BROOMAN, P. J. C., GRIFFITHS, G. J., ROBERTS, E. E., PEELING, W. B. & EVANS, K. T., 1981. Per-rectal ultrasound in the investigation of prostatic disease. *Clinical Radiology*, *32*, 669–676.

DAHNERT, W. F., HAMPER, U. M., EGGLESTON, J. C., WALSH, P. C. & SANDERS, R. C., 1986. Prostatic evaluation by transrectal sonography with histopathologic correlation: the echogenic appearance of early carcinoma. *Radiology*, *158*, 97–102.

DAVIES, R. LL., 1986. *Development and Application of Projection X-ray Microscopy*, PhD Thesis (University of Wales).

DAVIES, R. LL., JONES, D. R., HARRISON, T., GRIFFITHS, G. J. & EVANS, K. T., 1988. X-ray microscopy of the prostate gland. *British Journal of Urology*, *61*, 230–233.

GREENBERG, M., NEIMEN, H. L., BRANDT, T. D., FALKOWSKI, W. & CARTER, M., 1981. Ultrasound of the prostate. Analysis of tissue texture and abnormalities. *Radiology*, *141*, 757–762.

HARADA, K., TANAHASHI, Y., IGARI, D., NUMATA, I. & ORIKASA, S., 1980. Clinical evaluation of inside echo patterns in grey scale prostatic echography. *Journal of Urology*, *124*, 216–220.

JONES, D. R., GRIFFITHS, G. J., PARKINSON, M. C., EVANS, K. T., ROBERTS, E. E., DAVIES, R. LL., HARRISON, T. J. & PEELING, W. B., 1989. Comparative histopathology, microradiography and per-rectal ultrasonography of the prostate gland using cadaver specimens. *British Journal of Urology*, *63*, 508–511.

LEE, F., GRAY, J. M., MCLEARY, R. D., LEE, F. JNR, MCHUGH, T. A., SOLOMAN, M. H., KUMASAKA, G. H., STRAUB, W. H., BORLAZA, G. S. & MURPHY, G. P., 1986. Prostatic evaluation by transrectal sonography: criteria for diagnosis of early carcinoma. *Radiology*, *158*, 91–95.

PEELING, W. B., GRIFFITHS, G. J., EVANS, K. T. & ROBERTS, E. E. 1979. Diagnosis and staging of prostatic cancer by transrectal ultrasonography. A preliminary study. *British Journal of Urology*, *51*, 565–569.

RIFKIN, M. D., FRIEDLAND, G. W. & SHORTLIFFE, L., 1986. Prostatic evaluation by transrectal endosonography: detection of carcinoma. *Radiology*, *158*, 85–90.

RIFKIN, M. D., KURTZ, A. B., CHOI, H. Y. & GOLDBERG, B. B., 1983. Endoscopic ultrasonic evaluation of the prostate using a transrectal probe: prospective evaluation and acoustic characterisation. *Radiology*, *149*, 265–271.

1989, *The British Journal of Radiology*, *62*, 1063–1066

Low-field cine magnetic resonance imaging in aortic valve disease

By *Malcolm J. Metcalfe, MRCP, †‡Richard A. Jones, MSc, †§Thomas W. Redpath, PhD, **Francis W. Smith, MD, FFR, *Kevin Jennings, FRCP and *Stephen Walton, MD, MRCP

*Department of Cardiology and University Departments of †Bio-Medical Physics and **Nuclear Medicine, Aberdeen Royal Infirmary, Aberdeen AB9 2ZB

(*Received March 1989 and in revised form August 1989*)

Abstract. Cine magnetic resonance imaging (MRI) holds considerable promise as a means of detecting abnormal blood flow patterns within the heart and great vessels. To date, the majority of techniques employed have required moderate to high field strengths. We describe a novel, low-field-strength approach that is technically undemanding and faster than conventional methods, which we have applied to the detection of aortic valve disease. A series of 26 patients with aortic stenosis or aortic regurgitation was compared with 21 normal subjects. All 20 patients with aortic stenosis and 15 of 16 patients with aortic regurgitation were identified. There were four false positives in the aortic stenosis group; all these patients had significant aortic regurgitation. There were no false positives in the aortic regurgitation group. Low-field cine MRI is a practical and useful technique for the detection of aortic valve disease.

Since 1959 the sensitivity of magnetic resonance imaging (MRI) to flow has been appreciated (Singer, 1959), but it was not until the advent of whole-body imaging that associated cardiac blood flow could be appreciated (van Dijk, 1984). The majority of methods currently in use have the disadvantage of requiring medium- to high-field-strength machines. Recently, there has been a resurgence of interest in low-field-strength machines, which are less complicated, cheaper to buy and run and have certain advantages for cardiac work. To date, there has been only one report reliably identifying patients with significant aortic stenosis (Mitchell et al, 1988). There is, therefore, considerable interest in developing "fast-imaging" techniques to assess cardiac function and related anatomy. One such method of assessing aortic valvular function is described.

Patients and methods

Twenty-one normal controls (mean age 34 years, range 17–68 years) were compared with 26 patients with aortic valvular disease (mean age 58 years, range 17–84 years). All subjects with the exception of 11 normal volunteers had recently undergone cardiac catheterization to establish either their coronary anatomy or the severity of their aortic valvular disease. All patients were in sinus rhythm with no significant transient dysrhythmias.

Aortic stenosis was defined as a pressure difference of more than 19 mmHg from left ventricle to aorta recorded during cardiac catheterization. These measured pressure differences ranged from 20 to 140 mmHg with a mean of 61 mmHg. The severity of the aortic regurgitation was assessed by aortic root injection of 40 ml of contrast medium at 20 ml/s down a pigtail catheter. Care was taken to prevent the catheter prolapsing across the valve and causing spurious regurgitation. The severity was described as Grades 1 to 3. Grade 1 was taken as slight regurgitation of contrast medium in early diastole clearing completely in the next systole. Grade 2 was more severe regurgitation, which did not clear in the next systole. Grade 3 was severe regurgitation immediately filling and opacifying the ventricle at the end of the first diastole.

Magnetic resonance imaging was performed using a 3.4 MHz resistive magnet operating at 0.08 T (Redpath et al, 1987). A 16-frame cine MRI sequence was implemented using conventional electrocardiogram gating (Jones et al, 1989). The first line of data was acquired immediately after the QRS component. The repetition interval (TR) for the following 16 pulses was programmed in the range 35–75 ms, to encompass as much of the cardiac cycle as possible without over-running.

The patients were imaged using 20 mm contiguous transaxial slices from the aortic arch to the apex of the heart, typically taking six to seven slices. The patients were positioned using an ungated, fast saturation–recovery sequence. As no special setting up was required, the examination was usually completed within 30 min. The raw data were then transferred and processed using a VAX 750 computer. After processing, the 16 frames of each set were reviewed either separately or in the form of a movie-loop.

Using this method, blood flowing orthogonally to the imaging plane produces signal enhancement and turbulent flow results in a signal void on the images. The resulting sets of scans for each patient were then assessed blindly and independently and the results

---

*Author for correspondence and reprint requests.
Current addresses: ‡MR Senter, SINTEF, 7034 Trondheim, Norway; §Department of Clinical Physics, Walsgrave Hospital, Coventry CV2 2DX.

compared. The degree of observed aortic stenosis was recorded as normal, insignificant or significant by the following criteria. During systole, immediately proximal to and around the aortic arch, normal patients had uniform (non-turbulent) flow. Patients regarded as having insignificant aortic stenosis had partially turbulent flow and patients regarded as having significant aortic stenosis completely turbulent flow. The degree of aortic regurgitation was graded as normal, insignificant (a small area of turbulence just proximal to the aortic valve in diastole) and significant (more extensive turbulence extending at least to mid cavity).

In the case of aortic regurgitation the images were carefully viewed in the cine mode and unless the aortic valve was clearly demonstrated the images were excluded from analysis. This was done to prevent possible confusion arising from minor turbulence associated with the diastolic inflow, through the mitral valve, which is seen in all subjects.

Results

In the controls, signal enhancement resulting from laminar flow was seen in the proximal ascending aorta, descending aorta, right ventricular outflow tract, superior and inferior vena cavae and from left atrium to ventricle during diastole. In the proximal aorta, just above the aortic valve, a degree of turbulence was noted in some of the controls. In both controls and patients, a small degree of turbulence was noted just proximal to the aortic valve in systole but not in diastole. During diastole a variable degree of turbulence was seen in the ventricular cavity associated with the laminar flow through the mitral valve. In the normal patients, all of the above features were noted but the contrast was improved and consequently the images were of better quality than in the volunteers.

Visualization by continuous movie-loop clearly separated systolic and diastolic components of flow together with cardiac wall motion characteristics. Thus, in patients with aortic regurgitation, it was possible to visualize the start of aortic regurgitation just prior to diastolic inflow. It also helped to appreciate finer points of detail such as valve leaflets and smaller artery systolic flow.

Of the 26 patients with aortic valve disease, six patients had pure aortic regurgitation, 10 patients had pure aortic stenosis and 10 patients had both.

In the 20 patients with aortic stenosis, marked turbulence was observed within a variably dilated ascending aorta (Fig. 1). This turbulence was easily distinguished from the controls. Seven out of nine patients with a pressure difference of > 50 mmHg had significant turbulence; in the other two, turbulence was present but was graded as insignificant. On the other hand, turbulence was insignificant in nine out of 11 patients with a pressure difference of < 50 mmHg; in the other two it was graded as significant. Thus it was possible to gain a rough impression of the severity of the turbulence. Four false positives were also noted, occurring in patients with significant aortic regurgitation. Two of these patients were graded as having significant aortic stenosis and the remaining two as insignificant stenosis.

Fifteen out of 16 patients with aortic regurgitation were detected (Fig. 2) but in one patient (with minor regurgitation) the diagnosis was missed. Cine MRI correctly identified nine out of 11 patients with significant aortic regurgitation but underestimated two. Of the patients with minor aortic regurgitation, the diagnosis was overestimated in one patient and missed in another. Only one patient in this study was excluded from analysis because of technical failure in identifying the aortic valve. No false positives were identified.

Discussion

Magnetic resonance imaging is increasingly being regarded as a valuable tool for the assessment of cardiac disease. Unlike other imaging techniques that have their strengths in different areas and are to an extent comple-

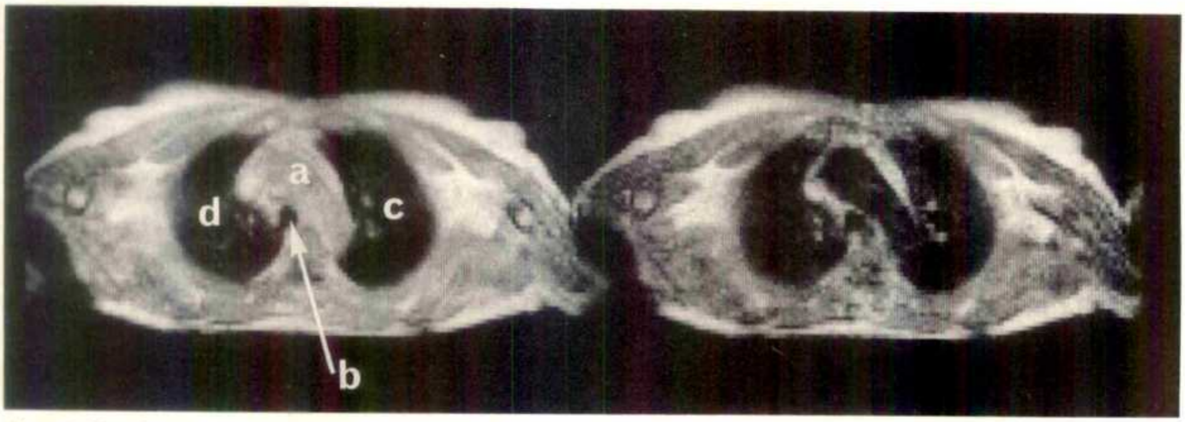

Figure 1. Two frames from a 16-frame cine MRI set of a patient with significant aortic stenosis. The section is at the level of the aortic arch. In the first frame (end diastole) the essentially neutral flow of blood can be seen and in the other frame (mid systole) the aortic arch is completely turbulent and consequently gives no signal. (a = aortic arch; b = trachea; c = left lung; d = right lung.)

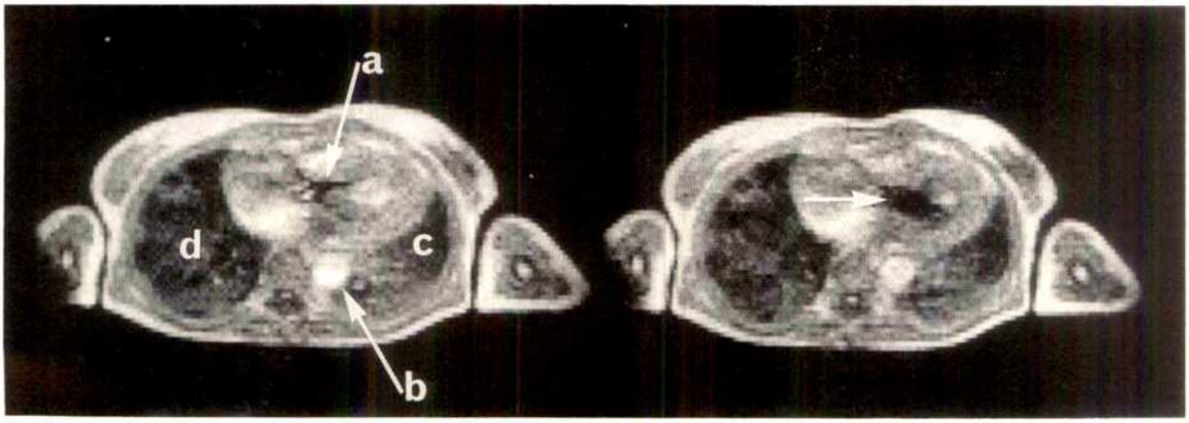

Figure 2. Two frames from a 16-frame cine MRI set of a patient with severe aortic regurgitation. The section is just proximal to the aortic outflow. The two frames show the progression of the regurgitant jet within the left ventricular cavity in early diastole. (a = aortic outflow tract; b = descending aorta; c = left lung; d = right lung.)

mentary, MRI has the ability to demonstrate related anatomy, function and blood flow (Margulis & Crooks, 1988). With regard to blood flow imaging it has been shown to be sensitive in assessing valvular regurgitation (Schiebler et al, 1987; Sechtem et al, 1987; Higgins et al, 1988), but to date has had only very limited application in assessing valvular stenosis (Sechtem et al, 1987; Mitchell et al, 1988).

The appearance of flowing blood on MRI depends on the technique used, with gradient echoes enhancing the signal due to flowing blood (Schiebler et al, 1987; Sechtem et al, 1987; Margulis & Crooks, 1988), whilst spin echoes suppress it (von Schulthess et al, 1985; Dilwath et al, 1987). Spin echoes are useful for assessing wall motion and intracardiac anatomy, whilst gradient echoes are superior for studying cardiac function such as regurgitant jets (Schiebler et al, 1987; Sechtem et al, 1987; Higgins et al, 1988).

Recently, the emphasis has been on trying to increase the speed of data acquisition by using cine MRI sequences (Waterton et al, 1985; Schiebler et al, 1987; Sechtem et al, 1987). These methods can acquire data in a fraction of the time required by conventional techniques but to date have only been applicable to medium- to high-field-strength machines. Our scans were obtained in the transaxial plane and consequently are nearest to a short-axis view.

Cine MRI techniques have previously demonstrated turbulence in the proximal aorta (Higgins et al, 1988), but, apart from our study, this feature has only been reported to be of clinical use in one previous report (Mitchell et al, 1988). Other methods of velocity mapping (Klipstein et al, 1987a,b; Underwood et al, 1987) have been employed but do not seem at present to be applicable to pathological aortic stenosis, presumably due to the eccentric jets and high velocity. These methods also have the disadvantage that they significantly prolong the imaging time.

The method used with our machine was deliberately kept simple so that the actual imaging time was as short as possible, typically 30 min. Although our machine is of low field strength, good-quality images were obtained without averaging, albeit of limited resolution. Low field strength has certain advantages for cardiac work, notably less motion artefact, lack of chemical shifts, less noise, shorter T_1 times and machines cheaper to buy, install and run (Margulis & Crook, 1988).

It is interesting that the images obtained in the normal controls were of better quality and definition than those of the normal volunteers. This is probably related to the increased age of the former population, as an increase in perivascular adipose tissue with age enhances the signal and therefore results in better definition. A secondary factor may be that increased atheroma lining the aorta in the older population may induce turbulence at the edges of the flowing blood with consequent increased definition.

All clinically important degrees of regurgitation were detected, but there was limited correlation, particularly of minor regurgitation, with the angiographic grading. The most likely reason for this is that a transaxial view was used. The regurgitant jet, therefore, was not in the optimum orientation for accurate assessment of the extent of the turbulence jet, as the left ventricular cavity was distorted. The majority of cine MRI techniques to date have used a long axis plane, through the aortic valve, to identify the regurgitant jet (Schiebler et al, 1987; Higgins et al, 1988). A further explanation, especially where minor degrees of regurgitation is concerned, is poor separation from the turbulence associated with mitral valve flow in diastole. In all subjects, during diastole, the laminar flow through the mitral valve is preceded by a small degree of turbulence. In minor degrees of aortic regurgitation it is possible that turbulence from both sources is poorly separated and perceived as more extensive aortic regurgitation than is actually the case. Development is currently under way to produce a post-processing steerable image slice to alleviate this without losing the inherent simplicity of the method.

The method is of particular interest in assessing the degree of aortic stenosis. Although, as previously observed in normal subjects, a small degree of turbulence is often present in the proximal aorta (Higgins et al. 1988), in practice it is clearly distinguishable from the turbulence generated by a stenotic valve. Cine MRI identified all patients with aortic stenosis. By using admittedly "soft" criteria to grade severity, there was only limited correlation with the measured pressure difference by cardiac catheterization.

The reason that these patients can be identified is possibly explained by the Bernoulli equation (Hatle & Angelson, 1985), which states that as a stenosis becomes more severe the velocity of blood through the stenosis increases as a square function. The more obstructive the stenosis the greater will be the velocity through it, and consequently the amount of generated turbulence distal to the valve will also be proportionally increased. In theory, if the jet is eccentric it could impinge on the aortic wall thus dissipating its kinetic energy and not producing as much turbulence as expected. This may be a contributary mechanism in those patients where there was underestimation of the stenosis.

In four patients with significant aortic regurgitation, abnormal turbulence was detected; the reason for this is probably two-fold. First, one patient had Marfan's disease with aneurysmal enlargement of the aortic root and grossly abnormal valve cusps, which could lead to increased turbulence across the valve. Secondly, in all four patients there was concomitant significant aortic regurgitation, which would lead to a marked increase in stroke volume across the valve, thereby generating increased turbulence.

These results demonstrate that this technique is sensitive for the detection of aortic stenosis or regurgitation. There is a limited correlation with severity as assessed by cardiac catheterization but further development may improve this with regard to aortic regurgitation. In view of its simplicity, speed and good blood-flow contrast, it is worthy of further investigation.

References

DILWATH, L. R., AISEN, A. M., MANCINI, G. B. J. & BUDA, A. J., 1987. Serial NMR imaging in acute MI. *American Journal of Cardiology, 59,* 1203–1205.

HATLE, L. & ANGELSON, B., 1985. Physics of blood flow. In *Doppler Ultrasound in Cardiology: Physical Principles and Clinical Applications* (Lea and Febiger, Philadelphia), p. 24.

HIGGINS, C. B., HOLT, W., PFLUGFELDER, P. & SECHTEM, U., 1988. Functional evaluation of the heart with MRI. *Magnetic Resonance in Medicine, 6,* 121–139.

JONES, R. A., METCALFE, M. J., REDPATH, T. W., SMITH, F. W. & WALTON, S., 1989. Low-field cine magnetic resonance imaging. *British Journal of Radiology, 62,* in press.

KLIPSTEIN, R. H., FIRMIN, D. N., UNDERWOOD, S. R., NAYLOR, G. L., REES, R. S. O. & LONGMORE, D. B., 1987a. Colour display of quantitative blood flow and cardiac anatomy in a single magnetic resonance cine-loop. *British Journal of Radiology, 60,* 105–111.

KLIPSTEIN, R. H., FIRMIN, D. N., UNDERWOOD, S. R., REES, R. S. O. & LONGMORE, D. B., 1987b. Blood flow patterns in the human aorta studied by magnetic resonance. *British Heart Journal, 58,* 316–323.

MARGULIS, A. R. & CROOKS, L. E., 1988. Present and future status of magnetic resonance imaging. *American Journal of Roentgenology, 150,* 487–492.

MITCHELL, L., JENKINS, J. P. R., ISHERWOOD, I. & ROWLANDS, D. J., 1988. Cine-flow magnetic resonance imaging in valvular heart disease. *British Journal of Radiology, 61,* 780.

REDPATH, T. W., HUTCHISON, J. M. S., EASTWOOD, L. M., SELBIE, R. D., JOHNSON, G., JONES, R. A. & MALLARD, J. R., 1987. A low field NMR imager for clinical use. *Journal of Physics E: Scientific Instruments, 20,* 1228–1234.

SCHIEBLER, M., AXEL, L., REICHEK, N., AURIGEMMA, G., YEAGER, B., DOUGLAS, P., BOGIN, K. & KRESSEL, H., 1987. Correlation of cine-MRI with two dimensional pulsed Doppler echocardiography in valvular insufficiency. *Journal of Computer Assisted Tomography, 11,* 627–632.

SECHTEM, U., PFLUGFELDER, P. W., WHITE, R. D., GOULD, R. G., HOLT, W., LIPTON, M. J. & HIGGINS, C. B., 1987. Cine-MR imaging: potential for the evaluation of cardiovascular function. *American Journal of Roentgenology, 148,* 239–246.

SINGER, J. R., 1959. Blood flow rates by nuclear magnetic resonance measurements. *Science, 130,* 1652–1653.

UNDERWOOD, S. R., FIRMIN, D. N., KLIPSTEIN, R. H., REES, R. S. O. & LONGMORE, D. B., 1987. Magnetic resonance velocity mapping: clinical application of a new technique. *British Heart Journal, 57,* 404–412.

VAN DIJK, P., 1984. Direct cardiac nuclear magnetic resonance imaging of heart wall and blood flow velocity. *Journal of Computer Assisted Tomography, 8,* 429–436.

VON SCHULTHESS, G. K., FISHER, M., CROOKS, L. E. & HIGGINS, C. B., 1985. Gated MR images of the heart: intracardiac signals in patients and healthy subjects. *Radiology, 156,* 125–132.

WATERTON, J. C., JENKINS, J. P. R., ZHU, X. P., LOVE, H. G., ISHERWOOD, I. & ROWLANDS, D. J., 1985. Magnetic resonance (MR) cine imaging of the human heart. *British Journal of Radiology, 58,* 711–716.

1989, *The British Journal of Radiology*, *62*, 1067–1074

Gadolinium-enhanced magnetic resonance imaging of spinal tumours

By C. I. Rothwell, FRCR, T. Jaspan, MRCP, FRCR, B. S. Worthington, BSc, FRCR and I. M. Holland, DMRD, FRCR

Department of Neuroradiology, University Hospital, Queen's Medical Centre, Nottingham NG7 2UH

(Received November 1988 and in revised form July 1989)

Abstract. The use of gadolinium diethylenetriamine-penta-acetic acid (Gd-DTPA) (Magnevist) enhanced magnetic resonance imaging (0.15 T) in the assessment of spinal tumours is described. Thirty-five patients were entered into the study and a total of 39 examinations were performed. The information obtained from unenhanced T_1- and T_2-weighted spin–echo sequences was compared with the Gd-DTPA-enhanced T_1 images. Thirty patients had intradural lesions and five had extradural lesions. A variable pattern of enhancement of intramedullary tumours was found, which in part reflected differences in the cystic component of the lesions. Extramedullary intra- and extradural lesions generally showed marked enhancement. The greatest contribution to management decisions was in the evaluation of intramedullary tumours where the use of contrast enhancement facilitated the precise localization of active tumour, differentiation of cystic and solid components of tumour, separation of tumour from peritumoral oedema and, in cases of suspected recurrence, aided distinction between tumour and both post-operative scarring and radiation damage.

Magnetic resonance imaging (MRI) has rapidly become the method of choice, when available, for the investigation of both intrinsic and extrinsic spinal cord disease. The advantages compared with myelography and computed tomography (CT) are now well established; these include the avoidance of ionizing radiation, lack of planar restriction and, above all, the wide range of tissue contrast that can be obtained by the appropriate choice of pulse sequence, providing excellent discrimination between intramedullary, extramedullary intradural and extradural disease processes. T_1-weighted spin–echo (SE) sequences provide good anatomical detail and T_2-weighted SE sequences are very sensitive for demonstrating pathology, which appears as areas of high signal intensity. However, the long repetition times of such sequences necessitates lengthy acquisition times making them more susceptible to artefact from cerebrospinal fluid (CSF) motion and patient movement. Furthermore, T_2-weighted SE sequences do not allow clear discrimination between tumour, peritumoral oedema, proteinaceous cystic change, reactive gliosis and post-radiotherapy changes.

The thrust to develop intravascular contrast agents in MRI was to allow discrimination between magnetically similar tissues, and, in the case of the brain and spinal cord, exploit differences in perfusion and breakdown of the barrier between the blood and neural tissue in a variety of pathologies. Gadolinium-DTPA was the first such contrast medium to be developed, and studies in the UK and Germany in 1983 and 1984 (Carr et al, 1984; Weinmann et al, 1984) proved the potential of the agent in diagnosing cerebral tumours. Further clinical trials have indicated that Gd-DTPA can improve the detection and characterization of intracranial lesions (Claussen et al, 1985; Curati et al, 1986; Stack et al, 1988) and have suggested that it is useful in the evaluation of spinal cord lesions (Bydder et al, 1985; Valk, 1988; Sze et al, 1988; Dillon et al, 1989). In this paper we present our experience of using Gd-DTPA in the investigation of suspected spinal cord tumours.

Patients and methods

Thirty-five patients with a clinically suspected diagnosis of spinal tumour were examined. A total of 39 examinations were performed, two patients having one follow-up scan and one patient being examined on three consecutive occasions. In each case a presumptive diagnosis had been made by an alternative examination technique, usually myelography complemented by computed tomography. Patients were aged between 18 and 75 years of age. Informed consent was obtained in all cases. Exclusion criteria included pregnancy, metallic implants and renal or hepatic failure.

Magnetic resonance imaging was performed on a Picker 0.15 T resistive system. The imaging protocol included pre-contrast T_1-weighted SE (repetition time (TR) = 500 ms, echo time (TE) = 40 ms) sequences in both the axial and sagittal planes and a T_2-weighted SE (TR = 1600 ms, TE = 80 ms) sequence in the sagittal plane. Gadolinium-DTPA (0.1 mmol/kg) was then injected intravenously as a bolus, followed by immediate re-scanning in both axial and sagittal planes, employing the same T_1-weighted sequence. A 128×128 acquisition matrix with two excitations was employed for the T_2-weighted sequences and a 256×256 matrix (192×192 towards the end of the study) with four excitations for the T_1-weighted sequences. A 30 cm field of view with dedicated surface coils and 7 mm thick contiguous slices were used routinely.

The T_1, T_2 and enhanced T_1 images were assessed by two neuroradiologists for their diagnostic quality, particular attention being paid to lesion conspicuity, separation of lesions from normal and oedematous cord and lesion signal characteristics. The enhancement of the lesion was graded as being none, moderate or marked. The images were then assessed to see if the gadolinium-enhanced images provided additional information, were of equal quality or provided less information than the comparable unenhanced MRI study.

Results

Table I provides the analysis of all the cases studied according to histological type. Operative histology was available in 27 patients (77.0%). A total of 30 patients with spinal tumours was examined and in each case the tumours showed a varying degree of enhancement with Gd-DTPA. There were 20 patients with intramedullary neoplasms (10 astrocytomas, six ependymomas, three haemangioblastomas and one spinal metastasis from a pineal germinoma), five intradural extramedullary neoplasms (four neurofibromas and one meningioma) and five extradural neoplasms (two chordomas, one malignant melanoma, one Hodgkin's lymphoma and one paraganglionoma). Three patients had benign lesions (one neuroepithelial cyst and two with hydrosyringomyelia); none of these lesions showed evidence of enhancement. Two patients were examined following surgery (one dermoid of the conus and one intramedullary ependymoma) to assess the extent of residual tumour. In both cases, post-operative changes only were shown with no evidence of enhancement.

Side-effects from Gd-DTPA were minimal. Two patients complained of slight warmth at the injection site, which lasted for a few minutes, possibly due to the hyperosmolality of the contrast medium. There were no other side-effects or adverse reactions.

The enhanced MRI scans provided more information than the plain MRI scans in 25 cases, were equivalent in nine cases and less informative in one. Most tumours, whether intra-axial or extra-axial, showed either homogeneously or heterogeneously strong enhancement. The main exceptions were the intramedullary gliomas, five of which showed only slight enhancement.

Intramedullary tumours

There were 20 intramedullary tumours and in all cases the T_2 images revealed an abnormality with areas of increased signal intensity. Contrast enhancement occurred in all cases but in 17 the Gd-DTPA images improved tumour delineation.

Of the 10 patients with cord astrocytomas, three were solid, four solid with a peritumoral cyst and three were predominantly cystic. Contrast enhancement of tumour tissue was variable being only slight in five and pronounced in five. In the three patients with a mainly cystic lesion (Fig. 1), there was definite rim enhancement, which excluded the diagnosis of a non-tumoral syrinx. In two patients who were examined after previous surgery and radiotherapy, tumour recurrence could only be positively identified after Gd-DTPA. In one case (Fig. 2) the T_2-weighted sequence demonstrated a thin atrophic cord with diffuse high signal consistent with either post-operative gliosis or tumour recurrence. However, Gd-DTPA administration revealed the presence of a nodule of enhancing tumour. In the other patient, focal expansion of the cord was demonstrated at the site of previous surgery with high signal on the T_2 sequence. The Gd-DTPA scan revealed the lesion to be predominantly cystic but with definite enhancing

Table I. Analysis of radiological findings according to histological type

Diagnosis	Patient no.	Findings on scan			Enhancement		
		Plain MR >Gd scan	Plain MR =Gd scan	Gd scan >Plain MR	None	Slight	Marked
Astrocytoma	10	—	3	7	—	5	5
Ependymoma	6	—	—	6	—	1	5
Haemangioblastoma	3	—	—	3	—	—	3
Intramedullary metastasis from pineal dysgerminoma	1	—	—	1	—	—	1
Residual ependymoma?	1	—	1	—	1	—	—
Syringomyelia	2	—	2	—	2	—	—
Neurofibroma	4	—	1	3	—	1	3
Meningioma	1	—	—	1	—	—	1
Neuroepithelial cyst	1	1	—	—	1	—	—
Residual dermoid	1	—	1	—	1	—	—
Chordoma	2	—	1	1	—	—	2
Extradural malignant melanoma	1	—	—	1	—	—	1
Mesenchymal giant cell tumour	1	—	—	1	—	—	1
Lymphoma	1	—	—	1	—	—	1
Total	35	1	9	25	5	7	23

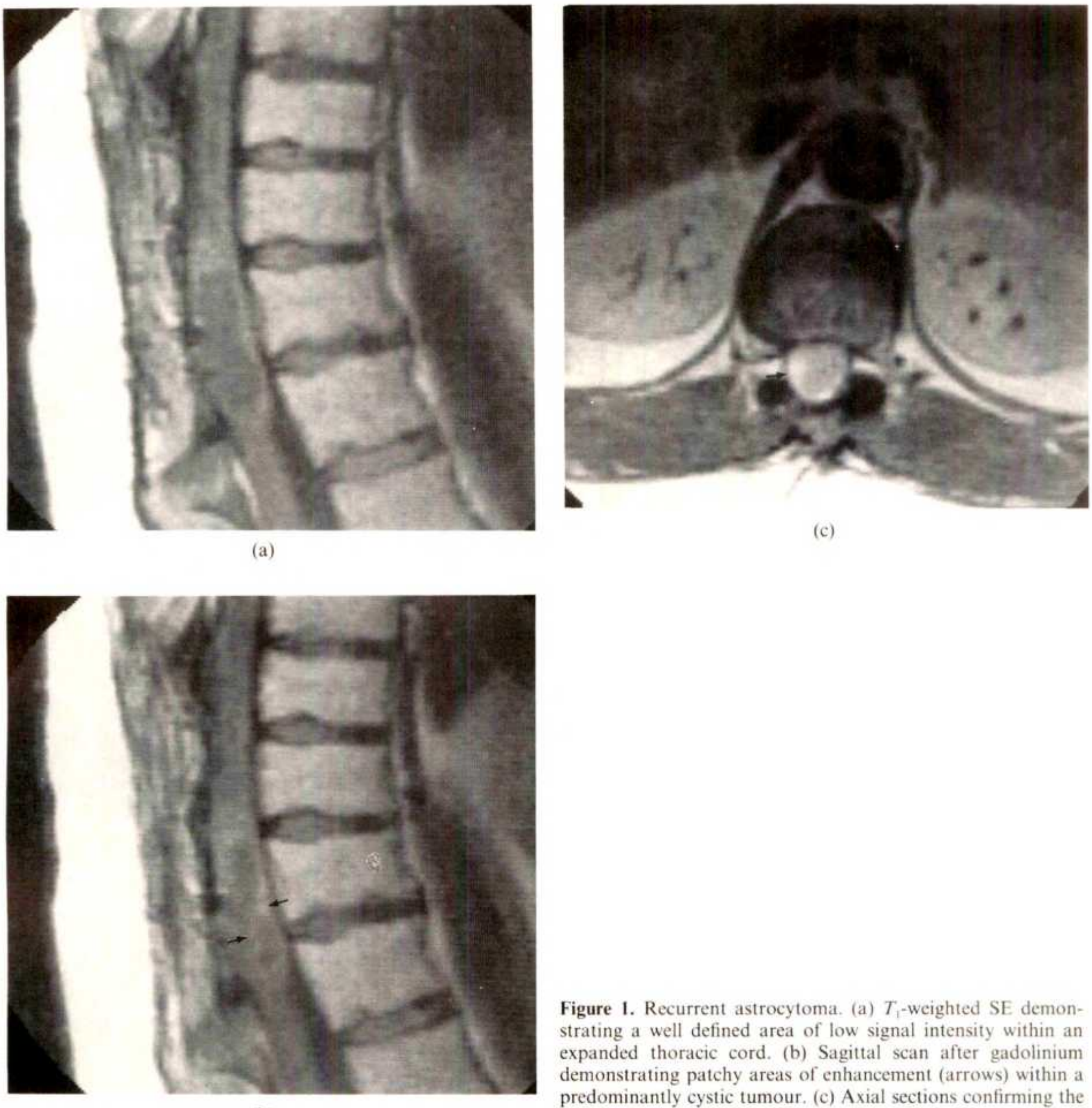

Figure 1. Recurrent astrocytoma. (a) T_1-weighted SE demonstrating a well defined area of low signal intensity within an expanded thoracic cord. (b) Sagittal scan after gadolinium demonstrating patchy areas of enhancement (arrows) within a predominantly cystic tumour. (c) Axial sections confirming the areas of enhancement within the cyst wall.

tumour in its wall. In this particular case the immediate post-contrast images revealed only slight enhancement but this was much more pronounced on a delayed scan taken 30 min after the injection of Gd-DTPA.

There were six patients with ependymomas (Fig. 3) and all except one showed strong enhancement of tumour tissue, which was homogeneous and sharply demarcated. Two of these patients had central cystic cavities, which were highlighted by the Gd-DTPA.

Three patients with haemangioblastomas were examined. In all cases the solid nodule of the tumour enhanced strongly and uniformly and could only be accurately identified on the Gd-DTPA images (Fig. 4). In one patient (Fig. 5) with a largely solid cervical haemangioblastoma, the Gd-DTPA sequences revealed further small, unsuspected, solid haemangioblastomas within the posterior fossa and the thoracic cord.

A single patient with intramedullary spinal metastasis from a pineal dysgerminoma was examined on three sequential ocasions. The extensive thoracic metastasis enhanced markedly, although heterogeneously, with Gd-DTPA. The contrast scans were of particular benefit in assessing the response of the tumour to radiotherapy and chemotherapy, demonstrating tumour regression.

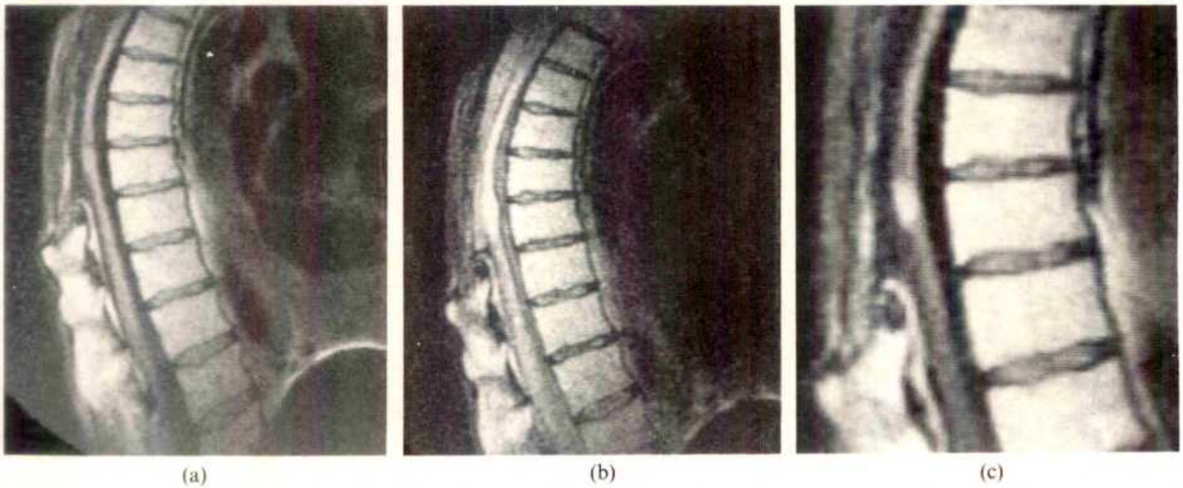

Figure 2. A 60-year-old man who had a macroscopic clearance of a dorsal intramedullary glioma 10 years previously, now presenting with severe thoracic backache. Myelogram revealed post-operative tethering of an atrophic cord. (a) T_1-weighted SE showed an atrophic cord with normal signal characteristics. (b) T_2-weighted SE. The mid-thoracic cord is of abnormal high signal intensity over several thoracic segments. (c) Post-gadolinium images demonstrate a definite focus of contrast enhancement within the thoracic cord consistent with tumour recurrence/residuum.

Extramedullary lesions

Six patients with intradural extramedullary lesions (four neurofibromas, one meningioma and one neuroepithelial cyst) were examined. The meningioma and three of the neurofibromas (Fig. 6) enhanced strongly and homogeneously with gadolinium. However, one patient with multiple neurofibromatosis showed only moderate and variable enhancement. The cervical neuroepithelial cyst did not enhance.

There were five patients with extradural tumours and in all cases at least part of the tumour enhanced strongly after Gd-DTPA. In all cases the extradural location of the tumour was identified on the unenhanced images but conspicuity and delineation of the extent of tumour was improved on the enhanced examinations.

Discussion

Gadolinium-DTPA has been shown to be safe and effective as a paramagnetic agent and several studies have reported on its clinical efficacy in the imaging of intracranial (Carr et al, 1984; Clausen et al, 1985; Curati et al, 1986; Valk, 1987; Stack et al, 1988) and spinal pathology (Bydder et al, 1985; Sze et al, 1988a, b; Valk, 1988; Dillon et al, 1989). The distribution and excretion of Gd-DTPA after intravenous injection is similar to that of conventional iodinated contrast media used in CT. In solution, Gd-DTPA exerts a paramagnetic effect due to the seven unpaired electrons of Gd^{3+}, which cause marked fluctuations of the local magnetic field. This results in a decrease in the T_1 and T_2 relaxation times of adjacent hydrogen protons through the proton–electron dipole–dipole phenomenon (Wolf et al, 1985; Gomori & Grossman, 1987). When present in tissues its effect is to produce a shortening of both T_1 and T_2 relaxation times, there being a reciprocal relationship between the degree of shortening and the local concentration. Since the T_1 of the particular tissue is always greater than its T_2, the absolute decrease of T_1 is always greater than that of T_2. In general, decreasing T_1 increases signal intensity with the optimal pulse sequences whilst decreasing T_2 leads to a reduction in signal intensity. The latter effect only comes to dominate the final signal intensity at high concentrations, and at the low concentration used in clinical practice following an intravenous injection of 0.1 mmol/kg, the T_1 effect predominates. It is on this account that highly T_1-dependent sequences such as an inversion–recovery (IR) sequence with a medium inversion time (TI) are most appropriate for the detection of contrast enhancement (Graif et al, 1985). These demonstrate greatest contrast enhancement when the TI of the IR sequence is intermediate between the T_1 of the tissue before and after enhancement with Gd-DTPA. Inversion–recovery sequences necessitate relatively long acquisition times and therefore, as a compromise, the shorter T_1-dependent forms of the SE can be used, which display moderate contrast enhancement that is generally greatest when the TR is between the tissue T_1 before and after contrast enhancement. Spin–echo sequences with long TR and TE values being relatively T_2-weighted are generally insensitive to contrast enhancement.

The enhancement demonstrated with intramedullary tumours is due to disruption of the barrier between blood and neural tissue, which allows Gd-DTPA to leak from the vascular compartment into the interstitial spaces. It would therefore seem reasonable to assume that the greater the degree of disruption of this barrier the greater the enhancement. Furthermore, if the disruption of the barrier is minimal, as may occur in low-grade gliomas, then enhancement might be slight initially but

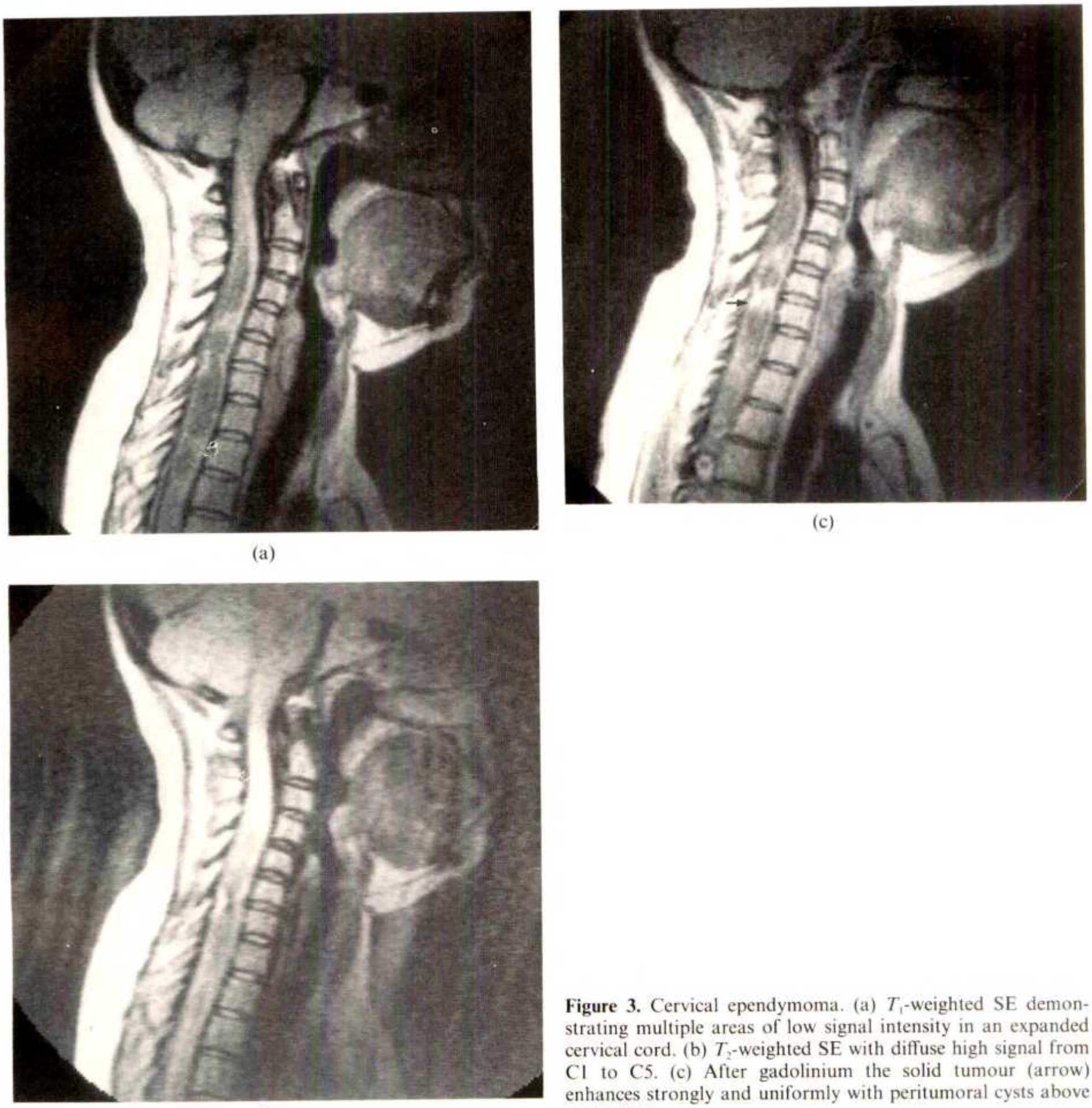

(a)

(c)

(b)

Figure 3. Cervical ependymoma. (a) T_1-weighted SE demonstrating multiple areas of low signal intensity in an expanded cervical cord. (b) T_2-weighted SE with diffuse high signal from C1 to C5. (c) After gadolinium the solid tumour (arrow) enhances strongly and uniformly with peritumoral cysts above and below.

increase progressively on delayed scans as the gadolinium slowly crosses the breach in the barrier. This feature of delayed enhancement of low-grade gliomas has been described (Laniado et al, 1986; Schorner et al, 1986) and was demonstrated in one of our patients with a Grade I astrocytoma where the enhancement at 15 min was equivocal but became obvious on the later scan at 30 min.

There were 20 patients with intramedullary tumours. On the preliminary T_1-weighted sequences, tumour boundaries were often difficult to discern, the tumour being almost isointense with the cord. On T_2-weighted sequences, both tumour and peritumoral oedema appeared as high signal. In 17 cases the enhanced scans were more informative, in particular in delineating tumour boundaries. Peritumoral cysts were identified in two of the ependymomas and in four of the astrocytomas. Their location could only be determined accurately on the enhanced scans as the proteinaceous cysts may have similar signal characteristics to the tumour. The enhancement characteristics did not permit accurate discrimination between astrocytomas and ependymomas, although five of the six ependymomas did show strong enhancement whereas this occurred in only five of the 10 astrocytomas and was slight in the remainder. The ependymomas were generally centrally situated,

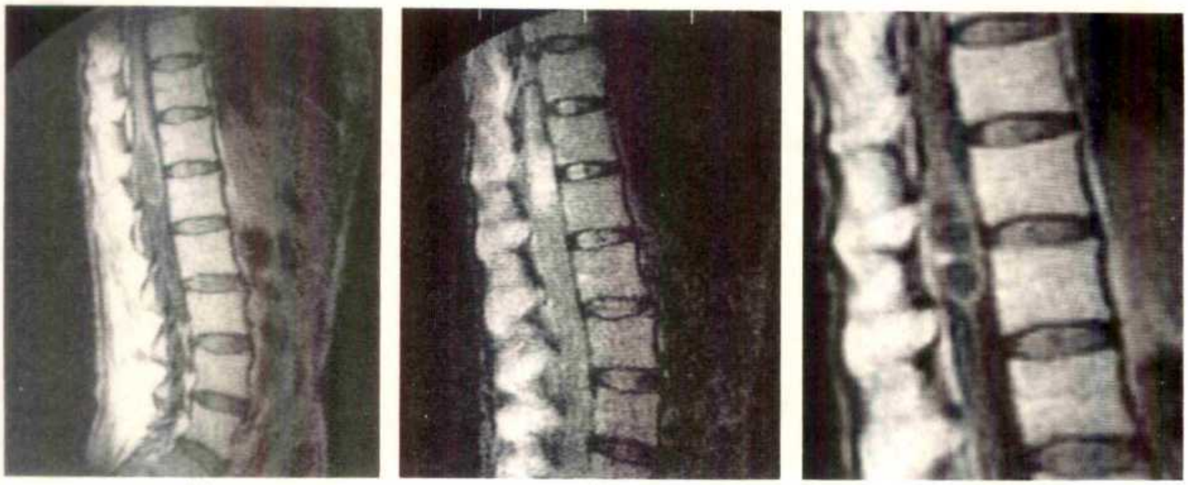
(a) (b) (c)

Figure 4. A 61-year-old woman with Von Hippel-Lindau disease. (a) T_1-weighted SE. There is fusiform expansion of the conus with a lesion of low signal intensity. (b) T_2-weighted SE. The lesion is of diffuse high signal intensity. (c) Sagittal images after gadolinium demonstrate the solid mural nodule of a cystic haemangioblastoma.

well demarcated and the enhancement was uniform, whereas the astrocytomas were often eccentrically placed and the enhancement was much more patchy and irregular, in keeping with a more diffuse infiltrating process.

The enhanced scans were particularly useful in the assessment of possible tumour residuum or recurrence after previous surgical intervention or radiotherapy. In this situation the unenhanced images can be difficult to interpret as there may be high signal within the cord on T_2-weighted images, which could be due to either tumour or gliotic scarring. If the cord is enlarged then one would favour tumour recurrence, but if the cord is atrophic gliosis would seem more likely. However, it is essential to proceed to enhanced scanning as residual tumour can be present in an atrophic cord, as demonstrated by one of our patients who had an incomplete resection of a Grade I astrocytoma followed by radiotherapy (Fig. 2). The enhanced images demonstrated a solid nodule of recurrent tumour situated centrally within the atrophic cord.

The enhancement characteristics of haemangioblastomas were virtually pathognomonic of the tumour (Figs 4, 5). The strong enhancement characteristics of the solid component of the tumour reflects both a combination of local disruption of the blood–neural tissue barrier and a highly vascular tumour bed as demonstrated by angiography. In all three cases the nodule of the tumour enhanced markedly and homogeneously. One of the haemangioblastomas was solid, one solid with a cystic component and one cystic with a small mural nodule. In all the cases the enhanced scans proved necessary for demonstrating the tumour nodule, which was isointense with the cord on the T_1-weighted images. On the T_2-weighted images, the tumour nodule, the peritumoral cyst (if present) and the surrounding cord all returned high signal (Fig. 4). In one patient with a large, predominantly solid haemangioblastoma of the cervical cord (Fig. 5), the enhanced scan revealed unsuspected further solid lesions of the thoracic cord and cerebellar hemisphere.

In this series, and in all other reported series, all tumours have enhanced to some degree. Enhancement has not been demonstrated in uncomplicated syringomyelia (Slasky et al, 1987), indicating the particular usefulness of gadolinium in differentiating an atypical syringomyelic cavity from a cystic cord tumour. This distinction was made in two of our patients with atypical syringomyelia who were both followed up over a 1-year period with no evidence of tumour appearance. This information is obviously of vital importance in determining patient management. Similarly, the gadolinium-enhanced images proved useful in excluding residual ependymoma in one post-operative patient. It must be remembered, however, that although no intrinsic tumours have yet been described that do not enhance, this possibility must exist. In the early stages of a low-grade glioma, immediate scanning following gadolinium administration may reveal only little or subtle enhancement, which could be easily overlooked. In the appropriate clinical context or the presence of equivocal MR appearances, we would advocate a further delayed scan 45 min after the administration of contrast medium.

Of the patients with intradural extramedullary tumours, the lesions were all demonstrated on the initial MR scans. Tumour conspicuity was, however, increased with the enhanced images and in one patient with a cervical meningioma, tumour definition was considerably improved with gadolinium. The numbers in this group were small, but the meningioma and three of the four neurofibromas enhanced markedly and homogeneously (Fig. 6). Enhancement of intradural extramedullary tumours and also extradural tumours is a reflection of the vascularity of the tumour as there is no

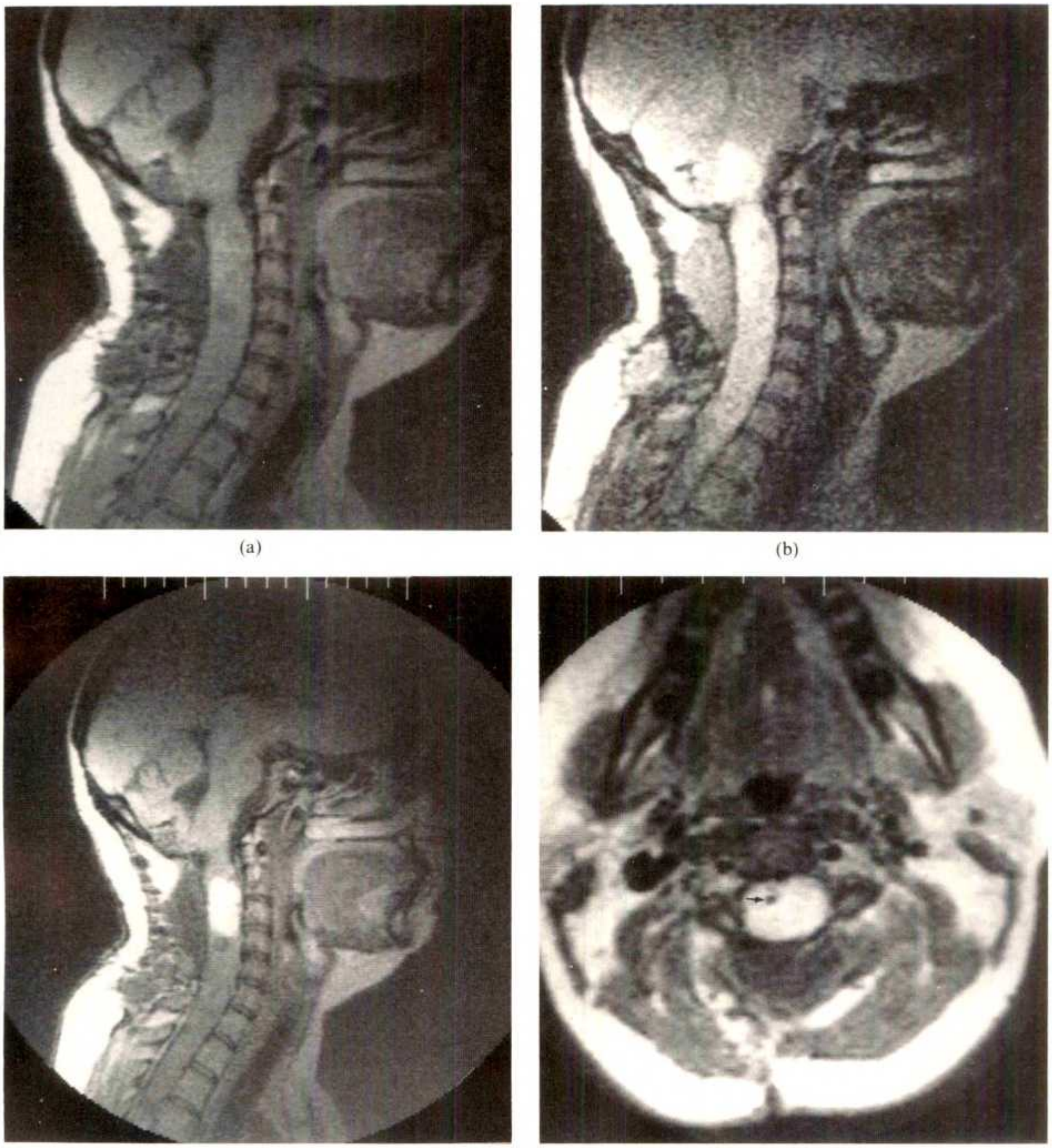
(a) (b) (c) (d)

Figure 5. Cervical haemangioblastoma. (a) T_1-weighted SE demonstrates an expanded cord with a small discrete area of low signal intensity. (b) T_2-weighted SE demonstrates intense high signal throughout the cervical cord extending into the medulla. (c) Sagittal and (d) axial sections after gadolinium demonstrate that the tumour is predominantly solid with only a small cystic component. The area of signal void (arrow) is consistent with a large feeding vessel.

disruption of the blood–neural tissue barrier. In this group of patients there was one cervical neuroepithelial cyst, which was demonstrated as a well circumscribed tumour with slight hypointensity on the T_1-weighted scan and moderate hyperintensity on the T_2-weighted scan, which showed no evidence of enhancement, features in keeping with an avascular proteinaceous cyst.

All of the extradural tumours enhanced, indicating their increased vascularity, and although in some cases

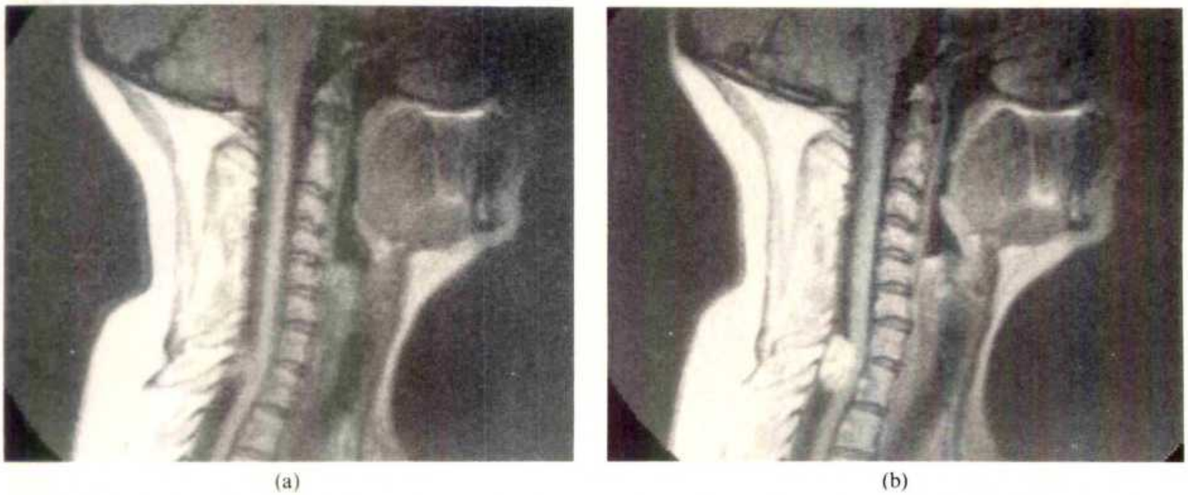
(a) (b)

Figure 6. Neurofibroma. (a) T_1-weighted SE showing an intradural extramedullary lesion of isointensity with the cervical cord at C7/T1. (b) After gadolinium the neurofibroma enhances markedly.

tumour delineation was improved with gadolinium, no significant additional information was provided with the enhanced images.

Conclusion

This study has shown that gadolinium-DTPA is safe and effective in the investigation of spinal tumours. It was of most benefit in separating the solid and cystic components of intramedullary tumours and in separating tumour from peritumoral cyst and oedema.

Acknowledgments

We would like to thank Schering for the supply of gadolinium used in this trial and the DHSS and MRC for the financial support of the MRI project.

References

BYDDER, G. M., BROWN, J., NIENDORF, H. P. & YOUNG, I. R., 1985. Enhancement of cervical intraspinal tumours in MR imaging with intravenous gadolinium-DTPA. *Journal of Computer Assisted Tomography*, *9*, 847–851.

CARR, D. H., BYDDER, G. M. & BROWN, J., 1984. Intravenous chelated gadolinium as a contrast agent in MRI. *American Journal of Roentgenology*, *143*, 215–244.

CLAUSEN, C., LANIADO, M., KAZNER, E., SCHORNER, W. & FELIX, R., 1985. Application of contrast agents in CT and MRI(NMR): their potential in imaging of brain tumours. *Neuroradiology*, *27*, 164–171.

CURATI, W. L., GRAIF, M., KINGSLEY, D. P. E., NIENDORF, H. P. & YOUNG, I. R., 1986. Acoustic neuromas: Gd-DTPA enhancement in MR imaging. *Radiology*, *158*, 447–451.

DILLON, P. D., NORMAN, D., HANS NEWTON, T., BOLLA, K. & MARK, A., 1989. Intradural spinal cord lesions: Gd-DTPA-enhanced MR imaging. *Radiology*, *170*, 229–237.

GOMORI, J. N. & GROSSMAN, R. I., 1987. Head and neck hemorrhage. In *Magnetic Resonance Annual*, ed. by H. Y. Kressel (Raven Press, New York), pp. 71–112.

GRAIF, M., BYDDER, G. M., STEINER, R. E., NIENDORF, P., THOMAS D. G. T. & YOUNG, I. R., 1985. Contrast-enhanced MR imaging of malignant brain tumours. *American Journal of Neuroradiology*, *6*, 855–862.

LANIADO, M., KORNMESSER, W., TREISCH, J., FELIX, R. & DEIMLING, M., 1986. Gd-DTPA enhanced fast magnetic resonance imaging of brain and spinal tumours: early clinical experience. In *Contrast Agents in Magnetic Resonance Imaging*. Proceedings of an international workshop, January 1986, San Diego, California, ed. by V. M. Runge et al (Excerpta Medica, Amsterdam), pp. 136–140.

SCHORNER, W., LANIADO, M., NIENDORF, H. P., SCHUBERT, C. & FELIX, R., 1986. Time-dependent changes in image contrast in brain tumours after gadolinium-DTPA. *American Journal of Neuroradiology*, *7*, 1013–1020.

SLASKY, B. S., BYDDER, G. M., NIENDORF, H. P. & YOUNG, I. R., 1987. MR imaging with gadolinium DTPA in the differentiation of tumour, syrinx and cyst of the spinal cord. *Journal of Computer Assisted Tomography*, *11*, 845–850.

STACK, J. P., ANTOUN, N. M., JENKINS, J. P. R., METCALFE, R. & ISHERWOOD, I., 1988. Gadolinium-DTPA as a contrast agent in magnetic resonance imaging of the brain. *Neuroradiology*, *30*, 145–154.

SZE, G., ABRAMSON, A., KROL, G., LIU, D., AMSTER, J., ZIMMERMAN, R. D. & DECK, M. D. F., 1988a. Gadolinium-DTPA in the evaluation of intradural extramedullary spinal disease. *American Journal of Neuroradiology*, *9*, 153–163.

SZE, J., KROL, G., ZIMMERMAN, R. D. & DECK, M. D. F., 1988. Intramedullary disease of the spine: diagnosis using gadolinium-DTPA-enhanced MR imaging. *American Journal of Neuroradiology*, *9*, 847–858.

VALK, J., 1987. Gadolinium DTPA in magnetic resonance imaging of the brain. *Acta Radiologica (Diagn)*, *28*, 430–436.

VALK, J., 1988. Gd-DTPA in MR of spinal lesions. *American Journal of Neuroradiology*, *9*, 345–350.

WEINMANN, H.-J., BRASCH, R. C., PRESS, W. R. & WESBEY, G. E., 1984. Characteristics of gadolinium-DTPA complex: a potential NMR contrast agent. *American Journal of Roentgenology*, *142*, 619–624.

WOLF, G. L., BURNETT, K. R., GOLDSTEIN, A. J. & JOSEPH, P. M., 1985. Contrast agents for magnetic resonance imaging. In *Magnetic Resonance Annual*, ed. by H. Y. Kressel (Raven Press, New York), pp. 231–266.

1989, *The British Journal of Radiology*, *62*, 1075–1078

Periventricular enhancement: a non-pathognomonic sign of intracerebral tumours

*†P. A. Murray, MRCP, FRCR, *‡A. N. Harnett, MRCP, FRCR, §P. I. Thompson, FRCR,
**M. Charlesworth, MB, FRCR and *P. N. Plowman, MD, FRCR

Departments of *Radiotherapy and **Neuroradiology, St Bartholomew's Hospital and §Department of Medical Oncology, Homerton Hospital, London

(*Received January 1989*)

Abstract. Four cases of periventricular contrast enhancement on computed tomography due to different tumours are reported, emphasizing that periventricular contrast enhancement is a non-specific radiological sign.

Periventricular contrast enhancement is a recognized feature of intracranial dysgerminoma and was once thought to be pathognomonic of this condition (Dupont et al, 1977). We present four cases of periventricular enhancement occurring in different pathological states and review the literature, which reveals that periventricular enhancement is a relatively non-specific radiological sign.

Case reports

Case 1

A 10-year-old boy presented in January 1987 with a 2-month history of frontal headaches and vomiting. Examination revealed bilateral papilloedema but was otherwise normal. A computed tomographic (CT) brain scan (Fig. 1) showed enhancing masses in the region of the pineal gland, the anterior recesses of the third ventricle and ependymaly over the body of the left lateral ventricle. A biopsy revealed a high-grade astrocytoma. Cerebrospinal fluid (CSF) levels of β-human chorionic gonadotrophin (HCG) and α-fetoprotein were not elevated. Owing to doubts about the diagnosis of astrocytoma because of these CT scan appearances, he was treated with neuraxis irradiation (50 Gy in 31 fractions to the primary site, 40 Gy in 25 fractions to the whole brain and 28 Gy in 18 fractions to the spine.) After 20 Gy there was marked clinical improvement and a repeat CT scan showed improvement with disappearance of the periventricular enhancement. In June 1987 he relapsed clinically and a CT scan demonstrated the presence of recurrent tumour in the region of the tectal plate. He was treated with *cis*-platinum, etoposide and bleomycin, but there was no response and he died in June 1987. At relapse the original presenting pathology was reviewed and stained positive for glial fibrillary acidic protein thus confirming the histological diagnosis of astrocytoma.

Case 2

A 12-year-old girl presented in June 1979 with a history of poor growth, polyuria, polydipsia and progressive visual loss in the right eye. Examination revealed that she was on the 10th percentile for height, there was bilateral optic atrophy, with a blind right eye and a left inferotemporal visual field defect. A CT scan demonstrated a small suprasellar mass, which, at biopsy, was histologically proven to be a dysgerminoma. She was treated with neuraxis irradiation (50 Gy to the primary site, 35 Gy to the whole brain and spine). She remained well until 1982 when she began to develop progressive visual loss. A CT scan at this time showed no evidence of recurrence. In 1984 she presented with drowsiness and loss of concentration. A CT scan showed a suprasellar mass, gross thickening of the right optic nerve and periventricular enhancement (Fig. 2). She received chemotherapy with *cis*-platinum, etoposide and bleomycin and after three cycles there was marked clinical improvement and complete radiological remission. At this stage, however, she developed a fulminant pneumonitis, which was fatal. Post-mortem examination confirmed the marked tumour regression with chemotherapy and only a small focus of persistent viable dysgerminoma was identified.

Case 3

A 65-year-old man presented in 1985 with cerebellar ataxia. A CT scan showed an enhancing cerebellar mass, which was largely resected at posterior craniotomy. Histological examination revealed a primary cerebral lymphoma and there was no evidence of extracranial disease following staging investigations. He received cranial irradiation (35 Gy to the whole brain with a 10 Gy boost to the posterior fossa). He improved clinically and remained well for 18 months when he represented in November 1987 with obtundation and signs of raised intracranial pressure. A CT scan showed a cerebellar recurrence with an enhancing lesion rostral to the third ventricle and periventricular enhancement (Fig. 3). He was retreated with further irradiation (30 Gy in 20

---

†Present address: The Royal Marsden Hospital, Sutton, Surrey. ‡Present address: Beatson Oncology Centre, Western Infirmary, Glasgow. Address reprint requests to Dr P. N. Plowman.

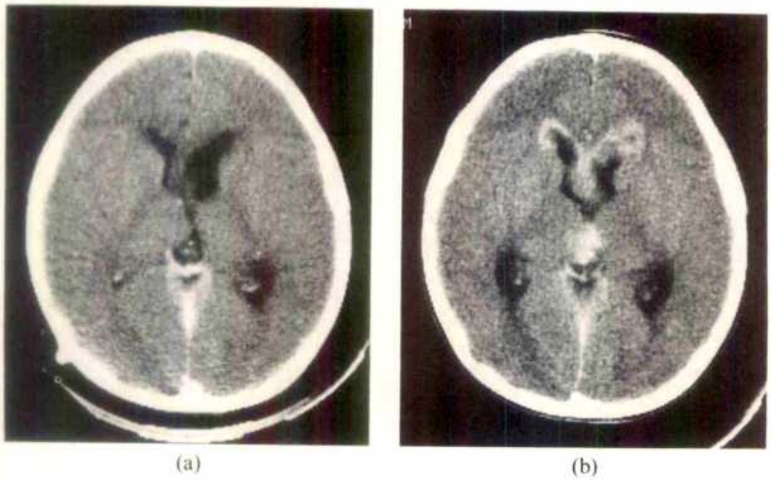

(a) (b)

Figure 1. *Case 1.* (a) Unenhanced and (b) enhanced CT scans. An enhancing mass in the region of the pineal with periventricular enhancement is seen.

fractions) with only a modest improvement over a short follow-up time to date.

Case 4

A 56-year-old woman presented in January 1987 with collapse of the left upper lobe, which, at bronchoscopy, was shown to be due to an undifferentiated large cell carcinoma of the upper lobe bronchus. She received external-beam irradiation (20 Gy in five fractions) to the mediastinum and left upper zone. In September 1987 she developed vertigo, drowsiness and bilateral nystagmus. A CT brain scan revealed a mass in the right parietal lobe with periventricular contrast enhancement around the right lateral ventricle. There were also a few subependymal nodules in the left lateral ventricle (Fig. 4). There was no response to steroid therapy and as her condition was rapidly deteriorating, radiotherapy was not prescribed. A post-mortem examination was not obtained.

Discussion

Periventricular spread of disease is recognized pathologically to occur in many tumours. It is well described in ependymoma (Rubenstein, 1970), medulloblastoma and germinoma (Rubinstein, 1972) and oligodendroglioma (Beck & Russell, 1942). Subependymal spread of tumour over long distances has been described in gliomas (Scherer, 1938). Vannier et al (1986) describe three pathological cases of small-cell carcinoma with extensive diffuse periventricular spread.

Periventricular spread in the subependymal region is thought to be relatively uncommon, and CT periventricular contrast enhancement a sign of this phenomenon. Each of the cases in this report demonstrated florid periventricular contrast enhancement. In Case 1, the CT appearances and rapid response to radiation were felt to be highly suggestive of germinoma despite the histological findings. The patient did not respond to germ cell chemotherapy and the positive glial fibrillary acidic protein stain confirmed the astrocyte lineage of this tumour. Perhaps the realization that subependymal spread occurs in many tumour types and that periventricular contrast enhancement on CT is non-specific would have prevented administration of this ineffective chemotherapy and spinal radiotherapy. The rapid resolution of the periventricular enhancement of this astrocytoma after 20 Gy is nevertheless of interest and should serve as an object lesson to clinicians who place a high reliability on "the 20 Gy therapeutic test" (Bloom, 1983). McGeachie et al (1977) report four cases of intracranial tumour with periventricular contrast enhancement demonstrated by CT. Three cases were due to malignant glioma and one non-pathological case was

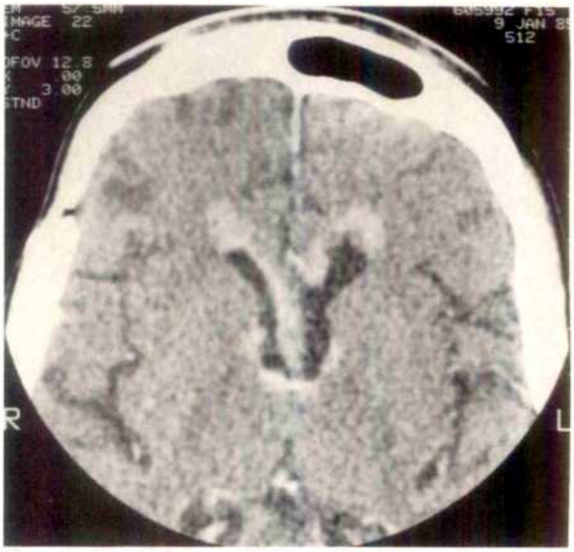

Figure 2. *Case 2.* Enhanced CT scan illustrating periventricular enhancement in recurrent dysgerminoma.

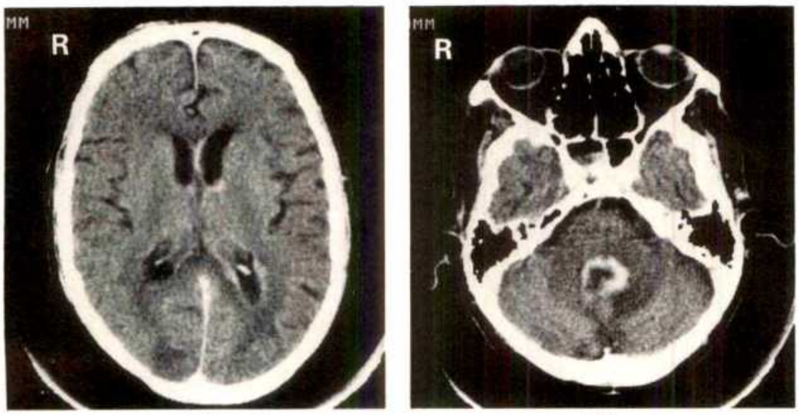

(a) (b)

Figure 3. *Case 3.* Periventricular enhancement of (a) the lateral ventricles and (b) the fourth ventricle in cerebral lymphoma.

presumed to be metastatic melanoma. In a series of 14 patients with leptomeningeal spread of glioma, four had obvious periventricular contrast enhancement demonstrated by CT (Awad et al, 1986).

Case 2 demonstrated the classic periventricular enhancement that was once regarded as pathognomonic of germinoma. The spread of the disease down the optic nerve was unique in our experience and the rapid response of the disease to systemic germ cell chemotherapy is particularly noteworthy.

Primary cerebral lymphoma is multifocal in approximately 50% of cases with a predeliction for the periventricular region, basal ganglia, thalamus and the corpus callosum (Lukın et al, 1980). Periventricular contrast enhancement has been reported in this condition by several authors (Neuwelt et al, 1984; Bogdahn et al, 1986). In addition, Ricevuti et al (1982) report a case of Hodgkin's disease with periventricular enhancing lesions.

The CT scan of Case 4 demonstrated remarkable periventricular contrast enhancement and although there was no histological confirmation, there is strong circumstantial evidence that this represented metastatic bronchial carcinoma. Although not widely recognized, this pattern of metastatic spread is reported in the literature. In the three cases of metastatic small cell carcinoma described by Vannier et al (1986), two demonstrated periventricular contrast enhancement. In a review of the CT findings in 50 cases of disseminated meningeal malignancy (metastatic disease 22, primary central nervous system tumours 18, lymphoma 7), there was periventricular contrast enhancement in 14 cases (Ascherl et al, 1981). This is similar to the incidence found by Ito et al (1986) who reviewed 25 cases of leptomeningeal tumour spread and found four cases with periventricular contrast enhancement. Periventricular enhancement is also described in a variety of non-malignant conditions including subacute periventricular encephalitis (Singh & Silberstein, 1980), pyogenic ependymitis (Zimmerman & Bilaniuk, 1976) and primary demyelinating disease (Reith et al, 1981). Neonatal subependymal haemorrhage will produce periventricular hyperdensities on the unenhanced scan (Pevsner et al, 1976).

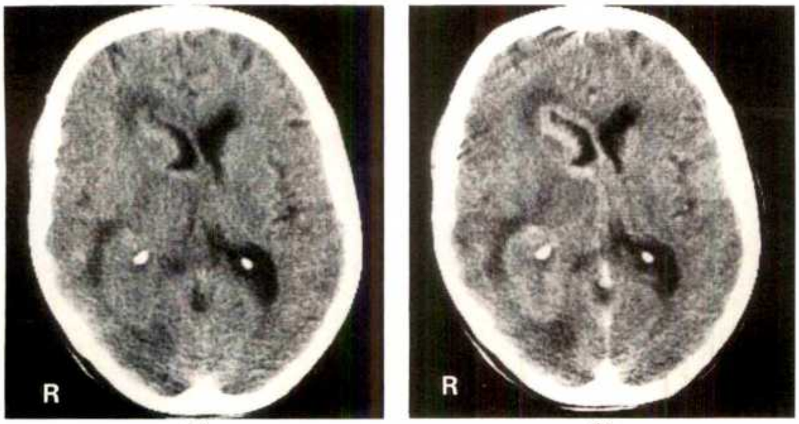

(a) (b)

Figure 4. *Case 4.* (a) Unenhanced and (b) enhanced CT scans showing periventricular contrast enhancement around the right lateral ventricle in metastatic carcinoma.

In summary, these four pathologically diverse cases demonstrate that periventricular enhancement is a non-specific sign of intracranial pathology.

References

ASCHERL, G. F., HILAL, S. K. & BRISMAN, R., 1981. Computed tomography of disseminated meningeal and ependymal malignant neoplasms. *Neurology, 31*, 567–574.

AWAD, A., BAY, J. W. & ROGERS, L., 1986. Leptomeningeal metastases from supratentorial malignant gliomas. *Neurosurgery, 19*, 247–251.

BECK, D. J. K. & RUSSELL, D. S., 1942. Oligodendrogliomatosis of the cerebrospinal pathways. *Brain, 65*, 352–372.

BLOOM, H. J. G., 1983. Intracranial germ cell tumours. *Clinics in Oncology, Vol. 2, 1*, 233–258.

BOGDAHN, U., BOGDAHN, S., MERTENS, H. G., DOMMASCH, D., WODARZ, R., WUNSCH, P. H., KUHL, P. & RICHTER, E., 1986. Primary non-Hodgkin's lymphomas of the CNS. *Acta Neurologica Scandinavica, 73*, 602–614.

DUPONT, M. G., GERARD, J. M., FLAMENT-DURAND, J., BALÉRIAUX-WAHA, D. & MARTELMANS, L. L., 1977. Pathognomonic aspects of germinoma on CT scan. *Neuroradiology, 14*, 209–211.

ITO, U., TOMITA, H., YAMAZAKI, S., TAKADA, Y. & INABA, Y., 1986. CT findings of leptomeningeal and periventricular dissemination of tumours. *Clinical Neurology Neurosurgery, 88*, 115–120.

LUKIN, R., TOMSICK, T. A. & CHAMBERS, A. A., 1980. Lymphoma and leukemia of the central nervous system. *Seminars in Roentgenology, 15*, 246–250.

MCGEACHIE, R. E., GOLD, H. A. & LATCHAW, R. E., 1977. Periventricular spread of tumor demonstrated by computed tomography. *Radiology, 125*, 407–410.

NEUWELT, E. A., GUMERLOCK, M. K., FRENKEL, E. L. & HILL, S. A., 1984. CNS lymphoma: diagnosis and treatment. *Journal of Neurooncology, 2*, 279.

PEVSNER, P. H., GARCIA-BUNEUL, R., LEEDS, N. & FINKELSTEIN, M., 1976. Subependymal and intraventricular hemorrhage in neonates. *Radiology, 119*, 111–114.

RIETH, K. G., DI CHIRO, G., CROMWELL, L. D., MCKEEVER, P. E., KORNBLITH, P. L., KUFTA, C. V. & PLEET, A. B., 1981. Primary demyelinating disease simulating glioma of the corpus callosum. *Journal of Neurosurgery, 55*, 620–624.

RICEVUTI, G., BALDUINA, C. L., GOLLOLI, L., PICCOLO, G., RICEVUTI, G. P., ROGNONE, F. & RIZZO, S. C., 1982. Computed tomography detection of a diffuse periventricular subependymal lesion in a case of Hodgkin's lymphoma (subependymal lymphoma). *Haematologica, 67*, 769–774.

RUBINSTEIN, L. J., 1970. The definition of ependymoblastoma. *American Journal of Pathology, 90*, 35–45.

——1972. Tumors of the central nervous system. In *Atlas of Tumor Pathology*, 2nd series, Fasc 6 (AFIP, Washington DC), pp. 328–332.

SCHERER, H. J., 1938. Structural development in gliomas. *American Journal of Cancer, 34*, 333–351.

SINGH, R. S. & SILBERSTEIN, E. B., 1980. Ventriculitis in an adult delineated by radionuclide brain scan. *Archives of Neurology, 37*, 381–383.

VANNIER, A., GRAY, F., GHERARDI, R., MARSAULT, C., DEGOS, J. D. & POIRIER, J., 1986. Diffuse subependymal periventricular metastases. *Cancer, 58*, 2720–2725.

ZIMMERMAN, R. A. & BILANIUK, L. T., 1976. Computed tomography of pyogenic intracranial infection. Scientific exhibit presented at the Scientific Assembly and the Radiological Society of North America, Chicago.

1989, *The British Journal of Radiology*, *62*, 1079–1083

Modulation in the radiosensitivity of MCF-7 human breast carcinoma cells by 17B-estradiol and tamoxifen

By *David E. Wazer, MD, †Oscar F. Tercilla, MD, †Peck-Sun Lin, PhD and †Rupert Schmidt-Ullrich, MD

Department of Radiation Oncology, New England Medical Center Hospital, Tufts University School of Medicine, 750 Washington Street, Boston, Massachusetts 02111, USA

(*Received February 1989 and in final form July 1989*)

Abstract. Colony-forming ability after exposure to ionizing irradiation was compared for proliferating hormone response MCF-7 breast carcinoma cells and cells whose growth was inhibited by tamoxifen or 17B-estradiol. As compared with controls ($D_o = 1.20$ Gy, $n = 3.1$), cells in 1 μM or 5 μM tamoxifen were less radiosensitive ($D_o = 1.20$ Gy, $n = 7.0$; $D_o = 1.22$ Gy, $n = 7.0$, respectively) with the predominant effect being a widened shoulder on the survival curve. This protective effect could be abolished by co-incubation of 5 μM tamoxifen with 100 nM or 5 μM 17B-estradiol ($D_o = 1.30$ Gy, $n = 2.6$; $D_o = 1.20$ Gy, $n = 2.6$, respectively). The decrease in radiosensitivity induced by tamoxifen was similar to that seen when replating of irradiated plateau-phase cultures was delayed for 24 h ($D_o = 1.30$ Gy, $n = 6.0$). In contrast, when proliferation of MCF-7 cultures was inhibited by 10 μM 17B-estradiol, radiosensitivity was increased with a markedly diminished survival curve shoulder ($D_o = 1.40$ Gy, $n = 1.0$). Different hormonal manipulations of cycling human breast carcinoma cells may have profound but disparate efects on radiosensitivity such that tamoxifen and estrogens may serve as useful agents with which to study the biochemical mechanisms of repair.

Hormonal agents such as high-dose estrogens and the anti-estrogen, tamoxifen, are believed to exert a direct growth-arresting effect on hormone-responsive, malignant mammary epithelial cells (MMEC) (Sutherland et al, 1983; Reddel & Sutherland, 1987). Estrogen concentrations of 5–50 μM inhibit proliferation of the estrogen receptor (ER) positive MMEC line, MCF-7. This is associated with a cell cycle phase specific re-assortment such that there is an increase in ploidy and marked depletion of G_1 cells with an accumulation in the S and G_2/M phases (Reddel & Sutherland, 1987).

Tamoxifen also interferes with the proliferation of MCF-7 cells, which can be explained partially by competition with estradiol (E_2) for binding to the estrogen receptor (Coezy et al, 1982; Rochefort et al, 1984). This interaction, however, is complex with both estradiol reversible and irreversible effects, which are dependent on the concentration of tamoxifen. At concentrations of 1–10 μM, tamoxifen arrests the growth of cultured MCF-7 cells with near complete segregation (>90%) into G_o/G_1 (Sutherland et al, 1983; Osborne et al, 1984).

Given recent trends in the management of early stage breast carcinoma, a significant number of patients will qualify to be treated with both hormonal manipulation and irradiation. As the radiosensitivity of mammalian cells can be affected significantly by cell cycle phase position and proliferative state (Sinclair & Morton, 1966; Berry et al, 1970), this will require an enhanced understanding of the combined hormone and irradiation effects on MMEC. In this study we have examined the effect of tamoxifen and 17B-estradiol on the radiosensitivity of the human MMEC line, MCF-7.

Materials and methods

Reagents

The reagents employed were of the highest purity grade available. Reagents and media were obtained from the following suppliers: RPMI 1640 medium, heat inactivated fetal calf serum (FCS) and glutamine from Gibco; porcine insulin and 17B-estradiol from Sigma; tamoxifen citrate from Stuart Pharmaceuticals (gift of Dr McCurdy); four-well culture plates from Linbro; 24-well culture plates and T-25 culture flasks from Costar; trypsin/EDTA from Irvine Scientific.

Cell culture

MCF-7 breast carcinoma cells were isolated initially at the Michigan Cancer Foundation from a metastatic pleural effusion and were obtained for these experiments from Dr Marc Lippman (National Cancer Institute, Bethesda, MD). The cells were cultured in RPMI 1640 and 10% (*v*/*v*) FCS (RPMI/10FCS) containing glutamine (3 μg/ml), insulin (10 ng/ml), penicillin (10 U/ml) and streptomycin (10 μg/ml), re-fed every 3 days and passaged once weekly. The experiments reported here were performed on passages 52–69 and cells seeded from stock cultures in log phase (30–70% confluent).

Drugs

Tamoxifen citrate was dissolved in ethanol and 17B-estradiol was dissolved in DMSO. Solvent concentration in the culture medium never exceeded 0.1% (*v*/*v*) and control experiments (data not shown) demonstrated no effect on culture growth or radiosensitivity. Stock solutions of drug were prepared fresh for each experiment and were shielded from prolonged exposure to light.

---

*Author for correspondence.

†Current address: Department of Radiation Oncology, Medical College of Virginia, Richmond, Virginia.

Growth kinetics and hormone response of MCF-7 cells

MCF-7 stock cultures were trypsinized and aliquoted into 24-well culture plates at a density of 10^4 cells/well. Vigorous pipetting following trypsin exposure resulted in a uniform population of single cells or small cell clumps consisting maximally of seven cells. The cells were maintained in RPMI/10FCS with or without drug and re-fed at least every 3 days in all experiments to assure sufficient drug levels in all cultures.

Growth curves of MCF-7 cells were established by comparing total cell numbers per well on Days 2, 5, 7 and 9 after plating. In parallel cultures, the effects of varying concentrations of tamoxifen, estradiol or combinations of both were compared with cultures without drug. Concentrations examined were: tamoxifen 1 μM, 5 μM; estradiol 10 nM, 100 nM, 10 μM; combined estradiol/tamoxifen 10 nM/5 μM, 100 nM/5 μM, 5 μM/5 μM. Each measurement point was obtained from triplicate samples and each haemocytometer count was repeated four times to minimize counting errors.

Irradiation experiments

The cloning efficiency of MCF-7 cells has been reported to range from 1 to 12% in exponentially growing stock cultures (Weichselbaum et al, 1980) and may range over two orders of magnitude depending on the relative density of stock cultures (Sutherland et al, 1983). Cloning efficiency in our cultures ranged from 5 to 17% (mean 12%) for control conditions, 2 to 14% (mean 8%) for tamoxifen-treated cells and 3 to 16% (mean 11%) for estradiol-treated cells.

Four-well culture plates containing RPMI/10FCS were inoculated with 5×10^2 to 10^5 MCF-7 cells obtained from exponentially growing stocks. After 8 h, the medium was replaced with fresh RPMI/10FCS with or without drug and the cells allowed to incubate an additional 48 h. Irradiation was then performed at room temperature in an ambient atmosphere using a 6 MV linear accelerator (Varian) at a dose-rate of 200 cGy/min. Single-dose exposures ranged from 0 to 10 Gy. The cultures were placed under a 1 cm tissue-equivalent bolus to ensure maximum dose delivery to all culture wells. Immediately after irradiation, the medium was replaced with drug-free RPMI/10FCS. Survival was assessed 21–28 days later by determining formation of colonies of greater than 50 cells. The surviving fraction was computed by dividing the colonies counted by the number of cells plated times the plating efficiency. A multiplicity correction was calculated for all irradiated cultures (Elkind & Whitmore, 1967).

In additional experiments we examined survival with the colony formation assay after delayed replating of irradiated confluent MCF-7 cells. Cultures were established by inoculating 10^6 cells in T-25 flasks with regular media changes every 3 days. On attaining confluence, the cells were maintained an additional 2 days with daily changes of fresh RPMI/10FCS or medium containing 5 μM tamoxifen. After irradiation, cultures were returned to the incubator for 24 h, trypsinized, counted and plated.

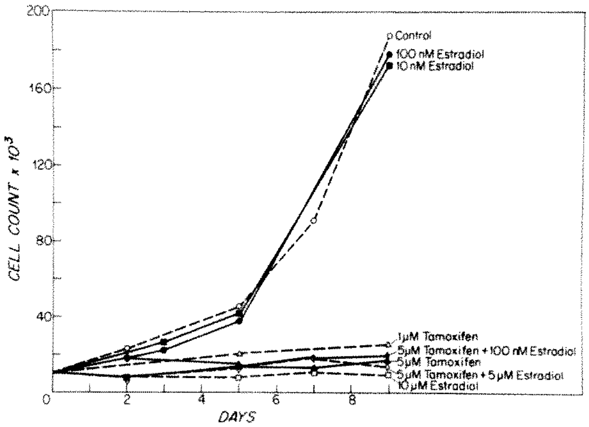

Figure 1. Effect of the duration of drug exposure on the proliferation of MCF-7 cells. Standard error of the mean (not depicted) was $<4\%$ for all points.

Curve fitting was performed by non-linear regression analysis using the UCLA-Biomedical Data Package on a PDP-11/RSX-11M operating system. The D_0 and n values were derived using least-squares regression analysis of data points above 200 cGy.

Results

Effect of 17B-estradiol and tamoxifen on the proliferation of MCF-7 cells

Requirements for the duration of drug exposure to exert growth inhibition were examined comparing control cultures with those exposed to varying concentrations of tamoxifen and estradiol or combinations of both drugs (Fig. 1). During a 9-day incubation, cells in RPMI/10FCS or medium containing 10 or 100 nM estradiol multiplied nearly 20-fold whereas growth arrest was obtained by the inclusion of 1 μM or 5 μM tamoxifen or 10 μM estradiol. Growth inhibition by 5 μM tamoxifen could not be reversed by co-incubation with 10 nM, 100 nM or 5 μM estradiol. The difference in cell numbers between the control and drug-treated cultures was not statistically significant on Day 2 but was so by Day 4 ($p < 0.02$).

Altered radiosensitivity of MCF-7 cells by tamoxifen and 17B-estradiol

In experiments comparing the radiosensitivity of proliferating MCF-7 cells with those inhibited by the presence of drug, irradiation was performed after 2 days because, at that time, control cultures appeared to be entering exponential growth relative to those arrested by tamoxifen or high concentrations of estradiol. Cells irradiated after exposure to 1 μM tamoxifen ($D_0 = 1.20 \pm 0.11$ Gy; $n = 7.0 \pm 1.2$) (mean ± SD) or 5 μM tamoxifen ($D_0 = 1.22 \pm 0.09$ Gy; $n = 7.0 \pm 1.7$) were less radiosensitive than controls ($D_0 = 1.20 \pm 0.09$ Gy;

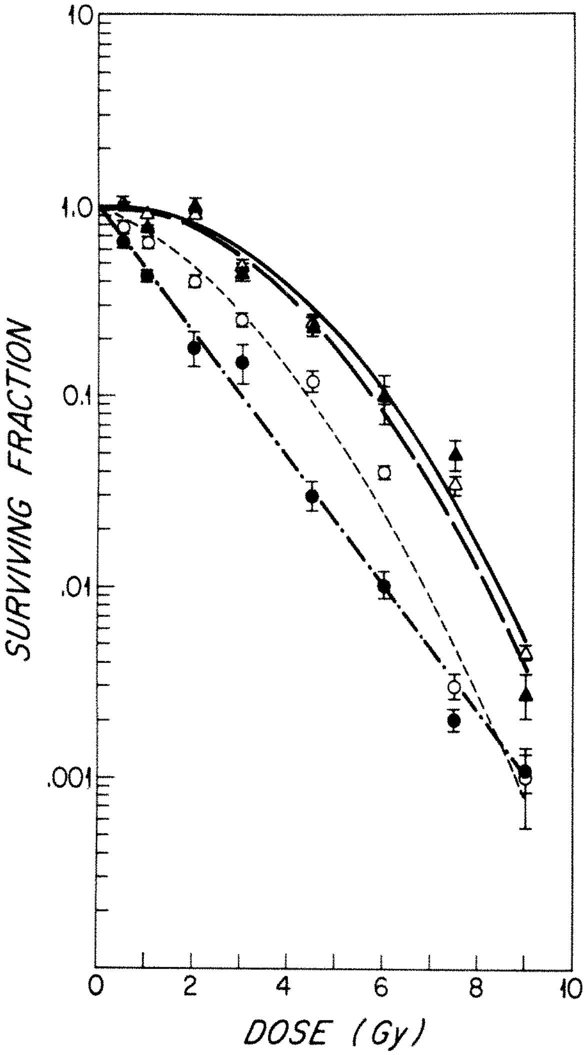

Figure 2. Survival curves after single doses for subconfluent cultures in the presence or absence of tamoxifen or estradiol. Control cultures (○), 1 μM tamoxifen (▲), 5 μM tamoxifen (△) and 10 μM estradiol (●).

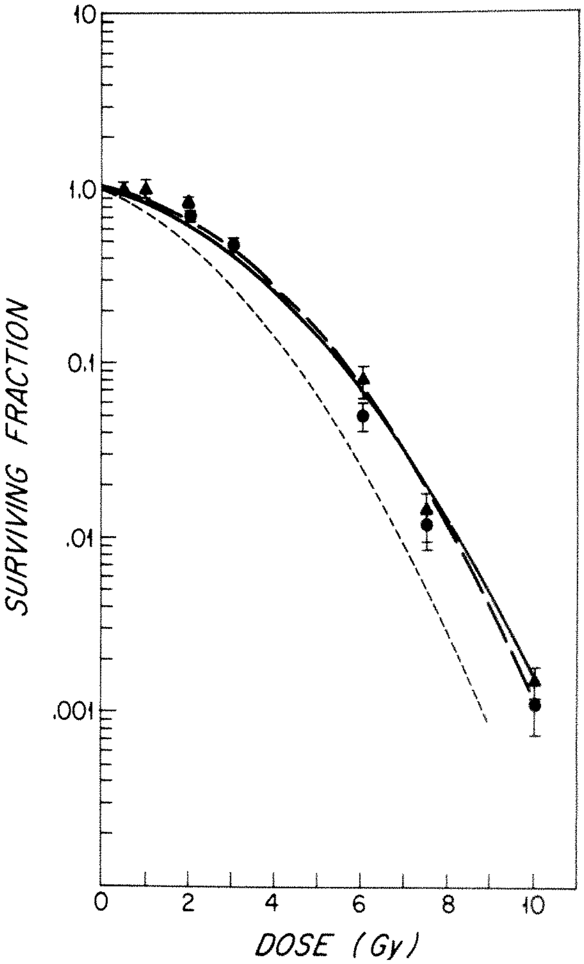

Figure 3. Survival curves after single doses for plateau-phase cultures in which replating was delayed for 24 h (DP). Control conditions from Fig. 2 (– – –), DP-plateau phase (●) and DP-plateau phase plus 5 μM tamoxifen (▲).

$n = 3.1 \pm 0.9$) (Fig. 2). The predominant effect appears to be a widening of the shoulder portion of the survival curve as the extrapolation numbers for tamoxifen-treated cells were significantly higher than for controls ($p < 0.02$). Modification of the culture conditions such that cells were grown to confluence prior to irradiation and delayed plating also decreased radiosensitivity. Delayed plating of irradiated plateau-phase cells ($D_0 = 1.30 \pm 0.12$ Gy; $n = 6.0 \pm 1.2$) or plateau-phase cells in 5 μM tamoxifen ($D_0 = 1.21 \pm 0.10$ Gy; $n = 6.0 \pm 1.7$) resulted in virtually identical survival curves (Fig. 3) with extrapolation numbers significantly higher than for controls ($p < 0.04$).

In contrast with the results for tamoxifen, growth arrest by 10 μM estradiol increased radiosensitivity ($D_0 = 1.40 \pm 0.13$ Gy; $n = 1.0 \pm 0.4$) relative to proliferating controls (Fig. 2). The predominant alteration of the survival curve appeared to be a markedly diminished shoulder with a significant decrease in the extrapolation number relative to controls ($p < 0.04$) and tamoxifen-treated cultures ($p < 0.01$). Lower concentrations of estradiol (10 or 100 nM) resulted in survival curves that were virtually identical to controls (data not shown).

Growth arrest of MCF-7 cells by 5 μM tamoxifen could not be reversed by the co-incubation of 100 nM or 5 μM estradiol (Fig. 1), whereas identical combinations of these drugs did reverse the tamoxifen-induced decrease in radiosensitivity. Cells irradiated in the presence of 5 μM tamoxifen/100 nM estradiol ($D_0 = 1.30 \pm 0.07$ Gy; $n = 2.6 \pm 0.8$) or 5 μM tamoxifen/5 μM estradiol ($D_0 = 1.20 \pm 0.09$ Gy; $n = 2.6 \pm 1.2$) had survival curves comparable to controls (Fig. 4).

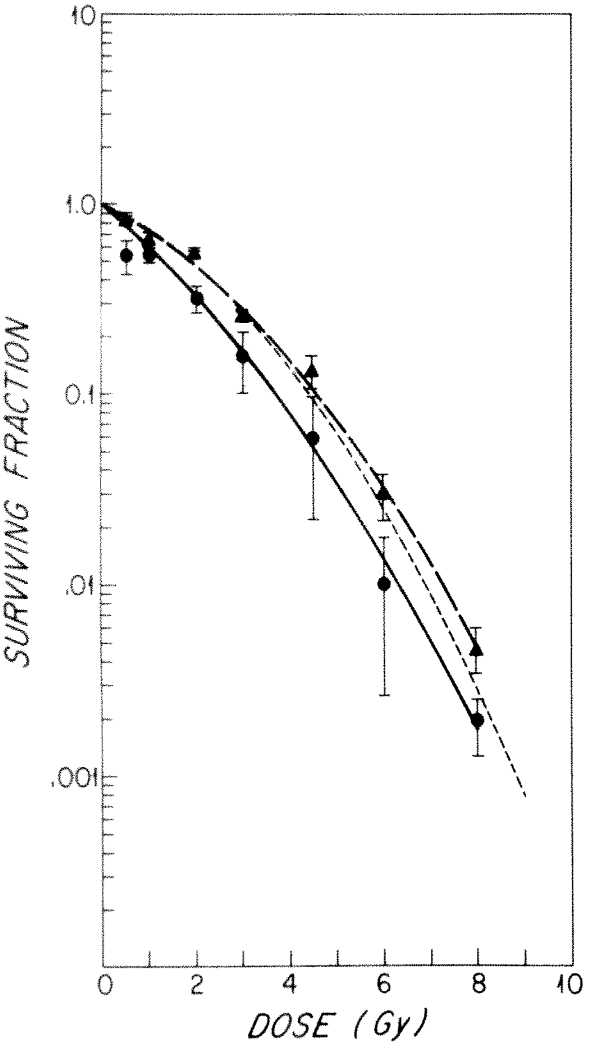

Figure 4. Survival curves after single doses for subconfluent cultures in the presence of tamoxifen and 17B-estradiol. Control (- - -), 5 μM tamoxifen/5 μM estradiol (●) and 5 μM tamoxifen/100 nM estradiol (▲).

Discussion

Responses of breast tumours to hormonal manipulation are generally associated with the presence of estrogen receptors, although the precise mode of the antiproliferative action is not understood. Growth arrest of hormone-responsive human breast carcinoma cells can be induced *in vitro* by the presence of the anti-estrogen, tamoxifen, or with high concentrations of 17B-estradiol. This is associated with a relative reassortment of cells within phases of the cell cycle such that tamoxifen increases the proportion in G_0/G_1 (Sutherland et al, 1983) whereas high concentrations of estrogens increase the proportion in G_2/M (Reddel & Sutherland, 1987).

It might be postulated that cells placed in a quiescent state would be less sensitive to the action of a cytocidal agent. This hypothesis has been tested recently where the cytotoxicity of 5-fluorouracil (5-FU) and adriamycin was evaluated in MCF-7 cells exposed to tamoxifen (Hug et al, 1985). It was reported that tamoxifen decreased the cytotoxicity of these drugs, particularly for the cell-cycle-dependent 5-FU. We have posed a similar question with regard to the effect of tamoxifen on radiosensitivity. While the lethal effects of radiation are not cell-cycle-phase specific, studies in synchronized populations have shown that there is considerable variation in radiosensitivity throughout the cell cycle such that cells in early G_1 are less radiosensitive than cells in G_2/M (Sinclair & Morton, 1966). In addition, survival is influenced by the relative proliferative potential of cells after irradiation where conditions that delay progression through the cell cycle may decrease lethality (for a review see Iliakis, 1988).

We observed that when proliferation is inhibited by tamoxifen, there is a marked reduction in the radiosensitivity of MCF-7 cells with widening of the shoulder on the survival curve. This protective effect could be reversed by the addition of a 15-fold less concentration of 17B-estradiol even though the overall population of cells remained in growth arrest. Decreased sensitivity of a similar magnitude was observed when confluent cultures were irradiated and replated 24 h later. Conversely, 10 μM 17B-estradiol inhibited proliferation to a degree comparable to tamoxifen, but radiosensitivity was increased with a marked reduction in the shoulder region. Lower concentrations of 17B-estradiol (100-fold or greater) did not affect proliferation and had no effect on radiosensitivity.

The cellular events that have decreased the radiosensitivity of tamoxifen-treated MCF-7 cells and increased the sensitivity of cells in high concentrations of 17B-estradiol are probably multifold. One possible explanation is that the relative redistribution of these cells in different phases of the cell cycle is reflected by a differential in radiosensitivity. Another explanation may relate to the proliferative potential of these cells after irradiation. Perhaps when cultures arrested in a high concentration of 17B-estradiol are irradiated then released into drug-free medium, cycling begins immediately with rapid fixation of damage. Alternatively, release from tamoxifen inhibition may result in slower cell-cycle progression allowing additional time for damage repair. This is supported by experiments in which delayed plating of irradiated plateau-phase cells resulted in a decreased radiosensitivity, which was not influenced by the presence or absence of tamoxifen. This suggests that an adverse interaction of radiation and tamoxifen occurs primarily in rapidly growing cell populations.

The importance of these results relates to the modulating effect of hormonal manipulation on the radiosensitivity of human breast carcinoma cells. One implication is that tamoxifen therapy during irradiation may result in a reduced fractional kill of hormone-sensitive cycling cells. Whether this has any clinical relevance remains to be tested. The differential in radiosensitivity induced by tamoxifen and high concentrations of 17B-estradiol may serve as a useful model system to elucidate better the biochemical mechanisms responsible for repair of radiation injury.

Acknowledgments

The authors thank Dr Hywel Madoc-Jones for his interest in this work and Michelle Teczar, RRT and the staff of the Department of Radiation Oncology for their technical assistance. This project was supported in part by funds for research development in the Department of Radiation Oncology, New England Medical Center Hospitals.

References

Berry, R. J., Hall, E. J. & Cavanaugh, J., 1970. Radiosensitivity and the oxygen effect for mammalian cells cultured *in vitro* in stationary phase. *British Journal of Radiology, 43,* 81–90.

Coezy, E., Borgra, J. L. & Rochefort, M., 1982. Tamoxifen and metabolites in MCF-7 cells: correlation between binding to estrogen receptor and cell growth inhibition. *Cancer Research, 42,* 317–323.

Elkind, M. & Whitmore, G., 1967. *The Radiobiology of Cultured Mammalian Cells* (Gordon and Breach, New York), pp. 24, 62–63.

Hug, V., Hortobagyi, G., Drewinko, B. & Finders, M., 1985. Tamoxifen-citrate counteracts the antitumor effects of cytotoxic drugs *in vitro. Journal of Clinical Oncology, 3,* 1672–1677.

Iliakis, G., 1988. Radiation-induced potentially lethal damage: DNA lesions susceptible to fixation. *International Journal of Radiation Biology, 53,* 541–584.

Osborne, C. K., Boldt, D. H., Clark, G. M. & Trent, J. M., 1984. Human breast cancer cell cycle synchronization by estrogens and anti-estrogens in culture. *Cancer Research, 44,* 1433–1439.

Reddel, R. R. & Sutherland, R. L., 1987. Effects of pharmacological concentrations of estrogens on proliferation and cell cycle kinetics of human breast cancer cell lines *in vitro. Cancer Research, 47,* 5323–5329.

Rochefort, H., Bordon, S., Chalbos, D. & Vignon, F., 1984, Steroidal and non-steroidal antiestrogens in breast cancer cells in culture. *Journal of Steroid Biochemistry, 20,* 105–110.

Sinclair, W. K. & Morton, R. A., 1966. X-ray sensitivity during the cell generation cycle of cultured chinese hamster cells. *Radiation Research, 29,* 450–474.

Sutherland, R. L., Hall, R. E. & Taylor, I. W., 1983. Cell proliferation kinetics of MCF-7 human mammary carcinoma cells in culture and effects of tamoxifen on exponentially growing and plateau phase cells. *Cancer Research, 43,* 3998–4006.

Weichselbaum, R. R., Little, J. B., Nove, J., Hellman, S. & Piro, A. J., 1980. Lack of selective killing by steroids in normal and malignant cells. *Journal of Cell Physiology, 103,* 429–433.

1989, *The British Journal of Radiology*, 62, 1084–1088

Sublethal damage repair and radiosensitivity of human squamous cell carcinoma cells grown with different culture techniques

By J. H. M. Schwachöfer, PhD, R. P. M. A. Crooijmans, J. van Gasteren, PhD, J. Hoogenhout, MD, PhD, *C. R. Jerusalem, MD, PhD and †H. B. Kal, PhD

Departments of Radiotherapy and *Cell Biology and Histology, University Hospital, Nijmegen, and †Radiobiological Institute TNO, Rijswijk, The Netherlands

(*Received March 1989 and in revised form May 1989*)

Abstract. In this study, cells of a human squamous cell carcinoma line, HN-1, were grown in monolayers and as multicellular tumour spheroids (MTS). Repair of radiation-induced damage was studied by irradiation with single and split doses of X rays (4–8 Gy). It was shown that the amount of sublethal damage that was repaired in this dose range was equal in cells growing in monolayers and as MTS. The radiosensitivity of spheroids, as expressed by spheroid "cure" dose, increased with increasing MTS diameter. It is postulated that, in MTS with no signs of hypoxia, radioresistance diminishes when MTS increase in diameter.

In 1973, Durand and Sutherland demonstrated that mammalian cells cultured *in vitro* as three-dimensionally growing multicellular tumour spheroids (MTS) may become more radioresistant than monolayers. Chinese hamster V79 cells, when grown for 1 day as spheroids, displayed an increased resistance to ionizing radiation, which was explained as a contact effect. This was primarily a shoulder-modifying effect, which resulted in an increase in the D_q value of the survival curve by 1–3 Gy (Durand & Sutherland, 1972, 1973). The reduced radiosensitivity was attributed to the three-dimensional contact of cells within the spheroid and thus denoted as "contact resistance" or "contact effect" (CE). The CE has since been reported in rodent tumours (Hill et al, 1979) and human tumour xenografts (Dertinger et al, 1984). The increased radioresistance of spheroid cells is independent of the proliferative status of the cells (Dertinger & Hülser, 1981).

When cultured under conditions as in spheroids, cells display an enhanced ability to accumulate sublethal radiation damage. In addition, it was shown, using split-dose regimens of low-linear-energy-transfer (LET) radiation, that cells from spheroids can repair sublethal damage more efficiently when grown as spheroids (Sutherland & Durand, 1976).

Limited data on sublethal damage repair in MTS are available from human tumour cell lines. In the present study, a human squamous cell carcinoma line, HN-1, (Easty et al, 1981) was used. With this cell line, spheroids in culture could be made using the method of Yuhas et al (1977). The responses to split- and single-dose irradiation were studied using the end-points of growth delay and cure for MTS, and colony-forming ability for monolayer cells. Repair of sublethal damage was quantified in exponentially growing monolayer cultures, and in spheroids of two different diameters.

Materials and methods

Cells were maintained in RPMI-1640 medium supplemented with 10% fetal bovine serum in 2 mM L-glutamine, 100 i.u./ml penicillin and 100 μg/ml streptomycin (Gibco), hereafter referred to as complete medium. Stock cultures of the cells were maintained at 37°C in 7.5% CO_2 in air with 100% humidity.

Cells were harvested from exponentially growing cultures by trypsinization with 0.25% trypsin/0.025% EDTA in buffered salt solution. Cells were washed by centrifugation and resuspended, counted, diluted and plated in six-well test plates (Nunc). Six wells (ϕ 35 mm) of one test plate per radiation dose were inoculated with 1000–10 000 cells each in 2 ml complete medium. The number of cells depended on the radiation dose. After allowing 4 h for cell attachment, the cells were irradiated as described below. Test plates were then incubated for 10 days at 37°C in 7.5% CO_2 in air. The colonies were then fixed and Giemsa-stained. Only those colonies consisting of 50 cells or more were scored as survivors. Experiments were performed in duplicate and results were analysed with the multitarget model.

To produce spheroids, the liquid-overlay technique was used (Yuhas et al, 1977). Single-cell suspensions were obtained by dissociation of monolayer cultures and 1×10^5 cells were seeded in 60 mm Petri dishes (Nunc) coated with 1% agarose to prevent attachment to the dishes. After 4 days incubation, small spheroids had developed that could be harvested using a Pasteur pipette.

Spheroids were selected and transferred to individual wells in 24-well test plates (Costar) pre-coated with 1% agarose. The plates were incubated as above with weekly changes of fresh complete medium (0.5 ml).

Address correspondence to: J. H. M. Schwachöfer, Department of Radiotherapy, University Hospital, PO Box 9101, 6500 HB Nijmegen, The Netherlands.

Irradiation was carried out using an 18 MV photon beam from a Saturne linear accelerator (CGR) at a dose-rate of 2 Gy/min, with a wax build-up to ensure homogenous energy deposition within each well. Radiation was applied either as a single dose or as split doses with a time interval of 6 h.

The growth of spheroids on test plates was determined twice weekly by measuring the diameter of individual spheroids using a calibrated scale in the eye-piece of an inverted microscope. Assuming spherical geometry, volumes were calculated and growth curves constructed by plotting the ratio volume/initial volume as a function of time after treatment.

Spheroids were irradiated at a diameter of 130 or 350 μm. Growth delay was estimated from the difference in time required for non-irradiated spheroids and the irradiated spheroids to reach a volume eight times (for the 130 μm spheroids) or four times (for the 350 μm spheroids) the original volume.

A "dose repaired" was calculated for irradiated cells, growing either as monolayers or as spheroids, from the survival and growth delay data, respectively. The dose-related repair capacity as expressed by this "dose repaired" is defined as the difference between the total dose administered in two equal fractions and the single dose required to achieve the same biological effect (iso-effect calculation). The "dose repaired" was determined as function of total dose.

Spheroids were considered to have been controlled or "cured" if they failed to regrow, *i.e.* to more than double in volume by the end of the 4–5 week observation period, following the irradiation. This criterion was chosen because, irrespective of the irradiation dose, all spheroids were able to obtain a doubling in volume. The percentage cured was calculated as the fraction of non-regrowing spheroids relative to the total number of MTS originally present in the treatment group. With probit analysis the spheroid cure dose (SCD_{50}) was calculated. Statistical analysis for differences in SCD_{50} values was performed as described by Litchfield and Wilcoxon (1949).

Results

Figure 1 shows growth curves of spheroids irradiated with single (a) and split (b) doses of X rays (4–8 Gy) at a diameter of 130 μm. Figure 2 shows growth curves of spheroids irradiated at 350 μm. A static phase in the growth was reached after doses in excess of 6 Gy (130 μm spheroids) and 4 Gy (350 μm spheroids).

The survival curves of monolayer cells irradiated either with single or split doses of X rays are shown in Fig. 3. An increase in survival after split-dose irradiation is exhibited. Multitarget survival curve parameters are: $D_0 = 0.53 \pm 0.09$ Gy, $D_q = 5.5 \pm 0.1$ Gy, for the single-dose data.

The growth delay calculated from the growth curves of the spheroids (Figs 1, 2) are shown in Fig. 4 [diameter = 130 μm (a) and 350 μm (b)]. After split-dose irradiation, the growth delay is significantly lower than after single doses, indicating repair of sublethal damage in spheroids of both diameters. The growth delay is more pronounced for the 350 μm spheroids than for the 130 μm spheroids.

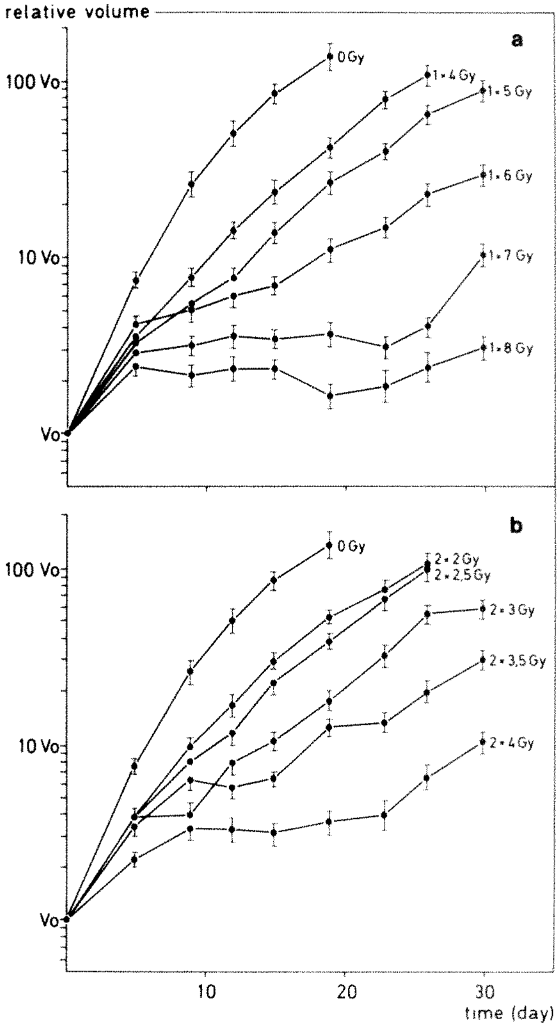

Figure 1. Growth curves of HN1 squamous cell carcinoma spheroids irradiated at a diameter of 130 μm with (a) single and (b) split doses of X rays. Growth is expressed as volume/initial volume as a function of time after treatment. Each point represents the average ± SD of at least 12 spheroids.

The "dose repaired" was calculated as described in the Materials and methods section from regrowth delay in spheroids and from the survival data for the monolayer irradiations. Figure 5 shows the "dose repaired" as a function of total dose for monolayer cells and spheroids. The "dose repaired" for monolayer cells and MTS with different diameters is not significantly different.

Figure 6 shows the results of the probit analysis of the proportion of cured spheroids after single dose irradiation as a function of total radiation dose. The dose necessary to sterilize 50% of the spheroids (SCD_{50}) is

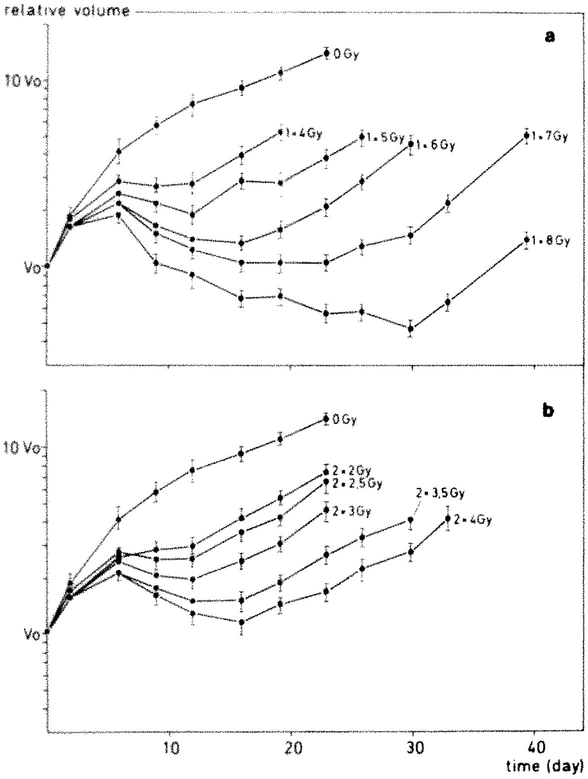

Figure 2. Growth curves of HN1 squamous cell carcinoma spheroids irradiated at a diameter of 350 μm with (a) single and (b) split doses of X rays. Growth is expressed as volume/initial volume as a function of time after treatment. Each point represents the average ± SD of at least 12 spheroids.

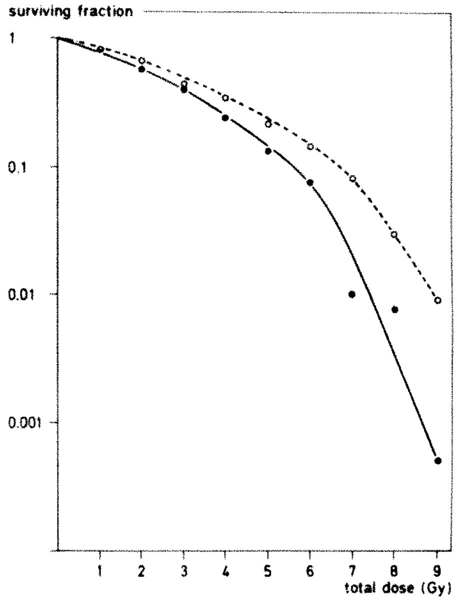

Figure 3. X-ray survival curve for HN-1 squamous cell carcinoma cells growing as monolayers. Cells were irradiated with single doses (solid line) and split doses (dashed line) 6 h apart. Error bars smaller than symbol size.

significantly larger for the spheroids with a 130 μm diameter (7.75 Gy, 7.38–8.46 Gy; 95% confidence limits) than for spheroids with a 350 μm diameter (6.87 Gy, 6.10–7.15 Gy; 95% confidence limits).

Discussion

Irradiation of human tumour cells of a squamous carcinoma cell line HN-1 growing as MTS and in monolayer culture revealed the same capacity for repair of sublethal damage. Also, there was no difference in repair capacity between cells growing as MTS when irradiated at different diameters. The reported increase in ability to repair sublethal damage in cells growing as spheroids (Sutherland & Durand, 1976) was not observed in the human tumour cells under consideration here. A similar effect has also been reported for 9L rat gliosarcoma spheroids (Rodriguez & Alpen, 1981).

In the pioneering studies by Durand and Sutherland (1972, 1973), the repair capacity of Chinese hamster V79 cells growing as MTS and as monolayers was compared. In contrast with our observations, they noticed an enhanced ability to repair sublethal damage for cells growing as MTS as compared with monolayer cells. However, their method was somewhat different from ours: the survival data were obtained from cells after disaggregation of MTS. In their study, cellular radiosensitivity of monolayer cells and small (150 μm) spheroids was of the same magnitude.

The question whether radiosensitivity of MTS of human cells can be expressed by parameters such as D_0 and D_q is difficult to address by evaluation of clonogenicity determined after irradiation. Cells of MTS derived from a number of human tumour lines have been found to be highly sensitive to artefactual cell killing during

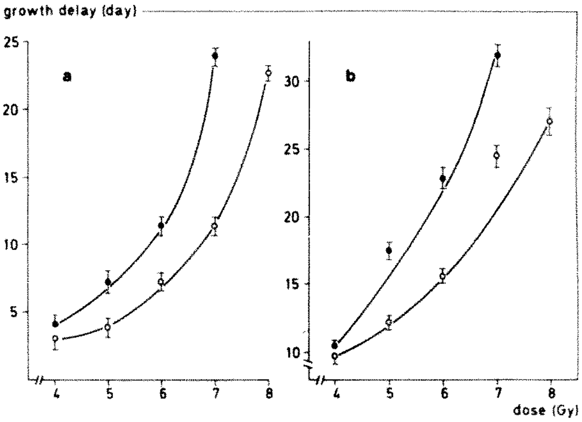

Figure 4. Growth delay as function of total dose for irradiated spheroids of squamous carcinoma cell line HN-1. Single (●) and split (○) doses administered to spheroids with a diameter of 130 μm (a) and 350 μm (b).

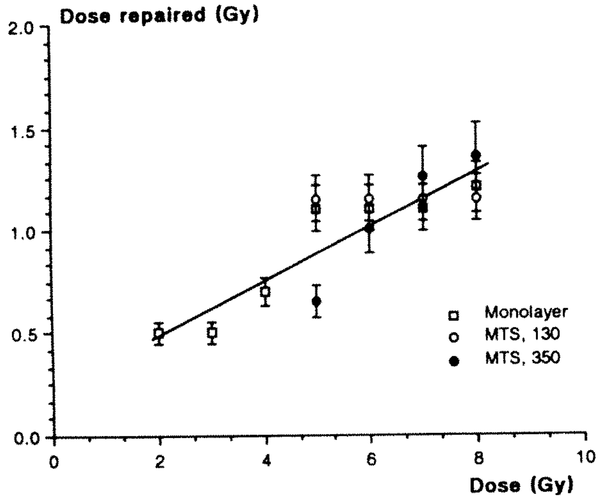

Figure 5. Dose repaired as a function of total dose, calculated on an iso-effect basis from growth delay data for spheroids and cell survival for monolayer cells.

disaggregation, making analysis of the survival of single cells obtained from MTS impractical. In addition, such determinations are often hampered by low plating efficiencies (Yuhas, 1983), as is also the case with HN-1 spheroids. The fact that after disaggregation of HN-1 MTS the plating efficiency of cells was too low for analysis of clonogenic survival prevented analysis of cure rate in terms of critical cell number (Kuwashima et al, 1988). The low clonogenic cell number in itself indicates that the critical cell number in HN-1 spheroids must be low.

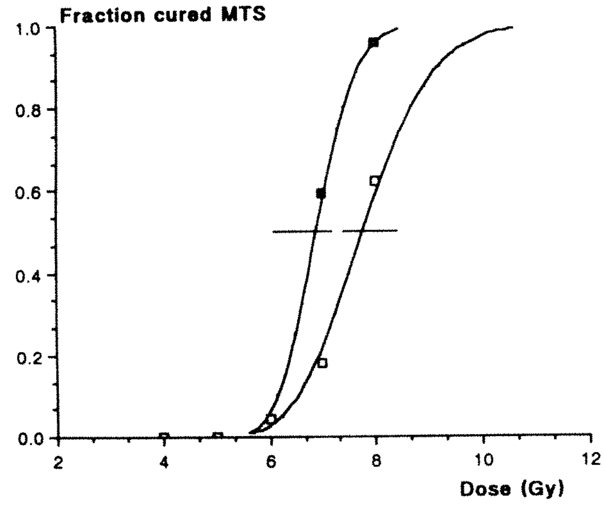

Figure 6. Fraction of "cured" HN-1 squamous cell carcinoma spheroids as a function of dose administered at two different diameters. Curves are fitted curves for actual cure data: □, 130 μm MTS; ■, 350 μm MTS. At 50% cure, 95% confidence intervals are shown.

In contrast with the results of Kuwashima et al (1988), who found an increasing SCD_{50} with increasing diameter for HMV-I melanoma MTS, the HN-1 squamous cell carcinoma cells growing as spheroids show 350 μm MTS to be more sensitive than 130 μm MTS.

The increase in radioresistance with increasing spheroid size has often been attributed in part to the presence of hypoxic cells (Sutherland & Durand, 1976; Sutherland, 1988). In HN-1 spheroids, polarographic oxygen tension measurements with microelectrodes showed no development of hypoxia with increasing spheroid diameter (Schwachöfer et al, 1989, submitted for publication). These observations deviate from the general finding that growing spheroids become increasingly hypoxic in their central regions, thus protecting tumour cells there from radiation damage (Carlsson & Acker, 1985; Sutherland, 1988). The absence of a hypoxic fraction in MTS has also been reported for rat 9L gliosarcoma (Gutin et al, 1982). Dertinger et al (1983) have suggested that contact effects and hypoxia in MTS might be related in that MTS with absence of hypoxia exhibit high contact resistance to radiation, and no contact effect with severe hypoxia. Electron microscopic study has shown the presence of gap-junctions (Schwachöfer, 1989, unpublished results), which are thought to determine cell–cell contacts in HN-1 cells of MTS. Our results might suggest that in the HN-1 squamous carcinoma cell line with the absence of hypoxia, contact resistance, as expressed by an increased ability to repair sublethal damage, is not developed. To our best knowledge, at present there are no other reports on MTS from human origin with no hypoxic centres that exhibit similar radiation responses as the HN-1 squamous cell carcinoma line.

Acknowledgments

Financial support from The Netherlands Cancer Foundation Koningen Wilhelmina Fonds is gratefully acknowledged. We are grateful to Prof. Dr H. Acker for valuable discussions.

References

Carlsson, J. & Acker, H., 1985. Influence of the oxygen pressure in the culture medium on the oxygenation of different types of multicellular spheroids. *International Journal of Radiation Oncology, Biology, Physics, 11*, 535–546.

Dertinger, H., Guichard, M. & Malaise, E. P., 1983. Is there a relationship between hypoxia, contact resistance, and intercellular communication? *Radiation and Environmental Biophysics, 22*, 209–214.

—— 1984. Relationship between intercellular communication and radiosensitivity of human tumour xenografts. *European Journal of Cancer and Clinical Oncology, 20*, 561–566.

Dertinger, H. & Hülser, D., 1981. Increased radioresistance of cells cultured in multicell spheroids. I: Dependence on cellular interaction. *Radiation and Environmental Biophysics, 19*, 101–107.

Durand, R. E. & Sutherland, R. M., 1972. Effects of intracellular contact on repair of radiation damage. *Experimental Cell Research, 71*, 75–80.

—— 1973. Growth and radiation survival characteristics of

V79-171b Chinese hamster cells: a possible influence of intercellular contact. *Radiation Research, 56*, 513–527.

Easty, D. M., Easty, G. C., Carter, R. L., Monaghan, P. & Butler, L. J.., 1981. Ten human carcinoma cell lines derived from squamous carcinomas of the head and neck. *British Journal of Cancer, 43*, 772–785.

Gutin, P. H., Barcellos, M. H., Shrieve, D. C., Sano, Y., Bernstein, M. & Deen, D. F., 1982. Further evidence for the absence of a hypoxic fraction in the 9L rat tumour multicellular spheroid system. *British Journal of Radiology, 55*, 688–690.

Hill, R. P., Ng, R., Warren, B. F. & Bush, R. S., 1979. The effect of intercellular contact on the radiation sensitivity of KHT sarcoma cells. *Radiation Research, 77*, 182–192.

Kuwashima, Y., Majima, H. & Okada, S., 1988. Cure, cell killing, growth delay and fragmentation of X-irradiated human melanoma HMV-I multicellular spheroids. *International Journal of Radiation Biology, 54*, 91–104.

Litchfield, J. T. & Wilcoxon, F., 1949. A simplified method of evaluating dose-effect experiments. *Journal of Pharmacology and Experimental Therapy, 96*, 99–113.

Rodriguez, A. & Alpen, E. L., 1981. Cell survival in spheroids irradiated with heavy ion beams. *Radiation Research, 85*, 24–37.

Rofstad, E. K., Wahl, A. & Brustad, T., 1986. Radiation response of multicellular spheroids initiated from five human melanoma xenograft lines. Relationship to the radioresponsiveness *in vivo*. *British Journal of Radiology, 59*, 1023–1029.

Sutherland, R. M., 1988. Cell and environment interactions in tumor microregions: the multicell spheroid model. *Science, 240*, 177–184.

Sutherland, R. M. & Durand, R. E., 1976. Radiation response of multicell spheroids: an *in vitro* tumor model. *Current Topics in Radiation Research Quarterly, 11*, 87–139.

Yuhas, J. M., 1983. Clonogenic assay for predicting the response of solid tumor to therapy. In *Biological Bases and Clinical Implications of Tumor Radioresistance*, ed. by G. A. Fletcher, C. Nervi & H. R. Withers (Masson, New York), pp. 383–390.

Yuhas, J. M., Li, A. P., Martinez, A. O. & Landman, A. J., 1977. A simplified method for production and growth of multicellular tumor spheroids. *Cancer Research, 37*, 3639–3643.

1989, *The British Journal of Radiology*, 62, 1089–1090

Case reports

Burkitt's lymphoma in a patient previously treated for Hodgkin's disease

By A. C. R. Robinson, MRCPI, FRCR, FFR, *G. G. Khoury, MB, MRCP, FRCR and D. Carney, MD, PhD, FRCPI

Department of Medical Oncology, St Luke's Hospital, Dublin, Eire and *University Department of Radiotherapy, Cookridge Hospital, Leeds LS16 6QB

(*Received March 1989 and in revised form June 1989*)

Treatment advances in Hodgkin's disease have resulted in many patients achieving long-term survival, and the late complication of second malignancies is being increasingly recognized. The occurrence of Burkitt's lymphoma following chemotherapy or combined-modality treatment for Hodgkin's disease has previously been documented. Its development has not, to the best of our knowledge, been described following irradiation alone. We report a male patient with Hodgkin's disease treated by mantle irradiation who subsequently died from Burkitt's lymphoma. Theories of pathogenesis are presented.

Case report

A 21-year-old Caucasian male presented with pathological Stage IIA (Ann Arbor) lymphocyte-predominant Hodgkin's disease. He was treated with mantle irradiation, a mid-plane dose of 3500 cGy in 16 fractions in 20 days being delivered to the mediastinum. Complete remission occurred and the patient remained well until 6 years later when he developed intestinal obstruction. Laparotomy revealed extensive malignancy involving the small bowel, mesentery and retroperitoneum, histology being Burkitt's lymphoma (Fig. 1). Bone marrow aspirate showed replacement with immature cells of Burkitt type and cytological findings on examination of cerebrospinal fluid showed malignant cells. The patient was commenced on systemic chemotherapy and intrathecal methotrexate, but died 2 days later of progressive disease. Autopsy confirmed the presence of Burkitt's lymphoma. There was no evidence of Hodgkin's disease.

Discussion

The occurrence of Burkitt's lymphoma following treatment of Hodgkin's disease is rare, a total of six cases being reported (Table I). Our patient is unusual in having lymphocyte-predominant Hodgkin's disease and receiving irradiation only for the management of his initial lymphoma.

The exact mechanism for the development of non-Hodgkin's lymphoma in this patient is unclear; one possible explanation is a natural propensity to develop lymphoid neoplasms. Recent monoclonal antibody studies suggest lymphocyte-predominant Hodgkin's disease is a separate entity from other forms of Hodgkin's disease (Pinkus & Said, 1985) and a disproportionate number of patients with this histological subtype have developed non-Hodgkin's lymphoma post-irradiation alone (Trenkner et al, 1986). The role of irradiation in inducing neoplasia in these subjects is unclear as Miettinen et al (1982) documented secondary non-Hodgkin's lymphoma in five out of 51 lymphocyte-predominant Hodgkin's disease patients. Only one had received irradiation supporting the theory that transformation may be part of the natural history of this histological subtype of Hodgkin's disease. Immunological abnormalities resulting from treatment and/or those inherent in the disease may also play a part as long-term survivors of Hodgkin's disease have persistent immunological dysfunction. The presence of this defect may allow abnormal lymphoid proliferation. The most frequent neoplasm developing after successfully treated Hodgkin's disease is acute non-lymphocytic leukaemia (ANLL). Combined treatment with chemotherapy and irradiation has most commonly been implicated. The risk post-irradiation alone appears to be negligible, but a direct relationship seems to exist between the risk of ANLL occurring and the cumulative dose of alkylating agents received (Pedersen-Bjergaard et al, 1987).

Increasingly, non-Hodgkin's lymphoma is being described following successful treatment of Hodgkin's

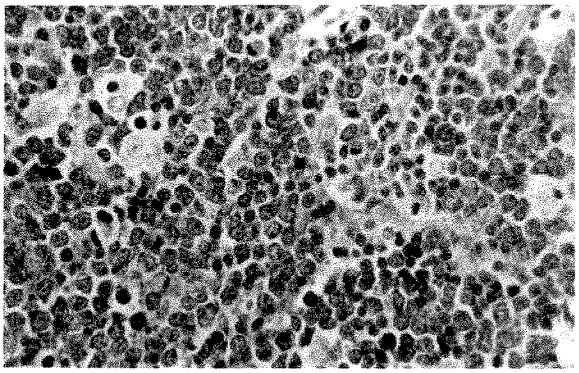

Figure 1. Burkitt's lymphoma showing characteristic starry sky appearance.

Address correspondence to: Dr A. C. R. Robinson, Christie Hospital & Holt Radium Institute, Wilmslow Road, Withington, Manchester M20 9BX.

Table I. Burkitt's lymphoma in Hodgkin's disease patients

Reference	Initial histology	Age at diagnosis (years)	Sex	Stage	Treatment			Latent	Outcome
					RT	CT	Both		
Magrath et al, 1975	Mixed cellularity	8	M	IA	–	+	–	9 months	Died
Mandelli et al, 1985	Mixed cellularity	38	M	IB	–	–	+	9 years	Died
Henry-Amar, 1983	NR	19	F	NR	–	–	+	13 years	Died
Case 6, 1980	Nodular sclerosis	24	M	IIA	–	–	+	11 years	Died
Andrieu et al, 1980	Nodular sclerosis	21	F	IIA	–	–	+	6 years	NR
This case report	Lymphocyte predominant	21	M	IIA	+	–	–	6 years	Died

RT = irradiation; CT = chemotherapy; NR = not reported.

disease. The therapy given may be of aetiological importance. The majority of patients affected have had combined-modality management and four of the six cases of Burkitt's lymphoma in this report had chemotherapy and irradiation. Non-Hodgkin's lymphoma may also develop post-chemotherapy alone as it has followed alkylating agents used in multiple myeloma (Gonzalez et al, 1977), carcinoma of the breast (Rosner et al, 1978) and carcinoma of the ovary (Reimer et al, 1977). Irradiation only may also be a factor as there appears to be an increased incidence of non-Hodgkin's lymphoma among survivors of the atomic bomb in Hiroshima (Anderson et al, 1972).

The major mortality for patients with Hodgkin's disease is still uncontrolled disease. As treatment improves, second malignancies will assume an increasingly significant role in determining survival.

Clinically, it is essential that no patient should be treated for presumed relapse of Hodgkin's disease without histological confirmation, since therapy aimed at producing cure varies with diagnosis and, in addition, prognosis may be significantly affected. Although the majority of non-Hodgkin's lymphomas complicating Hodgkin's disease are high-grade and have had a fatal course, a subset developing post-irradiation of the Hodgkin's lymphomas have been curable with chemotherapy (Trenkner et al, 1986).

Acknowledgments

We would like to thank Miss Amanda Smith for typing the manuscript.

References

ANDERSON, R. E., NISHIYANA, H., ISHIDAI, K. & OKABE, N., 1972. Pathogenesis of radiation related leukaemia and lymphoma. Speculation raised on experience of Hiroshima and Nagasaki. *Lancet*, *i*, 1060–1062.

ANDRIEU, J. M., CASASSUS, P., DEGOS, L., PREUD'HOMME, J. L., BERGER, R. & FLANDRIN, G., 1980. Burkitt's lymphoma occurring six years after Hodgkin's disease. *Acta Haematologica*, *63*, 330–332.

CASE 6, 1980. Case records of the Massachusetts General Hospital. *New England Journal of Medicine*, *302*, 389–395.

GONZALEZ, F., TRIYILLO, J. M. & ALEXANIAN, R., 1977. Acute leukaemia in multiple myeloma. *Annals of Internal Medicine*, *86*, 440–443.

HENRY-AMAR, M., 1983. Second cancers after radiotherapy and chemotherapy for early stages of Hodgkin's disease. *Journal of the National Cancer Institute*, *71*, 911–916.

MAGRATH, I., HENLE, W., OWOR, R. & OLWENY, C., 1975. Antibodies to Epstein Barr virus antigens before and after the development of Burkitt's lymphoma in a patient treated for Hodgkin's disease. *New England Journal of Medicine*, *292*, 621–623.

MANDELLI, F., MARELLI, M., CIMINO, G., ALIMENA, G., ANSELMO, A., DE CUIA, M. R., GASTALDI, R., ARCESE, W. & PAPA, G., 1985. A case of Burkitt's lymphoma—L$_3$ ALL with t (8;14) translocation, developed 10 years after Hodgkin's disease. *Scandinavian Journal of Haematology*, *34*, 97–100.

MIETTINEN, M., FRANSSILA, K. O. & SAXEN, E., 1982. Hodgkin's disease, lymphocyte predominance nodular. *Cancer*, *51*, 2293–2300.

PEDERSEN-BJERGAARD, J., LARSEN, S. O., STRUCK, J., HANSEN, H. H., SPECHT, L., ERSBOLL, J., HANSEN, M. M. & NISSEN, N. I., 1987. Risk of therapy related leukaemia and preleukaemia after Hodgkin's disease. *Lancet*, *ii*, 83–88.

PINKUS, G. S. & SAID, J. W., 1985. Hodgkin's disease, lymphocyte predominance, nodular—a distinct entity? *American Journal of Pathology*, *118*, 1–6.

REIMER, R. R., HOOVER, R., FRAUMENI, J. F. JR, YOUNG, R. C., 1977. Acute leukaemia after alkylating agent therapy of ovarian cancer. *New England Journal of Medicine*, *297*, 177–181.

ROSNER, F., CAREY, R. W. & ZARRABI, M. H., 1978. Breast cancer and acute leukaemia: report of 24 cases and review of the literature. *American Journal of Haematology*, *4*, 151–172.

TRENKNER, D. A., BROWNELL, M. & WASSERMAN, T. H., 1986. Non-Hodgkin's lymphomas following radiation therapy alone for Hodgkin's disease. *Radiotherapy and Oncology*, *6*, 199–206.

1989, *The British Journal of Radiology*, 62, 1091–1093

Case reports

Induced fluid movement within a giant ovarian cyst demonstrated by echo-planar imaging

By *B. S. Worthington, BSc, MB, BS, FRCR, B. Chapman, BSc, PhD, R. Ordidge BSc, PhD, R. Coxon, BSc, M. K. Stehling, DrMed, †E. M. Symonds, MD, FRCOG and P. Mansfield, BSc, PhD, FRS

Department of Physics, University of Nottingham and Departments of *Academic Radiology and †Obstetrics and Gynaecology, Queen's Medical Centre, Nottingham

(*Received May 1989*)

Over 50% of ovarian tumours are of epithelial origin occurring as solid carcinomas and mucinous or serous cysts, the majority of which can be readily categorized as benign or malignant. However, approximately one-fifth of the cysts, whilst showing some histological feature of malignancy, lack evidence of stromal invasion and are therefore reported as borderline malignancy. Serous cystadenomas may be unilocular or multilocular and vary in size from a few centimetres to enormous dimensions where they come to occupy most of the pelvis and abdominal cavity. In approximately 50% of cases the tumours are bilateral. Some have intracystic papillary ingrowths or solid areas in one or more loculi, and invasion of the cyst wall with tumour extension onto the serosal surface indicates the transition from a cystadenoma to a cystadenocarcinoma.

A giant serous cyst of the ovary has been imaged by echo-planar imaging (EPI) (Mansfield, 1977) and the features observed compared with the operative and pathological findings. The EPI technique permits the acquisition of single images in a time of 64 ms. On physical examination, a fluid thrill was readily elicited and deformation of the cyst during imaging induced flow patterns within the cyst contents which were clearly visualized and studied in real time.

Case report

A 71-year-old woman presented with a 4-month history of progressive abdominal distension and bilateral ankle swelling. She had also noted frequency of micturition. Eight years previously she had undergone a total hysterectomy for fibroids. On examination, a massive anteriorly situated tumour was present within the abdomen, extending downwards into the pelvis. On palpation the tumour was tense, cystic and a fluid thrill was readily elicited. A diagnosis of a giant ovarian cyst was made and this was confirmed on ultrasound examination.

Image quality on conventional magnetic resonance images (MRI) was suboptimal owing to patient movement during the data acquisition, but the scan showed a massive ovarian tumour with homogeneous contents, which had a high signal intensity on a T_2-weighted spin-echo sequence consistent with fluid content. No solid components were demonstrated within the cyst.

An examination of the abdomen and pelvis in the transverse axial plane was then carried out by EPI on a prototype machine operating at a magnetic field strength of 0.52 T. For data acquisition the MBEST (modulus-blipped echo-planar single-pulse technique) (Howseman et al, 1988), a variant of standard EPI, was used. A full description of the MRI system together with a discussion of this and other variants of EPI is given elsewhere (Mansfield & Morris, 1982; Stehling et al, 1989). The method allows the acquisition of a snapshot image in a single exposure of 64 ms and no signal averaging is required. The MBEST images are intrinsically T_2-weighted and the fluid within the cyst gave a high signal contrasting with the low signal from several small tumour nodules arising from the inner wall. A septum was also noted within the lower part of the cyst and a second smaller tumour was identified on the left side of the pelvis posteriorly on the lower sections.

This had a smooth outline and the majority of its contents returned a high signal apart from a small, anterior, low-signal nodule. This was interpreted as representing a concomitant cystadenoma of the other ovary. Motion of the fluid within the large cyst was induced by asking the patient to tap on her

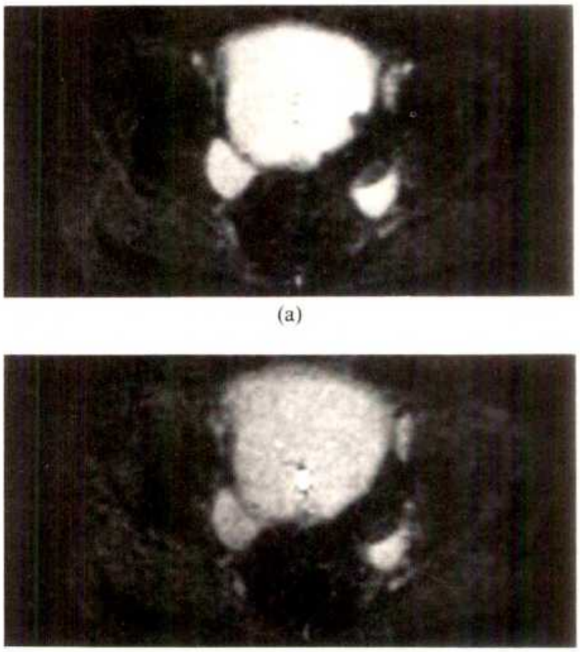
(a)

(b)

Figure 1. Two snapshot images from a series of transverse axial sections through the lower part of the large cyst. Two small tumour nodules are seen on the inner wall of the cyst in (a) but have moved out of the imaging plane in (b), which was taken during a different phase of respiration.

CENTRAL LIBRARY

anterior abdominal wall. The variations of signal intensity resulting from the flow patterns set up were visualized by taking a series of scans in rapid succession at the same level and displaying them as a movie loop.

Laparotomy confirmed the findings found by EPI and 4 litres of fluid were aspirated from the large cyst. Subsequent pathological examination confirmed that each tumour was a benign serous cystadenoma.

Discussion

Echo-planar imaging, which produces a snapshot image after a single excitation of the spin system, is superior to other fast imaging approaches in the study of abdominal pathology because the short imaging time minimizes motion artefact without sacrifice of the relaxation-time contrast. In the present case the patient found it difficult to lie completely still for the time of a conventional MRI scan and this resulted in blurred image detail. The examination failed to disclose any small tumour nodules arising from the inner wall of the cyst, whereas several were clearly shown on the EPI examination. The effect of respiratory movement on visualization of important structures is shown in Fig. 1 where a small tumour nodule enters and leaves the imaging plane during different parts of the respiratory cycle. The opportunity to study flow phenomena in real time is an important benefit of EPI. Induced intracavitary flow patterns within the large cyst were readily shown (Fig. 2).

The principles underlying this can be readily demonstrated by means of a simple phantom, which consists of a bottle containing water that is rotated briefly and the induced flow pattern imaged in the transverse axial plane (Fig. 3). Images 1 to 4 show 1 cm thick, cross-sectional slices through the water bottle. Images 1 and 2 show the first and second images, respectively, of a sequence of EPI experiments repeated at a rate of one per second. The water in the bottle is stationary. The second image appears less intense than the first because the interexperimental delay of 1 s only allows partial spin-lattice relaxation of the nuclear magnetic resonance (NMR) spins in the imaged slice. Images 3 and 4 show the first and second images, respectively, of a bottle that has been rotated. The first image is unchanged. However, Image 4 clearly demonstrates flow patterns

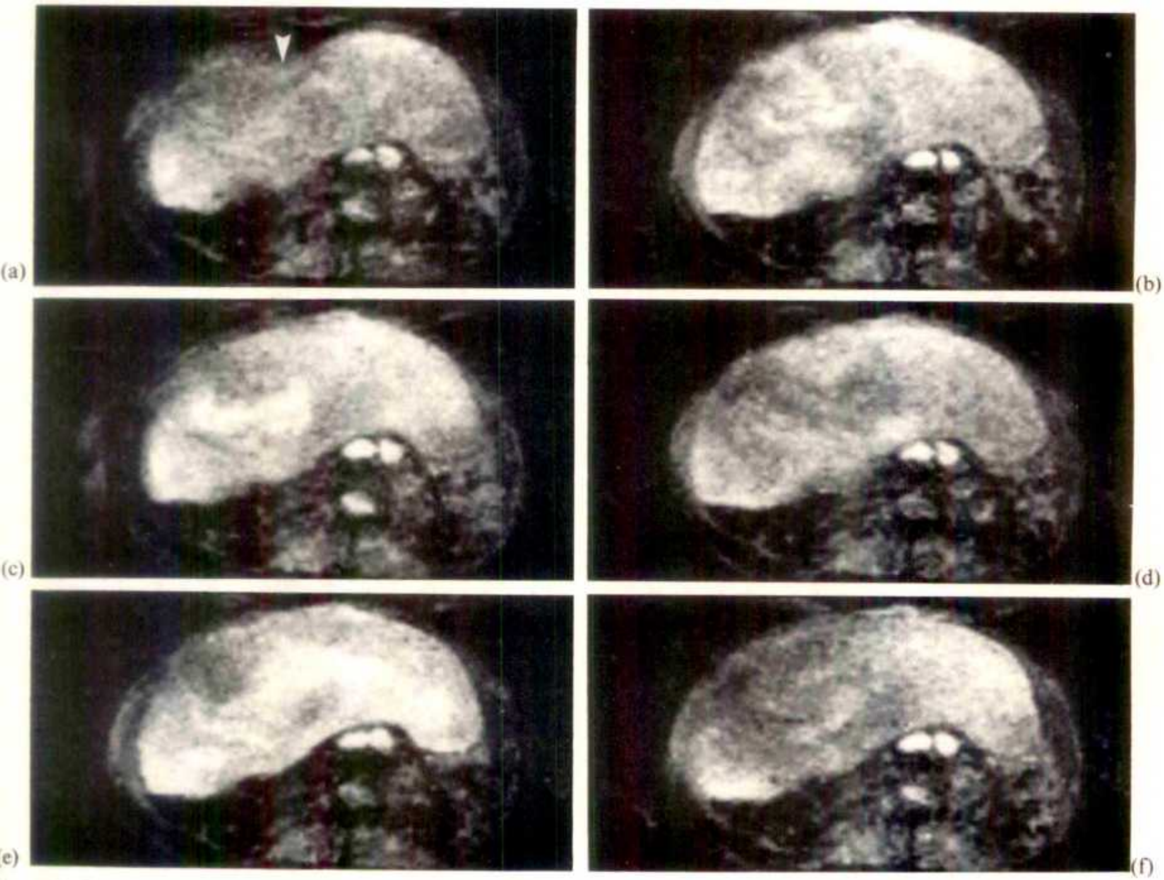

Figure 2. Six consecutive snapshots from a series of transverse axial sections taken through the cyst at the same level. In (a) the deformity of the anterior wall of the abdomen and underlying cyst is shown (arrow) following a firm tap by the patient. In (b)–(f) the development of flow patterns can be seen within the fluid contents of the cyst.

1989, *The British Journal of Radiology*, *62*, 1093–1095

Case reports

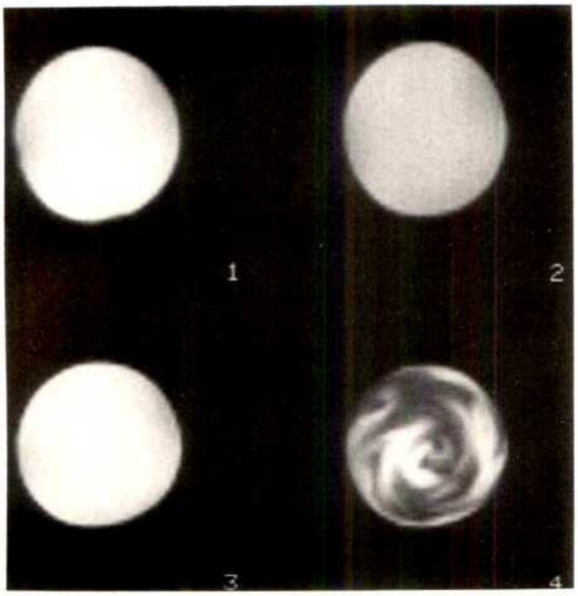

Figure 3. Images 1 and 2 are the first and second from a sequence of EPI images of a bottle containing stationary water. Image 2 appears less intense because of the T_1 weighting, which results from an interexperimental delay of 1 s. Images 3 and 4 are obtained from a similar sequence after the bottle has been rotated to induce flow inside the bottle. Image 4 shows flow patterns caused by motion of previously unperturbed NMR spins into the imaging plane during the interexperimental delay. The movie sequence was obtained at 1 frame/s in both cases.

caused by the motion of previously unperturbed NMR spins into the imaging plane during the interexperimental delay, which then appear with full signal intensity.

We conclude that the shorter examination time, which eliminates obtrusive movement artefact and gives better patient tolerance, plus the opportunity to study flow phenomena in real time are important benefits of ultra-high-speed imaging by EPI.

Acknowledgments

We thank the Medical Research Council, the Department of Health and Social Security of Great Britain and the British Heart Foundation for financial support of the echo-planar imaging programme. We also thank A. Howseman, A. Blamire and P. Gibbs for their valuable assistance in this project.

References

Howseman, A. M., Stehling, M. K., Chapman, B., Coxon, R., Turner, R., Ordidge, R. J., Cawley, M. G., Glover, P., Mansfield, P. & Coupland, R. E., 1988. Improvements in snap-shot nuclear magnetic resonance imaging. *British Journal of Radiology*, *61*, 822–823.

Mansfield, P., 1977. Multiplanar image formation using NMR spin echoes. *Journal of Physics*, *C10*, L55–L58.

Mansfield, P. & Morris, P., 1982. *NMR Imaging in Biomedicine* (Academic Press, New York).

Stehling, M. K., Howseman, A., Ordidge, R. J., Chapman, B., Turner, R., Coxon, R., Glover, P., Mansfield, P. & Coupland, R. E., 1989. Whole-body echo-planar MR imaging at 0.5 T. *Radiology*, *170*, 257–263.

Sonographic demonstration of renal tumour extension into the contralateral renal vein

By Preston Carvalho, BSc, MRCP, FRCR

Department of Radiology, Hammersmith Hospital, Du Cane Road, London W12 0HS

(*Received April 1989 and in revised form July 1989*)

Extension of renal tumour into the ipsilateral renal vein with or without inferior vena cava (IVC) extension is well recognized and it is mandatory to examine carefully the ipsilateral renal vein and IVC when there is evidence of a renal tumour (Goncharenko et al, 1979; Amis & Hartman, 1984). Extension of tumour into the contralateral renal vein, detected or imaged antemortem, has, however, not been described previously.

Case report

A 60-year-old Caucasian woman presented with a 2-week history of pyrexia, right loin pain, night sweats and malaise. On examination she had a tender right renal mass. Routine biochemistry was normal; the serum creatine was 69 mM/litre. Haemoglobin was 10.5 g/dl, the white cell count was 10 400 ml and the platelet count was 497 000/ml. The chest radiograph was unremarkable with no evidence of metastases. Ultrasound examination of the abdomen showed a 12 cm × 9 cm mass in the upper pole of the right kidney, which was of mixed echogenicity and was pushing the right lobe of the liver superiorly. No liver metastases were identified. The IVC contained echogenic solid material and was grossly expanded (Fig. 1). The IVC contained solid material up to 2.5 cm below the right atrium, where it regained its patency.

Address for correspondence: Dr P. Carvalho, Department of Diagnostic Radiology, Westminster Hospital, Dean Ryle St, London SW1 2AP.

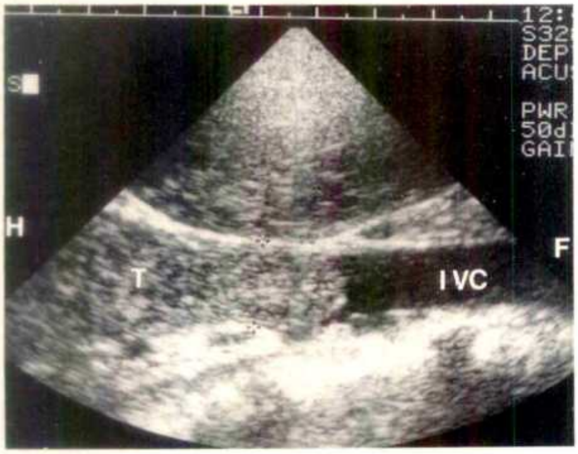

Figure 1. Longitudinal section through the upper inferior vena cava (IVC). Caudally the IVC is patent but cranially it is filled by echogenic tumour (T), which is expanding the IVC.

The ipsilateral right renal vein was engulfed by the tumour mass, which also extended into the IVC. The left renal vein, as it coursed into the IVC, was also expanded and filled with echogenic solid material (Figs 2, 3).

The left kidney appeared normal. Using duplex Doppler sonography, no Doppler signal could be obtained from the left renal vein but flow was demonstrated in renal vein branches at the left renal hilum with flow in the appropriate direction. However, the phasic component seen with normal renal venous Doppler signals was absent. Collateral veins were also present at the left renal hilum and the splenic hilum. In particular, a vein parallel to the long axis of the left kidney was seen consistent with an enlarged left ascending lumbar vein draining into the hemiazygous system (Fig. 4).

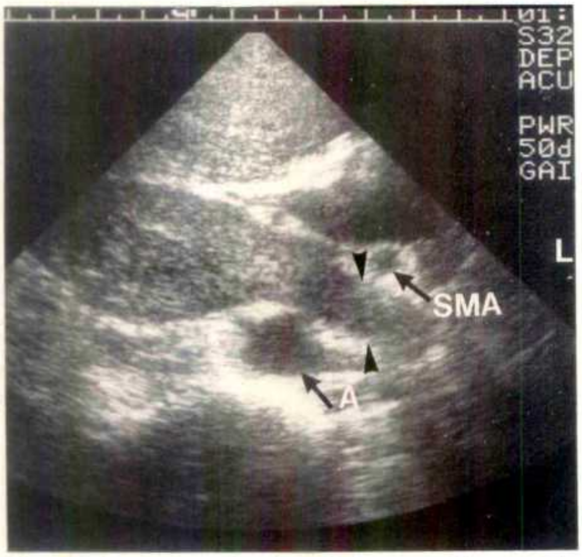

Figure 2. Transverse section through the upper abdomen at the level of the pancreas showing a dilated left renal vein (arrowheads) as it courses between the aorta (A) and superior mesenteric artery (SMA).

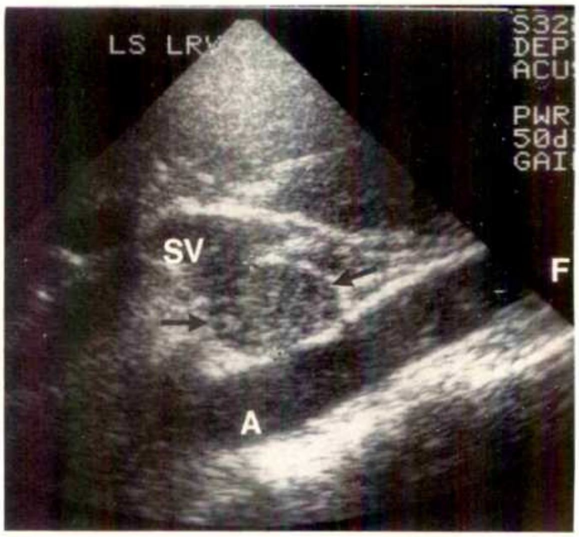

Figure 3. Longitudinal section of the upper abdomen through the aorta. The expanded left renal vein (arrows) lies between the aorta (A) and splenic vein (SV).

Computed tomography confirmed a large mass consistent with hypernephroma in the right kidney and cavography and renal angiography showed an obstructed upper IVC with collateral venous supply via the azygous and hemiazygous veins. In view of tumour extension into the IVC and both renal veins, the tumour was inoperable. Axillary lymphadenopathy subsequently developed and biopsy confirmed metastastic hypernephroma.

Discussion

Venous extension of hypernephromas varies in different series from 9% (Madayag et al, 1979) to 24% (Goncharenko et al, 1979). Inferior vena cava extension is more common with right-sided tumours and with larger tumours (Goncharenko et al, 1979). Precise

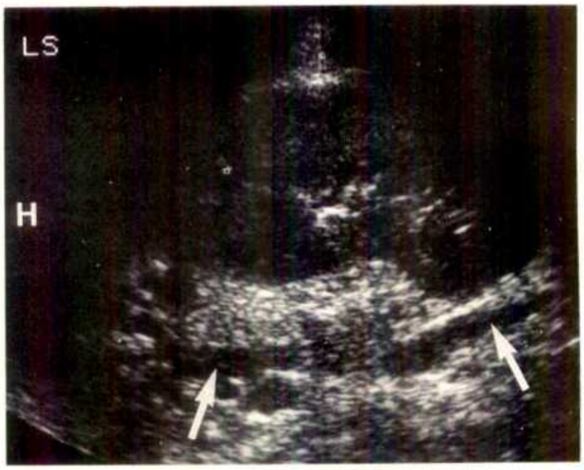

Figure 4. Longitudinal section through the left kidney showing collateral venous drainage by the left ascending lumbar vein (arrows).

evaluation of the renal veins and IVC is important preoperatively when radical surgery is proposed, both to plan surgery and to prevent intraoperative tumour embolization. Where tumour is invading the IVC with no evident metastases, radical IVC and renal vein block resections, together with resection of the affected kidney, have been carried out (McCullough & Gittes, 1974). If such surgery is contemplated, demonstration of patency of the contrarenal vein becomes important.

While tumour extension into the ipsilateral vein and vena cava have been previously described on both ultrasound and angiography, extension into the contralateral renal vein has only been described post-mortem (Svane, 1969). In the same study, tumour extension was also seen post-mortem into the right ventricle, pulmonary arteries and the iliac veins.

Presumably, tumour extension follows blood flow, and initial obstruction of the upper IVC and the right renal vein may result in flow reversal in a non-occluded left renal vein leading to tumour extension into the left renal vein. This patient's serum creatinine was normal and functioning of the left kidney was presumably dependent on the venous collateral drainage at the left renal hilum.

In summary, venous extension of hypernephroma can occur into the contralateral renal vein, and, where radical surgery is contemplated, it is important to examine carefully the contralateral renal vein as well as the ipsilateral renal vein and the inferior vena cava for tumour thrombus.

References

AMIS, E. S. & HARTMAN, D. S., 1984. Symposium on imaging and intervention in the renal fossa. *Radiologic Clinics of North America, 22,* 315–332.

GONCHARENKO, V., GERLOCK, A. J., JR, SAADOON, K. & TURNER, B., 1979. Incidence and distribution of venous extension of hypernephromas. *American Journal of Roentgenology, 133,* 263–265.

MADAYAG, M. A., AMBOS, M. A., LEFLEUR, R. S. & BOSNIAK, M. A., 1979. Involvement of the inferior vena cava in patients with renal cell carcinoma. *Radiology, 133,* 321–326.

MCCULLOUGH, D. L. & GITTES, R. F., 1974. Vena cava resection for renal cell carcinoma. *Journal of Urology, 112,* 162–167.

SVANE, S., 1969. Tumour thrombus of the IVC resulting from renal carcinoma. A report on 12 autopsied cases. *Scandinavian Journal of Urology and Nephrology, 3,* 241–256.

Spontaneous regression of multiple bone metastases in malignant melanoma

By M. E. A. O'Connell, MSc, MRCP, FRCR, *B. W. E. M. Powell, FRCS, *J. M. O'Connell, BSc, MB, BS and C. L. Harmer, MB, MRCP, FRCR

Departments of Radiotherapy and *Academic Surgery, The Royal Marsden Hospital, London SW3 6JJ

(Received May 1989)

Everson and Cole (1966) in their classic monograph defined spontaneous regression of malignant disease as "the partial or complete disappearance of a malignant tumour in the absence of all treatment or in the presence of therapy which is considered inadequate to exert a significant influence on neoplastic disease". It is generally agreed (Fauvet et al, 1960, 1964; Cappelaere et al, 1973) that regression of malignant melanoma must fulfil at least the following criteria:

1. clinical and histological diagnosis of melanoma;
2. no therapeutic manipulation that could account for the regression;
3. clinical observation of regression of existing lesions including radiographs, photographs, etc;
4. if possible, histopathological studies of tissue sites where regression has presumably occurred.

We describe a case of spontaneous regression of multiple bone metastases following palliative radiotherapy in a patient with malignant melanoma and discuss the possible mechanisms.

Case report

In September 1985, a 40-year-old Scotsman was referred to the Royal Marsden Hospital following local excision of a pigmented lesion on the dorsal surface of the distal part of the left forearm. The lesion had been present for 5 years and for the previous 6 months had increased in size and depth of colour and bled on trauma. The only other medical history of note was vagotomy for duodenal ulceration 20 years previously.

Examination revealed a generally fit man with a 1 cm transverse scar at the site of excision. There were no satellite nodules or clinical evidence of metastases. Review of histology (Fig. 1) revealed a malignant melanoma of the sessile nodular type, 1.3 mm thick (Clarke's level 3), with mitotic activity less than 1 in 5 per high-power field, sparse melanin, no ulceration, no upward dermal transmigration, no involution, moderate lymphocytic response, no lymphatic or vascular invasion and no lateral dermal component. The lateral and deep margins were clear. Full blood count, urea and electrolytes, liver function tests, gamma glutamyl transferase and alkaline phosphatase were within the normal ranges. Chest radiograph, liver ultrasound and radionuclide bone scan were normal. Wide

---

Address offprint requests to: Dr M. E. A. O'Connell, Academic Radiotherapy Unit, The Royal Marsden Hospital, Downs Road, Sutton, Surrey SM2 5PT.

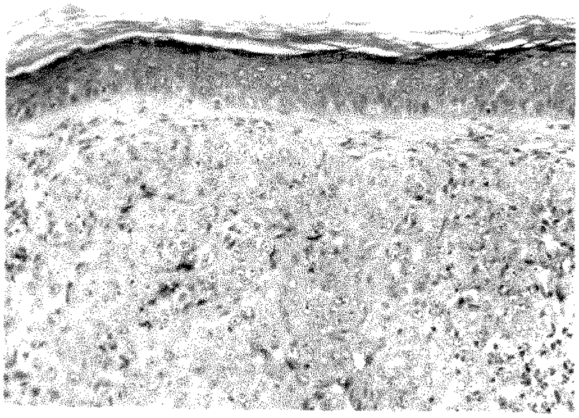

Figure 1. Histology showing infiltration of dermis by malignant melanoma. (Haematoxylin stain, magnification × 137.)

local re-excision with a 3 cm margin was performed together with exploration and sampling of the left axilla. Histology showed no residual tumour at the site of excision and no axillary lymphatic involvement.

In November 1985 he developed a 2 cm subcutaneous swelling 7 cm proximal to the original lesion. This was excised and histology showed an amelanotic undifferentiated lesion with high mitotic activity consistent with metastatic malignant melanoma. Two months later, a further deposit was excised from the left forearm. This recurrence appeared at the same site as that in December. Histology showed a firm grey nodule 2.8 cm × 2 cm × 1 cm with the microscopic appearances of an undifferentiated amelanotic melanoma (Fig. 2). There was no other clinical abnormality and a repeat chest radiograph was normal.

One month later a further 4.5 cm × 4 cm nodule occurred on the left forearm at the same site as the most recent lesion. In addition, the patient complained of indigestion. General clinical examination was otherwise negative. A barium meal showed a small, sliding, reducible hiatus hernia. Thoracic computed tomography (CT) showed no evidence of pulmonary metastases. Accordingly, in March 1986, a left axillary clearance and hyperthermic isolated limb perfusion of the left upper arm were performed. Sixty-five milligrams of Melphalan was given in three divided doses and the limb was perfused for 1 h. Post-operatively, he developed a marked reaction with oedema, erythema and pain, which settled slowly with complete resolution of the melanoma deposit. There was no evidence of systemic toxicity, the nadir white count being 4.7×10^9/litre. Histology showed no tumour in 12 axillary nodes sectioned.

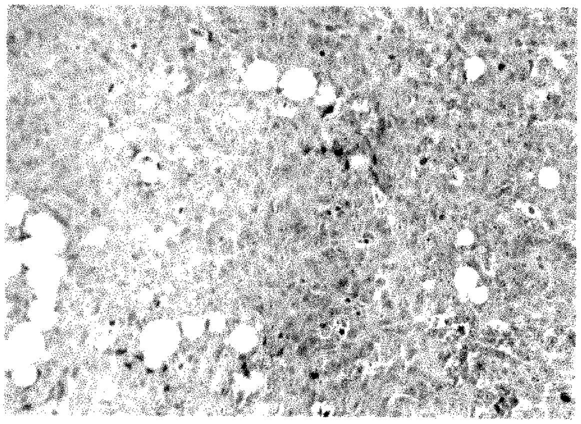

Figure 2. Histology showing infiltration of adipose tissue of the forearm by tumour histologically identical with that of primary lesion. (Haematoxylin stain, magnification × 137.)

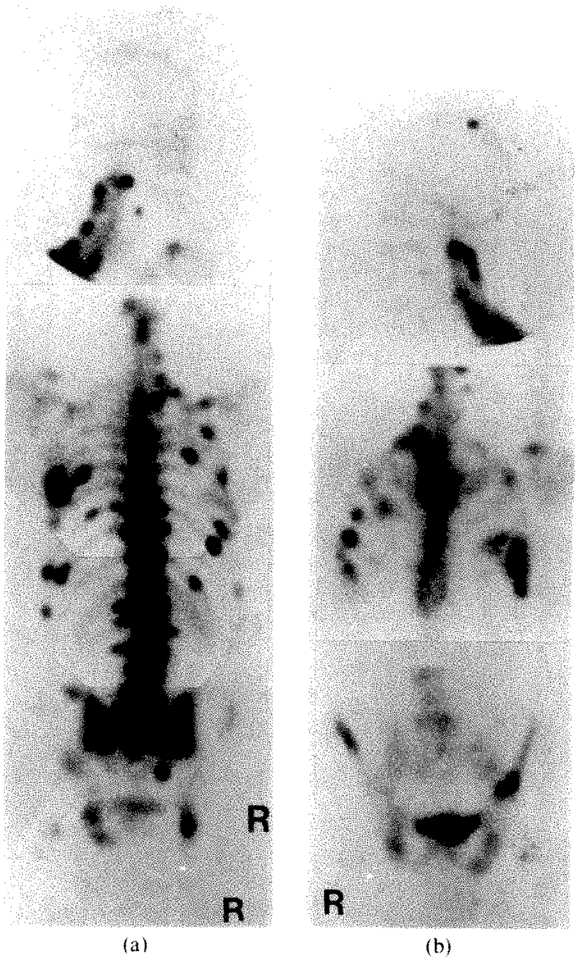

(a) (b)

Figure 3. Radionuclide bone scans (12 September 1986). (a) Postero-anterior and (b) antero-posterior scans showing abnormal increased uptake in the skull vault, multiple ribs, vertebrae and pelvis.

The patient remained well with no evidence of local or distant spread until June 1986 when he complained of low back pain. On examination there was no evidence of local recurrence, lymphadenopathy or hepatomegaly. There was marked spasm of the left erector spinae muscles but no neurological deficit in the limbs and no local bony tenderness. A radionuclide bone scan was equivocal. The bone pain progressed and by August involved the cervical spine, lower thoracic cage and the upper lumbar spine. The physical signs were unchanged but serum alkaline phosphatase was now grossly elevated at 321 i.u./litre (normal range 25–92 i.u./litre) and a radionuclide bone scan (Fig. 3) showed abnormal increased uptake in the skull vault and throughout the axial skeleton involving multiple ribs, vertebrae and pelvis. A radiograph of the lumbar

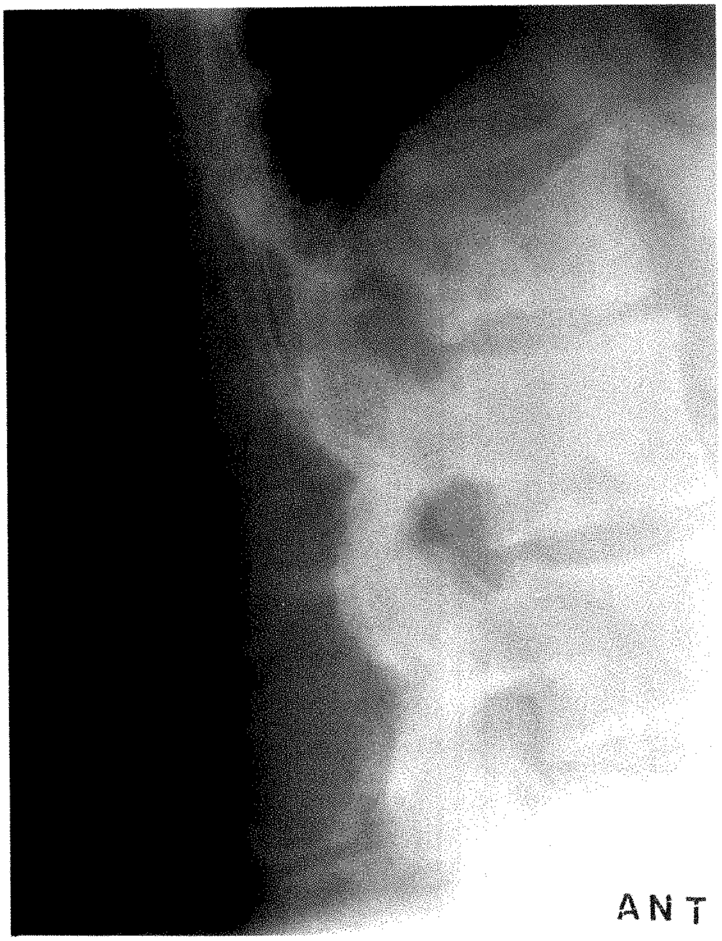

Figure 4. Lateral radiograph of the lumbar spine showing collapse of the first lumbar vertebra.

spine (Fig. 4) showed collapse of the first lumbar vertebra and a chest radiograph (Fig. 5) showed fractures of the left third, sixth and seventh ribs; the lung fields were clear.

Palliative external-beam radiotherapy (Harmer, 1976) was given to the painful lumbar deposit by a single direct posterior field measuring 9 cm × 6 cm and encompassing the 12th thoracic to second lumbar vertebrae inclusive (Fig. 6). A dose of 6.6 Gy at a depth of 6 cm was given once weekly on a telecobalt unit and repeated over a period of 1 month to give a total dose of 26.4 Gy. In addition, one single fraction of 8 Gy applied dose was given to the left lower ribs via a portal measuring 6 cm × 15 cm at 300 kV. His pain was relieved but 1 month later recurred in the lumbar spine. Repeat radiographs showed no significant change. Two further treatments each of 6.6 Gy were given to the previously treated lumbar field over a period of 8 days on the telecobalt unit.

By January 1987 the patient was well, back at full-time work and pain free. Clinically, there was no sign of recurrence in the left arm. Repeat radiographs showed healing fractures of the sixth and seventh ribs; the thoracic spine showed degenerative changes only and the lumbar spine showed scoliosis convex to the right with loss of definition of the pedicle and some collapse of the body of the first lumbar vertebra. In the pelvis, there was a sclerotic lesion projected over the left sacral ala (which had appeared since the radiograph of 2 September, 1986) and some increased sclerosis above the left acetabulum corresponding with an abnormal area of increased uptake on the radionuclide bone scan. There was an ill defined lucency in the proximal right femur below the intertrochanteric crest. The serum alkaline phosphatase level had returned to normal (81 i.u./litre).

In February 1988 he complained of intermittent lower thoracic and upper lumbar back pain present for the previous 2 months following trauma. On examination there was no sign of local or distant recurrence. There was tenderness over the lumbar spine particularly at the site of previous irradiation. Repeat radiographs of the lumbar spine showed no change compared with those of January 1987 and serum alkaline phosphatase remained within normal limits (54 i.u./litre). No further treatment was given and his symptoms completely resolved. A repeat radionuclide bone scan in June 1988 and again in September (Fig. 7) showed a photon-deficient area at the site of previous irradiation of the lumbar spine but no evidence of the previously demonstrated generalized areas of abnormal increased uptake. Serum alkaline phosphatase remains normal.

Discussion

Spontaneous regression of the primary lesion in malignant melanoma is not uncommon, the reported

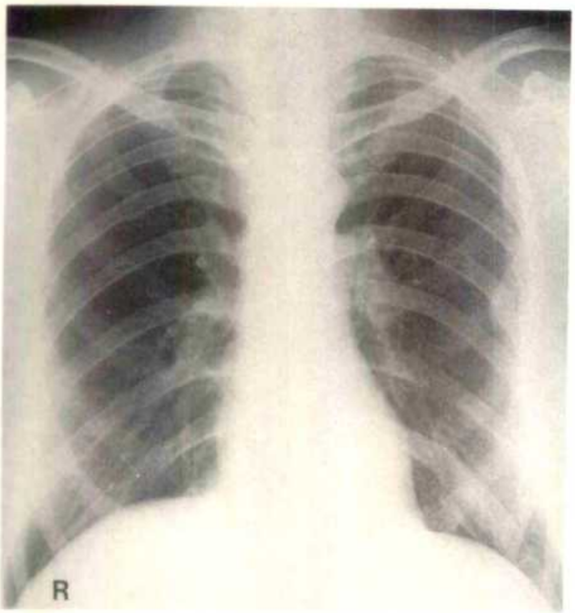

Figure 5. Antero-posterior radiograph of the chest showing fractures of left third, sixth and seventh ribs.

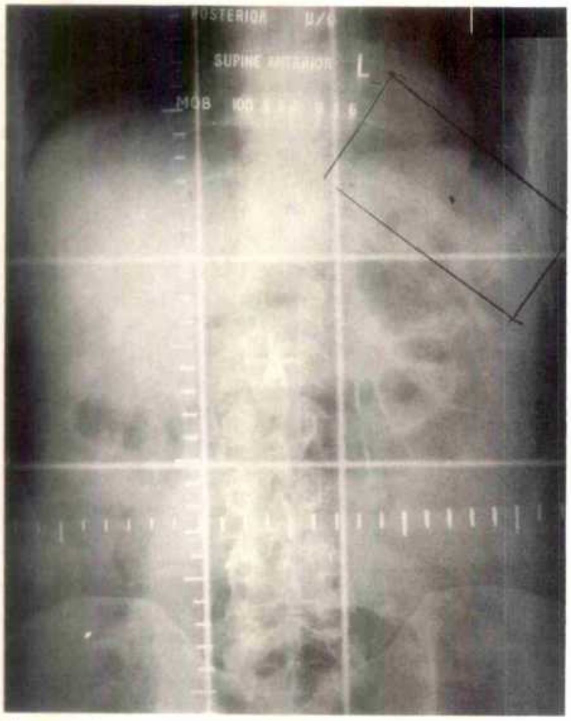

Figure 6. Antero-posterior radiography showing radiotherapy treatment portals to the lumbar spine (white rectangle) and left lower ribs (black rectangle).

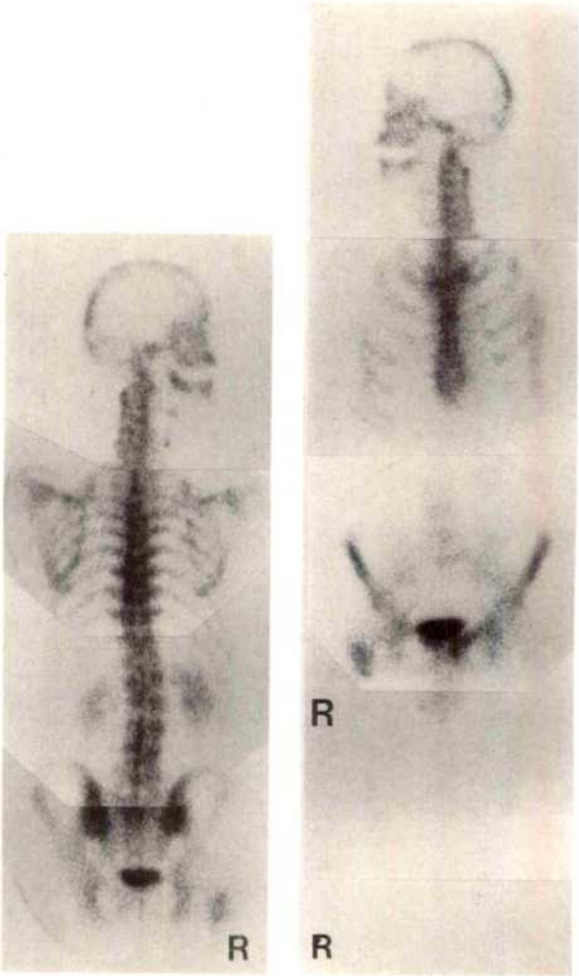

(a) (b)

Figure 7. Radionuclide bone scans (21 September 1988). (a) Postero-anterior and (b) antero-posterior scans showing a photon-deficient area in the lumbar spine at the site of previous irradiation but no evidence of widespread metastases.

incidence being from 3.7 to 8.7% (Das Gupta et al, 1963; Smith & Stehlin, 1965; Milton et al, 1977). Previous attention has also been drawn to the phenomenon of waxing and waning of multiple intransit metastases (Bodenham, 1968). However, spontaneous regression of metastatic melanoma is rare and less than 30 cases have been recorded in the literature since 1915 (Maurer et al, 1974; Bulkley et al, 1975; Bodurtha et al, 1976; Nathanson, 1976; Manelis et al, 1978; McCarthy et al, 1978; Rampen, 1979; Mikhail & Gorsulowsky, 1986). The incidence of spontaneous regression has been estimated by Bodurtha et al (1976) to be 0.3% from the literature and 0.4% from their own series. Although malignant melanoma represents less than 1% of all malignant neoplasms, it accounts for 11% of the reported cases of spontaneous regression (Everson & Cole, 1966) in which it is exceeded only by renal cell carcinoma (18%) and neuroblastoma (16%). Cutaneous metastases are the most common to show spontaneous regression followed in order by lymphatic, pulmonary, hepatic and cerebral metastases (Nathanson, 1976). However, spontaneous regression of bone metastases in malignant melanoma has not been previously reported.

A wide range of factors has been associated with spontaneous regression of metastatic melanoma including blood transfusion, anti-rabies inoculation, termination of pregnancy, abscess near tumour, consumption of garlic and administration of ^{131}I-labelled antibodies; regression has also been associated with diseases such as dermatomyositis and xeroderma pigmentosum (Nathanson, 1976). Spontaneous regression following irradiation to metastases other than those which regress has been described by Vogler et al (1958), Turner and Crawford (1961), Beswick and Quist (1963) and Kingsley (1975).

In the case described here, external-beam radiotherapy was administered to only two sites of metastatic disease, namely the left chest wall and lumbar spine. A radionuclide bone scan and radiographs, however, showed widespread dissemination bilaterally throughout the axial skeleton, skull vault and ribs. The appearance of these lesions was associated with a grossly elevated serum alkaline phosphatase level and although individual lesions were not subjected to biopsy, the diagnosis of disseminated osseous metastases from malignant melanoma seems in little doubt. Other possible causes of these scan appearances include: trauma with multiple fractures; demineralizing conditions leading to osteopenia and multiple fractures; hyperparathyroidism; multifocal osteomyelitis; bony abnormalities associated with high vascularity such as multiple haemangiomata (Maffucci's syndrome) and multiple bone metastases from another primary such as bronchus or prostate. However, these conditions are unlikely in view of the clinical findings together with normal lung fields on radiography and normal haematology and biochemistry (apart from elevated alkaline phosphatase). Furthermore, it is extremely unlikely that spontaneous regression of multiple deposits would have occurred as the result of radiotherapy to two localized involved sites. Indeed, in only four of the reported cases of spontaneous regression of visceral metastases had there been histological confirmation at the site of involvement (Bulkley et al, 1975; McCarthy et al, 1978; Rampen, 1979; Mikhail & Gorsulowsky, 1986).

This patient has apparently achieved spontaneous regression of his disease as shown by total resolution of symptoms and resumption of normal activities, return to normality of radionuclide bone scans (the photon-deficient area being consistent with previous radiotherapy), no evidence of active metastatic disease on radiographs and return to a normal level of serum alkaline phosphatase.

Immune mechanisms may play a role in the spontaneous regression of tumours and it is possible that destruction of tumour following radiotherapy stimulated an immune response in this patient. This could be the basis of the occasionally observed "abscopal effect" most commonly noted in lymphomas (Nobler, 1969). In this patient, tumour necrosis factor (TNF) (Carswell et al, 1975; Selby et al, 1987) was assayed using anti-TNF monoclonal antibodies but was not detected. Parvovirus titres were also measured (Siegel, 1983) but were within the normal range. Both of these assays were performed several months after the onset of the remission by which time levels, had they been elevated, may well have declined.

In conclusion, Everson and Cole (1966) warn that spontaneous remission is not synonymous with cure and in the series reviewed by Nathansan (1976) only 40% of patients with spontaneous regression of their metastases remained disease free for more than 5 years. This patient is well 2 years after remission but continued vigilance is clearly essential.

Acknowledgments

We are indebted to Professor Westbury for his encouragement and advice. We also thank Mr Paul Hyett of the Photographic Department for his skilled reproduction of the radiographs and scans and to Dr John Sloane, Consultant Pathologist, for the photomicrographs. We are also grateful to Mr John Southam, Senior Surgeon, Epsom District Hospital, who referred the patient and to Mrs Tina Haynes who kindly typed the manuscript.

References

BESWICK, I. P. & QUIST, G., 1963. Spontaneous regression of cancer. *British Medical Journal, ii*, 930.

BODENHAM, D. C., 1968. A study of 650 observed malignant melanomas in the South-West Region. *Annals of the Royal College of Surgeons, 43*, 218–239.

BODURTHA, A. J., BERKELHAMMER, J., KIM, Y. H., LAUCIUS, J. F. & MASTRANGELO, M. J., 1976. A clinical, histologic, and immunologic study of a case of metastatic melanoma undergoing spontaneous regression. *Cancer, 37*, 735–742.

BULKLEY, G. B., COHEN, M. H., BANKS, P. M., CHAR, D. H. & KETCHAM, A. S., 1975. Long-term spontaneous regression of malignant melanoma with visceral metastases. Report of a case with immunologic profile. *Cancer, 36*, 485–494.

CAPPELAERE, P., DEMAILLE, A. & ADENIS, L., 1973. L'exploration immunitaire des cancéreux. II. Immunité tumorale. *Lille Médical, 18*, 179–201.

CARSWELL, E. A., OLD, L. J., KASSEL, R. L., GREEN, S., FIORE, N. & WILLIAMSON, B., 1975. An endotoxin-induced serum factor that causes necrosis of tumours. *Proceedings of the National Academy of Science, 72*, 3666–3670.

DAS GUPTA, T., BOWDEN, L. & BERG, J. W., 1963. Malignant melanoma of unknown primary origin. *Surgery, Gynecology and Obstetrics, 117*, 341–345.

EVERSON, T. C. & COLE, W. H., 1966. *Spontaneous Regression of Cancer* (W. B. Saunders, Philadelphia).

FAUVET, J., CAMPAGNE, J., CHAVY, A. & PIET, G., 1960. Guérisons, régressions et rémissions spontanées des cancers. *La Revue du Practicien, 10*, 2349–2384.

FAUVET, J., ROUJEAU, J. & PIET, R., 1964. Les guérisons et régressions spontanées des cancers. *La Revue du Practicien, 14*, 2177–2180.

HARMER, C. L., 1976. The radiotherapy of melanoma. *Clinical and Experimental Dermatology, 1*, 29–36.

KINGSLEY, D. P. E., 1975. An interesting case of possible abscopal effect in malignant melanoma. *British Journal of Radiology, 48*, 863–866.

MANELIS, G., SHASHA, S. M., MANELIS, J., SUPRUN, H. &

1989, *The British Journal of Radiology*, *62*, 1100–1102

ROBINSON, E., 1978. Spontaneous regression of malignant melanoma. *Oncology*, *35*, 83–86.

MAURER, L. H., MCINTYRE, O. R. & RUECKERT, F., 1974. Spontaneous regression of malignant melanoma. Pathologic and immunologic study in a ten year survivor. *American Journal of Surgery*, *127*, 397–403.

MCCARTHY, W. H., SHAW, H. M. & MILTON, G. W., 1978. Spontaneous regression of metastatic malignant melanoma. *Clinical Oncology*, *4*, 203–207.

MIKHAIL, G. R. & GORSULOWSKY, D. C., 1986. Spontaneous regression of metastatic malignant melanoma. *Journal of Dermatological Surgical Oncology*, *12*, 497–500.

MILTON, G. W., SHAW, H. M. & MCCARTHY, W. H., 1977. Occult primary malignant melanoma: factors influencing survival. *British Journal of Surgery*, *64*, 805–808.

NATHANSON, L., 1976. Spontaneous regression of malignant melanoma: a review of the literature on incidence, clinical features and possible mechanisms. *National Cancer Institute Monograph*, *44*, 67–76.

NOBLER, M. P., 1969. The abscopal effect in malignant lymphoma and its relationship to lymphocyte circulation. *Radiology*, *93*, 410–412.

NOSSAL, G. J. V., 1976. Spontaneous regression of cancer: summary and profile for the future. *National Cancer Institute Monograph*, *44*, 145–148.

RAMPEN, F., 1979. Spontaneous regression of metastatic malignant melanoma. *Clinical Oncology*, *5*, 91–92.

SELBY, P., HOBBS, S., VINER, C., JACKSON, E., JONES, A., NEWELL, D., CALVERT, A. H., MCELWAIN, T., FEARON, K., HUMPHREYS, J. & SHIGA, T., 1987. Tumour necrosis factor in man: clinical and biological observations. *British Journal of Cancer*, *56*, 803–808.

SIEGL, G., 1983. Parvovirus infections and cancer. In *The Parvoviruses*, ed. by K. I. Berns (Plenum Press, New York), pp. 344–345.

SMITH, J. L. & STEHLIN, J. S., 1965. Spontaneous regression of primary malignant melanomas with regional metastases. *Cancer*, *18*, 1399–1415.

TURNER, F. P. & CRAWFORD, A. M., 1961. Malignant melanoma with brain metastasis case report with seven-year survival. *Journal of the Maine Medical Association*, *52*, 204–206.

VOGLER, W. R., PERDUE, G. D. & WILKINS, S. A., 1958. A clinical evaluation of malignant melanoma. *Surgery, Gynecology and Obstetrics*, *106*, 586–594.

Spontaneous pneumothorax with metastatic seminoma

By *A. J. Chippindale, BSc, MRCP, FRCR, B. Patel, MB, BCh, FRCR and B. Eddleston, FRCR

Department of Diagnostic Radiology, Christie Hospital and Holt Radium Institute, Wilmslow Road, Manchester

(*Received April 1989*)

Spontaneous pneumothorax is an uncommon manifestation of malignant neoplasm affecting the lung, and is seen mainly in cases of primary lung carcinoma and metastatic sarcoma, (Dines et al, 1973; Wright, 1976). We describe a patient who developed spontaneous, bilateral pneumothoraces whilst undergoing intensive chemotherapy for metastatic seminoma of the testis.

Case report

An 18-year-old male patient with widespread metastatic disease from seminoma testis was admitted for his third course of chemotherapy. He had presented to his general practitioner 3 months previously with episodes of haemoptysis, and was found to have Stage 4 testicular tumour. Orchidectomy revealed seminoma of the testis with large areas of necrosis. The chest radiograph (Fig. 1) demonstrated multiple pulmonary metastases. Further investigation showed intraocular metastases on the right and right-sided hydronephrosis due to pelvic lymphadenopathy.

On the day of his chemotherapy, a chest radiograph (Fig. 2) revealed a spontaneous right-sided pneumothorax. This was treated conservatively. In the following week, persistent gastointestinal haemorrhage necessitated venous cut-down for

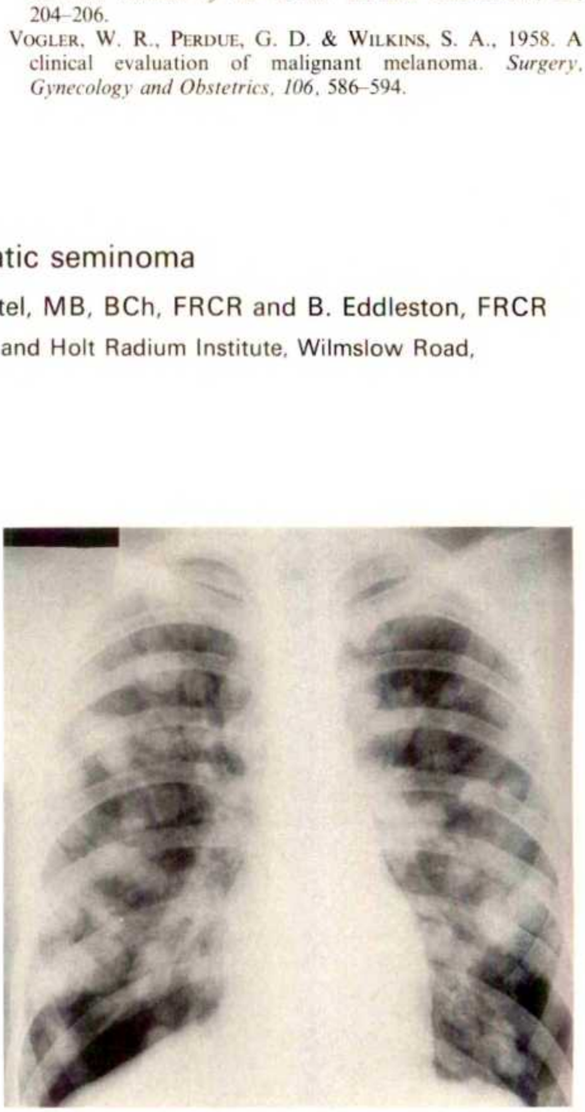

Figure 1. Chest radiograph at presentation shows multiple, bilateral pulmonary metastases.

---

*Author for correspondence.

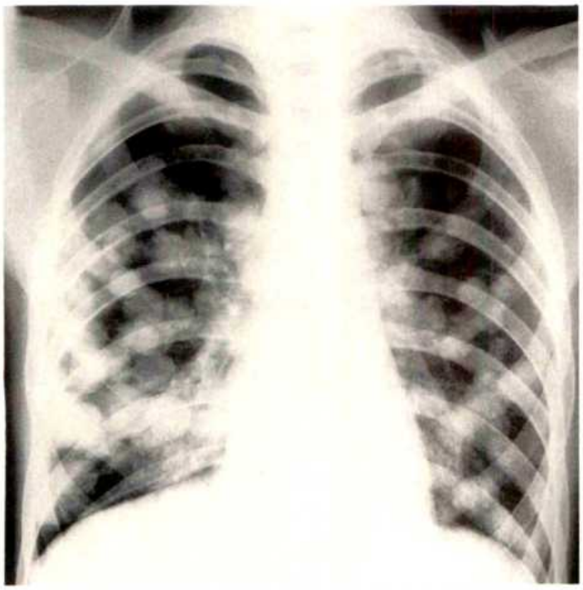

Figure 2. The patient has developed a pneumothorax on the right, which was treated conservatively.

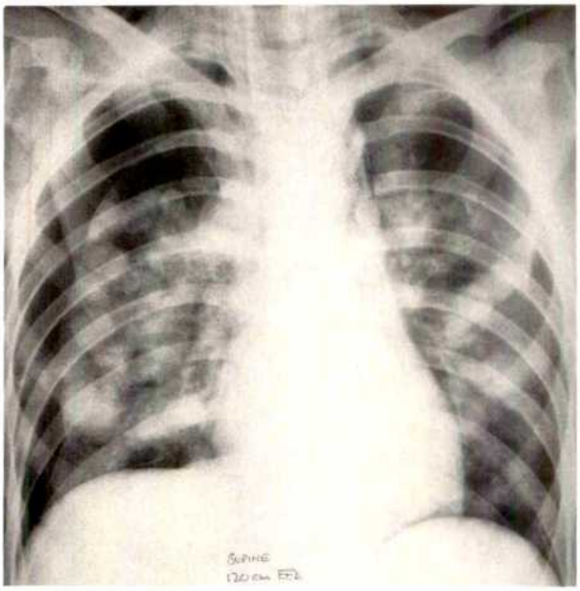

Figure 3. The patient had deteriorated clinically and became septicaemic. He has developed bilateral pneumothoraces.

blood transfusion. The patient later developed a spontaneous left pneumothorax (Fig. 3). He died after an episode of Gram-negative septicaemia.

Discussion

Spontaneous pneumothorax most commonly occurs in men in the third and fourth decades, and is thought to be secondary to rupture of a small subpleural air cyst or bulla. Spontaneous pneumothorax was a not uncommon presenting feature of pulmonary tuberculosis, and may complicate a number of lung diseases in which there is "honeycombing", such as tuberose sclerosis and histiocytosis X (Wright, 1976). Chronic bronchitis, emphysema, asthma and pneumoconiosis account for a proportion of cases, with occasional cases related to endometriosis.

Spontaneous pneumothorax is an uncommon manifestation of malignant neoplasm affecting the lung. In a review of 1143 patients with spontaneous pneumothorax (Dines et al, 1973), 10 cases were attributed to malignant pulmonary neoplasms. Four of these were related to primary lung carcinoma, with one case of lymphosarcoma and five of metastatic sarcoma. In two cases, pneumothorax preceded radiologically detected metastases. In spite of the fact that carcinomas account for the majority of lung metastases, spontaneous pneumothorax is reported more commonly in metastatic sarcoma (Brufman et al, 1977). Spontaneous pneumothorax is also described with other metastatic lung tumours, including Wilm's tumour (D'Angio & Iannaccone, 1961; Kassner et al, 1976; Siegel & McAlister, 1980), malignant melanoma (Yeung & Bonnet, 1977), carcinoma of the pancreas, kidney or adrenal (Wright, 1976), and one case of seminoma (Salzman et al, 1953).

The mechanism for the development of spontaneous pneumothorax with metastatic disease is incompletely understood. Necrosis of metastatic deposits may lead to the development of a malignant bronchopleural fistula (Shaw, 1951). As necrosis is a common feature of rapidly growing sarcoma metastases, this may account for the prevalence of reported cases of spontaneous pneumothorax in these patients. Tumour deposits may produce a check valve obstruction of an airway, leading to distension of distal lung tissue (Lodmell & Capps, 1949). Dissection of trapped air along interlobular septa to form subpleural bullae may lead to subsequent pneumothorax. D'Angio and Iannaccone (1961) observed such subpleural air trapping at autopsy in one child with metastatic osteosarcoma, although he had not developed pneumothorax.

The radiological diagnosis of spontaneous pneumothorax in patients with malignant disease presents no difficulty. Whilst pneumothorax is most commonly seen with primary lung carcinoma and metastatic sarcoma, other tumours including seminoma may give rise to this complication.

Acknowledgments

We would like to thank Mr Seamus Griffin for preparing the illustrations.

References

BRUFMAN, G., KRASNOKUKI, D., SCHWARTZ, A. & BIRAN, S., 1977. Spontaneous pneumothorax complicating lung metastases from carcinoma of the breast. *Radiologia Clinica (Basel)*, *46*, 38–41.

D'ANGIO, G. J. & IANNACCONE, G., 1961. Spontaneous pneumothorax as a complication of pulmonary metastases in malignant tumours of childhood. *American Journal of Roentgenology, 86,* 1092–1102.

DINES, D. E., CORTESE, D. A., BRENNAN, M. D., HAHN, R. G. & PAYNE, W. S., 1973. Malignant pulmonary neoplasms predisposing to spontaneous pneumothorax. *Mayo Clinic Proceedings, 48,* 541–544.

KASSNER, E. G., GOLDMAN, H. S. & ELGUEZABAL, A., 1976. Cavitating lung nodules and pneumothorax in children with metastatic Wilm's tumour. *American Journal of Roentgenology, 126,* 728–733.

LODMELL, E. A. & CAPPS, S. C., 1949. Spontaneous pneumothorax associated with metastatic sarcoma. *Radiology, 52,* 88–93.

SALZMAN, S., REID, J. H. & OGURA, G. I., 1953. Cavernous metastatic pulmonary carcinoma: a report of two cases. *Diseases of the Chest, 23,* 678–685.

SHAW, A. B., 1951. Spontaneous pneumothorax from secondary sarcoma of the lung. *British Medical Journal, i,* 278–280.

SIEGEL, M. J. & MCALISTER, W. H., 1980. Unusual intrathoracic complications in Wilm's tumour. *American Journal of Roentgenology, 134,* 1231–1234.

WRIGHT, F. W., 1976. Spontaneous pneumothorax and pulmonary metastatic disease—a syndrome sometimes associated with cavitating tumours. *Clinical Radiology, 27,* 211–222.

YEUNG, K. Y. & BONNETT, J. D., 1977. Spontaneous pneumothorax with metastatic malignant melanoma. *Chest, 71,* 435–436.

1989, *The British Journal of Radiology*, *62*, 1103–1104

Case of the month

A painful knee

By A. M. Davies, DMRD, FRCR and N. Evans, FRCR
Department of Radiology, Royal Orthopaedic Hospital, Birmingham

(*Received June 1988*)

A 37-year-old Asian woman presented with a 10-month history of periodic pain in the lateral aspect of the right knee becoming more severe over the past 2 weeks. Plain radiography revealed an expansile, lytic lesion in the head of the fibula, which had a well defined margin with a small cortical infraction posteriorly (Fig. 1). A bone scan showed a solitary, uniform focus of increased activity corresponding to the abnormality on the radiographs. Computed tomography (CT) demonstrated the expansile nature of the lesion (Fig. 2). All routine laboratory investigations were normal.

What is the differential diagnosis and what is the most likely diagnosis in this patient?

Address correspondence to: Dr A. M. Davies, Department of Radiology, Royal Orthopaedic Hospital, Woodlands, Northfield, Birmingham B31 2AP.

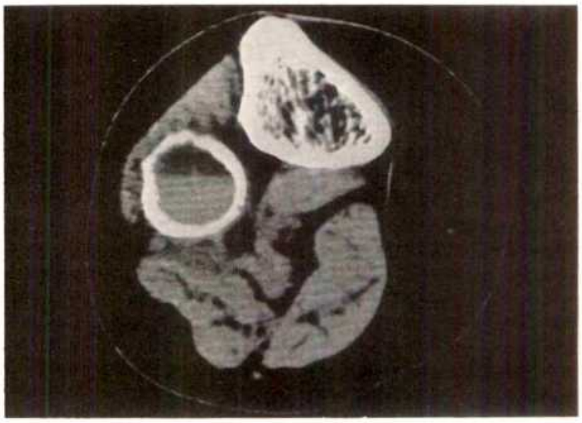

Figure 2. Axial CT scan through the proximal tibia and fibula.

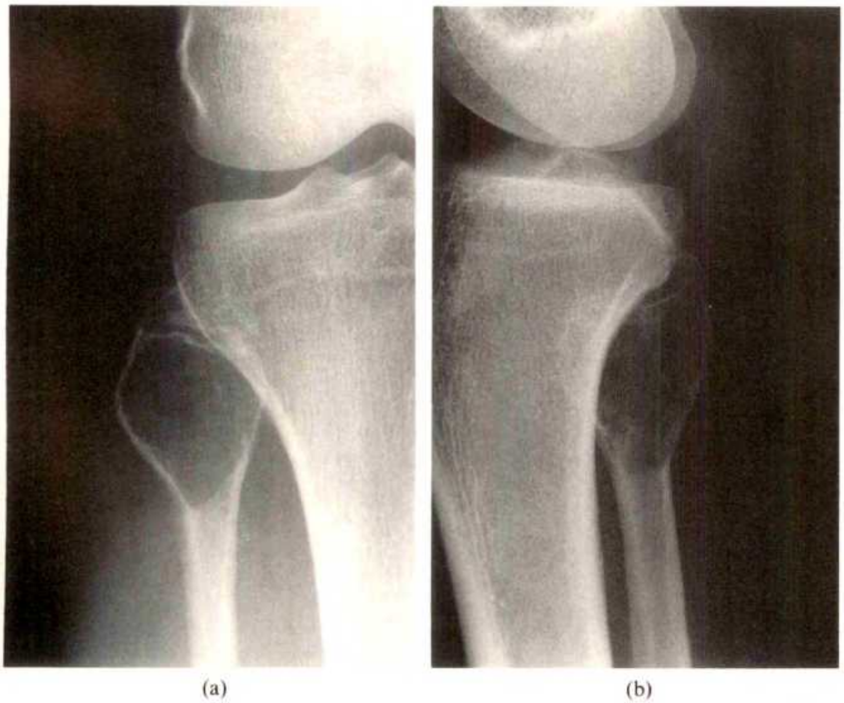

(a) (b)

Figure 1. (a) Antero-posterior and (b) lateral radiographs of the head of the fibula.

The differential diagnosis of an expansile, lytic lesion in the head of the fibula includes a giant cell tumour, aneurysmal bone cyst, simple bone cyst, enchondroma and a brown tumour.

The patient is rather old to present with a simple bone cyst and little activity would be expected on the bone scan, although a small cortical infraction was present. The absence of calcification within the matrix of the tumour makes an enchondroma less likely and, although the ethnic origin of the patient should alert one to the possibility of metabolic bone disease, the normal laboratory investigations and bone density exclude a brown tumour.

It is impossible in this case to distinguish on the plain radiographs between a giant cell tumour and an aneurysmal bone cyst. Computed tomography, however, reveals a fluid level within the tumour, which is a diagnostic feature of an aneurysmal bone cyst (ABC), and was subsequently confirmed histologically in this case.

Discussion

An ABC is a benign, non-neoplastic condition of bone consisting pathologically of varying amounts of vascular and fibrous tissue surrounding cavities containing a mixture of blood and serous fluid. Fluid levels have been described as a characteristic CT feature of an ABC (Hudson, 1984; Hertzanu et al, 1984) and are presumed to represent sedimentation of blood within the cystic cavities. The fluid levels may be single in unilocular lesions, as in this case, or multiple in multilocular lesions, as illustrated in a different patient in Fig. 3. To demonstrate the fluid level the examination must be performed in a plane perpendicular to the fluid level and the patient should remain motionless for at least 10 min prior to scanning to allow the contents of the cavity to settle (Hudson, 1984). Similar appearances have been described in ABCs imaged with magnetic resonance (Hudson et al, 1985; Beltran et al, 1986).

Although typical of an ABC, the presence on CT of a fluid level within a bone lesion should not be considered pathognomonic as it has also been described in a telangiectatic osteosarcoma (Hudson, 1984), a malignant tumour that also has a large vascular element, but does not have a well defined margin.

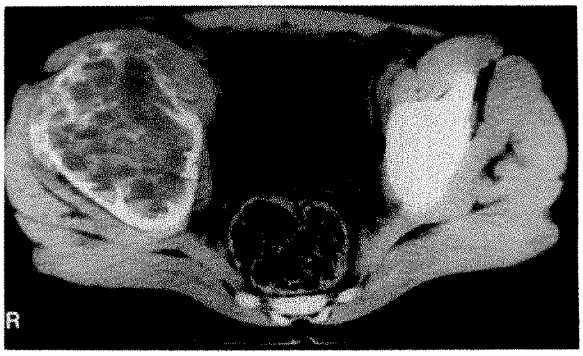

Figure 3. Large multilocular lesions in the right iliac bone of a 10-year-old boy showing multiple, small fluid levels within the individual loculi.

The precise aetiology of an ABC is unknown but it is now accepted that a significant proportion of cases, probably in excess of one-third, arise in pre-existing bone lesions. These include fibrous dysplasia (Diercks et al, 1986), giant cell tumour, non-ossifying fibroma, chondroblastoma and osteosarcoma. It is therefore important to appreciate that the identification of a fluid level on CT may be due to a secondary ABC (Diercks et al, 1986), although the underlying primary lesion may not be visible radiographically.

References

Beltran, J., Simon, D. C., Levy, M., Herman, L., Weis, L. & Mueller, C. F., 1986. Aneurysmal bone cysts: magnetic resonance imaging at 1.5T. *Radiology, 158,* 689–690.

Diercks, R. L., Sauter, A. J. M. & Mallens, W. M. C., 1986. Aneurysmal bone cyst in association with fibrous dysplasia. *Journal of Bone & Joint Surgery, 68B,* 144–146.

Hertzanu, Y., Mendelsohn, D. B. & Gottschalk, F., 1984. Aneurysmal bone cyst of the calcaneus. *Radiology, 151,* 51–52.

Hudson, T. M., 1984. Fluid levels in aneurysmal bone cysts: a CT feature. *American Journal of Roentgenology, 142,* 1001–1004.

Hudson, T. M., Hamlin, D. J. & Fitzsimmons, J. R., 1985. Magnetic resonance imaging of fluid levels in an aneurysmal bone cyst and in anticoagulated human blood. *Skeletal Radiology, 13,* 267–270.

1989, *The British Journal of Radiology*, 62, 1105–1106

Short communication

A radiological feature to assist in the diagnosis of intestinal obstruction

By Jenny Walker, ChM, FRCS and *Helen Carty, FRCPI, FRCR

Departments of Surgery and *Radiology, Alder Hey Children's Hospital, Liverpool L12 2AP

(*Received June 1989*)

Management of intestinal obstruction in neonates and infants is improved if accurate diagnosis of the site and cause of obstruction can be made pre-operatively. Contrast studies can be helpful in this context, especially when performed by a radiologist experienced in paediatric surgical conditions. We present two cases where an unusual radiological feature helped to identify the site and cause of intestinal obstruction.

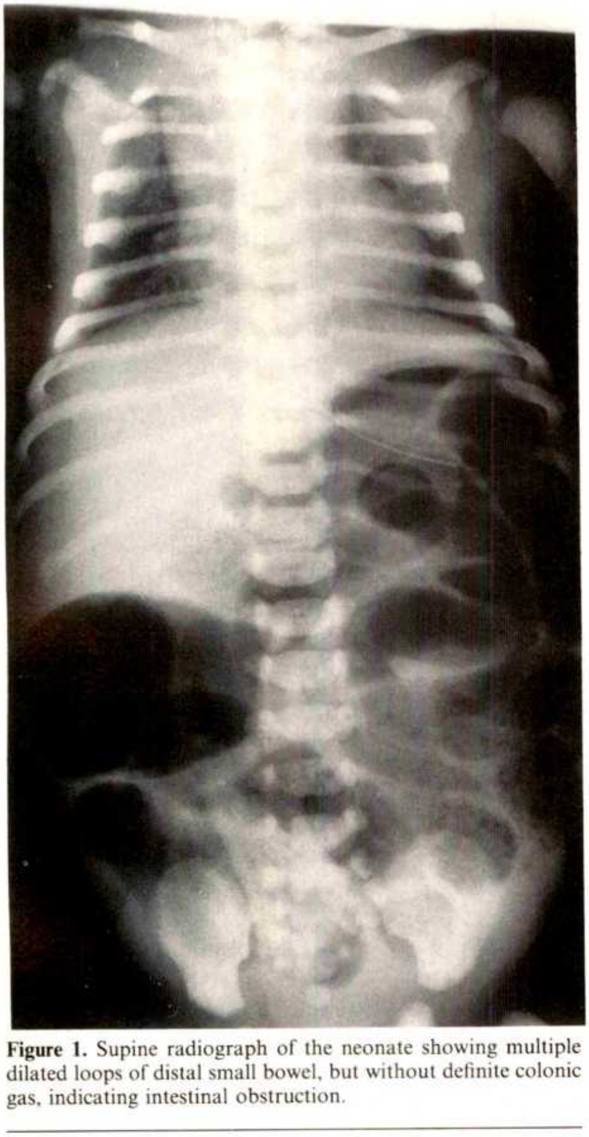

Figure 1. Supine radiograph of the neonate showing multiple dilated loops of distal small bowel, but without definite colonic gas, indicating intestinal obstruction.

Case 1

A male neonate presented to the Neonatal Surgical Unit at Alder Hey Children's Hospital on the first day of life. He had been born by normal delivery, weighing 3.9 kg. There had been

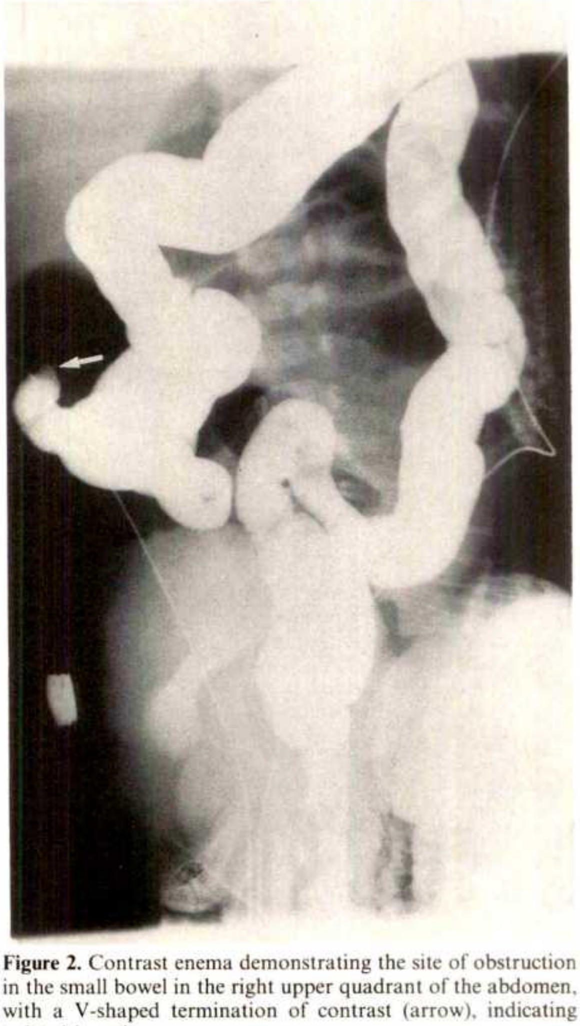

Figure 2. Contrast enema demonstrating the site of obstruction in the small bowel in the right upper quadrant of the abdomen, with a V-shaped termination of contrast (arrow), indicating twisted bowel.

Address correspondence to: Miss Jenny Walker, Senior Registrar in Paediatric Surgery, Alder Hey Children's Hospital, Liverpool L12 2AP.

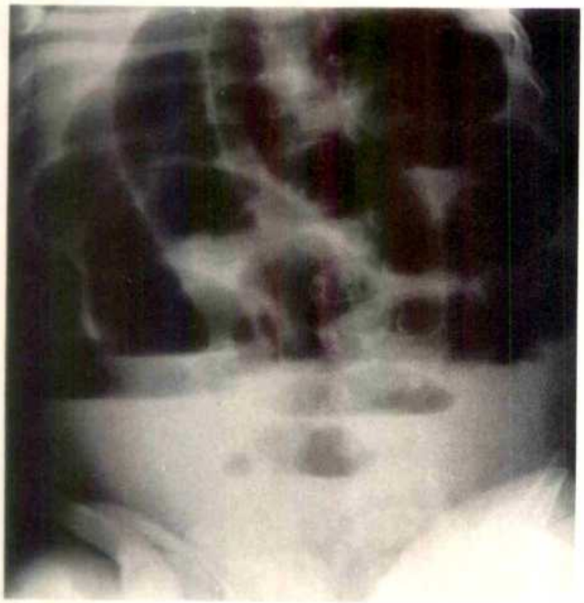

Figure 3. Erect abdominal radiograph demonstrating small bowel obstruction.

no antenatal problems, he was well at birth and he had one normal sibling. At 18 h of age he developed abdominal distension, bilious vomiting and had not passed meconium. A plain abdominal radiograph demonstrated intestinal obstruction, and Hirschsprung's disease or meconium ileus was considered (Fig. 1). A contrast enema was performed, and contrast medium quickly refluxed through a normal colon into the distal ileum, where the site of obstruction was demonstrated (Fig. 2). The contrast terminated with a "pointed" end resembling an inverted V, and this was interpreted as originating from a volvulus of the small bowel. At laparotomy, the obstruction was found to be due to an adhesion between a portion of ileum 20 cm from the caecum and the edge of the liver, there being a localized volvulus around the adhesion.

Case 2

An 8-week-old baby boy presented to his local hospital with a short history of diarrhoea and vomiting. Despite intravenous fluids and nothing by mouth over the next 24 h, the nasogastric aspirates and abdominal distension increased. A plain radiograph demonstrated intestinal obstruction (Fig. 3), and he was transferred to Alder Hey Children's Hospital for further management. The referring paediatric registrar observed that the patient had bilateral hydrocoeles, but that no herniae had been detected.

A contrast enema was performed, which demonstrated a normal colon and obstructed small bowel in the region of the right groin. The contrast stopped in an inverted V shape, and the diagnosis of a hernia reduction *en masse* was made, the constricting band of hernial sac resulting in the radiological feature (Fig. 4). This was confirmed at laparotomy when the bowel was released and the hernia repaired.

Discussion

Contrast enemas can be very useful in neonates and infants in identifying the site and possible cause of intestinal obstruction, even when the site of obstruction is in the small bowel. Contrast medium refluxes easily into the terminal ileum in these small patients, and a low small-bowel obstruction may be identifed. Modern non-ionic contrast medium is not dangerous as it has a low osmotic effect, nor is it hazardous if a perforation is discovered and contrast medium leaks into the peritoneal cavity.

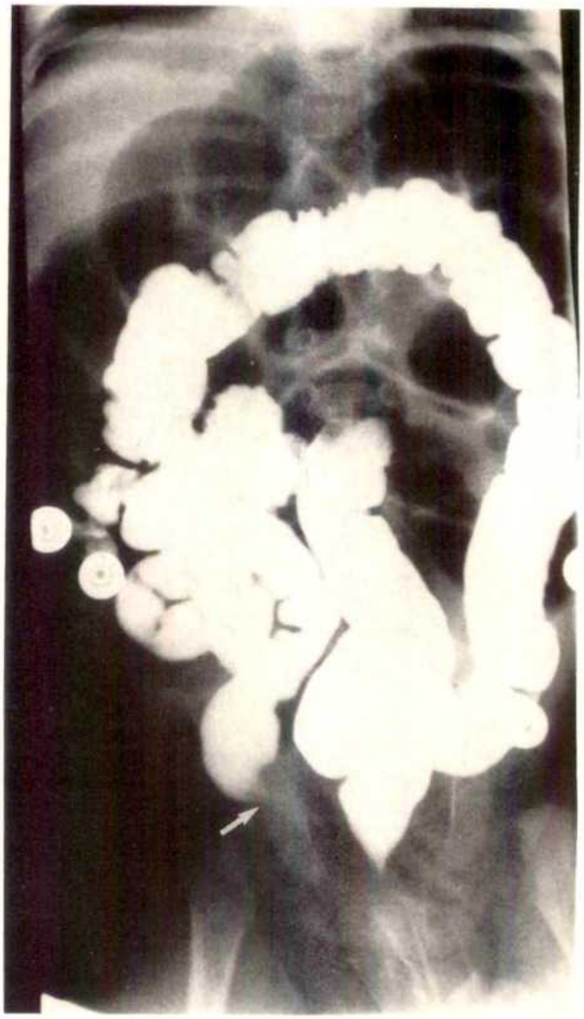

Figure 4. Contrast enema demonstrating the site of obstruction in the small bowel in the region of the right groin, with a V-shaped termination of contrast (arrow), indicating twisted bowel.

We have demonstrated two cases where the radiological feature of the inverted V sign was recognized at the site of obstruction, suggesting the cause as local twisting of normal bowel (unlike an atresia or an intussusception, or when impacted bowel contents are reached). Case 2 highlights again the dangers of an en-masse reduction of inguinal hernias.

Acknowledgments

We would like to thank Mr R. E. Cudmore for permission to report these two patients who were under his care.

1989, *The British Journal of Radiology*, *62*, 1107

Correspondence

(The Editors do not hold themselves responsible for opinions expressed by correspondents)

A localized hypersensitivity reaction to co-trimoxazole in a previously irradiated field simulating a recall phenomenon

THE EDITOR—SIR,

Recall of latent radiation reactions following subsequent administration of cytotoxic agents is a well recognized phenomenon mainly reported with actinomycin-D and adriamycin (D'Angio et al, 1959; Donaldson et al, 1974; Burdon et al, 1978). To our knowledge, similar reactions with non-cytotoxic antibiotics have not been reported. We present a case of a delayed localized hypersensitivity reaction to co-trimoxazole similar in nature to a recall phenomenon, 3 years following radiotherapy.

Case report

A 54-year-old woman was referred for radiotherapy in October 1986 after modified radical mastectomy and axillary dissection for an infiltrative ductal carcinoma of the left breast. A total dose of 5500 cGy in 28 fractions over 38 days was delivered to the chest wall using a cobalt-60 teletherapy unit through tangential fields. The regional lymphatics were irradiated through anterior internal mammary, supraclavicular and posterior axillary fields to a total dose of 5000 cGy in 25 fractions over 35 days, using the same unit. The patient did well in her follow-up until 8 February, 1989, when she presented with a localized maculopapular rash accompanied by itching, involving the irradiated chest wall, internal mammary region and the left arm (Fig. 1). It was ascertained from her history that she was on antibiotic therapy with co-trimoxazole (Bactrim forte, Roche, trimethoprim 160 mg + sulphamethoxazole 800 mg) for the last 2 days for an upper respiratory tract infection. The drug was discontinued immediately and she responded well to an oral antihistamine therapy. The reaction gradually subsided and completely disappeared within 5 days.

Comment

Sulfonamides are known to cause generalized hypersensitivity reactions in the form of maculopapular rashes (Schulz, 1983). Localized eruptions are also defined, mainly in male genitalia and mucosal surfaces (Talbot, 1980). However, skin eruptions confined to previously irradiated areas, similar to a recall phenomenon, have not previously been described as far as we know. The recall phenomenon was first described by D'Angio in 1959 with actinomycin-D, similar reactions were reported later with adriamycin administration (Donaldson et al, 1974; Burdon et al, 1978). Despite the wide usage of combined chemotherapy and radiotherapy, no such reactions are reported with cytotoxic agents other than antitumour

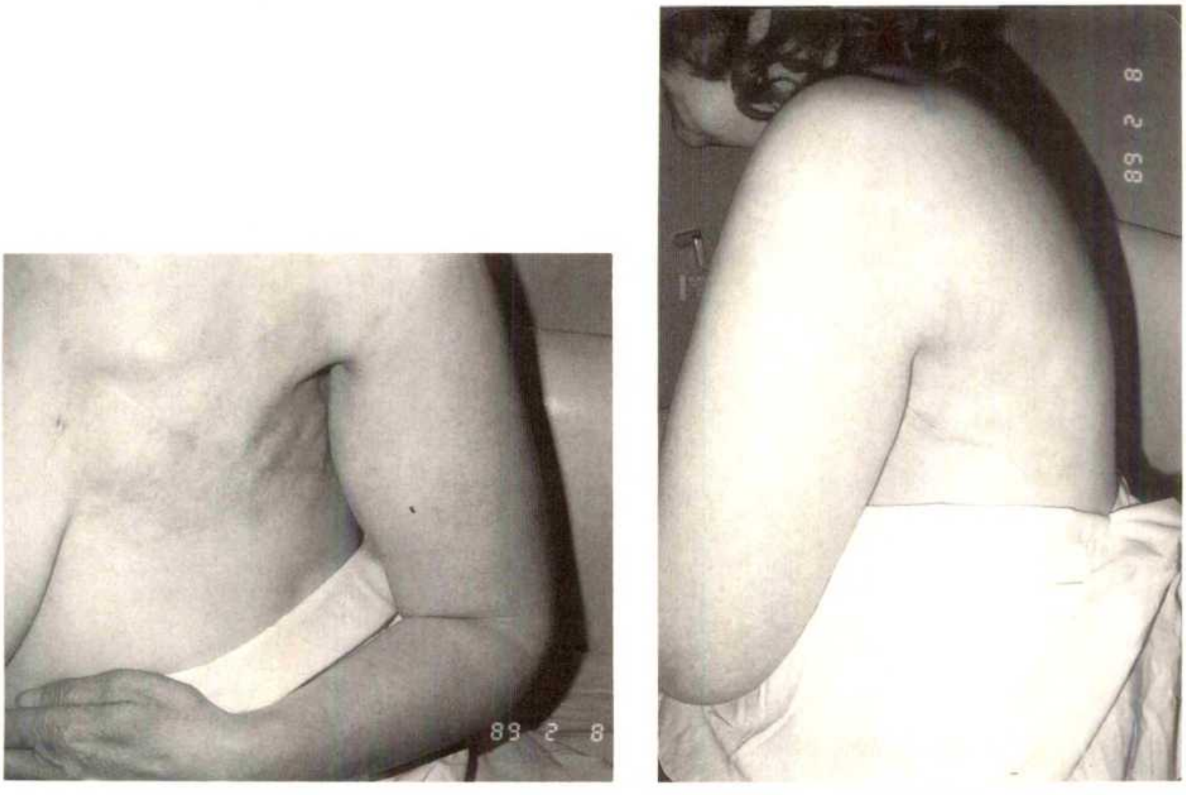

Figure 1. Localized maculopapular rash involving the chest wall, internal mammary region and left arm of the patient.

antibiotics. It is rather difficult to explain this observation on the basis of the mild folic acid antagonistic effect of co-trimoxazole causing a recall phenomenon, since this has not been described with methotrexate, which is a much stronger folic acid antagonist. It may be of interest to add that the reaction in our patient involved mainly the post-operatively irradiated chest wall and the left arm, which was not irradiated. This may be explained by the possible higher concentration of trimethoprim and sulphamethoxazole in the extracellular fluid in these two regions as a result of the additive effect of lymphatic stasis induced by surgical intervention.

Yours, etc.,

I. Lale Atahan
Fadil H. Akyol
Murat Gürkaynak
Hilmi F. Alanyali
Enis Özyar

Department of Radiology,
Division of Radiotherapy,
Hacettepe University Hospital,
Ankara 06100,
Turkey

(*Received May 1989*)

References

Burdon J., Bell, R., Sullivan, J. & Henderson, M., 1978. Adriamycin-induced recall phenomenon 15 years after radiotherapy. *Journal of the American Medical Association, 10*, 931.

D'Angio, G. J., Farber, S. & Maddock, C. L., 1959. Potentiation of X-ray effects by actinomycin-D. *Radiology, 73*, 175–177.

Donaldson, S. S., Glick, J. M. & Wilbur, J. R., 1974. Adriamycin activating a recall phenomenon after radiation therapy. *Annals of Internal Medicine, 3*, 407–408.

Schulz, K. H., 1983. Cutaneous manifestations of drug allergy. In *Allergic Reactions to Drugs*, ed. by A. L. de Weck & H. Bundgaard (Springer-Verlag, Berlin), pp. 139–140.

Talbot, M. D., 1980. Fixed genital drug eruption. *The Practitioner 224*, 823–824.

Kinetics of recovery from sublethal radiation damage

The Editor—Sir,

In an article published recently, Drs Hopewell and van den Aardweg (1988) re-analyse data on the kinetics of recovery from sublethal radiation damage (SLD). They question whether SLD repair follows mono-exponential kinetics and present a number of graphs that show fast repair in the beginning followed by slower repair. We have also noted that repair kinetics in human skin could be interpreted on the basis of two components (Turesson & Thames, 1989). In the latter study, however, direct analysis (Thames et al, 1986) was used and this differs from the method employed by Hopewell and van den Aardweg, which involved studying changes in the "percentage dose unrepaired." We wish to point out certain aspects of this analysis that must be considered when applying it.

First, data fitted with the "incomplete repair (IR) model" (Thames, 1985) give slightly bent curves if plotted as "percentage dose unrepaired" with increasing number of fractions n: $n=2$ results in a straight line, while $n=9$ shows moderate curvature (Fig. 1a and c, unlabelled curves). This is a small deviation from linearity, however, and would not explain the curvature found by Hopewell and van den Aardweg.

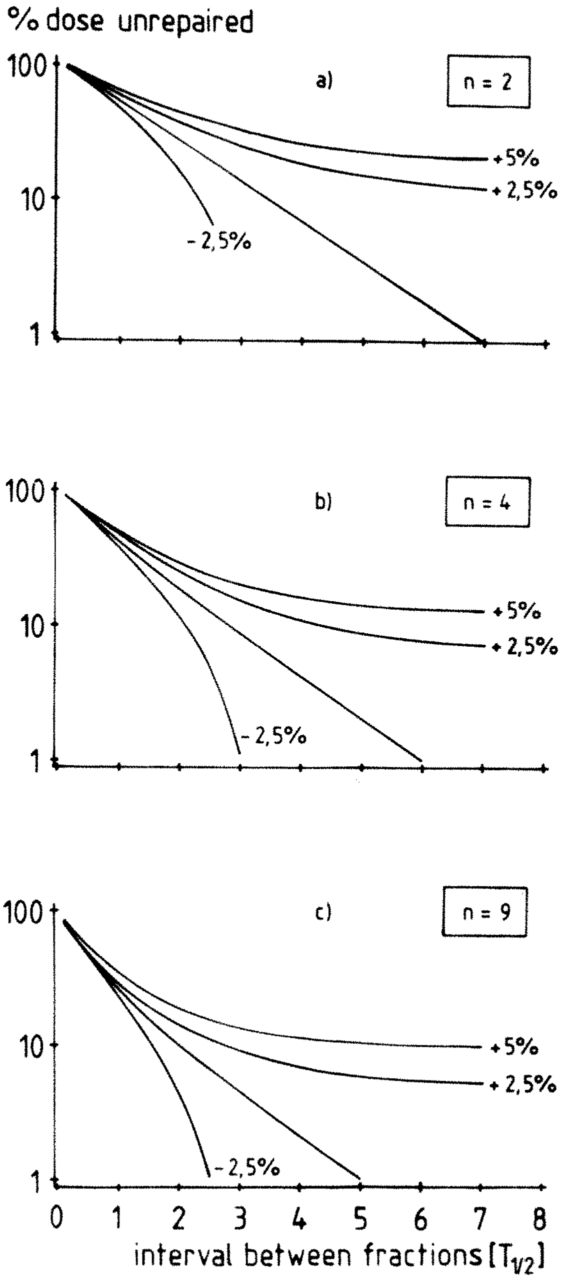

Figure 1. (a–c), "Percentage dose unrepaired" as used by Drs Hopewell and van den Aardweg plotted against the interval between fractions (in multiples of $T_{1/2}$). Hypothetical curves were calculated on the basis of the IR model (Thames, 1985). The parameters used are consistent with the pig skin data of Dr van den Aardweg with an α/β value of 10 Gy. Subsets a to c show the curves that result for the number of fractions n given in the panels. All isoeffect doses are calculated from the model, except the isoeffect dose for complete repair whose deviation from the expected value is indicated on the curves. The unlabelled curves are computed directly from the monoexponential IR model, and show that repair plots for percentage unrepaired dose are curved when the number of fractions is higher than two.

Secondly, isoeffect doses should be considered as estimates with confidence intervals. While isoeffect doses for shorter intervals are likely to be known with fair precision, the "complete repair" dose (D_∞) must be more or less guessed. It can be estimated from the isoeffect doses for the longest intervals, but in this case it could be intermediate among these, greater than some and less than others; intervals where D_∞ is less than the measured isoeffect dose must be omitted from the analysis since percentage unrepaired dose is plotted in logarithmic co-ordinates. On the other hand, D_∞ may be chosen larger than the measured isoeffect doses, and in this case no doses will be omitted from the analysis, but the curvature of the "repair plot" is increasing with increasing D_∞. This is illustrated in Fig. 1, which shows what happens if the isoeffect doses for incomplete repair (including the single doses) are determined correctly whereas the isoeffect dose for complete repair (D_∞) is up to 5% off the true value. Concave-up curves result if the repair capacity is overestimated, while concave-down curves indicate underestimates. Hopewell and van den Aardweg used as D_∞ the isoeffect doses at 24 h intervals (Hopewell, personal communication, 1989), and this happened to have been higher than isoeffect doses for shorter intervals. It is a matter for conjecture how well D_∞ was approximated by the isoeffect dose for 24-h intervals.

Why were only concave-up curves found by the authors? This could be because repair kinetics are truly biphasic, with the second phase being the slower one; it is interesting that there were no exceptions to the concave-up rule (see Thames et al, 1989, for an exception). However, this could also be because of overestimation of D_∞ (even by 5%), and its effect on the repair plots (Fig. 1).

Thirdly, it can be shown by Monte Carlo simulation that the points calculated for the percentage unrepaired-dose plot from isoeffect doses cannot be expected to be on a straight line. Assuming that the underlying isoeffect doses are normally distributed with a standard deviation of 5% around theoretical values that fit the IR model (half-time 1.25 h), not one out of 20 simulations gave a straight line. The intervals used were taken from the pig skin experiments of Dr van den Aardweg (Fig. 3 of Hopewell & van den Aardweg, 1988).

A final point concerns the use of doses and dose ratios in the analysis, as opposed to analyses based on the effect scale. The use of dose ratios such as percentage unrepaired dose, F_R and F_{rec} is plagued by dependence on the level of target-cell killing at isoeffect (Thames, 1984). This means that comparisons between tissues on the basis of such measures are invalid. Although this was not the objective of Drs Hopewell and van den Aardweg, it must be kept in mind when comparing repair kinetics in tissues, like lung and spinal cord, where the single doses for isoeffect are very different.

In conclusion, the use of percentage unrepaired dose in the analysis of repair kinetics in tissues should be discouraged. However, there is a trend in the presented data to suggest that repair kinetics slows down with longer intervals in some tissues.

Yours, etc.,

R. GUTTENBERGER
*H. D. THAMES

Gesellschaft für Strahlen und Umweltforschung,
GmbH München,
Institut für Strahlenbiologie,
8042 Neuherberg,
Federal Republic of Germany and
*Department of Biomathematics,
MD Anderson Cancer Center,
Houston, Texas 77030,
USA

(*Received July 1989*)

(Authors' reply)

THE EDITOR—SIR

We acknowledge with interest the letter from Drs Guttenberger and Thames commenting on our re-analysis of data on the kinetics of repair of sublethal radiation damage (Hopewell & van den Aardweg, 1988). We welcome this opportunity to respond since the topic has important implications for clinical radiotherapy. Reference to this very recently submitted letter was made in two previous publications by one of the authors (Thames, 1989; Thames et al, 1989).

Before discussing the important points raised by their letter, it is first essential to correct an unjustified assertion made in the above-mentioned publications (Thames, 1989; Thames et al, 1989), namely that any analyses based on plots of the percentage unrepaired dose are hampered by the selective exclusion of data points, specifically those with the longer interfraction intervals, and that this biases the results. In the studies carried out on pig skin, no data points were excluded or repeated to obtain a favourable result. It is our understanding that this was equally true for the crude data from the studies on the spinal cord of the rat, which were quoted by Ang et al (1987). It should be obvious that any analysis based on the use of selected data is strictly invalid.

Drs Guttenberger and Thames are perfectly correct to point out that the shape of the curve of the percentage unrepaired dose against interfraction interval will be influenced to some extent by the precision of the isoeffect dose for "complete repair" (D_∞), which was taken as the D_{24} in the analysis in question. The same is equally true of the isoeffect dose for "no-repair" (zero time interval), or the single dose in this particular instance. This has been found to be highly reproducible for the end-point of moist desquamation in pig skin (Hopewell & van den Aardweg, 1988). The finding that only concave curves were obtained from the data that was re-analysed was one reason for deducing that repair kinetics were possibly biphasic. However, in addition it was noted that the initial slope of the curves was much steeper than would have been predicted by an equation simply representing a monoexponential plus a constant term. This would have been the case only if the absolute amount of dose repaired had been overestimated.

It was our hope in re-analysing the data in the way that we did that we would encourage other investigators to reconsider their own findings. Of general concern is that biological data are frequently evaluated unthinkingly by specific models; indeed inadequate biological data are often "dressed up" by using such mathematical methods. Mathematical models should never be used as a substitute for poor biology: there is *no* substitute for a carefully devised and well conducted experiment. Specifically, valid information on the kinetics of repair of sublethal damage cannot be obtained when a single or limited number of interfraction intervals are used and the "incomplete repair" (IR) model (Thames, 1985) applied.

Although it does not provide an adequate description of results that we have re-analysed, and for which crude data were available, the IR model does nevertheless provide, on the basis of suggestions made by Dr Thames, further evidence for at least two components of repair. For the end-point of moist desquamation in pig skin and radiation given as three fractions, the half-time for repair ($T_{\frac{1}{2}}$) was found to increase significantly with increasing interfraction interval (van den Aardweg et al, in preparation). With interfraction intervals of 0.25 h and 4 h, direct analysis produced two separate estimates of $T_{\frac{1}{2}}$ (Table I). The short repair half-time of 0.26 h and the slower half-time of 1.17 h, which were highly significantly different from each other ($p < 0.001$), showed remarkable agreement with the values of 0.27 h (0.2–0.43) and 1.13 h (0.53–?) obtained by Turesson and

Table I. Dependence of interfraction interval on the half-time for repair ($T_{1/2}$) in the epidermis of the pig and the spinal cord of the rat, irradiated with three fractions and two fractions, respectively

Tissue	Interval (h)	$T_{1/2}$ (h)	α/β (Gy)
Epidermis[a]	0.25	0.26 (0.18–0.44)[c]	9.95
	0.5	0.42 (0.31–0.71)	10.07
	4.0	1.17 (0.74–2.72)	10.04
	$\leqslant 1.0$	0.41 (0.32–0.56)	7.32
	> 1.0	1.18 (0.91–1.64)	7.04
	all data	0.43 (0.32–0.66)	8.05
Spinal cord[b]	0.67	0.99 (0.79–1.33)	2.17
	4.0	1.89 (1.61–2.29)	2.13
	< 1.0	1.03 (0.77–1.52)	2.05
	$\geqslant 1.0$	1.88 (1.62–2.23)	2.20
	all data	1.90 (1.50–2.70)	2.70

[a]From Hopewell & van den Aardweg (1988), three fractions; [b]From Ang et al (1987), two fractions; [c]95% confidence limits.

Thames (1989) based on studies of moist desquamation on human skin. The α/β ratios were also similar in the two studies, ~10 Gy. In the studies on the pig both the short and long interfraction intervals involved three fractions, whereas in the investigations in man either three fractions/day or two fractions/day were used. This would appear to remove the one remaining reservation that Turesson and Thames (1989) had about accepting their own data as good evidence for biexponential repair kinetics. When the extensive data set from the studies on pig skin with three fractions (Hopewell & van den Aardweg, 1988) was grouped into intervals of $\leqslant 1$ h and > 1 h, significantly different $T_{1/2}$ values were again obtained. Application of the IR model to all data showed a bias towards the shorter of the two half-times (Table I).

The less extensive data for the spinal cord that was re-analysed in our earlier paper (Hopewell & van den Aardweg, 1988) involved irradiation with only two fractions. A similar analysis to that carried out above for skin also provided additional evidence for biexponential repair kinetics in the spinal cord (Table I). This confirms the recent finding of Thames, who proposed two components of repair after the analysis of the same data using an extension of the IR model (Thames, unpublished results: quoted by Turesson & Thames, 1989). The bias towards the larger $T_{1/2}$ value in the present evaluation, following direct analysis using all data, does not represent a fundamental difference between an early- and a late-responding tissue but is a reflection of the interfraction intervals used in the specific studies.

The different $T_{1/2}$ values that have been obtained using the IR model, which assumes monoexponential repair kinetics, should not be taken to represent the true values. The model will of necessity overestimate the short and underestimate the long half-times.

The argument as to whether repair is monoexponential or multiexponential is more than just of academic interest, but is of major importance in the practice of radiotherapy. Acceptance of monoexponential kinetics given an inappropriately short $T_{1/2}$ will seriously overestimate the amount of repair for long interfraction intervals with the subsequent overdosage of patients. Very short interfraction intervals, on the other hand, as might occur in complex multiple-field techniques (Turesson et al, 1984), could result in cases of patients being underdosed if a very fast component of repair was in operation.

The authors would like to thank Drs Guttenberger and Thames for many helpful discussions and we hope that these two letters contribute to the debate on the topic of repair kinetics.

Yours, etc.,

J. W. Hopewell
G. M. J. M. van den Aardweg
CRC Normal Tissue Radiobiology Research Group,
Research Institute (University of Oxford),
Churchill Hospital,
Headington,
Oxford OX3 7LJ

(*Received July 1989*)

References

Ang, K. K., Thames, H. D., van der Kogel, A. J. & van den Schueren, E., 1987. Is the rate of repair of radiation-induced sublethal damage in the rat spinal cord dependent on the size of dose per fraction? *International Journal of Radiation Oncology, Biology, Physics, 13*, 557–562.

Hopewell, J. W. & van den Aardweg, G. J. M. J., 1988. Current concepts of dose fractionation in radiotherapy: normal tissue tolerance. In *Megavoltage Radiotherapy 1937–1987, British Journal of Radiology*, Suppl. 22 (British Institute of Radiology, London), pp. 489–497.

Thames, H. D., 1984. Effect-independent measures of tissue responses to fractionated irradiation. *International Journal of Radiation Biology, 45*, 1–10.

———, 1985. An incomplete-repair model for survival after fractionated and continuous irradiation. *International Journal of Radiation Biology, 47*, 319–339.

———, 1989. Repair kinetics in tissues: alternative models. *Radiotherapy and Oncology, 14*, 321–327.

Thames, H. D., Mason, K. A., Bentzen, S. M., Ang, K. K. & Cundiff, J. H., 1989. Split-dose recovery in mouse jejunal crypt cells: characterization of repair kinetics. In *The Scientific Basis of Modern Radiotherapy*, ed. by N. J. McNally, BIR Report 19 (British Institute of Radiology, London), pp. 37–42.

Thames, H. D. Jr, Rozell, M. E., Tucker, S. L., Ang, K. K., Fisher, D. R. & Travis, E. L., 1986. Direct analysis of quantal radiation response data. *International Journal of Radiation Biology, 49*, 999–1009.

Turesson, I., Notter, G., Wickstrom, I., Johansson, K. A. & Eklund, S., 1984. The influence of irradiation time per treatment session on acute and late skin reactions: a study on human skin. *Radiotherapy and Oncology, 2*, 235–245.

Turesson, I. & Thames, K. D., 1989. Repair capacity and kinetics of human skin during fractionated radiotherapy: erythema, desquamation and telangiectasia after 3 and 5 year follow-up. *Radiotherapy and Oncology, 15*, 169–188.

The immediate film in intravenous urography

The Editor—Sir,

In routine examinations it is important to expose only those views that contribute to the diagnosis.

We reviewed 239 consecutive intravenous urographic examinations in all of which an "immediate film" had been exposed immediately after the end of the injection. This was a radiograph of the renal area, usually using a 25 cm × 30 cm film.

In no case was an abnormality seen that was not apparent on later radiographs. A radiograph taken of the renal areas 3 or 4 min after the end of the injection will show not only the nephrogram (which is seen also on an immediate film) but also the calyceal pattern: it is more useful than the immediate film.

Yours, etc.,
J. G. B. Russell
J. M. Weller

Department of Radiology,
Manchester Royal Infirmary,
Oxford Road,
Manchester M13 9WL
(*Received July 1989*)

Lung cancer: tissue characterization by magnetic resonance imaging T_1 and T_2 values *in vitro* and role of histopathology

The Editor—Sir

A wide variety of pulmonary disorders including neoplasms are amenable to characterization by magnetic resonance imaging (MRI) (Cohen et al, 1987). Shioya et al (1988) present a careful study favouring discrimination of normal and pathological lung tissues on the basis of T_1 and T_2 values *in vitro*, MRI intensity and histological correlation.

This paper brings out a facet of nuclear magnetic resonance (NMR) studies and histological correlations that has received limited attention. The need for generating information on relative MR intensity of tissues as an aid to clinical interpretation of MR images has recently been recognized (Ehman et al, 1986). Sundaram et al (1987) have reported association of increased MR signal intensity with cellularity in subclassification of histiocytomas. Bottomley et al (1987), in their comprehensive review assessing whether T_1 and T_2 values have diagnostic value, concede that the principal determinant of relaxation time is the "tissue type". We support this line of argument on the basis of the results of concomitant NMR, trace metal profiles and histopathological studies of involved and uninvolved regions of oral, respiratory and gastrointestinal tract tumours (Ranade, 1984, 1988a,b).

Specifically, carcinomas of lung and uninvolved regions in continuation with resected tumours showed the following pattern of T_1 values at 25 MHz and iron content.

The levels of iron in the uninvolved regions were higher than involved regions in carcinomas of lung, in keeping with the belief that levels of paramagnetic metals are reduced in malignancy. The T_1 values in a few cases were in the order of 900 ms higher than the mean T_1 values of the uninvolved region. Histological examination of these regions showed the presence of malignant cell clusters in the pulmonary tissues (Fig. 1). This observation was confirmed in more cases of uninvolved regions of lung as well as other regions from other body sites (Ranade, 1988a). It is therefore concluded that the presence of malignant cell clusters contributes to the unexpected rise in the T_1 value of the uninvolved region and supports the characterization of normal and pathological samples by NMR, relating the T_1 variation to the histological tissue constituents on a wider basis of evidence as detailed below.

In an NMR study of the transition zone between normal oesophagus and tumour in surgically resected samples, a gradient increase of T_1 values was observed. Duplicate samples of proximal uninvolved zones, involved zones and the distal uninvolved zones of gastric end designated as E1, E2, E3, E4, E5 and E6, respectively, showed mean T_1 values of 730, 815, 850, 803, 739 and 695 ms at 25 MHz. The T_1 values of normal zone E2 were close to T_1 values of tumour zones.

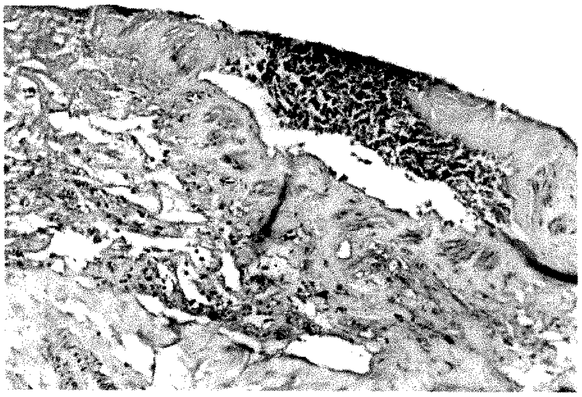

Figure 1. Histological section of uninvolved lung showing the presence of malignant cell clusters (× 140).

A histological study of E1 to E3 revealed the following dominant cell types: E1, normal; E2, malignancy associated changes (MAC) and E3, neoplastic cells.

The MAC types were encountered in a large number of samples that showed T_1 values close to tumour tissue. The MAC-positive regions were found to be associated with regions showing dysplasia (Ranade et al, 1985). It is contended that the MAC cell type provides another tissue constituent in addition to the multiple sample types studied by Shioya et al (1988), to which the T_1 variation can be ascribed.

Further to the results of NMR studies on isolated nuclei from normal and tumour tissues, normal and leukemic bone marrow and lymph nodes of normal and malignant lymphomas, it is hypothesized that the phenomenon of T_1 variation in these tumour models correlates well with the dominant cell type that constitutes them and is corroborated by the MRI of these tumour types. These have been summarized in recent publications (Ranade, 1987, 1988b).

Yours, etc.,
S. S. Ranade
P. N. Trivedi
V. S. Bamane

Radiobiology Unit,
Cancer Research Institute,
Tata Memorial Centre,
Parel, Bombay 400 012,
India
(*Received July 1989*)

References

Bottomley, P. A., Hardy, C. I., Argersinger, R. E. & Allen Moore, G., 1987. A review of ^{1}H NMR relaxation in pathology: are T_1 and T_2 diagnostic? *Medical Physics, 14,* 1–37.

Cohen, M. D., Scales, R. L., Eigen, H., Scott, P., Tepper, R., Cory, D. A. & Smith, J. A., 1987. Evaluation of pulmonary parenchymal disease by magnetic resonance imaging. *British Journal of Radiology, 60,* 223–230.

Ehman, R. L., Brasch, R. C., McNamara, M. T., Erikkson, U., Sosnovsky, G., Lukszo, J. & Li, S. W., 1986. Diradical nitroxyl spin-label contrast agents for magnetic resonance imaging: a comparison of relaxation effectiveness. *Investigative Radiology, 21,* 125–131.

Ranade, S. S. & Panday, V. K., 1984. Transition metals in human cancer II. *The Science of the Total Environment, 40,* 245–247.

RANADE, S. S., BHARADE, S. H., TALWALKAR, G. V., SUJATA, G. K., SHRINIVASAN, V. T. & SINGH, B. B., 1985. Significance of histopathology in pulsed NMR studies on cancer. *Magnetic Resonance in Medicine, 2,* 128–135.

RANADE, S. S., 1987. Cell type and proton relaxation. *Investigative Radiology, 22,* 346–347.

—— 1988a. Histopathologic correlation. In *Nuclear Magnetic Resonance Imaging,* Vol. II, ed. by C. L. Partain, R. R. Price, J. A. Patton, M. V. Kulkarni & A. E. James (W. B. Saunders, Philadelphia), pp. 1109–1130.

—— 1988b. Proton relaxation *in vivo, in vitro* and cellularity. *Acta Radiologica, 29,* 143.

SHIOYA, S., HAIDA, M., ONO, Y., FUKAZAKI, M. & YAMABAYASHI, H., 1988. Lung cancer: differentiation of tumour, necrosis and atelectasis by means of T_1 and T_2 values measured *in vitro. Radiology, 167,* 105–109.

SUNDARAM, M., MCGUIRE, M. H. & SCHAJOWICZ, F., 1987. Soft-tissue masses: histologic basis of increased signal (short T_2) on T_2-weighted MR imaging. *American Journal of Pathology, 148,* 1247–1250.

The potential value of hyperthermia in the management of human immunodeficiency virus infection

THE EDITOR—SIR,

A substantial record of clinical experience exists on the efficacy of zidovudine in symptomatic human immunodeficiency virus (HIV) infection. There is now a trend towards its expression at progressively earlier stages, embracing symptom-free subjects as reported by de Wolf et al (1988) and as proposed in the European Concorde trial (Lancet, 1989).

From the data available, zidovudine emerges as a potent retroviricide, but *in vivo* the action is incomplete and appears to be largely peripheral. Marrow depression is a prominent risk, and although there may be temporary subjective improvement in established illness, fatality is not avoided. Other agents, and their combinations, provide similar transient benefit. Treatment in the initial antigenaemic phase offers a greater chance of success, but since there is no specific primary lesion and any symptoms of invasion are likely to be misdiagnosed, many patients will miss the opportunity. Moreover, with long-term low dosage, viral resistance may be invited.

The crucial obstacle to curative therapy is the ability of the virus, neurotropic and lymphotropic, to establish inaccessible entrenchments in brain, bone marrow, bowel mucosa and lymphatic tissue, where it may replicate or remain latent. Of these reservoirs, the most secure is the central nervous system, which, because of the properties of the blood–brain barrier, is vascularly remote. A strategy capable of clearing virus from brain should effect general eradication.

We submit, in this context, that the potential of whole-body hyperthermia has been overlooked. We suggest that its application may serve to kill or inactivate the virus, accelerate the action of zidovudine and thus provide an abbreviated therapy.

Human immunodeficiency virus infection is the fourth major sexually transmitted disease. In this group, pyrexia is clinically rare, and the causal organisms are alike in possessing low thermal tolerance. Spire et al (1985) observed HIV, in culture, to be 100% inactivated at 56°C and 40% at 42°C after 30 min by employing reverse transcriptase assay. In sessions of artificial fever, temperatures of 41.8°C can be maintained for 5–6 h (Pettigrew et al, 1974; Bull et al, 1979).

We propose, therefore, the joint use of hyperthermia and zidovudine, in several sessions, on the following hypotheses.

(1) The organism may be eradicated by the new conditions.
(2) Alternatively, under adverse, but sublethal, thermal stress the virus will be more susceptible to the drug.
(3) Abnormal capillary dilatation with enhanced haemoperfusion will enhance drug access.
(4) Improved penetration of the lipid membrane blood–brain barrier by zidovudine is a possible effect.

Zidovudine ($C_{10}H_{13}N_5O_4$; molecular weight 267) shows quite high lipid solubility. With oral dosage of 1500 mg daily, cerebrospinal fluid concentrations of 30–50% of that in plasma are attained, *i.e.* 0.29–0.47 μmol/litre (Yarchoan et al, 1987). This is below the *in vitro* virustatic level of 1 μmol/litre.

According to Bradbury (1980), the rate of entry of highly lipid solubles to brain interstitial fluid rises with the rate of supply (*i.e.* blood flow) and with the capillary area exposed, but such an initial advantage may not persist in the steady state. Yarchoan et al (1987), however, remark that "even modest enhancement of penetration might have very important clinical consequences".

Systemic pyrexia has not previously been employed in viral infections, or where marrow compromise exists. Accordingly, clinical experiments will require a meticulous and cautious approach, but the need for a new strategy is compelling.

Yours, etc.,

K. D. COCHRAN
*H. WEATHERBURN

Viewfield,
Blebo Craigs,
Cupar, Fife and
*Department of Bio-Medical Physics and Bio-Engineering,
University of Aberdeen,
Foresterhill, Aberdeen

(*Received July 1989*)

References

BRADBURY, M. W., 1980. *The Concept of a Blood-Brain Barrier* (John Wiley & Sons, New York; Pitman Press, Bath).

BULL, J. M., LEES, D., SCHUETTE, W., WHANG-PENG, J., SMITH, R., BYNUM, G., ATKINSON, E. R., GOTTDIENER, J. S., GRALNICK, H. R., SHAWKER, T. H. & DE VITA, V. T., 1979. Whole-body hyperthermia: a phase-I trial of a potential adjuvant to chemotherapy. *Annals of Internal Medicine, 90,* 317–323.

LANCET, 1989. Zidovudine in symptomless HIV infection. Leading article. *Lancet, i,* 415–416.

PETTIGREW, R. T., GALT, J. M., LUDGATE, C. M. & SMITH, A. N., 1974. Clinical effects of whole-body hypothermia in advanced malignancies. *British Medical Journal, 4,* 679–682.

SPIRE, B., BARRE-SINOUSSI, F., DORMONT, D., MONTAGNIER, L. & CHERMANN, J. C., 1985. Inactivation of lymphadenopathy-associated virus by heat, gamma rays and ultraviolet light. *Lancet, i,* 188–189.

DE WOLF, F., GOUDSMIT, J., DE GANS, J., COUTINHO, R. A., LANGE, J. M., CLOAD, P., SCHELLEKENS, P. T. A., FIDDIAN, A. P. & VAN DER NOORDAR, J., 1988. Effect of zidovudine on serum human immunodeficiency virus antigen levels in symptom-free subjects. *Lancet i,* 373–376.

YARCHOAN, R., BROUWERS, P., SPITZER, A. R., GRAFMAN, J., SAFAI, B., PERNO, C. F., LARSON, S. M., BERG, G., FISCHL, M. A., WICHMAN, A., THOMAS, R. V., BRUNETTI, A., SCHMIDT, P. J., MYERS, C. E. & BRODER, S., 1987. Response of human immunodeficiency-virus-associated neurological disease to 3-azido-3-deoxythymidine. *Lancet, i,* 132–135.

Proceedings of The British Institute of Radiology

Clinical relevance of radiobiological models

Abstracts of papers presented at a BIR meeting, held at the British Institute of Radiology, 36 Portland Place, London W1N 4AT on Friday, 26 May 1989

Chairman: Dr I. J. Stratford

Radiobiological rationales in radiotherapy: the role of models, by T. E. Wheldon
A case for humoral radiopathology, by A. S. Michalowski
Are repair kinetics of radiation damage dose-rate dependent? by P. Nilsson, M. C. Joiner and H. Johns
The pathophysiology of the cardiopulmonary system after local heart irradiation in three strains of rats, by R. M. Pease and K. R. Trott
Pig lung: a model for the study of radiation pneumonitis, by M. Rezvani, J. W. Hopewell and M. E. C. Robbins
Acute radiation injury to the bladder: an experimental study of its pathogenesis, pathophysiology and treatment, by W. G. Bowsher and P. Blott
Radiation nephropathy and anaemia in mature pigs, by M. E. C. Robbins, D. Campling, M. Rezvani, S. Golding and J. W. Hopewell
The relevance of mouse tumour radiobiology for clinical radiotherapy, by G. G. Steel
Flow cytometric evaluation of hypoxic cells in solid experimental tumours, by R. J. Hodgkiss, G. Jones, J. Parrick, K. A. Smith, M. R. L. Stratford, T. Long and G. D. Wilson
Radiobiological studies of tumours in anaemic mice, by D. G. Hirst and A. C. Koong
The relevance of laboratory models to clinical practice, by M. I. Saunders
Close of meeting

Radiobiological rationales in radiotherapy: the role of models

T. E. Wheldon
Radiation Oncology Research Group, Beatson Oncology Centre, Belvidere Hospital, Glasgow G31 4PG and West of Scotland Health Boards, Department of Clinical Physics and Bio-Engineering, 11 West Graham Street, Glasgow G4 9LF

A radiobiological rationale may be described as a chain of reasoning that leads from some set of radiobiological data to its apparent implications for optimal treatment. Usually, the chain of reasoning involves the assumption that the radiobiological data set provides information on mechanisms that are common to the experimental and clinical situations, often that mechanisms revealed in the radiobiological study are the main ones (perhaps the only ones) operative in the clinical context. These assumptions are rarely true in practice but they may, sometimes, provide acceptable approximations. Experimental models (cell cultures, spontaneous or xenografted tumours in animals, non-tumour bearing animals for normal tissue studies) are useful if, and only if, they provide the opportunity to study, under controlled conditions, important mechanisms that are common to the experimental and clinical situations. Generally, the more basic the mechanism, the more plausible the expectation. It is important to recognize that phenomena will exist that are present in the experimental model but not the clinical situation, and *vice versa*. The usefulness of the model therefore depends on the *dominance* of the experimental results by mechanisms common to the experimental and clinical situations. Not all experimental models fulfil this requirement. Direct studies of optimal treatment scheduling for murine tumours are unlikely to enable reliable prediction of the corresponding clinical schedules, because phenomena peculiar to the experimental situation (*e.g.* rapid growth kinetics of murine tumours) will play an important part in determining the outcome. Appropriately designed studies may nevertheless provide useful generalities (*e.g.* the ubiquity of hypoxic cells in tumours of several species and their dominance in determining outcomes of single-fraction treatment).

Mathematical models essentially are tools for deriving the implications of a set of assumptions or axioms. They are used often because the implications of the axioms may be far from obvious. Usually, the axioms will themselves result from previous experimental or clinical studies suggesting the most important mechanisms operative in the situation to be modelled. Where the clinical implications of the radiobiological information are not immediately obvious, it is important to ensure that these implications are deduced correctly. The most common mistake is an over-generalization of the implications. For example, experimental studies may suggest that the α/β value for a group of tumours is greater than the corresponding values for late-responding normal tissues. This may lead to the over-generalized implication that hyperfractionation is the optimal treatment structure. Mathematical model studies show that parameters other than the α/β ratio enter into the derivation of the implications and that the influence of these parameters may be sufficient to negate the over-generalized conclusion. This might occur in the case of a resistant tumour (low individual values of α and β but high α/β ratio) with fast growth kinetics. The optimal schedule may then require larger-than-conventional fractions, despite the relationship of the ratios for tumour and tissue, considered in isolation. Other examples of possible over-generalizations include the use of single features (*e.g.* growth kinetic data) to deduce rationales (late-intensity schedules, accelerated regimes) whose consideration requires additional mechanisms to be taken into account. Mathematical model studies are useful in demonstrating the generality of such implications by mapping the circumstances in which the simplistic implications may fail. A simplistic implication may still be true in a statistical sense, with departures occurring only in special circumstances that can be defined by the model studies. Attention will then be focused on attempting to determine, in real applications, whether these special circumstances have occurred or not. Cautiously used, both experimental and mathematical models can be of great value in the design of treatment strategies that stand some chance of being superior to those in current use.

A case for humoral radiotherapy

A. S. Michalowski
MRC Cyclotron Unit, Hammersmith Hospital, London W12 0HS

The prevalent models of radiation damage to normal tissues focus on random sterilization of individual clonogenic cells. Evidence exists to suggest that such "autonomous clonogen" models may be incomplete and changes in the extracellular compartment after irradiation should be considered. Prodromal, acute and chronic effects of radiation are accompanied by excessive production of eicosanoids (prostaglandins, prostacyclin, thromboxanes and leukotrienes). These endogenous mediators of inflammatory reactions may be responsible for the vasodilatation, vasoconstriction, increased microvascular permeability, thrombosis and chemotaxis observed after radiation exposure. Glucocorticoids are well known to inhibit eicosanoid synthesis by interfering with phospholipase A_2 whilst non-steroid, anti-inflammatory drugs prevent prostaglandin/thromboxane synthesis by inhibiting cyclooxygenase. When administered after irradiation, drugs belonging to both groups have been shown to alleviate substantially a range of prodromal, acute and chronic effects of radiation in man and animals (Michalowski, 1989). Taken together, these two sets of observations are highly suggestive of a contribution of humoral factors to the overall radiation responses of normal tissues and organs. A full account of radiation damage should therefore consist of complementary humoral and cellular elements.

Reference

MICHALOWSKI, A., 1989. Martin Lindgren Lecture 1989. *Radiation Damage to Normal Tissues and its Treatment*, in preparation.

Are repair kinetics of radiation damage dose-rate dependent?

P. Nilsson, M. C. Joiner and H. Johns
CRC Gray Laboratory, PO Box 100, Mount Vernon Hospital, Northwood, Middlesex HA6 2JR

The rate of repair of radiation damage was investigated in mouse skin during protracted irradiation with single X-ray priming doses at dose-rates varying from 5 to 40 cGy/min followed by a single neutron top-up dose to bring the subthreshold X-ray damage into the measurable range. Two different experimental designs have been used so far: (i) a fixed priming X-ray dose of 15 Gy was given at varying dose-rates (5 to 280 cGy/min) or (ii) graded priming X-ray doses (0 to 30 Gy) were given at fixed low dose-rates of 10 and 20 cGy/min. Repair half-times ($T_{\frac{1}{2}}$) were determined by fitting the data (non-linear regression) with Thames' incomplete-repair (IR) model. Using the first experimental design and assuming that α/β does not change with the dose-rate and is equal to the value for acute exposure ($\alpha/\beta = 10.3$ Gy), $T_{\frac{1}{2}}$ was found to be 60 min at a dose-rate of 5 cGy/min, decreasing to 20 min at a dose-rate of 40 cGy/min, with a mean value of 43 ± 2 min. Thus, there was a trend of decreasing repair half-times with increasing dose-rate. However, using the second experimental design and the same assumptions, $T_{\frac{1}{2}}$ was found to be 50 ± 2 min and 60 ± 2 min at dose-rates of 10 and 20 cGy/min, respectively, *i.e.* a slight increase in $T_{\frac{1}{2}}$ with dose-rate. Thus, we did not find a conclusive dependence of repair kinetics on dose-rate in the experiments performed so far. The values of $T_{\frac{1}{2}}$ are, however, considerably shorter than those determined using acute fractionated X-ray doses (1–3 h) by varying the interfraction time interval, especially with high doses per fraction.

The pathophysiology of the cardiopulmonary system after local heart irradiation in three strains of rats

R. M. Pease and K. R. Trott
Department of Radiation Biology, Medical College of St Bartholomew's Hospital, Charterhouse Square, London EC1M 6BQ

Forty-five male rats of three strains (Fischer, Wistar and Sprague-Dawley) were locally X irradiated to the heart with doses of 20, 25 and 30 Gy. Animals were observed until they showed clinical signs of heart failure or other disease, whereupon they were killed. In 28 rats, large volumes of pleural effusions were observed at autopsy; these were considered to be a sign of heart failure. Another sign of heart failure was observed in 14 of the 28 rats, either ascites and/or subcutaneous oedema. The mean latency to death from heart failure was 226 ± 46 (mean $\pm$SD) ($n = 13$) days for the Fischer rats, 316 ± 54 ($n = 9$) days for the Wistar rats and 374 ± 66 ($n = 6$) for the Sprague-Dawley rats. The difference between the Fischer and the Wistar rats was significant. In all irradiated rats and some controls, cardiopulmonary function was tested at monthly intervals, commencing 100 days post-irradiation by measuring peripheral arterial blood pressure, heart rate and respiratory frequency in the conscious rat. The blood pressure of the control Wistar and Fischer rats ranged from 102 to 140 mmHg. Thirteen Wistar rats had periods of hypotension (78–100 mmHg) and nine later developed heart failure. Eight Fischer rats had periods of hypotension and seven later developed heart failure. The heart rate of control rats was between 300 and 450 beats/min; a rate of 270 or less was taken as pathological, and due to an anterio-venous block. Three of 13 irradiated Fischer, five of nine Wistar and three of six Sprague-Dawley rats had at least one episode of bradycardia prior to death from heart failure. Respiratory frequency at rest was between 100 and 150 breaths/min in the control rats. Twenty-six irradiated rats had a period prior to death from heart failure or other disease during which the breathing rate was equal to or higher than 160 breaths/min, some even above 250 breaths/min. In 19 of these, large volumes of pleural effusion were observed at autopsy and it was suggested that the pleural effusions limited tidal volume and thus the tachypnea became necessary to oxygenate the blood adequately. In all cases except four, hypotension preceded tachypnea. It is concluded that the pleural effusions arose as a result of heart failure after local heart irradiation, and that respiratory frequency could be used to predict their presence in life and also to serve as an end-point for radiation induced heart failure.

Pig lung: a model for the study of radiation pneumonitis

M. Rezvani, J. W. Hopewell and M. E. C. Robbins
CRC Normal Tissue Radiobiology Research Group, Research Institute (University of Oxford), Churchill Hospital, Headington, Oxford OX3 7LJ

A ^{133}Xe clearance technique has been used to assess the changes in the gas exchange capacity of the pig after the local irradiation of part of the lung with either single doses of ^{60}Co γ rays or fractionated doses of 250 kV X rays. Lung function tests were performed from 4 to 104 weeks after irradiation and functional changes in the irradiated volume of the lung were compared with a comparable volume of unirradiated lung in the same animal. The lung function results were computed into quantal data and ED_{50} values for a significant impairment of function ($\geqslant 15\%$) were obtained for both the early and late phases of damage. The ED_{50} values for early (10.12 ± 0.33 Gy) and late damage (9.73 ± 0.34 Gy) were not significantly different. At 104 weeks after irradiation the animals were killed. At this time the proportion of the lungs showing histologically defined fibrotic lesions was assessed. The dose–response curve for histological changes was not significantly different from those for both early and late functional damage. The dose–response curve for the early damage to pig lung was also compared with the published human data and a good agreement was found. This suggests that the pig might be an appropriate animal model for the study of radiation-induced lung damage in man. The linear-quadratic model did not provide a satisfactory fit to the fractionation results. The α/β ratios obtained by the application of this model were not significantly different from zero. A modified NSD equation did however provide a better description of the findings. A value for the N exponent of 0.44 ± 0.66 was obtained for both early and late damage to the lung.

Acute radiation injury to the bladder: an experimental study of its pathogenesis, pathophysiology and treatment

W. G. Bowsher and P. Blott
Department of Radiation Biology, Medical College of St Bartholomew's Hospital, Charterhouse Square, London EC1M 6BQ

Patients may suffer considerably from urinary frequency and incontinence early after irradiation of the bladder. Currently, the treatment of such symptoms is empirical, relying on drugs with an anti-cholinergic action. The role of anti-inflammatory drugs needs to be appraised. Under general anaesthetic, bladder pressure in female Wistar rats was measured at least weekly during filling with water at a rate of 0.05 ml/min. As a measure of compliance, the volume instilled for a 5 cm (water) pressure rise was recorded. Recordings were made in eight irradiated animals and four controls. Irradiated animals received 25 Gy (320 kV) locally to the bladder. A second experiment compared compliance changes in 10 animals treated with oral indomethacin (3 mg/kg/24 h), commenced 3 weeks after irradiation (25 Gy) and continued, with those in 10 untreated irradiated animals. In further experiments, bladder tissue was assayed for the prostaglandin PGE2, both pre- and post-irradiation, and bladders were examined by light and electron microscopy. Mean bladder compliance was maximally decreased by 33% in untreated irradiated animals compared with controls (no irradiation or drug) between 4 and 5 weeks after irradiation. Indomethacin-treated irradiated animals showed a 32% improvement in mean bladder compliance between 4 and 5 weeks post-irradiation compared with untreated irradiated animals. Histological examination of a limited amount of tissue taken between 1 and 5 weeks after irradiation was unremarkable. Electron microscopy showed marked degeneration of smooth muscle cells at 31 days after irradiation. Initial results of PGE2 assays show a maximum level 5 weeks after irradiation (48 ng/100 mg tissue) in untreated animals. The maximum decrease in bladder compliance at 4 and 5 weeks after irradiation correlates with maximally elevated levels of PGE2. This correlation, together with the observation that the compliance change was not as pronounced after treatment with indomethacin, supports the hypothesis that changes in bladder compliance early post-irradiation relate to elevated levels of prostaglandins within bladder muscle. A double-blind randomized clinical trial of indomethacin versus placebo in patients undergoing irradiation of the bladder is indicated.

Radiation nephropathy and anaemia in mature pigs

M. E. C. Robbins, D. Campling, M. Rezvani, *S. Golding and J. W. Hopewell
*CRC Normal Tissue Radiobiology Research Group, Research Institute (University of Oxford) and *Oxfordshire Regional CT Unit, Churchill Hospital, Oxford OX3 7LJ*

Renal irradiation has been reported to produce a pronounced reduction in both glomerular filtration rate (GFR) and effective renal plasma flow (ERPF) with concomitant anaemia. To help elucidate the physiological mechanisms involved in radiation nephropathy, both kidneys of mature 10-month-old pigs were irradiated with single doses of 7.8–14.0 Gy of ^{60}Co γ rays. Sequential measurements of individual kidney GFR and ERPF were made for up to 24 weeks after irradiation. Blood samples were also collected at regular intervals for (a) characterization of the radiation-induced anaemia and (b) estimation of plasma renin levels. Two weeks after irradiation, the ERPF and in particular the GFR increased. This was followed by a marked dose-dependent decline in renal function. Minimal function was observed 8–12 weeks after irradiation. Function then showed some evidence for recovery. There was a significant ($r \geqslant -0.98$; $p < 0.001$) inverse relationship between the mean GFR and ERPF values (noted 4–24 weeks after irradiation and expressed as a percentage of age-matched controls) and the radiation dose. In addition it was shown that after the lowest dose of 7.8 Gy, the reduction in ERPF was greater than that for the GFR. However, at higher doses, both parameters were equally reduced. Thus the slopes of the dose-effect curves showing the reduction in function against dose was significantly ($p < 0.001$) steeper for GFR than ERPF. Blood analyses showed a significant reduction ($p < 0.002$) in erythrocyte count, haematocrit and haemoglobin levels within 6–8 weeks of irradiation. The numbers of white blood cells and platelets were unchanged. The anaemia was characterized as a normochromic normocytic anaemia, as is found in clinical radiation nephritis. There were no changes in plasma renin levels following irradiation, indicating that the marked reduction in renal haemodynamics following irradiation was not a direct consequence of an activation of the renin angiotensin system.

The relevance of mouse tumour radiobiology for clinical radiotherapy

G. Gordon Steel
Radiotherapy Research Unit, Institute of Cancer Research, Sutton, Surrey SM2 5PX

Mouse tumours are not models of human cancer. Models are human creations, physically or mathematically. The appropriate question is what we can learn or have learned from studying mouse tumours that might have relevance for clinical radiotherapy. The experimental work includes not only spontaneous and transplanted murine tumours but also xenografts of human tumours in immune-suppressed mice. Tumours in animals are different from human tumours in many respects. They are often immunogenic. Metabolic rate and cell proliferation rates are higher and this has made it difficult to evaluate the role of repopulation during radiotherapy. The differences in oxygen diffusion and therefore hypoxia may be less. Nevertheless, experiments performed to test misonidazole as a radiosensitizer tended to exaggerate its potential. Xenografts retain some of the properties that determine response to chemotherapy and there are good grounds for using them in drug development. Since the stroma is derived from the host mouse there is no reason to believe that the degree of hypoxia or rate of reoxygenation of a xenograft will reflect that which exists in the patient. The value of xenografts for radiobiological studies is therefore in question. There are few examples of specific innovations in radiotherapy that can be attributed to work on tumours in rodents, but they have been useful in enabling some of the key concepts of radiobiology to be developed.

Flow cytometric evaluation of hypoxic cells in solid experimental tumours

R. J. Hodgkiss, G. Jones, J. Parrick, K. A. Smith, M. R. L. Stratford, T. Long and G. D. Wilson
Gray Laboratory, Mount Vernon Hospital, Northwood, Middlesex HA6 2JR

Poorly oxygenated, radioresistant cells in tumours are thought to contribute to local failure of radiotherapy and tumour regrowth. Such cells may be detected by the hypoxia-dependent binding of 2-nitroimidazoles labelled with a variety of radioactive isotopes followed by autoradiography. An alternative approach is to label a 2-nitroimidazole with an immunologically recognizable side-chain, theophylline. Bioreductive binding of the nitroimadazole also leads to binding and immobilization of the side-chain, which can then be detected by fluorescent immunochemical staining procedures. This staining procedure can be used to show more bioreductively bound theophylline in mammalian cells incubated *in vitro* with the drug under hypoxic compared with aerobic conditions. The oxygen-dependence of metabolic binding *in vitro* is similar to the oxygen dependence of radiosensitivity. Analysis of stained tumour cell suspensions by flow cytometry is greatly improved by the additional use of propidium iodide to stain DNA, which enables cell doublets, clumps and debris to be excluded on the basis of DNA content. This staining procedure has been used to evaluate the proportion of hypoxic cells in experimental tumours. Mice carrying subcutaneous tumours were treated with the drug (0.5 μmol g^{-1}), which appeared to be of low toxicity. Cell suspensions were prepared from excised tumours by mechanical disaggregation. A greater proportion of cells containing high levels of bound adducts can be found in tumours treated with the drug in air-breathing mice than from tumours treated in mice breathing carbogen (95% oxygen). The proportion of tumour cells staining for high levels of bound adducts does not depend greatly on cellular DNA content, and hence cell cycle position, although there is a small excess of hypoxic cells with a G2 DNA content. An immunoperoxidase staining procedure has been used to detect bioreductivity bound theophylline in tumour sections. There is little staining of the first five to six cell diameters surrounding most blood vessels; concentric rings of stained cells are found at greater distances but do not extend into the necrotic regions of the tumour.

Radiobiological studies of tumours in anaemic mice

David G. Hirst and Albert C. Koong
CRC Gray Laboratory, Mount Vernon Hospital, Northwood and Department of Radiation Oncology, Stanford University, Stanford, USA

Anaemia is frequently encountered as a complication in the treatment of malignant disease in some sites. There is also clear evidence from clinical studies that the anaemic patient treated with radiotherapy is more likely to fail locally than the patient with haemoglobin levels in the normal range. Furthermore, at least one study has indicated that variations in haemoglobin within what is usually thought to be the normal range can affect treatment outcome. We might expect, then, that tumours in anaemic mice would be similarly radioresistant. This has proved to be difficult to demonstrate convincingly in mouse tumour models and leads to the conclusion that the responses of a tumour or the host animal to altered haemodynamics must be rather complex. Our studies have focused on understanding these effects in the mouse and on developing appropriate models for studying the influence of anaemia on radiosensitivity. Two main points emerge from our studies. First, all the mouse tumours we have studied (four) became strikingly more radioresistant when anaemia is induced abruptly, such as by exchange plasma transfusion. Secondly, when anaemia is induced gradually, over several days, or if an interval elapses between transfusion and irradiation, tumours in anaemic mice show a radiosensitivity that is not greatly different from that in normal mice, with a trend towards greater sensitivity. These data imply that the poor response to radiotherapy seen in anaemic cancer patients may not be a direct consequence of reduced tumour oxygenation but is rather related to other tumour characteristics that also predispose towards anaemia.

The relevance of laboratory models to clinical practice

M. I. Saunders
Mount Vernon Hospital, Northwood, Middlesex HA6 2JR

Clinical research to improve the results of cancer treatment in patients is dependent on the ideas of scientists and clinicians. These ideas are tested in the laboratory and if they are effective in increasing the cure rate of tumours in animals then they may be applied to man; similarly, analysis of radiobiological data may lead to the formation of mathematical models that will look to the possibility of certain changes in treatment being effective. It is only when these scientific advances are put to the test in man can we know whether they will advance the cure of human cancer. Laboratory studies have led to explorations in the clinic of hypoxic cell sensitizers, hyperthermia and, most recently, fractionation. Mathematical models taking into account cell proliferation time and labelling indices have also been applied to the new fractionation studies. A novel scheme of radiotherapy using continuous, hyperfractionated, accelerated radiotherapy (CHART) was based on radiobiological science and has incorporated acceleration to overcome the possibilities of repopulation during a course of radiotherapy, hyperfractionation such that the dose per fraction is low to reduce late tissue morbidity and a 6-h interfraction interval to allow adequate recovery of sublethal injury. Initial results have shown local tumour control and survival superior to that observed in comparable previously treated groups of patients. Early normal-tissue reactions have been more intense, as predicted, but have all settled; late normal-tissue damage appears to be less to date. Mathematical models have suggested that this fractionation scheme should only be effective in a minority of rapidly proliferating tumours; however, the apparent success clinically would suggest a greater number of tumours. Randomized trials are to be conducted throughout the United Kingdom.

1989, *The British Journal of Radiology*, *62*, 1117

Radiology in AIDS

Additional abstract for proceedings of the above meeting, held at the BIR, 36 Portland Place, London W1N 4AT, on Thursday, 19 January 1989

Neuroradiological imaging in human immunodeficiency virus

Brian Kendall
The National Hospital for Nervous Diseases and The Middlesex Hospital, London

About 240 patients have been registered at The Middlesex Hospital, London, for AIDS and about one-third of these have had some symptoms indicating involvement of the nervous system. Over 50% of these patients have been subjected to computed tomography (CT) and, of these, 40% are normal, 40% show atrophy and 20% show focal pathology. Many of the radiological appearances are not specific, and confirmatory evidence of their nature is more frequently dependent on clinical evolution, response to therapy, serological testing and, occasionally, isolation of organisms, rather than biopsy or post-mortem histology, which is not commonly obtained. A normal CT scan has been shown to be associated with a better prognosis in relation to the development of progressive neurological disease and of focal lesions. Over 10% of patients with a normal CT scan have an abnormality shown on magnetic resonance imaging (MRI); whether absence of a lesion on MRI is of even better prognostic significance is not established.

Human immunodeficiency virus (HIV) itself may cause atrophy, which may be accompanied by patchy focal or ill defined, rather diffuse white matter of low density visible on CT and on a basis of demyelination and gliosis. Magnetic resonance imaging shows more extensive white matter abnormalities in such cases, and white matter changes may be present on MRI when CT shows only atrophy. There are to my knowledge no reports of abnormal spinal imaging associated with uncomplicated HIV infection. Indeed, even in the presence of proven secondary lesions, spinal imaging is frequently negative. Human immunodeficiency virus meningitis, both acute and chronic, is not associated with imaging abnormalities.

The immune system deficit results in increased susceptibility to both viral and non-viral pathogens. The commonest is cytomegalovirus (CMV) infection, but in the majority of cases the imaging appearances are non-specific or indistinguishable from uncomplicated HIV. Cytomegalovirus may cause multifocal, necrosing, encephalitic lesions and ependymitis, with enhancement after intravenous contrast medium injection. Progressive multifocal leucoencephalopathy, though much less frequent, produces more characteristic imaging abnormalities. There are circumscribed foci of low density on CT and of altered signal on MRI typically confined to the white matter. They are most commonly located in the parieto-occipital region, though not infrequent elsewhere in the cerebral white matter, and 10% are infratentorial. In AIDS patients, grey matter is not infrequently involved. Many of the foci enhance after intravenous contrast medium. Lesions of herpes simplex are similar to those occurring in non-AIDS patients, the temporal lobes being most frequently affected, though brain swelling may be diffuse. Varicella-zoster involving the trigeminal ganglion may spread to the carotid artery, and this was associated with lesions resembling infarcts in one patient in our series.

Non-viral opportunistic infections are present in about 45% of HIV-infected brains at autopsy. The commonest infecting organism is toxoplasma, which causes multifocal mass lesions. These are generally of low or brain density on CT and high signal on T_2-weighted MRI. Magnetic resonance may be particularly useful in revealing multiple lesions when only a single focus is evident on CT. Resolution on sulphonamide therapy may be rapid or relatively slow over a period of months. Premature discontinuation of the therapy may precipitate a rapid relapse. The cryptococcus is the next most frequently encountered infection. It most typically causes a subacute enhancing ependymitis and meningitis, with nodular foci extending into the adjacent brain. However, for prolonged periods, computed imaging may be normal. Other fungi and yeasts and tuberculosis occur much less frequently and cause appearances similar to toxoplasma. Microbacterium avium intercellularae, though frequent at post-mortem examination, is a very rare cause of granuloma formation shown on imaging studies. Primary neoplasms, particularly B-cell lymphoma, affect 6–8% of AIDS patients. They tend to be multicentric and are variable in density from heterogeneous with diffuse enhancement to low density with ring enhancement and surrounding oedema. Failure of a solitary lesion or of one or more of multiple lesions to respond to antitoxoplasma therapy should raise the possibility of lymphoma and the necessity for biopsy.

About 20% of systemic lymphomas occurring in AIDS patients cause metastases affecting the central nervous system (CNS). These may present as extra-axial mass(es), which may be relatively shallow and difficult to appreciate on routine imaging. Kaposi sarcoma rarely involves the CNS, but should be suspected if a haemorrhagic intraparenchymal mass is shown.

1989, *The British Journal of Radiology*, *62*, 1118–1122

Book reviews

Computed Tomography of the Abdomen in Adults. 85 Radiological Exercises for Students and Practitioners. By A. Wackenheim and A. Badoz (translated by M.-T. Wackenheim), pp. vi + 159, 1988 (Springer-Verlag, Berlin), DM 35.00.
ISBN 3–540–16540–1 (Berlin).
0–387–16540–1 (New York)

This little book contains 84 computed tomography (CT) exercises, each with one or more adequately reproduced half-tone images. The first eight illustrations demonstrate normal abdominal CT anatomy, the remainder cover a varied but by no means comprehensive collection of abdominal pathologies. The second half of the book contains line diagrams, descriptions and discussion for each of the studies, necessitating repetitive flipping from front to back to connect text with image. The layout of the images is not consistent, with frequent blank half-pages (useful for notes) and consecutive images sometimes one above the other and sometimes on facing pages. This, combined with an equally inconsistent text and line drawing layout makes correlation of text with image even more difficult.

The book is designed as a self-assessment exercise and is aimed at pre-Fellowship radiology trainees. It would be of greatest value for teaching purposes to those without regular access to CT.

The illustrations are rather small and required concentration and good lighting conditions for adequate viewing. Only one set of illustrations was missing its labelling, and I found one incorrectly annotated line diagram.

The original text, by Professor A. Wackenheim and Dr Badoz, was in French and has been translated by Marie-Therese Wackenheim. I suspect it has never had the benefit of an English, medically qualified proof reader. Some of the language is almost archaic, and amusing "near-misses" such as "repermeabilization of the umbilical vein" provide entertaining reading. Other translation errors are less easily forgiven and one or two sentences were self-contradictory.

Whilst I feel this is not an essential book for personal collections or libraries, it would partially compensate for lack of access to a CT film museum. A copy in each teaching hospital radiology department would not go amiss (though it might go missing).

The cost of approximately £10 is acceptable for a pocket book with many illustrations.

RICHARD W. WHITEHOUSE

Blood Flow in Artificial Organs and Cardiovascular Prostheses. Oxford Medical Engineering Series, No. 8. Ed. by J. C. Barbenel, A. C. Fisher, J. D. S. Gaylor, W. J. Anderson and C. D. Sheldon, pp. xvi + 266, 1989 (Oxford University Press, New York), £35.00.
ISBN 0–19–857647–1

This book is based on the proceedings of a conference on blood flow in artificial organs and cardiovascular prostheses. As such, it suffers from the problem often associated with this type of publication: the subject matter of individual chapters appears disjointed, author styles are disparate and there is inevitably some repetition. Some considerable time has elapsed since the conference took place, with the result that most of the contents of the book are readily available from other sources.

The title itself is not a fair reflection of the contents of the book. Indeed only a few of the chapters specifically mention blood flow. Thirty-one chapters are crammed into 260 pages. The chapters are of two types: those which review a particular topic and those which report research work. The first chapter is intended to be a "scene-setter" and gives a review of the haemodynamic factors of importance in improving design of vascular prostheses. The next seven chapters break from this theme and deal with clinical and laboratory assessment and some aspects of the design of prosthetic heart valves. Topics covered include leaflet design, mechanical properties of bovine pericardium, hydrodynamic testing and leakage design. The next two chapters describe a method for measuring lower limb blood flow and some of the anatomical and blood flow characteristics associated with the atrio-ventricular valves.

The theme changes abruptly again to deal with the interaction of blood with artificial surfaces. Topics discussed in chapters 11–19 include thrombosis, blood–membrane interaction, the immune response, platelet aggregation, a small animal model for evaluation of biomaterials and antithrombotic agents for chronic extracorporeal procedures (*e.g.* haemodialysis), pre-clotting of arterial graft implants, haemolysis in dacron grafts, platelet and fibrinogen kinetics in grafts and biocompatibility of haemodialysis membranes.

Chapters 20–22 are concerned with oxygen transfer in membrane oxygenators. The next seven chapters relate either to the measurement of whole blood viscosity or to the properties of its cellular constituents. Topics treated include a review of blood viscosity and cell deformability, variations in platelet count and volume following open heart surgery, whole blood viscometry, determination of red cell volume distribution and the relationship between red cell concentration and erythrocyte sedimentation rate. Chapter 30 discusses improved flow characteristics of Newtonian and non-Newtonian fluids in tapered tubes. The final chapter gives the briefest of accounts of a gamma camera based method of dynamic imaging of the flow distribution in membane oxgenators.

There are some spelling mistakes and some pieces of poor grammar, but, overall, the editorial standard is good. The illustrations have been well reproduced, though some of the anatomical photographs did not make their intended point very clearly (additional labelling would have helped non-clinical readers). At over £40 the book cannot be considered good value for money, especially as much of the material is already well known. In its favour, it does bring together many of the aspects that are important to the design of cardiovascular prostheses and should, therefore, be of interest to those working in this field.

T. COCHRANE

Anatomy and MRI of the Joints: A Multiplanar Atlas. Ed. by W. D. Middleton and T. L. Lawson, pp. xvi + 301, 1988 (Raven Press, New York), $156.50.
ISBN 0–88167–455–9

This atlas has been written as a ready reference for the identification of articular and periarticular structures seen on MR images. In this respect the book generally succeeds admirably. Indeed the photographs of the accompanying cytomicrotomes are beautiful to behold.

The MR images and microtomes do tally well on careful observation. It is, perhaps, an unfortunate fact of style that the microtomes and MRI scans are not "face-to-face", but run in small separate series. However, as stated in the preface, it is likely that the cytomicrotome photographs will outlast the MRI scans for reference purposes.

Whilst most of the MRI scans are of very high quality, it is noticeable that some are too dark.

The book covers in commendable detail the sectional anatomy of the temporomandibular joint, the shoulder, the elbow, the wrist, the finger, the hip, the knee and the ankle. Unfortunately, the section on the vertebral column is inadequate with only four MR images for the whole spine. It would, perhaps, have been better to have omitted the spine, which, if covered in the same detail as the other joints, could require a book in its own right. The book will be bought for the images of the other joints and not for the spinal images.

With this reservation in mind, this is an excellent atlas. It is up to date and good value for money. This book should be purchased by all users of MRI with an interest in the musculoskeletal system.

P. GODDARD

Nuclear Medicine. Self Assessment in Radiology and Imaging, No. 5. By S. Karimjee, A. Thomas and W. Taylor, pp. 192, 1989 (Wolfe Medical Publications, London), £19.50.
ISBN 0-7234-0999-4

This is a short, easy-to-read book, generally well illustrated, in which the reader is shown radionuclide images and then questioned on them. In each case, the images are shown again on the following pages with a discussion of the findings and outcome.

The cases are a reasonably good reflection of current nuclear medicine referrals, except I thought some monoclonal antibody studies should have been introduced and there are only two cardiac studies in the 54 cases. Almost half the cases are MDP bone studies. The level of the book is such that it is aimed at the fairly inexperienced, although some of the cases are quite complex.

Its main drawback, and a serious one, is the inclusion of a number of cases which are confusing, misleading or incompletely discussed. Some examples follow. Cases 3 and 18 are lung scans showing evidence of pulmonary embolism. In both cases there are, in addition, marked abnormalities of ventilation but these are not discussed. Case 17 is a captopril renogram. The renogram curves shown are first pass (flow) curves only, although they are described as though they were the complete curves. Captopril appears to have reduced the blood flow on the abnormal side. This is an unusual response, which is certainly not pathognomonic of renal artery stenosis as the authors state. This case is quite misleading and adds confusion to a subject which students usually have great difficulty understanding. Case 32 shows abnormal MIBG uptake in a neuroblastoma primary. The patient has, in addition, a grossly abnormal skeleton showing extensive diffuse infiltration. It is remarkable that this is not pointed out in the discussion. The quality of the bone scan is too poor to assess abnormalities, although some are probably present (and certainly would be expected on the evidence of the MIBG scan).

Case 33 is a renogram which shows appearances typical of acute tubular necrosis in a kidney. The discussion talks about a continuously rising renal curve, but the illustrations show it to be falling throughout, without a peak at any stage. Case 43 is another example of a poorly presented renal study in which the illustrations and text are out of step with each other.

Cases such as these seriously detract from the value of the book. It is imperative for a book aimed at beginners to be accurate in the fundamentals of the subject and for the reader to be absolutely confident in this accuracy. Unfortunately, this book cannot offer this confidence.

A. M. PETERS

Practical NMR Imaging. Ed. by M. A. Foster and J. M. S. Hutchison, pp. xv + 311, 1987 (IRL Press, Oxford), £36.00; $65.00.
ISBN 1-85221-011-7

The authors have aimed this book at those who are involved in the practical aspects of NMR within the clinical environment. The contributors are a well balanced team drawn from university departments of medical physics, industry and radiology.

The opening chapter condenses general principles into less than 50 pages. The second chapter, on siting and installation, is full of helpful and practical information for those involved in setting up NMR units. Other chapters consider a number of complex physical aspects of MRI. A chapter on contrast agents by G. M. Bydder is a model of clarity, as well as being particularly germane because of the recent introduction of gadolinium DTPA for clinical use. A short chapter by F. W. Smith introduces concisely the application of MRI to clinical practice. A balanced account of spectroscopy puts this modality into perspective. Finally, there is a chapter on safety considerations, and a short discourse on image artefacts, as an appendix.

This book is especially recommended for radiologists, as well as their colleagues in other disciplines, who are involved in the planning and installation of MR systems. It would, however, be a distinct advantage to have already a clear grasp of basic principles before reading this text. Those who are concerned with the running of an MR unit would also benefit.

In such a rapidly evolving field there are, inevitably, recent developments and trends which are not included in the book. Readers expecting advice on the most appropriate field strength, as well as other aspects of equipment for their particular needs, will be disappointed and have to look elsewhere. Notwithstanding these comments, the reader will gain a large amount of useful information.

G. H. WHITEHOUSE

Manual of Nuclear Medicine Procedures. By R. Mistry, pp. xviii + 197, 1988 (Chapman and Hall, London), £14.95.
ISBN 0-412-30240-3

The aim of this manual is to provide useful information to student nuclear medicine technicians and radiographers, and a practical reference text for departments wishing to widen the range of tests offered to the clinician.

The manual contains 11 chapters, each of which is devoted to a particular organ. Each chapter begins with an introduction to the organ, detailing the radiopharmaceuticals that can be used and the results that can be obtained, together with clinical indications for each test. The text then proceeds to give details of patient preparation, injection technique, radiopharmaceutical preparation and dose to be injected. Further sections contain details on equipment and collimator required for the test, line drawings of patient positioning under the gamma camera and layout of the views on a film formatter, and finally instruction on computer collection of the information together with relevant framing rates. The final section in each chapter deals with analysis of the information collected on the computer.

Two of the chapters in the manual deal with various common sample-counting procedures in detail. Information is also provided on adult and child injection doses, aseptic procedures and equipment and materials necessary for the preparation of the labelled radiopharmaceutical. Other sections detail sample collection, preparation of standards, counting of samples and calculation of results. All procedures in the manual are laid out in a format that is easy to follow so that a person who is not familiar with a particular test will be able to carry out the procedure and obtain the required results.

This book can be recommended as a useful addition to a departmental library, and is reasonably priced so that an individual could afford a copy for themselves.

A. M. CLAY

Assessing the Skeletal Maturity of the Hand–Wrist: Fels Method. By Alex F. Roche, Wm. Cameron Chumlea and David Thissen, pp. viii + 339, 1988 (Charles C. Thomas, Springfield, USA), $57.50.
ISBN 0–398–05452–5

As indicated by the title, the primary purpose of this book is to provide an improved method of assessing skeletal maturity based on radiographs of the hand and wrist. Additionally, the first two chapters describe the histological changes in bone maturation and a discussion of the many approaches to its assessment throughout this century and their relative values; there is an extensive bibliography. A rather cursory consideration of the need for skeletal age assessment is included but is of insufficient depth to be of value to the clinician.

The data were based on serial radiographs of the left wrist and hand of 355 boys and 322 girls born between 1928 and 1974, enrolled in the Fels Longitudinal Study of Growth and Development in Southwestern Ohio, USA. About 7000 radiographs were taken for each sex and the number for each child ranged from one to 38. As with scoring methods, each of several bones of the wrist and hand are evaluated individually and the skeletal age based on the total evaluation. The bones chosen are 22 in number, with the addition of the pisiform and adductor sesamoid to the 20 of the Tanner Whitehouse method. However, rather than give a score for each bone as an overall impression, several indicators of maturity for each bone are presented (totalling 98 for all ages combined) and judged on the basis of a few simple criteria, with two or three or occasionally four possible grades for each indicator (such as the simple presence or absence of a feature). The book includes a lengthy discussion on the way in which the system was developed, including its statistical basis and the criteria required of each indicator to justify its inclusion, *i.e.* discrimination, universality, reliability, validity and completeness.

At first sight this new approach to skeletal age assessment has much to recommend it. The recognition of the grades of each indicator is simple and precise, in contrast to many of the scoring criteria in the Tanner Whitehouse method. This latter system leaves much to be desired in matching up the textual description, radiographs and the drawings of the bone stages, whereas in the Fels method it is much easier to assign gradings, and the textual description and high-quality radiographs are easy to relate largely due to the simplicity of the features they are showing. This method, together with the complementary method of Roche–Wainer–Thissen for the knee (based on 34 maturity indicators), are the only methods that provide standard errors for the estimate for each radiograph.

However, sadly, when it comes to an honest appraisal of whether the system would be of use in practice on the Eastern side of the Atlantic, particularly in superseding the well established Tanner Whitehouse methods, there is little doubt that it would not. In a crucial 5½ page chapter, "Procedures for applying the Fels method", we learn first, not unreasonably, of the importance of applying the correct procedure in radiographic technique, but then "the person who will apply the Fels method should begin by reading this book. He or she should acquire a suitable ruler and must have access to an IBM PC compatible microcomputer with a memory of at least 48K and the computer program for the estimation of Fels skeletal ages (Appendix C). In addition, recording forms similar to the example in Appendix B are needed. Training should begin by assessing the test radiographs that are available . . . "

This method therefore involves other prerequisites, obtainable from the authors at a cost, and a fair assessment of the value of the method can clearly not be given without these extras needed to apply it appropriately.

It may well be that the Fels method (particularly when combined in many situations, as the authors advise, with the Roche–Wainer–Thissen skeletal age of the knee) is the most correct in the information it provides (though not necessarily appropriate for European children unless some correction is employed), but it will certainly not be quick and convenient. The descriptions of the 98 indicators based on 22 bones takes up 176 pages of the book, which presumably will need to be referred to in each skeletal age estimation. Unfortunately, about a third of the radiographs demonstrating indicators do not appear on the same page as the appropriate textual description. Not all indicators, however, are required each time and the relevant ones for the various sexes and ages up to 8 years are indicated on further tables. (Beyond the age of 8 there is no advice given on this point so presumably all 98 are required.) These grades are later entered into a computer to obtain the estimate of the skeletal age and the standard error of this estimate. References in the text to Tables XXI and XXIII on page 241 do not appear to be relevant to these particular tables (which are also referred to in more appropriate context elsewhere).

With experience, the procedure for the use of the method might become more straightforward, but it is doubtful if many European radiologists and clinicians would feel the financial investment in purchasing this expensive book and the other necessary extra items is worth the risk, and it is equally doubtful if the value of the information obtained by use of this method justifies its laboriousness. The Tanner Whitehouse systems have proved their value for British populations and will require more than this to supplant them.

J. M. H. BUCKLER

Glucagon in 1987: Gastrointestinal and Hepatobiliary Physiology Diagnosis and Treatment. Ed. by J. Picazo, pp. x + 175, 1987 (MTP Press, Lancaster), £30.00.
ISBN 0–7462–0055–2

This is a summary of the Third International Workshop on Glucagon held at Barcelona during March 1987. Eleven papers were presented relating to the use of glucagon in gastroenterology and hepatology. All the papers are reproduced in detail and it is clear that they stimulated a considerable amount of debate amongst the participants.

The meeting was divided into two approximately equal portions between gastroenterology and hepatology with naturally most of the diagnostic interest being centred on the gastroenterology section. Even here, however, interest for the diagnostic radiologist is limited, with a total of two chapters devoted to the use of glucagon in the investigation of the upper and lower GI tract. There is useful discussion in both chapters of the advantages and disadvantages of glucagon over anticholinergic drugs when inducing GI hypotonia and the reference section is very comprehensive. A similar debate is carried over into the chapter on glucagon in digestive endoscopy.

The only other chapter of passing interest to the diagnostic radiologist is one by Dr Carr-Locke on the effects of glucagon on the human biliary tree. This contains interesting data of the effects of glucagon on pancreatic and biliary duct pressure measurements and suggests some ways in which it might be used as a therapeutic drug rather than a diagnostic one. The rest of the book is really taken up by the use of glucagon in non-radiological areas and this would limit its value in diagnostic radiology departments. The book would be useful in big libraries as a reference source for both gastroenterologists and radiologists but its limited scope precludes its purchase by the individual radiologist.

Alan Freeman

Recent Developments in Nonionic Contrast Media. Ed. by V. Taenzer and S. Wende, pp. xvi + 240, 1989 (Georg Thieme Verlag, Stuttgart), DM 68.
ISBN 0–86577–300–9 (New York)
3–13–71921–3 (Stuttgart)
ISSN 0178–4609

This slim volume of some 240 pages is an up-to-date and well written review of the state of the art in non-ionic contrast media. It has been prepared under the auspices of Schering in Berlin and, as a result, is not surprisingly very much concerned with new Schering products. This is a perspective, not a criticism, since it must be said that Schering have a long tradition in contrast agent development and a large pool of talent and experience in this field. It is not recommended as a beginner's first introduction to the whole subject but it is an excellent survey of the field, covering studies in angiography, urography, myelography and lymphography with sections on pharmacokinetics and general pharmacology which contain much interesting and basic material. This is a book which will be useful to those who have an interest in contrast media, to those who wish to find out about the latest developments such as non-ionic dimers, to those who plan to carry out clinical studies and would like to read about how it is done, and as a reference source of basic pharmacology of contrast agents for any radiology department.

It is priced at DM 68 which seems reasonable using the current exchange rate but it is not clear how it will be priced in the UK. This will not endear me to Schering but, while we are waiting to hear the price in sterling, perhaps radiologists might ask their local Schering representative if he has the odd copy in his car boot!

P. Dawson

Imaging Techniques in Orthopaedics. Ed. by C. S. B. Galasko and I. Isherwood, pp. xii + 376, 1989 (Springer-Verlag, Berlin), £75.00.
ISBN 3–540–19523–8 (Berlin)
0–387–19523–8 (New York)

Orthopaedic radiology has moved irrevocably from "position as shown" plain film reports to a level of considerable sophistication, routinely using all the imaging techniques of any modern department. This book, edited by two well-known academics, brings together chapters on these techniques, with contributions from 33 authors from around the world. The book is in three sections: Radiological Techniques, Bone Mineral Studies and Clinical Indications. It is aimed at a broad audience, from both sides of the surgical/radiological divide.

Well written, illustrated, produced and referenced to 1986 it is a sensible length. However this inevitably leads to some superficiality of description, which often fails to deliver the promised indications, contraindications and complications of the techniques. Some areas seem redundant (for example epidurography and epidural venography); others out of place in an orthopaedic radiological book (such as arteriography for spinal AVMs) or scantily covered (only one short paragraph on bone biopsy). Some descriptions are heavy on author interest, but light on others, for example non-tumour ultrasound, outpatient radiculography, 3D CT (only one illustration) and non-vascular digital radiography. The final section in which a co-ordinated approach to technique-ulitization is advocated is disappointing, with few sensible management strategems. Personal series appear in the spinal trauma chapter (the purpose of this is unclear), and what about skeletal scintigraphy in painful scoliosis or MRI in avascular necrosis?

Repetition has largely been ironed out by the editors, but one wonders why a very full chapter on skeletal scintigraphy, including joint disease, is followed by another on the latter subject? "Clinical Indications" also contains a chapter on skeletal dysplasia, which seems curiously out of place, as it is organized in gamuts and does not address the role of imaging techniques. It is very difficult to produce a book that is all things to all readers. For the individual, purchase of this book will have to be weighed against others available with a similar purpose. It will be welcomed by staff in those hospitals who do not have a skeletal radiological service (the Skeletal Radiology Group of the Royal College of Radiologists currently comprises about 40 members) as a first-line reference book. Detailed information will require access to more sophisticated texts. It will also whet appetites for those comtemplating a career in skeletal radiology, and stimulate orthopaedic departments without a skeletal radiology service to know what they are missing!

Iain Watt

Appropriate Diagnostic Technology in the Management of Cardiovascular Diseases. Technical Report Series 772. Report of a WHO Expert Committee, pp. 44, 1988 (World Health Organization, Geneva) SFr6; $4.80.
ISBN 92–4–120772–8

This is a small-format paperback book with just over 40 pages. It considers the requirements for diagnostic equipment at primary, secondary and tertiary levels of care in systems of limited, intermediate and advanced states of development.

It asks important questions as to how useful a test is, how easy it is to get people to use the apparatus, and how easy it is to keep the apparatus running. In considering the answers to such questions it comes up with advice on the provision of such equipment at each level of care that is essentially common sense but usefully re-stated in this book.

M. J. Raphael

Radiology of the Foot and Ankle, Ed. by T. H. Berquist, pp. xvi + 511, 1988 (Raven Press, New York), $156.00.
ISBN 0–88167–445–1

This textbook is, quite simply, excellent. I had in fact already ordered a copy before being asked to review it! To have some 500 pages devoted to the radiology of the foot gives an indication of the comprehensive nature of this beautifully illustrated text. Chapters include Anatomy, Diagnostic Techniques, Trauma, The Arthritides, Neoplasms, Infections and Paediatric Disorders. The descriptions include all imaging modalities, including CT and NMR, with full explanations of the images obtained. This work is truly comprehensive and can be thoroughly recommended to all with an interest in the foot. It can, indeed, be used with profit as a reference text in any X-ray department.

I am only too conscious that this is an American book. The profuse illustrations using all imaging modalities on the foot are not available to the reviewer, who also has an interest in foot radiology and who works at one of the best known orthopaedic hospitals in Europe. I shouldn't grumble — we still have conventional radiography.

P. RENTON

Radiology of the Esophagus. By Dieter N. Hüpscher, pp. ix + 121, 1988 (Georg Thieme Verlag, Stuttgart), DM 133.
ISBN 3-13-711201-X (Stuttgart)
0-86577-275-4 (New York)

Considering its importance, the oesophagus remains a neglected organ often falling uncomfortably between the interests of the gastroenterologist, thoracic surgeon, general surgeon and the ENT specialist.

Likewise, although every general radiologist needs a good working knowledge of the oesophagus, specialist interest may be exhibited by the GI radiologist, thoracic radiologist as well as the "CT man". Practical accounts of its radiology are therefore to be found in all the standard speciality textbooks as well as the big general ones. It is relatively rare to encounter a monograph which is entirely devoted to this organ and which encompasses all aspects of its investigation. This is such a book and very well presented it is. It is by a single author and therefore uniformity of style is maintained throughout.

Dr Hüpscher has concentrated on contrast radiology of the oesophagus but devotes chapters to CT and other diagnostic tests. He begins with an outline of the radiological techniques and then details the anatomy and physiology of the pharynx and oesophagus. The subsequent chapters on contrast radiology are extremely comprehensive and very well illustrated. He then concludes with a useful chapter on the appearance of the oesophagus after various anti-reflux operations: a neglected topic.

The book is full of information and the text is complemented by an exhaustive and up-to-date reference section. Dr Hüpscher is to be congratulated on producing such a timely book which firmly reinforces the importance of good radiology of the oesophagus. Despite the relatively high price, its purchase by departmental libraries can be thoroughly recommended.

ALAN FREEMAN

Principles of Radiopharmacology. Ed. by H. Deckard and P. H. Cox, pp. 262, 1987 (Martinus Nijhoff, Dordrecht), Dfl.145.00; US$67.00; £48.25.
ISBN 0-89838-774-4

The book comprises 22 review articles based on lectures of the first and second training course in Radiopharmacology and Radiopharmacy, organized by the joint Committee on Radiopharmaceuticals (ENMS & SNME). The book covers a wide range of topics under the broad categories of Radiochemistry, Radiopharmacy, Radiopharmacology and Radiopharmaco-kinetics.

The editors state that it is aimed at readers from a wide range of disciplines, including pharmacists, radio-chemists, physicists, biochemists, mathematicians, electronic engineers, physicians and technicians. My first impression was that such a broad readership could not be catered for in 262 pages. However, the topics covered have been well chosen and assembled and provide "something" for everyone.

Not surprisingly for a multiauthor work, the style and grammar are variable, but do not unduly detract from the content. As pointed out by the editors, overlapping between the contents of the various papers has not been avoided thus providing different points of view on aspects of the same subject. Despite this disclaimer from the editors I feel that a good job has been done by them in obtaining cross referencing between the articles. Where there was repetition, I felt that it served a useful purpose in reiterating some of the subjects dealt with in previous chapters which is of particular importance for a reader who is not versed in the subject matter.

The figures were in general appropriate, although some would benefit from a clearer explanation in the legend. There are no colour illustrations. At £48.25 the book provides a good-value reference work for use by a departmental library rather than a book for the individual.

ALAN STUTTLE

An Atlas of Planar and SPECT Bone Scans. By I. Fogelman and B. D. Collier, pp. x + 320, 1989 (Martin Dunitz, London), £79.95.
ISBN 0-948269-77-4

The introduction of ^{99}Tc^{m}-labelled diphosphonates, together with the increasing sophistication of the gamma camera has revolutionized the diagnosis of bone disease over the past decade. Owing to the rapid development of this imaging technique, the requests for routine bone scans still continue to increase in most nuclear medicine departments and form the greatest part of the workload.

This atlas provides a comprehensive collection of ^{99}Tc^{m}-labelled diphosphonate bone scans drawn from the authors' wealth of experience in two busy hospitals, one either side of the Atlantic. Other imaging techniques are only mentioned when relevant to the cases presented. Most of the material is related to the adult skeleton although some paediatric examples are included. Over 900 high-quality illustrations are presented in a well set-out manner, aiming to provide a reference book for all who are involved with the diagnosis of skeletal abnormality.

After a brief introduction to the mechanism of tracer uptake and to the techniques of both planar and single photon emission computed tomography (SPECT), there is a section of "pattern recognition". This includes examples of normals of all ages; technical and positional artefacts and pitfalls both in conventional and SPECT scanning. This section will be most useful for those sitting the Part I FRCR. The rest of this section considers the importance of "pattern recognition" of disease processes, in that often the nature and distribution of tracer uptake will suggest the diagnosis. A symmetrical pattern of increased uptake is a feature of metabolic bone disease whereas trauma should be suspected with adjacent or clusters of lesions, especially in the thoracic cage.

Apart from the last chapter, which is a useful collection of miscellaneous topics and examples, the rest of the book is dedicated to solving clinical problems. The indications for requesting bone scans are divided into three categories: (a) investigation of bone pain; (b) investigation of malignancy and (c) investigation of benign bone disease.

"Teaching points" are found extensively throughout the text and these provide a wealth of condensed information particularly useful for Part II FRCR candidates.

The high sensitivity and low specificity of bone scanning presents a minefield for the inexperienced reporter, often resulting in over- rather than under-diagnosis. There has been a need for some time for an atlas of this type for all radiologists, nuclear medicine specialists and other doctors who report on bone scans.

I think this superb atlas is £80.00 well spent by any medical library and should be considered an essential bench copy for any department carrying out routine bone scanning. It is, after all, barely the cost of a single examination!

N. A. BARRINGTON

BJR THE BRITISH JOURNAL OF RADIOLOGY

Established 1896

The Editorial Committee

Honorary Editors
N. J. McNally, BSc, MSc, PhD
D. G. Shaw, FRCP, FRCR

Deputy Editors
C. K. Bomford, BSc, MPhil, FInstP
D. M. King, MB, BS, FRCR, DMRD

Associate Editors
P. Armstrong, MB, BS, FRCR, DMRD
H. Baddeley, MB, BS, DMRD, FRCR, MRACR
P. R. Blake, MB, BS, BSc, FRCR
J. A. Bullimore, MB, BS, MRCS, LRCP, DMRT, FRCR
R. G. Dale, MSc, PhD, CPhys, FInstP
P. Dawson, BSc, PhD, MB, BS, MRCP, MInstP, FRCR
S. Dische, MD, FRCR
F. A. Duck, PhD, MIEEE
A. H. Freeman, MB, BS, FRCR
R. M. Harrison, BSc, MSc, PhD, FInstP
J. W. Hopewell, BSc, PhD
H. W. C. Loose, DMRD, FRCR
A. M. Peters, BSc, MSc, MB, ChB, MRCPath
D. W. Pilling, MB, ChB, DCH, DMRD, FRCR
J. F. Reidy, MB, BS, FRCP, FRCR
J. R. K. Savage, DSc
R. A. Shields, PhD
D. M. Tait, MB, ChB, MRCP, FRCR
J. Tudor, MB, BS, FRCR
A. R. Valentine, MB, BS, MRCS, LRCP, FRCR, DMRD
G. H. Whitehouse, MB, BS, FRCP, FRCR, DMRD
A. G. Wilson, FRCP, FRCR
E. P. Wraight, MB, BChir, PhD, DMRT

Associate Editors Overseas
S. G. A. Chenery, PhD, FCCPM (North America)
B. J. Cremin, MD, FRCR, FRACR (South Africa)
R. Fox DPhil (Australia)
M. Takahashi, MD (Japan)
D. M. Taylor, DSc, CChem, FRSC (Continental Europe)

Managing Editor: T. R. Hogan, BSc, PhD

© 1989 The British Institute of Radiology, 1989

New Series
VOLUME 62
JANUARY TO DECEMBER, 1989

Published by
THE BRITISH INSTITUTE OF RADIOLOGY
36 Portland Place, London W1N 4AT

INDEX TO AUTHORS
1989

Adam, E. J. *See* Mills, P.
Adler, J. and Robey, G., 627
Afshar, F. *See* Thomson, E. S.
Agarwal, P. *See* Savit, R. M.
Aggarwal, S. *See* Sharma, S.
Ainslie, J. *See* Ashby, M. A.
Akyol, F. H. *See* Atahan, I. L.
Alanyali, H. *See* Atahan, I. L.
Alcock, C. J. *See* Wiernick, G.
Alevizaki, C., Georgiou, E., Nikiforakis, E. and Proukakis, C., 497
Alexander, M. S. M., Edelman, G. M., Man, K. and Randall, C. J., 724
Allan, P. L. *See* Loupas, T.
Allison, D. J. *See* Jackson, J. E.
Al-Mokhlef, J. *See* El-Khatib, E. L.
Amols, H. I. *See* Brenner, D. J.
Anderson, P. B. *See* Morcos, S. K.
Andersson, T., Ericsson, A., Eriksson, B., Hemmingsson, A., Lindh, E., Nyman, R. and Oberg, K., 433
Andreucci, V. E. *See* Iaccarino, V.
Armstrong, S. J., and Watt, I., 178
Arnot, R. N. *See* Peters, A. M.
Ash, D. V. *See* Robinson, A. C. R.
Ashby, M. A., Pacella, J. A., de Groot, R. and Ainslie, J., 608
Astor, M. *See* Bewley, D. K.
Atahan, I. L., Akyol, F., Gürkaynak, M., Alanyali, H. and Øzyar, E., 1107
Atahan, I. L., Akyol, F., Zorlu, F. and Gürkaynak, M. 854
Ayton, V. T. *See* Smith, M. A.
Ayyangar, K. M. *See* Palta, J. R.

Bader, D. *See* Baker, M. R.
Baker, E. J. *See* Smith, M. A.
Baker, M. R., Bader, D. and Hopewell, J. W., 830
Ball, P. *See* Turner, M. J.
Bamane, V. S. *See* Ranade, S. S.
Barber, C. J. *See* Choudri, A. H.
Barber, C. J. *See* Iaccarino, V.
Barber, C. *See* Stevens, J. M.
Barry, J. L. *See* Faulkner, K.
Barter, S. *See* Stevens, J. M.
Bates, T. D., 634
Bates, T. D. and Scott, O. C. A., 91, 956
Bates, T. D. *See* Wiernik, G.
Batinić, D. *See* Sarajlić, M.
Batty, V. *See* Herbetko, J.
Baudouin, S. V. *See* Morcos, S. K.
Bayliss, A. P. *See* Smith, F. W.
Becker, W., Schaefer, R. M. and Börner, W., 463
Becker, C. D. *See* Malone, D. E.
Beedie, R. *See* Morcos, S. K.
Behan, M. *See* Daly, B. D.
Bell, D., Millar, A. M., Grayshan, R. and Muir, A. L., 294
Bellemore, M. C. *See* Kozlowski, K.
Bellman, S. *See* Ng, Y. Y.
Bennett, I. C., Downes, M. O. and Collins, R. E. C., 489
Bentzen, S. M. and Thames, H. D., 633
Berry, R. J. *See* Wiernik, G.
Bewley, D. K., Cullen, B. M., Astor, M., Hall, E. J., Blake, S. W., Bonnett, D. E. and Zaider, M., 344
Bews, J. *See* Huda, W.
Bezirdjian, D. R. and Szucs, R., 171
Binns, P. J. *See* Slabbert, P. J.
Bisset, R., 953
Blake, N. S. and O'Connell, E., 443
Blake, P. *See* Constant, O.
Blake, P. R. *See* Burnet, N. G.
Blake, S. W. *See* Bewley, D. K.
Blakeborough, A. *See* Jeans, W. D.
Blekkenhorst, G. *See* Madhoo, J.
Bodley, R. N. *See* Todd, B. D.
Bol, A. *See* Vynckier, S.
Bonnett, D. E. *See* Bewley, D. K.
Borgstein, R. L., Shaw, J. J. and Pearson, R. H., 1019
Börner, W. *See* Becker, W.
Bougnoux, P. *See* Calais, G.
Bradić, I. *See* Sarajlić, M.
Bradnock, B. *See* Moss, J. G.
Bradshaw, A. *See* Dawson, P.
Bradshaw, C. R. *See* Buckland-Wright, J. C.
Breiter, N., Sassy, T. and Trott, K.-R., 381
Brenner, D. J. and Amols, H. I., 910
Brentanos, E. *See* Schouman-Claeys, E.
Bretland, P. M., 95
Brindle, J. M. *See* Wiernik, G.
Brownless, S. M. and Gimlette, T. M. D., 532
Brunton, F. J. *See* Rawlinson, J.
Buckland-Wright, J. C., 201
Buckland-Wright, J. C. and Bradshaw, C. R., 209
Budd, R. S., Hodgson, G. S. and Hare, W. S. C., 314, 318
Buirski, G., 274
Bundey, S. *See* Chapman, S.
Burhenne, H. J. *See* Malone, D. E.
Burnet, N. G. and Blake, P. R., 856
Burt, P. A., Notley, H. M. and Stout, R., 748
Burton, I. E. *See* Jackson, A.
Bury, R. W. *See* Morcos, S. K.

Cadigan, P., 82
Calais, G., Reynaud-Bougnoux, A., Bougnoux, P. and Le Flock, O., 849
Calder, C. J. *See* Duddy, M. J.
Calzado, A. *See* Vãńo, E.
Campell, I. R. and Warenius, H. M., 338
Cannon, R. *See* Given-Wilson, R.
Carney, D. *See* Robinson, A. C. R.
Carter, S. R., Davies, A. M., Evans, N. and Grimer, R. J., 269
Carter, S. R. *See* Davies, A. M.
Carty, H. *See* Walker, J.
Carvalho, P., 1094
Cassar-Pullicino, V. N. *See* Davies, A. M.
Catterall, M. 874
Chan, T. Y. K. and Davidson, T., 1034
Chandy, J. *See* Cook, J. V.
Chandy, J. *See* Davies, A. M.
Chang, H. *See* Chun, M.
Chang, H. *See* Wu, A.
Chapman, S., Gray, R. G. F., Constable, T. J. and Bundey, S., 491
Chapman, B. *See* Worthington, B. S.
Charlesworth, M. *See* Murray, P. A.
Chen, M.-S., Lin, F.-J., Tang, S. G., Leung, W.-M. and Leung, W., 739
Cherryman, G. R. *See* Williams, M. P.
Chippindale, A. J., 1101
Choi, B. I., Park, J. H., Kim, B. H., Kim, S. H., Han, M. C. and Kim, C.-W., 897
Choi, P. H. K. *See* Sham, J. S. T.

INDEX TO VOLUME 62

Choudhri, A. H., Rowlands, P. C., Barber, C. J., Johnson, J. and Stevens, J. M., 253
Choy, D. *See* Sham, J. S. T.
Chun, M., McKeough, P., Wu, A., Kasdon, D., Heros, D. and Chang, H., 158
Chun, M. *See* Wu, A.
Clarke, S. E. *See* West, D. J.
Clarkson, D. G., 94
Coakley, A. J. *See* Mountford, P. J.
Cobby, M. J. D., Culling, W., Jordan, S. C. and Hartnell, G. G., 371
Cobby, M., Duncan, A. and Hartnell, G., 561
Coffey, S. L. *See* Daly, B. D.
Cohen, P. *See* den Hartog Jager, F. C. A.
Colapinto, R. F. *See* Odurny, R. F.
Coldwell, D. M. Huff, J., Marcellus, H. and Coldwell, S. G., 234
Coldwell, S G. *See* Coldwell, D. M.
Collard, J.-M., *See* van Beers, B.
Collins, M. C. *See* Houston, J. P.
Collins, R. E. C. *See* Bennett, I. C.
Conere, T., Weatherburn, H. and Wassem, B., 1033
Constable, T. J. *See* Chapman, S.
Constant, O. and Blake, P., 623
Conway, J. *See* Sims, C.
Cook, J. V., Phelps, P. D. and Chandy, J., 74
Cook, J. V. and Tayar, R., 1043
Courdi, A., 298
Cowen, A. R., 999
Coxon, R. *See* Worthington, B. S.
Crawley, J. C. *See* Jain, D.
Creagh, M. F., MacDonald, L. M. and Garvie, D. C., 951
Crock, H. V., *See* Saywell, W. R.
Crofton, M. *See* Grech, P.
Crofton, M. E. *See* Tran, T.
Crooijmans, R. P. M. A. *See* Schwachöfer, J. H. M.
Crosher, G. A. *See* Smith, F. W.
Crowley, B. M. *See* Daly, B. D.
Crues, J. V. *See* Shellock, F. G.
Cruikshank, J. G. *See* Wardlaw, J. M.
Cullen, B. M. *See* Bewley, D. K.
Culling, W. *See* Cobby, M. J. D.
Cullum, I. D., Ell, P. J. and Ryder, J. P., 587

Dalby, J. E. *See* Wiernik, G.
Dale, R. G., 241
Daly, B. D., Coffey, S. L. and Behan, M., 1017
Daly, B. D. and Crowley, B. M., 256, 1034
Daly, B. D. and Moore, D. P., 859
Daly, L. *See* Logan, H.
Daly, B. D. *See* Robinson, A. C. R.
Dantas, R. O., 876
Darwin, C. J. *See* Warren, R. C.
Davidson, T. *See* Chan, T. Y. K.
Davies, A. M., 877
Davies, A. M., Carter, S. R., Grimer, R. J. and Sneath, R. S., 893
Davies, A. M. and Cassar-Pullicino, V. N., 1050
Davies, A. M. and Evans, N., 1103
Davies, A. M., Evans, N. and Chandy, J., 716
Davies, A. M., Evans, N. and Grimer, R. J., 183
Davies, A. M. *See* Carter, S. R.
Davies, P. *See* McCullough, M.
Davies, P. *See* Stinchcombe, S. J. Davies, R. Ll. *See* Jones, D. R.
Dawes, P. J. D. K., Dean, E. M. and Lambert, G. D., 64
Dawes, P. J. D. K., Patrick, D. and Hall, K., 729
Dawson, P. and Bradshaw, A., 631
Day, M. J., 498
Dean, E. M. *See* Dawes, P. J. D. K.
Deans, H. E., Smith, F. W., Lloyd, D. J., Law, A. N. and Sutherland, H. W., 603
de Belder, M. A. *See* Page, J. E.
Deehan, C., 874
Deehan, C. and O'Donoghue, J. A., 566, 874
de Groot, R. *See* Ashby, M. A.
Delgado, V. *See* Vãno, E.
den Hartog Jager, F. C. A., Cohen, P. and van Haastert, M., 807
den Hollander, J. C. *See* Schipper, J.
Devière, J. *See* van Gansbeke, D.
Dewbury, K. C., 293
Dixon, A. K. *See* Moore, N. R.
Dobrowsky, W., 53
Dock, W., Hajek, P., Wittich, G., Kumpan, W. and Grabenwöger, F., 940
Dodd, N. J. F. *See* Moore, J. V.
Dodds, W. J. *See* Taylor, A. J.
Doughty, D. *See* Plowman, P. N.
Downes, M. O. *See* Bennett, M. O.
Doyle, A. J., 176
Duck, F. A., Starritt, H. C., ter Haar, G. R. and Lunt, M. J., 1005
Duddy, M. J. and Calder, C. J., 180
Duncan, A. *See* Cobby, M.
Dunscombe, P. B. and Fox, K., 48
Durst-Zivković, B. *See* Sarajlić, M.
du Toit, J. P. *See* Smit, B. J.

Eddelston, B. *See* Chippindale, A. J.
Edelman, G. M. *See* Alexander, M. S. M.
Edwards, S. *See* Nisbet, A. P.
Eikelboom, B. C. *See* Teeuwen, C.
El-Khatib, E. G., Rymel, J. and Al-Mokhlef, J., 744
Ell, P. J. *See* Cullum, I. D.
Elliott, V. *See* Pye, S. D.
Ellis, F., 954
England, J. P. S. *See* Saywell, J. P. S.
Erdentug, M. A. *See* Parkin, A.
Ericsson, A. *See* Andersson, T.
Eriksson, B. *See* Andersson, T.
Evans, N. *See* Carter, S. R.
Evans, N. *See* Davies, A. M.
Evans, N. *See* Morgan, A.
Evans, K. T. *See* Jones, D. R.
Ewen, C. and Hendry, J. H., 283
Faulkner, K., Barry, J. L. and Smalley, P., 230
Faulkner, K. *See* Law, J.
Feola, J. *See* Yaes, R. J.
Finstone, H. *See* Goldfarb, C. R.
Fitzgerald Finch, O. P. *See* Mahendran, M.
Fitzgerald, R., Mackie, G. and Manns, R., 293
Fogelman, I. *See* West, D. J.
Fønstelien, E. *See* Høiseth, A.
Ford, E. H. *See* Hong, S. S.
Forman, A. G. G. *See* Jeans, W. D.
Forrest, A. P. M., 695
Fowler, J. F., 679
Fowler, J. F. *See* Wiernik, G.
Fox, P. *See* Dunscombe, P. B.
Freer, C. E. L. *See* Moore, N. R.
Frija, G. *See* Schouman-Claeys, E.
Fritz, P., Rieden, K., Lenarz, T., Haels, J. and zum Winkel, K., 107

Gaffney, C. C. *See* Shirato, H.
Gaines, P. A. and Sampson, M. A., 335
Gainey, G. T. *See* Litten, R. Z.
Gajek, W. R. *See* Wiernik, G.
Garrett, A. *See* Scally, J.

INDEX TO AUTHORS—continued

Garvie, D. C. *See* Creagh, M. F.
Gattamaneni, H. R. *See* Wallace, W. H. B.
Gelin, M. *See* van Gansbeke, S.
Gemmell, H. G. *See* Smith, D. F.
Georgiou, E. *See* Alevizaki, C.
Gibbon, W. W. and Jackson, A., 487
Gimlette, T. M. D. *See* Brownless, S. M.
Given-Wilson, R., Pope, R. M., Michell, M. J., Cannon, R. and McGregor, A. M., 705
Glaholm, J. and Harmer, C., 298, 876
Glenthøj, A. *See* Karstrup, S.
Goddard, B. A., 1033
Godfrey, L. W. *See* Todd, B. D.
Goldfarb, C. R., Ongseng, F. and Finestone, H., 387
González, L. *See* Vãño, E.
Goodman, G. G. *See* Shirato, H.
Goodman, S. *See* Wiernik, G.
Gordon, I. *See* Peters, A. M.
Goulatia, R. K. *See* Sharma, S.
Grabenwöger, F. *See* Dock, W.
Graham, N. *See* Guest, P. J.
Gray, R. G. F. *See* Chapman, S.
Graysham, R. *See* Bell, D.
Grech, P., Rowlands, P. and Crofton, M., 753
Grech, P. *See* Tran, T.
Greenspan, B. *See* Hong, S. S.
Griffiths, G. J. *See* Jones, D. R.
Grimer, R. J. *See* Carter, S. R.
Grimer, R. J. *See* Davies, A. M.
Groenewald, W. A. *See* Smit, B. J.
Grundy, A. *See* Harrison, A.
Guest, P. J., McLean, A. and Graham, N., 629
Gürkaynak, M. *See* Atahan, I. L.
Guttenberger, R. and Thames, H. D., 1107
Gwilt, D. J. *See* Mahendran, M.

Haels, J. *See* Fritz, P.
Hainau, B. *See* Karstrup, S.
Hajek, P. *See* Dock W.
Hall, A. J. *See* Parkin, A.
Hall, E. J., 765
Hall, E. J. *See* Bewley, D. K.
Hall, K. *See* Dawes, P. J. D. K.
Halliwell, M., Key, H., Jenkins, D., Jackson, P. C. and Wells, P. N. T., 824
Han, M. C. *See* Choi, B. I.
Hansell, D. M. and Strickland, B., 1
Hanson, M. E. *See* Tait, W. H.
Hare, W. S. C. *See* Budd, R. S.
Harmer, C. *See* Glaholm, J.
Harmer, C. L. *See* O'Connell, M. E. A.
Harnett, A. N. *See* Murray, P. A.
Harnett, A. N. *See* Plowman, P. N.
Harrison, A., Machin, L. and Grundy, A., 85
Harrison, T. J. *See* Jones, D. R.
Hartnell, G., 1034
Hartnell, G. G. *See* Cobby, M. J. D.
Hartnell, G. *See* Cobby, M.
Havard, A. C., 295
Haybittle, J. L. *See* Wiernik, G.
Hayward, M. W. J. *See* Whyte, A. M.
Hegedüs, L. *See* Karstrup, S.
Hekali, P. E. *See* Lamminen, A. E.
Heller, M. *See* Spielmann, R. P.
Hemmingsson, A. *See* Andersson, T.
Hendry, J. H. *See* Ewen, C.
Hendry, J. H. *See* Wallace, W. H. B.
Henk, J. M. *See* Wiernik, G.
Henson, J. H. L. *See* Jeans, W. D.
Herbetko, J., Batty, V. and Millar, J. G. B., 1026
Hering, E. R., Sealy, R., Korrubel, J. B. and Hill, J., 266
Hernandez, J. C. *See* Maruyama, Y.
Heron, C. W. *See* Williams, M. P.
Heros, D. *See* Chun, M.
Heros, D. *See* Wu, A.
Hiles, P. A. *See* Ramsdale, M. L.
Hill, J. *See* Hering, E. R.
Ho, C. M. *See* Sham, J. S. T.
Hodgson, G. S. *See* Budd, R. S.
Høiseth, A., Reikers, O. and Fønstelien, E., 114
Holland, I. M. *See* Rothwell, C. I.
Holloway, T. M. A. *See* Jeans, W. D.
Holm, H. H. *See* Karstrup, S.
Hong, S. S., Ford, E. H. and Greenspan, B., 468
Hoogenhout, J. *See* Schwachöfer, J. H. M.
Hopewell, J. W. and van den Aardweg, G. M. J. M., 1109
Hopewell, J. W. *See* Baker, M. R.
Hopewell, J. W. *See* Morris, G. M.
Hopewell, J. W. *See* Simmonds, R. H.
Hopewell, J. W. *See* Wiernik, G.
Horiuchi, J.-I. *See* Hoshina, M.
Hornsey, S., 765
Horrow, M. M. *See* Savit, R. M.
Hoshina, M., Shibuya, H., Horiuchi, J.-I., Matsubara, S., Suzuki, S. and Takeda, M., 59
Hough, J. H. *See* Slabbert, J. P.
Hounsell, A. R. *See* Walker, A.
Hourihan, M. D. *See* Whyte, A. M.
Houston, J. P., Sampson, M. A. and Collins, M. C., 273
Howard, N. *See* Wiernik, G.
Huda, W., Bews, J. and Saydak, A. P., 921
Huda, W., Sandison, G. A. and Lee, T. Y., 138
Huff, J. *See* Coldwell, D. M.
Hughes, M. *See* Nicholson, D. A.
Hughes, P. L. *See* Lewis-Jones, H. G.
Husband, J. E. *See* Williams, M. P.
Hussey, J. K. *See* Smith, F. W.

Iaccarino, V., Russo, D., Niola, R., Muto, R., Testa, A., Andreucci, V. E. and Porta, E., 593
Inglis, J. A. *See* Law, J.
Ipinyomi, J. and Watt, I., 279
Isherwood, I. *See* Taylor, P. M.

Jackson, A. and Burton, I. E., 944
Jackson, A. *See* Gibbon, W. W.
Jackson, J. E. and Allison, D. J., 379
Jackson, J. E. and O'Donnell, C. J., 867
Jackson, P. C. *See* Halliwell, M.
Jain, D., Lahiri, A., Crawley, J. C. and Raftery, E. B., 294
Jalloh, S. *See* Mahendran, M.
Janeczek, J. *See* Mustafa, A. A.
Jaspan, T. *See* Rothwell, C. I.
Jeans, W. D., 194
Jeans, W. D. *See* Smithson, P. H.
Jeans, W. D., Henson, J. H. L., Holloway, T. M. A., Forman, A. G. G. and Blakeborough, A., 121
Jenkins, D. *See* Halliwell, M.
Jennings, K. *See* Metcalfe, M. J.
Jerusalem, C. R. *See* Schwachöfer, J. H. M.
Johnson, J. *See* Choudhri, A. H.
Jones, C. H., 69
Jones, D. R., Griffiths, G. J., Parkinson, M. C., Evans, K. T., Roberts, E. E., Davies, R. Ll., Harrison, T. J. and Peeling, W. B., 1059
Jones, H. L. *See* Slabbert, J. P.
Jones, R. A. *See* Metcalfe, M. J.

INDEX TO VOLUME 62

Jones, S. N. *See* Rickards, D. R.
Jordan, S. C. *See* Cobby, M. J. D.
Joseph, A. E. A. *See* Mills, P.

Kagan, A. R. *See* Rao, A.
Kaiser, A. M. *See* Peters, A. M.
Kal, H. B. *See* Schwachöfer, J. H. M.
Kälebo, P. and Strid, K.-G., 883
Kalifa, G. *See* Schouman-Claeys, E.
Kartstrup, S., I. Transbøl, Holm. H. H., Glenthøj, A. and Hegedüs, L., 1037
Karstrup, S., Glenthøj, A., Hainau, B., Hegedüs, L., Torp-Pedersen, S. and Holm, H. H., 981
Kasdon, D. *See* Wu, A.
Kasdon, D. *See* Chun, M.
Kenney, I. J. and Lutkin, J. E., 497
Kerslake, R. *See* Stevens, J. M.
Key, H. *See* Halliwell, M.
Khosla, A. *See* Sharma, S.
Khoury, G. G. *See* Robinson, A. C. R.
Kim, B. H. *See* Choi, B. I.
Kim, C.-W. *See* Choi, B. I.
Kim, S. H. *See* Choi, B. I.
Kim, Y. T. *See* Ward, W. F.
Kirkbride, P. and Plowman, P. N., 457
Kirkpatrick, A. E. *See* Law, J.
Klosok, J. *See* Stuttle, A. W. J.
Knight, R. S. G. *See* Smith, D. F.
Knowles, J. F. and Nimmon, C. C., 87
Korhola, O. A. *See* Lamminen, A. E.
Korrubel, J. B. *See* Herring, E. R.
Koslin, D. B. *See* Williams, M. P.
Koslowski, K. and Tsuruta, T., 376
Kozlowski, K. and Bellemore, M. C., 862
Kumpan, W. *See* Dock W.
Kung, E. E. *See* Spielmann, R. P.

Lacert, P. *See* Schouman-Claeys, E.
Ladusans, E. J. *See* Smith, M. A.
Lahiri, A. *See* Jain, D.
Lalande, G. *See* Schouman-Claeys, E.
Lamb, G. H. R. *See* Lewis-Jones, H. G.
Lambert, G. D. *See* Dawes, P. J. D. K.
Lamminen, A. E., Hekali, P. E., Tiula, E., Suramo, I. and Korhola, O. A., 326
LaRiviere, P. D., 473
Laurence, V. M. and Robinson, A. C. R., 83
Lavender, J. P. *See* Peters, A. M.
Lavender, J. P. *See* Stuttle, A. W. J.
Law, J. and Kirkpatrick, A. E., 163, 565
Law, J., Faulkner, K. and Smith, S., 192
Law, J., Inglis, J. A. and Tolley, D. A., 185
Law, A. N. *See* Deans, H. E.
Lawinski, C. P. *See* Ramsdale, M. L.
Le Floch, O. *See* Calais, G.
Lee, T. Y. *See* Huda, W.
Lee, S. H., 495
Lenarz, T. *See* Fritz, P.
Leung, W.-M. *See* Chen M.-S.
Leung, W. *See* Chen, M.-S.
Lewis-Jones, H. G., Lamb, G. H. R. and Hughes, P. L., 977
Lin, F.-J. *See* Chen, M.-S.
Lin, P.-S. *See* Wazer, D. E.
Lindh, E. *See* Andersson, T.
Lindup, R. *See* Wiernik, G.
Litten, R. Z., Walden, T. L., Gainey, G. T. and Nagai, R., 189
Lloyd, D. J. *See* Deans, H. E.
Logan, H., Daly, L. and Masterson, J., 237
Loupas, T., Allan, P. L. and McDicken, W. N., 761
Ludwig, J. W. *See* Teeuwen, C.
Lunt, M. J. *See* Duck, F. A.
Lutkin, J. E. *See* Kenney, I. J.

MacDonald, L. M. *See* Creagh, M. F.
Machin, L. *See* Harrison, A.
Mackie, G. *See* Fitzgerald, R.
Madhoo, J. and Blekkenhorst, J., 281
Mahendran, M., Gwilt, D. J., Fitzgerald Finch, O. P. and Jalloh, S., 174
Maisey, M. N. *See* Nisbet, A. P.
Maisey, M. N. *See* Smith, M. A.
Maisey, M. N. *See* West, D. J.
Malone, D. E., Becker, C. D., Reich, K. D., Quenville, N. F. and Burhenne, H. J., 843
Man, K. *See* Alexander, M. S. M.
Manhire, A. R. *See* Rocker, G. M.
Manifold, I. H. *See* Sims, C.
Manns, R. *See* Fitzgerald, R.
Mansfield, P. *See* Worthington, B. S.
Marcellus, H. *See* Coldwell, D. M.
Marshall, I. *See* Pye, S. D.
Martin, D. F. and Nicholson, D., 953
Martin, D. F. *See* Nicholson, D. A.
Martin-Smith, *See* P. Mills, J. A.
Maruyama, Y., Yaes, R. J., Urano, M., Patel, P. and Hernandez, J. C., 386
Maruyama, Y. *See* Yaes, R. J.
Mashiter, G. *See* Nisbet, A. P.
Masterson, J. *See* Logan, H.
Matos, C. *See* van Gansbeke, D.
Matsubara, S. *See* Hoshina, M.
Maurer, H.-J., 498
Maurice, H. and Watt, I., 31
McCullough, M., Davies, P. and Richardson, R., 260
McDicken, W. N. *See* Loupas, T.
McDicken, W. N. *See* Pye, S. D.
McGregor, A. M. *See* Given-Wilson, R.
McKeough, P. *See* Wu, A.
McKeough, P. *See* Chun, M.
McLean, A. *See* Guest, P. J.
McLoughlin, M. J. *See* Odurny, A.
McMillan, M. A. *See* Straiton, J. A.
Melange, M. *See* van Beers, B.
Meng, Q. and Watt, I., 321
Metcalfe, M. J., Jones, R. A., Redpath, T. W., Smith, F. W., Jennings, K. and Walton, S., 1063
Michel, C. *See* Vynckier, S.
Michell, M. J. *See* Given-Wilson, R.
Miles, K. A., 871
Millar, A. M. *See* Bell, D.
Millar, D. *See* Pye, S. D.
Millar, J. G. B. *See* Herbetko, J.
Mills, P. and Parsons, C. A., 287
Mills, J. A. and Martin-Smith, P., 565
Mills, P., Joseph, A. E. A. and Adam, E. J., 974
Misra, N. *See* Sharma, S.
Mistry, R. *See* West, D. J.
Molteni, A. *See* Ward, W. F.
Moore, N. R., Dixon, A. K. and Freer, C. E. L., 710
Moore, D. P. *See* Daly, B. D.
Moore, J. V., Dodd, N. J. F. and Wood, B., 869
Moran, P. *See* Vãño, E.
Morcos, S. K., 293
Morcos, S. K., Baudouin, S. V., Anderson, P. B., Beedie, R. and Bury, R. W., 383
Moreman, B. *See* Taylor, P. M.
Morgan, A. and Evans, N., 78
Morley, P. *See* Straiton, J. A.
Morris, G. M. and Hopewell, J. W., 41

INDEX TO AUTHORS—continued

Morris-Jones, P. H. *See* Wallace, W. H. B.
Moseley, I. F. *See* Travis, R. C.
Moskovic, E. and Ramachandra, S., 1021
Moss, J. G., Sellar, R. J. and Bradnock, B., 755
Mountford, P. J. and Coakley, A. J., 388
Muir, A. L. *See* Bell, D.
Muller, P. *See* van Gansbeke, D.
Murphy, P. *See* Smithson, P. H.
Murray, P. I. *See* Travis, R. C.
Murray, P. A., Harnett, A. N., Thompson, P. I., Charlesworth, M. and Plowman, P. N., 1075
Mustafa, A. A. and Janeczek, J., 838
Muto, R. *See* Iaccarino, V.

Nagai, R. *See* Litten, R. Z.
Najm, Y. C. *See* West, D. J.
Nakajima, T., 148
Nanda Kumar, E. *See* Nicholson, D. A.
Ng, Y. Y., Bellman, S. and Phelps, P. D., 947
Nias, A. H. W. and Perry, P. M., 932
Nicholson, D. A., Zammit-Maempel, I., Hughes, M., Nandar Kumar, E. and Martin, D. F., 447
Nicholson, D. *See* Martin, D. F.
Nikiforakis, E. *See* Alevizaki, C.
Nimmon, C. C. *See* Knowles, J. F.
Niola, R. *See* Iaccarino, V.
Nisbet, A. P., Shaw, P., Taube, D., Edwards, S., Maisey, M. N. and Mashiter, G., 438
Norwood, H. *See* Parkin, A.
Notley, H. M. *See* Burt, P. A.
Nyman, R. *See* Andersson, T.

Oberg, K. *See* Andersson, T.
O'Connell, E. *See* Blake, N. S.
O'Connell, M. E. A., Powell, B. W. E. M., O'Connell, J. M. and Harmer, C. L., 1096
O'Connell, J. M. *See* O'Connell, M. E. A.
O'Donnell, C. J. *See* Jackson, J. E.
O'Donoghue, J. A. *See* Deehan, C.
Odurny, A., McLoughlin, M. J., Colapinto, R. F. and Sniderman, K. W., 6
Onseng, F. *See* Goldfarb, C. R.
Ordidge, R. *See* Worthington, B. S.
Ott, R. J., 421
Ozyar, E. *See* Atahan, I. L.

Pacella, J. A. *See* Ashby, M. A.
Page, J. E., Wilson, A. G. and de Belder, M. A., 986
Palta, J. R., Ayyangar, K. M., Suntharalingham, N. and Tupchong, L., 927
Panzer, W. and Zankl, M., 936
Park, J. H. *See* Choi, B. I.
Parkin, A., Norwood, H., Erdentug, M. A. and Hall, A. J., 620
Parkinson, M. C. *See* Jones, D. R.
Parsons, C. A. *See* Mills, P.
Parsons, J. M. *See* Smith, M. A.
Patel, P. *See* Maruyama, Y.
Patel, B. *See* Chippindale, A. J.
Patrick, D. *See* Dawes, P. J. D. K.
Pearson, D. *See* Rocker, G. M.
Pearson, R. H. *See* Borgstein R. L.
Peeling, W. B. *See* Jones, D. R.
Perry P. M. *See* Nias, A. H. W.
Peters, A. M., 536
Peters, A. M. *See* Stuttle, A. W. J.
Phelps, P. D. *See* Cook, J. V.
Phelps, P. D. *See* Ng, Y. Y.
Phillips, D. L. *See* Wiernik, G.
Picard, A. *See* Schouman-Claeys, E.
Plowman, P. N., Doughty, D. and Harnett, A. N., 218
Plowman, P. N. *See* Kirkbride, P.
Plowman, P. N. *See* Murray, P. A.
Plowman, P. N. *See* Thomson, E. S.
Pointon, R. C. S. *See* Slevin, N. J.
Pointon, R. S. *See* Wiernik, G.
Pope, R. M. *See* Given-Wilson, R.
Porta, E. *See* Iaccarino, V.
Powell, B. W. E. M. *See* O'Connell, M. E. A.
Powell-Jackson, P. R., 387
Pratt, T. A. and Sweeney, J. K., 734
Proukakis, C. *See* Alevizaki, C.
Pye, S. D., Elliott, V., Marshall, I., Millar, D., Robertson, S., McDicken, W. N. and Wild, S. R., 1014

Quenville, N. F. *See* Malone, D. E.

Raftery, E. B. *See* Jain, D.
Rajani, M. *See* Sharma, S.
Ramachandra, S. *See* Moskovic, E.
Ramachandran, T. P. *See* Wilkinson, J. M.
Ramsdale, M. L., Hiles, P. A. and Lawinski, C. P., 484
Ranade, S. S., Trivedi, P. N. and Bamane, V. S., 1111
Randall, C. J. *See* Alexander, M. S. M.
Rao, A., Kagan, A. R. and Steckel, R. J., 864
Rawlinson, J. and Brunton, F. J., 27
Read, M. R. T. F., 194
Redpath, T. W. *See* Metcalfe, M. J.
Reich, K. D. *See* Malone, D. E.
Reikers, O. *See* Høiseth, A.
Reynaud-Bougnoux, A. *See* Calais, G.
Rezvani, M. *See* Wiernik, G.
Richard, F. *See* Vynckier, S.
Richardson, R. *See* McCullough, M.
Rickards, D. and Jones, S. N., 573
Rieden, K. *See* Fritz, P.
Rimmer, S. *See* Taylor, P. M.
Robbins, M. E. C. *See* Simmonds, R. H.
Roberts, E. E. *See* Jones, D. R.
Roberts, R. C. *See* Smith, D. F.
Robertson, G., 366
Robertson, E. M. *See* Smith, F. W.
Robertson, S. *See* Pye, S. D.
Robey, G. *See* Adler, G.
Robinson, A. C. R., Khoury, G. G., Ash, D. V. and Daly, B. D., 245
Robinson, A. C. R., Khoury, G. G. and Carney, D., 1089
Robinson, A. C. R. *See* Laurence, V. M.
Rocker, G. M., Rose, D. H., Manhire, A. R., Pearson, D. and Shale, D. J., 582
Rose, D. H. *See* Rocker, G. M.
Rostom, A. Y. and Sunderland, K., 173
Rostom, A. Y. *See* Stockdale, A. D.
Rothwell, C. I., Jaspan, T., Worthington, B. S. and Holland, I. M., 1067
Rowlands, P. C. *See* Choudhri, A. H.
Rowlands, P. *See* Grech, P.
Russell, J. G. B., 92, 94, 635, 765
Russell, J. G. B. and Weller, J. M., 1111
Russo, D. *See* Iaccarino, V.
Ryder, J. P. *See* Cullum, I. D.
Rymel, J. *See* El-Khatib, E. G.

Sampson, M. A. *See* Gaines, P. A.
Sampson, M. A. *See* Houston, J. P.
Sandison, G. A. *See* Huda, W.

INDEX TO VOLUME 62

Sarajlić, M., Durst-Zivković, B., Svoren, E., Vitković, M., Batinić, D., Bradić, I. and Vučković, I., 551
Sassy, T. *See* Breiter, N.
Savage, J. R. K., 507
Savit, R. M., Horrow, M. M. and Agarwal, P., 79
Saydak, A. P. *See* Huda, W.
Saywell, W. R., 276
Saywell, W. R., Crock, H. V., England, J. P. S. and Steiner, R. E., 290
Scally, J. and Garrett, A., 81
Schaefer, D. J. *See* Shellock, F. G.
Schaefer, R. M. *See* Becker, W.
Schipper, J., van Oostayen, J. A., den Hollander, J. C. and van Seyen, A. J., 35
Schmidt-Ullrich, R. *See* Wazer, D. E.
Schneidau, A. *See* Stevens, J. M.
Schouman-Claeys, E., Picard, A., Lalande, G., Kalifa, G., Lacert, P., Brentanos, E. and Frija, G., 248
Schwachöfer, J. H. M., Crooijmans, R. P. M. A., van Gesteren, J., Hoogenhout, J., Jerusalem, C. R. and Kal, H. B., 1084
Scott, O. C. A. *See* Bates, T. D.
Sealy, R. *See* Hering, E. R.
Sellar, R. J. *See* Moss, J. G.
Shah, K. J. *See* Walsh, M. T.
Shale, D. J. *See* Rocker, G. M.
Shalet, S. M. *See* Wallace, W. H. B.
Sham, J. S. T., Wei, W. I., Choy, D., Ho, C. M., Tai, P. T. H. and Choi, P. H. K., 355
Sharma, S., Sggarwal, S., Talwar, K. K. and Rajani, M., 117
Sharma, S., Rajani, M., Khosla, A., Misra, N. and Goulatia, R. K., 1056
Shaw, J. J. *See* Borgstein, R. L.
Shaw, P. *See* Nisbet, A. P.
Shellock, F. G., Schaefer, D. J. and Crues, J. V., 904
Shibuya, H. *See* Hoshina, M.
Shirato, H., Gaffney, C. C. and Goodman, G. B., 285
Simmonds, R. H., Hopewell, J. W. and Robbins, M. E. C., 915
Sims, C., Manifold, I. H. and Conway, J., 785
Singcharoen, T., 168
Slabbert, J. P., Binns P. J., Jones, H. L. and Hough, J. H., 989
Slevin, N. J. and Pointon, R. C. S., 145
Smalley, P. *See* Faulkner, K.
Smit, B. J., du Toit, J. P. and Groenewald, W. A., 68
Smith, M. A., Baker, E. J., Ayton, V. T., Parsons, J. M., Ladusans, E. J. and Maisey, M. N., 367
Smith, D. F., Smith, F. W., Knight, R. S. G., Roberts, R. C. and Gemmell, H. G., 970
Smith, F. W., Bayliss, A. P., Hussey, J. K., Robertson, E. M., Weir, J. and Crosher, G. A., 796
Smith, F. W. *See* Deans, H. E.
Smith, F. W. *See* Smith, D. F.
Smith, F. W. *See* Metcalfe, M. J.
Smith, S. *See* Law, J.
Smithson, P. H., Jeans, W. D. and Murphy, P., 71
Sneath, R. S. *See* Davies, A. M.
Sniderman, K. W. *See* Odurny, A.
Spielmann, R. P., Küng, E. E., Witte, G. and Heller, M., 373
Starritt, H. C. *See* Duck, F. A.
Steckel R. J. *See* Rao, A.
Stehling, M. K. *See* Worthington, B. S.
Steiner, R. E. *See* Saywell, W. R.
Stevens, J. M. *See* Choudhri, A. H.
Stevens, J. M., Barter, S., Kerslake, R., Schneidau, A., Barber, C. and Thomas, D. J., 813
Stewart, E. T. *See* Taylor, A. J.
Stinchcombe, S. J. and Davies, P., 949
Stockdale, A. D. and Rostom, A. Y., 563
Stout, R. *See* Burt, P. A.
Straiton, J. A., McMillan, M. A. and Morley, P., 803
Strickland, B. *See* Hansell, D. M.
Strid, K.-G. *See* Kälebo, P.
Struyven, J. *See* van Gansbeke, D.
Stuttle, A. W. J., Klosok, J., Peters, A. M. and Lavender, J. P., 963
Sunderland, K. *See* Rostom, A. Y.
Suntharalingam, N. *See* Palta, J. R.
Suramo, I. *See* Lamminen, A. E.
Sutherland, H. W. *See* Deans, H. E.
Suzuki, S. *See* Hoshina, M.
Svoren, E. *See* Sarajlić, M.
Sweeney, J. K. *See* Pratt, T. A.
Symonds, E. M. *See* Worthington, B. S.
Szucs, R. *See* Bezirdjian, D. R.

Tai, P. T. H. *See* Sham, J. S. T.
Tait, W. H. and Hanson, M. E., 613
Takeda, M. *See* Hoshina, M.
Talwar, K. K. *See* Sharma, S.
Tang, S. G. *See* Chen, M.-S.
Taube, D. *See* Nisbet, A. P.
Tawn, D. J. and Watt, I., 790
Tayar, R. *See* Cook, J. V.
Taylor, P. M., Moreman, B., Rimmer, S. and Isherwood, I., 331
Taylor, A. J., Dodds, W. J. and Stewart, E. T., 890
Teeuwen, C., Eikelboom, B. C. and Ludwig, J. W., 13
ter Haar, G. R. *See* Duck, F. A.
Tercilla, O. F. *See* Wazer, D. E.
Testa, A. *See* Iaccarino, V.
Thames, H. D. *See* Bentzen, S. M.
Thames, H. D. *See* Guttenberger, R.
Thomas, D. J. *See* Stevens, J. M.
Thomas, N. B., 635
Thompson, P. I. *See* Murray, P. A.
Thomson, E. S., Afshar, F. and Plowman, P. N., 223
Thomson, J. L. G., 134
Tiula, E. *See* Lamminen, A. E.
Tobias, J. S. *See* Wiernik, G.
Todd, B. D., Godfrey, L. W. and Bodley, R. N., 187
Todd, B., 635
Tolley, D. A. *See* Law, J.
Tomlinson, M. J., 91
Torp-Pedersen, S. *See* Karstrup, S.
Tran, T., Grech, P. and Crofton, M. E., 942
Transbøl, I. *See* Karstrup, S.
Travis, R. C., Murray, P. I., Moseley, I. F. and Wright, J. E., 521
Trigaux, J.-P. *See* van Beers, B.
Trivedi, P. N. *See* Ranade, S. S.
Trott, K.-R. *See* Breiter, N.
Ts'ao, C. *See* Ward, W. F.
Tsuruta, T. *See* Kozlowski, K.
Tung, K. T. and Wilson, G. F., 1029
Tupchong, L. *See* Palta, J. R.
Turner, M. J. and Ball, P., 193

Urano, M. *See* Maruyama, Y.
Urano, M. *See* Yaes, R. J.

van Beers, B., Trigaux, J.-P., Weynants, P., Collard, J.-M. and Melange, M., 558

INDEX TO AUTHORS—continued

van de Geijn, J., 296
van den Aardweg, G. M. J. M. *See* Hopewell, J. W.
van Gansbeke, D., Matos, C., Gelin, P., Müller, P., Zalcman, M., Devière, J. and Struyven, J., 127
van Gesteren, J. *See* Schwachöfer, J. H. M.
van Haastert, M. *See* den Hartog Jager, F. C. A.
Vanneste, F. *See* Vynckier, S.
Vãńo, E., González, L., Calzado, A., Morán, P. and Delgado, V., 20
van Oostayen, J. A. *See* Schipper, J.
van Seyen, A. J. *See* Schipper, J.
Vitković, M. *See* Sarajlić, M.
Vučković, I. *See* Sarajlić, M.
Vynckier, S., Vanneste, F., Richard, F., Bol, A., Michel, C. and Wambersie, A, 1031

Wait, I. *See* Armstrong, S. J.
Wait, I. *See* Ipinyomi, J.
Wait, I. *See* Maurice, H.
Wait, I. *See* Meng, Q.
Wait, I. *See* Tawn, D. J.
Walden, T. N. *See* Litten, R. Z.
Walker, A. and Hounsell, A. R., 554
Walker, J. and Carty, H., 1105
Wallace, W. H. B., Shalet, S. M., Hendry, J. H., Morris-Jones, P. H. and Gattamaneni, H. R., 995
Walsh, M. T. and Shah, K. J., 624
Walton, S. *See* Metcalfe, M. J.
Wambersie, A. *See* Vynckier, S.
Ward, W. F., Molteni, A., Kim, Y. T. and Ts'ao, C., 348
Wardlaw, J. M. and Cruikshank, J. G., 759
Warenius, H. M. *See* Campell, I. R.
Warren, R. C. and Darwin, C. J., 817
Wassem, B. *See* Conere, T.
Wazer, D. E., Tercilla, O. F., Lin, P.-S. and Schmidt-Ullrich, R., 1079
Weatherburn, H. *See* Conere, T.
Wei, W. I. *See* Sham, J. S. T.
Weir, J. *See* Smith, F. W.
Weller, J. M. *See* Russell, J. G. B.
Wells, P. N. T.,399
Wells, P. N. T. *See* Halliwell, M.
West, D. J., Najm, Y. C., Mistry, R., Clarke, S. E., Fogelman, I. and Maisey, M. N., 303
Weston, M. J. and Wilde, P., 751
Weynants, P. *See* van Beers, B.
Whyte, A. M. and Hourihan, M. D., 526
Whyte, A. M. and Hayward, A. M., 1023
Wiernik, G., Alcock, C. J., Bates, T. D., Berry, R. J., Brindle, J. M., Dalby, J. E., Fowler, J. F., Gajek, W. R., Goodman, S., Haybittle, J. L., Henk, J. M., Hopewell, J. W., Howard, N., Lindup, R., Phillips, D. L., Pointon, R. S., Rezvani, M. and Tobias, J. S., 450
Wierzbicki, J. *See* Yaes, R. J.
Wild, S. R. *See* Pye, S. D.
Wilde, P. *See* Weston, M. J.
Wilkinson, J. M. and Ramachandran, T. P., 362
Williams, M. P., Husband, J. E., Heron, C. W., Cherryman, G. R. and Koslin, D. B., 544
Wilson, A. G. *See* Page, J. E.
Wilson, G. F. *See* Tung, K. T.
Witte, G. *See* Spielmann, R. P.
Wittich, G. *See* Dock, W.
Wood, B. *See* Moore, J. V.
Worthington, B. S., Chapman, B., Ordidge, R., Coxon, R., Stehling, M. K., Symonds, E. M. and Mansfield, P., 1092
Worthington B. S. *See* Rothwell C. I.
Wright, J. E. *See* Travis, R. C.
Wu, A., Chun, M., Kasdon, D., Heros, D., McKeough, P. and Chang, H., 154
Wu, A. *See* Chun, M.

Yaes, R. J., Feola, J., Wierzbicki, J., Urano, M. an Maruyama, Y., 873
Yaes, R. J. *See* Maruyama, Y.

Zaider, M. *See* Bewley, D. K.
Zalcman, M. *See* van Gansbeke, D.
Zammit-Maempel, I. *See* Nicholson, D. A.
Zankl, M. *See* Panzer, W.
Zorlu, F. *See* Atahan, I. L.
zum Winkel, K. *See* Fritz, P.

SUBJECT INDEX
1989

List of sections:
- Radiodiagnosis
  - Bones and joints (excluding skull)
  - Neuroradiology (including skull)
  - Cardiovascular system
  - Respiratory tract
  - Digestive tract
  - Liver and biliary tract, spleen, pancreas
  - Urinary tract
  - Haemopoietic, lymphatic, reticulo-endothelial systems
  - Reproductive system
  - Endocrine system
  - Ear, nose, throat, mouth, eyes
  - Breast and soft tissues
  - Paediatrics
  - Contrast media and other drugs
  - Apparatus and technical aspects
  - Organization, statistics and economics
  - Computed tomography (head)
  - Computed tomography (whole body)
  - Computed tomography (apparatus and technical aspects)
  - Interventional radiology
- Ultrasound
  - Clinical aspects
  - Apparatus and technical aspects
- Nuclear medicine
  - Clinical aspects
  - Apparatus and technical aspects
- Nuclear magnetic resonance
- Physics
  - Applied to radiodiagnosis
  - Applied to radiotherapy
  - Applied to nuclear medicine
- Radiotherapy
  - Results and clinical aspects
  - Apparatus and technical aspects
- Cancer chemotherapy
- Radiobiology
  - Applied to radiotherapy
  - Effects of radiation quality
  - Fractionation studies
  - Hyperthermia and irradiation
  - Sensitizers and protectors
  - Other studies
- Hyperthermia
- Hazards and radiation protection
- Lectures and addresses
- Education
- Proceedings
- Obituaries
- Awards
- Book reviews
- Instructions to authors

RADIODIAGNOSIS
Bones and joints
(excluding skull)

Technetium-99m hydroxymethylene diphosphonate scanning of acute injuries to the lateral ligaments of the ankle, 31
Van Buchem's disease with classical radiological features and appearances on cranial computed tomography (Case report), 74
Basic concepts of femoral neck anteversion: comparison of two definitions, 114
Unusual long bone changes in thalassaemia: findings on plain radiography and computed tomography (Case report), 168
Sickle-shaped scapulae in a patient with the Pierre Robin syndrome (Case report), 171
Intraoperative radioactive localization of an osteoid osteoma: a useful variation in technique (Short communication), 187
Intraoperative localization of an osteoid osteoma (Correspondence), 635
Stress changes of the wrist in adolescent gymnasts (Correspondence), 194
Clinical applications of high-definition microfocal radiography, 209
A comparison of two different T-grain films in rare-earth screens with a standard film–screen combination for intravenous pyelography and bone examinations, 237
Value of bone scanning and computed tomography in fibrodysplasia ossificans progressiva (Case report), 269
Giant central disc prolapse: a pitfall in computed tomographic diagnosis (Case report), 274
The misleading pre-operative chest radiograph (Case of the month), 279
Demonstration of vertebral body end plate veins by magnetic resonance imaging (Short communication), 290
The relation of radionuclide uptake by bone to the rate of calcium mineralization. I: Experimental studies using ^{45}Ca, ^{32}P and ^{99}Tc-MDP, 314
The relation of radionuclide uptake by bone to the rate of calcium mineralization. II: Patient studies using ^{99}Tc-MDP, 318
Phalangeal osteoid osteoma, 321
Dysplastic cortical hyperostosis: a new form of lethal neonatal dwarfism (Case report), 376
Chromium-51 EDTA/technetium-99m MDP ratio: a simple non-invasive method for assessing renal osteodystrophy, 438
An isolated capitate fracture in a nine-year-old boy (Case report), 487
X-ray dual-photon absorptiometry: a new method for the measurement of bone density, 587
Bone marrow scintigraphy in the diagnosis of post-traumatic avascular necrosis of bone, 790
Spondylo-metaphyseal dysplasia of Sutcliffe type (Case report), 859
Atypical amyloidosis of bone (Case report), 861
Radiographic videodensitometry for quantitative monitoring of experimental bone healing, 883
Fatigue fractures of the femoral diaphysis in the skeletally immature simulating malignancy, 893
Primary malignant fibrous histiocytoma of a metacarpal bone: a new localization (Case report), 940
Double-contrast CT arthrography of the shoulder joint, 1043
Demonstration of osteochondritis dissecans of the talus by coronal CT arthrography, 1050
Spontaneous regression of multiple bone metastases in malignant melanoma (Case report), 1096

CENTRAL LIBRARY

INDEX TO VOLUME 62

Neuroradiology
(including skull)

Van Buchem's disease with classical radiological features and appearances on cranial computed tomography (Case report), 74
Radiological evaluation of temporal bone disease: high-resolution computed tomography versus conventional X-ray diagnosis, 107
Outpatient myelography: an acceptable and cost-effective technique, 253
Outpatient myelography: an acceptable and cost-effective technique (Correspondence), 877
Giant central disc prolapse: a pitfall in computed tomographic diagnosis (Case report), 274
Orbital intraconal haematic cysts in young people: computed tomography and magnetic resonance imaging, 521
The diagnosis of tumours involving the parapharyngeal space by computed tomography, 525
Outpatient lumbar radiculography: comparison of iopamidol and iohexol and a literature review, 716
Atlanto-axial rotary fixation: diagnosis by functional computed tomography (Case report), 756
Relative safety of intravenous digital subtraction angiography over other methods of carotid angiography and impact on clinical management of cerebrovascular disease, 813
Retroperitoneal mass and spinal cord compression due to extramedullary haemopoiesis in polycythaemia rubra vera (Case report), 944
^{99}Tc-HMPAO single photon emission computed tomography in partial epilepsy: a preliminary report, 970
Gadolinium-enhanced magnetic resonance imaging of spinal tumours, 1067
Periventricular enhancement: a non-pathognomonic sign of intracerebral tumours, 1075

Cardiovascular system

Clinically unsuspected complications of arterial surgery shown by post-operative digital subtraction angiography, 13
Aortic tumours: report of a case and review of the literature, 35
Anomalous superior vena cava causing non-visualization of the lungs in perfusion scintigraphy (Case report), 78
Intravenous digital subtraction angiography in non-specific aorto-arteritis, 117
Assessment of angioplasty balloon catheters: further studies, 121
Sickle-shaped scapulae in a patient with the Pierre Robin syndrome (Case report), 171
Autopsy assessment of the Gunther vena caval filter (Case report), 174
New developments in the field of acute myocardial infarct imaging (Correspondence), 294
The localization of myocardial ischaemia with technetium-99m methoxy isobutyl isonitrile and single photon emission computed tomography, 303
Magnetic resonance imaging of the infant heart at 1.5 T (Technical note), 367
Balloon embolization of a congenital arterio-venous fistula between the internal mammary artery and a portal vein radicle (Case report), 371
Magnetic resonance imaging of ruptured aneurysm of the ascending aorta (Case report), 373
Total or partial percutaneous renal ablation in the treatment of renovascular hypertension: radiological and clinical aspects, 593
Central venous catheter placement for intravenous digital subtraction angiography: an assessment of technical problems and success rate, 599
Acute aorto-iliac thrombosis in a young man shown on unenhanced computed tomography (Case report), 627
Echocardiographic diagnosis of pulmonary embolism (Case report), 751
Aneurysm of the inferior pancreaticoduodenal artery diagnosed by real-time ultrasound and pulsed Doppler (Case report), 753
Sequential imaging of post-operative thrombus using the In-111-labelled platelet-specific monoclonal antibody P256, 963
Low-field cine MRI in aortic valve disease, 1063

Respiratory tract

High-resolution computed tomography in pulmonary cystic fibrosis, 1
Anomalous superior vena cava causing non-visualization of the lungs in perfusion scintigraphy (Case report), 78
Submarine escape training: lung cysts and tension pneumothorax (Case report), 276
The misleading pre-operative chest radiograph (Case of the month), 279
Sarcoidosis mimicking metastatic testicular tumour (Correspondence), 293
Haemoptysis in a laundry worker (Case of the month), 379
Iotrolan in selective bronchography via the fibreoptic bronchoscope (Short communication), 383
Effect of cirrhosis on accuracy of ^{99}Tc-tin colloid scintigraphy and ultrasound scanning in diangosis of hepatocellular carcinoma (Correspondence), 387
Spontaneous abrupt changes in the distribution of ventilation: a cause for apparent mismatching on ventilation/perfusion scintigraphy, 536
Foregut cyst of the mediastinum: fluid re-accumulation after transbronchial needle aspiration (Case report), 558
Jekyll and Hyde chest radiographs (Case of the month), 561
The radiographic differentiation of pulmonary oedema, 582
The value of transoesophageal ultrasonography in the management of a mediastinal foregut cyst, 986
Spontaneous pneumothorax with metastatic seminoma (Case report), 1101

Digestive tract

Transient diverticula of the colon, 27
Ossified leiomyoma of the stomach: demonstration on computed tomography (Case report), 79
Radiological appearances of colonic ring staple anastomoses, 256
Radiological appearances of colonic ring staple anastomoses (Correspondence), 1034
The influence of type of tube and experience of the operator on performance of small bowel enema, 447
Distal bowel infarction following angioplasty of the internal iliac artery (Case report), 489
A pressure valve for pneumatic reduction of intussusception (Correspondence), 499

INDEX TO SUBJECTS—continued

Foregut cyst of the mediastinum: fluid re-accumulation after transbronchial needle aspiration (Case report), 558
Dysphagia after fast neutron therapy to the head and neck, 724
Late radiation injury of the rectum and sigmoid colon: barium enema findings in 92 patients, 807
Transient circular narrowing of the cervical oesophagus (Correspondence), 876
Alimentary tract lesions in Cowden's disease, 890
The influence of tube type and operator experience on performance of small bowel enema (Correspondence), 953
Agenesis of the salivary gland: a report of two cases (Case reports), 1023
A radiological feature to assist in the diagnosis of intestinal obstruction (Short communication), 1105

Liver and biliary tract, spleen, pancreas
Hepatic venography in the surgical assessment of hepatic tumours, 6
Cystic haemangioma of the spleen: findings on ultrasound and computed tomography (Case report), 180
Ultrasound diagnosis of gallbladder perforation in a case of xanthogranulomatous cholecystitis (Case report), 273
The prevalence and characterization of simple hepatic cysts by ultrasound examination, 335
Balloon embolization of a congenital arterio-venous fistula between the internal mammary artery and a portal vein radicle (Case report), 371
Relative proton density and relaxation times in liver metastases during interferon treatment, 433
Splenic accumulation of ^{99}Tc-methylene diphosphonate (Correspondence), 499
Small hepatocellular carcinoma: detection with sonography, computed tomography (CT), angiography and Lipiodol-CT, 897

Urinary tract
Renal neoplasms in a family (Case report), 83
Radiation dose to urological surgeons during X-ray fluoroscopy for percutaneous stone extraction (Short communication), 185
A comparison of two different T-grain films in rare-earth screens with a standard film–screen combination for intravenous pyelography and bone examinations, 237
Chromium-51 EDTA/technetium-99m MDP ratio: a simple non-invasive method for assessing renal osteodystrophy, 438
Endoscopic correction of vesico-ureteric reflux by subureteric Teflon injection: follow-up ultrasound and voiding cystography, 443
Congenital ureteric diverticula in children and adults: classification, radiological and clinical features, 551
Percutaneous interventional uroradiology (Review article), 573
Total or partial percutaneous renal ablation in the treatment of renovascular hypertension: radiological and clinical aspects, 593
Ultrasound in suspected obstruction complicating renal transplantation, 803
Asymptomatic haematuria and abnormal urine cytology (Case report), 864
Can ultrasound replace the intravenous urogram in preliminary investigation of renal tract disease? A prospective study, 977
Sonographic demonstration of renal tumour extension into the contralateral renal vein (Case report), 1094
The immediate film in intravenous urography (Correspondence), 1111

Haemopoietic, lymphatic, reticulo-endothelial systems
Primary extranodal lymphoma in muscle (Case report), 81
Retroperitoneal mass and spinal cord compression due to extramedullary haemopoiesis in polycythaemia rubra vera (Case report), 944
Burkitt's lymphoma following treatment for Hodkin's disease (Case report), 1089

Reproductive system
Costing imaging procedures (Correspondence), 94
Sarcoidosis mimicking metastatic testicular tumour (Correspondence),293
Magnetic resonance imaging in recurrent carcinoma of the cervix, 544
Primary malignant melanoma of the vagina (Case report), 623
Computed tomographic staging of testicular tumours: an unexpected source of error (Case report), 942 Uterine leiomyomata: sonographic mimicry (Case report), 1019
The correlation of histopathological, microradiographic and ultrasound features in diseases of the prostate gland, 1059
Induced fluid movement within a giant ovarian cyst demonstrated by echo-planar imaging (Case report), 1092
Spontaneous pneumothorax with metastatic seminoma (Case report), 1101

Endocrine system
Comparison of techniques for thallium-201-technetium-99m parathyroid imaging, 532
Ultrasound-guided, histological, fine-needle biopsy from suspect parathyroid tumours: success-rate and reliability of histological diagnosis, 981
Ultrasonographic appearances of parathyroid carcinoma (Case report), 1017
An illustrative case: enough to raise one's blood pressure (Case report), 1026
Ultrasound-guided, histological, fine-needle biopsy from suspect parathyroid tumours: success-rate and reliability of histological diagnosis, 981

Ear, nose, throat, mouth, eyes
Orbital intraconal haematic cysts in young people: computed tomography and magnetic resonance imaging, 521
The diagnosis of tumours involving the parapharyngeal space by computed tomography, 525

Breast and soft tissues
Primary extranodal lymphoma in muscle (Case report), 81
Films, screens and cassettes for mammography, 163
Films, screens and cassettes for mammography (Correspondence), 565
Acute rhabdomyolysis: evaluation with magnetic resonance imaging compared with computed tomography and ultrasonography, 326
The effects of angiotensin II on Doppler signals from a soft-tissue tumour, 331

INDEX TO VOLUME 62

X-ray protection considerations for mammography screening centres (Technical note), 554
Screening for breast cancer: the UK scene (The 69th Mackenzie Davidson Memorial Lecture), 695
Enhanced risk from low-energy screen-film mammography X-rays, 910
Ductal adenoma of the breast: mammographic appearances and pathological correlation (Case report), 1021

Paediatrics
Stress changes of the wrist in adolescent gymnasts (Correspondence), 194
Radiation dose to neonates on a Special Care Baby Unit, 230
Contribution of computed tomography in the aetiology and prognosis of cerebral palsy in children, 248
Magnetic resonance imaging of the infant heart at 1.5 T (Technical note), 367
Dysplastic cortical hyperostosis: a new form of lethal neonatal dwarfism (Case report), 376
An isolated capitate fracture in a nine-year-old boy (Case report), 487
Congenital ureteric diverticula in children and adults: classification, radiological and clinical features, 551
Fetal fat measurement by magnetic resonance imaging, 603
Neuroblastoma presenting with obstructive jaundice (Case report), 624
Radio-opaque hemithorax in a neonate (Case of the month), 951

Contrast media and other drugs
Variation of image quality with X-ray tube potential in mammography (Correspondence), 191
A large trial of intravenous Conray 325 and Niopam 300 to assess immediate and delayed reactions, 260
The effects of angiotensin II on Doppler signals from a soft-tissue tumour, 331
Iotrolan in selective bronchography via the fibreoptic bronchoscope (Short communication), 383
Effect of cirrhosis on accuracy of ^{99}Tc-tin colloid scintigraphy and ultrasound scanning in diangosis of hepatocellular carcinoma (Correspondence), 387
Secretion of radioactivity in breast milk following administration of ^{123}I hippuran (Correspondence), 388
Radiocontrast agents are contact activators of coagulation (Short communication), 631
Outpatient lumbar radiculography: comparison of iopamidol and iohexol and a literature review, 716
Acute toxic myopathy: a delayed adverse effect of intravenous urography with iopamidol 370 (Case report), 949
The influence of Buscopan on adverse reactions to intravascular contrast media, 1056

Apparatus and technical aspects
Installation requirements for an argon laser angioplasty system (Technical note), 71
Assessment of angioplasty balloon catheters: further studies, 121
Variation of image quality with X-ray tube potential in mammography (Correspondence), 191
A new high-definition microfocal X-ray unit, 201
Clinical applications of high-definition microfocal radiography, 209
A comparison of two different T-grain films in rare-earth screens with a standard film–screen combination for intravenous pyelography and bone examinations, 237
An alignment test jig for measuring the effective focal-spot size of mammographic X-ray tubes (Technical note), 484
A pressure valve for pneumatic reduction of intussusception (Correspondence), 499
Microcomputer processing of film radiographs, 613
Pioneer discovery of rare-earth fluorescence (Correspondence), 765
Relative safety of intravenous digital subtraction angiography over other methods of carotid angiography and impact on clinical management of cerebrovascular disease, 813
Assessment of feature size abnormalities using receiver operating characteristic analysis, 817
Soft-tissue effects of biliary extracorporeal shockwave lithotripsy in swine, 843
Radiographic videodensitometry for quantitative monitoring of experimental bone healing, 883
A physical evaluation of the imaging performance of a high-resolution fluorography system, 999
British standards specification for balloon dilatation catheters, 1034

Organization, statistics and economics
Some indicative parameters on diagnostic radiology in Spain: first dose estimations, 20
Costing imaging procedures (Correspondence), 94
Experiences at the new magnetic resonance imaging centre at Bristol, 134
The cost of imaging procedures (Correspondence), 194
An analysis of referrals for primary diagnostic ultrasound to a general X-ray department (Correspondence), 293
'Out of hours radiography' (Correspondence), 498
The cost of imaging procedures (Correspondence), 498
A flexible image archiving system using a personal computer and optical disk (Technical note), 620
The cost of imaging procedures (Correspondence), 635
Screening for breast cancer: the UK scene (The 69th Mackenzie Davidson Memorial Lecture), 695

Computed tomography
(head)
Radiological evaluation of temporal bone disease: high-resolution computed tomography versus conventional X-ray diagnosis, 107
Contribution of computed tomography in the aetiology and prognosis of cerebral palsy in children, 248
Orbital intraconal haematic cysts in young people: computed tomography and magnetic resonance imaging, 521
The diagnosis of tumours involving the parapharyngeal space by computed tomography, 525
The use of real-time orbital ultrasound in Graves' ophthalmopathy: a comparison with computed tomography, 705
The role of computed tomography and coronal plane tomography in radiotherapy for laryngeal tumours, 729

Atlanto-axial rotary fixation: diagnosis by functional computed tomography (Case report), 756
Treatment of tumours of the parotid gland and middle ear using obliquely reconstructed computed tomographic images, 785
Computed tomography of earpits-deafness syndrome (Case report), 947

Computed tomography
(whole body)
High-resolution computed tomography in pulmonary cystic fibrosis, 1
Ossified leiomyoma of the stomach: demonstration on computed tomography (Case report), 79
Unusual long bone changes in thalassaemia: findings on plain radiography and computed tomography (Case report), 168
Demonstration on computed tomography of tracheomalacia in tracheobronchomegaly (Mounier-Kuhn syndrome) (Case report), 176
Lipoma arborescens of the knee, (Case report), 178
Cystic haemangioma of the spleen: findings on ultrasound and computed tomography (Case report), 180
Evaluation of response following irradiation of juvenile angiofibromas, 245
Value of bone scanning and and computed tomography in fibrodysplasia ossificans progressiva (Case report), 269
Giant central disc prolapse: a pitfall in computed tomographic diagnosis (Case report), 274
Primary orbital lymphoma: staging by computed tomographic scanning (Short communication), 287
Acute rhabdomyolysis: evaluation with magnetic resonance imaging compared with computed tomography and ultrasonography, 326
Acute aorto-iliac thrombosis in a young man shown on unenhanced computed tomography (Case report), 627
The anatomy of the first sacral nerve root sheath shown by computed tomography, 710
Low-field (0.08T) magnetic resonance imaging of the pancreas: comparison with computed tomography and ultrasound, 796
Small hepatocellular carcinoma: detection with sonography, computed tomography (CT), angiography and Lipiodol-CT, 897
A method for estimating embryo doses resulting from computed tomographic examinations (Technical note), 936
Computed tomographic staging of testicular tumours: an unexpected source of error (Case report), 942
Ultrasound-guided chemical parathyroidectomy in patients with primary hyperparathroidism: a prospective study, 1037
Double-contrast CT arthrography of the shoulder joint, 1043
Demonstration of osteochondritis dissecans of the talus by coronal CT arthrography, 1050
Periventricular enhancement: a non-pathognomonic sign of intracerebral tumours, 1075

Computed tomography
(Apparatus and technical aspects)
Patient doses from computed tomography in Manitoba from 1977 to 1987, 138
Aid to localization for computed tomographic biopsy and aspiration procedures (Correspondence), 193

Interventional radiology
Percutaneous drainage of subphrenic abscesses, 127
Radiation dose to urological surgeons during X-ray fluoroscopy for percutaneous stone extraction (Short communication), 185
Foregut cyst of the mediastinum: fluid re-accumulation after transbronchial needle aspiration (Case report), 558
Percutaneous interventional uroradiology (Review article), 573
Central venous catheter placement for intravenous digital subtraction angiography: an assessment of technical problems and success rate, 599

ULTRASOUND
Clinical aspects
Polyorchidism diagnosed by ultrasound (Case report), 82
Cystic haemangioma of the spleen: findings on ultrasound and computed tomography (Case report), 180
Ultrasound diagnosis of gallbladder perforation in a case of xanthogranulomatous cholecystitis (Case report), 273
New developments in the field of acute myocardial infarct imaging (Correspondence), 294
Acute rhabdomyolysis: evaluation with magnetic resonance imaging compared with computed tomography and ultrasonography, 326
The effects of angiotensin II on Doppler signals from a soft-tissue tumour, 331
The prevalence and characterization of simple hepatic cysts by ultrasound examination, 335
Doppler ultrasound in medical diagnosis (Review article), 399
The use of real-time orbital ultrasound in Graves' ophthalmopathy: a comparison with computed tomography, 705
Echocardiographic diagnosis of pulmonary embolism (Case report), 751
Aneurysm of the inferior pancreaticoduodenal artery diagnosed by real-time ultrasound and pulsed Doppler (Case report), 753
Clinical evaluation of a digital signal processing device for real-time speckle suppression in medical ultrasonics (Short communication), 761
Low-field (0.08T) magnetic resonance imaging of the pancreas: comparison with computed tomography and ultrasound, 796
Ultrasound in suspected obstruction complicating renal transplantation, 803
New scans from old: digital reformatting of ultrasound images, 824
Ultrasound demonstration of vocal cord movements (Short communication), 871
Small hepatocellular carcinoma: detection with sonography, computed tomography (CT), angiography and Lipiodol-CT, 897
Total abdominal and pelvic ultrasound: incidental findings and a comparison between outpatient and general practice referrals in 1000 cases, 974
Can ultrasound replace the intravenous urogram in preliminary investigation of renal tract disease? A prospective study, 977
Ultrasound-guided, histological, fine-needle biopsy from suspect parathyroid tumours: success-rate and reliability of histological diagnosis, 981
The value of transoesophageal ultrasonography in the management of a mediastinal foregut cyst, 986
Ultrasonographic appearances of parathyroid carcinoma (Case report), 1017

INDEX TO VOLUME 62

Uterine leiomyomata: sonographic mimicry (Case report), 1019
The correlation of histopathological, microradiographic and ultrasound features in diseases of the prostate gland, 1059
Sonographic demonstration of renal tumour extension into the contralateral renal vein (Case report), 1094

Apparatus and technical aspects
The unseen radiation hazards of ultrasound (Correspondence), 295
Doppler ultrasound in medical diagnosis (Review article), 399
Clinical evaluation of a digital signal processing device for real-time speckle suppression in medical ultrasonics (Short communication), 761
New scans from old: digital reformatting of ultrasound images, 824
Surface heating of diagnostic ultrasound transducers, 1005
The use of an infrared touch screen to control the sensitivity of ultrasound scanners in clinical practice (Technical note), 1014

NUCLEAR MEDICINE
Clinical aspects
Technetium-99m hydroxymethylene diphosphonate scanning of acute injuries to the lateral ligaments of the ankle, 31
Intraoperative radioactive localization of an osteoid osteoma: a useful variation in technique (Short communication), 187
Value of bone scanning and computed tomography in fibrodysplasia ossificans progressiva (Case report), 269
The localization of myocardial ischaemia with technetium-99m methoxy isobutyl isonitrile and single photon emission computed tomography, 303
The relation of radionuclide uptake by bone to the rate of calcium mineralization. I: Experimental studies using ^{45}Ca, ^{32}P and ^{99}Tc-MDP, 314
The relation of radionuclide uptake by bone to the rate of calcium mineralization. II: Patient studies using ^{99}Tc-MDP, 318
Phalangeal osteoid osteoma, 321
Nuclear medicine in the 1990s: a quantitative physiological approach (1988 Mayneord Lecture), 421
Chromium-51 EDTA/technetium-99m MDP ratio: a simple non-invasive method for assessing renal osteodystrophy, 438
Splenic accumulation of ^{99}Tc-methylene diphosphonate (Correspondence), 499
Comparison of techniques for thallium-201-technetium-99m parathyroid imaging, 532
Spontaneous abrupt changes in the distribution of ventilation: a cause for apparent mismatching on ventilation/perfusion scintigraphy, 536
Bone marrow scintigraphy in the diagnosis of post-traumatic avascular necrosis of bone, 790
Proton nuclear magnetic resonance imaging as a predictor of the outcome of photodynamic therapy of tumours (Short communication), 869
Sequential imaging of post-operative thrombus using the In-111-labelled platelet-specific monoclonal antibody P256, 963
^{99}Tc-HMPAO single photon emission computed tomography in partial epilepsy: a preliminary report, 970
Lung cancer: tissue characterization by MRI T_1, T_2 values *in vitro* and role of histopathology (Correspondence), 1111

Apparatus and technical aspects
New developments in the field of acute myocardial infarct imaging (Correspondence), 294

NUCLEAR MAGNETIC RESONANCE
Experiences at the new magnetic resonance imaging centre at Bristol, 134
Demonstration of vertebral body end plate veins by magnetic resonance imaging (Short communication), 290
Acute rhabdomyolysis: evaluation with magnetic resonance imaging compared with computed tomography and ultrasonography, 326
Magnetic resonance imaging of the infant heart at 1.5 T (Technical note), 367
Magnetic resonance imaging of ruptured aneurysm of the ascending aorta (Case report), 373
Relative proton density and relaxation times in liver metastases during interferon treatment, 433
Orbital intraconal haematic cysts in young people: computed tomography and magnetic resonance imaging, 521
Magnetic resonance imaging in recurrent carcinoma of the cervix, 544
Fetal fat measurement by magnetic resonance imaging, 603
Low-field (0.08T) magnetic resonance imaging of the pancreas: comparison with computed tomography and ultrasound, 796
Alterations in body and skin temperatures caused by magnetic resonance imaging: is the recommended exposure for radiofrequency radiation too conservative? 904
Low-field cine MRI in aortic valve disease, 1063
Gadolinium-enhanced magnetic resonance imaging of spinal tumours, 1067
Induced fluid movement within a giant ovarian cyst demonstrated by echo-planar imaging (Case report), 1092

PHYSICS
Applied to radiodiagnosis
A new high-definition microfocal X-ray unit, 201
X-ray dual-photon absorptiometry: a new method for the measurement of bone density, 587
Assessment of feature size abnormalities using receiver operating characteristic analysis, 817
A physical evaluation of the imaging performance of a high-resolution fluorography system, 999

Applied to radiotherapy
Precision of determining compliance with prescribed fields from conventional portal films, 48
A source localizing technique for the microSelectron-HDR afterloading system (Technical note), 69
Leakage from a caesium-137 needle (Correspondence), 92
Interstitial iridium-192 implantation for malignant brain tumours. Part I: Techniques of dosimetry planning, 154
An iodine-125 applicator designed for irradiating blood vessels growing into the cornea of the eye (Technical note), 266
Autoradiographic imaging of pion stopping distribution utilizing scanning laser stimulated luminescence (Short communication), 285

INDEX TO SUBJECTS—continued

The quality of high-energy X-ray beams, 473
Asymmetric field arc rotations, 927
A quality assessment of the effects of a hydrogenous filter on a p(66)Be(40) neutron beam, 989
Control of patient positioning for fast neutron therapy using positron emission tomography (Short communication), 1031

Applied to nuclear medicine
X-ray dual-photon absorptiometry: a new method for the measurement of bone density, 587

RADIOTHERAPY
Results and clinical aspects
Radiotherapy of epidermoid anal canal cancer, 53
Discriminant analysis on the treatment results of interstitial radium tongue implants, 59
Results of treatment of carcinoma of the uterine cervix using the Newcastle afterloading technique, 64
Late normal tissue reactions in patients with breast carcinoma (Correspondence), 91
Radical radiotherapy for carcinoma of the vulva, 145
Interstitial iridium-192 implantation for malignant brain tumours. Part II: Clinical experience, 158
Re-irradiation of astrocytoma of the brain (Case report), 173
Paediatric brachytherapy. I. The role of brachytherapy in the multidisciplinary therapy of localized cancers, 218
Paediatric brachytherapy. II. Brain implantation, 223
Evaluation of response following irradiation of juvenile angiofibromas, 245
Post-operative neutron irradiation (Correspondence), 298
Treatment of persistent and recurrent nasopharyngeal carcinoma by brachytherapy, 355
First interim progress report on the second British Institute of Radiology fractionation study: short versus long overall treatment times for radiotherapy of carcinoma of the laryngopharynx, 450
Upper-half body irradiation for oat cell carcinoma of the bronchus (Short communication), 563
Use of a radon mould technique for skin cancer: results from the Peter MacCallum Cancer Institute (1975-1984), 608
Are the results of the St Thomas' trial of post-mastectomy radiotherapy inconsistent with the predictions from the linear-quadratic model (Correspondence), 633
Dysphagia after fast neutron therapy to the head and neck, 724
The role of computed tomography and coronal plane tomography in radiotherapy for laryngeal tumours, 729
Clinical significance of cranial nerve deficit in the therapy of nasopharyngeal carcinoma, 739
Treatment of tumours of the parotid gland and middle ear using obliquely reconstructed computed tomographic images, 785
Late radiation injury of the rectum and sigmoid colon: barium enema findings in 92 patients, 807
Squamous cell carcinoma of the base of the tongue: results of treatment in 115 cases, 849
Radiotherapy in the management of aggressive fibromatosis (Case report), 854
Sustained complete remission of Stage IVb carcinoma of the cervix with *cis*-platinum, methotrexate and bleomycin chemotherapy (Case report), 856
Proton nuclear magnetic resonance imaging as a predictor of the outcome of photodynamic therapy of tumours (Short communication), 869
Soft-tissue sarcoma: neutrons versus photons for post-operative irradiation (Correspondence), 874
Ten-year results of a post-operative trial: NSD and LQ correspondence (Correspondence), 954
Ovarian failure following abdominal irradiation in childhood: the radiosensitivity of the human oocyte, 995
A localized hypersensitivity reaction to co-trimoxazole in a pre-irradiated field simulating recall phenomenon (Correspondence), 1107

Apparatus and technical aspects
An indwelling intrauterine tube to facilitate intracavitary radiotherapy of carcinoma of the cervix (Technical note), 68
A source localizing technique for the microSelectron-HDR afterloading system (Technical note), 69
Interstitial iridium-192 implantation for malignant brain tumours. Part I: Techniques of dosimetry planning, 154
Paediatric brachytherapy. I. The role of brachytherapy in the multidisciplinary therapy of localized cancers, 218
Paediatric brachytherapy. II. Brain implantation, 223
The ICRU recommendations for reporting intracavitary therapy in gynaecology and the Manchester method of treating cancer of the cervix uteri, 362
Radiotherapy simulators and independent field wire movement (Technical note), 366
Stem-cell depletion and grid therapy (Correspondence), 386
Platinum chemotherapy, radiotherapy and the inner ear: implications for 'standard' radiation portals, 457
The role of computed tomography and coronal plane tomography in radiotherapy for laryngeal tumours, 729
A technique for total skin electron irradiation using six large flattened electron beams: implementation on linear accelerators having different modes of electron beam production (Technical note), 744
A simple technique for intraluminal irradiation in oesophageal tumours using the high-dose-rate Microselectron (Technical note), 748
Treatment of tumours of the parotid gland and middle ear using obliquely reconstructed computed tomographic images, 785

CANCER CHEMOTHERAPY
Platinum chemotherapy, radiotherapy and the inner ear: implications for 'standard' radiation portals, 457
Sustained complete remission of Stage IVb carcinoma of the cervix with *cis*-platinum, methotrexate and bleomycin chemotherapy (Case report), 856

INDEX TO VOLUME 62

RADIOBIOLOGY

Applied to radiotherapy

Radiobiological assessment of permanent implants using tumour repopulation factors in the linear-quadratic model, 241
Precipitation of radiation injury in kidney epithelium reveals a high fractionation sensitivity (Short communication), 283
Incorporating the time factor into the linear-quadratic model (Correspondence), 296
Stem-cell depletion and grid therapy (Correspondence), 386
Biological equivalence between fractionated radiotherapy treatments (Correspondence), 565
The linear quadratic formula and progress in fractionated radiotherapy (Review article), 679
Biological equivalence between frctionated radiotherapy treatments using the linear-quadratic model (Correspondence), 873
Residual radiation-induced injury in dermal tissue: implications for retreatment, 915
Ten-year results of a post-operative trial: NSD and LQ correspondence (Correspondence), 954
Kinetics of recovery from sublethal radiation damage (Correspondence), 1107

Effects of radiation quality

Changes in biological effectiveness of the neutron beam at Clatterbridge (62 MeV p on Be) measured with cells *in vitro*, 344
Changes in relative biological effectiveness with depth of neutron beams (Correspondence), 765

Fractionation studies

Cell kinetic changes in the follicular epithelium of pig skin after irradiation with single and fractionated doses of X rays, 41
Effects of inhibition of intercellular communication on repair of damage induced by ionizing radiation (Short communication), 281
First interim progress report on the second British Institute of Radiology fractionation study: short versus long overall treatment times for radiotherapy of carcinoma of the laryngo-pharynx, 450
Biological equivalence between fractionated radiotherapy treatments (Correspondence), 565
The linear quadratic formula and progress in fractionated radiotherapy (Review article), 679
Sublethal damage repair and radiosensitivity of human squamous cell carcinoma cells grown with different culture techniques, 1084

Hyperthermia and irradiation

The potential value of hyperthermia-induced high fever in the management of HIV infection (Correspondence), 1112

Sensitizers and protectors

Experimental intra-arterial administration of SR-2508 in the rabbit V2 carcinoma model, 234
Tetrachlorodecaoxygen anion complex treatment after localized X irradiation of the rat colon (Short communication), 381
Radiation toxicity of indium-111-2-mercaptopyridine-N-oxide on HeLa S-3 cells, 468
Variation of tumour radiosensitivity with time after anaesthetic, 932
Modulation in the radiosensitivity of MCF-7 human breast carcinoma cells by 17B-estradiol and tamoxifen, 1079

Other studies

Functional changes in the irradiated rat ureter: assessment by transit-time renography (Short communication), 87
Alteration of cardiac myosin isozymes after whole-body irradiation (Short communication), 189
Effects of inhibition of intercellular communication on repair of damage induced by ionizing radiation (Short communication), 281
Precipitation of radiation injury in kidney epithelium reveals a high fractionation sensitivity (Short communication), 283
Radiation-induced cell death by chromatin loss, 338
Structure-function analysis of angiotensin-converting enzyme inhibitors as modifiers of radiation-induced pulmonary endothelial dysfunction in rats, 348
Tetrachlorodecaoxygen anion complex treatment after localized X irradiation of the rat colon (Short communication), 381
In vivo viability of ^{111}In-labelled granulocytes demonstrated in a sham-dialysis model, 463
Radiation toxicity of indium-111-2-mercaptopyridine-N-oxide on HeLa S-3 cells, 468
Atypical radiological features of beta-glucuronidase deficiency (mucopolysaccharidosis VII) occurring in an elderly patient from an inbred kindred (Case report), 493
The production of chromosome structural changes by radiation: an update of Lea, 1946, Chapter VI (Review article), 507
The effects of single doses of X rays on the mechanical properties of pig skin *in vivo*, 830
Soft-tissue effects of biliary extracorporeal shockwave lithotripsy in swine, 843
Radiation doses in extracorporeal shock wave lithotripsy, 921
Sublethal damage repair and radiosensitivity of human squamous cell carcinoma cells grown with different culture techniques, 1084

HYPERTHERMIA

The potential value of hyperthermia-induced high fever in the management of HIV infection (Correspondence), 1112

HAZARDS AND RADIATION PROTECTION

Some indicative parameters on diagnostic radiology in Spain: first dose estimations, 20
Diagnostic radiation, pregnancy and termination (Correspondence), 92
Costing imaging procedures (Correspondence), 94
Patient doses from computed tomography in Manitoba from 1977 to 1987, 138
Possibility of retrospective dosimetry for persons accidentally exposed to ionizing radiation using electron spin resonance of sugar and mother-of-pearl, 148
Films, screens and cassettes for mammography, 163
Radiation dose to urological surgeons during X-ray fluoroscopy for percutaneous stone extraction (Short communication), 185
Radiation dose to neonates on a Special Care Baby Unit, 230
The unseen radiation hazards of ultrasound (Correspondence), 295
Secretion of radioactivity in breast milk following administration of ^{123}I hippuran (Correspondence), 388

INDEX TO SUBJECTS—continued

Memorandum from the British Committee on Radiation Units and Measurements. Quantities for environmental monitoring, 482
X-ray protection considerations for mammography screening centres (Technical note), 554
A review of the occupational exposure in the North-Western Region, 734
Organ doses from cardiac and carotid digital subtraction angiography, 838
Alterations in body and skin temperatures caused by magnetic resonance imaging: is the recommended exposure for radiofrequency radiation too conservative? 904
Enhanced risk from low-energy screen–film mammography X-rays, 910
Radiation doses in extracorporeal shock wave lithotripsy, 921
Ovarian failure following abdominal irradiation in childhood: the radiosensitivity of the human oocyte, 995
An interesting radiation protection finding around a linear accelerator (Correspondence), 1033

LECTURES AND ADDRESSES

Nuclear medicine in the 1990s: a quantitative physiological approach (1988 Mayneord Lecture), 421
Screening for breast cancer: the UK scene (The 69th Mackenzie Davidson Memorial Lecture), 695

EDUCATION

A colonic double bubble (Case of the month), 85
The jockey with a mass in the thigh (Case of the month), 183
The misleading pre-operative chest radiograph (Case of the month), 279
Haemoptysis in a laundry worker (Case of the month), 379
The warm and tender hip (Case of the month), 497
Jekyll and Hyde chest radiographs (Case of the month), 561
No way out (Case of the month), 629
A rare diversion? (Case of the month), 759
A real headache! (Case of the month), 867
Radio-opaque hemithorax in a neonate (Case of the month), 951
Common symptom: uncommon cause (Case of the month), 1029
Visits to controlled areas in X-ray departments (Correspondence), 1033
A painful knee (Case of the month), 1103

PROCEEDINGS

Too much radiation in radiodiagnosis? March 9, 1988, 96
Imaging in stroke: how, why and when? October 13, 1988, 389
Paediatric nuclear medicine. November 23, 1988, 499
British Medical Ultrasound Society, 20th Annual Meeting, 6–8 December 1988, 636
Radiology in AIDS, 19 January 1988, 878, 1116
Radiobiology work in progress; Normal tissue radiation reactions Nuclear medicine in gastroenterology, 14 February 1989, 772
The impact of magnetic resonance imaging on imaging strategies: issues and future directions, 21 February 1989, 878
Clinical relevance of radiobiological models, 26 May 1989, 1113

OBITUARIES

I. G. Williams, B147
J. B. Massey, B150
H. Thomlinson, B170

AWARDS

BIR Awards 1989, B127, B143

BOOK REVIEWS

Amplatz, K. and Lange, P. H. *Atlas of endourology*, 395
Angerson, W. J., Sheldon, C. D., Barbenel, J. C., Fisher, A. C. and Gaylor, J. D. S. (Eds). *Oxford medical engineering series, 7: Blood flow in the brain*, 960
Armstrong, P. and Wastie, M. L. *Diagnostic imaging, 2nd edn*, 397
Baert, A. L., Boijsen, E., Fuchs, W. A. and Heuck, F. H. W. (Eds). *Frontiers in European radiology 5*, 1035
Barbenel, J. C., Fisher, A. C., Gaylor, J. D. S. and Sheldon, C. D. (Eds). *Blood flow in artificial organs and cardiovascular prostheses. Oxford Medical Engineering Series, No. 8*, 1118
Bassett, L. W. and Gold, R. H. (Eds). *Breast cancer detection: mammography and other methods in breast imaging, 2nd edn*, 1036
Berquist, T. H. (Ed.). *Radiology of the foot and ankle*, 1121
Brant-Zawadzki, M. and Norman, D. (Eds). *Magnetic resonance imaging of the central nervous system*, 101
Bisese, J. H. *MRI: a teaching approach*, 198
Bradley, W. G. Jr, Adey, W. R. and Hasso, A. N. *Magnetic resonance imaging of the brain, head and neck. A text atlas*, 198
Bragg, D. G. (Ed.). *1988 yearbook of diagnostic radiology*, 782
Broecker, B. H. and Klein, F. A. (Eds). *Pediatric tumors of the genitourinary tract*, 197
Bruneton, J.-N. *Ultrasonography of the neck*, 300
Bruneton, J.-N. *Ultrasonography of the spleen*, 678
Bury, R. F. *Practical guides for general practice 3. Radiology*, 959
Cabanis, E. A., Doyon, D., Halimi, Ph., Iba-Zizen, M. T., Sigal, R. and Tamraz, J. *Atlas d'IRM de l'encephale et de la moelle*, 780
Calder, J. and Chessell, G. *An atlas of radiological interpretation: the bones*, 568
Carr, D. H. (Ed.). *Contrast media*, 960
Chard, T. *Computing for clinicians*, 570
Christoforidis, A. J. (Ed.). *Atlas of axial, sagittal and coronal anatomy (with CT and MRI)*, 199
Clark, D. A. *Coronary angioplasty*, 677
Coleman, B. G. *Genitourinary ultrasound. A text/atlas*, 676
Cox, P. H. (Ed.). *Radiopharmacy and radiopharmacology yearbook 2*, 781
Cox, P. H. (Ed.). *Radiopharmacy and radiopharmacology yearbook 3*, 962
Dacie, J. E. *MCQs on diagnostic imaging*, 570
Daniels, D. L., Haughton, V. M. and Naidich, T. P. *Cranial and spinal magnetic resonance imaging. An atlas and guide*, 199
Datz, F. L. *Gamuts in nuclear medicine, 2nd edn*, 504
Deckard, H. and Cox, P. H. *Principles of radiopharmacology*, 1122
Dickinson, H. G. and Goodhew, P. J. (Eds). *Eurem 88. Volume 1: Tutorials, instrumentation and techniques. Volume 2: Physics and materials. Volume 3: Biology*, 777

INDEX TO VOLUME 62

Diebler, C. and Dulac, O. *Pediatric neurology and neuroradiology. Cerebral and cranial diseases*, 675
Dixon, R. L. (Ed.). *MRI: acceptance testing and quality control. The role of the clinical physicist*, 881
Drings, P. and Vogt-Moykopf (Eds). *Therapy of lung metastases—contributions to oncology*, 881
Eisenberg, R. L. *Clinical imaging. An atlas of differential diagnosis*, 397
Eisenberg, R. L. (Ed.). *Diagnostic imaging: an algorithmic approach*, 398
Eisenberg, R. L. *Diagnsotic imaging: an algorithmic approach*, 957
Elster, A. D. *Cranial magnetic resonance imaging*, 783
Evans, K. T., Gravelle, I. H., Roberts, G. M. and Hayward, C. *Clinical radiology for medical students, 2nd edn*, 569
Falke, T. H. M. (Ed.). *Essentials of clinical MRI*, 197
Federle, M. P., Megibow, A. J. and Naidich, D. P. (Eds). *Radiology of AIDS*, 958
Feinstein, A. R. *Clinimetrics*, 196
Felix, W. R. Jr (Ed.). *Non-invasive diagnosis of peripheral vascular disease*, 677
Fischer, H. W. *Radiographic anatomy: a working atlas*, 675
Fischer, H. W. *The radiologist's first reader*, 781
Fishman, E. K. and Jones, B. *Contemporary issues in computed tomography. Computed tomography of the gastrointestinal tract*, 782
Fogelman, I. and Maisey, M. *An atlas of clinical nuclear medicine*, 571
Foster, M. A. and Hutchison, J. M. S. (Eds). *Practical NMR imaging*, 1119
Freedman, M. *Clinical imaging: an introduction to the role of imaging in clinical practice*, 567
Freeman, L. M. and Weissmann, H. S. (Eds). *Nuclear medicine annual 1988*, 957
Fuller, L. M., Hagemeister, F. B., Sullivan, M. P. and Velasquez, W. S. (Eds). *Hodgkin's disease and non-Hodgkin's lymphomas in adults and children*, 777
Galasko, C. S. B. and Isherwood, I. (Eds). *Imaging techniques in orthopaedics*, 1121
Galasko, C. S. B. and Noble, J. (Eds). *Current trends in orthopaedic surgery*, 958
Gale, M. E. and Karlinsky, J. B. *Computed tomography of the chest: a teaching file*, 301
Galperin, E. I., Kuzovlev, N. F. and Karagiulian, S. R. *Benign strictures of bile ducts*, 676
Gelfand, M. J. and Thomas, S. R. (Eds). *Effective use of computers in nuclear medicine. Practical clinical applications in the imaging laboratory*, 778
Godden, T. J. *Physical aspects of brachytherapy*, 197
Gogelman, I. and Collier, B. D. *An atlas of planar and SPECT bone scans*, 1122
Gordon, I. (Ed.). *Diagnostic imaging in paediatrics*, 396
Grossman, Z. D. and Rosebrough, S. F. *Clinical radioimmunoimaging*, 505
Hornsby, V. P. L. and Winter, R. K. *Aids to Part I FRCR*, 570
Hüpscher, D. N. *Radiology of the oesophagus*, 1122
IAEA. *Nuclear and atomic data for radiotherapy and related radiobiology. Proceedings of a meeting at Rijswijk, 16–20 September, 1985*, 196
IAEA. *Dosimetry in radiotherapy, Vols 1 and 2. Proceedings of a symposium organized by IAEA and WHO*, 962
IARC. *International Agency for Research on Cancer. Biennial report 1986/87*, 106
ICRP. *Radiation dose to patients from radiopharmaceuticals: a report of a task group of Committee 2 of the ICRP. ICRP Publication 53*, 195
Isaacson, G., Mintz, M. C. and Crelin, E. S. *Atlas of fetal sectional anatomy. With ultrasound and magnetic resonance*, 395
James, R., Knowles, R. and Markisz, J. A. *Quality assurance and image artefacts in magnetic resonance imaging*, 196
Javadpour, N. and Murphy, G. P. (Eds). *Advances in urologic oncology. Progress in clinical and biological research, Vol. 277*, 961
Karasick, S. and Karasick, D. *Atlas of hysterosalpingography*, 504
Karimjee, S., Thomas, A. and Taylor, W. *Nuclear medicine. Self-assessment in radiology and imaging, No. 5.*, 1119
Keats, T. E. *Atlas of normal roentgen variants that may simulate disease, 4th edn*, 1035
Keats, T. E. and Smith, T. H. *An atlas of normal developmental roentgen anatomy, 2nd edn*, 567
Kessel, L. and Boundy, U. F. *Diagnostic picture tests in orthopaedics*, 569
Kittle, C. F. *Mesothelioma. Diagnosis and management*, 106
Kristensen K. and Norbygaard, E. (Eds). *Safety and efficacy of radiopharmaceuticals 1987*, 102
Kurtz, A. B. and Goldberg, B. B. *Obstetrical measurements in ultrasound. A reference manual*, 783
Kurtz, A. B. and Goldberg, B. B. (Eds). *Clinics in gastrointestinal ultrasound 23*, 957
Labovitz, A. J. and Williams, G. A. *Doppler echocardiography. The quantitative approach, 2nd edn*, 300
Landay, M. J. *Interpretation of the chest roentgenogram*, 101
Layfer, L. F., Petasnick, J. and Katz, R. S. *Rheumatologic disorders. Advanced exercises in diagnostic radiology 19*, 960
Lee, F. and McLeary, R. D. (Eds). *The use of transrectal ultrasound in the diagnosis and management of prostate cancer*, 300
Lee, S. H. and Rao, K. C. V. G. *Cranial computed tomography and MRI, 2nd edn*, 959
Letourneau, J. G., Elyaderani, M. K. and Castañeda-Zuñiga, W. R. *Percutaneous biopsy, aspiration and drainage*, 102
Lloyd, G. A. S. *Diagnostic imaging of the nose and paranasal sinuses*, 572
Logemann, J. A. *Manual for the videofluorographic study of swallowing*, 101
Löhr, E. and L.-D. Leder (Eds). *Renal and adrenal tumors: pathology, radiology, ultrasonography, magnetic resonance (MRI), therapy, immunology, 2nd edn*, 301
Manton, D. J., Roebuck, E. J. and Fordham, G. L. *Building and extending a radiology department—A practical guide to planning and project management*, 882
McMinn, R. M. H. and Hutchings, R. T. *A colour atlas of human anatomy, 2nd edn*, 570
Meire, H. B., Dewbury, K. C. and Cosgrove, D. O. *Ultrasound teaching cases, Vol. 1, 2nd edn*, 395
Mettler, F. A. Jr. *Contemporary issues in nuclear imaging. Radionuclide bone imaging and densitometry*, 882
Meyers, M. A. *Dynamic radiology of the abdomen. Normal and pathologic anatomy, 3rd edn*, 676
Middleton, W. D. and Lawson, T. L. (Eds).

INDEX TO SUBJECTS—continued

Anatomy and MRI of the joints. A multiplanar atlas, 1118

Miller, D. D. *Clinical cardiac imaging*, 571

Mink, J. H., Reicher, M. A. and Crues, J. V. III. *Magnetic resonance imaging of the knee*, 200

Mistry, R. *Manual of nuclear medicine prodedures*, 1119

Moseley, H. *Non-ionising radiaion: microwaves, ultraviolet and laser radiation*, 195

Moseley, I. *Magnetic resonance imaging in diseases of the nervous system: an introduction*, 779

Mould, R. F. *Chernobyl: the real story*, 103

Mould, R. F. and Rose, A. (Eds). *International strategies for the eradication of carcinoma of the cervix in developing areas: proceedings of the International Working Party meeting in India 1987*, 504

Murphy, C. H. and Murphy, M. R. (Eds). *Radiology for anaesthesia and critical care*, 506

NCRP. *Ionizing radiation exposure of the population of the United States. NRCP Report No. 93*, 103

Newton, T. H., Hasso, A. N. and Dillon, W. P. *Modern neuroradiology. Volume 3: Computed tomography of the head and neck*, 958

Nisbet, P., Gedroyc, W. and Rankin, S. *Case studies in diagnostic imaging: film interpretation for postgraduate examinations*, 882

Patterson, J. T. *The dread disease: cancer and modern Americal culture*, 397

Perry, N. and Chauhan, A. *Radiological casebook: 75 cases with clinico-radiological discussion*, 569

Picazo, J. (Ed.). *Glucagon in 1987: gastrointestinal and hepatobiliary physiology diagnosis and treatment*, 1120

Raghavan, D. (Ed.). *The management of bladder cancer*, 105

Ramsey, R. G. *Neuroradiology, 2nd edn*, 506

Raval, B., Yeakley, J. W. and Harris, J. H. Jr. *Normal anatomy for multiplanar imaging. I. The trunk and extremities. II. Head, neck and spine*, 301

Redel, D. A. *Colour blood flow imaging of the heart*, 784

Reed, K. L., Anderson, C. F. and Shenker, L. *Fetal echocardiography. An atlas*, 783

Riccabona, G. *Thyroid cancer. Its epidemiology, clinical features and treatment*, 678

Roche, A. F., Chumlea, W. C. and Thissen, D. *Assessing the skeletal maturity of the hand wrist: Fels method*, 1120

Rott, H.-D. *Bioeffect literature reviews 1980–1987*, 393

Roy, C. *Ultrasound of the abdomen. Exercises in radiological diagnosis*, 779

Sadamoto, K. and Fukui, K. *Cerebral angio-CT*, 301

Sakuma, S., Ishigaki, T. and Takeuchi, T. *Diagnostic imaging of the liver, biliary tract and pancreas. Data analysis and diagnostic procedures*, 782

Seward, J. B., Tajik, A. J., Edwards, W. D. and Hagler, D. J. *Two-dimensional echocardiographic atlas. Volume 1: Congenital heart disease*, 782

Sick, H. and Burquet, J.-L. *Imaging anatomy of the knee region*, 957

Sim, F. H. (Ed.). *Diagnosis and management of metastatic bone disease: a multidisciplinary approach*, 567

Simpkins, K. C. (Ed.). *A textbook of radiological diagnosis, Vol. 4. The alimentary tract: the hollow organs and salivary glands*, 504

Smith, H. (Ed.). *Lung cancer risk from indoor exposure to radon daughters. ICRP Publication 50*, 104

Smith, H. (Ed.). *Data for use in protection against external radiation. ICRP Publication 51*, 104

Smith, H. (Ed.). *Protection of the patient in nuclear medicine. ICRP Publication 52*, 104

Smith, P. H. and Pavone-Macaluso, M. (Eds).*Management of advanced cancer of prostate and bladder*, 105

Staudach, A. *Sectional fetal anatomy in ultrasound*, 393

Stevens, J. M., Valentine, A. R. and Kendall, B. E. *Computed cranial and spinal imaging. A practical introduction*, 394

Taenzer, V. and Wende, S. (Eds). *Recent developments in nonionic contrast media*, 1121

Taylor, K. J. W., Burns, P. N. and Wells, P. N. T. (Eds). *Clinical applications of Doppler ultrasound*, 200

Testa, N. G. and Gale, R. P. (Eds). *Haematopoiesis: long term effects of chemotherapy and radiation* , 778

Thomas, R. H. and Stevenson, G. R. *Radiological safety aspects of the operation of proton accelerators. Technical report series No. 283*, 961

Thron, A. K. *Vascular anatomy of the spinal cord. Neuroradiological investigations and clinical syndromes*, 1036

Timor-Tritsch, I. E. and Rottem, S. (Eds). *Transvaginal sonography*, 102

Tonnis, D. *Congenital dysplasia and dislocation of the hip in children and adults*, 396

Toombs, B. D. and Sandler, C. M. *Computed tomography in trauma*, 393

Umali, C. B. *Basics of chest film interpretation*, 568

Unger, J. M. *Head and neck imaging. Handbooks of diagnostic imaging*, 101

Vaeth, J. M. and Meyer, J. (Eds). *Time, dose and fractionation in the radiation therapy of cancer: a frontier revisited*, 778

Valavanis, A., Schubiger, O. and Naidich, T. P. *Clinical imaging of the cerebello-pontine angle*, 1036

Valk, J. *MRI of the brain, head, neck and spine. A teaching atlas of clinical applications*, 198

van Nieuwenhuizen, O. *Cerebral visual disturbance in infantile encephalopathy*, 960

Veiga-Pires, J. A. and Grainger, R. G. (Eds). *Pioneers in angiography. The Portuguese School of Angiography, 2nd edn*, 1035

Velchik, M. G., Alavi, A., Cohen, S. and Soloway, R. D. (Eds). *Contemporary issues in gastroenterology, Vol. 7. Gastrointestinal nuclear imaging*, 677

Wackenheim, A. and Badoz, A. *Computed tomography of the abdomen in adults. 85 radiological exercises for students and practitioners*, 1118

Wall, B. F., Harrison, R. M. and Spiers, F. W. *Patient dosimetry techniques in diagnostic radiology. IPSM Report No. 53*, 881

World Health Organization. *Rational use of diagnostic imaging in paediatrics. Report of a WHO study group. WHO Technical Report Series 757*, 302

World Health Organization. *Quality assurance in radiotherapy*, 780

World Health Organization. *Appropriate diagnostic technology in the management of cardiovascular diseases, Technical Report Series 771*, 1121

Williams, J. G. P. *Diagnostic picture tests in injury in sport*, 568

Wilmot, D. M. and Sharko, G. A. (Eds). *Pediatric*

imaging for the technologist, 675
Yasargil, M. G., Teddy, P. J. and Valavanis, A. *Microneurosurgery, Vol. IIIA*, 505
Zonneveld, F. W. *Computed tomography of the temporal bone and orbit. Technique of direct multiplanar, high resolution CT and correlative cryosectional anatomy*, 394

Instructions to authors, 99

BIR Bulletin

Honorary Editor, BIR Bulletin: D. Rickards, LRCP, MRCS, FFR(D)SA, FRCR
Please address all correspondence to: Honorary Editor, BIR Bulletin, The British Institute of Radiology,
36 Portland Place, London W1N 4AT
The British Institute of Radiology is not responsible for opinions expressed in the BIR Bulletin

Curt Westman Scholarship 1989

Early in 1989, after having been appointed as Consultant in ultrasound and mammography in Sheffield, it was suggested to me that I should apply for the 1989 Curt Westman Scholarship, to study mammography. I duly filled out the application form and took out the recently filed CV, and later I was informed that my application was successful; thus I have recently returned from Stockholm after observing various aspects of radiology there.

I was greeted in Sweden by Dr Bertil Lamke who was wearing a Royal Navy Sweatshirt, hoping, he explained, to aid my recognition of him. This was the first time (but not the last) I was to feel overdressed during my stay in Sweden. It was also my first experience, after a tour of Stockholm and a delightful dinner, of the warmth and hospitality that I was to receive during my stay.

Accommodation had been arranged for me in a private flat with a balcony overlooking a lake surrounded by forest. The flat was just a few minutes' tube-ride from the clinic in Vallingby, where I was based. This clinic is basically a private hospital with a Diagnostic Radiology Department situated on the ground floor. The latter contains the only CT scanner owned privately in Sweden, the government apparently believing that this sort of facility is best contained within the public sector.

I arrived early the next morning and passed through a brightly decorated waiting-room containing not only new magazines, sculpture and a high-tec clock, but even comfortable chairs. I wore a blazer and tie, wishing to appear fairly casual but smart, and realized that this was not the norm when I was introduced to the other radiologists, who were wearing jeans and t-shirts. As I visited several departments during my stay, I saw that this mode of dress was the standard; however, it does not seem to detract from the quality of medicine practised.

Mammography, which is the financial engine of the Radiology Department at the clinic, is a mix of clinical, symptomatic and screening. They have been screening for 10 years, and I felt embarrassed that they could take out mammograms from 10 years ago that are of the same diagnostic quality as today's, whereas we in Britain can hardly do that for films of 2 years ago. In a session, 25 women are X-rayed, examined by the radiologist, have further views including magnification, are ultrasounded if necessary and talked to. This was the first time (but again not the last) I was to see how much radiology in Sweden is more at the front of clinical management and of the decision-making process than it is here in the UK.

The pattern of mammography followed here was much as I saw elsewhere in Sweden, and that was: under 50 years, two views per breast every 18 months; over 50, one view every 2 years, or two views if the breasts were dense. Those women who are normal are given a ticket and asked to return in 18 or 24 months. Those that have an abnormality return to a weekly assessment clinic where stereotactic biopsy is made, or if having had a positive biopsy previously, are seen by an oncologist rather than a surgeon (this being the traditional route of primary referral).

In the afternoon, I visited the Huddinge University Hospital which is a suburb of Stockholm. It could best be described as a general teaching hospital. It has a radiology department comprising 28 diagnostic rooms. There are 50 (50!) film alternators for film display and reporting. Each major specialty has its own demonstration room within the department, with a set of film alternators where all the current cases are kept.

I made two visits to the Karolinska Hospital during my stay. It is in the centre of Stockholm and layed out with a number of buildings spread out over extensive grounds with large areas of grass, trees and shrubbery. Each building, however, houses a separate specialty, *e.g.* cardiothoracic or neurological, and each contains its own radiology. Thus the chest radiologists in one building are essentially totally separate from the neuroradiologists in another building, perhaps not such a bad idea at that!

It was at the Karolinska that I met Dr Gunilla Svane and Dr Edvard

Azavedo who have written extensively on mammography, and in particular about their experience with stereotactic fine-needle aspiration (FNA). They have performed literally thousands of biopsies using this technique, which they carry out on the prone-lying breast-hanging table. Dr Azavedo came along to one of the assessment sessions at the Vallingby Clinic and performed a number of stereotactic biopsies using their CGR unit. There is no doubt that using an electronic built-in calculator with the stereotactic facility makes biopsy or localization both quick and easy. The FNA slide smears were made by Dr Azavedo in the mammography room as soon as they had been taken, a process he felt was within the capability of most radiologists, but having spent his early career as a pathologist before he switched to radiology he may be a little biased.

While I was in Sweden, Dr Laslo Tabar was taking a visiting party of approximately 30 Americans to various mammography centres around Sweden. I wish to thank profusely Dr Cristina Hedborg-Melander and Dr Eva Frodis who allowed me to visit their mammography unit in Vasteras just the day after they had "entertained" Dr Tabar and group, an experience they described as exhausting. These two radiologists have, with their radiographers, nurses, secretaries and assistants a warm, close-knit working atmosphere which one had to experience only briefly in order to appreciate and see its value, particularly when working in a small field such as mammography.

Vasteras has a screening population of 47 000 women. Using a combination of a mobile and a static screening unit, these women have been screened in just over 18 months: this is approximately twice "Forrest rate". The two radiologists are, perhaps unlike in most places in the UK, both full-time mammographers, but they evidently get great satisfaction from their work and do not feel that this is a negative point. A list of women for screening is sent form the central government source, and timed and dated appointments are then sent out by the mammography clinic.

Approximately 160 women are screened each day at the two screening centres and the films are returned, undeveloped, in a light tight box, to the central clinic where the developing, reading and assessment take place. It takes about 1 hour to process the films and 2–3 hours to place all the films on a mammography film alternator. All the films are double read and if 1 day is lost, for example because of visiting radiologists, then it takes a considerable effort to catch up.

They estimated that about 4-5% of women were recalled. This is the first time that I have really seen screening in action on a large scale, and it can work if done by people who are dedicated and believe that screening mammography is a viable concept. Adequate central government funding is, however, an essential prerequisite. If I wished to provoke a little mirth amongst our Swedish colleagues, I would talk about single-view, 3-yearly screening: it never failed.

On my final working day, I visited Dr Per Sundin at the Danderyds Hospital, Stockholm. Here, although a new mammography centre was being built at the hospital, screening mammography was being performed in the department with screening unit and processor in the same room. Viewing took place on an alternator in a space about 6 feet by 6 feet: it was a little cramped, but again I found great enthusiasm for the concept of screening.

Lunch at the top of the Kaknas tower, at over 500 feet the tallest structure in Scandinavia, on a beautiful summer's day, with superb views over Stockholm, brought my working visit to a close.

Stockholm is, without doubt, one of the most beautiful and interesting cities that I have visited. Elegant buildings, clear lakes and canals crossed by wide bridges make an excellent walking environment. It is impossible to visit Stockholm without taking a boat ride during the long summer's evenings out into the archipelago to the east where there are thousands of tree-covered islands. The city has some superb museums, art galleries and a world famous opera house, although to listen to an opera about an American, based on an English musical comedy, composed by an Italian, set in Japan and sung in Swedish provides an interesting cultural mix. The music (Madame Butterfly) was familiar, however, and thus most enjoyable.

Finally, while I was visiting the Huddinge University Hospital, I attended the Radiology Department lunchtime film discussions. I found this nerve-wracking, as the visiting radiologist is inevitably seated in the front row and asked unanswerable questions. There was one small problem, however, as the two most interesting cases of the day had been pinched by the orthopaedic surgeons—this familiar tune is also heard in Sweden.

I wish to thank Dr Bertil Lamke and Dr Christian Hardstedt for showing such interest and hospitality during my visit to Stockholm, and thanks also to the other radiologists who took time to show me around the many departments I visited. I can recommend without reservation the experience that the Curt Westman Scholarship allowed me to enjoy. I wish, also, to thank the Edinburgh E.A.R. Trust who helped to finance my trip.

R. J. Peck

Curt Westman Scholarship

Members wishing to visit the clinic in Vallingby, Sweden, of the late Dr Curt Westman, now owned by AB Medicinsk Rontgen, should write to the General Secretary of the BIR. Return air ares and 2 weeks' accommodation are generously provided by AB Medicinsk Rontgen, and the BIR provides a sum towards expenses.

BIR Company Subscribers

The BIR company subscriber scheme was launched at the end of 1987 and is aimed at all companies who advertise in the BJR or exhibit at the MED X RAY technical exhibition.

For a subscription of just £250 per annum for an initial period of 3 years, an attractive package of benefits is offered (see March 1988 Bulletin for details).

If your company is interested in joining the scheme, please contact: Miss Susan Johnstone, General Secretary, British Institute of Radiology, 36 Portland Place, London W1N 4AT; Tel: 01 580 4085. Companies which have enrolled to date are listed below.

Agfa-Gevaert Ltd
27 Great West Road, Brentford, Middlesex TW8 9AX; tel. 01-560 2131. Product Areas 1. Contact Mr G. Mountford, Director.

Amersham International PLC
Lincoln Place, Green End, Aylesbury, Bucks HP20 2TP; tel. 0296-395222. Product areas 4, 5, 6. Contact Mr James McLaughlin, Sales and Marketing Manager.

British Nuclear Fuels plc
Room 525, Hinton House, Risley, Warrington, Cheshire WA3 6AS; tel. 0925-835022. Product areas 8, 11. Contact Dr R. J. Berry, Director of Health and Safety and Environmental Protection.

Cardiac Services Ltd
95A Finaghy Road, South Belfast BT10 OBY; tel. 0232-625566. Product areas 1, 3, 4, 5, 6. Contact Mr R J Brown. Managing Director.

Central Electricity Generating Board
15 Newgate Street, London EC1A 7AU; tel. 01-634 6898. Product areas 7, 8. Contact Mr R. V. Brierley, Office Services Manager.

E. G. & G. Astrophysics Research Ltd
Vale Road, Windsor, Berkshire SL4 5JP; tel 0753-855611. Product areas 1, 6, 7, 8,. Contact Miss Susan Holgate, Sales Executive (Therapy).

Elscint (GB) Ltd
Tower Road, Berinsfield, Oxfordshire OX9 8LW; tel 0865-340900 . Product areas 1, 3, 4. Contact Ms Faith Gorman, Managing Director.

E-Z-EM Ltd
1230 High Road, Whetstone, London N20; tel 01-446 9714. Product areas 1, 2, 8. Contact Mr D. F. Wills, Sales and Marketing Manager.

Fugi Photo Film (UK) Ltd
125 Finchley Road, London NW3 6JH; tel 01-586 9351. Product areas 1, 3. Contact Mr R. G. Brown, Marketing and Administration Manager.

Gammex-RMI Ltd
4 Clarendon Chambers, Clarendon Street, Nottingham NG1 5LN; tel. 0602-483807. Product areas 1, 3, 4, 5, 6. Contact Miss Eileen Parr, Commercial Manager.

IGE Medical Systems Ltd
352 Buckingham Avenue, Slough, Berks SL1 4ER; tel. 0753-874000. Product areas 1, 3, 4, 5, 6, 8. Contact Mr Jack Strange, Sales Administration.

Kodak Ltd
PO Box 66, Station Road, Hemel Hempstead, Herts HP1 1JU; tel. 0442-61122. Product areas 1. Contact Mr P. E. Blackwell, Manager, Health Sciences Division.

Mallinckrodt Diagnostica (UK) Ltd
11 North Portway Close, Round Spinney, Northampton NN3 4RQ. tel. 0604-46132. Product areas 4, 5. Contact Mr D. G. L. Wood, Business Manager.

Medical XraySupplies Ltd
Unit 12, Kingsbury Industrial Estate, Church Lane, Kingsbury, London NW9 8AU; tel. 01-205 9500. Product areas 1. Contact Mr R. J. Laird, Sales Director/Managing Director.

Nuclear Associates
100 Voice Road, Carle Place, New York 11514-1593, USA; tel 516-741 7614. Product areas 1, 3, 4, 5, 6, 8. Contact Mr H. Glasser, General Manager.

Nycomed (UK) Ltd
Nycomed House, 2111 Coventry Road, Sheldon, Birmingham B26 3EA; tel 021-742 2444. Product areas 1, 3. Contact Mr L. Birch Hansen, Managing Director.

Polaroid (UK) Ltd
Ashley Road, St Albans, Herts AL1 5PR; tel 0727 59191. Product areas 1, 3. Contact Ms Tina Thompstone, Product Supervisor.

Premise Engineering Ltd
Tibbs Hill Road, Abbots Langley, Watford, Herts WD5 ODR; tel. 09277-67433/63320. Product areas 8. Contact Mr R. K. Beach, Director.

Quantel Ltd
Administration Centre, Kiln Road, Newbury, Berkshire RG13 2HA; tel. 0635-32222. Product areas 2, 10. Contact Mr Christopher Trim, Publicity Officer.

Schering Health Care Ltd
The Brow, Burgess Hill, West Sussex RH15 9NE; tel. 04446-6011. Product areas 1, 2, 3. Contact Mr A. Greaves, Product Manager.

3M UK PLC
3M House, Bracknell, PO Box 1, Berks RG12 1JU; tel. 0344 426726. Product areas 1. Contact Mr Alan Budge, Marketing Manager.

Toshiba Medical Systems Europe BV
Schieweg 1, 2627 An Delft, The Netherlands; tel. 015 61 0121. Product areas 1, 6. Contact Mr. P Blonk, Office Manager, X-ray BU.

Wardray Products Ltd
Hampton Court Estate, Summer Road, Thames Ditton, Surrey KT7 OSP; 01-398 9911. Product areas 8. Contact Mr R. B. Wardley, Managing Director.

Key to product areas:

1. Diagnostic X-ray inc. NMR and CT.
2. Interventional radiology.
3. Ultrasound.
4. Nuclear medicine.
5. Radiopharmaceuticals.
6. Radiotherapy and oncology.
7. Radiobiology.
8. Radiation protection.
9. PACS.
10. Image processing.
11. Nuclear fuel cycle services.

Product News

Monitoring system for radon and neutron dosimetry

Vinten Instruments has introduced a computer-controlled PN3 system for the measurement of radon concentrations and neutron fields. PN3 is a high quality polymer track-etch material developed for dosimetry applications. For personal or environmental monitoring, PN3 elements are exposed in holders for predetermined periods, and are then chemically etched in 100-element magazines before passing to an automatic processor for readout. The special optical and lighting system results in greatly magnified alpha particle tracks which are visible to the naked eye. Complete data management systems are supplied by Vinten to suit individual customer needs.

For further information contact: Vinten Analytical Systems Ltd, Sunderland Road, Sandy, Bedfordshire SG19 1RB. Tel: (0767) 82222

Rapid response call point system for X-ray departments

Teltronic Communications have devised a system which enables nursing staff to summon assistance quickly and simply. Loud Speaking units are sited at strategic points throughout the department, each with a "Speak" button which when operated transmits speech to all units on the System. The called person can quickly confirm that they have received the message and will be attending.

For further information please contact: Kevin Cain at Teltronic Communications. Tel: (0377) 830265

The push-button cyclotron

The rapid development of nuclear medicine has increased the need for radioisotopes. Traditionally these have been produced either in nuclear reactors or in cyclotrons operated by research departments at major universities and hospitals. Demand has now reached the level where it requires industrial scale facilities.

Ion Beam Applications SA (a joint venture between the Belgian National Institute for Radioelements and the Catholic University of Louvain) has recently introduced a Cyclone 30 cyclotron which is able to operate for long periods without the main cyclotron chamber having to be opened. A high performance vacuum pumping system enables the cyclotron's external ion beam source, stripper probes and target assemblies to be cycled between high vacuum and atmosphere to allow these subsystems to be maintained and operated. The pumping systems have been supplied by Edwards.

The Cyclone 30 is so named because it is a fixed field, fixed frequency machine capable of accelerating H-minus ions up to 30 MeV. This allows the production of all the cyclotron-based isotopes commonly used for nuclear medicine.

For further information contact: Mr J. F. Fowler, Edwards High Vacuum International Tel: (0293) 28833

In brief

Vinten Analytical Systems Ltd has been appointed exclusive UK distributor for the range of therapy treatment products made by Theratronics International Ltd of Ontario. Products include the fully computerized Radiotherapy Treatment Planning System (Theraplan), Therasim Simulator System, Theratron Series Cobalt 60 units and resourcing and a capability beam data acquisition system (Therascan).

For further information contact: Vinten Analytical Systems Ltd, Sunderland Road, Sandy, Bedfordshire SG19 1RB. Tel: (0767) 82222.

BIR

Conference Services

Is there a seminar, conference or evening get-together you want to organize, but you don't have the time? The BIR Conference Office may be able to help you. Please call Nelleke van Helfteren, Conference Manager, to discuss possibilities.

01-580 4085

A Philips Gyroscan T5 Magnetic Resonance Imager was delivered to the King Edward VII Hospital at Midhurst in West Sussex at the end of August. Costing £1 million, the Gyroscan T5 is the first of a new, lighter, more compact generation of MRI units which are more cost effective in operation.

For further information contact: Dr E. H. Burrows, MRI Unit, King Edward VII Hospital, Midhurst, West Sussex GU29 OBL. Tel: (073081) 2341

The IGP Durr Med 260 X-ray film processor is ideally suited for use in a mobile breast screening operation as it needs only 1 x 1/2 m standing area. It is fully automatic and has an integral replenishment system controlled by microprocessor. A full range of Daylight Attachments are available for daylight processing.

For further information contact: IGP (UK) Ltd, 1-5 Cutler's Road, South Woodham Ferrers, Chelmsford, Essex CM3 5JS. Tel: (0245) 323555

BIR Calendar

Unless otherwise indicated, enquiries about the following events should be addressed to the Conference Manager, British Institute of Radiology, 36 Portland Place, London W1N 4AT (Tel. 01-580 4085).

Vascular effects in tumour therapy
November 10, 1989
Chairman: Dr I. J. Stratford

What shall we do about osteoporosis?
November 22, 1989
Middlesex Hospital, London
Joint BIR/NOS all day meeting
Chairman: Prof. P. J. Ell
Speakers: J. Adams, I. Cullum, M. Fischer (Kassel), I. Fogelman, M. Hall, A. Horsman, H. Jacobs, P. Meunier (Lyon) L. Rosenthall (Montreal), G. Russell and R. Valkema (Leiden)

Radiation protection — sense or nonsense?
December 13, 1989
All day meeting at Middlesex Hospital, London
Chairmen:Dr R. J. Berry and Prof. K. Boddy
Speakers: R. J. Berry, T. Godden, P. Green, D. Henshaw, G. Kendall, B. A. Lindskoug (Halmstad), N. Pearce, R. Phillip, E. Radford, G. Russell, B. Wall and S. J. Wozniak

Impact of modern imaging techniques in everyday ENT practice
January 18, 1990
Joint BIR/RCR/RSM evening meeting organized by the BIR
Chairman: Dr P. Anslow
Speakers: P. Anslow, T. Alun-Jones, L. Watson and H. Whittet

Methods of determining blood flow using radionuclides
February 13, 1990
Joint IPSM/BIR all day meeting organized by IPSM

Quantification in imaging—what has it achieved and what is its future?
February 21, 1990
Chairmen: Drs R. Speller and W. Hateley

Radiobiology proffered papers
February 23, 1990
All day work-in-progress meeting

Imaging towards 2000 — practical integration of new technologies
March 21, 1990
All day meeting at the Scientific Societies, London
Chairmen: Profs P. N. T. Wells and I. Isherwood
Speakers: R. Frakowiak, A. Hemingway, J. Howart, W. R. Lees, H. Nunnerly, M. Smith and J. Williams

Photodynamic therapy
April 4, 1990
Joint BIR/IPSM all day meeting organized by the BIR
Chairman: Dr D. Ash

BIR Annual General Meeting
May 3, 1990 at 5 p.m.
36 Portland Place, London
BIR members only

The combination of chemotherapy and radiotherapy in clinical practice
May 10, 1990
All day meeting
Chairman: Prof. A. Horwich

The repair of radiation damage — molecules to man
May 11, 1990
All day work-in-progress meeting

Radiology 90

Harrogate, 11-13 June 1990
Deadlines for receipt of proffered abstracts 12 January 1990 Contact the Conference Office for an abstract form.

Library News

The BIR Library is open weekdays 9 a.m.–5 p.m. (7 p.m. on Tuesdays).

The Librarian, Mrs Gunnel Ingham, is in attendance Tuesdays 11 a.m.–7 p.m. and Thursdays 11 a.m.–5p.m. In her absence, assistance will be given by Miss Helen Smith. (Tel: 01-580 4085.)

The journal stock includes more than 100 titles. Though journals may not be taken out of the library, there is a photocopy service, also available by post or FAX. A list of current journals is available on request and is also published in the March and September issues of the Bulletin. Most books (excepting the historical collection) are available on loan.

There is an agreement which allows Institute members limited use of the Royal Society of Medicine Library for reference purposes. Members should apply to the Librarian for a visitor's card.

Recent additions to the library

D. M. Taylor, C. W. Mays, G. B. Gerber and R. G. Thomas (Eds). BIR Report 21: Risks from radium and thorotrast. Proceedings. 1989

C. K. Bomford, P. D. K. Dawes S. C. Lillicrap and J. Young. BJR Supplement 23: Treatment simulators. 1989

Halperin, E. C., Kun, L. E., Constine, L. S. and Tarbell, N. J.: Pediatric radiation oncology. 1989

Roberts, D. P. and Smith, N. L. Radiographic imaging—a practical aproach. 1988.

Staudach, A. Sectional fetal anatomy in ultrasound. 1987.

Taenzer, V. and Wende, S. (Eds). Recent developments in nonionic contrast media. 1989

Meetings and Courses

NPL Course on Measurement Techniques for Colorimetry and Spectrophotometry
November 21–22, 1989
NPL, Teddington
Further details: J. F. Verrill, National Physical Laboratory, Teddington, Middlesex TW11 0LW. Tel: 01-977 3222, Ext. 6646.

Biliary Lithotripsy
December 7–9, 1989
January 11–13, 1990
February 1–3, 1990
March 1–3, 1990
May 3–5, 1990
June 7–9, 1990
Baltimore, Maryland, USA
Further details: Program Coordinator, The Johns Hopkins Medical Institutions, Office of Continuing Education, Turner Building, 720 Rutland Avenue, Baltimore, Maryland 21205, USA. Tel: 301 955 2959.

Strontium 89 Chloride in Prostatic Cancer—A Major Advance in the Treatment of Metastatic Bone Pain?
December 13, 1989
London
Further details: Dr V. R. McCready, Nuclear Medicine Department, The Royal Marsden Hospital, Downs Road, Sutton, Surrey SM2 5PT.

Health Physics Experience in Decommissioning Contaminated Plant and Buildings
January 23, 1990
St Bartholomew's Hospital, London
Further details: Dr D. N. S. Dixon, Programme Committee Secretary, 67 Oatlands Park, Linlithgow, West Lothian EH49 6AS. Tel: 031-244 2253.

International Symposium in Physics of Medical Imaging and Advances in Computer Applications
February 21–23, 1990
New Delhi, India
Further details: Dr M. M. Rehani, Organizing Secretary, ISPMICA, Medical Physics Unit, IRCH, All India Institute of Medical Sciences, New Delhi-110029, India.

Impact of Personal Computers on Radiation Oncology Departments 4th Workshop of the European Association of Radiology Commission Informatique
April 23–25, 1990
Geneva, Switzerland
Further details: Dr P. Minet, Service de Radiothérapie, CHU Sart-Tilman, 4000 Liege, Belgium. Tel: 041-30 71 11.

Spectrum of Developmental Disabilities XII: Prematurity: Neuro-Developmental Assessment and Intervention Issues
March 19–21
Maryland, USA
Further details: Program Coordinator, The Johns Hopkins Medical Institutions, Office of Continuing Education, Turner Building,720 Rutland Avenue, Baltimore, Maryland 21205. Tel: 301 955 2959.

1st International Confrontations Ultrasound Locomotor Apparatus
March 30–April 1, 1990
Montpellier, France
Further details: R Fonquernie, Laboratoire de Chirurgie Experimentale, Institut de Biologie, Faculté de Médecine, 4 Boulevard Henri IV, 34000 Montpellier, France.

Health Physics Objectives in the Design of Plant and Equipment
April 3, 1990
City University, London
Further details: Dr D. N. S. Dixon, Programme Committee Secretary, 67 Oatlands Park, Linlithgow, West Lothian EH49 6AS. Tel: 031-244 2253.

2nd International Brachytherapy and Remote Afterloading Symposium and Workshop
April 19–21, 1990
St Louis, Missouri
Further details: Carlos A. Perez, Director, Radiation Oncology Centre, Mallinckrodt Institute of Radiology, 4511 Forest Park Boulevard, Suite 411, St Louis, Missouri 63108, USA.

72nd Annual Meeting of the American Radium Society
April 21–25, 1990
Scottsdale, Arizona
Further details: Ms Suzanne Bohn, Administrative Director, American Radium Society, 1101 Market Street, 14th Floor, Philadelphia, PA 19107, USA.

British Nuclear Energy Society Conference on Occupational Exposure
April 29–May 3, 1990
Guernsey, Channel Islands
Further details: Mr G. A. M. Webb, National Radiological Protection Board, Chilton, Didcot, Oxon OX11 ORQ. Tel: 0235 833891.

Diagnostic Imaging in Musculo-Skeletal Radiology
May 10–11
Glasgow
Further details: The Honorary Secretary,Royal College of Physicians & Surgeons of Glasgow, 242 St Vincent Street, Glasgow G2 5RJ. Tel: 041 221 6072

6th International Congress on Breast Diseases
June 10–14, 1990
Boston, USA
Further details: Congress Secretariat, Office of Continuing Education, Tufts University School of Medicine, 136 Harrison Avenue, Box 36, Boston, Massachusetts 02111, USA.

International Skeletal Society — 4th Annual Meeting of the European Society of Head and Neck Radiology September 12–15, 1990
Brescia, Italy
Further details: The Organizing Secretariat, Clas International S. r. l., Via Pace, 8, 25122 Brescia, Italy. Tel: 9 30 48006.

Ultrasound Angiography
September 25–28,1990
London
Further details: The Conference Secretariat, P.O. Box 15, Eastleigh, Hampshire S05 5XG.

16th L.H. Gray Memorial Conference Vasculature as a Target for Anti-Cancer Therapy
September 17–21, 1990
Manchester
Further details: Dr J. V. Moore, Paterson Institute of Cancer Research, Christie Hospital and Holt Radium Institute, Wilmslow Road, Manchester M20 9BX. Tel: 061-445 8123, Ext. 518.

As a service to our readers, notice of meetings or courses will be inserted free of charge. Please send full details to the Honorary Editor, BIR Bulletin.

BIR Bulletin

Honorary Editor, BIR Bulletin: D. Rickards, LRCP, MRCS, FFR(D)SA, FRCR
Please address all correspondence to: Honorary Editor, BIR Bulletin, The British Institute of Radiology,
36 Portland Place, London W1N 4AT
The British Institute of Radiology is not responsible for opinions expressed in the BIR Bulletin

An introduction to Radiology 90

By V. Ralph McCready, Scientific Programme Chairman

Next year's Annual Congress of the British Institute of Radiology promises to be the best ever. Taking place at the same time as The College of Radiographers' Annual Conference, over 1500 delegates are expected to attend the meetings and visit MED X RAY—the premier exhibition of medical X-ray equipment in the UK.

The scientific programme has a new format which will provide something for everybody, as well as specialized sessions for the real expert. Most sessions throughout the meeting will begin with a review lecture given by an expert in his or her field. The international faculty of lecturers has been chosen to provide up-to-date reviews which will interest equally the trainee for higher examinations and established consultants and scientists who wish to refresh their memories. Reviews include subjects of topical interest in diagnostic radiology, ultrasound, nuclear medicine, physics and radiotherapy.

In diagnostic radiology, the modern approach to the assessment of spinal disorders will be reviewed, comparing and contrasting the newer methods such as magnetic resonance imaging. Other radiological topics will include the radiology of chest trauma, the radiology of the liver, joint disease and paediatric renal disease.

Radiotherapists will be interested in latest thoughts on the use of PET oncology, the treatment of soft-tissue sarcomas and current techniques for their diagnosis. Conformation radiotherapy will be discussed and a special session will be devoted to the effect on radiotherapy dose distribution of tumour control probability.

Radiology 90

Harrogate, 11-13 June 1990

Ultrasound enthusiasts will be able to hear how colour Doppler works, while the clinical applications of colour Doppler will be reviewed. Other review lectures will include rectal endoscopic ultrasound and the use of ultrasound in paediatrics.

Radio-isotope reviews will include studies in the heart and the endocrine glands. With the current media interest in bone density, a review of clinical bone densitometry will be compulsive listening for both radiologists and nuclear medicine physicians.

Following the popularity of last year's teach-ins, Radiology 90 will include tutorials on diagnosis and radiotherapy treatment planning in head and neck cancer.

A new concept to be tried at Radiology 90 is the consensus workshop. Subjects of current debate such as the evaluation of skeletal metastases and the best techniques for the diagnosis of testicular tumours will be discussed by leading experts with opposing views. If a consensus can be reached, a paper will be prepared for publication to guide the rest of us! Enough time will be allowed for in-depth discussion which should provide interest and perhaps entertainment for the audience.

During the three day meeting, plenary sessions will include lectures by interventional ultrasound expert Hans Holm from Denmark; Fred Lizzi from the USA will present his experience with ultrasound therapy in the eye and Juliana Denekamp from the CRC Gray Laboratory will talk on tumour vasculation.

Harrogate is set in Brontë or Herriot country, depending on whether you read or watch television. It provides an excellent conference venue and promises a pleasant social programme which will include (for the outdoor types) a golf match, a fishing competition, and trips to York, Castle Howard, Ripley Castle and through the Yorkshire Dales—some of the most striking landscape in the British Isles. For the not-so-energetic, the civic reception, buffet and disco and BIR annual dinner will provide entertainment and opportunity to meet up with old friends and make new ones.

So, in the words of the President, Kit Hill, COME AND JOIN THE PARTY!

Dr R.H. Thomlinson died unexpectedly on 13 August 1989. There can be few radiobiologists or radiotherapists who have not, at some time, quoted the Thomlinson and Gray model of diffusion limited oxygen penetration leading to hypoxia in tumours. The following tribute to Hugh Thomlinson was kindly provided by Dr Oliver Scott.

Hugh Thomlinson, 1922–1989. A personal tribute

Hugh was an original. Throughout his life, he set his own mark on each of his multitudinous activities. I remember him at Cambridge, 50 years ago, studying anatomy. The other medical students were struggling with Gray's textbook and a pile of bones; not so Hugh. He decided to make an exact model of the human organs in polychromatic plasticene and a most elegant construction gradually took shape in the bottom of a large cardboard box. It was never finished.

I have memories of Hugh as a rock-climber; before we reached the rock-face, he would check every aspect of our equipment. When the climb began, he would move slowly and deliberately, each action calculated in advance, and I always had total confidence that we would arrive safely at the summit. He was passionate about the importance of good equipment. When Alan Conger announced his intention of climbing the Matterhorn and bought himself an ice-axe, Hugh took hold of it, carefully placed the steel blade on a raised hearth and leapt onto the handle with his full weight. "Stop!" cried Alan. But "Better to break it in South Kensington than on the mountain" replied Hugh with episcopal gravity. Climbing, medicine and religion were all linked in Hugh's mind. As a schoolboy, he was inspired by the story of T. Howard Somervell, whose book *After Everest—the Experiences of a Mountaineer and Medical Missionary* was published in 1936.

Hugh was educated at Rugby and studied medicine at Cambridge and St. Thomas' Hospital, to which he returned after his National Service in the Army. A turning point in Hugh's life was in the autumn of 1953, when he first met L.H. Gray. Hal Gray was intensely interested in the problem of tumour hypoxia and had calculated a diffusion path of around 145 microns for oxygen. Hugh had been studying the pattern of necrosis in tumours and Hal naturally asked the vital question "How thick are the layers of tumour before necrosis sets in?" Hugh replied "Around 160 microns". There was electricity in the air. The consequences of this meeting are well known to radiobiologists and "Thomlinson and Gray, 1955" is still quoted today. It is a curious fact that the BJR referees blocked publication and the manuscript went elsewhere. Perhaps this rejection was a measure of the originality of this work?

Hugh was converted to the idea of becoming a radiobiologist and joined the MRC Experimental Pathology Unit under G. J. Popjak and later Tikvah Alper. Another landmark in Hugh's career was the appearance of his paper with Elizabeth Craddock in 1967. They introduced a new method of plotting growth delay in irradiated tumours and demonstrated the effect of oxygen combined with irradiation over a wide range of oxygen pressures. Hugh was extremely interested in the work of Luke van Putten and Bob Kallman on reoxygenation, and a strong friendship arose between Hugh and Bob, broken only by Hugh's death.

Hugh's contribution to the development of radiobiology cannot be related to the number of his published papers and it may be that he exerted his greatest influence as a teacher. He organized a teaching course in radiobiology for the Royal College of Radiologists at Mount Vernon Hospital. It was written, "He had planned the five days with enormous care and attention to detail regarding what speakers should cover. He sat through the whole course himself and raised questions of clarification throughout. He showed us, as a group of clinicians, that it was possible to think logically and usefully about the subject in relation to clinical radiotherapy. He did this by explaining the basis of the scientific method in relation to data and hypothesis and showed how they worked in practice".

The last decade of Hugh's life, when he was working at Mount Vernon Hospital, was devoted to the development of measurement based sequential therapy (MBST). This involved making and recording thousands of measurements of tumour size, a task calling for great patience (a virtue with which Hugh was generously endowed). It has to be said that MBST has not as yet been accepted by the scientific community and Hugh did feel isolated and, to some extent, misunderstood. Hugh was on dangerous ground when he questioned the necessity for randomized clinical trials, but perhaps we should remember that good clinical observation often precedes a trial. It is to be hoped that somewhere, sometime, the outcome of MBST will be compared with conventional methods in a fully randomized trial and then this brilliant foray into the unknown may be vindicated.

Hugh will also be remembered for

his skills and activities outside the realm of science: for his woodwork, his photography, his love of history and music and, in particular, for the barn concerts which he and Shelagh organized so beautifully and which gave his friends so many memorable evenings.

O. C. A. Scott

Meeting Report BIR Welsh Branch

The summer meeting of the Welsh Branch of the British Institute of Radiology took place at the Cwrt Bleddyn Hotel, Llangybi, Gwent on June 9 and 10 1989. The meeting was a combined event with the South West Radiologists' Association and was very well attended by members of both organizatons.

Also present was the President of the BIR, Professor Brian Worthington. He was a principal speaker, and the Welsh Branch were very pleased that he was able to take part.

The meeting was preceded by a dinner on Friday evening which was a great success; in spite of this, the scientific meeting on the following day was well attended. The meeting was preceded by a short business meeting for the Welsh Branch of the BIR.

The main scientific meeting opened with a lecture by Professor Worthington entitled "In the twinkling of an eye" in which he gave an overview of the problems due to artefact in magnetic resonance imaging. His entertaining and illuminating lecture covered the approaches adopted by his team in Nottingham to shorten the acquisition time for imaging. The acquisition of the data in only 64 ms without the need for signal averaging had permitted study of flow and motional activity of body organs in real time. The audience found his lecture stimulating and it gave an exciting insight into current developments in this field.

Professor Worthington's talk was followed by a contribution from the South West Radiologists's Association. Dr Iain Birchall of Frenchay Hospital, Bristol gave a paper called "Thyroid ultrasound: what's the point?". He began with a review of the current status of ultrasound of the thyroid in most hospitals. He felt that the technique, sometimes employed by clinicians, was underused and in many cases answered only very limited questions. He was of the view that ultrasound examination of the thyroid was extremely cost effective and could answer a much wider range of questions in both nodular disease and hyperthyroidism. He presented the results of scanning over 2000 thyroids and besides demonstrating from this material the usefulness of the technique, he was careful to point out limitations and pitfalls that the less experienced ultrasonographer might encounter.

The pre-coffee slot was occupied by another member of the South West Radiologists' Association, Dr G. Hartnell of Bristol Royal Infirmary. Dr Hartnell gave a paper entitled "Is coronary angioplasty a good investment?". Dr Hartnell also pointed out that angioplasty has not been shown to improve life expectancy, which would make it unreasonable to apply it to those groups of patients in which coronary bypass grafting has been shown to improve long term prognosis. In terms of the relief of symptoms in patients who have angina with one or two vessels involved, angioplasty remains a worthwhile procedure.

Following coffee the first speaker was Mr R. L. Gower, a urological surgeon at St Woolos Hospital, Newport. The topic covered was "The current status of lithotripsy in the management of renal stones". He presented a balanced view of the position of this technique in the treatment of renal calculi and proposed guidelines as to which stones would be suitable for therapy, particularly if lithotripter were immediately available. The relative merits of equipment were discussed and he completed his presentation with cautionary comments on the complications that arise from inappropriate lithotripsy.

Dr Anthony Jones, consultant radiologist at the Royal Gwent Hospital, Newport, and experienced ultrasonographer presented "Some difficult diagnoses in prenatal ultrasound". The basis for the paper was Dr Jones' experience of prenatal scanning in an area of a high incidence of neural tube defects. In Gwent all pregnant women are offered prenatal screening and over 90% choose to enter the screening programme. Scans are performed at 16 weeks though personal preference was for an 18–20 week fetal survey. Dr Jones then shared his experience over the last few years of some of the difficult diagnostic problems he had encountered. Included were the difficulties of assessing mild cerebral ventriculomegaly, minor variants of spina bifida, bone density in the fetus, diaphragmatic hernia and pleural effusions. The limited time available did not allow discussion of the difficulties related to the urinary tract and gastrointestinal tract in fetal ultrasonography. The paper was concluded with the proposition that the screening programme would change in a few years' time from that of neural tube defects as the prime consideration to congenital cardiac abnormalities which would require scanning at a later gestational age in order to demonstrate adequately cardiac anatomy.

The meeting was closed with a session of members' cases which stimulated discussion on a variety of topics.

The event was concluded with a buffet lunch. It had been a great success and was a tribute to the hard work of the Gwent and South West Radiologists.

N. Powell
Secretary
BIR Welsh Branch

President's Dinner

The BIR Library set the scene for the annual President's Dinner, at which the badge of office is passed to the new president, this year held on 28 September 1989. Pictured from left to right are: the retiring president, Professor Brian Worthington with his wife Margaret and Mrs Susan Hill with the new president, Professor Kit Hill.

Product news

New imaging system from Varian

Varian has developed a new radiation therapy imaging system which enables radiation oncologists to verify instantly exact X-ray beam placement in relation to anatomical landmarks. This results in improved treatment quality and eliminates the time, labour and costs associated with acquiring X-ray port films, the conventional means for verifying treatments.

Varian's easy-to-use system enables high quality portal images to be displayed digitally on-line on a computer monitor. Within seconds of turning the medical linear accelerator's radiation beam on, the radiation oncologist has exact verification of in-progress treatment. Images can be enhanced, manipulated, made into hard copy and stored, all at the push of a button.

The complete imaging system includes the image detector unit, a microprocessor, and an easy-to-use operator interface.

The portable image detector unit easily attaches to the medical linear accelerator and forms a transmission image from the X-rays that pass through the patient's body. The unit is similar in size and shape to a standard film cassette and is used and positioned the same way. The central processing unit is equipped with additional special-purpose boards for controlling the image detector as well as image acquisition, processing and display. The video processor and monitor can display up to 265 shades of grey with an additional colour overlay. Standard, high-resolution images can be acquired and displayed within one to six seconds.

For further information, please contact Varian International AG, Steinhauserstrasse/Kollerstrasse 38, CH-6300 Zug, Switzerland or your local Varian office.

Dynamic Imaging have just introduced the CONCEPT 2000 ultrasound system. The CONCEPT series is a system of cross-related products that enable the clinician to have a greater choice in the selection of scanners, transducers and accessories. Transducers are comprised of annular, convex, linear and mechanical sector types including transvaginal and transrectal formats. Frequencies vary from 3.5 MHz to 7.5 MHz, and modules include action replay and computer controlled adaptive scanning (CCAS). This is a significant advance in ultrasound scanning and was developed in response to the limitations of the manual adjustment of time gain compensation (TGC) controls. Echo information is used by the scanner to set up the TGC releasing the operator from time-consuming and often suboptimal adjustment of manual TGC; CCAS provides a unique TGC vector for every scan line and adjusts each lines' TGC several times per second according to the type of tissue encountered by the ultrasound beam.

For further information contact Linda Robichaud, Dynamic Imaging Ltd, Young Square, Brucefield Industrial Park, Livingstone, EH54 9BX. Tel: 0506 415282.

Pixel Machine speeds body scanning

Nottingham University are using an AT&T Pixel Machine, supplied by computer graphics and imaging specialists CGI Ltd, to provide enhanced real time image capability for their magnetic resonance imaging body scanning system.

Echo planar imaging (EPI) was developed for body scanning by Professor Peter Mansfield in 1977 and the University leads the world in this method of scanning. EPI uses nuclear magnetic resonance to provide high speed scans which gives faster patient positioning and the ability to freeze motion, for example in unborn children or in the lungs, and enables real-time monitoring of physical movements, for example of heart-valve motion. To display motion in real time requires the power of the Pizel machine.

For more information contact Ron Coxon, Nottingham University. Tel: 0602 484848 or Greg Paul, CFI Ltd, Lychgate House 24 High Street, Ramsbury, Wiltshire SN8 2PB. Tel: 0672 20777.

New digital imaging system for Ireland

The first bi-plane DCI system in Great Britain and Ireland was recently installed in St James's Hospital, Dublin. It is capable of acquiring two images simultaneously by using short X-ray pulses that are beamed through the patient, so as to freeze the motion of the beating heart. These X-ray images are then converted into a visual image by an image intensifier, and the images are displayed immediately on the monitors in the room. During review, the synchronous display of the images of both channels shows the actual and complete position. The introduction of DCI into routine cardiology procedures creates new possibilities in this field.

For further information contact: Philips Medical Systems UK Ltd, Kelvin House, 63-75 Glenthorne Road, Hammersmith, London W6 0LJ. Tel: 01-741 1666.

Improved pocket Doppler probe

Oxford Sonicaid have introduced a new "pencil-tipped" probe to give easier accessibility to the awkward examination sites such as the supraorbital region. The new probe design is also ideal for measuring blood pressures in neonates.

The Sonicaid BV105 allows the clinician to complete a full non-invasive assessment of blood flow in both deep and superficial vessels. Applications include detection of peripheral arterial and venous disease, evaluation of impotence, pre- and post-surgical evaluation of blood flow in limbs and assessment of any low flow state such as in neonates or hypotensive patients. With the addition of the optional 2 MHz probe this pocket Doppler can also be used as a fetal heart detector.

For further information contact Christine Price, Oxford Sonicaid Ltd, Quarry Lane, Chichester, West Sussex PO19 2LP. Tel: 0243 775022.

In brief

Distribution of Epi-C (colon administration units) and the Bubble Breaker has been transferred from Bioglan Laboratories to Smith & Nephew Pharmaceuticals Limited. The Bioglan sales team, headed by Mrs Annette Drake, has joined Smith & Nephew Pharmaceuticals to continue to provide the support for these products.

All enquiries to Smith & Nephew Pharmaceuticals Ltd, Bampton Road, Harold Hill, Romford, Essex RM3 8SL. Tel: 04023 49333.

North West mobile MRI unit: first in Europe

The first MRI mobile service in Europe started recently at the AMI Alexander Hospital in Cheadle, Cheshire. The £1 million unit, in its specially constructed vehicle, represents the very latest in body scanning technology and will initially be available one day a week at Cheadle for both NHS patients and those with private medical insurance. However, it is expected that the demand will result in an increase in the number of days that the unit is operational.

For further information contact Andrew Cameron, Executive Director, ALMI Alexander Hospital, Mill Lane, Cheadle, Cheshire SK8 2PX. Tel: 061-428 3656

BIR Company Subscribers

The BIR company subscriber scheme was launched at the end of 1987 and is aimed at all companies who advertise in the BJR or exhibit at the MED X RAY technical exhibition.

For a subscription of just £250 per annum for an initial period of 3 years, an attractive package of benefits is offered (see March 1988 Bulletin for details).

If your company is interested in joining the scheme, please contact: Miss Susan Johnstone, General Secretary, British Institute of Radiology, 36 Portland Place, London W1N 4AT; Tel: 01-580 4085. Companies that have enrolled to date are listed below.

Agfa-Gevaert Ltd
27 Great West Road, Brentford, Middlesex TW8 9AX; tel. 01-560 2131. Product Areas 1. Contact Mr G. Mountford, Director.

Amersham International PLC
Lincoln Place, Green End, Aylesbury, Bucks HP20 2TP; tel. 0296-395222. Product areas 4, 5, 6. Contact Mr James McLaughlin, Sales and Marketing Manager.

British Nuclear Fuels plc
Room 525, Hinton House, Risley, Warrington, Cheshire WA3 6AS; tel. 0925-835022. Product areas 8, 11. Contact Dr R. J. Berry, Director of Health and Safety and Environmental Protection.

Cardiac Services Ltd
95A Finaghy Road, South Belfast BT10 0BY; tel. 0232-625566. Product areas 1, 3, 4, 5, 6. Contact Mr R J Brown, Managing Director.

Central Electricity Generating Board
15 Newgate Street, London EC1A 7AU; tel. 01-634 6898. Product areas 7, 8. Contact Mr R. V. Brierley, Office Services Manager.

E. G. & G. Astrophysics Research Ltd
Vale Road, Windsor, Berkshire SL4 5JP; tel 0753-855611. Product areas 1, 6, 7, 8,. Contact Miss Susan Holgate, Sales Executive (Therapy).

Elscint (GB) Ltd
Tower Road, Berinsfield, Oxfordshire OX9 8LW; tel 0865-340900 . Product areas 1, 3, 4. Contact Ms Faith Gorman, Managing Director.

E-Z-EM Ltd
1230 High Road, Whetstone, London N20; tel 01-446 9714. Product areas 1, 2, 8. Contact Mr D. F. Wills, Sales and Marketing Manager.

Fuji Photo Film (UK) Ltd
125 Finchley Road, London NW3 6JH; tel 01-586 9351. Product areas 1, 3. Contact Mr R. G. Brown, Marketing and Administration Manager.

Gammex-RMI Ltd
4 Clarendon Chambers, Clarendon Street, Nottingham NG1 5LN; tel. 0602-483807. Product areas 1, 3, 4, 5, 6. Contact Miss Eileen Parr, Commercial Manager.

IGE Medical Systems Ltd
352 Buckingham Avenue, Slough, Berks SL1 4ER; tel. 0753-874000. Product areas 1, 3, 4, 5, 6, 8. Contact Mr Jack Strange, Sales Administration.

Kodak Ltd
PO Box 66, Station Road, Hemel Hempstead, Herts HP1 1JU; tel. 0442-61122. Product areas 1. Contact Mr P. E. Blackwell, Manager, Health Sciences Division.

Mallinckrodt Diagnostica (UK) Ltd
11 North Portway Close, Round Spinney, Northampton NN3 4RQ. tel. 0604-46132. Product areas 4, 5. Contact Mr D. G. L. Wood, Business Manager.

Medical XraySupplies Ltd
Unit 12, Kingsbury Industrial Estate, Church Lane, Kingsbury, London NW9 8AU; tel. 01-205 9500. Product areas 1. Contact Mr R. J. Laird, Sales Director/Managing Director.

Nuclear Associates
100 Voice Road, Carle Place, New York 11514-1593, USA; tel 516-741 7614. Product areas 1, 3, 4, 5, 6, 8. Contact Mr H. Glasser, General Manager.

Nycomed (UK) Ltd
Nycomed House, 2111 Coventry Road, Sheldon, Birmingham B26 3EA; tel 021-742 2444. Product areas 1, 3. Contact Mr L. Birch Hansen, Managing Director.

Polaroid (UK) Ltd
Ashley Road, St Albans, Herts AL1 5PR; tel 0727 59191. Product areas 1, 3. Contact Ms Tina Thompstone, Product Supervisor.

Premise Engineering Ltd
Tibbs Hill Road, Abbots Langley, Watford, Herts WD5 0DR; tel. 09277-67433/63320. Product areas 8. Contact Mr R. K. Beach, Director.

Quantel Ltd
Administration Centre, Kiln Road, Newbury, Berkshire RG13 2HA; tel. 0635-32222. Product areas 2, 10. Contact Mr Christopher Trim, Publicity Officer.

Schering Health Care Ltd
The Brow, Burgess Hill, West Sussex RH15 9NE; tel. 04446-6011. Product areas 1, 2, 3. Contact Mr A. Greaves, Product Manager.

3M UK PLC
3M House, Bracknell, PO Box 1, Berks RG12 1JU; tel. 0344 426726. Product areas 1. Contact Mr Alan Budge, Marketing Manager.

Toshiba Medical Systems Europe BV
Schieweg 1, 2627 An Delft, The Netherlands; tel. 015 61 0121. Product areas 1, 6. Contact Mr. P Blonk, Office Manager, X-ray BU.

Wardray Products Ltd
Hampton Court Estate, Summer Road, Thames Ditton, Surrey KT7 0SP; 01-398 9911. Product areas 8. Contact Mr R. B. Wardley, Managing Director.

Key to product areas:

1. Diagnostic X-ray inc. NMR and CT.
2. Interventional radiology.
3. Ultrasound.
4. Nuclear medicine.
5. Radiopharmaceuticals.
6. Radiotherapy and oncology.
7. Radiobiology.
8. Radiation protection.
9. PACS.
10. Image processing.
11. Nuclear fuel cycle services.

BIR

Conference Services

Is there a seminar, conference or evening get-together you want to organize, but you don't have the time? The BIR Conference Office may be able to help you. Please call Nelleke van Helfteren, Conference Manager, to discuss possibilities.

01-580 4085

Library News

The BIR Library is open weekdays 9 a.m.–5 p.m. (7 p.m. on Tuesdays).

The Librarian, Mrs Gunnel Ingham, is in attendance Tuesdays 11 a.m.–7 p.m. and Thursdays 11 a.m.–5p.m. In her absence, assistance will be given by Miss Helen Smith. (Tel: 01-580 4085.)

The journal stock includes more than 100 titles. Though journals may not be taken out of the library, there is a photocopy service, also available by post or FAX. A list of current journals is available on request and is also published in the March and September issues of the Bulletin. Most books (except the historical collection) are available on loan.

Recent additions to the library

Bom, N. & Roelandt, J. (Eds). Intravascular ultrasound: techniques, developments and clinical perspectives. 1989

Mould, R. F. (Ed). Brachytherapy 2. Proceedings of the 5th International Selectron User's Meeting, The Hague, 1988

BIR Calendar

Unless otherwise indicated, enquiries about the following events should be addressed to the Conference Manager, British Institute of Radiology, 36 Portland Place, London W1N 4AT (Tel. 01-580 4085).

Radiation protection — sense or nonsense?
December 13, 1989
All day meeting at Middlesex Hospital, London
Chairmen: Dr R. J. Berry and Prof. K. Boddy
Speakers: R. J. Berry, P. Green, D. Henshaw, G. Kendall, B. A. Lindskoug (Halmstad), N. Pearce, E. Radford, G. Russell, B. Wall and S. J. Wozniak

Impact of modern imaging techniques in everyday ENT practice
January 18, 1990
Joint BIR/RCR/RSM evening meeting organized by the BIR
Chairman: Dr P. Anslow
Speakers: P. Anslow, T. Alun-Jones, S. Barker, L. Watson and H. Whittet

Methods of determining blood flow using radionuclides
February 13, 1990
Joint IPSM/BIR all day meeting organized by IPSM

Quantitation of argon blood flow using nuclear medicine techniques
February 21, 1990
Chairmen: Drs R. Speller and W. Hately

Radiobiology proffered papers
February 23, 1990
All day work-in-progress meeting

Imaging towards 2000 — practical integration of new technologies
March 21, 1990
All day meeting at the Scientific Societies, London
Chairmen: Profs P. N. T. Wells and I. Isherwood
Speakers: R. Frakowiak, A. Hemingway, J. Howart, W. R. Lees, H. Nunnerly, M. Smith and J. Williams

Photodynamic therapy
April 4, 1990
Joint BIR/IPSM all day meeting organized by the BIR
Chairman: Dr D. Ash
Speakers: D. Ash, S. Brown, J. Colles, A. Mackenzie, W. Starr, J. Carruth and J. Lowdell

BIR Annual General Meeting
May 3, 1990 at 5 p.m.
36 Portland Place, London
BIR members only

The combination of chemotherapy and radiotherapy in clinical practice
May 10, 1990
All day meeting
Chairman: Prof. A. Horwich, Dr J. Tobias and Dr S. Arnott

The repair of radiation damage — molecules to man
May 11, 1990
All day work-in-progress meeting

Radiology 90

Harrogate, 11-13 June 1990

Deadlines for receipt of proffered abstracts 12 January 1990. Contact the Conference Office for an abstract form.

FAX at the BIR

A FAX machine has been installed at the BIR. The number is: 01-255 3209. This can be used for urgent business, including library photocopies for which there will be an extra charge.

Meetings and courses

Bart's (FRCR II) Course: MCQ, Film Reporting and Vivas
February 12–14, 1990
St Bartholomew's Hospital, London
Further details: Mrs C. Burrage, Course Secretary, Room 26, Dunn Laboratories, St Bartholomew's Hospital, West Smithfield, London EC1A 7BE. Tel: 01-601 7531.

International Symposium in Physics of Medical Imaging and Advances in Computer Applications
February 21–23, 1990
New Delhi, India
Further details: Dr M. M. Rehani, Organizing Secretary, ISPMICA, Medical Physics Unit, IRCH, All India Institute of Medical Sciences, New Delhi-110029, India.

Drugs, Behaviour and the Brain: Advances in PET and SPECT Imaging of the Brain
March 15–17, 1990
Maryland, USA
Further details: Patty Campbell, Program Coordinator, The John Hopkins Medical Institutions, Office of Continuing Education, 720 Rutland Avenue, Baltimore, Maryland 21205, USA. Tel: (301) 955 8582.

Ob/Gyn and Abdominal Sonography: Update 1990
March 16, 1990
San Francisco, USA
Further details: Radiology Postgraduate Education, University of California, 521 Parnassus Avenue, Room C-324, San Francisco, CA 94143, USA. Tel: (415) 476 5731.

33rd Annual Diagnostic Radiology, Postgraduate Course
March 19–23, 1990
San Fransisco, USA
Further details: Radiology Postgraduate Education, University of California, 521 Parnassus Avenue, Room C-324, San Francisco, CA 94143, USA. Tel: (415) 476 5731.

Diagnostic Imaging: 1990
March 26–30, 1990
Kauai, HI, USA
Further details: Radiology Postgraduate Education, University of California, 521 Parnassus Avenue, Room C-324, San Francisco, CA 94143, USA. Tel: (415) 476 5731.

MR Imaging Update: Correlation with Ultrasound and CT Course and Symposium—1990
April 2–6, 1990
Bora Bora, Tahiti, USA
Further details: Radiology Postgraduate Education, University of California, 521 Parnassus Avenue, Room C-324, San Francisco, CA 94143, USA. Tel: (415) 476 5731.

Health Physics Objectives in the Design of Plant and Equipment
April 10, 1990
London
Further details: Dr D. N. S. Dixon, Programme Committee Secretary, 67 Oatlands Park, Linlithgow, West Lothian EH49 6AS. Tel: 031-244 2253.

Radiation Protection Applied to Low-Energy Beta Emitters
April 19, 1990
London
Further details: Philip Nicholson, Hon. Secretary, Institute of Radiation Protection, 64 Dalkeith Road,Harpenden, Herts AL5 5PW.

The Sixth Midlands Course in Otoradiology and MRI in ENT
April 19–21, 1990
Coventry
Further details: Miss M. Adams, Centre Administrator, Warwickshire Post-graduate Medical Centre, Stoney Stanton Road, Coventry CV1 4FG.

Radiology Review Course
April 29–May 4, 1990
Florida, USA
Further details: Carol Lamarre, Program Coordinator, University of Miami School of Medicine, Department of Radiology, PO Box 016960 (R-109), Miami, Florida 33101 USA. Tel: 305 549 6894.

27th Congress of the European Society of Paediatric Radiology
May 14–19, 1990
Munich, West Germany
Further details: Dr H. Fendel, Universität Kinderklinik, Röntgenabteilung, Lindwurmstr. 4, D-8000 München 2, FRG. Tel: 089 5160 3102. Deadline for submission of papers, posters: December 31, 1989.

Blood Vessel Imaging Using Ultrasound Techniques
May 16–18, 1990
Southampton
Further details: Mr K. N. Humphries, Blood Vessel Imaging Course, 10 Swale Drive, Chandlers Ford, Hampshire SO5 3QY.

1st World Congress on Safety in Medical Practice: Prevention and Compensation of Iatrogenic Complications
May 28–31, 1990
Elsinore, Denmark
Further details: Secretariat, ISPIC, University of Copenhagen, 21 Blegdamsvej, DK-2100 Copenhagen, Denmark.

CT and MR in Body Imaging: a Comprehensive Course
May 22–25, 1990
Monterey, CA, USA
Further details: Radiology Postgraduate Education, University of California, 521 Parnassus Avenue, Room C-324, San Francisco, CA 94143, USA. Tel: (415) 476 5731.

14th Leeds Gastroenterology Course for Radiologists
July 2–6, 1990
Leeds
Further details: Miss P. Kentley, Postgraduate Dean's Office, Level 7, Worsley Medical Building, University of Leeds, Leeds LS2 9JT. Tel: 0532 431751.

Killingbeck Cardiovascular II
July 11–13, 1990
Leeds
Further details: Dr M. R. Rees, Course Organizer, Killingbeck Hospital, York Road, Leeds LS14 6UQ. Tel: 0532 648164.

Brachytherapy Working Conference 6th International Selectron Users' Meeting
September 9–11, 1990
Florence, Italy
Further details: Conference Secretariat, Nucletron International B. V., PO Box 110, 3956 ZT Leersum, The Netherlands. Tel: 31 0 3434 54224.

International Skeletal Society — 17th Annual Refresher Course
September 9–15, 1990
Salzburg, Austria
Further details: Secretary/Treasurer, International Skeletal Society, Radiology Hospital of the University of Pennsylvania, 3400 Spruce Street, Philadelphia PA19104, USA.

As a service to our readers, notice of meetings or courses will be inserted free of charge. Please send full details to the Honorary Editor, BIR Bulletin.